

Point Beach Nuclear Plant Units 1 and 2
Dockets 50-266 and 50-301
NRC 2020-0032 Enclosure 4

Enclosure 4

Non-proprietary Reference Documents and Redacted Versions of Proprietary Reference Documents

(Public Version) (21 Attachments)

(850 Total Pages, including cover sheets)

Enclosure 4 Document List

- Attachment 1** – Westinghouse LTR-REA-20-28-NP, Revision 0, “Reactor Vessel, Reactor Vessel Supports, and Concrete Bioshield Exposure Data in Support of the Point Beach Unit 2 Subsequent License Renewal (SLR) Time-Limited Aging Analysis (TLAA),” July 31, 2020
- Attachment 2** – WCAP-18554-NP, Revision 1, “Fracture Mechanics Assessment of Reactor Pressure Vessel Structural Steel Supports for Point Beach Units 1 and 2,” September 2020
- Attachment 3** – Westinghouse WCAP-18555-NP, Revision 1, “Point Beach Units 1 and 2 Time-Limited Aging Analyses on Reactor Vessel Integrity for Subsequent License Renewal,” August 2020
- Attachment 4** – Framatome Topical Report BAW-2192, Revision 0, Supplement 3NP, Revision 0, “Low Upper-Shelf Toughness Fracture Mechanics Analysis of Reactor Vessels of B&W Owners Reactor Vessel Working Group for Levels A & B Service Loads,” October 2020
- Attachment 5** – Framatome Topical Report BAW-2178, Revision 0, Supplement 2NP, Revision 0, “Low Upper-Shelf Toughness Fracture Mechanics Analysis of Reactor Vessels of B&W Owners Reactor Vessel Working Group for Levels C & D Service Loads,” October 2020
- Attachment 6** – Framatome Technical Report ANP-3886NP, Revision 0, PWROG-20043-NP, “PWROG – PBN Unit 1 IS Plate A9811-1 Equivalent Margins Analysis for SLR,” October 2020
- Attachment 7** – Structural Integrity Associates, Inc. Report No.2000088.401, Revision 2, “Cycle Counts and Fatigue Projections for 80 Years of Plant Operation for Point Beach Nuclear Units 1 and 2,” October 19, 2020
- Attachment 8** – Westinghouse LTR-SDA-II-20-05-NP, Revision 2, “Environmentally Assisted Fatigue Screening Results for Point Beach Unit 1 and Unit 2 Safety Class 1 Primary Equipment,” June 30, 2020
- Attachment 9** – Structural Integrity Associates, Inc. Report No. 2000088.402, Revision 1, “Environmentally-Assisted Fatigue Evaluation for 80 Years of Plant Operation for Point Beach Nuclear Units 1 and 2,” September 25, 2020
- Attachment 10** – Westinghouse LTR-SDA-II-20-08-NP, Revision 1, “Environmentally Assisted Fatigue Evaluation Results for the Point Beach Unit 1 and Unit 2 Primary Equipment Sentinel Locations for Subsequent License Renewal,” July 15, 2020

Point Beach Nuclear Plant Units 1 and 2
Dockets 50-266 and 50-301
NRC 2020-0032 Enclosure 4

Attachment 11 – Westinghouse LTR-SDA-II-20-13-NP, Revision 2, “Environmentally Assisted Fatigue Evaluation Results for the Point Beach Unit 1 and Unit 2 Pressurizer Lower Head for Subsequent License Renewal,” September 23, 2020

Attachment 12 - Structural Integrity Associates, Inc. File No. 2000088.310P – REDACTED, Revision 1, “EAF Refined Analyses (Charging Nozzle, Hot Leg Surge Nozzle, SI Nozzle, SI/RHR Tee),” August 14, 2020

Attachment 13 - Structural Integrity Associates, Inc. Calculation No. PBCH-03Q-301, Revision 3, “Evaluation of Thermal Stratification Due to Valve Leakage,” September 25, 2020

Attachment 14 – Westinghouse LTR-SDA-20-064-NP, Revision 1, “ASME Section XI Appendix L Evaluation Results for the Point Beach Units 1 and 2 Pressurizer Spray Nozzles,” October 7, 2020

Attachment 15 – Structural Integrity Associates Calculation PBCH-06Q-301, Revision 1, “Containment Penetration Fatigue Evaluation,” November 11, 2003

Attachment 16 – Westinghouse WCAP-14439-NP, Revision 4, “Technical Justification for Eliminating Large Primary Loop Pipe Rupture as the Structural Design Basis for the Point Beach Nuclear Plant Units 1 and 2 for the Subsequent License Renewal Program (80 Years),” June 2020

Attachment 17 – Westinghouse LTR-SDA-II-20-06, Revision 1, “Leak-Before-Break Reconciliation of the Point Beach Units 1 and 2 Pressurizer Surge Line, Residual Heat Removal Line, and Accumulator Line Piping Systems for the Subsequent License Renewal Program,” May 4, 2020

Attachment 18 – Westinghouse LTR-PAFM-05-58-NP, Revision 3, “Flaw Tolerance Evaluation for Susceptible Reactor Coolant Loop Cast Austenitic Stainless Steel Piping Components in Point Beach Units 1 and 2 for 80 years,” July 2020

Attachment 19 – Westinghouse LTR-SDA-20-020-NP, Revision 1, “Point Beach Units 1 and 2 Reactor Coolant Pump Casings ASME Code Case N-481 Analysis for 80-year Subsequent License Renewal (SLR),” July 2020

Attachment 20 – Westinghouse LTR-AMLR-20-26-NP, Revision 1, “Transmittal of Results from the MRP-191 Revision 2 Review in Support of Subsequent License Renewal for Point Beach Units 1 and 2,” June 11, 2020

Attachment 21 – Westinghouse LTR-REA-20-29-NP, Revision 0, “Comparison of Point Beach Unit 1 Reactor Internals Fluence Values to the Representative 3-Loop Plant for MRP-191, Revision 2”, July 7, 2020

Enclosure 4
Non-proprietary Reference Documents and
Redacted Versions of Proprietary Reference
Documents
(Public Version)
Attachment 1

**Westinghouse LTR-REA-20-28-NP, Revision 0,
“Reactor Vessel, Reactor Vessel Supports, and
Concrete Bioshield Exposure Data in Support of the
Point Beach Unit 2 Subsequent License Renewal
(SLR) Time-Limited Aging Analysis (TLAA),” July 31,
2020**

(63 Total Pages, including cover sheets)



To: John T. Ahearn
Cc: Alexandria M. Carolan
Benjamin E. Mays
Anees Udyawar

Date: July 31, 2020

From: Nuclear Operations & Radiation Analysis
Phone: (724) 940-8119
Email: nedwidfm@westinghouse.com
Our Ref: **LTR-REA-20-28-NP, Revision 0**

Subject: **Reactor Vessel, Reactor Vessel Supports, and Concrete Bioshield Exposure Data in Support of the Point Beach Unit 2 Subsequent License Renewal (SLR) Time-Limited Aging Analysis (TLAA)**

Reference(s): 1. CN-REA-20-17, Revision 0, "Point Beach Unit 2 Reactor Vessel, Vessel Supports, and Bioshield Concrete Exposure for Subsequent License Renewal (SLR)," July 2020.

Attachment(s): 1. Reactor Vessel, Reactor Vessel Supports, and Concrete Bioshield Exposure Data in Support of the Point Beach Unit 2 Subsequent License Renewal (SLR) Time-Limited Aging Analysis (TLAA) (60 pages)

Attachment 1 provides select exposure data applicable to the Point Beach Unit 2 reactor pressure vessel (RPV), RPV supports, concrete bioshield, and in-vessel and ex-vessel dosimetry. The exposure data in Attachment 1 were taken from CN-REA-20-17 (Reference 1). These data are to be provided to NextEra Energy in support of their SLR project. Exposure projections to 72 effective full-power years (EFPY) are provided in Attachment 1.

The RPV neutron fluence results will be used by Westinghouse to assess pressure-temperature limit curves for the RPV, the RPV support iron atom displacement results will be used by Westinghouse to assess embrittlement of the RPV supports, and the concrete gamma dose results will be used by Enercon to assess degradation of the bioshield concrete. Conclusions based on the results of these downstream evaluations will be summarized in the analyses in which the evaluations are performed.

Please contact the undersigned if there are any questions regarding this information.

Author: *(Electronically Approved)**
Frank M. Nedwidek
Nuclear Operations & Radiation
Analysis

Reviewer: *(Electronically Approved)**
Andrew E. Hawk
Nuclear Operations & Radiation
Analysis

Approver: *(Electronically Approved)**
Laurent P. Houssay
Nuclear Operations & Radiation
Analysis

* *Electronically approved records are authenticated in the Process, Records and Information Management Environment*

Attachment 1

Reactor Vessel, Reactor Vessel Supports, and Concrete Bioshield Exposure Data in Support of the Point Beach Unit 2 Subsequent License Renewal (SLR) Time-Limited Aging Analysis (TLAA)

Table of Contents

1.0	Introduction.....	3
2.0	Discrete Ordinates Model	4
3.0	Dosimetry Comparisons.....	11
4.0	Exposure Results.....	19
4.1	Reactor Pressure Vessel	19
4.2	Surveillance Capsules	34
4.3	RPV Supports.....	45
4.4	Concrete Bioshield.....	53
5.0	References.....	60

1.0 Introduction

This attachment describes a discrete ordinates transport analysis performed for Point Beach Unit 2. The results of this analysis are intended to support the Point Beach Unit 2 80-year subsequent license renewal (SLR) time-limited aging analysis (TLAA).

The neutron transport methodology used to generate the data provided in this attachment followed the guidance of Regulatory Guide 1.190 (Reference 1), and was consistent with the United States Nuclear Regulatory Commission (NRC) approved methodology described in WCAP-18124-NP-A (Reference 2). This methodology has been generically approved for calculations of exposure of the reactor pressure vessel (RPV) beltline (generally, RPV materials opposite the active fuel). No method, generic or specific to Point Beach Unit 2, has been approved by the NRC for the other calculations performed (i.e., exposure of RPV extended beltline materials, RPV supports, and bioshield concrete).

2.0 Discrete Ordinates Model

Discrete ordinates transport calculations were performed on a fuel-cycle-specific basis to determine the neutron and gamma ray environment within the Point Beach Unit 2 reactor geometry. The specific methods applied are consistent with those described in WCAP-18124-NP-A (Reference 2).

All the transport calculations were carried out using the three-dimensional discrete ordinates code RAPTOR-M3G and the BUGLE-96 cross-section library. The BUGLE-96 library provides a 67-group coupled neutron-gamma ray cross-section data set produced specifically for light water reactor applications. In these analyses, anisotropic scattering was treated with a P_5 Legendre expansion and the angular discretization was modeled with an S_{16} order of angular quadrature. Energy- and space-dependent core power distributions, as well as system operating temperatures were treated on a fuel-cycle-specific basis.

A top view of the RAPTOR-M3G model for Point Beach Unit 2 at the core midplane is shown in Figure 2-1. In this figure, a single quadrant is depicted. A top view of the RAPTOR-M3G model just above the nozzle support shoes is shown in Figure 2-2. This figure shows the ring girder, support column, and cutout in the bioshield surrounding the support column. A top view of the RAPTOR-M3G model through the nozzle centerline is shown in Figure 2-3. Side views of the RAPTOR-M3G model of the reactor are shown in Figure 2-4 through Figure 2-6. The model extends radially from the centerline of the reactor core out to a location interior to the concrete bioshield, and over an axial span from an elevation nine feet below the active fuel to eight feet above the active fuel.

In addition to the core, reactor vessel internals, RPV, and concrete bioshield, the RAPTOR-M3G model developed for this quadrant geometry includes explicit representations of the surveillance capsules, RPV cladding, and the insulation located external to the RPV. The RPV supports extending through the bioshield, and various cut-outs in the bioshield are included as well.

From a neutronic standpoint, the inclusion of the surveillance capsules and associated support structure in the analytical model is significant. Since the presence of the capsules and structure has a marked impact on the magnitude of the neutron flux as well as on the relative neutron and gamma ray spectra at dosimetry locations within the capsules, a meaningful evaluation of the radiation environment internal to the capsules can be made only when these perturbation effects are properly accounted for in the analysis.

In developing the RAPTOR-M3G model of the reactor geometry shown in Figure 2-1 through Figure 2-6, nominal design dimensions were employed for the various structural components. Coolant above the active core assumed the same density as the core outlet conditions, and coolant below the active core assumed the same density as the core inlet conditions. These coolant temperatures were varied on a cycle-specific basis. The reactor core itself was treated as a homogeneous mixture of fuel, cladding, water, and miscellaneous core structures.

The RAPTOR-M3G model consisted of 256 radial by 214 azimuthal by 377 axial intervals. Mesh sizes were chosen to assure that proper convergence of the inner iterations was achieved on a pointwise basis. The pointwise inner iteration flux convergence criterion utilized in the calculations was set at a value of 0.001. A review of the results indicates that all the neutron and gamma groups fully converged for all cycles.

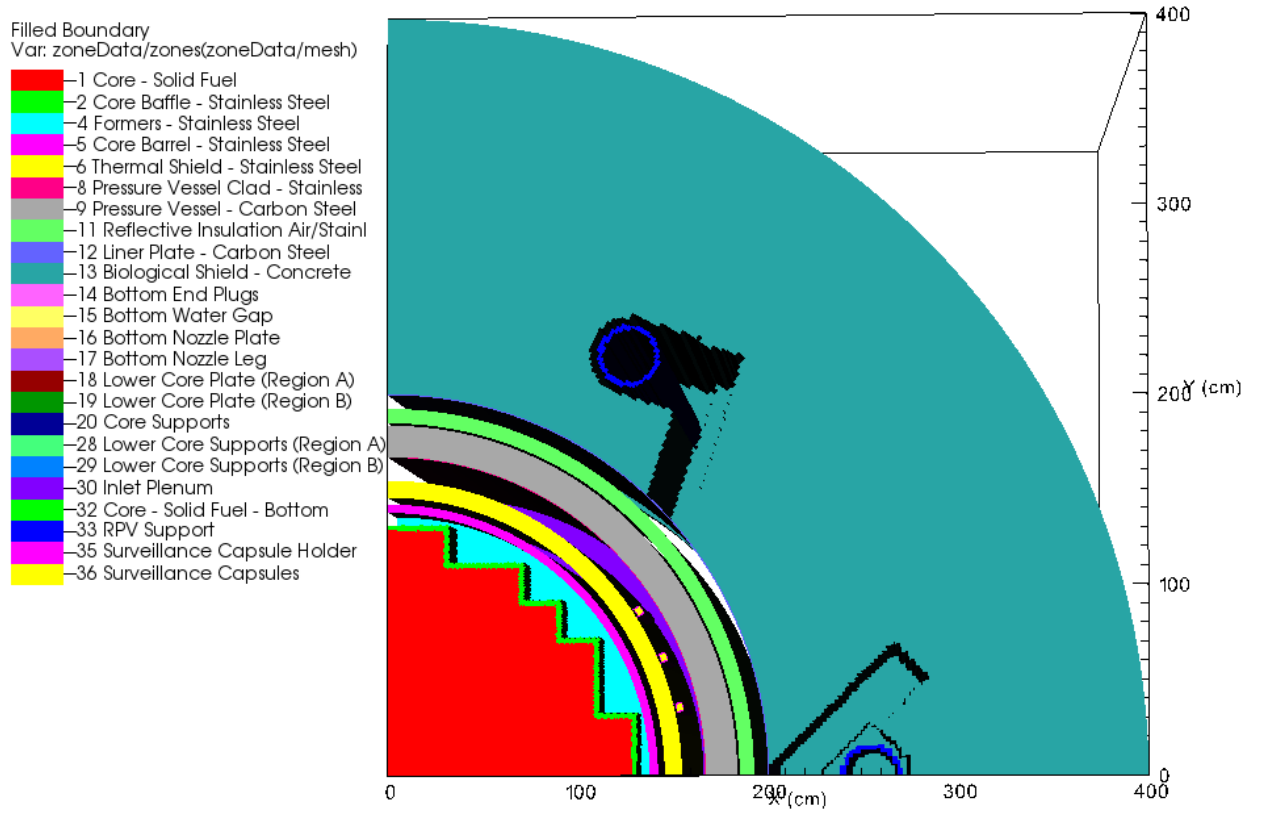


Figure 2-1
Top View of RAPTOR-M3G Model, Core Midplane (Z = 0 cm)

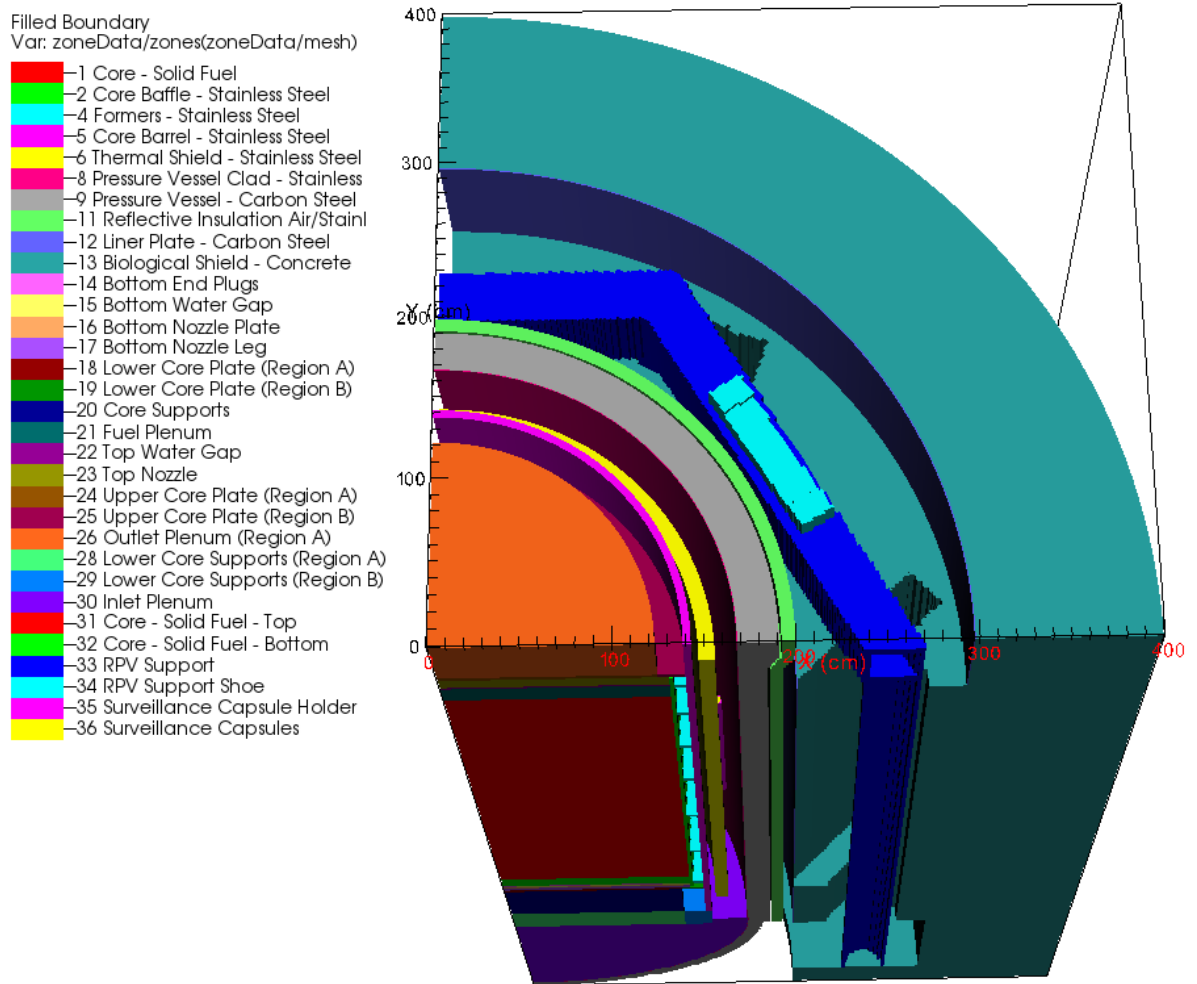


Figure 2-2
Top View of RAPTOR-M3G Model, above Ring Girder (Z = 264 cm)

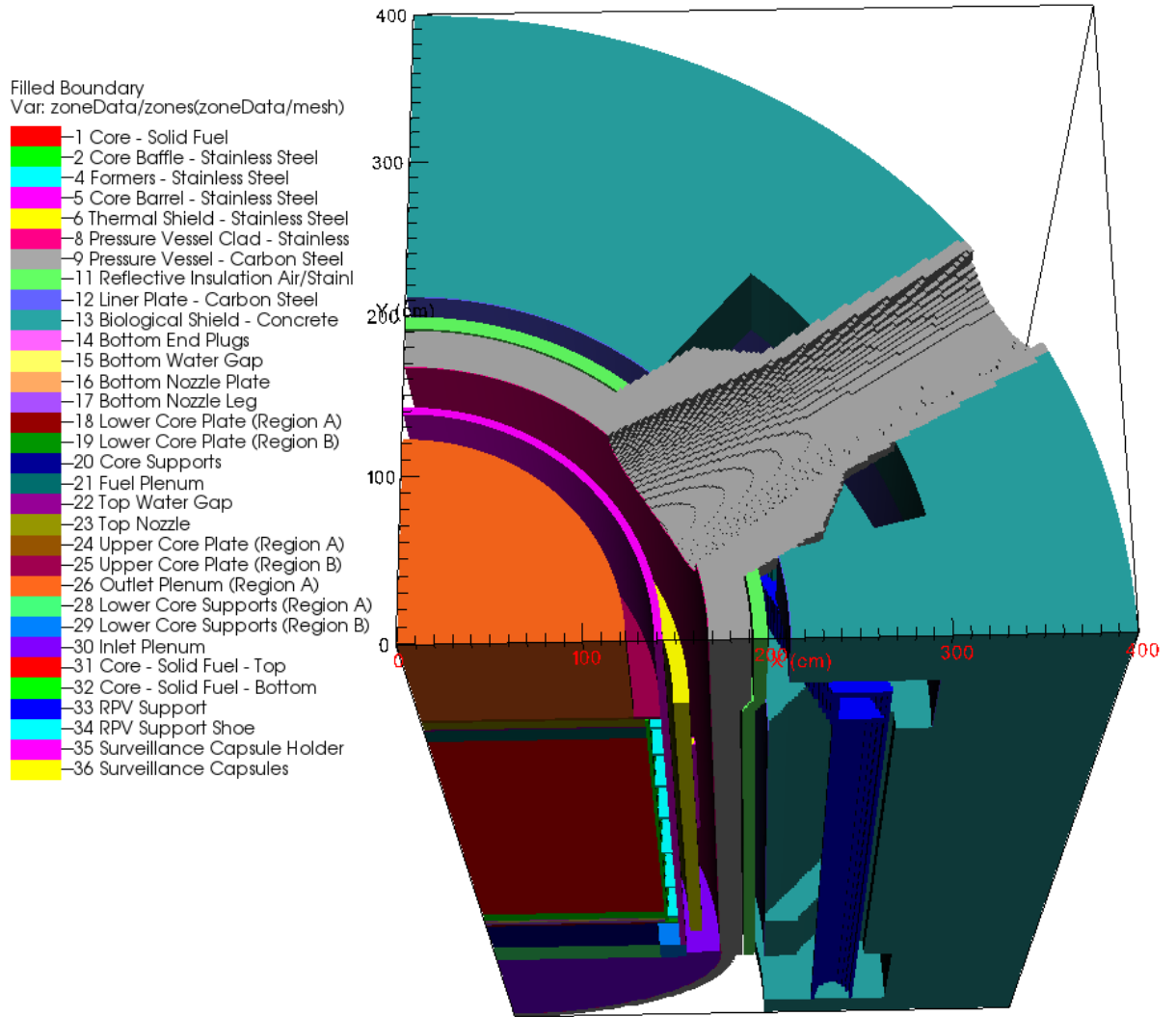


Figure 2-3
Top View of RAPTOR-M3G Model, through Nozzle Centerline (Z = 332 cm)

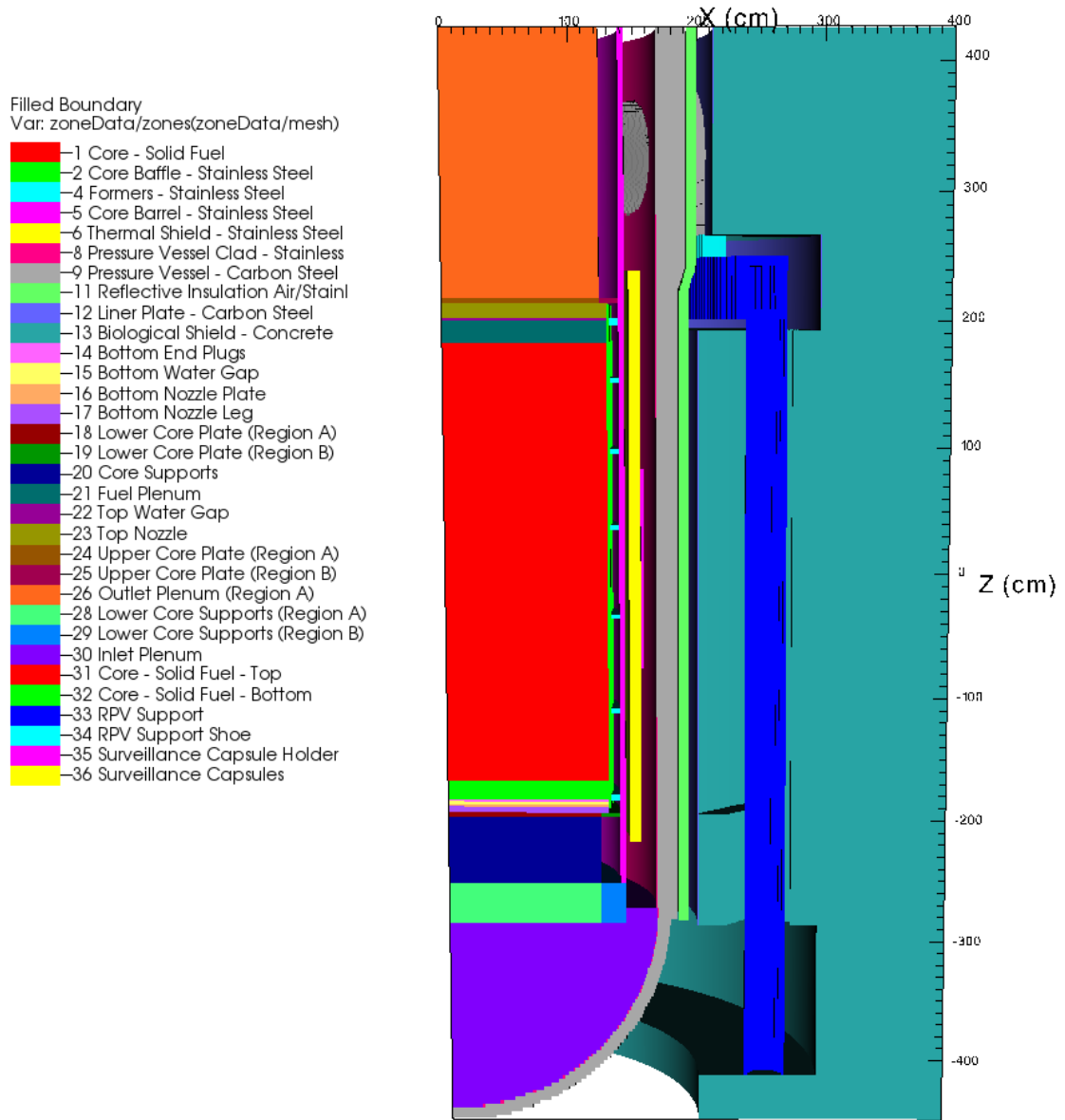


Figure 2-4
Side View of RAPTOR-M3G Model, through Support Column ($\theta = 0^\circ$)

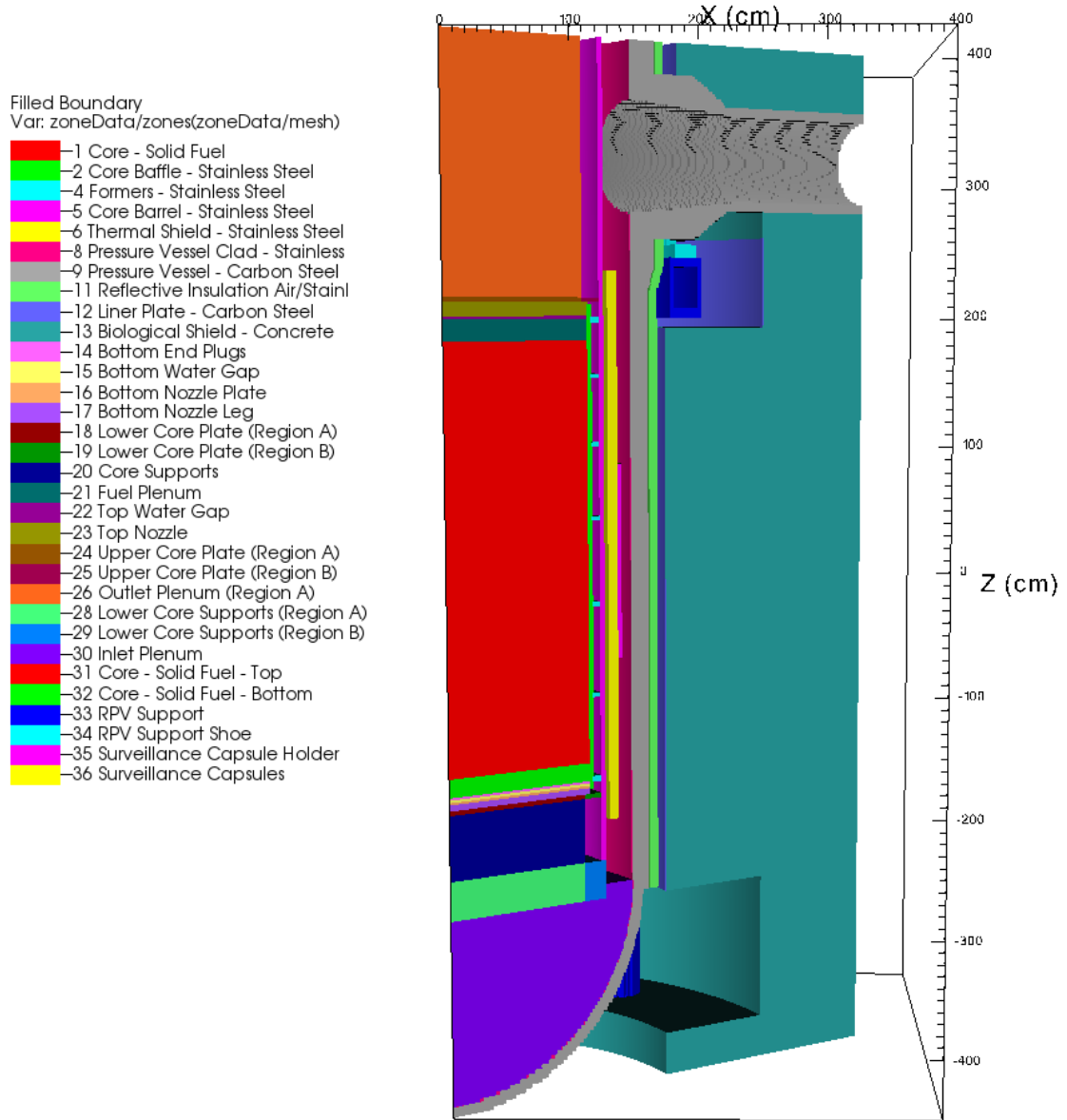


Figure 2-5
Side View of RAPTOR-M3G Model, through Inlet Nozzle ($\theta = 31.5^\circ$)

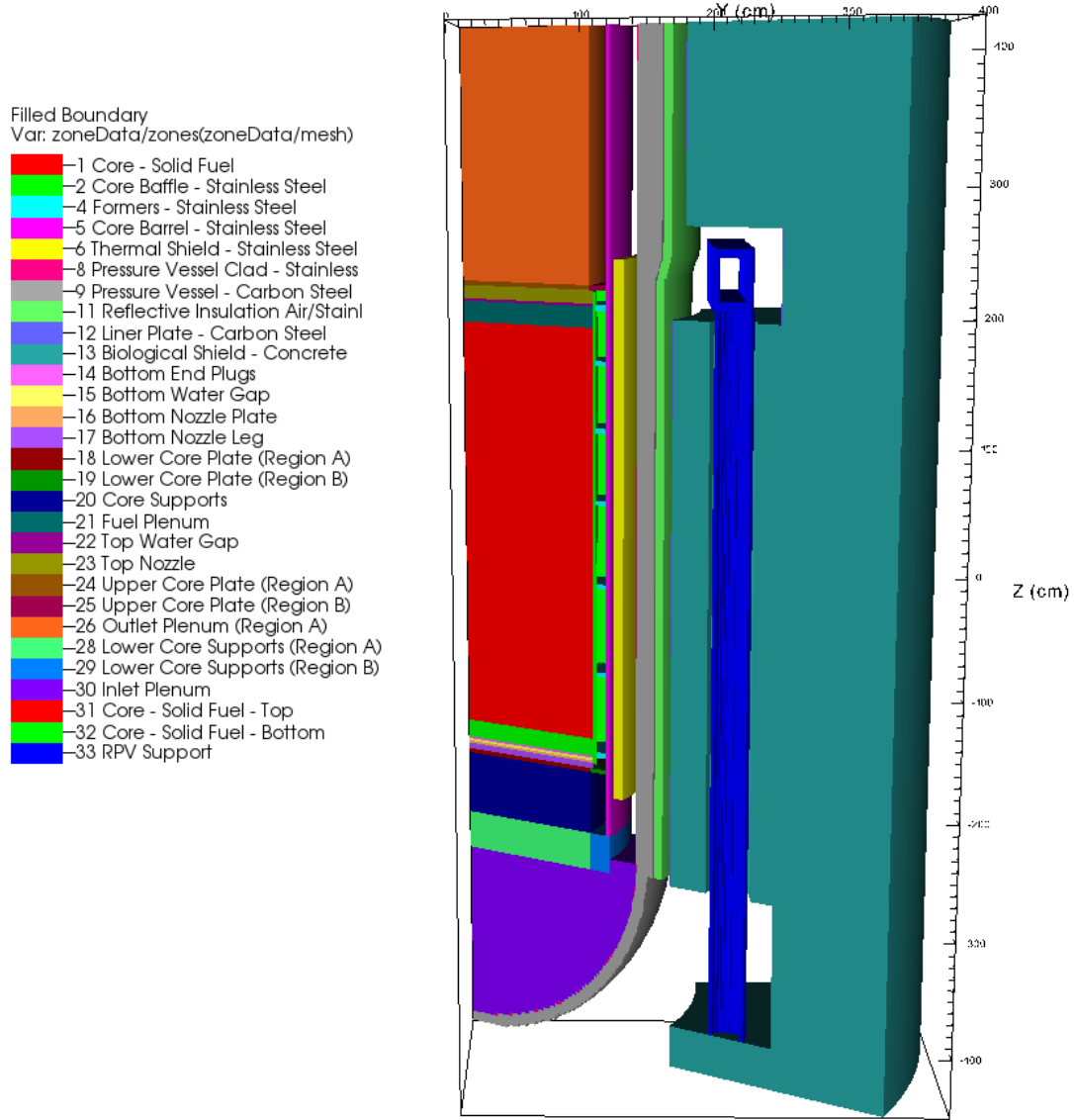


Figure 2-6
Side View of RAPTOR-M3G Model, through Support Column ($\theta = 60^\circ$)

3.0 Dosimetry Comparisons

Six in-vessel surveillance capsules attached to the thermal shield were included in the Point Beach Unit 2 reactor design. The capsules were located at azimuthal angles of 77° and 257° (13° from the core cardinal axis), 67° and 247° (23° from the core cardinal axis), and 57° and 237° (33° from the core cardinal axis). In addition to these six in-vessel surveillance capsules included in the original Reactor Vessel Surveillance Program, a seventh capsule was inserted into a 13° capsule holder location prior to Cycle 26. A summary of the surveillance capsules is given in Table 3-1.

To supplement the neutron dosimetry provided by the sensor sets contained in the in-vessel surveillance capsules, multiple foil sensors were installed at several locations in the annular region located between the RPV thermal insulation and the concrete bioshield. These multiple foil sets were designed to provide measured reaction rate data sufficient to characterize the neutron spectra at these measurement locations. The ex-vessel neutron dosimetry (EVND) was installed prior to Cycle 15 at azimuthal locations of 0°, 15°, 30°, and 45° relative to the core cardinal axis. A summary of the EVND capsules irradiated during Cycles 15 through 20 is given in Table 3-2.

Comparisons of the measurement results from each of the four in-vessel surveillance capsules and 25 ex-vessel sensor set irradiations with corresponding analytical predictions were used to demonstrate compliance with the requirements of Regulatory Guide 1.190 (Reference 1) as well as to support the uncertainty estimates associated with the calculated exposure levels. These comparisons were examined on two levels. In the first instance, calculations of individual sensor reaction rates were compared directly with the measurement data from the counting laboratory. This level of comparison was not impacted by the least-squares evaluations of the sensor sets. In the second case, calculated values of neutron exposure rates in terms of fast neutron fluence rate ($E > 1.0$ MeV) and iron atom displacement rate were compared with the best estimate exposure rates obtained from the least-squares evaluation.

In Table 3-3, comparisons of measurement-to-calculation (M/C) ratios are listed for the threshold sensors contained in the in-vessel surveillance capsules. From Table 3-3 it is noted that for the individual threshold reaction foils, the average M/C ratio ranges from 0.96 to 1.08 with an overall average of 1.01 and an associated standard deviation of 5.9%.

In Table 3-4, similar comparisons are provided for the 16 sensor sets withdrawn from the midplane axial elevation measurement locations in the reactor cavity. From Table 3-4, it is noted that for the individual threshold reaction foils the average M/C ratio ranges from 0.86 to 1.06 with an overall average of 0.90 and an associated standard deviation of 6.8%. The overall average was based on an equal weighting of the sensor types with no account taken of the spectral coverage of the individual sensors. Comparisons of the M/C ratios for the nine sensor sets withdrawn from the off-midplane measurement locations in the reactor cavity are provided in Table 3-5.

In Table 3-6 and Table 3-7, best-estimate-to-calculation (BE/C) ratios for fast neutron fluence rate ($E > 1.0$ MeV) and iron atom displacement rate resulting from the least-squares evaluation of each sensor set are provided for both the in-vessel and midplane ex-vessel irradiations. For the in-vessel capsules, the average BE/C ratio is seen to be 1.01 with an associated standard deviation of 1.2% for fast neutron fluence rate ($E > 1.0$ MeV) and 1.02 with an associated standard deviation of 1.3% for iron atom displacement rate. The corresponding average BE/C ratios from the midplane ex-vessel irradiations are 0.87 with a standard

deviation of 4.4% for fast neutron fluence rate ($E > 1.0$ MeV) and 0.89 with a standard deviation of 4.8% for iron atom displacement rate.

The data sets listed in Table 3-3 through Table 3-7 provide a validation of the results of the plant-specific neutron transport calculations. These data comparisons show that for the in-vessel locations, the measurements and calculations agree within the 20% criterion specified in Regulatory Guide 1.190. For the ex-vessel locations, the measurements and calculations agree within the 30% criterion specified in Regulatory Guide 1.190.

The total database summary of the M/C comparisons based on the individual sensor reactions without recourse to the least-squares adjustment procedure is summarized in Table 3-8. A similar comparison for exposure rates expressed in terms of fast neutron fluence rate ($E > 1.0$ MeV) and iron atom displacement rate is summarized in Table 3-9.

These data comparisons show similar results, with the linear average M/C ratio of 0.96 in good agreement with the resultant least-squares BE/C ratios of 0.94 for fast neutron fluence rate ($E > 1.0$ MeV) and 0.96 for iron atom displacement rate. The comparisons show that the $\pm 20\%$ (1σ) agreement between calculation and measurement required by Regulatory Guide 1.190 is met.

Table 3-1
Surveillance Capsule Summary

Capsule ID	Azimuthal Location ^[1]	Withdrawal Time
V	13°	EOC 1
T	23°	EOC 3
R	13°	EOC 5
S	33°	EOC 16
P	23°	EOC 22 ^[2]
N	33°	-
W	13°	-
Note(s):		
1. Relative to cardinal axis.		
2. Surveillance capsule has not been analyzed.		

Table 3-2
Ex-Vessel Neutron Dosimetry Summary

Cycle 15 Irradiation				
Capsule Set 2 Identification				
Azimuth (degrees)	Vessel Support	Core Top	Core Midplane	Core Bottom
0	XX	G	H	I
15			J	
30			K	
45			L	

Cycle 16 Irradiation				
Capsule Set 3 Identification				
Azimuth (degrees)	Vessel Support	Core Top	Core Midplane	Core Bottom
0		M	N	O
15			P	
30			Q	
45			R	

Cycle 17 Irradiation				
Capsule Set 5 Identification				
Azimuth (degrees)	Vessel Support	Core Top	Core Midplane	Core Bottom
0		AA	BB	CC
15			DD	
30			EE	
45			FF	

Cycles 18-20 Irradiation				
Capsule Set 7 Identification				
Azimuth (degrees)	Vessel Support	Core Top	Core Midplane	Core Bottom
0		MM	NN	OO
15			PP	
30			QQ	
45			RR	

Table 3-3
Comparison of Measured to Calculated Threshold Reaction Rates – In-Vessel Capsules

Capsule	Reaction					
	⁶³ Cu (n,α)	⁵⁴ Fe (n,p) Rear	⁵⁴ Fe (n,p) Front	⁵⁸ Ni (n,p)	²³⁸ U (n,f)	²³⁷ Np (n,f)
V	0.92	0.95	0.89		1.09	1.07
T	0.97	1.02	1.01	0.99	0.99	1.08
R	1.03	0.98	0.98	1.01	1.04	1.09
S	1.07			0.94	1.10	1.07
Average	1.00	0.99	0.96	0.98	1.05	1.08
% std dev	6.4	3.5	6.7	3.6	4.8	0.9

Reaction	Average M/C	% Standard Deviation
⁶³ Cu (n,α)	1.00	6.4
⁵⁴ Fe (n,p) Rear	0.99	3.5
⁵⁴ Fe (n,p) Front	0.96	6.7
⁵⁸ Ni (n,p)	0.98	3.6
²³⁸ U (n,f)	1.05	4.8
²³⁷ Np (n,f)	1.08	0.9
Linear Average	1.01	5.9

Table 3-4
Comparison of Measured to Calculated Threshold Reaction Rates – Ex-Vessel Midplane Capsules

Capsule	Reaction						
	⁶³ Cu (n,α)	⁴⁶ Ti (n,p)	⁵⁴ Fe (n,p)	⁵⁴ Fe (n,p) (Cd)	⁵⁸ Ni (n,p)	²³⁸ U (n,f)	²³⁷ Np (n,f)
H	0.86	0.89	0.82	0.84	0.85	0.84	1.00
J	0.98	1.01	0.91	0.89	0.90	0.90	1.07
K	0.92	0.96	0.94	0.87	0.88	0.88	1.00
L	0.98	1.03	0.90	0.88	0.93	0.96	1.16
N	0.84	0.86	0.82	0.79	0.82	0.82	
P	0.91	0.91	0.86	0.82	0.86	0.86	
Q	0.97	0.96	0.89	0.91	0.90	0.87	
R	0.99	0.97	0.94	0.92	0.94	0.91	
BB	0.87	0.87	0.85	0.82	0.83	0.81	
DD	0.96	0.95	0.89	0.88	0.88	0.87	
EE	0.94	0.96	0.88	0.88	0.88	0.90	
FF	0.98	0.97	0.91	0.90	0.91	0.89	
NN	0.88	0.89	0.83	0.81	0.83	0.84	
PP	0.95	0.93	0.83	0.85	0.85	0.88	
QQ	0.95	0.95	0.85	0.84	0.86	0.86	
RR	0.95	0.92	0.84	0.85	0.87	0.90	
Average	0.93	0.94	0.87	0.86	0.87	0.87	1.06
% std dev	5.0	5.1	4.7	4.4	4.0	4.2	7.4

Reaction	Average M/C	% Standard Deviation
⁶³ Cu (n,α)	0.93	5.0
⁴⁶ Ti (n,p)	0.94	5.1
⁵⁴ Fe (n,p)	0.87	4.7
⁵⁴ Fe (n,p) Cd	0.86	4.4
⁵⁸ Ni (n,p)	0.87	4.0
²³⁸ U (n,f)	0.87	4.2
²³⁷ Np (n,f)	1.06	7.4
Linear Average	0.90	6.8

Table 3-5
Comparison of Measured to Calculated Threshold Reaction Rates – Ex-Vessel Off-Midplane Capsules

Capsule	Reaction						
	⁶³ Cu (n,α)	⁴⁶ Ti (n,p)	⁵⁴ Fe (n,p)	⁵⁴ Fe (n,p) Cd	⁵⁸ Ni (n,p)	²³⁸ U (n,f)	²³⁷ Np (n,f)
G	0.76	0.87	0.71	0.81	0.81	0.86	0.97
I	0.79	0.89	0.77	0.77	0.82	0.88	1.03
XX	0.77	0.82	0.71	0.74	0.72	0.95	1.04
M	0.94	1.00	0.93	0.92	0.97	1.03	
O	0.87	0.94	0.87	0.85	0.92	0.98	
AA	0.99	1.05	0.96	0.96	1.02	1.09	
CC	0.92	0.99	0.90	0.88	0.95	0.98	
MM	0.86	0.95	0.82	0.83	0.91	0.94	
OO	0.79	0.94	0.81	0.80	0.87	0.92	

Table 3-6
Comparison of Best-Estimate to Calculated Exposure Rates – In-Vessel Capsules

Capsule	Neutron Fluence Rate (E > 1.0 MeV)		Iron Displacement Rate	
	BE/C	% std dev	BE/C	% std dev
V	0.99	6	1.00	7
T	1.02	6	1.02	7
R	1.02	6	1.03	7
S	1.01	6	1.02	7
Average	1.01	1.2	1.02	1.3

Table 3-7
Comparison of Best-Estimate to Calculated Exposure Rates – Ex-Vessel Midplane Capsules

Capsule	Neutron Fluence Rate (E > 1.0 MeV)		Iron Displacement Rate	
	BE/C	% std dev	BE/C	% std dev
H	0.87	6	0.91	9
J	0.92	6	0.95	9
K	0.91	6	0.93	9
L	0.95	6	0.99	9
N	0.82	7	0.84	10
P	0.84	7	0.86	11
Q	0.88	7	0.89	10
R	0.91	7	0.91	10
BB	0.83	7	0.84	10
DD	0.86	7	0.88	11
EE	0.88	7	0.89	10
FF	0.89	7	0.89	10
NN	0.83	7	0.85	10
PP	0.84	7	0.86	11
QQ	0.84	7	0.86	11
RR	0.86	7	0.87	10
Average	0.87	4.4	0.89	4.8

Table 3-8
Total Database Summary (M/C Reaction Rate Ratios)

Reaction	In-Vessel Database		Midplane Ex-Vessel Database		Combined Database	
	Average M/C	% Unc. (1 σ)	Average M/C	% Unc. (1 σ)	Average M/C	% Unc. (1 σ)
⁶³ Cu (n, α)	1.00	6.4	0.93	5.0	0.97	4.1
⁴⁶ Ti (n,p)	-	-	0.94	5.1	-	-
⁵⁴ Fe (n,p)	0.97	5.0	0.87	4.5	0.92	3.4
⁵⁸ Ni (n,p)	0.98	3.6	0.87	4.0	0.93	2.7
²³⁸ U (n,f)	1.05	4.8	0.87	4.2	0.96	3.2
²³⁷ Np (n,f)	1.08	0.9	1.06	7.4	1.07	3.7
Linear Average	1.01	5.9	0.90	6.8	0.96	4.3

Table 3-9
Total Database Summary (Integral Exposure Rate Ratios)

Parameter	In-Vessel Database		Midplane Ex-Vessel Database		Combined Database	
	Average BE/C	% Unc. (1 σ)	Average BE/C	% Unc. (1 σ)	Average BE/C	% Unc. (1 σ)
Fluence Rate (E > 1.0 MeV)	1.01	1.2	0.87	4.4	0.94	2.3
dpa/s	1.02	1.3	0.89	4.8	0.96	2.5

4.0 Exposure Results

4.1 Reactor Pressure Vessel

Neutron exposure data pertinent to the RPV clad/base metal interface are given in Table 4-1 and Table 4-2 for neutron fluence rate ($E > 1.0$ MeV) and fluence ($E > 1.0$ MeV), respectively, and in Table 4-3 and Table 4-4 for dpa/s and dpa, respectively. In each case, the data are provided for each operating cycle of the Point Beach Unit 2 reactor. Neutron fluence ($E > 1.0$ MeV) and dpa are also projected to future operating times extending to 72 EFPY. Two projections are provided: one using Cycle 38 as the basis for future projections with no bias on peripheral assembly power, and the second using Cycle 38 as the basis for future projections with a 10% positive bias on peripheral assembly power. The RPV exposure data are presented in terms of the maximum exposure experienced by the pressure vessel at azimuthal angles of 0° , 15° , 30° , 45° , 60° , 75° , and 90° , and at the azimuthal location providing the maximum exposure relative to the core cardinal axes.

In Table 4-5 and Table 4-6, maximum projected fast neutron fluence ($E > 1.0$ MeV) and dpa, respectively, of the various RPV materials are given. The neutron exposure data provided in Table 4-5 and Table 4-6 are the maximum values at either the RPV clad/base metal interface or the RPV outer surface. Note that for regions and materials above and below the core (e.g., inlet nozzle to nozzle belt forging weld and lower shell to lower head ring circumferential weld), the neutron exposure values at the RPV outer surface can be greater than those at the clad/base metal interface (Reference 3).

Table 4-1
Calculated Maximum Fast Neutron Fluence Rate ($E > 1.0$ MeV) at the RPV Clad/Base Metal Interface

Cycle	Cycle Length (EFPY)	Total Time (EFPY)	Fluence Rate (n/cm ² -s)								Elevation of Max. (cm)
			0°	15°	30°	45°	60°	75°	90°	Maximum ^[1]	
1	1.52	1.52	4.66E+10	2.70E+10	1.82E+10	1.59E+10	1.83E+10	2.77E+10	4.66E+10	4.66E+10	1.0
2	1.05	2.57	4.60E+10	2.70E+10	1.90E+10	1.69E+10	1.92E+10	2.74E+10	4.60E+10	4.60E+10	-65.0
3	0.87	3.44	4.53E+10	2.62E+10	1.85E+10	1.65E+10	1.86E+10	2.65E+10	4.52E+10	4.53E+10	-67.0
4	0.87	4.31	4.20E+10	2.44E+10	1.75E+10	1.54E+10	1.76E+10	2.50E+10	4.19E+10	4.20E+10	1.0
5	0.89	5.20	4.25E+10	2.57E+10	1.78E+10	1.43E+10	1.78E+10	2.58E+10	4.17E+10	4.25E+10	1.0
6	0.87	6.06	3.20E+10	2.09E+10	1.83E+10	1.52E+10	1.86E+10	2.16E+10	3.22E+10	3.22E+10	1.0
7	0.89	6.96	3.53E+10	2.05E+10	1.53E+10	1.47E+10	1.53E+10	2.06E+10	3.47E+10	3.53E+10	1.0
8	0.86	7.81	3.69E+10	2.08E+10	1.48E+10	1.42E+10	1.50E+10	2.16E+10	3.74E+10	3.74E+10	-1.0
9	0.79	8.60	3.76E+10	2.13E+10	1.49E+10	1.43E+10	1.51E+10	2.19E+10	3.76E+10	3.76E+10	1.0
10	1.20	9.80	3.32E+10	1.95E+10	1.51E+10	1.43E+10	1.53E+10	2.02E+10	3.35E+10	3.35E+10	-1.0
11	0.85	10.65	2.69E+10	1.89E+10	1.51E+10	1.30E+10	1.51E+10	1.88E+10	2.58E+10	2.69E+10	-1.0
12	0.80	11.45	2.94E+10	1.94E+10	1.43E+10	1.19E+10	1.46E+10	1.99E+10	2.94E+10	2.94E+10	3.0
13	0.81	12.25	2.68E+10	1.79E+10	1.37E+10	1.15E+10	1.38E+10	1.85E+10	2.70E+10	2.70E+10	5.0
14	0.86	13.12	2.74E+10	1.87E+10	1.48E+10	1.36E+10	1.49E+10	1.93E+10	2.75E+10	2.75E+10	1.0
15	0.80	13.92	2.69E+10	1.83E+10	1.38E+10	1.12E+10	1.40E+10	1.86E+10	2.67E+10	2.69E+10	7.0
16	0.85	14.78	2.64E+10	1.64E+10	1.17E+10	1.05E+10	1.18E+10	1.67E+10	2.64E+10	2.64E+10	71.0
17	0.84	15.62	2.66E+10	1.65E+10	1.20E+10	1.13E+10	1.21E+10	1.68E+10	2.66E+10	2.66E+10	71.0
18	0.85	16.46	2.56E+10	1.64E+10	1.25E+10	1.16E+10	1.26E+10	1.66E+10	2.55E+10	2.56E+10	71.0
19	0.83	17.29	2.60E+10	1.63E+10	1.23E+10	1.14E+10	1.24E+10	1.62E+10	2.55E+10	2.60E+10	71.0
20	0.88	18.18	2.63E+10	1.64E+10	1.27E+10	1.21E+10	1.28E+10	1.67E+10	2.63E+10	2.63E+10	71.0

Table 4-1 (continued)
Calculated Maximum Fast Neutron Fluence Rate ($E > 1.0$ MeV) at the RPV Clad/Base Metal Interface

Cycle	Cycle Length (EFPY)	Total Time (EFPY)	Fluence Rate (n/cm ² -s)								Elevation of Max. (cm)
			0°	15°	30°	45°	60°	75°	90°	Maximum ^[1]	
21	0.90	19.08	2.51E+10	1.58E+10	1.20E+10	1.14E+10	1.23E+10	1.63E+10	2.53E+10	2.53E+10	71.0
22	0.75	19.82	2.39E+10	1.58E+10	1.45E+10	1.57E+10	1.47E+10	1.61E+10	2.38E+10	2.39E+10	71.0
23	0.92	20.74	2.44E+10	1.52E+10	1.17E+10	1.14E+10	1.18E+10	1.56E+10	2.44E+10	2.44E+10	71.0
24	1.57	22.31	2.54E+10	1.62E+10	1.24E+10	1.13E+10	1.24E+10	1.65E+10	2.54E+10	2.54E+10	71.0
25	1.27	23.58	2.48E+10	1.56E+10	1.31E+10	1.30E+10	1.32E+10	1.67E+10	2.57E+10	2.57E+10	71.0
26	1.35	24.93	2.76E+10	1.76E+10	1.39E+10	1.29E+10	1.38E+10	1.76E+10	2.72E+10	2.76E+10	71.0
27	1.33	26.27	2.56E+10	1.56E+10	1.10E+10	9.92E+09	1.11E+10	1.59E+10	2.56E+10	2.56E+10	71.0
28	1.25	27.52	2.67E+10	1.68E+10	1.27E+10	1.18E+10	1.28E+10	1.71E+10	2.67E+10	2.67E+10	71.0
29	1.37	28.89	2.67E+10	1.66E+10	1.25E+10	1.16E+10	1.26E+10	1.70E+10	2.67E+10	2.67E+10	71.0
30	1.42	30.31	2.21E+10	1.45E+10	1.32E+10	1.26E+10	1.33E+10	1.48E+10	2.21E+10	2.21E+10	71.0
31	1.19	31.50	2.65E+10	1.59E+10	9.88E+09	8.24E+09	9.97E+09	1.66E+10	2.70E+10	2.70E+10	71.0
32	1.33	32.83	3.02E+10	1.90E+10	1.55E+10	1.49E+10	1.58E+10	1.92E+10	2.98E+10	3.02E+10	71.0
33	1.28	34.11	3.55E+10	2.04E+10	1.42E+10	1.32E+10	1.43E+10	2.07E+10	3.55E+10	3.55E+10	71.0
34	1.45	35.56	3.34E+10	2.14E+10	1.63E+10	1.48E+10	1.65E+10	2.13E+10	3.28E+10	3.34E+10	71.0
35	1.37	36.93	3.72E+10	2.19E+10	1.49E+10	1.37E+10	1.50E+10	2.24E+10	3.76E+10	3.76E+10	-73.0
36	1.46	38.40	3.75E+10	2.17E+10	1.44E+10	1.35E+10	1.46E+10	2.18E+10	3.73E+10	3.75E+10	-73.0
37	1.40	39.80	3.39E+10	2.05E+10	1.48E+10	1.44E+10	1.48E+10	2.07E+10	3.38E+10	3.39E+10	-73.0
38	1.52	41.32	3.70E+10	2.15E+10	1.45E+10	1.37E+10	1.46E+10	2.17E+10	3.70E+10	3.70E+10	-73.0

Note(s):

1. Maximum occurs at an azimuthal angle of 0°, or the octant symmetric angle, 90°.

Table 4-2
Calculated Maximum Fast Neutron Fluence (E > 1.0 MeV) at the RPV Clad/Base Metal Interface

Cycle	Cycle Length (EFPY)	Total Time (EFPY)	Fluence (n/cm ²)								Elevation of Max. (cm)
			0°	15°	30°	45°	60°	75°	90°	Maximum ^[1]	
1	1.52	1.52	2.24E+18	1.30E+18	8.74E+17	7.63E+17	8.80E+17	1.33E+18	2.24E+18	2.24E+18	1.0
2	1.05	2.57	3.75E+18	2.18E+18	1.50E+18	1.32E+18	1.51E+18	2.23E+18	3.75E+18	3.75E+18	-1.0
3	0.87	3.44	4.99E+18	2.89E+18	2.00E+18	1.77E+18	2.02E+18	2.96E+18	4.98E+18	4.99E+18	-3.0
4	0.87	4.31	6.14E+18	3.56E+18	2.48E+18	2.19E+18	2.50E+18	3.64E+18	6.13E+18	6.14E+18	-1.0
5	0.89	5.20	7.32E+18	4.28E+18	2.98E+18	2.59E+18	3.00E+18	4.36E+18	7.30E+18	7.32E+18	-1.0
6	0.87	6.06	8.20E+18	4.85E+18	3.48E+18	3.00E+18	3.50E+18	4.95E+18	8.18E+18	8.20E+18	-1.0
7	0.89	6.96	9.19E+18	5.42E+18	3.91E+18	3.42E+18	3.94E+18	5.53E+18	9.16E+18	9.19E+18	-1.0
8	0.86	7.81	1.02E+19	5.99E+18	4.31E+18	3.80E+18	4.34E+18	6.11E+18	1.02E+19	1.02E+19	-1.0
9	0.79	8.60	1.11E+19	6.52E+18	4.68E+18	4.16E+18	4.72E+18	6.66E+18	1.11E+19	1.11E+19	-1.0
10	1.20	9.80	1.24E+19	7.25E+18	5.25E+18	4.70E+18	5.29E+18	7.42E+18	1.24E+19	1.24E+19	-1.0
11	0.85	10.65	1.31E+19	7.76E+18	5.66E+18	5.05E+18	5.70E+18	7.93E+18	1.31E+19	1.31E+19	-1.0
12	0.80	11.45	1.38E+19	8.24E+18	6.02E+18	5.34E+18	6.07E+18	8.43E+18	1.38E+19	1.38E+19	-1.0
13	0.81	12.25	1.45E+19	8.69E+18	6.37E+18	5.64E+18	6.42E+18	8.90E+18	1.45E+19	1.45E+19	-1.0
14	0.86	13.12	1.53E+19	9.19E+18	6.77E+18	6.01E+18	6.83E+18	9.43E+18	1.52E+19	1.53E+19	-1.0
15	0.80	13.92	1.60E+19	9.65E+18	7.12E+18	6.29E+18	7.18E+18	9.90E+18	1.59E+19	1.60E+19	-1.0
16	0.85	14.78	1.65E+19	1.00E+19	7.43E+18	6.57E+18	7.49E+18	1.03E+19	1.65E+19	1.65E+19	3.0
17	0.84	15.62	1.71E+19	1.04E+19	7.75E+18	6.87E+18	7.81E+18	1.07E+19	1.71E+19	1.71E+19	5.0
18	0.85	16.46	1.76E+19	1.08E+19	8.08E+18	7.18E+18	8.15E+18	1.11E+19	1.76E+19	1.76E+19	7.0
19	0.83	17.29	1.83E+19	1.12E+19	8.40E+18	7.48E+18	8.47E+18	1.14E+19	1.83E+19	1.83E+19	63.0
20	0.88	18.18	1.90E+19	1.16E+19	8.76E+18	7.82E+18	8.83E+18	1.19E+19	1.90E+19	1.90E+19	63.0

Table 4-2 (continued)
Calculated Maximum Fast Neutron Fluence ($E > 1.0$ MeV) at the RPV Clad/Base Metal Interface

Cycle	Cycle Length (EFPY)	Total Time (EFPY)	Fluence (n/cm ²)								Elevation of Max. (cm)
			0°	15°	30°	45°	60°	75°	90°	Maximum ^[1]	
21	0.90	19.08	1.97E+19	1.20E+19	9.10E+18	8.14E+18	9.18E+18	1.23E+19	1.97E+19	1.97E+19	63.0
22	0.75	19.82	2.03E+19	1.24E+19	9.44E+18	8.51E+18	9.52E+18	1.27E+19	2.03E+19	2.03E+19	63.0
23	0.92	20.74	2.10E+19	1.28E+19	9.78E+18	8.84E+18	9.86E+18	1.31E+19	2.10E+19	2.10E+19	65.0
24	1.57	22.31	2.23E+19	1.36E+19	1.04E+19	9.40E+18	1.05E+19	1.40E+19	2.22E+19	2.23E+19	65.0
25	1.27	23.58	2.33E+19	1.43E+19	1.09E+19	9.92E+18	1.10E+19	1.46E+19	2.32E+19	2.33E+19	65.0
26	1.35	24.93	2.44E+19	1.50E+19	1.15E+19	1.05E+19	1.16E+19	1.54E+19	2.44E+19	2.44E+19	65.0
27	1.33	26.27	2.55E+19	1.57E+19	1.20E+19	1.09E+19	1.21E+19	1.60E+19	2.55E+19	2.55E+19	65.0
28	1.25	27.52	2.66E+19	1.63E+19	1.25E+19	1.14E+19	1.26E+19	1.67E+19	2.65E+19	2.66E+19	65.0
29	1.37	28.89	2.77E+19	1.70E+19	1.30E+19	1.19E+19	1.31E+19	1.75E+19	2.77E+19	2.77E+19	65.0
30	1.42	30.31	2.87E+19	1.77E+19	1.36E+19	1.24E+19	1.37E+19	1.81E+19	2.87E+19	2.87E+19	67.0
31	1.19	31.50	2.97E+19	1.83E+19	1.40E+19	1.27E+19	1.41E+19	1.87E+19	2.97E+19	2.97E+19	67.0
32	1.33	32.83	3.10E+19	1.91E+19	1.46E+19	1.33E+19	1.47E+19	1.95E+19	3.09E+19	3.10E+19	67.0
33	1.28	34.11	3.24E+19	1.99E+19	1.52E+19	1.39E+19	1.53E+19	2.04E+19	3.24E+19	3.24E+19	67.0
34	1.45	35.56	3.39E+19	2.08E+19	1.59E+19	1.45E+19	1.60E+19	2.14E+19	3.39E+19	3.39E+19	67.0
35	1.37	36.93	3.55E+19	2.17E+19	1.65E+19	1.51E+19	1.67E+19	2.23E+19	3.54E+19	3.55E+19	67.0
36	1.46	38.40	3.71E+19	2.27E+19	1.72E+19	1.57E+19	1.73E+19	2.33E+19	3.71E+19	3.71E+19	67.0
37	1.40	39.80	3.86E+19	2.36E+19	1.78E+19	1.63E+19	1.80E+19	2.41E+19	3.86E+19	3.86E+19	67.0
38	1.52	41.32	4.03E+19	2.45E+19	1.85E+19	1.70E+19	1.86E+19	2.51E+19	4.03E+19	4.03E+19	67.0

Table 4-2 (continued)
Calculated Maximum Fast Neutron Fluence ($E > 1.0$ MeV) at the RPV Clad/Base Metal Interface

Cycle	Cycle Length (EFPY)	Total Time (EFPY)	Fluence (n/cm ²)								Elevation of Max. (cm)
			0°	15°	30°	45°	60°	75°	90°	Maximum ^[1]	
<i>Projection with no bias on peripheral fuel assemblies</i>											
		42	4.11E+19	2.50E+19	1.88E+19	1.73E+19	1.90E+19	2.56E+19	4.10E+19	4.11E+19	67.0
		48	4.78E+19	2.88E+19	2.15E+19	1.98E+19	2.17E+19	2.95E+19	4.78E+19	4.78E+19	67.0
		54	5.46E+19	3.28E+19	2.42E+19	2.24E+19	2.44E+19	3.35E+19	5.45E+19	5.46E+19	67.0
		60	6.13E+19	3.69E+19	2.70E+19	2.50E+19	2.72E+19	3.74E+19	6.13E+19	6.13E+19	67.0
		66	6.81E+19	4.10E+19	2.97E+19	2.76E+19	3.00E+19	4.14E+19	6.80E+19	6.81E+19	67.0
		72	7.48E+19	4.50E+19	3.25E+19	3.02E+19	3.28E+19	4.53E+19	7.48E+19	7.48E+19	67.0
<i>Projection with 10% bias on peripheral fuel assemblies</i>											
		42	4.11E+19	2.50E+19	1.88E+19	1.73E+19	1.90E+19	2.56E+19	4.11E+19	4.11E+19	67.0
		48	4.85E+19	2.92E+19	2.18E+19	2.01E+19	2.20E+19	2.99E+19	4.85E+19	4.85E+19	67.0
		54	5.59E+19	3.36E+19	2.48E+19	2.29E+19	2.50E+19	3.42E+19	5.58E+19	5.59E+19	67.0
		60	6.33E+19	3.81E+19	2.78E+19	2.57E+19	2.80E+19	3.86E+19	6.32E+19	6.33E+19	67.0
		66	7.06E+19	4.25E+19	3.08E+19	2.86E+19	3.11E+19	4.29E+19	7.06E+19	7.06E+19	67.0
		72	7.80E+19	4.69E+19	3.38E+19	3.14E+19	3.41E+19	4.72E+19	7.80E+19	7.80E+19	67.0
Note(s):											
1. Maximum occurs at an azimuthal angle of 0°.											

Table 4-3
Calculated Maximum Iron Atom Displacement Rate at the RPV Clad/Base Metal Interface

Cycle	Cycle Length (EFPY)	Total Time (EFPY)	Displacement Rate (dpa/s)								Elevation of Max. (cm)
			0°	15°	30°	45°	60°	75°	90°	Maximum ^[1]	
1	1.52	1.52	7.64E-11	4.60E-11	3.02E-11	2.59E-11	3.00E-11	4.59E-11	7.64E-11	7.64E-11	1.0
2	1.05	2.57	7.52E-11	4.53E-11	3.14E-11	2.74E-11	3.13E-11	4.53E-11	7.52E-11	7.52E-11	-63.0
3	0.87	3.44	7.39E-11	4.39E-11	3.05E-11	2.68E-11	3.03E-11	4.38E-11	7.39E-11	7.39E-11	-65.0
4	0.87	4.31	6.85E-11	4.13E-11	2.89E-11	2.50E-11	2.87E-11	4.12E-11	6.85E-11	6.85E-11	1.0
5	0.89	5.20	6.94E-11	4.33E-11	2.93E-11	2.33E-11	2.90E-11	4.25E-11	6.83E-11	6.94E-11	-1.0
6	0.87	6.06	5.23E-11	3.52E-11	3.02E-11	2.47E-11	3.03E-11	3.56E-11	5.27E-11	5.27E-11	1.0
7	0.89	6.96	5.75E-11	3.47E-11	2.53E-11	2.39E-11	2.50E-11	3.39E-11	5.67E-11	5.75E-11	1.0
8	0.86	7.81	6.01E-11	3.50E-11	2.45E-11	2.30E-11	2.44E-11	3.57E-11	6.11E-11	6.11E-11	-3.0
9	0.79	8.60	6.13E-11	3.61E-11	2.46E-11	2.31E-11	2.46E-11	3.61E-11	6.15E-11	6.15E-11	1.0
10	1.20	9.80	5.42E-11	3.29E-11	2.50E-11	2.32E-11	2.49E-11	3.33E-11	5.48E-11	5.48E-11	-1.0
11	0.85	10.65	4.40E-11	3.16E-11	2.49E-11	2.11E-11	2.46E-11	3.10E-11	4.22E-11	4.40E-11	-3.0
12	0.80	11.45	4.80E-11	3.28E-11	2.35E-11	1.93E-11	2.38E-11	3.28E-11	4.80E-11	4.80E-11	3.0
13	0.81	12.25	4.37E-11	3.02E-11	2.26E-11	1.86E-11	2.25E-11	3.04E-11	4.42E-11	4.42E-11	5.0
14	0.86	13.12	4.47E-11	3.16E-11	2.44E-11	2.21E-11	2.43E-11	3.17E-11	4.49E-11	4.49E-11	1.0
15	0.80	13.92	4.39E-11	3.09E-11	2.28E-11	1.83E-11	2.27E-11	3.06E-11	4.36E-11	4.39E-11	65.0
16	0.85	14.78	4.30E-11	2.75E-11	1.92E-11	1.71E-11	1.92E-11	2.75E-11	4.30E-11	4.30E-11	73.0
17	0.84	15.62	4.33E-11	2.76E-11	1.98E-11	1.82E-11	1.97E-11	2.77E-11	4.34E-11	4.34E-11	71.0
18	0.85	16.46	4.17E-11	2.75E-11	2.06E-11	1.88E-11	2.05E-11	2.74E-11	4.16E-11	4.17E-11	71.0
19	0.83	17.29	4.24E-11	2.73E-11	2.02E-11	1.85E-11	2.01E-11	2.67E-11	4.16E-11	4.24E-11	71.0
20	0.88	18.18	4.29E-11	2.76E-11	2.09E-11	1.97E-11	2.08E-11	2.75E-11	4.29E-11	4.29E-11	71.0

Table 4-3 (continued)
Calculated Maximum Iron Atom Displacement Rate at the RPV Clad/Base Metal Interface

Cycle	Cycle Length (EFPY)	Total Time (EFPY)	Displacement Rate (dpa/s)								Elevation of Max. (cm)
			0°	15°	30°	45°	60°	75°	90°	Maximum ^[1]	
21	0.90	19.08	4.09E-11	2.65E-11	1.98E-11	1.85E-11	1.99E-11	2.68E-11	4.12E-11	4.12E-11	71.0
22	0.75	19.82	3.89E-11	2.67E-11	2.39E-11	2.54E-11	2.38E-11	2.65E-11	3.89E-11	3.89E-11	71.0
23	0.92	20.74	3.97E-11	2.56E-11	1.93E-11	1.84E-11	1.91E-11	2.56E-11	3.98E-11	3.98E-11	71.0
24	1.57	22.31	4.13E-11	2.72E-11	2.04E-11	1.83E-11	2.02E-11	2.72E-11	4.15E-11	4.15E-11	71.0
25	1.27	23.58	4.04E-11	2.62E-11	2.15E-11	2.10E-11	2.15E-11	2.74E-11	4.20E-11	4.20E-11	73.0
26	1.35	24.93	4.50E-11	2.96E-11	2.28E-11	2.09E-11	2.24E-11	2.89E-11	4.44E-11	4.50E-11	71.0
27	1.33	26.27	4.17E-11	2.62E-11	1.80E-11	1.61E-11	1.80E-11	2.62E-11	4.17E-11	4.17E-11	71.0
28	1.25	27.52	4.35E-11	2.81E-11	2.10E-11	1.91E-11	2.09E-11	2.81E-11	4.36E-11	4.36E-11	71.0
29	1.37	28.89	4.36E-11	2.79E-11	2.05E-11	1.88E-11	2.04E-11	2.79E-11	4.36E-11	4.36E-11	71.0
30	1.42	30.31	3.60E-11	2.43E-11	2.16E-11	2.04E-11	2.16E-11	2.43E-11	3.61E-11	3.61E-11	73.0
31	1.19	31.50	4.32E-11	2.67E-11	1.62E-11	1.34E-11	1.62E-11	2.73E-11	4.41E-11	4.41E-11	71.0
32	1.33	32.83	4.92E-11	3.19E-11	2.54E-11	2.41E-11	2.57E-11	3.16E-11	4.87E-11	4.92E-11	71.0
33	1.28	34.11	5.79E-11	3.42E-11	2.34E-11	2.15E-11	2.32E-11	3.42E-11	5.80E-11	5.80E-11	71.0
34	1.45	35.56	5.45E-11	3.58E-11	2.68E-11	2.41E-11	2.68E-11	3.51E-11	5.36E-11	5.45E-11	73.0
35	1.37	36.93	6.07E-11	3.64E-11	2.45E-11	2.23E-11	2.45E-11	3.70E-11	6.14E-11	6.14E-11	-71.0
36	1.46	38.40	6.10E-11	3.60E-11	2.37E-11	2.18E-11	2.38E-11	3.60E-11	6.09E-11	6.10E-11	-73.0
37	1.40	39.80	5.51E-11	3.40E-11	2.44E-11	2.34E-11	2.41E-11	3.40E-11	5.52E-11	5.52E-11	-73.0
38	1.52	41.32	6.03E-11	3.57E-11	2.39E-11	2.21E-11	2.38E-11	3.57E-11	6.04E-11	6.04E-11	-73.0

Note(s):

1. Maximum occurs at an azimuthal angle of 0°, or the octant symmetric angle, 90°.

Table 4-4
Calculated Maximum Iron Atom Displacements at the RPV Clad/Base Metal Interface

Cycle	Cycle Length (EFPY)	Total Time (EFPY)	Displacements (dpa)								Elevation of Max. (cm)
			0°	15°	30°	45°	60°	75°	90°	Maximum ^[1]	
1	1.52	1.52	3.67E-03	2.21E-03	1.45E-03	1.24E-03	1.44E-03	2.21E-03	3.67E-03	3.67E-03	1.0
2	1.05	2.57	6.14E-03	3.70E-03	2.48E-03	2.15E-03	2.47E-03	3.70E-03	6.15E-03	6.15E-03	-3.0
3	0.87	3.44	8.16E-03	4.90E-03	3.31E-03	2.88E-03	3.29E-03	4.89E-03	8.16E-03	8.16E-03	-3.0
4	0.87	4.31	1.00E-02	6.03E-03	4.10E-03	3.56E-03	4.08E-03	6.02E-03	1.00E-02	1.00E-02	-3.0
5	0.89	5.20	1.20E-02	7.24E-03	4.92E-03	4.21E-03	4.89E-03	7.21E-03	1.19E-02	1.20E-02	-3.0
6	0.87	6.06	1.34E-02	8.20E-03	5.75E-03	4.88E-03	5.71E-03	8.18E-03	1.34E-02	1.34E-02	-3.0
7	0.89	6.96	1.50E-02	9.18E-03	6.46E-03	5.56E-03	6.42E-03	9.13E-03	1.50E-02	1.50E-02	-1.0
8	0.86	7.81	1.66E-02	1.01E-02	7.12E-03	6.18E-03	7.08E-03	1.01E-02	1.66E-02	1.66E-02	-1.0
9	0.79	8.60	1.82E-02	1.10E-02	7.74E-03	6.76E-03	7.69E-03	1.10E-02	1.82E-02	1.82E-02	-1.0
10	1.20	9.80	2.02E-02	1.23E-02	8.68E-03	7.63E-03	8.63E-03	1.23E-02	2.02E-02	2.02E-02	-1.0
11	0.85	10.65	2.14E-02	1.31E-02	9.35E-03	8.20E-03	9.29E-03	1.31E-02	2.14E-02	2.14E-02	-1.0
12	0.80	11.45	2.26E-02	1.39E-02	9.94E-03	8.68E-03	9.89E-03	1.39E-02	2.26E-02	2.26E-02	-1.0
13	0.81	12.25	2.37E-02	1.47E-02	1.05E-02	9.16E-03	1.05E-02	1.47E-02	2.37E-02	2.37E-02	-1.0
14	0.86	13.12	2.49E-02	1.56E-02	1.12E-02	9.76E-03	1.11E-02	1.55E-02	2.49E-02	2.49E-02	-1.0
15	0.80	13.92	2.61E-02	1.64E-02	1.18E-02	1.02E-02	1.17E-02	1.63E-02	2.60E-02	2.61E-02	-1.0
16	0.85	14.78	2.70E-02	1.70E-02	1.23E-02	1.07E-02	1.22E-02	1.70E-02	2.70E-02	2.70E-02	3.0
17	0.84	15.62	2.79E-02	1.76E-02	1.28E-02	1.12E-02	1.27E-02	1.76E-02	2.79E-02	2.79E-02	7.0
18	0.85	16.46	2.88E-02	1.83E-02	1.33E-02	1.17E-02	1.33E-02	1.82E-02	2.88E-02	2.88E-02	7.0
19	0.83	17.29	2.99E-02	1.89E-02	1.39E-02	1.22E-02	1.38E-02	1.89E-02	2.99E-02	2.99E-02	61.0
20	0.88	18.18	3.11E-02	1.96E-02	1.45E-02	1.27E-02	1.44E-02	1.95E-02	3.11E-02	3.11E-02	61.0

Table 4-4 (continued)
Calculated Maximum Iron Atom Displacements at the RPV Clad/Base Metal Interface

Cycle	Cycle Length (EFPY)	Total Time (EFPY)	Displacements (dpa)								Elevation of Max. (cm)
			0°	15°	30°	45°	60°	75°	90°	Maximum ^[1]	
21	0.90	19.08	3.23E-02	2.03E-02	1.50E-02	1.32E-02	1.50E-02	2.03E-02	3.22E-02	3.23E-02	61.0
22	0.75	19.82	3.32E-02	2.10E-02	1.56E-02	1.38E-02	1.55E-02	2.09E-02	3.31E-02	3.32E-02	63.0
23	0.92	20.74	3.43E-02	2.17E-02	1.61E-02	1.44E-02	1.61E-02	2.17E-02	3.43E-02	3.43E-02	63.0
24	1.57	22.31	3.64E-02	2.31E-02	1.71E-02	1.53E-02	1.71E-02	2.30E-02	3.63E-02	3.64E-02	63.0
25	1.27	23.58	3.80E-02	2.41E-02	1.80E-02	1.61E-02	1.79E-02	2.41E-02	3.80E-02	3.80E-02	65.0
26	1.35	24.93	3.99E-02	2.54E-02	1.90E-02	1.70E-02	1.89E-02	2.53E-02	3.99E-02	3.99E-02	65.0
27	1.33	26.27	4.16E-02	2.65E-02	1.97E-02	1.77E-02	1.96E-02	2.64E-02	4.16E-02	4.16E-02	65.0
28	1.25	27.52	4.33E-02	2.76E-02	2.06E-02	1.84E-02	2.05E-02	2.76E-02	4.34E-02	4.34E-02	65.0
29	1.37	28.89	4.52E-02	2.88E-02	2.15E-02	1.92E-02	2.13E-02	2.88E-02	4.52E-02	4.52E-02	65.0
30	1.42	30.31	4.68E-02	2.99E-02	2.24E-02	2.01E-02	2.23E-02	2.98E-02	4.69E-02	4.69E-02	65.0
31	1.19	31.50	4.85E-02	3.09E-02	2.30E-02	2.06E-02	2.29E-02	3.09E-02	4.85E-02	4.85E-02	65.0
32	1.33	32.83	5.05E-02	3.22E-02	2.41E-02	2.16E-02	2.39E-02	3.22E-02	5.05E-02	5.05E-02	67.0
33	1.28	34.11	5.29E-02	3.36E-02	2.50E-02	2.25E-02	2.49E-02	3.36E-02	5.29E-02	5.29E-02	67.0
34	1.45	35.56	5.53E-02	3.52E-02	2.62E-02	2.36E-02	2.61E-02	3.52E-02	5.53E-02	5.53E-02	67.0
35	1.37	36.93	5.79E-02	3.67E-02	2.72E-02	2.45E-02	2.71E-02	3.67E-02	5.79E-02	5.79E-02	67.0
36	1.46	38.40	6.06E-02	3.84E-02	2.83E-02	2.55E-02	2.82E-02	3.83E-02	6.06E-02	6.06E-02	67.0
37	1.40	39.80	6.30E-02	3.98E-02	2.94E-02	2.65E-02	2.92E-02	3.98E-02	6.30E-02	6.30E-02	67.0
38	1.52	41.32	6.58E-02	4.15E-02	3.05E-02	2.75E-02	3.04E-02	4.14E-02	6.58E-02	6.58E-02	67.0

Table 4-4 (continued)
Calculated Maximum Iron Atom Displacements at the RPV Clad/Base Metal Interface

Cycle	Cycle Length (EFPY)	Total Time (EFPY)	Displacements (dpa)								Elevation of Max. (cm)
			0°	15°	30°	45°	60°	75°	90°	Maximum ^[1]	
<i>Projection with no bias on peripheral fuel assemblies</i>											
		42	6.70E-02	4.22E-02	3.10E-02	2.80E-02	3.09E-02	4.22E-02	6.70E-02	6.70E-02	67.0
		48	7.80E-02	4.87E-02	3.54E-02	3.21E-02	3.53E-02	4.87E-02	7.81E-02	7.81E-02	67.0
		54	8.90E-02	5.52E-02	3.99E-02	3.63E-02	3.98E-02	5.52E-02	8.91E-02	8.91E-02	67.0
		60	1.00E-01	6.17E-02	4.44E-02	4.05E-02	4.43E-02	6.17E-02	1.00E-01	1.00E-01	67.0
		66	1.11E-01	6.82E-02	4.89E-02	4.47E-02	4.88E-02	6.82E-02	1.11E-01	1.11E-01	67.0
		72	1.22E-01	7.47E-02	5.34E-02	4.89E-02	5.33E-02	7.47E-02	1.22E-01	1.22E-01	67.0
<i>Projection with 10% bias on peripheral fuel assemblies</i>											
		42	6.71E-02	4.23E-02	3.10E-02	2.81E-02	3.09E-02	4.22E-02	6.71E-02	6.71E-02	67.0
		48	7.91E-02	4.94E-02	3.59E-02	3.25E-02	3.57E-02	4.93E-02	7.92E-02	7.92E-02	67.0
		54	9.12E-02	5.65E-02	4.08E-02	3.71E-02	4.07E-02	5.65E-02	9.12E-02	9.12E-02	67.0
		60	1.03E-01	6.36E-02	4.57E-02	4.17E-02	4.56E-02	6.36E-02	1.03E-01	1.03E-01	67.0
		66	1.15E-01	7.07E-02	5.06E-02	4.63E-02	5.05E-02	7.07E-02	1.15E-01	1.15E-01	67.0
		72	1.27E-01	7.78E-02	5.56E-02	5.09E-02	5.55E-02	7.78E-02	1.27E-01	1.27E-01	67.0
Note(s):											
1. Maximum occurs at an azimuthal angle of 0°, or the octant symmetric angle, 90°.											

Table 4-5
Calculated Maximum Fast Neutron Fluence (E > 1.0 MeV) at RPV Welds and Shells

<i>Projection with no bias on peripheral fuel assemblies</i>				
Material	Fluence (n/cm²)			
	41.32 EFPY	42 EFPY	48 EFPY	54 EFPY
Inlet nozzle to nozzle belt forging weld (lowest extent) ^[1]	3.64E+16	3.70E+16	4.23E+16	4.76E+16
Nozzle belt forging (lowest extent) [123V352]	3.53E+18	3.59E+18	4.11E+18	4.64E+18
Nozzle belt forging to intermediate shell circumferential weld [21935]	4.01E+18	4.08E+18	4.68E+18	5.28E+18
Intermediate shell forging [123V500]	4.03E+19	4.11E+19	4.78E+19	5.46E+19
Intermediate shell to lower shell circumferential weld [SA-1484]	3.55E+19	3.62E+19	4.30E+19	4.98E+19
Lower shell forging [122W195]	3.83E+19	3.91E+19	4.60E+19	5.29E+19
Lower shell to lower head ring circumferential weld	2.69E+16	2.74E+16	3.17E+16	3.60E+16

<i>Projection with no bias on peripheral fuel assemblies</i>				
Material	Fluence (n/cm²)			
	60 EFPY	66 EFPY	72 EFPY	
Inlet nozzle to nozzle belt forging weld (lowest extent) ^[1]	5.30E+16	5.83E+16	6.36E+16	
Nozzle belt forging (lowest extent) [123V352]	5.17E+18	5.70E+18	6.23E+18	
Nozzle belt forging to intermediate shell circumferential weld [21935]	5.88E+18	6.48E+18	7.09E+18	
Intermediate shell forging [123V500]	6.13E+19	6.81E+19	7.48E+19	
Intermediate shell to lower shell circumferential weld [SA-1484]	5.66E+19	6.34E+19	7.02E+19	
Lower shell forging [122W195]	5.99E+19	6.68E+19	7.38E+19	
Lower shell to lower head ring circumferential weld	4.03E+16	4.46E+16	4.89E+16	

Table 4-5 (continued)
Calculated Maximum Fast Neutron Fluence (E > 1.0 MeV) at RPV Welds and Shells

<i>Projection with 10% bias on peripheral fuel assemblies</i>				
Material	Fluence (n/cm²)			
	41.32 EFPY	42 EFPY	48 EFPY	54 EFPY
Inlet nozzle to nozzle belt forging weld (lowest extent) ^[1]	3.64E+16	3.70E+16	4.28E+16	4.86E+16
Nozzle belt forging (lowest extent) [123V352]	3.53E+18	3.59E+18	4.16E+18	4.74E+18
Nozzle belt forging to intermediate shell circumferential weld [21935]	4.01E+18	4.08E+18	4.74E+18	5.39E+18
Intermediate shell forging [123V500]	4.03E+19	4.11E+19	4.85E+19	5.59E+19
Intermediate shell to lower shell circumferential weld [SA-1484]	3.55E+19	3.63E+19	4.37E+19	5.11E+19
Lower shell forging [122W195]	3.83E+19	3.92E+19	4.67E+19	5.43E+19
Lower shell to lower head ring circumferential weld	2.69E+16	2.75E+16	3.21E+16	3.68E+16

<i>Projection with 10% bias on peripheral fuel assemblies</i>				
Material	Fluence (n/cm²)			
	60 EFPY	66 EFPY	72 EFPY	
Inlet nozzle to nozzle belt forging weld (lowest extent) ^[1]	5.45E+16	6.03E+16	6.61E+16	
Nozzle belt forging (lowest extent) [123V352]	5.31E+18	5.89E+18	6.46E+18	
Nozzle belt forging to intermediate shell circumferential weld [21935]	6.04E+18	6.70E+18	7.35E+18	
Intermediate shell forging [123V500]	6.33E+19	7.06E+19	7.80E+19	
Intermediate shell to lower shell circumferential weld [SA-1484]	5.85E+19	6.60E+19	7.34E+19	
Lower shell forging [122W195]	6.19E+19	6.95E+19	7.71E+19	
Lower shell to lower head ring circumferential weld	4.15E+16	4.62E+16	5.08E+16	
Note(s):				
1. Also applicable to outlet nozzle/nozzle belt forging weld and safety injection nozzle/nozzle belt forging weld.				

Table 4-6
Calculated Maximum Iron Atom Displacements at RPV Welds and Shells

<i>Projection with no bias on peripheral fuel assemblies</i>				
Material	Displacements (dpa)			
	41.32 EFPY	42 EFPY	48 EFPY	54 EFPY
Inlet nozzle to nozzle belt forging weld (lowest extent) ^[1]	3.01E-04	3.06E-04	3.51E-04	3.95E-04
Nozzle belt forging (lowest extent) [123V352]	6.00E-03	6.10E-03	7.01E-03	7.91E-03
Nozzle belt forging to intermediate shell circumferential weld [21935]	6.77E-03	6.89E-03	7.91E-03	8.93E-03
Intermediate shell forging [123V500]	6.58E-02	6.70E-02	7.81E-02	8.91E-02
Intermediate shell to lower shell circumferential weld [SA-1484]	5.83E-02	5.95E-02	7.07E-02	8.18E-02
Lower shell forging [122W195]	6.26E-02	6.39E-02	7.52E-02	8.65E-02
Lower shell to lower head ring circumferential weld	1.24E-04	1.26E-04	1.46E-04	1.65E-04

<i>Projection with no bias on peripheral fuel assemblies</i>				
Material	Displacements (dpa)			
	60 EFPY	66 EFPY	72 EFPY	
Inlet nozzle to nozzle belt forging weld (lowest extent) ^[1]	4.40E-04	4.85E-04	5.29E-04	
Nozzle belt forging (lowest extent) [123V352]	8.81E-03	9.71E-03	1.06E-02	
Nozzle belt forging to intermediate shell circumferential weld [21935]	9.95E-03	1.10E-02	1.20E-02	
Intermediate shell forging [123V500]	1.00E-01	1.11E-01	1.22E-01	
Intermediate shell to lower shell circumferential weld [SA-1484]	9.30E-02	1.04E-01	1.15E-01	
Lower shell forging [122W195]	9.78E-02	1.09E-01	1.21E-01	
Lower shell to lower head ring circumferential weld	1.85E-04	2.05E-04	2.24E-04	

Table 4-6 (continued)
Calculated Maximum Iron Atom Displacements at RPV Welds and Shells

<i>Projection with 10% bias on peripheral fuel assemblies</i>				
Material	Displacements (dpa)			
	41.32 EFPY	42 EFPY	48 EFPY	54 EFPY
Inlet nozzle to nozzle belt forging weld (lowest extent) ^[1]	3.01E-04	3.07E-04	3.56E-04	4.04E-04
Nozzle belt forging (lowest extent) [123V352]	6.00E-03	6.11E-03	7.09E-03	8.07E-03
Nozzle belt forging to intermediate shell circumferential weld [21935]	6.77E-03	6.90E-03	8.01E-03	9.12E-03
Intermediate shell forging [123V500]	6.58E-02	6.71E-02	7.92E-02	9.12E-02
Intermediate shell to lower shell circumferential weld [SA-1484]	5.83E-02	5.96E-02	7.18E-02	8.40E-02
Lower shell forging [122W195]	6.26E-02	6.40E-02	7.63E-02	8.87E-02
Lower shell to lower head ring circumferential weld	1.24E-04	1.26E-04	1.48E-04	1.69E-04

<i>Projection with 10% bias on peripheral fuel assemblies</i>				
Material	Displacements (dpa)			
	60 EFPY	66 EFPY	72 EFPY	
Inlet nozzle to nozzle belt forging weld (lowest extent) ^[1]	4.53E-04	5.01E-04	5.50E-04	
Nozzle belt forging (lowest extent) [123V352]	9.06E-03	1.00E-02	1.10E-02	
Nozzle belt forging to intermediate shell circumferential weld [21935]	1.02E-02	1.13E-02	1.24E-02	
Intermediate shell forging [123V500]	1.03E-01	1.15E-01	1.27E-01	
Intermediate shell to lower shell circumferential weld [SA-1484]	9.62E-02	1.08E-01	1.20E-01	
Lower shell forging [122W195]	1.01E-01	1.13E-01	1.26E-01	
Lower shell to lower head ring circumferential weld	1.91E-04	2.12E-04	2.34E-04	
Note(s):				
1. Also applicable to outlet nozzle/nozzle belt forging weld and safety injection nozzle/nozzle belt forging weld.				

4.2 Surveillance Capsules

Results of the discrete ordinates transport analyses pertinent to the surveillance capsule evaluations are provided in Table 4-7 through Table 4-11. In Table 4-7, the calculated fast neutron fluence rate ($E > 1.0$ MeV) is provided at the geometric center of capsule locations as a function of irradiation time for the Point Beach Unit 2 reactor. In Table 4-8, the calculated fast neutron fluence ($E > 1.0$ MeV) is provided for the individual capsules. Similar data presented in terms of iron atom displacement rate and integrated iron atom displacements are given in Table 4-9 and Table 4-10, respectively.

In Table 4-11, lead factors associated with surveillance capsules are provided as a function of operating time for the Point Beach Unit 2 reactor. The lead factor is defined as the ratio of the neutron fluence ($E > 1.0$ MeV) at the geometric center of the surveillance capsule to the maximum neutron fluence ($E > 1.0$ MeV) at the RPV clad/base metal interface. Note that Capsule W was inserted into the reactor in a 13° capsule holder location after Cycle 25.

Table 4-7
Calculated Fast Neutron Fluence Rate (E > 1.0 MeV) at Surveillance Capsule Locations

Cycle	Cycle Length (EFPY)	Total Time (EFPY)	Fluence Rate (n/cm ² -s)		
			13°	23°	33°
1	1.52	1.52	1.36E+11	7.85E+10	7.40E+10
2	1.05	2.57	1.36E+11	8.06E+10	7.88E+10
3	0.87	3.44	1.32E+11	7.77E+10	7.69E+10
4	0.87	4.31	1.25E+11	7.49E+10	7.32E+10
5	0.89	5.20	1.31E+11	7.83E+10	7.30E+10
6	0.87	6.06	1.01E+11	7.52E+10	7.62E+10
7	0.89	6.96	1.01E+11	6.54E+10	6.36E+10
8	0.86	7.81	1.02E+11	6.45E+10	6.09E+10
9	0.79	8.60	1.06E+11	6.52E+10	6.13E+10
10	1.20	9.80	9.53E+10	6.39E+10	6.28E+10
11	0.85	10.65	8.96E+10	6.58E+10	6.11E+10
12	0.80	11.45	9.40E+10	6.44E+10	5.68E+10
13	0.81	12.25	8.56E+10	6.11E+10	5.47E+10
14	0.86	13.12	9.00E+10	6.43E+10	6.04E+10
15	0.80	13.92	8.79E+10	6.23E+10	5.49E+10
16	0.85	14.78	6.62E+10	4.87E+10	4.74E+10
17	0.84	15.62	6.67E+10	5.03E+10	4.94E+10
18	0.85	16.46	6.59E+10	5.16E+10	5.13E+10
19	0.83	17.29	6.60E+10	5.07E+10	5.06E+10
20	0.88	18.18	6.69E+10	5.15E+10	5.28E+10
21	0.90	19.08	6.47E+10	4.94E+10	4.99E+10
22	0.75	19.82	6.33E+10	5.55E+10	6.24E+10
23	0.92	20.74	6.25E+10	4.73E+10	4.89E+10
24	1.57	22.31	6.55E+10	5.18E+10	5.09E+10
25	1.27	23.58	6.26E+10	5.14E+10	5.52E+10
26	1.35	24.93	7.18E+10	5.63E+10	5.80E+10
27	1.33	26.27	6.41E+10	4.64E+10	4.49E+10
28	1.25	27.52	6.80E+10	5.23E+10	5.31E+10
29	1.37	28.89	6.76E+10	5.13E+10	5.18E+10
30	1.42	30.31	5.95E+10	5.07E+10	5.50E+10

Table 4-7 (continued)
Calculated Fast Neutron Fluence Rate ($E > 1.0$ MeV) at Surveillance Capsule Locations

Cycle	Cycle Length (EFPY)	Total Time (EFPY)	Fluence Rate (n/cm ² -s)		
			13°	23°	33°
31	1.19	31.50	6.63E+10	4.42E+10	3.85E+10
32	1.33	32.83	7.90E+10	6.08E+10	6.29E+10
33	1.28	34.11	8.43E+10	5.83E+10	5.75E+10
34	1.45	35.56	8.84E+10	6.68E+10	6.59E+10
35	1.37	36.93	1.06E+11	6.35E+10	5.95E+10
36	1.46	38.40	1.05E+11	6.16E+10	5.79E+10
37	1.40	39.80	9.85E+10	6.14E+10	6.05E+10
38	1.52	41.32	1.04E+11	6.15E+10	5.84E+10

Table 4-8
Calculated Fast Neutron Fluence (E > 1.0 MeV) at Surveillance Capsules

Cycle	Cycle Length (EFPY)	Total Time (EFPY)	Fluence (n/cm ²)						
			V	T	R	S	P	N	W
1	1.52	1.52	6.54E+18	3.77E+18	6.54E+18	3.55E+18	3.77E+18	3.55E+18	
2	1.05	2.57		6.44E+18	1.10E+19	6.17E+18	6.44E+18	6.17E+18	
3	0.87	3.44		8.58E+18	1.47E+19	8.28E+18	8.58E+18	8.28E+18	
4	0.87	4.31			1.81E+19	1.03E+19	1.06E+19	1.03E+19	
5	0.89	5.20			2.17E+19	1.23E+19	1.28E+19	1.23E+19	
6	0.87	6.06				1.44E+19	1.49E+19	1.44E+19	
7	0.89	6.96				1.62E+19	1.67E+19	1.62E+19	
8	0.86	7.81				1.78E+19	1.85E+19	1.78E+19	
9	0.79	8.60				1.94E+19	2.01E+19	1.94E+19	
10	1.20	9.80				2.17E+19	2.25E+19	2.17E+19	
11	0.85	10.65				2.34E+19	2.43E+19	2.34E+19	
12	0.80	11.45				2.48E+19	2.59E+19	2.48E+19	
13	0.81	12.25				2.62E+19	2.74E+19	2.62E+19	
14	0.86	13.12				2.78E+19	2.92E+19	2.78E+19	
15	0.80	13.92				2.92E+19	3.08E+19	2.92E+19	
16	0.85	14.78				3.05E+19	3.21E+19	3.05E+19	
17	0.84	15.62					3.34E+19	3.18E+19	
18	0.85	16.46					3.48E+19	3.32E+19	
19	0.83	17.29					3.61E+19	3.45E+19	
20	0.88	18.18					3.76E+19	3.60E+19	
21	0.90	19.08					3.90E+19	3.74E+19	
22	0.75	19.82					4.03E+19	3.89E+19	
23	0.92	20.74						4.03E+19	
24	1.57	22.31						4.28E+19	
25	1.27	23.58						4.50E+19	
26	1.35	24.93						4.75E+19	3.06E+18
27	1.33	26.27						4.94E+19	5.76E+18
28	1.25	27.52						5.15E+19	8.44E+18
29	1.37	28.89						5.37E+19	1.14E+19
30	1.42	30.31						5.62E+19	1.40E+19

Table 4-8 (continued)
Calculated Fast Neutron Fluence (E > 1.0 MeV) at Surveillance Capsules

Cycle	Cycle Length (EFPY)	Total Time (EFPY)	Fluence (n/cm ²)						
			V	S	R	T	P	N	W
31	1.19	31.50						5.76E+19	1.65E+19
32	1.33	32.83						6.03E+19	1.98E+19
33	1.28	34.11						6.26E+19	2.33E+19
34	1.45	35.56						6.56E+19	2.73E+19
35	1.37	36.93						6.82E+19	3.19E+19
36	1.46	38.40						7.09E+19	3.68E+19
37	1.40	39.80						7.36E+19	4.11E+19
38	1.52	41.32						7.64E+19	4.61E+19
<i>Projection with no bias on peripheral fuel assemblies</i>									
		42						7.76E+19	4.83E+19
		48						8.87E+19	6.80E+19
		54						9.97E+19	8.76E+19
		60						1.11E+20	1.07E+20
		66						1.22E+20	1.27E+20
		72						1.33E+20	1.47E+20
<i>Projection with 10% bias on peripheral fuel assemblies</i>									
		42						7.77E+19	4.85E+19
		48						8.98E+19	7.00E+19
		54						1.02E+20	9.15E+19
		60						1.14E+20	1.13E+20
		66						1.26E+20	1.35E+20
		72						1.38E+20	1.56E+20

Table 4-9
Calculated Iron Atom Displacement Rate at Surveillance Capsule Locations

Cycle	Cycle Length (EFPY)	Total Time (EFPY)	Displacement Rate (dpa/s)		
			13°	23°	33°
1	1.52	1.52	2.51E-10	1.38E-10	1.31E-10
2	1.05	2.57	2.49E-10	1.42E-10	1.40E-10
3	0.87	3.44	2.42E-10	1.37E-10	1.36E-10
4	0.87	4.31	2.28E-10	1.31E-10	1.30E-10
5	0.89	5.20	2.39E-10	1.37E-10	1.29E-10
6	0.87	6.06	1.83E-10	1.32E-10	1.35E-10
7	0.89	6.96	1.84E-10	1.14E-10	1.12E-10
8	0.86	7.81	1.87E-10	1.13E-10	1.07E-10
9	0.79	8.60	1.93E-10	1.14E-10	1.08E-10
10	1.20	9.80	1.74E-10	1.12E-10	1.11E-10
11	0.85	10.65	1.63E-10	1.15E-10	1.08E-10
12	0.80	11.45	1.71E-10	1.12E-10	1.00E-10
13	0.81	12.25	1.56E-10	1.06E-10	9.64E-11
14	0.86	13.12	1.64E-10	1.12E-10	1.06E-10
15	0.80	13.92	1.60E-10	1.08E-10	9.68E-11
16	0.85	14.78	1.20E-10	8.47E-11	8.33E-11
17	0.84	15.62	1.21E-10	8.75E-11	8.69E-11
18	0.85	16.46	1.19E-10	8.96E-11	9.02E-11
19	0.83	17.29	1.20E-10	8.81E-11	8.90E-11
20	0.88	18.18	1.21E-10	8.96E-11	9.28E-11
21	0.90	19.08	1.17E-10	8.59E-11	8.77E-11
22	0.75	19.82	1.14E-10	9.65E-11	1.10E-10
23	0.92	20.74	1.13E-10	8.23E-11	8.60E-11
24	1.57	22.31	1.19E-10	9.01E-11	8.95E-11
25	1.27	23.58	1.13E-10	8.93E-11	9.73E-11
26	1.35	24.93	1.30E-10	9.80E-11	1.02E-10
27	1.33	26.27	1.16E-10	8.08E-11	7.90E-11
28	1.25	27.52	1.23E-10	9.09E-11	9.35E-11
29	1.37	28.89	1.23E-10	8.93E-11	9.12E-11
30	1.42	30.31	1.08E-10	8.81E-11	9.68E-11

Table 4-9 (continued)
Calculated Iron Atom Displacement Rate at Surveillance Capsule Locations

Cycle	Cycle Length (EFPY)	Total Time (EFPY)	Displacement Rate (dpa/s)		
			13°	23°	33°
31	1.19	31.50	1.20E-10	7.69E-11	6.78E-11
32	1.33	32.83	1.43E-10	1.06E-10	1.11E-10
33	1.28	34.11	1.53E-10	1.02E-10	1.01E-10
34	1.45	35.56	1.61E-10	1.16E-10	1.16E-10
35	1.37	36.93	1.93E-10	1.11E-10	1.05E-10
36	1.46	38.40	1.92E-10	1.08E-10	1.02E-10
37	1.40	39.80	1.79E-10	1.07E-10	1.07E-10
38	1.52	41.32	1.89E-10	1.07E-10	1.03E-10

Table 4-10
Calculated Iron Atom Displacements at Surveillance Capsules

Cycle	Cycle Length (EFPY)	Total Time (EFPY)	Displacements (dpa)						
			V	T	R	S	P	N	W
1	1.52	1.52	1.20E-02	6.63E-03	1.20E-02	6.31E-03	6.63E-03	6.31E-03	
2	1.05	2.57		1.13E-02	2.03E-02	1.09E-02	1.13E-02	1.09E-02	
3	0.87	3.44		1.51E-02	2.69E-02	1.47E-02	1.51E-02	1.47E-02	
4	0.87	4.31			3.32E-02	1.82E-02	1.87E-02	1.82E-02	
5	0.89	5.20			3.99E-02	2.18E-02	2.25E-02	2.18E-02	
6	0.87	6.06				2.55E-02	2.61E-02	2.55E-02	
7	0.89	6.96				2.87E-02	2.93E-02	2.87E-02	
8	0.86	7.81				3.16E-02	3.24E-02	3.16E-02	
9	0.79	8.60				3.43E-02	3.52E-02	3.43E-02	
10	1.20	9.80				3.85E-02	3.94E-02	3.85E-02	
11	0.85	10.65				4.13E-02	4.25E-02	4.13E-02	
12	0.80	11.45				4.39E-02	4.53E-02	4.39E-02	
13	0.81	12.25				4.63E-02	4.80E-02	4.63E-02	
14	0.86	13.12				4.92E-02	5.11E-02	4.92E-02	
15	0.80	13.92				5.17E-02	5.38E-02	5.17E-02	
16	0.85	14.78				5.39E-02	5.61E-02	5.39E-02	
17	0.84	15.62					5.84E-02	5.62E-02	
18	0.85	16.46					6.08E-02	5.86E-02	
19	0.83	17.29					6.31E-02	6.10E-02	
20	0.88	18.18					6.56E-02	6.36E-02	
21	0.90	19.08					6.81E-02	6.61E-02	
22	0.75	19.82					7.04E-02	6.87E-02	
23	0.92	20.74						7.11E-02	
24	1.57	22.31						7.56E-02	
25	1.27	23.58						7.95E-02	
26	1.35	24.93						8.38E-02	5.55E-03
27	1.33	26.27						8.72E-02	1.04E-02
28	1.25	27.52						9.08E-02	1.53E-02
29	1.37	28.89						9.48E-02	2.06E-02
30	1.42	30.31						9.91E-02	2.54E-02

Table 4-10 (continued)
Calculated Iron Atom Displacements at Surveillance Capsules

Cycle	Cycle Length (EFPY)	Total Time (EFPY)	Displacements (dpa)						
			V	S	R	T	P	N	W
31	1.19	31.50						1.02E-01	2.99E-02
32	1.33	32.83						1.06E-01	3.60E-02
33	1.28	34.11						1.10E-01	4.22E-02
34	1.45	35.56						1.16E-01	4.95E-02
35	1.37	36.93						1.20E-01	5.79E-02
36	1.46	38.40						1.25E-01	6.68E-02
37	1.40	39.80						1.30E-01	7.47E-02
38	1.52	41.32						1.35E-01	8.38E-02
<i>Projection with no bias on peripheral fuel assemblies</i>									
		42						1.37E-01	8.78E-02
		48						1.56E-01	1.24E-01
		54						1.76E-01	1.60E-01
		60						1.95E-01	1.95E-01
		66						2.15E-01	2.31E-01
		72						2.34E-01	2.67E-01
<i>Projection with 10% bias on peripheral fuel assemblies</i>									
		42						1.37E-01	8.82E-02
		48						1.58E-01	1.27E-01
		54						1.80E-01	1.67E-01
		60						2.01E-01	2.06E-01
		66						2.22E-01	2.45E-01
		72						2.44E-01	2.84E-01

Table 4-11
Calculated Surveillance Capsule Lead Factors

Cycle	Cycle Length (EFPY)	Total Time (EFPY)	Lead Factor						
			V	T	R	S	P	N	W
1	1.52	1.52	2.92	1.68	2.92	1.59	1.68	1.59	
2	1.05	2.57		1.72	2.94	1.64	1.72	1.64	
3	0.87	3.44		1.72	2.94	1.66	1.72	1.66	
4	0.87	4.31			2.95	1.68	1.73	1.68	
5	0.89	5.20			2.97	1.68	1.75	1.68	
6	0.87	6.06				1.76	1.81	1.76	
7	0.89	6.96				1.76	1.82	1.76	
8	0.86	7.81				1.75	1.81	1.75	
9	0.79	8.60				1.74	1.81	1.74	
10	1.20	9.80				1.76	1.82	1.76	
11	0.85	10.65				1.78	1.85	1.78	
12	0.80	11.45				1.79	1.87	1.79	
13	0.81	12.25				1.80	1.89	1.80	
14	0.86	13.12				1.82	1.91	1.82	
15	0.80	13.92				1.83	1.93	1.83	
16	0.85	14.78				1.85	1.94	1.85	
17	0.84	15.62					1.96	1.86	
18	0.85	16.46					1.97	1.88	
19	0.83	17.29					1.97	1.89	
20	0.88	18.18					1.97	1.89	
21	0.90	19.08					1.97	1.89	
22	0.75	19.82					1.98	1.92	
23	0.92	20.74						1.92	
24	1.57	22.31						1.92	
25	1.27	23.58						1.94	
26	1.35	24.93						1.95	0.13
27	1.33	26.27						1.94	0.23
28	1.25	27.52						1.94	0.32
29	1.37	28.89						1.94	0.41
30	1.42	30.31						1.96	0.49

Table 4-11 (continued)
Calculated Surveillance Capsule Lead Factors

Cycle	Cycle Length (EFPY)	Total Time (EFPY)	Lead Factor						
			V	S	R	T	P	N	W
31	1.19	31.50						1.94	0.56
32	1.33	32.83						1.95	0.64
33	1.28	34.11						1.93	0.72
34	1.45	35.56						1.94	0.80
35	1.37	36.93						1.92	0.90
36	1.46	38.40						1.91	0.99
37	1.40	39.80						1.91	1.07
38	1.52	41.32						1.89	1.14
<i>Projection with no bias on peripheral fuel assemblies</i>									
		42						1.89	1.18
		48						1.85	1.42
		54						1.83	1.61
		60						1.81	1.75
		66						1.79	1.86
		72						1.78	1.96
<i>Projection with 10% bias on peripheral fuel assemblies</i>									
		42						1.89	1.18
		48						1.85	1.44
		54						1.82	1.64
		60						1.80	1.79
		66						1.79	1.90
		72						1.77	2.00

4.3 RPV Supports

The components of the RPV supports for which radiation exposure was calculated are the ring girder and the support columns. Exposure of these components was calculated on a point-wise basis. For the ring girder, points were distributed at 5° increments as shown in Figure 4-1. Exposure was calculated on the lower inner edge, upper inner edge, lower outer edge, and upper outer edge of the ring girder.

For the support columns, points were distributed at 10° increments around the outer radius of the support columns, as shown in Figure 4-1. When determining maximum exposure, points were distributed at 10-cm increments over the central 200-cm length of the active core.

Maximum projected exposures of the RPV support structures are given in Table 4-12 through Table 4-14. Neutron exposure is given for both energies greater than 1.0 MeV and energies greater than 0.1 MeV; these exposures are given in Table 4-12 and Table 4-13, respectively. Similar data presented in terms of iron atom displacements is given in Table 4-14 and visually represented in Figure 4-2.

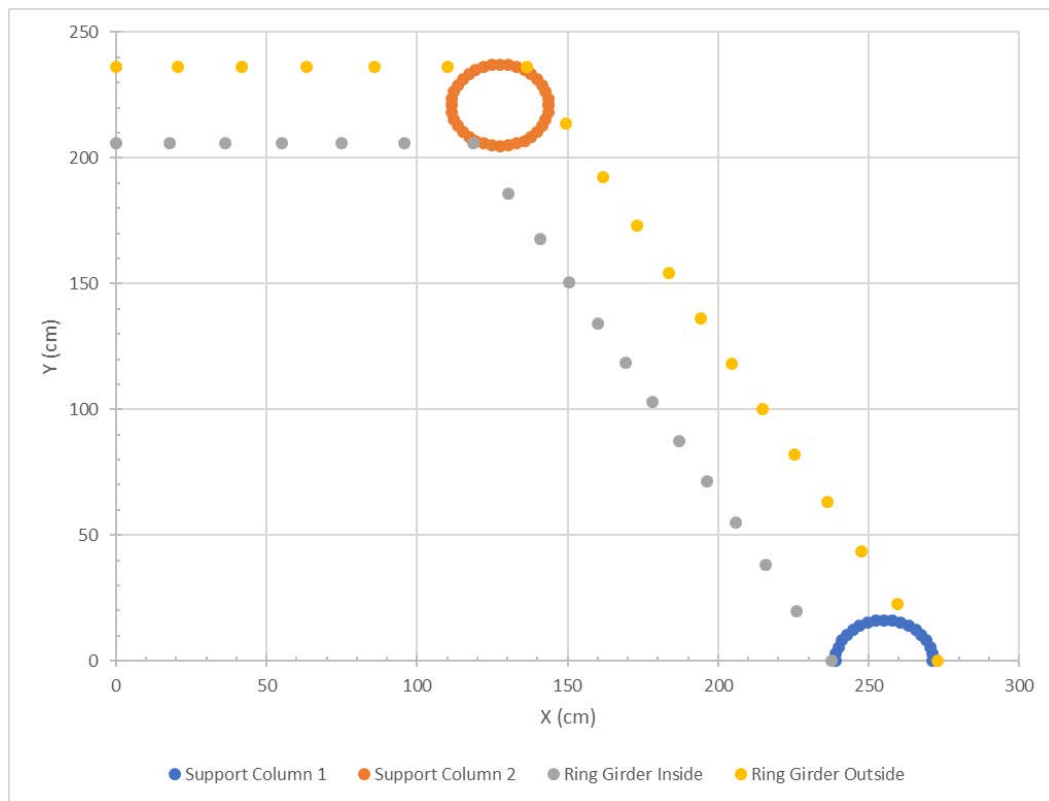


Figure 4-1
Pointwise Locations to Determine RPV Support Exposure

Table 4-12
Calculated Maximum Fast Neutron Fluence (E > 1.0 MeV) at RPV Support Components

<i>Projection with no bias on peripheral fuel assemblies</i>				
Material	Fluence (n/cm²)			
	41.32 EFPY	42 EFPY	48 EFPY	54 EFPY
Support Column 1 – maximum	1.12E+18	1.14E+18	1.33E+18	1.52E+18
Support Column 1 – top of support foot	2.48E+15	2.53E+15	2.91E+15	3.28E+15
Support Column 1 – bottom of column	2.04E+15	2.08E+15	2.39E+15	2.69E+15
Support Column 2 – maximum	7.82E+16	7.95E+16	9.13E+16	1.03E+17
Support Column 2 – top of support foot	2.59E+15	2.63E+15	3.03E+15	3.42E+15
Support Column 2 – bottom of column	2.36E+15	2.40E+15	2.77E+15	3.13E+15
Ring Girder – inside bottom edge	5.76E+17	5.86E+17	6.75E+17	7.64E+17
Ring Girder – inside top edge	1.50E+17	1.52E+17	1.75E+17	1.99E+17
Ring Girder – outside bottom edge	1.87E+17	1.90E+17	2.21E+17	2.51E+17
Ring Girder – outside top edge	2.83E+16	2.88E+16	3.32E+16	3.76E+16

<i>Projection with no bias on peripheral fuel assemblies</i>				
Material	Fluence (n/cm²)			
	60 EFPY	66 EFPY	72 EFPY	
Support Column 1 – maximum	1.72E+18	1.91E+18	2.10E+18	
Support Column 1 – top of support foot	3.66E+15	4.04E+15	4.42E+15	
Support Column 1 – bottom of column	3.00E+15	3.31E+15	3.61E+15	
Support Column 2 – maximum	1.15E+17	1.26E+17	1.38E+17	
Support Column 2 – top of support foot	3.81E+15	4.21E+15	4.60E+15	
Support Column 2 – bottom of column	3.49E+15	3.86E+15	4.22E+15	
Ring Girder – inside bottom edge	8.53E+17	9.42E+17	1.03E+18	
Ring Girder – inside top edge	2.22E+17	2.45E+17	2.68E+17	
Ring Girder – outside bottom edge	2.81E+17	3.11E+17	3.41E+17	
Ring Girder – outside top edge	4.19E+16	4.63E+16	5.07E+16	

Table 4-12 (continued)
Calculated Maximum Fast Neutron Fluence (E > 1.0 MeV) at RPV Support Components

<i>Projection with 10% bias on peripheral fuel assemblies</i>				
Material	Fluence (n/cm²)			
	41.32 EFPY	42 EFPY	48 EFPY	54 EFPY
Support Column 1 – maximum	1.12E+18	1.14E+18	1.35E+18	1.56E+18
Support Column 1 – top of support foot	2.48E+15	2.53E+15	2.94E+15	3.35E+15
Support Column 1 – bottom of column	2.04E+15	2.08E+15	2.42E+15	2.75E+15
Support Column 2 – maximum	7.82E+16	7.97E+16	9.25E+16	1.05E+17
Support Column 2 – top of support foot	2.59E+15	2.63E+15	3.06E+15	3.49E+15
Support Column 2 – bottom of column	2.36E+15	2.41E+15	2.80E+15	3.20E+15
Ring Girder – inside bottom edge	5.76E+17	5.87E+17	6.84E+17	7.81E+17
Ring Girder – inside top edge	1.50E+17	1.53E+17	1.78E+17	2.03E+17
Ring Girder – outside bottom edge	1.87E+17	1.91E+17	2.24E+17	2.57E+17
Ring Girder – outside top edge	2.83E+16	2.89E+16	3.36E+16	3.84E+16

<i>Projection with 10% bias on peripheral fuel assemblies</i>				
Material	Fluence (n/cm²)			
	60 EFPY	66 EFPY	72 EFPY	
Support Column 1 – maximum	1.77E+18	1.98E+18	2.19E+18	
Support Column 1 – top of support foot	3.77E+15	4.18E+15	4.59E+15	
Support Column 1 – bottom of column	3.09E+15	3.42E+15	3.76E+15	
Support Column 2 – maximum	1.18E+17	1.31E+17	1.44E+17	
Support Column 2 – top of support foot	3.92E+15	4.35E+15	4.78E+15	
Support Column 2 – bottom of column	3.60E+15	3.99E+15	4.39E+15	
Ring Girder – inside bottom edge	8.78E+17	9.75E+17	1.07E+18	
Ring Girder – inside top edge	2.28E+17	2.53E+17	2.79E+17	
Ring Girder – outside bottom edge	2.90E+17	3.22E+17	3.55E+17	
Ring Girder – outside top edge	4.32E+16	4.79E+16	5.27E+16	

Table 4-13
Calculated Maximum Fast Neutron Fluence ($E > 0.1$ MeV) at RPV Support Components

<i>Projection with no bias on peripheral fuel assemblies</i>				
Material	Fluence (n/cm²)			
	41.32 EFPY	42 EFPY	48 EFPY	54 EFPY
Support Column 1 – maximum	7.53E+18	7.68E+18	8.97E+18	1.03E+19
Support Column 1 – top of support foot	4.45E+16	4.53E+16	5.22E+16	5.90E+16
Support Column 1 – bottom of column	3.65E+16	3.72E+16	4.27E+16	4.83E+16
Support Column 2 – maximum	8.11E+17	8.25E+17	9.46E+17	1.07E+18
Support Column 2 – top of support foot	4.52E+16	4.60E+16	5.29E+16	5.99E+16
Support Column 2 – bottom of column	4.02E+16	4.09E+16	4.71E+16	5.33E+16
Ring Girder – inside bottom edge	4.97E+18	5.06E+18	5.83E+18	6.60E+18
Ring Girder – inside top edge	1.83E+18	1.86E+18	2.14E+18	2.42E+18
Ring Girder – outside bottom edge	1.63E+18	1.66E+18	1.92E+18	2.18E+18
Ring Girder – outside top edge	5.71E+17	5.81E+17	6.69E+17	7.58E+17

<i>Projection with no bias on peripheral fuel assemblies</i>				
Material	Fluence (n/cm²)			
	60 EFPY	66 EFPY	72 EFPY	
Support Column 1 – maximum	1.16E+19	1.29E+19	1.42E+19	
Support Column 1 – top of support foot	6.58E+16	7.27E+16	7.95E+16	
Support Column 1 – bottom of column	5.39E+16	5.94E+16	6.50E+16	
Support Column 2 – maximum	1.19E+18	1.31E+18	1.43E+18	
Support Column 2 – top of support foot	6.68E+16	7.38E+16	8.07E+16	
Support Column 2 – bottom of column	5.95E+16	6.57E+16	7.20E+16	
Ring Girder – inside bottom edge	7.37E+18	8.13E+18	8.90E+18	
Ring Girder – inside top edge	2.70E+18	2.99E+18	3.27E+18	
Ring Girder – outside bottom edge	2.45E+18	2.71E+18	2.97E+18	
Ring Girder – outside top edge	8.46E+17	9.34E+17	1.02E+18	

Table 4-13 (continued)
Calculated Maximum Fast Neutron Fluence (E > 0.1 MeV) at RPV Support Components

<i>Projection with 10% bias on peripheral fuel assemblies</i>				
Material	Fluence (n/cm²)			
	41.32 EFPY	42 EFPY	48 EFPY	54 EFPY
Support Column 1 – maximum	7.53E+18	7.69E+18	9.11E+18	1.05E+19
Support Column 1 – top of support foot	4.45E+16	4.54E+16	5.29E+16	6.03E+16
Support Column 1 – bottom of column	3.65E+16	3.72E+16	4.33E+16	4.94E+16
Support Column 2 – maximum	8.11E+17	8.26E+17	9.59E+17	1.09E+18
Support Column 2 – top of support foot	4.52E+16	4.61E+16	5.36E+16	6.12E+16
Support Column 2 – bottom of column	4.02E+16	4.09E+16	4.77E+16	5.45E+16
Ring Girder – inside bottom edge	4.97E+18	5.07E+18	5.91E+18	6.75E+18
Ring Girder – inside top edge	1.83E+18	1.86E+18	2.17E+18	2.48E+18
Ring Girder – outside bottom edge	1.63E+18	1.66E+18	1.95E+18	2.24E+18
Ring Girder – outside top edge	5.71E+17	5.82E+17	6.79E+17	7.75E+17

<i>Projection with 10% bias on peripheral fuel assemblies</i>				
Material	Fluence (n/cm²)			
	60 EFPY	66 EFPY	72 EFPY	
Support Column 1 – maximum	1.19E+19	1.34E+19	1.48E+19	
Support Column 1 – top of support foot	6.78E+16	7.53E+16	8.28E+16	
Support Column 1 – bottom of column	5.55E+16	6.15E+16	6.76E+16	
Support Column 2 – maximum	1.22E+18	1.36E+18	1.49E+18	
Support Column 2 – top of support foot	6.88E+16	7.64E+16	8.40E+16	
Support Column 2 – bottom of column	6.13E+16	6.81E+16	7.49E+16	
Ring Girder – inside bottom edge	7.59E+18	8.43E+18	9.26E+18	
Ring Girder – inside top edge	2.79E+18	3.09E+18	3.40E+18	
Ring Girder – outside bottom edge	2.52E+18	2.81E+18	3.09E+18	
Ring Girder – outside top edge	8.71E+17	9.67E+17	1.06E+18	

Table 4-14
Calculated Maximum Iron Atom Displacements at RPV Support Components

<i>Projection with no bias on peripheral fuel assemblies</i>				
Material	Displacements (dpa)			
	41.32 EFPY	42 EFPY	48 EFPY	54 EFPY
Support Column 1 – maximum	2.98E-03	3.04E-03	3.55E-03	4.06E-03
Support Column 1 – top of support foot	1.45E-05	1.48E-05	1.70E-05	1.93E-05
Support Column 1 – bottom of column	1.23E-05	1.25E-05	1.43E-05	1.62E-05
Support Column 2 – maximum	3.10E-04	3.15E-04	3.61E-04	4.08E-04
Support Column 2 – top of support foot	1.47E-05	1.50E-05	1.73E-05	1.95E-05
Support Column 2 – bottom of column	1.35E-05	1.37E-05	1.58E-05	1.79E-05
Ring Girder – inside bottom edge	1.80E-03	1.83E-03	2.11E-03	2.38E-03
Ring Girder – inside top edge	6.15E-04	6.26E-04	7.21E-04	8.16E-04
Ring Girder – outside bottom edge	6.03E-04	6.14E-04	7.11E-04	8.08E-04
Ring Girder – outside top edge	1.84E-04	1.87E-04	2.16E-04	2.44E-04

<i>Projection with no bias on peripheral fuel assemblies</i>				
Material	Displacements (dpa)			
	60 EFPY	66 EFPY	72 EFPY	
Support Column 1 – maximum	4.57E-03	5.09E-03	5.60E-03	
Support Column 1 – top of support foot	2.15E-05	2.37E-05	2.60E-05	
Support Column 1 – bottom of column	1.81E-05	1.99E-05	2.18E-05	
Support Column 2 – maximum	4.54E-04	5.00E-04	5.47E-04	
Support Column 2 – top of support foot	2.18E-05	2.41E-05	2.63E-05	
Support Column 2 – bottom of column	1.99E-05	2.20E-05	2.41E-05	
Ring Girder – inside bottom edge	2.66E-03	2.94E-03	3.22E-03	
Ring Girder – inside top edge	9.11E-04	1.01E-03	1.10E-03	
Ring Girder – outside bottom edge	9.05E-04	1.00E-03	1.10E-03	
Ring Girder – outside top edge	2.73E-04	3.01E-04	3.29E-04	

Table 4-14 (continued)
Calculated Maximum Iron Atom Displacements at RPV Support Components

<i>Projection with 10% bias on peripheral fuel assemblies</i>				
Material	Displacements (dpa)			
	41.32 EFPY	42 EFPY	48 EFPY	54 EFPY
Support Column 1 – maximum	2.98E-03	3.04E-03	3.60E-03	4.16E-03
Support Column 1 – top of support foot	1.45E-05	1.48E-05	1.73E-05	1.97E-05
Support Column 1 – bottom of column	1.23E-05	1.25E-05	1.45E-05	1.66E-05
Support Column 2 – maximum	3.10E-04	3.16E-04	3.66E-04	4.17E-04
Support Column 2 – top of support foot	1.47E-05	1.50E-05	1.75E-05	2.00E-05
Support Column 2 – bottom of column	1.35E-05	1.37E-05	1.60E-05	1.83E-05
Ring Girder – inside bottom edge	1.80E-03	1.83E-03	2.14E-03	2.44E-03
Ring Girder – inside top edge	6.15E-04	6.27E-04	7.31E-04	8.34E-04
Ring Girder – outside bottom edge	6.03E-04	6.15E-04	7.21E-04	8.27E-04
Ring Girder – outside top edge	1.84E-04	1.88E-04	2.19E-04	2.50E-04

<i>Projection with 10% bias on peripheral fuel assemblies</i>				
Material	Displacements (dpa)			
	60 EFPY	66 EFPY	72 EFPY	
Support Column 1 – maximum	4.72E-03	5.28E-03	5.84E-03	
Support Column 1 – top of support foot	2.21E-05	2.46E-05	2.70E-05	
Support Column 1 – bottom of column	1.86E-05	2.07E-05	2.27E-05	
Support Column 2 – maximum	4.68E-04	5.18E-04	5.69E-04	
Support Column 2 – top of support foot	2.24E-05	2.49E-05	2.74E-05	
Support Column 2 – bottom of column	2.05E-05	2.28E-05	2.51E-05	
Ring Girder – inside bottom edge	2.74E-03	3.04E-03	3.35E-03	
Ring Girder – inside top edge	9.38E-04	1.04E-03	1.15E-03	
Ring Girder – outside bottom edge	9.33E-04	1.04E-03	1.14E-03	
Ring Girder – outside top edge	2.81E-04	3.12E-04	3.43E-04	

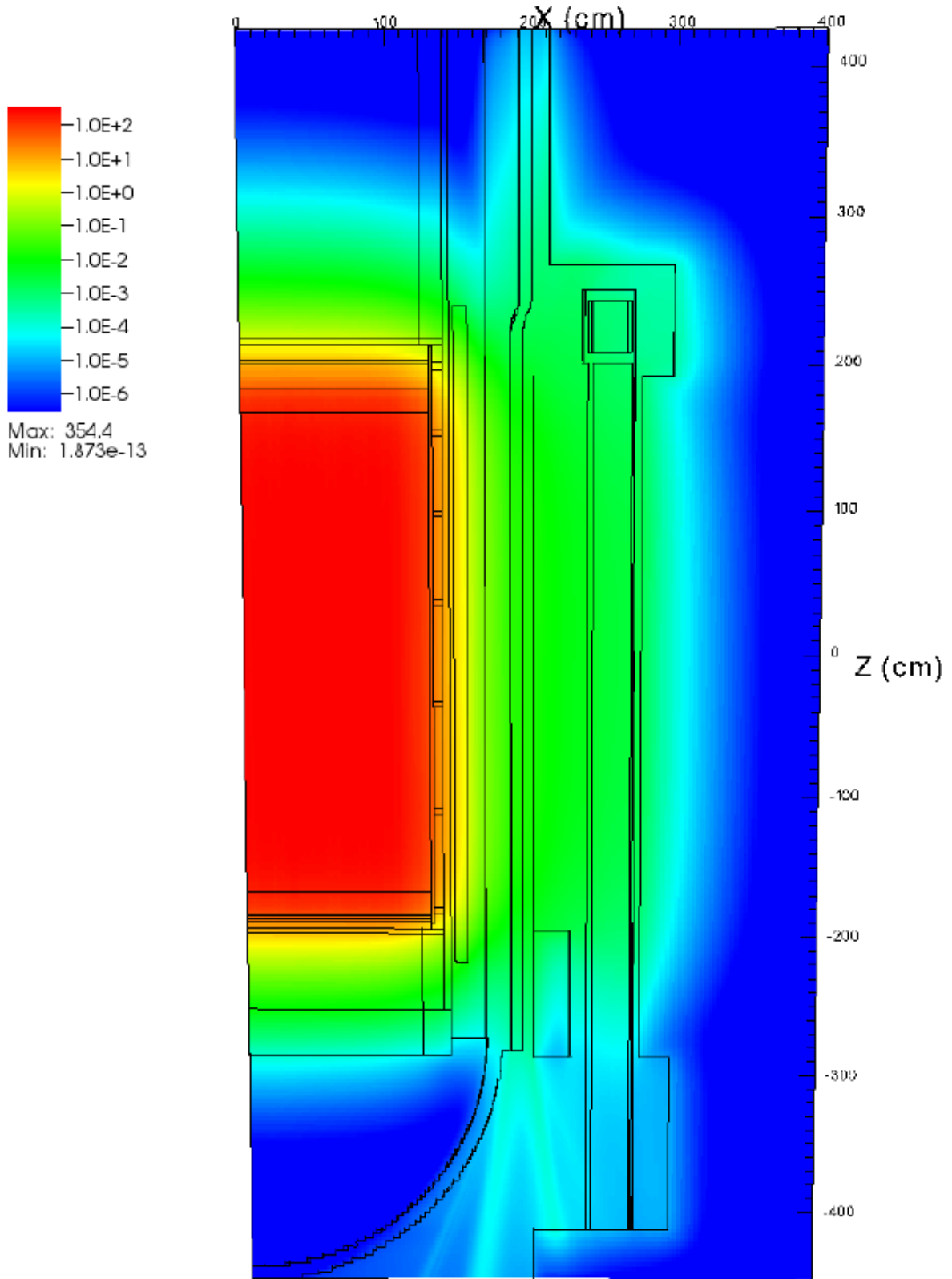


Figure 4-2
Side View through Support Column ($\theta = 0^\circ$) of Iron Atom Displacements

4.4 Concrete Bioshield

Maximum projected exposures of the bioshield concrete are given in Table 4-15 through Table 4-17. Neutron exposure is given for both energies greater than 1.0 MeV and energies greater than 0.1 MeV; these exposures are given in Table 4-15 and Table 4-16, respectively. Maximum gamma exposure of bioshield concrete is given in Table 4-17. The concrete exposure data are presented in terms of the maximum exposure experienced by the bioshield at azimuthal angles of 15°, 30°, 60°, 75°, and 90°, and at the azimuthal location providing the maximum exposure relative to the core cardinal axes. No data are reported for azimuthal angles of 0° or 45°, as these locations correspond to ex-core detector wells, as shown in Figure 2-1. There is an ex-core detector well centered at 90° as well that is not relevant to RPV support column exposure, so it is not modeled. Reported data at 90° are therefore slightly conservative, because azimuthal locations beyond 85° would correspond to an ex-core detector well.

As shown in Table 4-17, the concrete gamma dose threshold value for consideration of radiation exposure effects of 1×10^8 Gy (1×10^{10} rad) has already been exceeded. It was reached at approximately 34.5 EFPY, during Cycle 34.

Table 4-15
Calculated Maximum Fast Neutron Fluence (E > 1.0 MeV) at the Bioshield Concrete

Cycle	Cycle Length (EFPY)	Total Time (EFPY)	Fluence (n/cm ²)						Elevation of Max. (cm)
			15°	30°	60°	75°	90°	Maximum ^[1]	
1	1.52	1.52	1.24E+17	8.18E+16	8.35E+16	1.27E+17	1.80E+17	1.80E+17	-3.0
2	1.05	2.57	2.10E+17	1.40E+17	1.43E+17	2.14E+17	3.03E+17	3.03E+17	-5.0
3	0.87	3.44	2.78E+17	1.87E+17	1.91E+17	2.84E+17	4.02E+17	4.02E+17	-5.0
4	0.87	4.31	3.43E+17	2.32E+17	2.36E+17	3.50E+17	4.95E+17	4.95E+17	-5.0
5	0.89	5.20	4.11E+17	2.78E+17	2.83E+17	4.18E+17	5.90E+17	5.90E+17	-5.0
6	0.87	6.06	4.66E+17	3.22E+17	3.29E+17	4.75E+17	6.63E+17	6.63E+17	-5.0
7	0.89	6.96	5.23E+17	3.63E+17	3.70E+17	5.32E+17	7.42E+17	7.42E+17	-5.0
8	0.86	7.81	5.77E+17	4.01E+17	4.09E+17	5.88E+17	8.23E+17	8.23E+17	-5.0
9	0.79	8.60	6.29E+17	4.36E+17	4.45E+17	6.41E+17	8.98E+17	8.98E+17	-5.0
10	1.20	9.80	7.01E+17	4.89E+17	5.00E+17	7.15E+17	1.00E+18	1.00E+18	-5.0
11	0.85	10.65	7.48E+17	5.26E+17	5.37E+17	7.63E+17	1.06E+18	1.06E+18	-5.0
12	0.80	11.45	7.95E+17	5.59E+17	5.72E+17	8.10E+17	1.12E+18	1.12E+18	-5.0
13	0.81	12.25	8.38E+17	5.91E+17	6.04E+17	8.55E+17	1.18E+18	1.18E+18	-5.0
14	0.86	13.12	8.86E+17	6.29E+17	6.42E+17	9.04E+17	1.24E+18	1.24E+18	-3.0
15	0.80	13.92	9.30E+17	6.61E+17	6.75E+17	9.48E+17	1.30E+18	1.30E+18	-3.0
16	0.85	14.78	9.67E+17	6.89E+17	7.05E+17	9.86E+17	1.34E+18	1.34E+18	-1.0
17	0.84	15.62	1.00E+18	7.19E+17	7.35E+17	1.02E+18	1.39E+18	1.39E+18	5.0
18	0.85	16.46	1.04E+18	7.49E+17	7.66E+17	1.06E+18	1.44E+18	1.44E+18	7.0
19	0.83	17.29	1.08E+18	7.79E+17	7.96E+17	1.10E+18	1.49E+18	1.49E+18	15.0
20	0.88	18.18	1.12E+18	8.11E+17	8.29E+17	1.14E+18	1.54E+18	1.54E+18	19.0
21	0.90	19.08	1.16E+18	8.42E+17	8.61E+17	1.18E+18	1.60E+18	1.60E+18	43.0
22	0.75	19.82	1.19E+18	8.74E+17	8.93E+17	1.21E+18	1.64E+18	1.64E+18	45.0
23	0.92	20.74	1.23E+18	9.05E+17	9.25E+17	1.25E+18	1.70E+18	1.70E+18	51.0
24	1.57	22.31	1.30E+18	9.61E+17	9.82E+17	1.33E+18	1.80E+18	1.80E+18	55.0
25	1.27	23.58	1.36E+18	1.01E+18	1.03E+18	1.39E+18	1.88E+18	1.88E+18	55.0
26	1.35	24.93	1.43E+18	1.06E+18	1.09E+18	1.46E+18	1.97E+18	1.97E+18	57.0
27	1.33	26.27	1.49E+18	1.10E+18	1.13E+18	1.52E+18	2.06E+18	2.06E+18	57.0
28	1.25	27.52	1.55E+18	1.15E+18	1.18E+18	1.58E+18	2.14E+18	2.14E+18	59.0
29	1.37	28.89	1.62E+18	1.20E+18	1.23E+18	1.65E+18	2.23E+18	2.23E+18	59.0
30	1.42	30.31	1.68E+18	1.25E+18	1.28E+18	1.71E+18	2.31E+18	2.31E+18	59.0

Table 4-15 (continued)
Calculated Maximum Fast Neutron Fluence (E > 1.0 MeV) at the Bioshield Concrete

Cycle	Cycle Length (EFPY)	Total Time (EFPY)	Fluence (n/cm ²)						Elevation of Max. (cm)
			15°	30°	60°	75°	90°	Maximum ^[1]	
31	1.32	29.56	1.74E+18	1.29E+18	1.32E+18	1.77E+18	2.39E+18	2.39E+18	59.0
32	1.27	30.83	1.81E+18	1.35E+18	1.38E+18	1.85E+18	2.49E+18	2.49E+18	59.0
33	1.48	32.31	1.89E+18	1.40E+18	1.43E+18	1.92E+18	2.61E+18	2.61E+18	61.0
34	1.22	33.53	1.98E+18	1.47E+18	1.50E+18	2.02E+18	2.73E+18	2.73E+18	61.0
35	1.43	34.96	2.07E+18	1.53E+18	1.56E+18	2.10E+18	2.85E+18	2.85E+18	61.0
36	1.34	36.30	2.16E+18	1.59E+18	1.62E+18	2.20E+18	2.99E+18	2.99E+18	61.0
37	1.50	37.79	2.24E+18	1.65E+18	1.69E+18	2.28E+18	3.10E+18	3.10E+18	59.0
38	1.37	39.17	2.34E+18	1.71E+18	1.75E+18	2.38E+18	3.24E+18	3.24E+18	59.0
<i>Projection with no bias on peripheral fuel assemblies</i>									
		42	2.38E+18	1.74E+18	1.78E+18	2.42E+18	3.30E+18	3.30E+18	59.0
		48	2.75E+18	2.00E+18	2.04E+18	2.80E+18	3.84E+18	3.84E+18	59.0
		54	3.12E+18	2.26E+18	2.31E+18	3.18E+18	4.38E+18	4.38E+18	57.0
		60	3.50E+18	2.51E+18	2.57E+18	3.56E+18	4.92E+18	4.92E+18	57.0
		66	3.87E+18	2.77E+18	2.83E+18	3.94E+18	5.47E+18	5.47E+18	55.0
		72	4.24E+18	3.03E+18	3.10E+18	4.33E+18	6.01E+18	6.01E+18	55.0
<i>Projection with 10% bias on peripheral fuel assemblies</i>									
		42	2.38E+18	1.75E+18	1.78E+18	2.43E+18	3.31E+18	3.31E+18	59.0
		48	2.79E+18	2.03E+18	2.07E+18	2.84E+18	3.90E+18	3.90E+18	59.0
		54	3.20E+18	2.31E+18	2.36E+18	3.26E+18	4.49E+18	4.49E+18	57.0
		60	3.60E+18	2.59E+18	2.65E+18	3.67E+18	5.08E+18	5.08E+18	57.0
		66	4.01E+18	2.87E+18	2.93E+18	4.09E+18	5.67E+18	5.67E+18	55.0
		72	4.42E+18	3.15E+18	3.22E+18	4.51E+18	6.26E+18	6.26E+18	55.0
Note(s):									
1. Maximum occurs at an azimuthal angle of 90°.									

Table 4-16
Calculated Maximum Fast Neutron Fluence (E > 0.1 MeV) at the Bioshield Concrete

Cycle	Cycle Length (EFPY)	Total Time (EFPY)	Fluence (n/cm ²)						Elevation of Max. (cm)
			15°	30°	60°	75°	90°	Maximum ^[1]	
1	1.52	1.52	1.13E+18	7.48E+17	7.43E+17	1.13E+18	1.53E+18	1.53E+18	-5.0
2	1.05	2.57	1.91E+18	1.28E+18	1.27E+18	1.89E+18	2.57E+18	2.57E+18	-13.0
3	0.87	3.44	2.53E+18	1.70E+18	1.69E+18	2.51E+18	3.41E+18	3.41E+18	-15.0
4	0.87	4.31	3.11E+18	2.10E+18	2.09E+18	3.09E+18	4.19E+18	4.19E+18	-13.0
5	0.89	5.20	3.73E+18	2.52E+18	2.50E+18	3.70E+18	4.99E+18	4.99E+18	-13.0
6	0.87	6.06	4.22E+18	2.91E+18	2.89E+18	4.19E+18	5.61E+18	5.61E+18	-13.0
7	0.89	6.96	4.73E+18	3.27E+18	3.25E+18	4.69E+18	6.27E+18	6.27E+18	-5.0
8	0.86	7.81	5.22E+18	3.62E+18	3.59E+18	5.18E+18	6.95E+18	6.95E+18	-5.0
9	0.79	8.60	5.68E+18	3.93E+18	3.91E+18	5.65E+18	7.58E+18	7.58E+18	-5.0
10	1.20	9.80	6.33E+18	4.41E+18	4.38E+18	6.29E+18	8.44E+18	8.44E+18	-5.0
11	0.85	10.65	6.75E+18	4.73E+18	4.70E+18	6.70E+18	8.93E+18	8.93E+18	-5.0
12	0.80	11.45	7.16E+18	5.03E+18	4.99E+18	7.11E+18	9.45E+18	9.45E+18	-5.0
13	0.81	12.25	7.54E+18	5.31E+18	5.27E+18	7.50E+18	9.93E+18	9.93E+18	-5.0
14	0.86	13.12	7.97E+18	5.63E+18	5.60E+18	7.92E+18	1.05E+19	1.05E+19	-5.0
15	0.80	13.92	8.36E+18	5.92E+18	5.88E+18	8.31E+18	1.09E+19	1.09E+19	-5.0
16	0.85	14.78	8.68E+18	6.17E+18	6.13E+18	8.63E+18	1.13E+19	1.13E+19	-1.0
17	0.84	15.62	9.01E+18	6.43E+18	6.39E+18	8.96E+18	1.18E+19	1.18E+19	5.0
18	0.85	16.46	9.34E+18	6.69E+18	6.65E+18	9.29E+18	1.22E+19	1.22E+19	7.0
19	0.83	17.29	9.67E+18	6.95E+18	6.91E+18	9.60E+18	1.26E+19	1.26E+19	19.0
20	0.88	18.18	1.00E+19	7.23E+18	7.19E+18	9.96E+18	1.30E+19	1.30E+19	25.0
21	0.90	19.08	1.04E+19	7.51E+18	7.46E+18	1.03E+19	1.35E+19	1.35E+19	31.0
22	0.75	19.82	1.07E+19	7.78E+18	7.73E+18	1.06E+19	1.38E+19	1.38E+19	31.0
23	0.92	20.74	1.10E+19	8.05E+18	8.00E+18	1.09E+19	1.43E+19	1.43E+19	33.0
24	1.57	22.31	1.17E+19	8.54E+18	8.49E+18	1.16E+19	1.51E+19	1.51E+19	43.0
25	1.27	23.58	1.22E+19	8.95E+18	8.90E+18	1.21E+19	1.58E+19	1.58E+19	45.0
26	1.35	24.93	1.28E+19	9.42E+18	9.36E+18	1.27E+19	1.65E+19	1.65E+19	47.0
27	1.33	26.27	1.33E+19	9.80E+18	9.74E+18	1.32E+19	1.72E+19	1.72E+19	49.0
28	1.25	27.52	1.38E+19	1.02E+19	1.01E+19	1.37E+19	1.79E+19	1.79E+19	51.0
29	1.37	28.89	1.44E+19	1.06E+19	1.06E+19	1.43E+19	1.87E+19	1.87E+19	53.0
30	1.42	30.31	1.49E+19	1.11E+19	1.10E+19	1.49E+19	1.93E+19	1.93E+19	55.0

Table 4-16 (continued)
Calculated Maximum Fast Neutron Fluence (E > 0.1 MeV) at the Bioshield Concrete

Cycle	Cycle Length (EFPY)	Total Time (EFPY)	Fluence (n/cm ²)						Elevation of Max. (cm)
			15°	30°	60°	75°	90°	Maximum ^[1]	
31	1.19	31.50	1.54E+19	1.14E+19	1.13E+19	1.54E+19	2.00E+19	2.00E+19	55.0
32	1.33	32.83	1.61E+19	1.19E+19	1.18E+19	1.60E+19	2.08E+19	2.08E+19	55.0
33	1.28	34.11	1.68E+19	1.24E+19	1.23E+19	1.67E+19	2.17E+19	2.17E+19	55.0
34	1.45	35.56	1.75E+19	1.30E+19	1.29E+19	1.75E+19	2.27E+19	2.27E+19	57.0
35	1.37	36.93	1.83E+19	1.35E+19	1.34E+19	1.82E+19	2.38E+19	2.38E+19	55.0
36	1.46	38.40	1.91E+19	1.41E+19	1.40E+19	1.91E+19	2.49E+19	2.49E+19	55.0
37	1.40	39.80	1.99E+19	1.46E+19	1.45E+19	1.98E+19	2.59E+19	2.59E+19	55.0
38	1.52	41.32	2.07E+19	1.52E+19	1.51E+19	2.06E+19	2.70E+19	2.70E+19	55.0
<i>Projection with no bias on peripheral fuel assemblies</i>									
		42	2.11E+19	1.55E+19	1.54E+19	2.10E+19	2.75E+19	2.75E+19	55.0
		48	2.45E+19	1.78E+19	1.77E+19	2.43E+19	3.21E+19	3.21E+19	51.0
		54	2.78E+19	2.01E+19	1.99E+19	2.77E+19	3.66E+19	3.66E+19	47.0
		60	3.12E+19	2.24E+19	2.22E+19	3.10E+19	4.11E+19	4.11E+19	45.0
		66	3.45E+19	2.47E+19	2.45E+19	3.44E+19	4.56E+19	4.56E+19	43.0
		72	3.79E+19	2.70E+19	2.68E+19	3.77E+19	5.02E+19	5.02E+19	43.0
<i>Projection with 10% bias on peripheral fuel assemblies</i>									
		42	2.11E+19	1.55E+19	1.54E+19	2.11E+19	2.76E+19	2.76E+19	55.0
		48	2.48E+19	1.80E+19	1.79E+19	2.47E+19	3.25E+19	3.25E+19	51.0
		54	2.85E+19	2.05E+19	2.04E+19	2.83E+19	3.75E+19	3.75E+19	47.0
		60	3.22E+19	2.30E+19	2.29E+19	3.20E+19	4.24E+19	4.24E+19	45.0
		66	3.58E+19	2.55E+19	2.54E+19	3.57E+19	4.74E+19	4.74E+19	43.0
		72	3.95E+19	2.81E+19	2.79E+19	3.93E+19	5.23E+19	5.23E+19	43.0
Note(s):									
1. Maximum occurs at an azimuthal angle of 90°.									

Table 4-17
Calculated Concrete Gamma Dose at the Bioshield Concrete

Cycle	Cycle Length (EFPY)	Total Time (EFPY)	Gamma Dose (Gy)						Elevation of Max. (cm)
			15°	30°	60°	75°	90°	Maximum ^[1]	
1	1.52	1.52	5.12E+06	3.65E+06	3.81E+06	5.40E+06	6.95E+06	6.95E+06	-9.0
2	1.05	2.57	8.65E+06	6.26E+06	6.53E+06	9.13E+06	1.17E+07	1.17E+07	-13.0
3	0.87	3.44	1.15E+07	8.35E+06	8.71E+06	1.21E+07	1.56E+07	1.56E+07	-15.0
4	0.87	4.31	1.42E+07	1.03E+07	1.08E+07	1.49E+07	1.92E+07	1.92E+07	-13.0
5	0.89	5.20	1.70E+07	1.24E+07	1.29E+07	1.79E+07	2.29E+07	2.29E+07	-13.0
6	0.87	6.06	1.93E+07	1.43E+07	1.49E+07	2.03E+07	2.57E+07	2.57E+07	-13.0
7	0.89	6.96	2.16E+07	1.61E+07	1.67E+07	2.27E+07	2.88E+07	2.88E+07	-13.0
8	0.86	7.81	2.38E+07	1.77E+07	1.85E+07	2.51E+07	3.18E+07	3.18E+07	-13.0
9	0.79	8.60	2.59E+07	1.93E+07	2.01E+07	2.73E+07	3.47E+07	3.47E+07	-13.0
10	1.20	9.80	2.89E+07	2.16E+07	2.25E+07	3.05E+07	3.86E+07	3.86E+07	-13.0
11	0.85	10.65	3.08E+07	2.32E+07	2.42E+07	3.24E+07	4.09E+07	4.09E+07	-13.0
12	0.80	11.45	3.27E+07	2.46E+07	2.57E+07	3.44E+07	4.33E+07	4.33E+07	-13.0
13	0.81	12.25	3.44E+07	2.60E+07	2.71E+07	3.63E+07	4.54E+07	4.54E+07	-13.0
14	0.86	13.12	3.63E+07	2.76E+07	2.88E+07	3.83E+07	4.79E+07	4.79E+07	-13.0
15	0.80	13.92	3.81E+07	2.90E+07	3.02E+07	4.02E+07	5.00E+07	5.00E+07	-11.0
16	0.85	14.78	3.96E+07	3.02E+07	3.15E+07	4.17E+07	5.19E+07	5.19E+07	-7.0
17	0.84	15.62	4.11E+07	3.14E+07	3.28E+07	4.33E+07	5.37E+07	5.37E+07	7.0
18	0.85	16.46	4.26E+07	3.27E+07	3.41E+07	4.49E+07	5.56E+07	5.56E+07	13.0
19	0.83	17.29	4.41E+07	3.39E+07	3.54E+07	4.64E+07	5.74E+07	5.74E+07	17.0
20	0.88	18.18	4.57E+07	3.53E+07	3.68E+07	4.82E+07	5.95E+07	5.95E+07	37.0
21	0.90	19.08	4.73E+07	3.66E+07	3.82E+07	4.98E+07	6.16E+07	6.16E+07	37.0
22	0.75	19.82	4.87E+07	3.79E+07	3.96E+07	5.13E+07	6.32E+07	6.32E+07	37.0
23	0.92	20.74	5.02E+07	3.92E+07	4.09E+07	5.29E+07	6.53E+07	6.53E+07	37.0
24	1.57	22.31	5.32E+07	4.16E+07	4.34E+07	5.60E+07	6.90E+07	6.90E+07	37.0
25	1.27	23.58	5.55E+07	4.36E+07	4.55E+07	5.85E+07	7.20E+07	7.20E+07	37.0
26	1.35	24.93	5.82E+07	4.59E+07	4.79E+07	6.14E+07	7.54E+07	7.54E+07	37.0
27	1.33	26.27	6.06E+07	4.77E+07	4.98E+07	6.39E+07	7.85E+07	7.85E+07	37.0
28	1.25	27.52	6.30E+07	4.97E+07	5.18E+07	6.65E+07	8.16E+07	8.16E+07	37.0
29	1.37	28.89	6.57E+07	5.18E+07	5.40E+07	6.92E+07	8.49E+07	8.49E+07	39.0
30	1.42	30.31	6.81E+07	5.40E+07	5.63E+07	7.18E+07	8.79E+07	8.79E+07	39.0

Table 4-17 (continued)
Calculated Concrete Gamma Dose at the Bioshield Concrete

Cycle	Cycle Length (EFPY)	Total Time (EFPY)	Gamma Dose (Gy)						Elevation of Max. (cm)
			15°	30°	60°	75°	90°	Maximum ^[1]	
31	1.19	31.50	7.03E+07	5.55E+07	5.79E+07	7.41E+07	9.09E+07	9.09E+07	53.0
32	1.33	32.83	7.33E+07	5.79E+07	6.05E+07	7.72E+07	9.47E+07	9.47E+07	53.0
33	1.28	34.11	7.63E+07	6.02E+07	6.28E+07	8.05E+07	9.88E+07	9.88E+07	53.0
34	1.45	35.56	7.99E+07	6.31E+07	6.58E+07	8.42E+07	1.03E+08	1.03E+08	53.0
35	1.37	36.93	8.35E+07	6.57E+07	6.86E+07	8.80E+07	1.08E+08	1.08E+08	53.0
36	1.46	38.40	8.72E+07	6.84E+07	7.14E+07	9.19E+07	1.13E+08	1.13E+08	53.0
37	1.40	39.80	9.06E+07	7.11E+07	7.42E+07	9.55E+07	1.18E+08	1.18E+08	53.0
38	1.52	41.32	9.45E+07	7.39E+07	7.72E+07	9.96E+07	1.23E+08	1.23E+08	39.0
<i>Projection with no bias on peripheral fuel assemblies</i>									
		42	9.62E+07	7.52E+07	7.85E+07	1.01E+08	1.25E+08	1.25E+08	39.0
		48	1.11E+08	8.64E+07	9.02E+07	1.17E+08	1.46E+08	1.46E+08	37.0
		54	1.27E+08	9.77E+07	1.02E+08	1.34E+08	1.67E+08	1.67E+08	37.0
		60	1.42E+08	1.09E+08	1.14E+08	1.50E+08	1.87E+08	1.87E+08	37.0
		66	1.57E+08	1.20E+08	1.26E+08	1.66E+08	2.08E+08	2.08E+08	37.0
		72	1.72E+08	1.31E+08	1.37E+08	1.82E+08	2.29E+08	2.29E+08	37.0
<i>Projection with 10% bias on peripheral fuel assemblies</i>									
		42	9.63E+07	7.53E+07	7.86E+07	1.02E+08	1.25E+08	1.25E+08	39.0
		48	1.13E+08	8.76E+07	9.15E+07	1.19E+08	1.48E+08	1.48E+08	37.0
		54	1.30E+08	9.99E+07	1.04E+08	1.37E+08	1.71E+08	1.71E+08	37.0
		60	1.46E+08	1.12E+08	1.17E+08	1.54E+08	1.93E+08	1.93E+08	37.0
		66	1.63E+08	1.25E+08	1.30E+08	1.72E+08	2.16E+08	2.16E+08	37.0
		72	1.80E+08	1.37E+08	1.43E+08	1.90E+08	2.39E+08	2.39E+08	37.0
Note(s):									
1. Maximum occurs at an azimuthal angle of 90°.									

5.0 References

1. NRC Regulatory Guide 1.190, "Calculational and Dosimetry Methods for Determining Pressure Vessel Neutron Fluence," Office of Nuclear Regulatory Research, March 2001.
2. Westinghouse Report WCAP-18124-NP-A, Rev. 0, "Fluence Determination with RAPTOR-M3G and FERRET," July 2018.
3. Westinghouse InfoGram IG-13-2, "Fluence Attenuation Profile in Reactor Pressure Vessel Shell and Inlet/Outlet Nozzle Regions," July 2013.

This page was added to the quality record by the PRIME system upon its validation and shall not be considered in the page numbering of this document.

Approval Information

Author Approval Nedwidek Frank M Jul-30-2020 14:54:33

Reviewer Approval Hawk Andrew E Jul-30-2020 15:48:06

Approver Approval Houssay Laurent Jul-30-2020 17:02:44

Files approved on Jul-30-2020

*** This record was final approved on 7/30/2020 5:02:44 PM. (This statement was added by the PRIME system upon its validation)

Point Beach Nuclear Plant Units 1 and 2
Dockets 50-266 and 50-301
NRC 2020-0032 Enclosure 4, Attachment 2

Enclosure 4

**Non-proprietary Reference Documents and
Redacted Versions of Proprietary Reference
Documents**

(Public Version)

Attachment 2

**WCAP-18554-NP, Revision 1, “Fracture Mechanics
Assessment of Reactor Pressure Vessel Structural
Steel Supports for Point Beach Units 1 and 2,”
September 2020**

(106 Total Pages, including cover sheets)

Fracture Mechanics Assessment of Reactor Pressure Vessel Structural Steel Supports for Point Beach Units 1 and 2



WCAP-18554-NP
Revision 1

**Fracture Mechanics Assessment of Reactor Pressure Vessel
Structural Steel Supports for Point Beach Units 1 and 2**

September 2020

Alexandria M. Carolan*
RV/CV Design and Analysis

Verifier: Xiaolan Song*
RV Upper Internals Design Analysis

Reviewers: Benjamin W. Amiri*
J. Brian Hall*
Stephen K. Longwell*
Anees Udyawar*

Approved: Lynn A. Patterson*, Manager
RV/CV Design and Analysis

*Electronically approved records are authenticated in the electronic document management system.

Westinghouse Electric Company LLC
1000 Westinghouse Drive
Cranberry Township, PA 16066, USA

© 2020 Westinghouse Electric Company LLC
All Rights Reserved

FOREWORD

This document contains Westinghouse Electric Company LLC proprietary information and data which has been identified by brackets. Coding ^(a,c,e) associated with the brackets sets forth the basis on which the information is considered proprietary.

The proprietary information and data contained in this report were obtained at considerable Westinghouse expense and its release could seriously affect our competitive position. This information is to be withheld from public disclosure in accordance with the Rules of Practice 10CFR2.390 and the information presented herein is to be safeguarded in accordance with 10CFR2.390. Withholding of this information does not adversely affect the public interest.

This information has been provided for your internal use only and should not be released to persons or organizations outside the Directorate of Regulation and the ACRS without the express written approval of Westinghouse Electric Company LLC. Should it become necessary to release this information to such persons as part of the review procedure, please contact Westinghouse Electric Company LLC, which will make the necessary arrangements required to protect the Company's proprietary interests.

The proprietary information in the brackets is provided in the proprietary version of this report (WCAP-18554-P Revision 1).

RECORD OF REVISIONS

Revision	Date	Revision Description
0	August 2020	Original Issue
1	September 2020	Revision 1 incorporates comments from NextEra Energy (Point Beach) on Revision 0 of this report. The comments are saved within Westinghouse's internal documentation system.

TABLE OF CONTENTS

	EXECUTIVE SUMMARY	v
1	INTRODUCTION	1-1
2	GENERAL METHODOLOGY	2-1
3	SUPPORT CONFIGURATION, MATERIAL, AND GEOMETRY	3-1
4	LOADING CONDITIONS AND STRESS ANALYSIS	4-1
4.1	COLUMN STRESS	4-4
4.2	BOX RING GIRDER STRESS	4-5
4.3	SHEAR BRACE: I-BEAM STRESS.....	4-7
4.4	SHEAR BRACE: BOLT STRESS.....	4-9
4.5	SHEAR BRACE: KEY SHEAR STRESS.....	4-10
4.6	BOLTS (AT BOX RING GIRDER) STRESS	4-11
4.7	PINS (AT BOTTOM OF COLUMN) STRESS	4-12
4.8	SUPPORT SHOE STRESS.....	4-13
4.9	LEVELING SCREW STRESS.....	4-15
4.10	BASE PLATE STRESS	4-16
5	FRACTURE MECHANICS METHODOLOGY	5-1
5.1	FRACTURE TOUGHNESS DETERMINATION	5-1
5.1.1	Fracture Toughness for the Point Beach Supports.....	5-1
5.1.2	Bulk Material Temperature.....	5-14
5.1.3	Neutron Embrittlement and Nil-Ductility Transition Temperature of RPV Supports.....	5-16
5.2	STRESS INTENSITY FACTORS AND POSTULATED FLAWS	5-28
5.2.1	Cylinder Model (for Columns).....	5-29
5.2.2	Plate Model (for Box Ring Girder, I-beam, Support Shoe Box, Base Plate, and Key Shear).....	5-30
5.2.3	Round Bar Model (for Bolts, Leveling Screw and Pin)	5-34
6	ALLOWABLE FLAW SIZES	6-1
7	CRITICAL FLAW SIZE CALCULATION RESULTS	7-1
7.1	COLUMNS.....	7-4
7.2	BOX RING GIRDER	7-6
7.3	SHEAR BRACE: I-BEAM.....	7-8
7.4	SHEAR BRACE: BOLT	7-11
7.5	SHEAR BRACE: SHEAR KEY	7-13
7.6	BOLTS (AT BOX RING GIRDER).....	7-15
7.7	PINS (AT BOTTOM OF COLUMNS).....	7-17
7.8	SUPPORT SHOE BOX MEMBER	7-18
7.9	LEVELING SCREW	7-19
7.10	BASE PLATE	7-20
8	DISCUSSION OF CONCLUSIONS	8-1
8.1	EVALUATION OF CURRENT CONDITIONS	8-1
8.2	CHANGE IN EMBRITTLEMENT OVER TIME	8-1
8.3	CRITICAL FLAW SIZE CONCLUSIONS	8-2
9	REFERENCES	9-1

EXECUTIVE SUMMARY

As plants apply for 80 year licensure (Subsequent License Renewal-SLR), the United States (U.S.) Nuclear Regulatory Commission (NRC) has queried the nuclear power plant industry to investigate the impact of neutron embrittlement (radiation effects) on the reactor pressure vessel (RPV) supports due to extended plant operation past 60 years. The radiation effects on RPV supports were previously investigated and resolved as part of GSI-15 in NUREG-0933, Revision 3 [1], NUREG-1509 (published in May 1996) [2] and NUREG/CR-5320 (published in 1989) [3]. The conclusions in NUREG-0933, Revision 3 [1] stated that the supports were acceptable for continued operation and GSI-15 was resolved. However, for plants applying for 80 year life licensure, the U.S. NRC has requested a re-assessment of the RPV structural steel supports based on a fracture mechanics evaluation to account for neutron embrittlement (radiation effects).

Therefore, in this report, a detailed fracture mechanics evaluation is performed on Point Beach Units 1 and 2 reactor pressure vessel structural steel supports to calculate the critical flaw sizes following the general guidance of ASME Section XI [4] to investigate brittle fracture of the structural steel supports per NUREG-0933, Revision 3 [1] and NUREG-1509 [2]. Ten separate structural steel components within the Point Beach Units 1 and 2 RPV support system were evaluated which included the column, box ring girder, I-beam, bolts at shear brace, key shear, bolts at ring girder, pins at bottom of columns, support shoe box, leveling screw and base plate. The critical flaw sizes are determined by equating the applied stress intensity factor to the material specific fracture toughness. The stress intensity factor was determined for the various loading combinations at Point Beach Units 1 and 2 RPV supports and for an array of flaw shapes and orientations. The impact of neutron embrittlement on the RPV structural steel supports was determined for various EFPY (effective full power years). As a sensitivity study, 72 EFPY and 42 EFPY of neutron embrittlement were incorporated in the material specific fracture toughness.

Based on the magnitude of the critical flaw sizes calculation as discussed in Section 8 of this report, it can be demonstrated that the calculated critical flaw size based on 80 years (72 EFPY) of neutron embrittlement are sufficiently large (i.e., flaw tolerant) as compared to [

] ^{a,c,e}

For the column, bolts at the shear brace, key shear, support shoe box, and the base plate, the critical flaw sizes are larger than the [^{a,c,e}] by a large margin and are of larger or similar size to the [^{a,c,e}]. The leveling screw and the pins at bottom of the columns critical flaw sizes are above the [^{a,c,e}] by a lesser margin compared to the previously mentioned components. For the bolts at the ring girder, I-beam, and box ring girder, justification of stability is concluded based on the [

^{a,c,e} It is concluded that the critical Point Beach Units 1 and 2 RPV structural steel support components continue to be structurally stable (i.e., flaw tolerant) considering 80 years of radiation embrittlement effects on the supports, and a sufficient level of flaw tolerance is demonstrated to justify continuing the current visual examination (VT-3) of the RPV structural steel supports.

1 INTRODUCTION

As plants apply for 80 year licensure (Subsequent License Renewal-SLR), the United States Nuclear Regulatory Commission (NRC) has queried the nuclear power plant industry to investigate the impact of neutron embrittlement (radiation effects) on the reactor pressure vessel (RPV) supports due to extended plant operation past 60 years. The radiation effects on RPV supports were previously investigated and resolved as part of GSI-15 in NUREG-0933, Revision 3 [1], NUREG-1509 (published in May 1996) [2] and NUREG/CR-5320 (published in 1989) [3]. The conclusions in NUREG-0933, Revision 3 [1] stated that the supports were acceptable for continued operation and GSI-15 was resolved, as follows:

The preliminary conclusion indicated that the potential problem [embrittlement of supports due to radiation effects] did not pose an immediate threat to public health and safety... The above tentative results indicated that plant safety could be maintained despite RVSS [reactor vessel support structures] radiation damage... In order to encompass the uncertainties in the various analyses and provide an overall conservative assessment, several structural analyses conducted demonstrated the following:

1. Postulating that one of the four RPV supports was broken in a typical PWR, the remaining supports would carry the reactor vessel load even under SSE [safe-shutdown earthquake] seismic loads;
2. If all supports were assumed to be totally removed (i.e., broken), the short span of piping between the vessel and the shield wall would support the load of the vessel.

The results of the analyses virtually eliminated the concern for both radiation embrittlement and significant structural damage from a postulated RPV failure... Based on the staff's regulatory analysis, the issue was RESOLVED with no new requirements. Consideration of a license renewal period of 20 years did not change this conclusion.

Based on conclusions in NUREG-0933 and NRC Memorandums on GSI-15 [5], it was concluded that the RPV supports were not a concern for the entirety of its plant life (i.e., 40 and 60 years) even in the extreme case where all the supports were totally removed (i.e., broken), the piping has acceptable margin to carry the load of the vessel. However, for plants applying for 80 year life licensure, the NRC has requested a re-assessment of the RPV structural steel supports based on a fracture mechanics evaluation to account for neutron embrittlement [6].

There are two potential fracture mechanics strategies that are identified to resolve the radiation embrittlement concern based on NUREG-0933 and NUREG-1509. One option was to compare the lowest service temperature (LST) with the material adjusted reference temperature, with incorporation of irradiation effects. If the lowest service temperature is higher than the material adjusted reference temperature, then the RPV supports are acceptable. Historically, it was determined that the LST method would not provide sufficient margin, hence this methodology will not be completed for Point Beach RPV structural steel supports.

The second method to investigate brittle fracture of the structural steel supports per NUREG-0933 and NUREG-1509 is to perform a detailed fracture mechanics evaluation in order to calculate the critical flaw sizes similar to the general guidance of ASME Section XI Appendix A. Based on the magnitude of the critical flaw sizes calculation, the analysis could be used to demonstrate that the calculated critical flaw

size based on 80 years of neutron embrittlement are sufficiently large (i.e., flaw tolerant) as compared to [

] ^{a,c,e} Note that current ASME Section XI IWF in-service inspection for supports require only a visual examination (VT-3). The objective of the analysis is to demonstrate sufficient level of flaw tolerance to justify continuing the current visual examination (VT-3).

It should be noted, as part of the overall resolution of GSI-15 in NUREG-1509, a detailed fracture mechanics evaluation was performed in 1989 for one of the pilot plants in NUREG/CR-5320, namely, Turkey Point Unit 3 (the other plant was Trojan). The conclusions in NUREG/CR-5320 indicated that for the most severe credible loading (deadweight plus large break LOCA) at 32 EFPY (40 years), the best-estimated minimum critical flaw size depth is 0.3 inches for the structural support beams. Furthermore, the study had concluded that calculated flaw size is insensitive to reactor operating time after ~10 EFPY, and at startup (0 EFPY) the size is 0.6 inches. The study in NUREG/CR-5320 also demonstrated that considering uncertainties in the fracture toughness, initial nil-ductility transition temperature (NDTT_o), and the operating temperature of the support components, the $\pm 1\sigma$ (one standard deviation) values of the critical flaw size at 32 EFPY are ~0.2 and 0.6 inches. For the loading case of deadweight plus safe shutdown earthquake, the critical flaw size is substantially larger (1.1 inches as compared with 0.3 inches) at 32 EFPY.

Even though the fracture mechanics study performed for Turkey Point Unit 3 and Trojan in NUREG/CR-5320 (conducted in 1989) had calculated small critical flaw sizes that could be of a source of concern for brittle fracture, the NRC staff in 1996 had reviewed several other structural analyses, in addition to the fracture mechanics evaluation. Based on the NRC's review of other structural consequence analysis, a final conclusion (as stated in NUREG-0933 of GSI-15) was reached that even if one of the RPV supports were broken in a PWR, the remaining supports would safely carry the reactor vessel load under seismic events. The structural analyses also concluded that even if all the RPV supports were broken, the short span of piping between the vessel and the shield wall would support the load of the reactor vessel.

As a result, the fracture mechanics evaluation in NUREG/CR-5320 can be considered a defense-in-depth study of the structural integrity of the RPV supports, as supplemented by the structural analysis which demonstrated that the piping can withstand the load of the RPV after failure of all vessel supports. It should be noted that the flaw sizes postulated in the NUREG/CR-5320 would have been identified during original fabrication (pre-service inspection) of the support welds either by dye penetrate testing, magnetic particle or even ultrasonic equipment as required by AISC (American Institute of Steel Construction) and AWS (American Welding Society).

The goal of the analysis herein for Point Beach Units 1 and 2 for the 80 year license renewal is to keep consistent with the overall methodology that had been previously accepted by the industry and NRC in NUREG-0933, NUREG-1509, and NUREG/CR-5320, while at the same time demonstrate that the RPV supports are structurally safe with consideration of neutron embrittlement for plant life extension to 80 years. The objective of the analysis is to demonstrate sufficient level of flaw tolerance to justify continuing the current visual examination (VT-3) into the future.

Thus, the assessment in this report for Point Beach Units 1 and 2 determines the critical flaw sizes based on a fracture mechanics evaluation for the RPV structural steel supports to investigate the impact of neutron embrittlement (radiation effects) for an operating life of 80 years. The general methodology of the fracture mechanics evaluation is described in Section 2. Point Beach support configuration, materials, and geometry are provided in Section 3 of this report. Section 4 describes the plant-specific loading conditions and the stresses used in the evaluation, while Section 5 will provide information regarding fracture toughness, plant-specific neutron embrittlement, and postulation of flaw sizes. Section 6 describes the allowable flaw sizes which are compared to the critical flaw sizes. Section 7 will provide the calculated critical flaw sizes that were determined for the supports to demonstrate structural stability based on the linear elastic fracture mechanics evaluations and Section 8 provides the final conclusions of the fracture mechanics evaluation. All cited references are provided in Section 9.

2 GENERAL METHODOLOGY

The goal of the fracture mechanics evaluation is to demonstrate that brittle fracture is not a concern for the RPV structural steels at Point Beach Units 1 and 2 (i.e., the calculated critical flaw sizes are sufficiently large or flaw tolerant) based on 80 years (72 EFPY) of neutron embrittlement. Linear elastic fracture mechanics (LEFM) will be used as a conservative methodology to evaluate the structural integrity of the supports. The LEFM methodology is illustrated in a flow chart format (see Figure 2-1) based on the guidance provided in NUREG-1509 for a fracture mechanics approach to account for radiation effects on RPV support steels. The LEFM methodology is briefly described in the following paragraphs.

The limiting component for the fracture mechanics analysis is based on a combination of component geometry, operating condition, stress, material property, and neutron embrittlement. Point Beach support configuration, materials, and geometry are provided in Section 3 of this report. The critical flaw size will be calculated by equating the material specific fracture toughness to the applied stress intensity factors for various postulated flaw sizes in the support components based on different loading conditions (i.e., normal, upset, faulted-1 and faulted-2; there is no emergency loading condition at Point Beach). Consideration of all applicable loading conditions, such as deadweight, seismic, loss-of-coolant accident, welding residual stresses and thermal stresses are accounted for in the analysis as described in Section 4 of this report. [

]a,c,e

Based on the component geometry and loading types, various stress intensity factors will be considered as described in Section 5.2 of this report. Stress intensity factors based on semi-elliptical postulated flaws with various aspect ratios (AR, flaw length over flaw depth) will be considered at the RPV support components with plate-like structures; these AR will range from 2:1 to infinity. Quarter-circular corner flaws are also considered at the edge of the plates. Continuous circumferential flaws are postulated for the column component. For bolts/bars/screws, the stress intensity factors will be based on a 360° continuous circumferential flaw, straight front and semi-circular front flaws in a bar model. The stress intensity factors are then compared to the material specific fracture toughness to determine critical flaw size.

The material specific fracture toughness will be [

]a,c,e

Sections 7 and 8 provide the calculated critical flaw sizes that were determined for the RPV structural steel supports and the comparison to the allowable flaw sizes to demonstrate structural stability based on the linear elastic fracture mechanics evaluations.

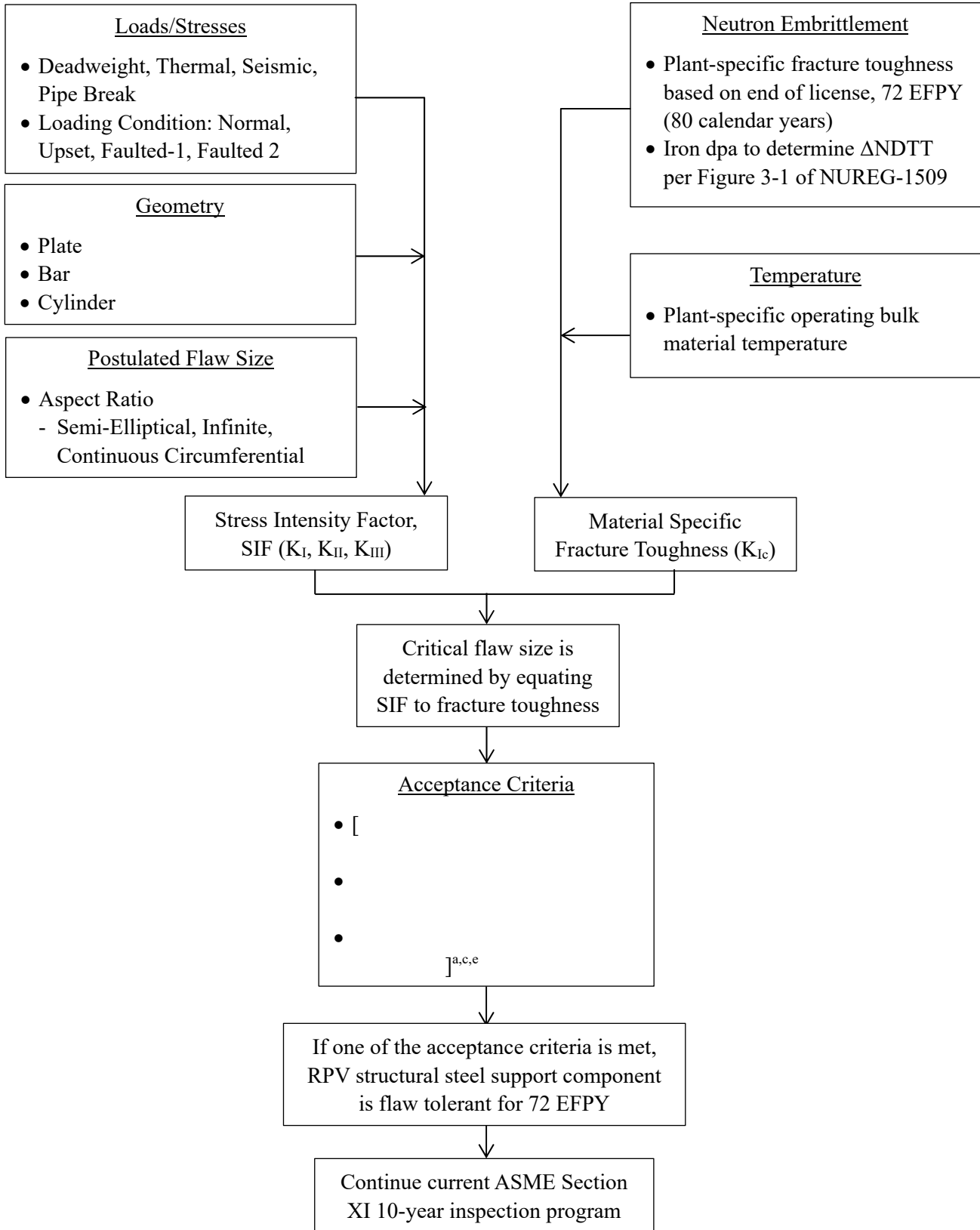


Figure 2-1: Fracture Toughness Approach Flowchart

3 SUPPORT CONFIGURATION, MATERIAL, AND GEOMETRY

This section of the report describes the general Point Beach RPV support configuration, material designation and geometry such as thickness and diameter.

The Point Beach Unit 1 loop layout and RPV support location and orientation are provided in Figure 3-1 and in Figure 3-2 for Point Beach Unit 2. The RPV support structure (long-columns) consists of a six-sided structural steel ring girder supported at each apex by approximately 19' long steel columns extending downward to the interior concrete structure below the RPV. The columns are 12" diameter steel cylinders and support the box ring girder. The Point Beach Unit 2 RPV and ring girder layout is provided in Figure 3-3, which is also applicable to Point Beach Unit 1. The six columns of the support structure are bolted at the top to the ring girder and pinned at the bottom to the floor anchor (see Figure 3-4). A close-up of the shear brace system and the bolts which fasten the box ring girder to the columns is provided in Figure 3-5 and a close up of the pin at the bottom of the column and the base plate is shown in Figure 3-6.

The center of each segment of the box ring girder provides lateral and rotational restraint by structural members embedded in the surrounding primary shield wall concrete. The RPV has six supports pads, one at each of the four nozzles, and two additional gusset-braced support pads that are welded directly to the RPV (see Figure 3-1 and Figure 3-2). Each vessel support bears on a support shoe, which is fastened to the support structure. The support shoe is a structural member that transmits the support loads to the supporting structure. It is designed to restrain vertical, lateral, and rotational movement of the RPV but to allow for thermal growth by permitting radial sliding on the bearing plates at each support. An exploded view of the support shoe assembly is shown in Figure 3-7. The inside surface of the reactor cavity is lined with steel plate and is 3'-3" from the external surface of the RPV. Point Beach Unit 1 and Unit 2 RPV supports are detailed, fabricated and delivered per the Design Specification 6118-C-10 [7].

The following ten RPV structural steel support components are considered for the critical flaw size calculations as these locations could experience tensile stresses and high embrittlement effects: column, box ring girder, I-beam at shear brace, bolts at shear brace, key shear, bolts at ring girder, pins at bottom of column, support shoe box, leveling screw, and base plate. The geometry of interest and the type of material for the previously mentioned components is provided below per the RPV support drawings [8].

Column (see Figure 3-4)

Material: ASTM A-53-63T Type S Grade B

Outside Diameter (OD) = 12.75"

Thickness (t) = 1"

Inside Radius (R_i) = 5.375"

Box Ring Girder (see Figure 3-4)

Material: U.S. Steel T-1 ¹ (Composed of 4 steel plates welded into a box shape)

Flange Width = 12"

Flange Thickness = 3"

Web Width = 13.5"

Web Thickness = 1.5"

¹All material noted as U.S. Steel T-1 are ASTM A-514-65 or A-517-65, Type F for 4" thick components and under.

Shear Brace: I-Beam (see Figure 3-5)

Material: U.S. Steel T-1 (Composed of flange and web welded into I-beam)

Flange Width = 10"

Flange Thickness = 1.75"

Web Width = 9"

Web Thickness = 1"

Bolts (at Shear Brace) (see Figure 3-5)

Material: ASTM A-490

Outside Diameter = 1.6012"

Shear Brace: Shear Key (see Figure 3-5)

Material: U.S. Steel T-1

Thickness = 2"

Width = 2.5"

Length = 14"

Bolts (at the apex of box ring girder) (see Figure 3-5)

Material: ASTM A-490

Outside Diameter = 1.6012"

Pins (at bottom of column) (see Figure 3-6)

Material: ASTM A-490

Outside Diameter = 3.994"

Support Shoe Box Member (see Figure 3-7)

[

] ^{a,c,e}

Leveling Screw (see Figure 3-7)

[

] ^{a,c,e}

Base Plate (at the bottom of the columns) (see Figure 3-6)

Material: U.S. Steel T-1

Thickness = 2"

Width = 22"

Length = 22"



Figure 3-1: Point Beach Unit 1 Loop Layout, RPV Support Location, and Orientation



Figure 3-2: Point Beach Unit 2 Loop Layout, RPV Support Location, and Orientation



a,c,e

**Figure 3-3: Point Beach Unit 2 RPV and Ring Girder Layout
(Applicable to Point Beach Unit 1)**

a,c,e

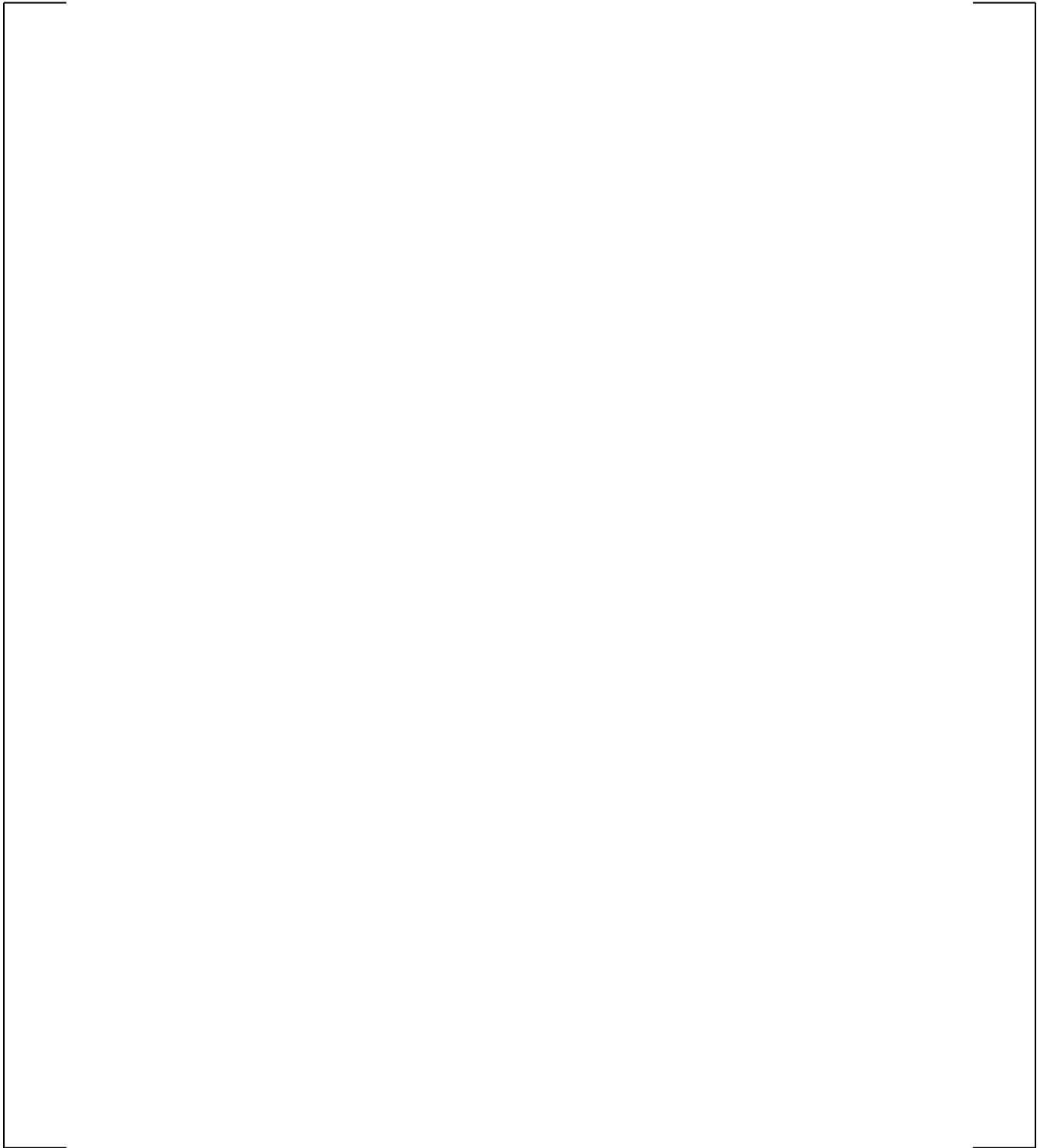


Figure 3-4: Point Beach Units 1 and 2 RPV Support Assembly

a,c,e



Figure 3-5: Close-up – Point Beach Units 1 and 2 RPV Support Assembly

[

]a,c,e



Figure 3-6: Elevation View of Pin and Base Plate

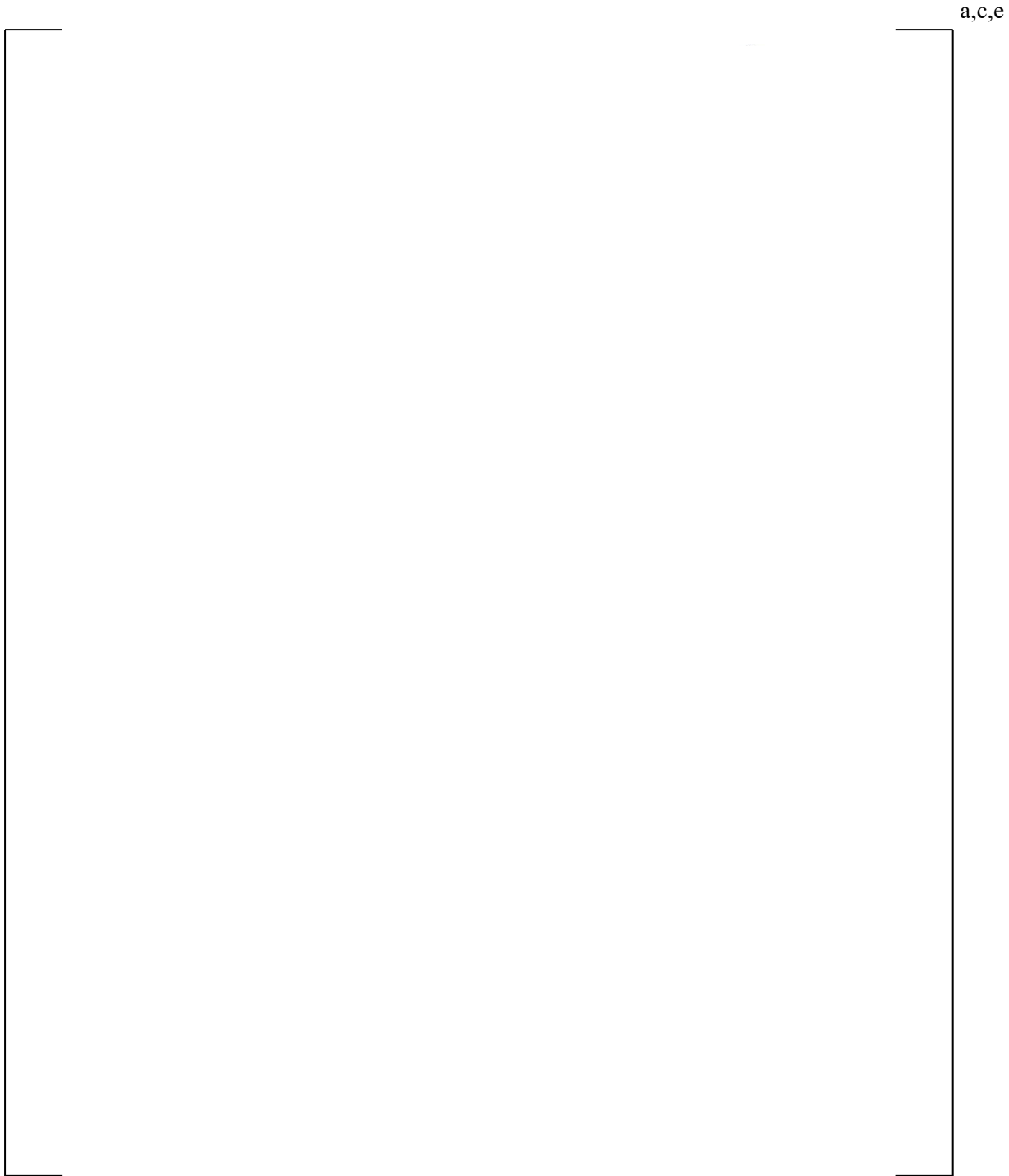


Figure 3-7: Exploded View - RPV Support Shoe Assembly

[

]a,c,e

4 LOADING CONDITIONS AND STRESS ANALYSIS

The critical flaw sizes are determined by equating the applied stress intensity factor to the material specific fracture toughness. The stress intensity factor is determined for the various loading combinations at Point Beach Units 1 and 2 RPV supports components. The design basis load combinations for the Point Beach RPV supports are based on the Updated Final Safety Analysis Report (UFSAR) [9], and are as follows:

Normal:	DW + THM	DW = deadweight stress
Upset:	Normal + OBE	THM = thermal stress
Faulted-1:	Normal + SSE	OBE = operational basis earthquake stress
Faulted-2:	Normal + SSE + LOCA	SSE = safe shutdown earthquake stress
		LOCA = loss-of-coolant accident stress

There are ten components within the Point Beach Units 1 and 2 RPV support system that are evaluated which includes the column, box ring girder, I-beam, bolts at shear brace, key shear, bolts at ring girder, pins at bottom of column, support shoe box, leveling screw and base plate. These support components represent the locations of highest stresses within the RPV support system and/or are located near the RPV active core and subjected to high neutron irradiation. The stresses are plant specific and bound both Point Beach Units 1 and 2. [

The stresses at the ten RPV support components are provided in Table 4-1 through Table 4-11.

The typical stress components [

The stress intensity factor methodology for each of the ten components is described in Section 5.2 of this report.

Welding residual stress (WRS) is also considered for applicable components. The box ring girder is welded with full penetration welds at the four corners of box as shown in [8.a, 8.e]. The drawings and design specification [7] do not specify that the box ring girder welds are post weld heat treated (PWHT); thus the welding residual stress is considered and [

]a,c,e

[]^{a,c,e}

The flanges and web within the I-beam are welded together with 3/4" fillet welds as shown in [8.a, 8.e]. The drawings and design specification [7] do not specify that the I-beam welds are PWHT; thus the WRS is considered and [

]^{a,c,e}

The WRS described in the previous two paragraphs for the I-beam and box ring girder semi-elliptical flaws near the welds is conservatively applied as constant through the wall thickness. For a more representative case, the through-wall welding residual stress profile from [

] ^{a,c,e} In this more representative case to account for WRS, the limiting Faulted-2 stresses for the I-beam are added to the through-wall WRS and critical flaw sizes are determined.

The following sections in this report provide the stress for each of the ten components analyzed and a figure of the postulated flaws which are analyzed to determine the critical flaw sizes:

- Section 4.1: Column
- Section 4.2: Box Ring Girder
- Section 4.3: I-beam at the Shear Brace
- Section 4.4: Bolt at the Shear Brace
- Section 4.5: Key Shear at the Shear Brace
- Section 4.6: Bolts at the Box Ring Girder
- Section 4.7: Pins at the Bottom of the Column
- Section 4.8: Support Shoe
- Section 4.9: Leveling Screw
- Section 4.10 Base Plate



a,c,e

Figure 4-1: [

]a,c,e

4.1 COLUMN STRESS

The applied stresses on the columns are provided in Table 4-1. A drawing of the column and the postulated flaws is shown in Figure 4-2. The membrane stress (i.e., axial stress in Table 4-1) on the column is compressive; when the compressive stress is combined with the stress due to bending of the column, [

]a,c,e

**Table 4-1: Stress Values for Column
Point Beach Units 1 and 2 Reactor Vessel Supports System**

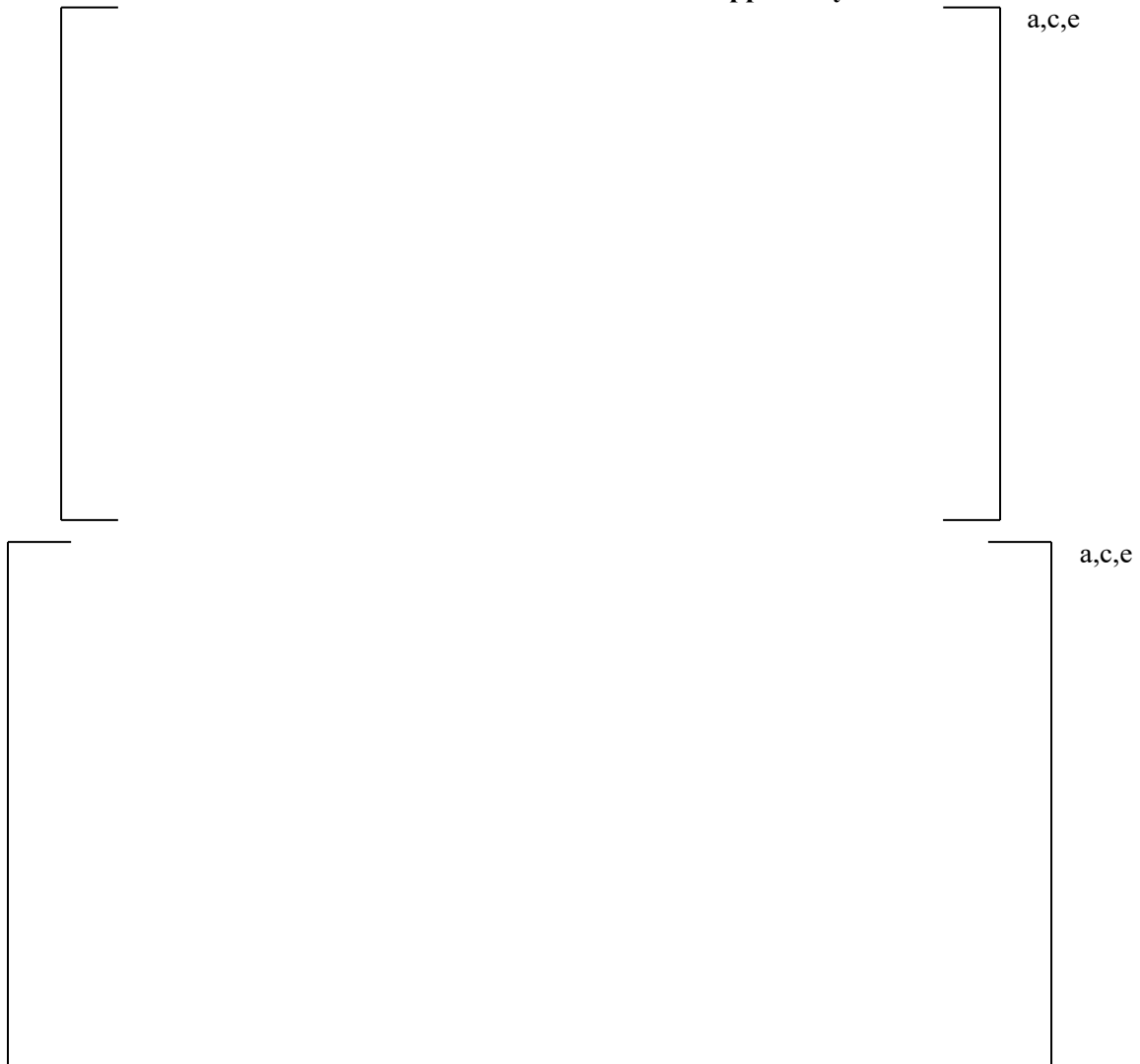


Figure 4-2: Postulated Circumferential Flaw ^(a) and Loads in Column

Note:
(a) [

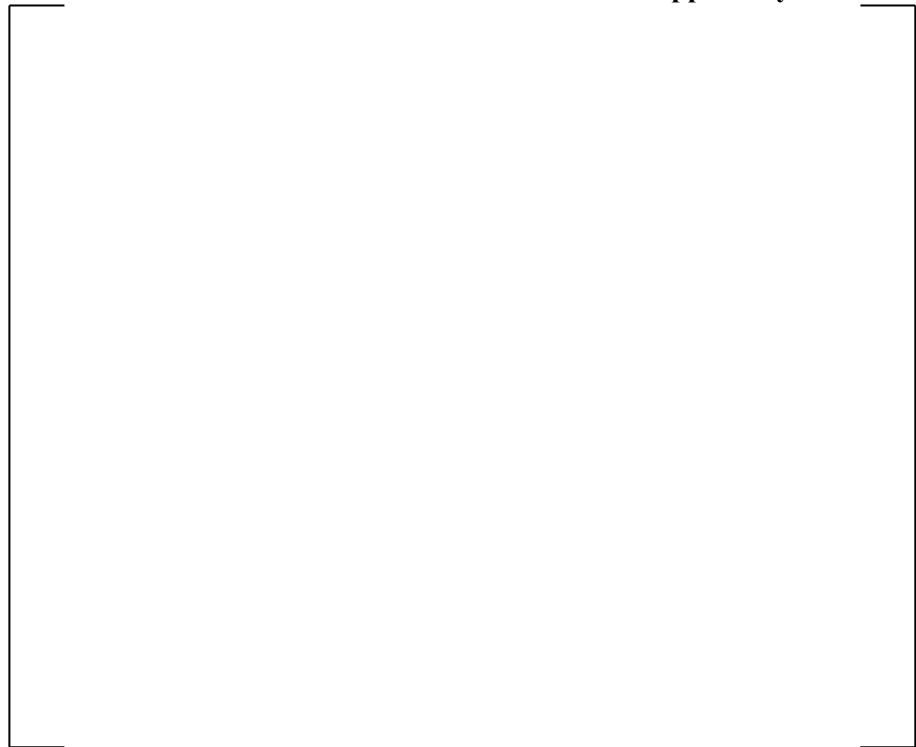
]a,c,e

4.2 BOX RING GIRDER STRESS

The applied stresses on the box ring girder are provided in Table 4-2. A drawing of the box ring girder and the postulated flaws is shown in Figure 4-3. [

] ^{a,c,e} Welding residual stress is added to the operating stress for the postulated semi-elliptical flaws located near the welded portion of the box ring girder. The semi-elliptical flaws are analyzed with aspect ratios (AR, flaw length over flaw depth) of 6:1 and 2:1 as a parametric study. In addition, infinitely long edge flaws are postulated in top edge and side edge of the flange, the side edge of the web and a corner flaw is postulated in the flange for the parametric study.

**Table 4-2: Stress Values for Box Ring Girder
Point Beach Units 1 and 2 Reactor Vessel Supports System**



a,c,e



Figure 4-3: Postulated Flaws ^(c) and Loads in Box Ring Girder

[

] ^{a,c,e}

4.3 SHEAR BRACE: I-BEAM STRESS

The applied stresses on the I-beam are provided in Table 4-3. A drawing of the I-beam and the postulated flaws is shown in Figure 4-4. [

] ^{a,c,e} Welding residual stress is added to the operating stress for the postulated semi-elliptical flaws located near the welded portion of the I-beam. The semi-elliptical flaws are analyzed with aspect ratios (AR, flaw length over flaw depth) of 6:1 and 2:1 as a parametric study. In addition, infinitely long edge flaws are postulated in top edge and side edge of the flange, the side edge of the web and a corner flaw is postulated in the flange for the parametric study.

**Table 4-3: Stress Values for I-Beam in Shear Brace
Point Beach Units 1 and 2 Reactor Vessel Supports System**

	a,c,e
--	-------



Figure 4-4: Postulated Flaws ^(c) and Loads in Shear Brace I-Beams

[

]a,c,e

4.4 SHEAR BRACE: BOLT STRESS

The applied loads on the bolts are provided in Table 4-4. A drawing of the bolts and the postulated flaws is shown in Figure 4-5. Critical flaw size is determined based on a postulated 360° continuous circumferential, straight front and semi-circular front flaw in the bolt. These three flaw sizes are analyzed as a parametric study. []^{a,c,e}

Table 4-4: Axial Tensile Force Values for Bolts of the Shear Brace Point Beach Units 1 and 2 Reactor Vessel Supports System

[] ^{a,c,e}



Figure 4-5: Postulated Flaws and Force in Bolts of the Shear Brace

4.5 SHEAR BRACE: KEY SHEAR STRESS

The applied shear loads on the key shear are provided in Table 4-5. A drawing of the key shear and the postulated flaws is shown in Figure 4-6. [

] ^{a,c,e} An edge flaw is postulated on two faces of the key shear as shown in Figure 4-6 to account for Mode II and Mode III stress intensity factor (K_{II} and K_{III}). The Mode II and Mode III stress intensity factors are conservatively compared to Mode I fracture toughness to determine critical flaw size.

Table 4-5: Shear Load Values for Key Shear in Shear Brace Point Beach Units 1 and 2 Reactor Vessel Supports System

	a,c,e
--	-------



Figure 4-6: Postulated Flaws and Shear Load in Key Shear in Shear Brace

4.6 BOLTS (AT BOX RING GIRDER) STRESS

The applied loads and moment on the bolts are provided in Table 4-6. A drawing of the bolts and the postulated flaws is shown in Figure 4-7. The shear load and tensile load are converted to stresses [

] ^{a,c,e}

**Table 4-6: Loads and Moment Values for Bolts at Box Ring Girder
Point Beach Units 1 and 2 Reactor Vessel Supports System**



^{a,c,e}



^{a,c,e}

Figure 4-7: Postulated Flaws and Loads in Bolts at Box Ring Girder

4.7 PINS (AT BOTTOM OF COLUMN) STRESS

The applied forces and moments on the pin at bottom of column are provided in Table 4-7. A drawing of the pin and the postulated flaw is shown in Figure 4-8. [

] ^{a,c,e}

**Table 4-7: Force and Moment Values for Pins at Bottom of Column
Point Beach Units 1 and 2 Reactor Vessel Supports System**

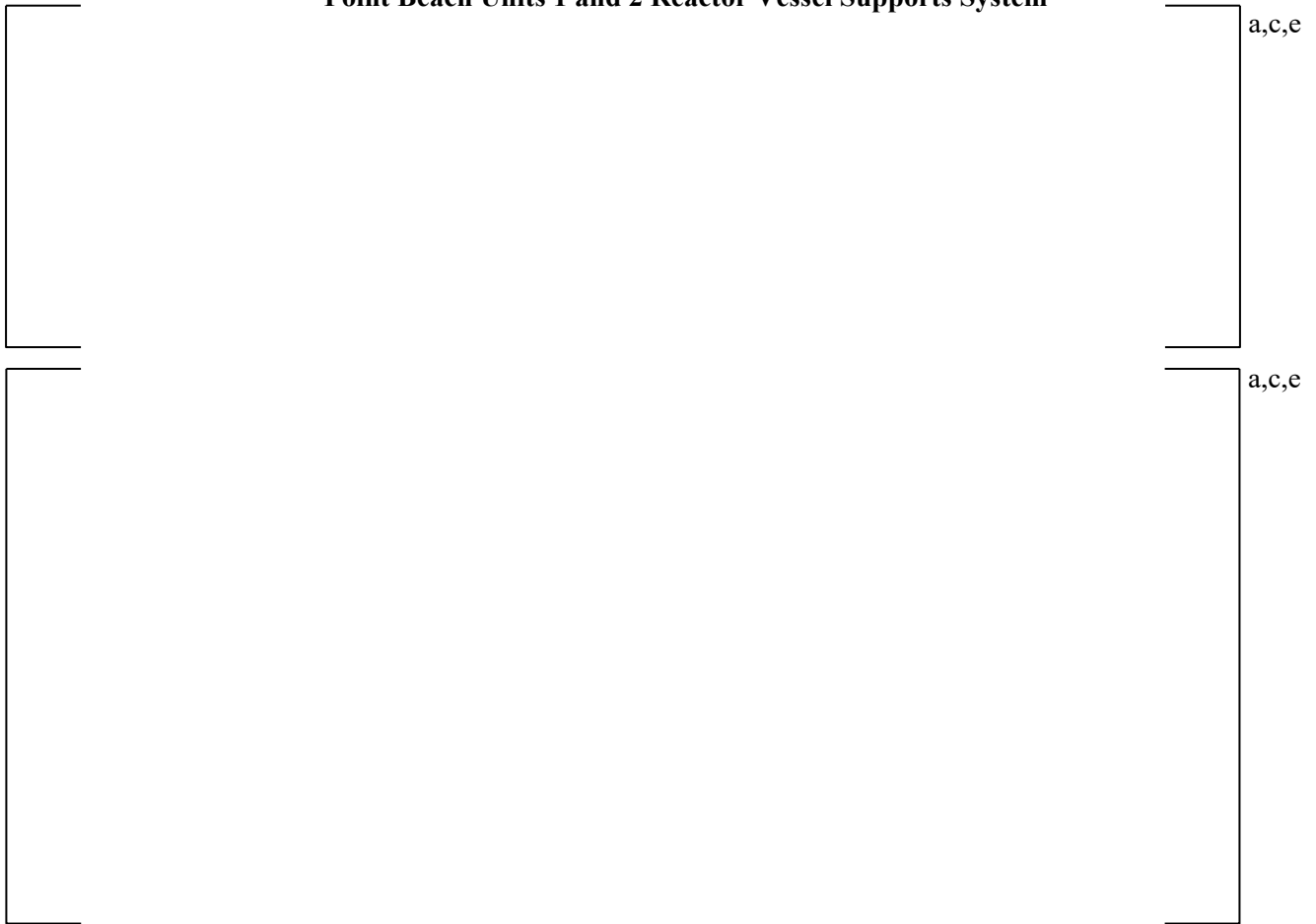


Figure 4-8: Postulated Edge Flaw and Loads in Pins at Bottom of Column

4.8 SUPPORT SHOE STRESS

The applied stresses on the support shoe are provided in Table 4-8 and Table 4-9 for Cut 1/Cut 2 and Cut 5/Cut 6, respectively. A drawing of the support shoe, postulated flaws, and cut locations are shown in Figure 4-9. Cut 3/Cut 4 and Cut 7 are [


] ^{a,c,e} An infinitely long top and side edge flaw are analyzed for Cut 1/Cut 2 and a through-wall double edge flaw at the hole in the support shoe is analyzed for Cut 5/ Cut 6.

**Table 4-8: Stress Values for Support Shoe (Cut 1/Cut 2)
Point Beach Units 1 and 2 Reactor Vessel Supports System**

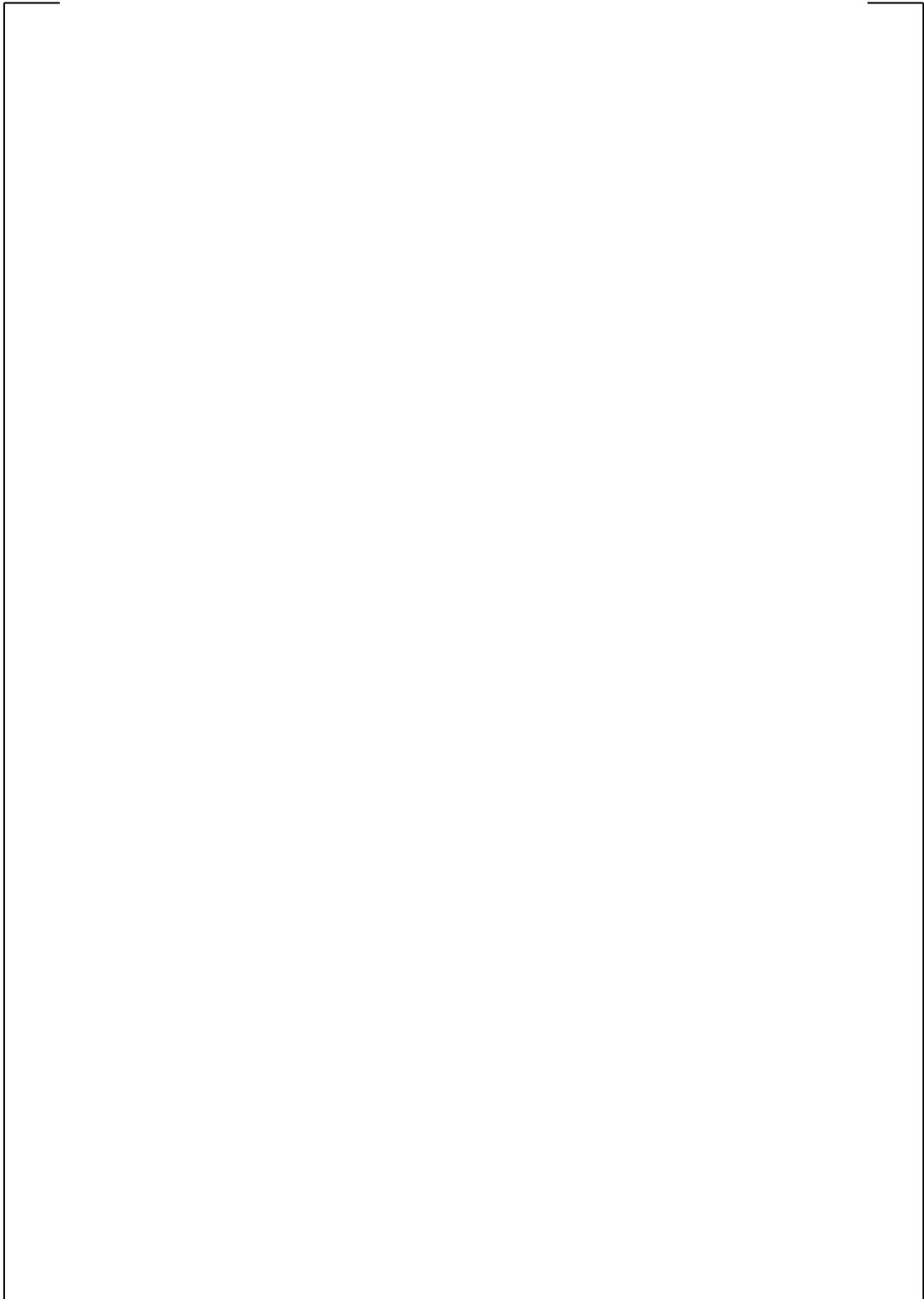


a,c,e

**Table 4-9: Stress Values for Support Shoe (Cut 5/Cut 6)
Point Beach Units 1 and 2 Reactor Vessel Supports System**



a,c,e



a,c,e

Figure 4-9: Postulated Flaws and Loads in Support Shoe

4.9 LEVELING SCREW STRESS

The applied forces and moments on the leveling screw are provided in Table 4-10. A drawing of the leveling screw and the postulated flaws is shown in Figure 4-10. The shear load and tensile load are converted to stresses [

]a,c,e

**Table 4-10: Force and Moment Values for Leveling Screw
Point Beach Units 1 and 2 Reactor Vessel Supports System**



a,c,e



a,c,e

Figure 4-10: Postulated Flaws and Loads in Leveling Screw

4.10 BASE PLATE STRESS

The applied stresses to the base plate are provided in Table 4-11. A drawing of the base plate and the postulated flaw is shown in Figure 4-11. The stresses shown in Table 4-11 are the result of a conservative analysis without the consideration of axial compressive forces from the column to maximize the bending in the base plate. The tensile stresses in Table 4-11 are []^{a,c,e} As a conservative study, a semi-elliptical flaw with aspect ratio (AR, flaw length over flaw depth) of 10:1 is analyzed to determine the critical flaw sizes of the base plate.

**Table 4-11: Stress Values for Base Plate
Point Beach Units 1 and 2 Reactor Vessel Supports System**

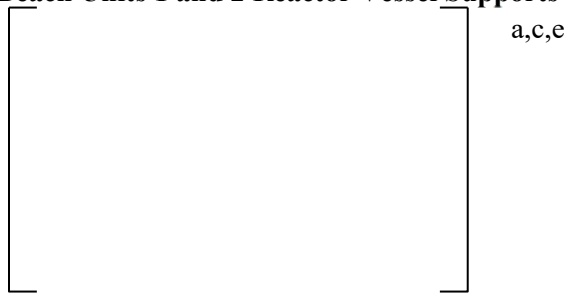


Figure 4-11: Postulated Flaw in Base Plate

5 FRACTURE MECHANICS METHODOLOGY

As discussed in Section 2, the linear elastic fracture mechanics methodology is used to evaluate the structural integrity of the Point Beach Units 1 and 2 RPV supports. The goal of the evaluation in this report is to demonstrate that the calculated critical flaw size based on 80 years of neutron embrittlement are sufficiently large (i.e., flaw tolerant) as compared to [

]^{a,c,e} A detailed description of the allowable flaw sizes is provided in Section 6.

The critical flaw sizes are calculated based on equating the stress intensity factor to the material specific fracture toughness with consideration of neutron embrittlement. The discussion for stress intensity factors will be provided in Section 5.2, while the determination of fracture toughness values is discussed in Section 5.1.

5.1 FRACTURE TOUGHNESS DETERMINATION

The critical flaw size is determined by equating the applied stress intensity factor to fracture toughness. For pressure vessel steels, it would be appropriate to use the K_{Ic} or K_{IR} fracture toughness curves in ASME Section XI [4] and ASME Section III Appendix G-2000 [11], respectively; however, the RPV support materials (which are high strength materials) are not comparable to the steels which were tested to generate the ASME Section XI and Section III curves (SA-533 Grade B Class 1, SA-508 Class 2, and SA-508 Class 3). Instead of using the ASME K_{Ic} or K_{IR} fracture toughness curves, material specific fracture toughness is used to calculate critical flaw size as described in detail in Section 5.1.1. Briefly stated, [

]^{a,c,e}

5.1.1 Fracture Toughness for the Point Beach Supports

The fracture toughness used to determine the critical flaw size of the RPV support components, as well as the inclusion of embrittlement and strain rate effects is discussed in this section. Each material for the RPV support component is discussed in detail to determine the appropriate fracture toughness value at 72 EFPY and 42 EFPY. The box ring girder also considered irradiated fracture toughness at 60 EFPY. The 42 EFPY and 60 EFPY fracture toughness results are provided to compare the change in fracture toughness due to neutron embrittlement over time and its resulting effect on ductility of the material.

5.1.1.1 U.S. Steels T-1 (Box Ring Girder, I-beam, Shear Key, Base Plate)

The box ring girder, I-beam, shear key and base plate are US steel T-1 material which are specified as ASTM A-514 or A-517 Type F. The T-1 steel plates are quenched and tempered with high yield strength (minimum yield strength is 100 ksi for thickness 2.5" and under or 90 ksi for thickness over 2.5" to 6") per ASTM A-517 [12]; thus, the K_{Ic} and K_{IR} fracture toughness curves in ASME Sections XI and III may not be applicable.

[

]a,c,e

5.1.1.2 ASTM A-53 (Column)

The columns in the RPV support system are made of ASTM A-53 Grade B material, with a minimum yield strength of 35 ksi per ASTM A-53-64 [14]. NUREG-1509 [2] states on page 43, note (1).d, that the minimum fracture toughness values contained in Table 4-3 of [2] may be used if the RPV supports are the same as those listed in Group III in Table 4.6 of NUREG/CR-3009 [22]. Note that A-53 is listed as a Group I (highest susceptibility to brittle fracture) material in Table 4.6 of NUREG/CR-3009. However, the column is in a [

]a,c,e

5.1.1.3 []a,c,e (Support Shoe)

The support shoes which hold the RPV inlet and outlet nozzles and vessel support brackets are [

]a,c,e

[

] ^{a,c,e}**5.1.1.4 [^{a,c,e} (Leveling Screw)**

The leveling screws within the support shoe are [

] ^{a,c,e}**5.1.1.5 ASTM A-490 (Bolts and Pins at Bottom of Column)**

The following components within the RPV support systems are made of A-490 material: the bolts at the shear brace, the bolts at the apex of the box ring girder above the top of the columns, and the pins at the bottom of the columns. [

] ^{a,c,e}

[

]a,c,e

5.1.1.6 Strain Rate Effects

Per the guidance in Section 4.3.3.1 of NUREG-1509 [2] strain rates associated with dynamic loading for earthquake or pipe break scenarios should be addressed (i.e., the rate of load application). Per [

]a,c,e

¹ [

]a,c,e

[

]a.c.e

Table 5-1: Fracture Toughness for Point Beach RPV Support Components

a,c,e





a,c,e



a,c,e

Figure 5-1: [

]a,c,e

[

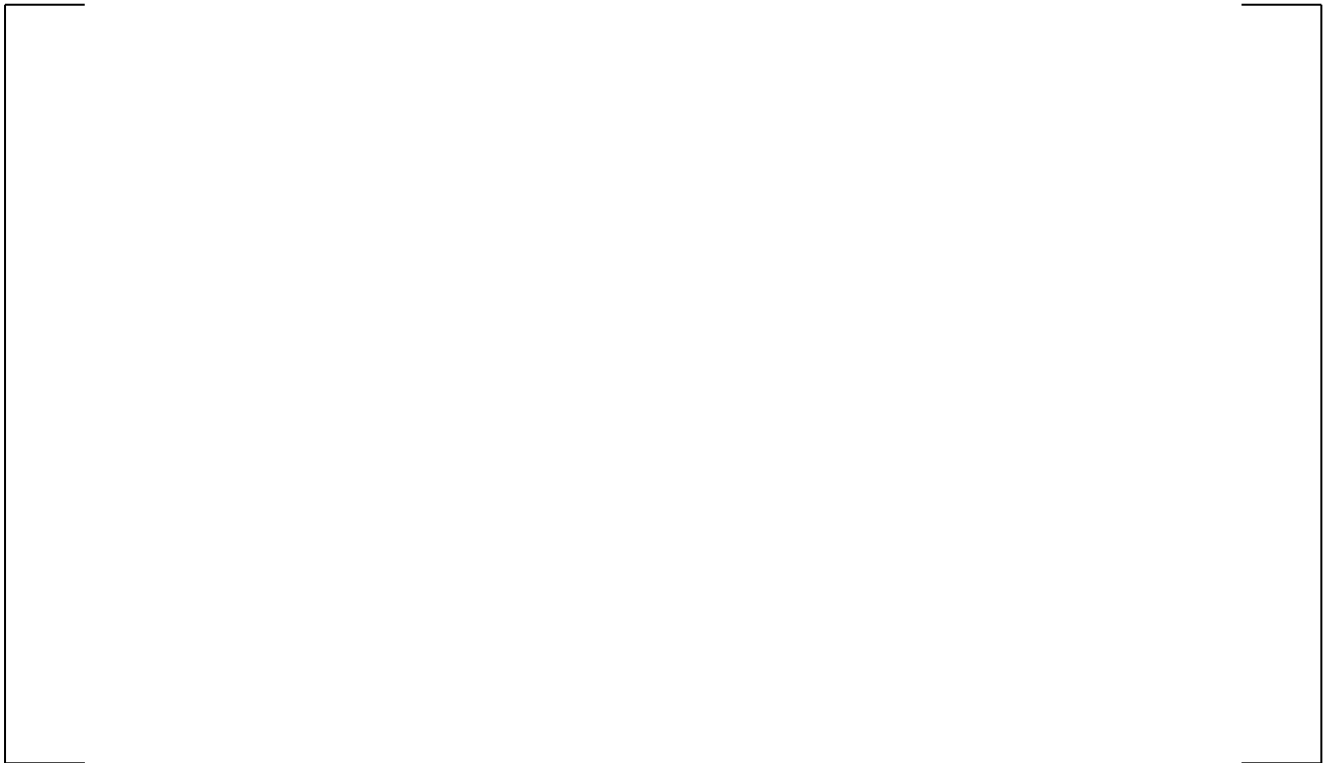
]a,c,e



a,c,e

Figure 5-2.a: [

]a,c,e



a,c,e

Figure 5-2.b: [

]a,c,e



Figure 5-2.c: [

]a,c,e



Figure 5-3: [

]a,c,e



a,c,e

Figure 5-4: [

]a,c,e

5.1.2 Bulk Material Temperature

The containment operating temperature of the supports is used for the RPV support components in lieu of bulk material temperature (T) of the Point Beach reactor vessel support components to determine fracture toughness. As described in PBNWEC-20-0023 [27], the containment operating temperature is not measured. The vertical legs of the supports and the corners of the hexagonal ring-beam support (box ring girder) are exposed to considerable movement of ambient temperature air and are, therefore, close to ambient temperatures (~65°F-100°F). The minimum operating temperature for the Point Beach supports is listed in Table 4.2 of NUREG/CR-3009 [22] to be 85°F.

The reactor cavity has cooling air circulated from below in order to maintain the concrete temperatures at or below the design requirement of [

] ^{a,c,e}

The minimum operating temperature from NUREG/CR-3009 (85°F) is used for components with sufficient margin between critical flaw size and allowable flaw size. When additional margin is required, the operating temperatures are used to determine fracture toughness. [

] ^{a,c,e} The operating temperatures for each component are provided in Table 5-2.

Table 5-2: Operating Temperature for Point Beach Units 1 and 2

	a,c,e
--	-------

5.1.3 Neutron Embrittlement and Nil-Ductility Transition Temperature of RPV Supports

A Westinghouse Owners Group (WOG) (now known as Pressurized Water Reactor Owners Group [PWROG]) program was performed in WCAP-14422 Revision 2-A [28] during the late 1990s and completed in the year 2000 that reassessed the aging effects from neutron embrittlement on the reactor vessel supports for the first license renewal program (60 years). The assessment in WCAP-14422 referenced the extensive industry research and plant specific evaluations performed in NUREG-1509, NUREG/CR-5320 and the resolution of GSI-15 in NUREG-0933 to conclude that aging management is not a concern for the RPV supports for 60 years of plant life operation.

In the final NRC safety evaluation for WCAP-14422, the NRC staff concluded “the staff considers that neutron embrittlement is not a concern for the supports, and does not warrant an aging management program” [28]. The conclusion was based on an evaluation that shows that if all the supports failed, the short span of piping between the vessel and the shield wall would support the load of the vessel. This eliminated the staff’s concern with RPV support embrittlement.

The embrittlement prediction models developed in NUREG/CR-5320 and used in the fracture mechanics analysis of Trojan and Turkey Point, were discussed in Section 2.3 of NUREG-1509. The major issue of the embrittlement curve in NUREG/CR-5320 was that only fast neutron fluence ($E > 1.0$ MeV) was considered to cause embrittlement damage. Sections 2 and 3 of NUREG-1509 concluded that low-energy neutron irradiation (below 1 MeV) could potentially make a significant contribution to the observed embrittlement. Therefore, the guidance provided in NUREG-0933 GSI-15 resolution is to utilize Figure 3-1 of NUREG-1509 (reproduced herein as Figure 5-5) to calculate the change in nil-ductility transition temperature (Δ NDTT) based on dpa for the energy spectrum $E > 0.1$ MeV.

[

^{a,c,e} The Point Beach RPV supports evaluation in this report conservatively considers iron dpa from all energy levels – the iron dpa values include contributions of fast neutrons above 0.1 MeV as well as thermal neutrons below 0.1 MeV.

The impact of neutron embrittlement (radiation effects) on the Point Beach Units 1 and 2 RPV supports was determined for 42 EFPY, 60 EFPY and 72 EFPY (80 calendar years of operation). The neutron embrittlement is defined as a function of iron displacement per atom (dpa) consistent with Figure 3-1 of

NUREG-1509 (reproduced herein as Figure 5-5) to determine change in nil-ductility transition temperature (Δ NDTT). The neutron transport methodology used to generate the iron dpa data followed the guidance of NRC Regulatory Guide 1.190 [29], and was consistent with the NRC approved methodology described in WCAP-18124-NP-A [30]. Although this methodology has not been approved by the NRC for the RPV supports, the methodology has been generically approved for calculations of exposure of the RPV beltline (generally, RPV materials opposite the active fuel). The following paragraphs describe the neutron transport methodology for Point Beach Units 1 and 2.

[

]a.c.e

[

]a,c,e

Maximum projected exposures, in terms of iron dpa, of the RPV support structures at 42, 60, and 72 EFPY are provided in Table 5-3 for Point Beach Unit 1 and in Table 5-4 for Point Beach Unit 2. Neutron embrittlement is conservatively based on iron dpa from all energy levels – the iron dpa values include contributions of fast neutrons above 0.1 MeV as well as thermal neutrons below 0.1 MeV. The iron dpa projections beyond the most recent fuel cycles were calculated using a conservative 10% bias on power in peripheral fuel assemblies (i.e., for future operation, the assemblies are modeled as producing 10% more power than the cycles used for projections - Cycle 37 for Point Beach Unit 1 and Cycle 38 for Point Beach Unit 2).

The iron dpa values that were used to determine Δ NDTT at 42, 60 and 72 EFPY are provided in Table 5-5 and bound Point Beach Units 1 and 2. The resulting Δ NDTT calculated based on Figure 3-1 of NUREG-1509 (reproduced herein as Figure 5-5) using the upper bound curve is also provided in Table 5-5. The applicable Δ NDTT value for each component is provided in Table 5-6.

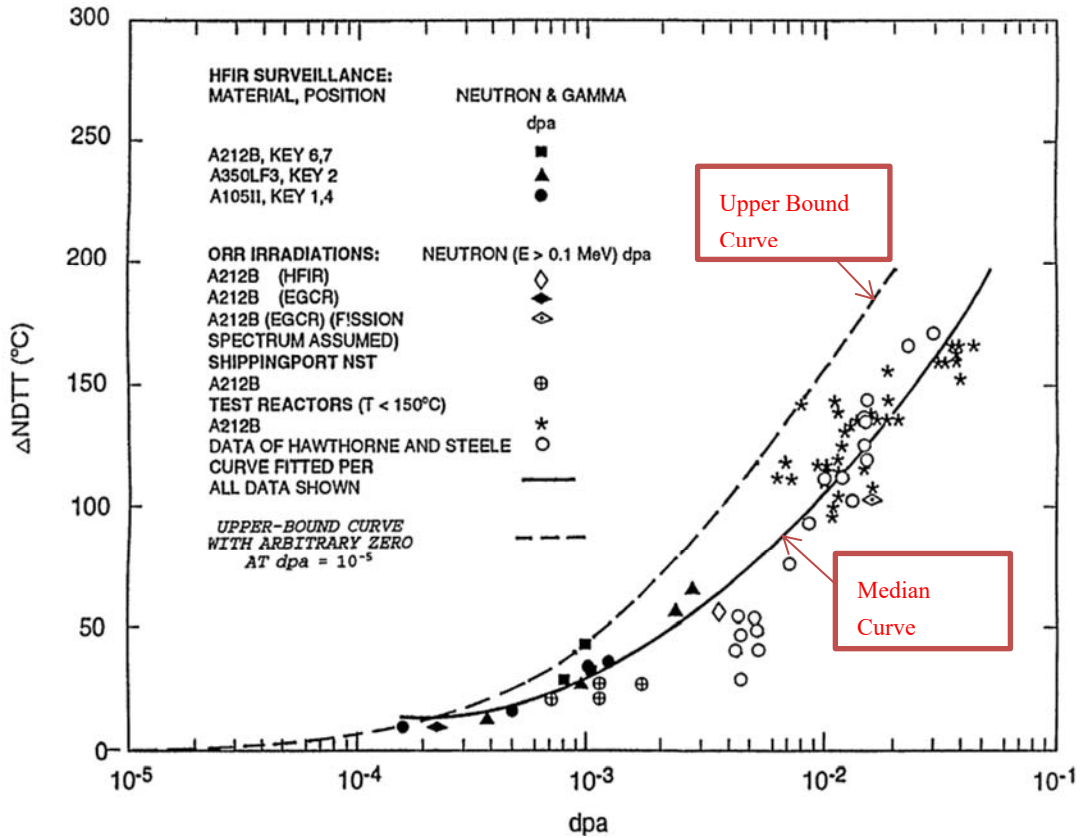


Figure 5-5: Change in Nil-Ductility Transition Temperature, ΔNDTT as a Function of dpa [Figure 3-1 of 2]



Figure 5-6: Top View of RAPTOR-M3G Model, Core Midplane ($Z = 0$ cm)

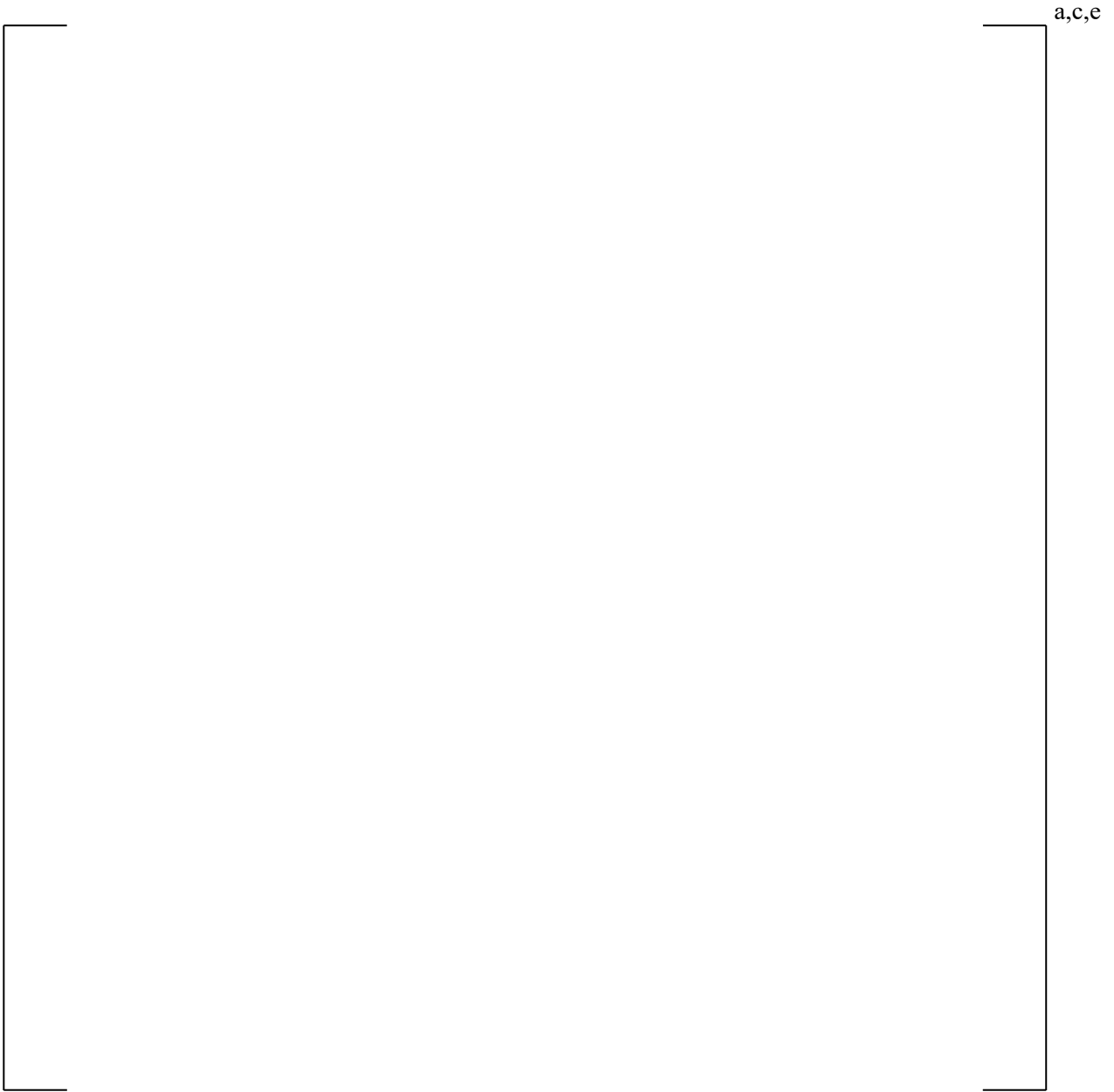


Figure 5-7: Side View of RAPTOR-M3G Model, through Support Column ($\theta = 0^\circ$)

a,c,e

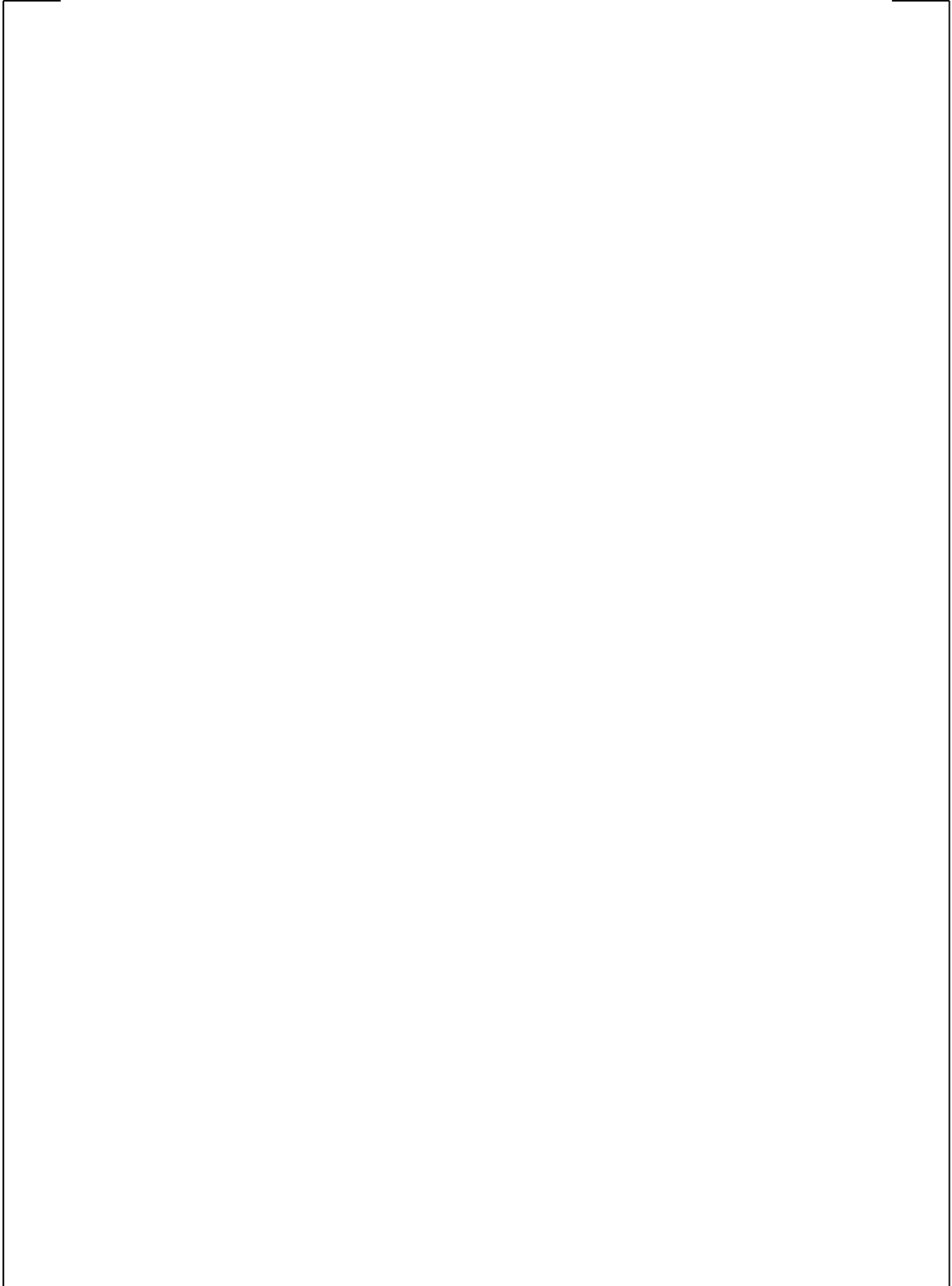


Figure 5-8: Side View of Iron Displacement per Atom at 72 EFPY ($\theta = 0^\circ$)

Table 5-3: Point Beach Unit 1 Maximum Iron Atom Displacement at RPV Support Components

<i>Projection with 10% bias on peripheral fuel assemblies</i>			
Location	Displacements (dpa) ^(a)		
	42 EFPY	60 EFPY	72 EFPY
Support Column 1 – maximum	3.09E-03	4.69E-03	5.76E-03
Support Column 1 – top of support foot	1.37E-05	2.07E-05	2.53E-05
Support Column 1 – bottom of column	1.17E-05	1.75E-05	2.14E-05
Support Column 2 – maximum	3.13E-04	4.58E-04	5.54E-04
Support Column 2 – top of support foot	1.39E-05	2.09E-05	2.56E-05
Support Column 2 – bottom of column	1.26E-05	1.91E-05	2.34E-05
Ring Girder – inside bottom edge	1.76E-03	2.63E-03	3.21E-03
Ring Girder – inside top edge	6.10E-04	9.08E-04	1.11E-03
Ring Girder – outside bottom edge	6.01E-04	9.04E-04	1.11E-03
Ring Girder – outside top edge	1.83E-04	2.72E-04	3.31E-04

Note:

- (a) Neutron embrittlement is conservatively based on dpa from all energy levels, it includes contributions of fast neutrons above 0.1 MeV as well as thermal neutrons below 0.1 MeV.

Table 5-4: Point Beach Unit 2 Maximum Iron Atom Displacement at RPV Support Components

<i>Projection with 10% bias on peripheral fuel assemblies</i>			
Location	Displacements (dpa) ^(a)		
	42 EFPY	60 EFPY	72 EFPY
Support Column 1 – maximum	3.04E-03	4.72E-03	5.84E-03
Support Column 1 – top of support foot	1.48E-05	2.21E-05	2.70E-05
Support Column 1 – bottom of column	1.25E-05	1.86E-05	2.27E-05
Support Column 2 – maximum	3.16E-04	4.68E-04	5.69E-04
Support Column 2 – top of support foot	1.50E-05	2.24E-05	2.74E-05
Support Column 2 – bottom of column	1.37E-05	2.05E-05	2.51E-05
Ring Girder – inside bottom edge	1.83E-03	2.74E-03	3.35E-03
Ring Girder – inside top edge	6.27E-04	9.38E-04	1.15E-03
Ring Girder – outside bottom edge	6.15E-04	9.33E-04	1.14E-03
Ring Girder – outside top edge	1.88E-04	2.81E-04	3.43E-04

Note:

- (a) Neutron embrittlement is conservatively based on dpa from all energy levels, it includes contributions of fast neutrons above 0.1 MeV as well as thermal neutrons below 0.1 MeV.

**Table 5-5: Iron Displacement per Atom and Corresponding Δ NDTT at RPV Support Components
Bounds Point Beach Units 1 and 2**

Item ^(a)	Location	42 EFY			60 EFY			72 EFY		
		Displacements (dpa)	Upper Bound Curve Δ NDTT		Displacements (dpa)	Upper Bound Curve Δ NDTT		Displacements (dpa)	Upper Bound Curve Δ NDTT	
1	Support Column 1 – maximum	3.09E-03	164.27°F	91.26°C	4.72E-03	200.81°F	111.56°C	5.84E-03	223.70°F	124.28°C
2	Support Column 1 – top of support foot	1.48E-05	12.60°F	7.00°C	2.21E-05	12.60°F	7.00°C	2.70E-05	12.60°F	7.00°C
3	Support Column 1 – bottom of column	1.25E-05	12.60°F	7.00°C	1.86E-05	12.60°F	7.00°C	2.27E-05	12.60°F	7.00°C
4	Support Column 2 – maximum	3.16E-04	31.50°F	17.50°C	4.68E-04	43.34°F	24.08°C	5.69E-04	52.38°F	29.10°C
5	Support Column 2 – top of support foot	1.50E-05	12.60°F	7.00°C	2.24E-05	12.60°F	7.00°C	2.74E-05	12.60°F	7.00°C
6	Support Column 2 – bottom of column	1.37E-05	12.60°F	7.00°C	2.05E-05	12.60°F	7.00°C	2.51E-05	12.60°F	7.00°C
7	Ring Girder – inside bottom edge	1.83E-03	119.92°F	66.62°C	2.74E-03	154.44°F	85.80°C	3.35E-03	172.33°F	95.74°C
8	Ring Girder – inside top edge	6.27E-04	56.21°F	31.23°C	9.38E-04	75.89°F	42.16°C	1.15E-03	87.62°F	48.68°C
9	Ring Girder – outside bottom edge	6.15E-04	55.40°F	30.78°C	9.33E-04	75.60°F	42.00°C	1.14E-03	87.16°F	48.42°C
10	Ring Girder – outside top edge	1.88E-04	21.81°F	12.12°C	2.81E-04	30.24°F	16.80°C	3.43E-04	31.50°F	17.50°C

Note:

(a) The location of the dpa values are provided in Figure 5-9 via the item number.

Table 5-6: Applicable Item Number for each Support Component and Corresponding Neutron Embrittlement Shift, Δ NDTT

Component	Item	Upper Bound Curve ΔNDTT, °F at 72 EFPY	Upper Bound Curve ΔNDTT, °F at 42 EFPY
Column	Maximum of 1 and 4	223.70	164.27
Box Ring Girder	Maximum of 7, 8, 9, and 10	172.33	119.92
Bolts at Box Ring Girder ^(a)	Maximum of 7, 8, 9 and 10	172.33	119.92
Shear Brace (I-Beam and Key Shear)	Maximum of 9 and 10	87.16	55.40
Support Shoe	Maximum of 8 and 10	87.62	56.21
Leveling Screw	Maximum of 8 and 10	87.62	56.21
Bolts at Shear Brace	Maximum of 9 and 10	87.16	55.40
Pins at Bottom of Column	Maximum of 2 and 5	12.60	12.60
Base plate	Maximum of 2 and 5	12.60	12.60

Note:

- (a) There is an additional analysis completed for the box ring girder component with neutron embrittlement effects at 60 EFPY. The resulting Δ NDTT for 60 EFPY is based on the maximum of Items 7 through 10 to be 154.44°F.

a,c,e



Figure 5-9: Location of dpa Values within Support System

Note the numbers in red boxes are 'Item' numbers which represent the location of the dpa values in Table 5-5 and Table 5-6.

5.2 STRESS INTENSITY FACTORS AND POSTULATED FLAWS

A wide range of stress intensity factor (SIF) methodologies were considered in the analysis of linear elastic fracture mechanics to account for the support geometry (bolt, cylinder and flat plate models) and also for different loading types (tensile stresses, stresses due to bending moment, and shear stresses) and for flaw shapes (edge flaw, semi-elliptical flaw, continuous flaw and corner flaw). The prevalent crack-opening stress components are the stresses normal to the face of the flaws; however, shear stresses are also present in the supports. [

$K_{I,c,e}$ are then used to calculate the Mode I stress intensity factors, which can be equated to the fracture toughness of the material to back-calculate the critical flaw sizes (discussed in Section 7). Stress intensity factors for Mode II and Mode III crack opening, also denoted as K_{II} and K_{III} , respectively, are considered for the shear key component where the main load is based on shear stress. A general description of the SIF methodologies is provided in Table 5-7 for each of the ten RPV support components and the following sections provide more detail for each stress intensity factor correlations.

The crack tip stress intensity factors are determined based on the stress intensity factor expressions from API-579 2016 Edition [10], Raju/Newman/NASA database [31], and Tada [32]. The stress intensity factor databases are industry accepted solutions and have been used frequently for previous fracture mechanics projects. [

$K_{I,c,e}$

A variety of flaw shapes are considered in the fracture mechanics analysis based on the three previously mentioned SIF databases to provide a parametric study of critical flaw sizes within each of the RPV support components. The flaw shapes which are appropriate for the various support geometry (bolt, cylinder, flat plate models) are described in Table 5-7. These flaw shapes include infinitely long edge flaws in plates, semi-elliptical flaws with aspect ratio (AR, flaw length/flaw depth) of 2, 6 and 10 (AR of 10 is used for base plate component), and corner flaws as discussed in Section 5.2.2. Corner flaws are analyzed for historical comparison with the RPV supports in NUREG/CR-5320, which included this type of flaw. Note the semi-elliptical flaws in the box flange and I-beam are subjected to welding residual stress as described in Section 4. The cylindrical column is conservatively analyzed with a 360° continuous circumferential inside and outside surface flaw as discussed in Section 5.2.1. The bar shaped components are analyzed with a 360° continuous circumferential, straight front and semi-circular front flaw shapes as discussed in Section 5.2.3.

5.2.1 Cylinder Model (for Columns)

A variety of circumferential flaws, ranging in size from an aspect ratio of 2 to continuous, on the inside and outside surface of the cylindrical columns can be postulated to determine critical flaw size. The driving force to cause Mode I crack opening in axial flaws is hoop stress which is not present in the column; thus, axial flaws are not analyzed. The 360° continuous circumferential flaw stress intensity factor model will bound a smaller semi-elliptical flaw; thus, only 360° continuous circumferential flaw on the inside and outside diameter of the column is analyzed (see Figure 5-10 for a graphical representation of the flaws).

The stress provided in Section 4.1 for the column is conservatively applied as constant through-the-wall thickness (i.e., as a pure membrane stress). The loads on the column are shown in Figure 4-2. The stress intensity factor correlations for the 360° continuous circumferential flaw in a cylinder is provided in API-579 [10] Section 9B.5.8 as follows:

$$K_I = G_0 \sigma_m \sqrt{\pi a}$$

Where:

K_I = stress intensity factor (ksi-in^{0.5})

G_0 = factor to account for aspect ratio, geometry, and flaw location

σ_m = membrane stress (ksi)

a = flaw depth or size (in.)

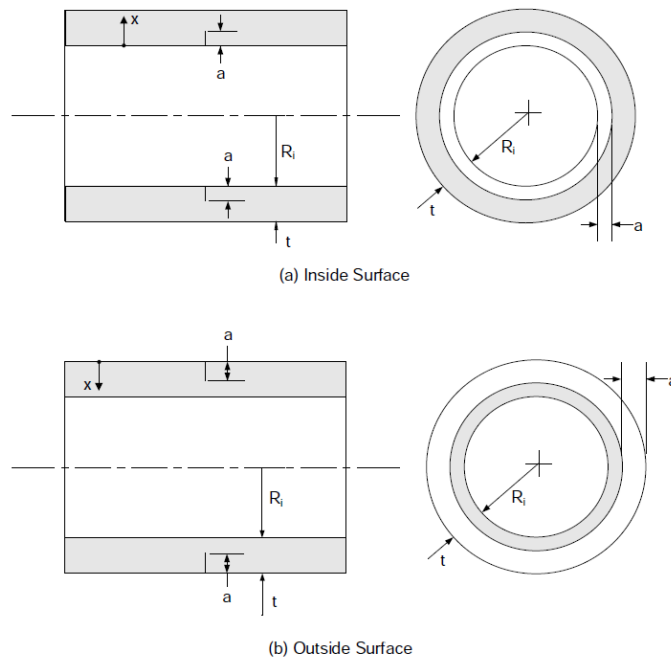


Figure 5-10: Cylinder Model – 360° Continuous Circumferential Flaw on Inside and Outside Surface

5.2.2 Plate Model (for Box Ring Girder, I-beam, Support Shoe Box, Base Plate, and Key Shear)

The box ring girder, I-beam, support shoe box, base plate and key shear can all be modeled as a flat plate (see discussion at the end of this section for key shear). The first postulated flaw case in the flat plate model is a semi-elliptical flaw with an aspect ratio (flaw length / flaw depth) of 2 and 6 for the box ring girder and I-beam as a parametric study of critical flaw sizes. The base plate conservatively considers a larger aspect ratio of 10. See Figure 5-11.a for a graphical representation of a semi-elliptical flaw in a plate model.

The stress provided in Section 4.2, Section 4.3 and Section 4.10 for the box ring girder, I-beam and base plate is conservatively applied as constant through-the-wall thickness (i.e., as a pure membrane stress). The loads on the box ring girder, I-beam and base plate are shown in Figure 4-3, Figure 4-4, and Figure 4-11, respectively. Note that the box ring girder and I-beam semi-elliptical flaws included welding residual stress since the flaws are postulated near the welds of the components. The stress intensity factor correlation for the semi-elliptical flaw with pure membrane stress is provided in API-579 [10] Section 9B.3.4 as follows:

$$K_I = M_m \sigma_m \sqrt{\frac{\pi a}{Q}}$$

Where:

K_I = stress intensity factor (ksi-in^{0.5})

M_m = factor to account for flaw size, aspect ratio, and geometry

σ_m = membrane stress (ksi)

a = flaw depth or size (in.)

$Q = 1 + 1.464(a/c)^{1.65}$ for $a/c < 1$

The box ring girder, I-beam, and support shoe also considered an infinitely long 'top edge' flaw and 'side edge' flaw on the various plates within the components (flange and web components of the box ring girder and I-beam); see Figure 4-3 as an example of top edge and side edge flaws. Note that the box ring girder and I-beam infinitely long edge flaws do not include welding residual stress since all or a majority of the postulated flaw is outside of the weld. See Figure 5-11.b for a graphical representation of an infinitely long edge flaw in a plate model.

The stress provided in Section 4.2, Section 4.3 and Section 4.8 for the box ring girder, I-beam and support shoe is conservatively applied as constant through-the-wall thickness (i.e., as a pure membrane stress). The loads on the box ring girder, I-beam and support shoe are shown in Figure 4-3, Figure 4-4, and Figure 4-9, respectively. The stress intensity factor for the infinitely long edge flaw in a plate with pure membrane stress is provided in API-579 [10] Section 9B.3.2 as follows:

$$K_I = G_o \sigma_o \sqrt{\pi a}$$

Where:

K_I = stress intensity factor (ksi-in^{0.5})

G_o = influence coefficient to account for flaw size and geometry

σ_o = membrane stress (ksi)

a = flaw depth or size (in.)

The box ring girder and I-beam component also consider a quarter circular corner flaw in a flat plate model for historical comparison with the RPV supports in NUREG/CR-5320, which included this type of flaw (see Figure 5-11.c for a graphical representation of corner flaw in a plate model). The stress intensity factor for the corner crack is based on Raju/Newman/NASA [31], and is correlated as follows:

$$K_I = S_t F_c \sqrt{\frac{\pi a}{Q}}$$

Where:

K_I = stress intensity factor (ksi-in^{0.5})

F_c = influence coefficient to account for flaw size and geometry

S_t = uniform tension stresses (membrane) (ksi)

a = flaw depth or size (in.)

$Q = 1 + 1.464(a/c)^{1.65}$ for $a/c \leq 1$, for the analysis herein $a = c$, therefore $Q = 2.464$

The support shoe component also considers a through-wall double edge crack in a plate model with a hole (see Figure 5-12) to account for the holes in the support shoe for the leveling screws. The stress intensity factor was based on the correlation in API-579 [10] Section 9B.4.2 and is correlated as follows:

$$K_I = M_m \sigma_m \sqrt{\pi c}$$

Where:

K_I = stress intensity factor (ksi-in^{0.5})

M_m = influence coefficient to account for flaw size and geometry

σ_m = membrane stress (ksi)

c = flaw depth or size (in.)

The key shear component is considered as a plate model; however, the stress is defined as a shear stress which causes Mode II and Mode III stress intensity factor (see Figure 5-13 for a graphical representation of an edge flaw in a plate model). The shear load on the key shear is shown in Figure 4-6. The Mode II and Mode III stress intensity factor is based on the correlation in Section 2.31 of Tada [32] as follows:

$$K_{II} = F_{II(a/b)} \tau \sqrt{\pi a}$$

$$K_{III} = F_{III(a/b)} \tau_l \sqrt{\pi a}$$

Where:

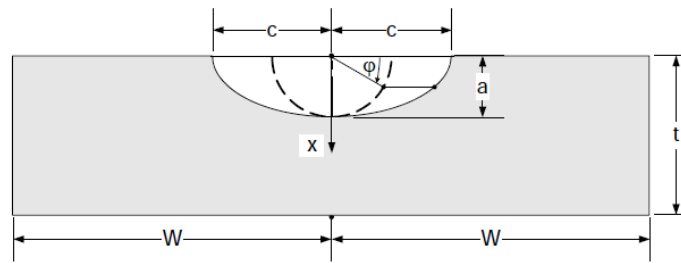
K_{II} and K_{III} = Mode II and Mode III stress intensity factor (ksi-in^{0.5})

$F_{II(a/b)}$ and $F_{III(a/b)}$ = influence coefficient to account for flaw size (a) and geometry (thickness)

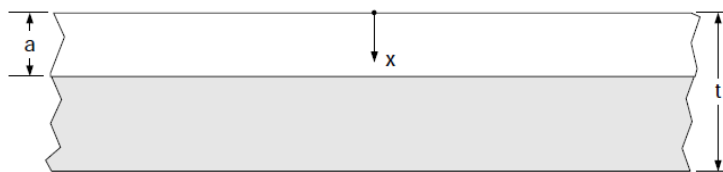
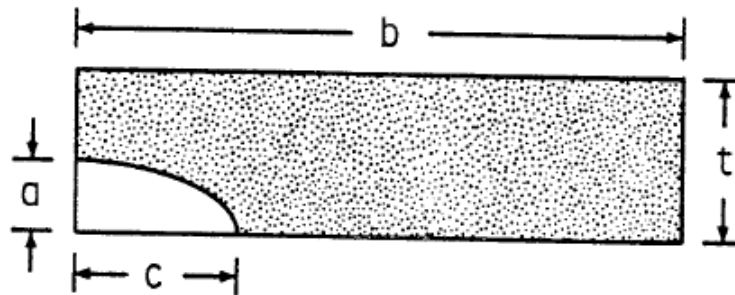
τ and τ_l = shear stress (ksi)

a = flaw depth or size (in.)

b = thickness of component (in.)



(a) Finite Length Surface Crack

(b) Infinitely Long Surface Crack ($c \gg a$)

(c) Corner crack

Figure 5-11: Postulated Surface Flaw in a Plate Model

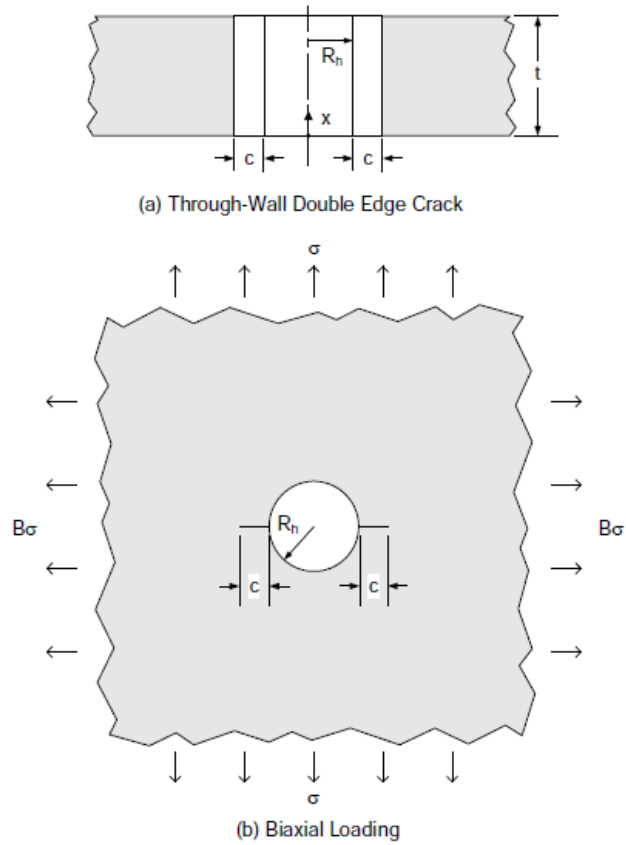


Figure 5-12: Postulated Through-Wall Double Edge Flaw in Plate with Hole Model

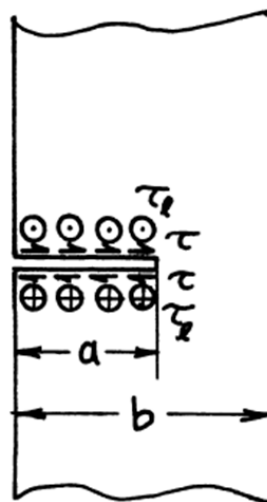


Figure 5-13: Postulated Edge Flaw with Shear Stress in a Plate Model

5.2.3 Round Bar Model (for Bolts, Leveling Screw and Pin)

The leveling screws, bolts at the shear brace, and bolts at the column to box ring girder connection were conservatively assumed to have completely 360° circumferential flaws oriented perpendicular to the bolt centerlines and therefore responsive to bolt tensile loading. In addition, the straight front and semi-circular crack models are postulated as a parametric study and for less limiting critical flaw size results. See Figure 5-14 for a graphical representation of the three flaw types in a bar model.

The axial force, shear stress, and moments on the bar components are provided in Section 4.4, Section 4.6 and Section 4.9 for the bolt at the shear brace, bolt and the ring girder, and leveling screw, respectively. The loads on the bolt at the shear brace, bolt and the ring girder, and leveling screw are provided in Figure 4-5, Figure 4-7, and Figure 4-10, respectively. The stress intensity factor for the bolts are based on API-579 [10] Sections 9B.11.1, 9B.11.2, and 9B.11.3 for round bar, surface circumferential crack - 360°, straight front crack, and semi-circular front crack, respectively with through-wall membrane stress as follows:

$$K_I = M_m \sigma_m \sqrt{\pi a}$$

Where:

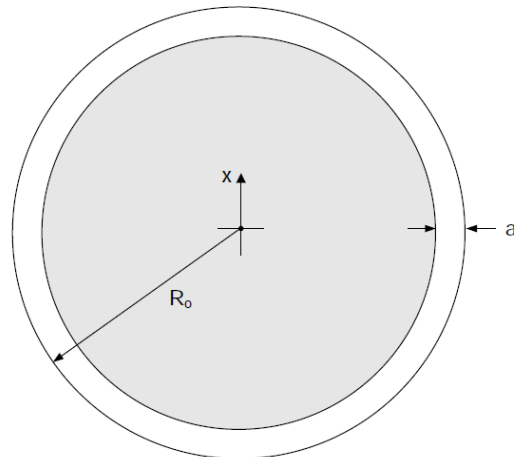
- K_I = stress intensity factor (ksi-in^{0.5})
- M_m = influence factor to account for flaw size and geometry
- σ_m = membrane stress (ksi)
- a = flaw depth or size (in.)

The pins at the bottom of the columns are constricted as a three point bending specimen, thereby causing the large force acting in the middle of the pin to cause high bending stress to open a flaw on the bottom of the pin (see Figure 5-15 for a graphical representation of the edge flaw in the pin). The forces and moments on the pin are provided in Section 4.7 and the loads are shown in Figure 4-8. The stress intensity factor for an edge flaw in a pin is based on Section 2.16 in Tada [32] as follows:

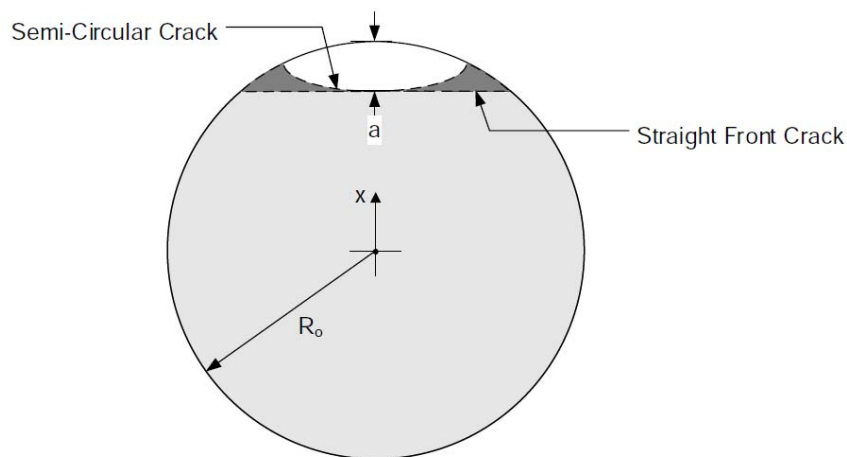
$$K_I = F_{a/b} \sigma \sqrt{\pi a}$$

Where:

- K_I = stress intensity factor (ksi-in^{0.5})
- $F_{a/b}$ = influence factor to account for flaw size and geometry
- σ = membrane stress (ksi)
- a = flaw depth or size (in.)



(a). 360° Continuous Surface Flaw



(b). Straight Front and Semi-Circular Surface Crack

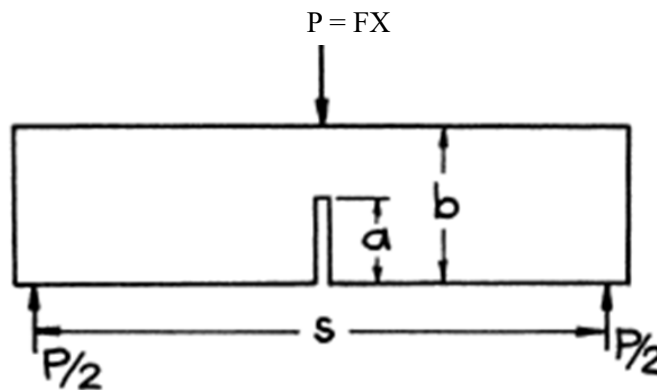
Figure 5-14: Postulated Flaws in a Round Bar Model**Figure 5-15: Postulated Edge Flaw in a Three Point Bending Model**

Table 5-7: Mode I, II and Mode III Stress Intensity Factor Description

Component	Model Shape	Flaw Configuration	SIF Reference and Section No.	Figure of Postulated Flaw Shape
Column	Cylinder Mode I SIF	360° Continuous Circumferential on Inside and Outside Surface	API-579 Section 9B.5.8 [10]	Figure 5-10
Box Ring Girder I-beam (in Shear Brace) Support Shoe Box Base Plate	Plate Mode I SIF	Semi-Elliptical	API-579 Section 9B.3.4 [10]	Figure 5-11
		Infinite	API-579 Section 9B.3.2 [10]	
		Corner	Raju/Newman/NASA (1984) [31]	
	Plate with Hole ^(a) Mode I SIF	Through-Wall Double Edge Crack	API-579 Section 9B.4.2 [10]	Figure 5-12
Key Shear (in Shear Brace)	Plate Mode II and III SIF	Edge Crack	Tada Part 2.31 Section A [32]	Figure 5-13
Leveling Screw Bolts (at Shear Brace) Bolts (at Column to Box Ring Girder)	Bar Mode I SIF	360° Continuous Circumferential	API-579 Section 9B.11.1 [10]	Figure 5-14
		Straight Front	API-579 Section 9B.11.2 [10]	
		Semi-Circular Front	API-579 Section 9B.11.3 [10]	
Pins (at Bottom of Column)	Rectangular Bar Mode I SIF	Edge Crack	Tada Part 2.16 Section A [32] ^(b)	Figure 5-15

Notes:

(a) [

(b)

]a,c,e

6 ALLOWABLE FLAW SIZES

The goal of the fracture mechanics analysis is to demonstrate that the calculated critical flaw sizes based on 80 years of neutron embrittlement are sufficiently large as compared to [

]a,c,e

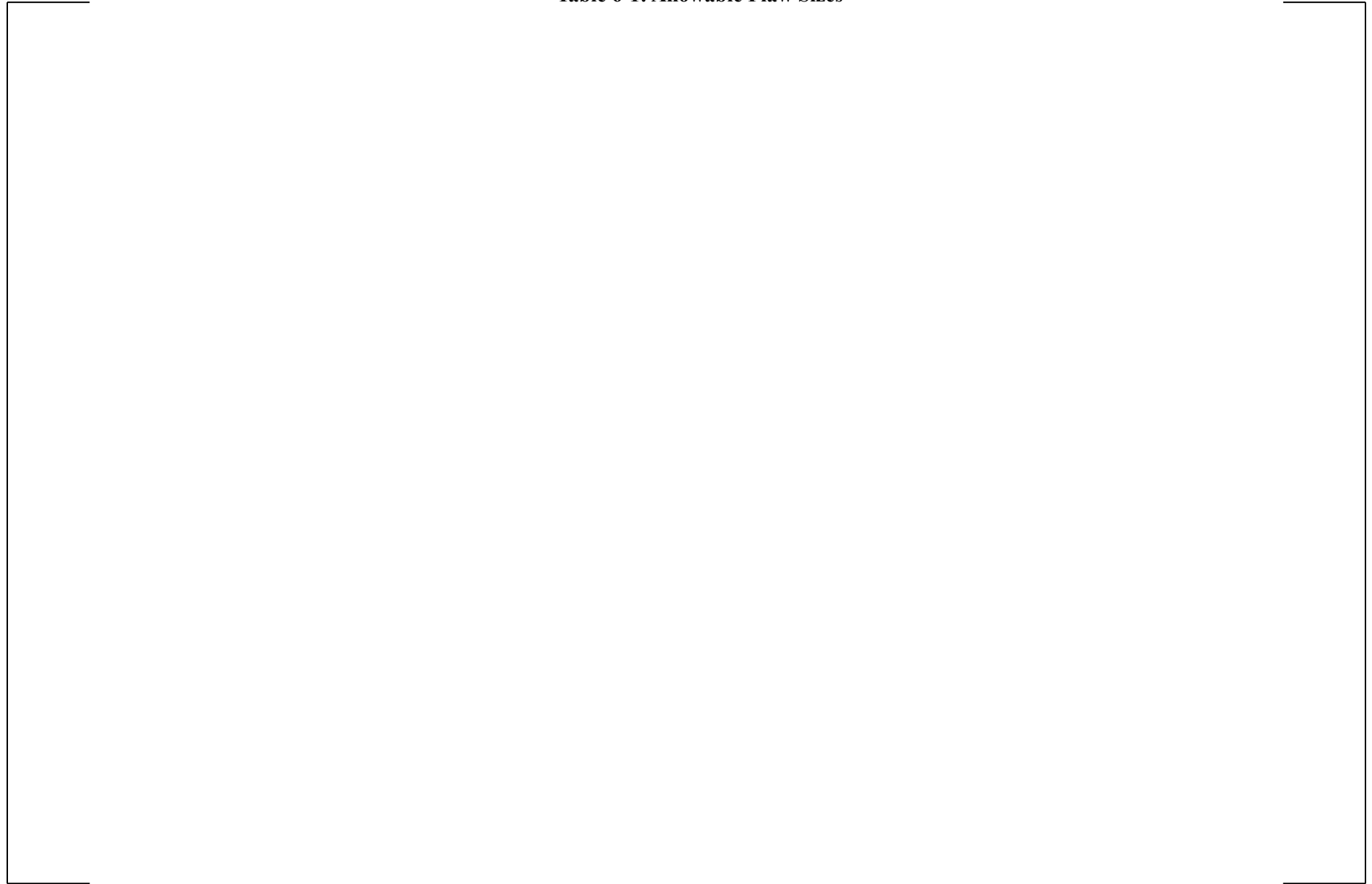
[

] ^{a,c,e}

The allowable flaw sizes in Table 6-1 are compared against the calculated critical flaw sizes in Section 7 to demonstrate that the Point Beach Units 1 and 2 RPV supports are flaw tolerant for 80 years of service (i.e., that a large flaw size is required to fail the support system).

Table 6-1: Allowable Flaw Sizes

a,c,e



a,c,e





Figure 6-1: [

] a,c,e

7 CRITICAL FLAW SIZE CALCULATION RESULTS

As discussed in several previous sections of this report, the goal of the fracture mechanics analysis for Point Beach Units 1 and 2 RPV supports is to justify that plant life extension to 80 years does not cause a structural integrity concern based on radiation embrittlement. One technique to demonstrate continued operability of the RPV supports past 60 years is to compare the critical flaw sizes calculated in the analysis herein to [

] ^{a,c,e} These previously mentioned allowable flaw sizes are described in detail in Section 6 of this report.

Per Section 4.2.4 of NUREG-1509 if the following criteria are met, the supports would demonstrate safe operation with consideration of neutron radiation embrittlement:

1. The initial nil-ductility transition temperature of the RPV supports is well below the minimum operating temperature.
2. The radiation exposure at the supports is low.
3. The peak tensile stresses are 6 ksi, or less.

The component specific evaluation considering the three criteria above is provided in the following sections; if these criteria are not met, a fracture mechanics evaluation is completed. Note that for Point Beach RPV structural steel components which meet the three criteria, a fracture mechanics evaluation is still completed for a conservative defense in depth basis.

This section provides the critical flaw sizes for each of the ten components based on latest plant specific stresses, welding residual stress, operating conditions temperatures, neutron embrittlement for 42 EFPY and 72 EFPY of operation, shift in NDTT based on Figure 3-1 of NUREG-1509 (reproduced as Figure 5-5 herein), and latest stress intensity factors used in the industry. [

] ^{a,c,e} The Δ NDTT based on the neutron embrittlement at 42 and 72 EFPY is calculated in Table 5-6 for various locations around the Point Beach RPV supports. The Δ NDTT for each component is conservative based on a representative location to account for embrittlement effects.

It should be noted that the RPV supports experience various loading conditions (normal, upset, faulted-1 and faulted-2) as discussed in Section 4. [

]a,c,e

[

]a,c,e

Furthermore, many components in the fracture mechanics analysis have large margin between the allowable flaw size and the critical flaw size (see Section 7.1 through Section 7.10).

7.1 COLUMNS

There are six columns which support the box ring girder (see Figure 3-4). The maximum embrittlement in the column is applied to the columns, resulting in fracture toughness values of 23 ksi√in and 24 ksi√in for 72 EFPY and 42 EFPY, respectively (see Table 5-1). The axial stress in the columns is highly compressive (see Table 4-1), causing the [

] ^{a,c,e} Since the tensile stress is small, there would be large margin between fracture toughness and applied stress intensity factor and no further investigation should be required. Although the column is subjected to the highest impact of embrittlement, neutron embrittlement is not a concern due to the low tensile stress and the change in fracture toughness from 42 EFPY to 72 EFPY is also small. [

] ^{a,c,e}

However, a conservative study is completed in which the compressive axial stress is removed and the critical flaw sizes are determined for a postulated 360° continuous circumferential flaw, which bounds the results for a semi-elliptical flaw. The resulting 360° continuous circumferential critical flaw sizes are shown in Table 7-1 for 72 and 42 EFPY. Axial flaws are not required to be analyzed since hoop stress is not present. The calculated critical flaw sizes for this conservative case are larger than the [

] ^{a,c,e} thus, the columns continue to be structurally stable considering 80 years of radiation embrittlement effects on the supports.

As shown in Table 7-1, the change in embrittlement from 42 to 72 EFPY results in critical flaw sizes that varies on average by 1% to 2%. Thus, it is determined that the effect of the change in embrittlement over time is minor on the critical flaw sizes.

Table 7-1: Summary of Column Critical Flaw Size for 72 EFPY

Component	Fracture Toughness	Loading Condition	Critical Flaw Size (a/t), % ^(a)	
			360° Continuous Circumferential on Inside Surface	360° Continuous Circumferential on Outside Surface
Column	$K_{Ic} = 23 \text{ ksi}\sqrt{\text{in}}$ for 72 EFPY	Normal	64.2	59.6
		Upset	67.8	62.9
		Faulted-1	61.9	57.0
		Faulted-2	48.0	44.4
	$K_{Ic} = 24 \text{ ksi}\sqrt{\text{in}}$ for 42 EFPY	Normal	66.2	61.4
		Upset	70.0	64.7
		Faulted-1	63.8	59.2
		Faulted-2	50.1	46.2
Section XI Allowable Flaw Size			3.1	3.1

Note:

- (a) The critical flaw sizes are determined by setting applied stress intensity factor equal to fracture toughness and back-calculating flaw size. Cylinder thickness = 1".

7.2 BOX RING GIRDER

The box ring girder is located under the support shoe which supports the RPV inlet/outlet nozzles and brackets (see Figure 3-4). A portion of the ring girder is subjected to high embrittlement (inside bottom edge per Table 5-5), resulting in a fracture toughness value of 57 ksi√in at 72 EFPY, 62 ksi√in at 60 EFPY and 72 ksi√in at 42 EFPY, respectively (see Table 5-1).

In addition to the applied stresses on the ring girder (see Table 4-2), welding residual stress is considered for the postulated semi-elliptical flaw in the web and flange per Section 4 of this report. There was insufficient information to demonstrate that the box ring girder was post weld heat treated; thus, [$J^{a,c,e}$] was added to the applied stresses which resulted in small critical flaw sizes for the semi-elliptical flaw in the web and flange which are postulated near the welds.

Various postulated flaw shapes in a plate model were analyzed, including a study of semi-elliptical flaws with aspect ratio (flaw length over flaw depth) of 6 and 2, infinite length flaws in the web and flange and a corner flaw in the flange. The calculated critical flaw sizes are shown in Table 7-2 for the previously mentioned postulated flaw shapes, as well as the [

] $J^{a,c,e}$

As shown in Table 7-2, the change in embrittlement from 42, 60 and 72 EFPY results in critical flaw sizes that varies on average by 1% to 2% for the limiting semi-elliptical flaw shapes. Thus, it is determined that the effect of the change in embrittlement over time is minor on the critical flaw sizes. Based on the conclusions described in the previous paragraphs, the box ring girders continue to be structurally stable considering 80 years of radiation embrittlement effects on the supports.

Table 7-2: Summary of Box Ring Girder Critical Flaw Size

Component	Fracture Toughness	Loading Condition	Critical Flaw Size (a/t), % ^(a)							
			Semi-Elliptical Web (AR = 6) ^(b)	Semi-Elliptical Web (AR = 2) ^(b)	Semi-Elliptical Flange (AR = 6) ^(b)	Semi-Elliptical Flange (AR = 2) ^(b)	Top Edge Flange	Side Edge Web	Side Edge Flange	Corner Flange
Box Ring Girder	$K_{Ic} = 57 \text{ ksi}\sqrt{\text{in}}$ for 72 EFPY	Normal	3.9	8.8	2.2	5.1	27.0	35.7	10.7	67.3
		Upset	4.1	9.1	2.4	5.3	30.5	38.5	13.1	76.0
		Faulted-1	3.8	8.4	2.2	4.9	25.0	32.9	9.3	62.0
		Faulted-2	3.4	7.5	1.9	4.3	18.6	26.0	5.8	45.4
	$K_{Ic} = 62 \text{ ksi}\sqrt{\text{in}}$ for 60 EFPY	Normal	4.6	10.4	2.7	6.0	29.1	37.9	12.2	72.9
		Upset	4.8	10.7	2.8	6.3	32.7	40.7	14.8	81.7
		Faulted-1	4.5	10.0	2.6	5.8	27.1	35.1	10.7	67.5
		Faulted-2	4.0	8.9	2.3	5.1	20.5	28.1	6.7	50.5
	$K_{Ic} = 72 \text{ ksi}\sqrt{\text{in}}$ for 42 EFPY	Normal	6.2	14.0	3.6	8.1	33.0	41.9	15.2	83.1
		Upset	6.5	14.5	3.8	8.5	36.7	44.6	18.1	92.5
		Faulted-1	6.0	13.4	3.5	7.8	31.0	39.1	13.5	77.5
		Faulted-2	5.4	12.0	3.1	6.9	24.2	32.0	8.8	59.8
Section XI Allowable Flaw Size			4.3	8.7	3.7 ^(d)	7.5 ^(d)	2.7 ^(d)	3.1	1.9	12.1 ^(c)

Notes:

(a) The critical flaw sizes are determined by setting applied stress intensity factor equal to fracture toughness and back-calculating flaw size. Web thickness = 1.5". Flange thickness = 3". For side edge flaws in the flange, the width of the flange (12") represents the thickness.

(b) The semi-elliptical flaws are postulated at the weld of the ring girder; thus, [

] ^{a,c,e}

(c) [

] ^{a,c,e}

(d) [

] ^{a,c,e}

7.3 SHEAR BRACE: I-BEAM

The six shear brace configurations consist of two key shears, five bolts and two I-beams in the shape of an 'A-frame' (see Figure 3-5). The shear brace bolts are analyzed in Section 7.4 and the shear keys are analyzed in Section 7.5. The analysis for the I-beam conservatively considers embrittlement at the outside top and bottom edge of the ring girder (embrittlement at the I-beam would be less since this component is further from the RV), resulting in a fracture toughness value of 50 ksi√in and 58 ksi√in for 72 EFPY and 42 EFPY, respectively (see Table 5-1).

In addition to the applied stresses on the I-beam (see Table 4-3), welding residual stress is considered for the postulated semi-elliptical flaw in the web and flange per Section 4 of this report. There was insufficient information to demonstrate that the Point Beach Unit 2 I-beam was post weld heat treated; thus, []^{a,c,e} was added to the applied stresses which resulted in small critical flaw sizes for the semi-elliptical flaw in the web and flange which are postulated near the welds.

Various postulated flaw shapes in a plate model were analyzed, including a study of semi-elliptical flaws with aspect ratio (flaw length over flaw depth) of 6 and 2, infinite length flaws in the web and flange and a corner flaw in the flange. The calculated critical flaw sizes are shown in Table 7-3 for the previously mentioned postulated flaw shapes, as well as the []^{a,c,e}

[]^{a,c,e}

As a sensitivity case, the WRS through-wall stress distribution (see Section 4) for a semi-elliptical flaw in the I-beam flange is considered with an aspect ratio of 2 and 6. The faulted-2 stress is conservatively applied as constant through-the-wall thickness. []^{a,c,e}

The critical flaw size is the flaw size which sets applied stress intensity factor equal to the fracture toughness (50 ksi√in for 72 EFPY of embrittlement is used). The critical flaw size for a semi-elliptical flaw with an aspect ratio of 2 is 55% through-the-wall thickness and the critical flaw size for a semi-elliptical flaw with an aspect ratio of 6 is 4% through-the-wall thickness. This sensitivity case demonstrates that a small flaw size (AR = 2) and through-wall welding residual stress will result in a critical flaw size larger than the []^{a,c,e}

As shown in Table 7-3, the change in embrittlement from 42 to 72 EFPY results in critical flaw sizes that varies on average by 2% to 5% for the limiting semi-elliptical flaw shapes. Thus, it is determined that the

effect of the change in embrittlement over time is minor on the critical flaw sizes. Based on the conclusions described in the previous paragraphs, the I-beams continue to be structurally stable considering 80 years of radiation embrittlement effects on the supports.

Table 7-3: Summary of I-Beam Critical Flaw Size

Component	Fracture Toughness	Loading Condition	Critical Flaw Size (a/t), % ^(a)							
			Semi-Elliptical Web (AR = 6) ^(b)	Semi-Elliptical Web (AR = 2) ^(b)	Semi-Elliptical Flange (AR = 6) ^(b)	Semi-Elliptical Flange (AR = 2) ^(b)	Top Edge Flange	Side Edge Web	Side Edge Flange	Corner Flange ^(e)
I-Beam	K _{Ic} = 50 ksi√in for 72 EFPY	Normal	6.6	14.8	3.8	8.5	80.0 ^(c)	80.0 ^(c)	80.0 ^(d)	99.9
		Upset	5.9	13.2	3.4	7.6	60.9	66.1	40.7	99.9
		Faulted-1	5.3	11.9	3.0	6.8	45.5	52.3	22.9	99.9
		Faulted-2	5.0	11.2	2.8 ^(g)	6.4 ^(g)	38.9	46.2	17.0	99.9
	K _{Ic} = 58 ksi√in for 42 EFPY	Normal	8.9	19.8	5.1	11.4	80.0 ^(c)	80.0 ^(c)	80.0 ^(d)	99.9
		Upset	7.9	17.7	4.5	10.2	63.7	68.6	44.5	99.9
		Faulted-1	7.1	15.9	4.1	9.1	49.2	55.7	26.6	99.9
		Faulted-2	6.7	15.0	3.8	8.6	42.8	49.9	20.4	99.9
Section XI Allowable Flaw Size			4.3	8.7	4.3	8.7	3.1	3.1	1.9	12.1 ^(f)

Notes:

- (a) The critical flaw sizes are determined by setting applied stress intensity factor equal to fracture toughness and back-calculating flaw size. Web thickness = 1". Flange thickness = 1.75".
- (b) The semi-elliptical flaw is postulated at the weld of the I-beam; thus, [
]a,c,e
- (c) Per API-579 [10], the edge flaw SIF methodology is limited by $a/t \leq 80\%$.
- (d) Per API-579 [10], the edge flaw SIF methodology is limited by $a/t \leq 80\%$. The width of the flange (10") represents the thickness.
- (e) Per [31], the corner flaw SIF methodology is limited by $a/t < 1$ (i.e., critical through-wall flaws are allowed).
- (f) [
]a,c,e
- (g) As a sensitivity study, the through-wall WRS distribution in Section 4 is analyzed. The critical flaw size for a semi-elliptical flaw with an aspect ratio of 2 is 55% through-the-wall thickness and the critical flaw size for a semi-elliptical flaw with an aspect ratio of 6 is 4% through-the-wall thickness. This sensitivity case demonstrates that a small flaw size (AR = 2) and through-wall residual stress will result in a critical flaw size larger than the Section XI allowable.

7.4 SHEAR BRACE: BOLT

There are five bolts within the shear brace (see Figure 3-5); the centroid bolt does not provide any support during operation; thus, only the four adjacent bolts are analyzed. The analysis for the bolts conservatively considers embrittlement at the outside top and bottom edge of the ring girder (embrittlement at the bolts would be less since this component is further from the RPV), resulting in a fracture toughness value of 32 ksi√in and 37 ksi√in at 72 EFPY and 42 EFPY, respectively (see Table 5-1). The change in neutron embrittlement over time is not significant as the change in fracture toughness is small from 42 EFPY to 72 EFPY. The bolts are only subjected to a tensile axial force shown in Table 4-4 which results in favorable calculated circumferential critical flaw sizes shown in Table 7-4. As a parametric study, there are three postulated flaws which are analyzed: 360° continuous circumferential, straight front, and semi-circular front. Axial flaws are not required to be analyzed since hoop stress is not present. The calculated circumferential critical flaw sizes are larger than the [

] ^{a,c,e}

In addition, per Section 6, [

] ^{a,c,e}

As shown in Table 7-4, the change in embrittlement from 42 to 72 EFPY results in critical flaw sizes that varies on average by 1% to 2%. Thus, it is determined that the effect of the change in embrittlement over time is minor on the critical flaw sizes. Based on the conclusions described in the previous paragraphs, the bolts at the shear brace continue to be structurally stable considering 80 years of radiation embrittlement effects on the supports.

Table 7-4: Summary of Shear Brace Bolts Critical Flaw Size

Component	Fracture Toughness	Loading Condition	Critical Flaw Size, % ^(a)		
			Circumferential 360° Continuous, a/R _o	Straight Front, a/OD	Semi-Circular Front, a/OD
Shear Brace Bolt	K _{Ic} = 32 ksi√in for 72 EFPY	Normal	99.8	62.5 ^(b)	60.0 ^(c)
		Upset	51.5	62.5 ^(b)	60.0 ^(c)
		Faulted-1	41.5	54.7	60.0 ^(c)
		Faulted-2	37.4	50.1	57.9
	K _{Ic} = 37 ksi√in for 42 EFPY	Normal	99.8	62.5 ^(b)	60.0 ^(c)
		Upset	53.4	62.5 ^(b)	60.0 ^(c)
		Faulted-1	43.7	57.1	60.0 ^(c)
		Faulted-2	39.8	52.8	60.0 ^(c)
Section XI Allowable Flaw Size			9.4	0.61	0.61

Notes:

- (a) The critical flaw sizes are determined by setting applied stress intensity factor equal to fracture toughness and back-calculating flaw size. Bolt outside diameter = 1.6012”.
- (b) Per API-579 [10], the flaw size is limited by $0.065 < \zeta < 0.625$, where $\zeta = a/2 \cdot \text{radius of bolt}$. The radius of the bolt is 0.8006”; thus, flaw depth is limited to 1” or 62.5% through the bolt diameter.
- (c) Per API-579 [10], the flaw size is limited by $\zeta < 0.6$, where $\zeta = a/2 \cdot \text{radius of bolt}$. The radius of the bolt is 0.8006”; thus, flaw depth is limited to 0.96” or 60% through the bolt diameter.

7.5 SHEAR BRACE: SHEAR KEY

There are two shear keys within the shear brace (see Figure 3-5). The analysis for the shear key conservatively considers embrittlement at the outside top and bottom edge of the ring girder (embrittlement at the shear keys would be less since this component is further from the RV), resulting in a fracture toughness value of 50 ksi√in and 58 ksi√in for 72 EFPY and 42 EFPY, respectively (see Table 5-1). The change in neutron embrittlement over time is not significant as the change in fracture toughness is small from 42 EFPY to 72 EFPY. The key shears are subjected to a shear force shown in Table 4-5 which are converted to shear stress. Note that the shear stress in Table 4-5 is less than the 6 ksi stress criteria per NUREG-1509; however, the location of the key shears are near the active core of the RPV with high radiation exposure; thus, the key shears are analyzed. The small shear stress in the key shear components results in favorable critical flaw sizes shown in Table 7-5. The calculated critical flaw sizes (infinitely long edge flaws in a plate model) are larger than the [

] ^{a,c,e} thus, the shear keys continue to be structurally stable considering 80 years of radiation embrittlement effects on the supports. [

] ^{a,c,e}

As shown in Table 7-5, the change in embrittlement from 42 to 72 EFPY results in critical flaw sizes that varies less than 1%. Thus, it is determined that the effect of the change in embrittlement over time is minor on the critical flaw sizes.

Table 7-5: Summary of Shear Brace Shear Key Critical Flaw Size

Component	Fracture Toughness	Loading Condition	Critical Flaw Size (a/t), % ^(a)	
			Edge Flaw in Plate K _{II} Model ^{(b) (c)}	Edge Flaw in Plate K _{III} Model ^{(b) (d)}
Shear Brace	K _{Ic} = 50 ksi√in for 72 EFPY	Normal	99.9	99.9
		Upset	99.5	99.6
		Faulted-1	98.3	98.7
		Faulted-2	97.2	97.8
Shear Key	K _{Ic} = 58 ksi√in for 42 EFPY	Normal	99.9	99.9
		Upset	99.6	99.7
		Faulted-1	98.7	99.0
		Faulted-2	97.9	98.4
Section XI Allowable Flaw Size			3.1	3.1

Notes:

- (a) The critical flaw sizes are determined by setting applied stress intensity factor equal to fracture toughness and back-calculating flaw size. The Mode II and Mode III stress intensity factors are conservatively compared to Mode I fracture toughness.
- (b) There are no limits of applicability for the K_{II} and K_{III} models provided in Tada [32]; however, it is noted that as the flaw depth (a) reaches the thickness dimension (i.e., a/thickness nears 1), the influence coefficient (F_{II} and F_{III}) become infinite. The shear stress in Table 4-5 is small enough to permit essentially through-wall critical flaw sizes.
- (c) An edge flaw in the 2" thickness of the key shear results in Mode II crack opening.
- (d) An edge flaw in the 2.5" thickness of the key shear results in Mode III crack opening.

7.6 BOLTS (AT BOX RING GIRDER)

There are three bolts at the apexes of the ring girder which connect the girder to the columns (see Figure 3-5). The analysis for these bolts considers embrittlement of the ring girder, resulting in a fracture toughness value of 36 ksi√in and 47 ksi√in for 72 EFPY and 42 EFPY, respectively (see Table 5-1). Based on fracture toughness, the change in neutron embrittlement over time is significant since these bolts are close to the outside surface of the RPV and near the active core region. [

]^{a,c,e} and bending moment in Table 4-6 are applied to the bolts and the calculated critical flaw sizes are shown in Table 7-6. As a parametric study, there are two postulated flaws which are analyzed: 360° continuous circumferential and semi-circular front. The straight front circumferential flaw sizes are not reported since the limits of applicability of the stress intensity factor model are not met due to the large loads. Axial flaws are not required to be analyzed since hoop stress is not present.

The postulated 360° continuous circumferential critical flaw size is less than the [

]^{a,c,e}

As shown in Table 7-6, the change in embrittlement from 42 to 72 EFPY results in critical flaw sizes that varies on average by 1% to 4% for the postulated 360° continuous circumferential and up to 8% for the postulated semi-circular front flaw. Thus, it is determined that the effect of the change in embrittlement over time is minor on the critical flaw sizes. Based on the conclusions described in the previous paragraphs, the bolts at the ring girder continue to be structurally stable considering 80 years of radiation embrittlement effects on the supports.

Table 7-6: Summary of Box Ring Girder Bolts Critical Flaw Size

Component	Fracture Toughness	Loading Condition	Critical Flaw Size, % ^(a)	
			Circumferential 360° Continuous, a/R _o	Semi-Circular Front, a/OD
Bolt at Box Ring Girder	K _{Ic} = 36 ksi√in for 72 EFPY	Normal	16.9	38.9
		Upset	4.8	7.6
		Faulted-1	3.4	4.8
		Faulted-2	2.1	2.7
	K _{Ic} = 47 ksi√in for 42 EFPY	Normal	20.4	46.9
		Upset	7.0	12.9
		Faulted-1	5.1	8.3
		Faulted-2	3.4	4.7
Section XI Allowable Flaw Size			9.4	0.61

Note:

- (a) The critical flaw sizes are determined by setting applied stress intensity factor equal to fracture toughness and back-calculating flaw size. Bolt outside diameter = 1.6012”.

7.7 PINS (AT BOTTOM OF COLUMNS)

The pins at the bottom of the columns connect the columns and the baseplate together (see Figure 3-6). Since the pins are far from the active core of the reactor vessel, the embrittlement at the base plate is small, resulting in a fracture toughness value of 45 ksi√in for 72 EFPY and 42 EFPY (i.e., the change in embrittlement between 42 EFPY and 72 EFPY is negligible, see Table 5-1). [

] ^{a,c,e} The calculated critical flaw sizes are shown in Table 7-7 for an edge flaw at the bottom of the pin. The calculated critical flaw sizes are larger than the [^{a,c,e} thus, the pins continue to be structurally stable considering 80 years of radiation embrittlement effects on the supports.

In addition, per Section 6, [

] ^{a,c,e}

As previously mentioned, the change in embrittlement between 42 to 72 EFPY is negligible; thus, the critical flaw sizes in Table 7-7 are the same for 42 and 72 EFPY.

Table 7-7: Summary of Pins Critical Flaw Size

Component	Fracture Toughness	Loading Condition	Critical Flaw Size (a/OD), % ^(a)
			Edge Flaw
Pin at Bottom of Column	K _{Ic} = 45 ksi√in for 72 EFPY	Normal	3.8
		Upset	1.8
		Faulted-1	1.3
		Faulted-2	0.7
	K _{Ic} = 45 ksi√in for 42 EFPY	Normal	3.8
		Upset	1.8
		Faulted-1	1.3
		Faulted-2	0.7
Section XI Allowable Flaw Size			0.20

Note:

- (a) The critical flaw sizes are determined by setting applied stress intensity factor equal to fracture toughness and back-calculating flaw size. Pin outside diameter = 3.994".

7.8 SUPPORT SHOE BOX MEMBER

The support shoes are located under the RPV inlet/outlet nozzles and brackets (see Figure 3-7). The embrittlement is based on top inside and outside edge of ring girder, resulting in a fracture toughness value of 110 ksi $\sqrt{\text{in}}$ and 147 ksi $\sqrt{\text{in}}$ for 72 EFPY and 42 EFPY, respectively (see Table 5-1). Two cuts are analyzed within the support shoe: Cut 1/Cut 2 (within the bulk of the steel) and Cut 5/Cut 6 (across the leveling screw hole). The stresses are provided in Table 4-8 and Table 4-9 for Cut 1/Cut 2 and Cut 5/Cut 6, respectively. [

]^{a,c,e} and the resulting calculated critical flaw sizes are shown in Table 7-8. An infinitely long top and side edge flaw are analyzed for Cut 1/Cut 2 and a through-wall double edge flaw at the hole in the support shoe is analyzed for Cut 5/Cut 6. The calculated critical flaw sizes are larger than the [

]^{a,c,e} thus, the support shoes continue to be structurally stable considering 80 years of radiation embrittlement effects on the supports.

As shown in Table 7-8, the change in embrittlement from 42 to 72 EFPY results in critical flaw sizes that varies on average by 4% to 8%. Thus, it is determined that the effect of the change in embrittlement over time is minor on the critical flaw sizes.

Table 7-8: Summary of Support Shoe Critical Flaw Size

Component	Fracture Toughness	Loading Condition	Critical Flaw Size (a/t), % ^(a)		
			Cut 5/Cut 6: Plate with Hole ^(b)	Cut 1/Cut 2: Top Edge Flaw	Cut 1/Cut 2: Side Edge Flaw
Support Shoe	K _{Ic} = 110 ksi $\sqrt{\text{in}}$ for 72 EFPY	Normal	34.5	70.9	65.4
		Upset	34.5	50.5	42.2
		Faulted-1	34.5	36.7	28.1
		Faulted-2	34.5	29.9	21.6
	K _{Ic} = 147 ksi $\sqrt{\text{in}}$ for 42 EFPY	Normal	34.5	75.4	70.3
		Upset	34.5	57.0	49.5
		Faulted-1	34.5	44.3	35.6
		Faulted-2	34.5	37.6	28.9
Section XI Allowable Flaw Size			1.9 ^(c)	1.9	1.9

Notes:

- The critical flaw sizes are determined by setting applied stress intensity factor equal to fracture toughness and back-calculating flaw size.
- Per the limits of applicability of the SIF methodology in API-579 [10], the flaw size is limited to half the support shoe width minus radius of the hole []^{a,c,e}
- An allowable flaw size is not provided since the calculated critical flaw size is through the shoe wall thickness, which is represented by two edge flaws that are 34.5% through-the-wall thickness; however, 1.9% is reported.

7.9 LEVELING SCREW

There are two leveling screws located inside each of the six support shoes which are directly below the RPV nozzles and support brackets (see Figure 3-7). The embrittlement based on top inside and outside edge of ring girder are conservatively applied to the leveling screw, resulting in fracture toughness values of 56 ksi $\sqrt{\text{in}}$ and 70 ksi $\sqrt{\text{in}}$ for 72 EFPY and 42 EFPY, respectively (see Table 5-1). [

] ^{a,c,e} and bending moment in Table 4-10 are applied to the leveling screw and the calculated circumferential critical flaw sizes are shown in Table 7-9. As a parametric study, there are three postulated flaws which are analyzed: 360° continuous circumferential, straight front, and semi-circular front. Axial flaws are not required to be analyzed since hoop stress is not present. The calculated critical flaw sizes are larger than the [

] ^{a,c,e}

In addition, per Section 6, [

] ^{a,c,e}

As shown in Table 7-9, the change in embrittlement from 42 to 72 EFPY results in critical flaw sizes that varies on average by 3% to 7%. Thus, it is determined that the effect of the change in embrittlement over time is minor on the critical flaw sizes. Based on the conclusions described in the previous paragraphs, the leveling screws continue to be structurally stable considering 80 years of radiation embrittlement effects on the supports.

Table 7-9: Summary of Leveling Screws Critical Flaw Size

Component	Fracture Toughness	Loading Condition	Critical Flaw Size (a/t), % ^(a)		
			Circumferential 360° Continuous, a/R _o	Straight Front, a/OD	Semi-Circular Front, a/OD
Leveling Screw	K _{Ic} = 56 ksi $\sqrt{\text{in}}$ for 72 EFPY	Normal	16.4	30.6	39.6
		Upset	21.3	41.3	49.2
		Faulted-1	12.4	18.9	27.9
		Faulted-2	9.5	12.1	19.8
	K _{Ic} = 70 ksi $\sqrt{\text{in}}$ for 42 EFPY	Normal	19.3	38.3	46.5
		Upset	24.3	47.3	55.2
		Faulted-1	15.2	25.9	35.2
		Faulted-2	12.1	18.1	26.9
Section XI Allowable Flaw Size			4.2	0.12	0.12

Note:

- (a) The critical flaw sizes are determined by setting applied stress intensity factor equal to fracture toughness and back-calculating flaw size. [

] ^{a,c,e}

7.10 BASE PLATE

The base plate is located at the bottom of the RPV support structure and supports the columns (see Figure 3-6). Since the base plates are far from the active core of the reactor vessel, the embrittlement at the base plate is small, resulting in a fracture toughness value of 70 ksi√in for both 72 EFPY and 42 EFPY (see Table 5-1). The force on the base plate is highly compressive; resulting in [

] ^{a,c,e} (see Table 4-11) on the base plate which is less than the 6 ksi stress criteria discussed in the beginning of Section 6. In addition, the base plate initial NDTT_o is -20°F (per Table 4-1 of NUREG-1509 for A-517 material) which is well below the minimum operating temperature of 85°F. Thus, the three criteria in NUREG-1509 are met (i.e., the base plate is free from radiation embrittlement and the integrity may be reasonably assured) and no further investigation should be required.

However, a conservative study is completed in which the compressive load due to the column is removed and the critical flaw sizes are determined. [

] ^{a,c,e} The resulting critical flaw sizes are shown in Table 7-10 for a semi-elliptical flaw (with aspect ratio of 10). The applied stress is small and results in a critical flaw size of 80% through the plate thickness, which is an applicability limit on the stress intensity factor methodology. The calculated critical flaw sizes for this conservative case are larger than the [

] ^{a,c,e} thus, the base plates continue to be structurally stable considering 80 years of radiation embrittlement effects on the supports.

As previously mentioned, the change in embrittlement between 42 to 72 EFPY is negligible; thus, the critical flaw sizes in Table 7-10 are the same for 42 and 72 EFPY.

Table 7-10: Summary of Base Plate Critical Flaw Size

Component	Fracture Toughness	Loading Condition	Critical Flaw Size (a/t), % ^(a)
			Semi-Elliptical Flaw AR = 10 ^(b)
Base Plate	K _{Ic} = 70 ksi√in for 72 EFPY	Normal	80.0
		Upset	80.0
		Faulted-1	80.0
		Faulted-2	80.0
	K _{Ic} = 70 ksi√in for 42 EFPY	Normal	80.0
		Upset	80.0
		Faulted-1	80.0
		Faulted-2	80.0
Section XI Allowable Flaw Size			3.6

Notes:

- The critical flaw sizes are determined by setting applied stress intensity factor equal to fracture toughness and back-calculating flaw size. Thickness = 2".
- Per API-579 [10], the semi-elliptical SIF methodology in a plate is limited by $a/t \leq 80\%$.

8 DISCUSSION OF CONCLUSIONS

8.1 EVALUATION OF CURRENT CONDITIONS

Per Section 4.3.1 of NUREG-1509 [2], physical examination of the structural components is essential to the reevaluation completed herein and an assessment of the overall condition of the RPV support structure. Based on PBNWEC-20-0023 [27], the supports for the RPV are examined during the ISI inspection interval as part of the normal ASME ISI examinations as required by 10CFR50.55a. Point Beach Unit 1 RPV supports were examined most recently in 2005, 2007, and 2016. In the 2016 exam, there were no relevant indications identified. Point Beach Unit 2 RPV supports were examined most recently in 2006, 2008, and 2015. In the 2015 exam, there were no relevant indications identified. The visual exams (VT-3) are best effort due to limited access to the RPV supports.

Based on the ISI examination, Point Beach NDE Level III personnel have concluded that the discoloration at the base plate and bolts was due to staining from cavity seal leakage from the reactor vessel flange during outage (this leakage is not present after plant start-up). The NDE Level III personnel concluded that while there was some light surface corrosion, there was no degradation of the base plate or associated bolting. Any degradation would have to be evaluated by the design team at Point Beach and re-analysis of the AISC margins for the structural steel components (base plate, bolts, and nuts) would be needed.

To date, there had been no re-design or analysis needed for this region of the support. As such, Point Beach has concluded that the discoloration is not related to general corrosion or degradation of the support; furthermore, there was no loss of capacity of the load bearing members at the lower base plate, nuts, and bolts. Therefore, no degradation or reduced load carrying capability due to corrosion is required to be considered in the fracture evaluation of the RPV supports. The discussion of the current conditions of the Point Beach RPV supports is provided in PBNWEC-20-0023 [27].

8.2 CHANGE IN EMBRITTLEMENT OVER TIME

[

]a.c.e

8.3 CRITICAL FLAW SIZE CONCLUSIONS

Based on conclusions in NUREG-0933, it was determined that the RPV supports were not a concern for the entirety of its plant life (i.e., 40 or 60 years), even if all the supports were totally removed (i.e., broken), the piping has acceptable margin to carry the load of the vessel. Nevertheless, for plants applying for 80 year life licensure, the NRC has requested a re-assessment of the RPV structural steel supports based on a fracture mechanics evaluation to account for neutron embrittlement.

The goal of the fracture mechanics analysis in this report for Point Beach Units 1 and 2 will be to demonstrate that the calculated critical flaw sizes based on 80 years of neutron embrittlement are sufficiently large (i.e., flaw tolerant) as compared to [

] ^{a,c,e} These previously mentioned allowable flaw sizes were described in detail in Section 6 of this report. Based on this comparison of the critical flaw size, it can be demonstrated that Point Beach RPV supports are flaw tolerant for an operating life of 80 years.

There are ten components within the Point Beach Units 1 and 2 RPV support system that were evaluated: column, box ring girder, I-beam, bolts at shear brace, key shear, bolts at ring girder, pins at the bottom of the columns, support shoe box, leveling screw, and base plate. These ten components are considered for the critical flaw size calculations as these locations could experience tensile stresses and high embrittlement effects. The critical flaw sizes for each of the ten components are based on latest plant specific stresses, welding residual stress, operating conditions temperatures, neutron embrittlement for 42 EFPY and 72 EFPY of operation, shift in NDTT based on Figure 3-1 of NUREG-1509 (reproduced as Figure 5-5 herein), and latest stress intensity factors used in the industry. [

] ^{a,c,e}

The critical flaw sizes for each Point Beach Units 1 and 2 RPV support component are determined in Sections 7.1 through 7.10 for various flaw shapes and orientation for 42 and 72 EFPY; the limiting critical flaw size for each component is provided in Table 8-1. The critical flaw size represents the largest flaw size which would equate applied stress intensity factor to the component specific material fracture toughness. The critical flaw sizes are compared against [

] ^{a,c,e} In most cases, the critical flaw sizes are larger than the Section XI allowable flaw sizes by a large margin; thereby concluding that the Point Beach Units 1 and 2 reactor vessel support components continue to be structurally stable (i.e., flaw tolerant) considering 80 years of radiation embrittlement effects on the supports. The five components which fall into this category are:

- columns
- bolts at the shear brace
- shear key
- support shoe box
- base plate

Other cases where the margin with respect to the ASME Section XI allowable flaw sizes is small or not met will be discussed in the following paragraphs.

The leveling screw and pin critical flaw sizes are all above the [

] ^{a,c,e}

The 360° continuous circumferential critical flaw sizes for the bolts at the ring girder are less than the Section XI allowable flaw size. However, these critical flaw sizes, as well as the flaw sizes for all the bolts including the leveling screw and pin, [

] ^{a,c,e}

The critical flaw sizes for the limiting semi-elliptical flaws in the I-beam and box ring girder are less than the Section XI allowable flaw sizes. For both components, large welding residual stress is applied to the semi-elliptical flaw in the web and flange (near the welds), resulting in small critical flaw sizes. However, these flaws [

] ^{a,c,e} The infinite length flaws in the web and flange and a corner flaw in the flange critical flaw sizes are well above the Section XI allowable flaw sizes by a large margin; thereby concluding that the Point Beach Units 1 and 2 I-beam and box ring girder support components continue to be structurally stable (i.e., flaw tolerant) considering 80 years of radiation embrittlement effects on the supports.

Based on the discussions above and the results provided in this report, it is concluded that the RPV supports at Point Beach Units 1 and 2 are structurally stable (i.e., flaw tolerant) considering 80 calendar years (72 EFPY) of radiation embrittlement effects and a sufficient level of flaw tolerance is demonstrated to justify continuing the current visual examination (VT-3) of the RPV structural steel supports. In conclusion, the loss of fracture toughness due to neutron embrittlement over 80 years is not significant and therefore, the Point Beach Units 1 and 2 RPV structural steel supports do not require more frequent inspections than those required by the current ASME Section XI inspection program.

Table 8-1: Summary of Point Beach Units 1 and 2 RPV Support Critical Flaw Sizes

Loading Condition	Fracture Toughness	Critical Flaw Size (a/t, flaw depth over thickness) ^(a)									
		Column	Box Ring Girder Flange ^(b)	I-Beam Web ^(b)	Shear Brace: Bolt	Shear Brace: Shear Key	Bolts at Box Ring Girder	Pin at Bottom of Column	Support Shoe Box	Leveling Screw	Base Plate
Normal	Fracture Toughness for 72 EFPY	59.6 %	2.2 % ^(c)	3.8 % ^(c)	99.8 %	99.9 %	16.9 %	3.8 %	65.4 %	16.4 %	80.0 %
Upset		62.9 %	2.4 % ^(c)	3.4 % ^(c)	51.5 %	99.5 %	4.8 % ^(c)	1.8 %	42.2 %	21.3 %	80.0 %
Faulted-1		57.0 %	2.2 % ^(c)	3.0 % ^(c)	41.5 %	98.3 %	3.4 % ^(c)	1.3 %	28.1 %	12.4 %	80.0 %
Faulted-2		44.4 %	1.9 % ^(c)	2.8 % ^(c)	37.4 %	97.2 %	2.1 % ^(c)	0.7 %	21.6 %	9.5 %	80.0 %
Normal	Fracture Toughness for 42 EFPY	61.4 %	3.6 % ^(c)	5.1 %	99.8 %	99.9 %	20.4 %	3.8 %	70.3 %	19.3 %	80.0 %
Upset		64.7 %	3.8 %	4.5 %	53.4 %	99.6 %	7.0 % ^(c)	1.8 %	49.5 %	24.3 %	80.0 %
Faulted-1		59.2 %	3.5 % ^(c)	4.1 % ^(c)	43.7 %	98.7 %	5.1 % ^(c)	1.3 %	35.6 %	15.2 %	80.0 %
Faulted-2		46.2 %	3.1 % ^(c)	3.8 % ^(c)	39.8 %	97.9 %	3.4 % ^(c)	0.7 %	28.9 %	12.1 %	80.0 %
Section XI Allowable Flaw Size		3.1 %	3.7 %	4.3 %	9.4 %	3.1 %	9.4 %	0.20 %	1.9 %	4.2 %	3.6 %

Notes:

- (a) The critical flaw sizes are determined by setting applied stress intensity factor equal to fracture toughness and back-calculating flaw size. There are no significant transients or thermal cycling that would cause any crack growth over time. The calculated critical flaw sizes are compared against the Section XI allowable flaw sizes (permissible per Section 4.3.4.1 of NUREG-1509) and any approved design specification requirements. In most cases, the critical flaw sizes are larger than the Section XI allowable flaw sizes by a large margin; thereby concluding that the Point Beach reactor vessel support components continue to be structurally stable (i.e., flaw tolerant) considering 80 years of radiation or embrittlement effects on the supports.
- (b) This location considers welding residual stress.
- (c) The critical flaw sizes are less than the Section XI allowable flaw sizes. However, the installed welds or fabricated components will be free from flaws on the order of the critical flaw sizes, as determined in this table per its representative design specification, which would require repair of flaw sizes of this magnitude during initial fabrication.

9 REFERENCES

1. NUREG-0933, "Resolution of Generic Safety Issues (Formerly entitled "A Prioritization of Generic Safety Issues)," Main Report with Supplements 1-34. Generic Issue No: 15, "Radiation Effects on Reactor Vessel Supports (Rev. 3)."
2. NUREG-1509, "Radiation Effects on Reactor Pressure Vessel Supports," May 1996.
3. NUREG/CR-5320, "Impact of Radiation Embrittlement on Integrity of Pressure Vessel Supports for Two PWR Plants." January 1989.
4. ASME Boiler & Pressure Vessel Code, 2007 Edition with 2008 Addenda Section XI, "Rules for Inservice Inspection of Nuclear Power Plant Components."
5. Memorandums by the NRC Regarding Resolution of GSI-15 as cited in NUREG-0933 [NRC Adams Accession No.: ML003749352]
 - a. Memorandum for James M. Taylor from David L. Morrison, "Resolution of Generic Safety Issue 15, 'Radiation Effects on Reactor Vessel Supports'", May 29, 1996. (3 pages).
 - b. Memorandum for John T. Larkins from Joseph A. Murphy, "Proposed Resolution of GSI-15, 'Radiation Effects on Reactor Pressure Vessel Supports'", June 22, 1994 (3 pages) (Enclosures: 206 pages).
6. NRC Lessons Learned for SLR:
 - a. NRC Public Meeting: "SLR Change - DRAFT New FE SRP-SLR Section 3.5.2.2.2.7 and AMR for Irradiation of RV Steel Supports," Meeting Held 02/20/20. [ADAMS Accession Number ML20049H359]
 - b. U.S. NRC Report, "Summary of April 7, 2020 Teleconference on Topics Related to Lessons Learned from the Review of the First Subsequent License Renewal Application," April 27, 2020. [ADAMS Accession Number ML20107F699]
7. [
8. [

]a,c,e

]a,c,e

[

]a,c,e

- 9. Updated Final Safety Analysis Report (UFSAR) for Point Beach Units 1 and 2, Table A.5-3, Date Released: December 2, 2016. [NRC Adams Accession No.: ML16251A147]
- 10. American Petroleum Institute, API-579-1/ASME FFS-1, "Fitness-For-Service," June 2016.
- 11. ASME Code Section III, Division 1 – Appendices, "Rules for Construction of Nuclear Power Plant Components," 1989 Edition.
- 12. ASTM A-517-84, "Standard Specification for Pressure Vessel Plates, Alloy Steel, High-Strength, Quenched and Tempered."
- 13. ASTM A-300-68, "Standard Specification for Notch Toughness Requirements for Normalized Steel Plates for Pressure Vessels."
- 14. ASTM A-53-64, "Standard Specification for Welded and Seamless Steel Pipe."
- 15. ASTM A-508-64, "Standard Specification for Quenched and Tempered Vacuum Treated Carbon and Alloy Steel Forgings for Pressure Vessels."
- 16. ASTM A-434-76, "Standard Specification for Steel Bars, Alloy, Hot-Rolled or Cold-Finished, Quenched and Tempered."
- 17. ASTM A-490-76a, "Standard Specification for Quenched and Tempered Alloy Steel Bolts for Structural Steel Joints."
- 18. ASTM A-354-86, "Standard Specification for Quenched and Tempered Alloy Steel Bolts, Studs, and other Externally Threaded Fasteners."

19. [

]a,c,e

20. [

]a,c,e

21. ASME Code Section II – Part D, “Materials,” 2007 Edition with 2008 Addenda.
22. NUREG/CR-3009, SAND78-2347, “Fracture Toughness of PWR Components Supports,” February 1983.
23. ASME Section XI Code Case N-830, “Direct Use of Master Fracture Toughness Curve for Pressure-Retaining Materials of Class 1 Vessels Section XI, Division 1,” Approval Date: September 4, 2014.
24. “Technical Basis for ASME Code Case N-830, Revision 1 (MRP-418) Direct Use of Master Curve Fracture Toughness Curve for Pressure-Retaining Materials of Class 1 Vessels, Section XI,” October 2017.
25. Toll Bridge Program Oversight Committee, “Report on the A354 Grade BD High-Strength Steel Rods on the New East Span of the San Francisco-Oakland Bay Bridge, With Findings and Decisions,” California Department of Transportation, 2013.
26. []^{a,c,e}
27. NextEra Energy Point Beach Letter PBNWEC-20-0023, “Point Beach Nuclear Plant Units 1 and 2 Subsequent License Renewal Project Response to Westinghouse Letter WEC-NEE-PB-SLR-20-003, NEXT-20-33,” April 27, 2020.
28. Westinghouse Report WCAP-14422, Revision 2-A, “Licensing Renewal Evaluation: Aging Management for Reactor Coolant System Supports,” December 2000.
29. USNRC Regulatory Guide 1.190, “Calculational and Dosimetry Methods for Determining Pressure Vessel Neutron Fluence,” Office of Nuclear Regulatory Research, March 2001.
30. Westinghouse Report WCAP-18124-NP-A, Rev. 0, “Fluence Determination with RAPTOR-M3G and FERRET,” July 2018.
31. J. C. Newman, Jr. and I. S. Raju, National Aeronautics and Space Administration (NASA), “Stress-Intensity Factor Equations for Cracks in Three-Dimensional Finite Bodies subjected to Tension and Bending Loads,” NASA Technical Memorandum 85793, April 1984.
32. Hiroshi Tada, Paul C. Paris, George R. Irwin, “The Stress Analysis of Cracks Handbook,” Third Edition, ASME Press, New York, 2000.
33. AWS D2.0-66, “Specifications for Welded Highway and Railway Bridges,” American Welding Society, Seventh Edition.
34. “Specifications for Structural Joints Using ASTM A325 or A490 Bolts,” Research Council on Structural Connections, March 1964.

This page was added to the quality record by the PRIME system upon its validation and shall not be considered in the page numbering of this document.

Approval Information

Author Approval Carolan Alexandria M Sep-10-2020 14:44:41

Verifier Approval Song Xiaolan Sep-10-2020 15:53:00

Reviewer Approval Hall J Brian Sep-11-2020 07:48:17

Reviewer Approval Longwell Stephen K Sep-14-2020 06:31:10

Reviewer Approval Amiri Benjamin W Sep-14-2020 09:24:44

Reviewer Approval Udyawar Anees Sep-14-2020 12:13:52

Manager Approval Patterson Lynn Sep-14-2020 12:23:24

Files approved on Sep-14-2020

*** This record was final approved on 9/14/2020 12:23:24 PM. (This statement was added by the PRIME system upon its validation)

Point Beach Nuclear Plant Units 1 and 2
Dockets 50-266 and 50-301
NRC 2020-0032 Enclosure 4, Attachment 3

Enclosure 4

**Non-proprietary Reference Documents and
Redacted Versions of Proprietary Reference
Documents**

(Public Version)

Attachment 3

**Westinghouse WCAP-18555-NP, Revision 1, “Point
Beach Units 1 and 2 Time-Limited Aging Analyses on
Reactor Vessel Integrity for Subsequent License
Renewal,” August 2020**

(108 Total Pages, including cover sheets)

Point Beach Units 1 and 2 Time-Limited Aging Analyses on Reactor Vessel Integrity for Subsequent License Renewal



WCAP-18555-NP
Revision 1

**Point Beach Units 1 and 2 Time-Limited Aging Analyses on
Reactor Vessel Integrity for Subsequent License Renewal**

D. Brett Lynch*

Reactor Vessel/Containment Vessel (RV/CV) Design and Analysis

August 2020

Reviewers: Benjamin E. Mays*
License Renewal, Radiation Analysis, and Nuclear Operations

Andrew E. Hawk*
Nuclear Operations & Radiation Analysis

Approved: Lynn A. Patterson*, Manager
RV/CV Design and Analysis

Laurent P. Houssay*, Manager
Nuclear Operations & Radiation Analysis

*Electronically approved records are authenticated in the electronic document management system.

Westinghouse Electric Company LLC
1000 Westinghouse Dr.
Cranberry Township, PA 16066

© 2020 Westinghouse Electric Company LLC
All Rights Reserved

RECORD OF REVISIONS

Revision 0: Original Issue

Revision 1: Revision 1 is issued to incorporate NextEra comments on Revision 0 and to incorporate updated Point Beach Unit 2 fluence results. It is noted that the conclusions of the report remain unchanged, as the fluence values utilized in Revision 0 were either unchanged or bounding compared to the Revision 1 values. Changes are marked with change bars.

TABLE OF CONTENTS

LIST OF TABLES iv

LIST OF FIGURES vii

1 TIME-LIMITED AGING ANALYSIS..... 1-1

2 CALCULATED NEUTRON FLUENCE FOR POINT BEACH UNITS 1 AND 2.....2-1

 2.1 INTRODUCTION.....2-1

 2.2 DISCRETE ORDINATES ANALYSIS.....2-1

 2.3 DOSIMETRY COMPARISONS2-3

 2.4 POINT BEACH UNIT 1 NEUTRON FLUENCE DATA TABLES.....2-12

 2.5 POINT BEACH UNIT 2 NEUTRON FLUENCE DATA TABLES.....2-33

3 FRACTURE TOUGHNESS PROPERTIES 3-1

4 SURVEILLANCE DATA.....4-1

5 CHEMISTRY FACTORS.....5-1

6 PRESSURIZED THERMAL SHOCK EVALUATION6-1

7 HEATUP AND COOLDOWN PRESSURE-TEMPERATURE LIMIT CURVES7-1

 7.1 ADJUSTED REFERENCE TEMPERATURES CALCULATION.....7-1

 7.2 P-T LIMIT CURVES APPLICABILITY7-12

8 SURVEILLANCE CAPSULE WITHDRAWAL SCHEDULES8-1

9 REFERENCES.....9-1

APPENDIX A POINT BEACH UNITS 1 AND 2 SURVEILLANCE PROGRAM CREDIBILITY
EVALUATIONA-1

LIST OF TABLES

Table 1-1	Evaluation of Time-Limited Aging Analyses Per the Criteria of 10 CFR 54.3	1-1
Table 2.4-1	Point Beach Unit 1 Calculated Maximum Fast Neutron Fluence Rate ($E > 1.0$ MeV) at the RPV Clad/Base Metal Interface.....	2-12
Table 2.4-2	Point Beach Unit 1 Calculated Maximum Fast Neutron Fluence ($E > 1.0$ MeV) at the RPV Clad/Base Metal Interface.....	2-14
Table 2.4-3	Point Beach Unit 1 Calculated Maximum Iron Atom Displacement Rate at the RPV Clad/Base Metal Interface.....	2-16
Table 2.4-4	Point Beach Unit 1 Calculated Maximum Iron Atom Displacements at the RPV Clad/Base Metal Interface.....	2-18
Table 2.4-5	Point Beach Unit 1 Calculated Maximum Fast Neutron Fluence ($E > 1.0$ MeV) at RPV Welds and Shells.....	2-20
Table 2.4-6	Point Beach Unit 1 Calculated Maximum Iron Atom Displacements at RPV Welds and Shells.....	2-21
Table 2.4-7	Point Beach Unit 1 Calculated Fast Neutron Fluence Rate ($E > 1.0$ MeV) at Surveillance Capsule Locations.....	2-22
Table 2.4-8	Point Beach Unit 1 Calculated Fast Neutron Fluence ($E > 1.0$ MeV) at Surveillance Capsules.....	2-23
Table 2.4-9	Point Beach Unit 1 Calculated Iron Atom Displacement Rate at Surveillance Capsule Locations.....	2-24
Table 2.4-10	Point Beach Unit 1 Calculated Iron Atom Displacements at Surveillance Capsules.....	2-25
Table 2.4-11	Point Beach Unit 1 Calculated Surveillance Capsule Lead Factors	2-26
Table 2.4-12	Point Beach Unit 1 Ex-Vessel Neutron Dosimetry Summary.....	2-27
Table 2.4-13	Point Beach Unit 1 Comparison of Measured to Calculated Threshold Reaction Rates–In-Vessel Capsules.....	2-28
Table 2.4-14	Point Beach Unit 1 Comparison of Measured to Calculated Threshold Reaction Rates – Ex-Vessel Midplane Capsules.....	2-29
Table 2.4-15	Point Beach Unit 1 Comparison of Measured to Calculated Threshold Reaction Rates – Ex-Vessel Off-Midplane Capsules.....	2-30
Table 2.4-16	Point Beach Unit 1 Comparison of Best-Estimate to Calculated Exposure Rates – In-Vessel Capsules.....	2-30
Table 2.4-17	Point Beach Unit 1 Comparison of Best-Estimate to Calculated Exposure Rates – Ex-Vessel Midplane Capsules.....	2-31
Table 2.4-18	Point Beach Unit 1 Total Database Summary (M/C Reaction Rate Ratios).....	2-32
Table 2.4-19	Point Beach Unit 1 Total Database Summary (Integral Exposure Rate Ratios).....	2-32

Table 2.5-1	Point Beach Unit 2 Calculated Maximum Fast Neutron Fluence Rate ($E > 1.0$ MeV) at the RPV Clad/Base Metal Interface.....	2-33
Table 2.5-2	Point Beach Unit 2 Calculated Maximum Fast Neutron Fluence ($E > 1.0$ MeV) at the RPV Clad/Base Metal Interface.....	2-35
Table 2.5-3	Point Beach Unit 2 Calculated Maximum Iron Atom Displacement Rate at the RPV Clad/Base Metal Interface.....	2-37
Table 2.5-4	Point Beach Unit 2 Calculated Maximum Iron Atom Displacements at the RPV Clad/Base Metal Interface.....	2-39
Table 2.5-5	Point Beach Unit 2 Pressure Vessel Maximum Fast Neutron Fluence	2-41
Table 2.5-6	Point Beach Unit 2 Calculated Maximum Iron Atom Displacements at RPV Welds and Shells.....	2-42
Table 2.5-7	Point Beach Unit 2 Calculated Fast Neutron Fluence Rate ($E > 1.0$ MeV) at Surveillance Capsule Locations.....	2-43
Table 2.5-8	Point Beach Unit 2 Calculated Neutron Fluence ($E > 1.0$ MeV) at the Surveillance Capsule Center.....	2-44
Table 2.5-9	Point Beach Unit 2 Calculated Iron Atom Displacement Rate at Surveillance Capsule Locations.....	2-45
Table 2.5-10	Point Beach Unit 2 Calculated Iron Atom Displacements at Surveillance Capsules.....	2-46
Table 2.5-11	Point Beach Unit 2 Calculated Surveillance Capsule Lead Factors	2-47
Table 2.5-12	Point Beach Unit 2 Ex-Vessel Neutron Dosimetry Summary.....	2-48
Table 2.5-13	Point Beach Unit 2 Comparison of Measured to Calculated Threshold Reaction Rates – In-Vessel Capsules.....	2-49
Table 2.5-14	Point Beach Unit 2 Comparison of Measured to Calculated Threshold Reaction Rates – Ex-Vessel Midplane Capsules.....	2-50
Table 2.5-15	Point Beach Unit 2 Comparison of Measured to Calculated Threshold Reaction Rates – Ex-Vessel Off-Midplane Capsules.....	2-51
Table 2.5-16	Point Beach Unit 2 Comparison of Best-Estimate to Calculated Exposure Rates – In-Vessel Capsules.....	2-51
Table 2.5-17	Point Beach Unit 2 Comparison of Best-Estimate to Calculated Exposure Rates – Ex-Vessel Midplane Capsules.....	2-52
Table 2.5-18	Point Beach Unit 2 Total Database Summary (M/C Reaction Rate Ratios).....	2-53
Table 2.5-19	Point Beach Unit 2 Total Database Summary (Integral Exposure Rate Ratios).....	2-53
Table 3-1	Point Beach Units 1 and 2 Reactor Vessel Beltline and Surveillance Material Properties and Chemistry	3-3
Table 4-1	Point Beach Unit 1 Surveillance Program Results.....	4-2

Table 4-2	Point Beach Unit 2 Surveillance Program Results.....	4-2
Table 5-1	Calculation of Chemistry Factors Using Point Beach Unit 1 Surveillance Capsule Data	5-2
Table 5-2	Calculation of Chemistry Factors Using Point Beach Unit 2 Surveillance Capsule Data	5-3
Table 5-3	Position 1.1 and 2.1 Chemistry Factors for Point Beach Units 1 and 2.....	5-4
Table 6-1	RT _{PTS} Calculations for Point Beach Units 1 and 2 Reactor Vessel Beltline Materials.....	6-2
Table 7-1	Point Beach Units 1 and 2 Fluence and Fluence Factor Values for the Surface, 1/4T, and 3/4T Locations at 50 EFPY.....	7-2
Table 7-2	Point Beach Units 1 and 2 Fluence and Fluence Factor Values for the Surface, 1/4T, and 3/4T Locations at 72 EFPY.....	7-3
Table 7-3	Calculation of the Point Beach Units 1 and 2 ART Values at the 1/4T Location for the Reactor Vessel Beltline Materials at EOLE (50 EFPY).....	7-4
Table 7-4	Calculation of the Point Beach Units 1 and 2 ART Values at the 3/4T Location for the Reactor Vessel Beltline Materials at EOLE (50 EFPY).....	7-6
Table 7-5	Calculation of the Point Beach Units 1 and 2 ART Values at the 1/4T Location for the Reactor Vessel Beltline Materials at SLR (72 EFPY).....	7-8
Table 7-6	Calculation of the Point Beach Units 1 and 2 ART Values at the 3/4T Location for the Reactor Vessel Beltline Materials at SLR (72 EFPY).....	7-10
Table 7-7	Summary of the Limiting ART Values.....	7-12
Table 8-1	Point Beach Unit 1 Recommended Surveillance Capsule Withdrawal Schedule	8-3
Table 8-2	Point Beach Unit 2 Recommended Surveillance Capsule Withdrawal Schedule	8-3
Table A-1	Regulatory Guide 1.99, Revision 2, Credibility Criteria	A-1
Table A-2	Calculation of Interim Chemistry Factors for the Credibility Evaluation Using Point Beach Unit 1 Surveillance Capsule Data Only	A-4
Table A-3	Point Beach Unit 1 Surveillance Capsule Data Scatter about the Best-Fit Line.....	A-5
Table A-4	Calculation of Residual versus Fast Fluence	A-6
Table A-5	Calculation of Interim Chemistry Factors for the Credibility Evaluation Using Point Beach Unit 2 Surveillance Capsule Data Only	A-9
Table A-6	Point Beach Unit 2 Surveillance Capsule Data Scatter about the Best-Fit Line Using All Available Surveillance Data.....	A-10
Table A-7	Calculation of Residual versus Fast Fluence	A-11

LIST OF FIGURES

Figure 2-1	Point Beach Units 1 and 2 Top View of RAPTOR-M3G Model – Core Midplane ($Z = 0$ cm)	2-6
Figure 2-2	Point Beach Units 1 and 2 Top View of RAPTOR-M3G Model Above Ring Girder ($Z = 264$ cm).....	2-7
Figure 2-3	Point Beach Units 1 and 2 Top View of RAPTOR-M3G Model Through Nozzle Centerline ($Z = 332$ cm).....	2-8
Figure 2-4	Point Beach Units 1 and 2 Side View of RAPTOR-M3G Model Through Support Column ($\theta = 0^\circ$).....	2-9
Figure 2-5	Point Beach Units 1 and 2 Side View of RAPTOR-M3G Model Through Support Column ($\theta = 31.5^\circ$).....	2-10
Figure 2-6	Point Beach Units 1 and 2 Side View of RAPTOR-M3G Model Through Support Column ($\theta = 60^\circ$).....	2-11
Figure 4-1	RPV Base Metal Material Identifications for Point Beach Units 1 and 2.....	3-2

EXECUTIVE SUMMARY

This report presents the time-limited aging analyses (TLAAs) for the Point Beach Units 1 and 2 reactor pressure vessels (RPVs) with respect to reactor vessel integrity (RVI) in accordance with the requirements of the License Renewal Rule, 10 CFR Part 54. TLAAs are calculations that address safety-related aspects of the RPV within the bounds of the current 60-year license. These calculations must also be evaluated to account for an extended period of operation (80 years) also termed subsequent (or second) license renewal (SLR) period.

Point Beach Units 1 and 2 are currently licensed through 60 years of operation; therefore, with a 20-year license extension, the SLR term is applicable through 80 years of operation. The evaluations in this report for 60 years of operation are applicable through 50 effective full-power years (EFPY) for Units 1 and 2, which is deemed end-of-license extension (EOLE). Similarly, evaluations in this report performed at 80 years of operation are applicable through 72 EFPY, which is deemed the end of SLR. Updated neutron fluence evaluations were used to identify the Point Beach Units 1 and 2 beltline materials, i.e., materials with a SLR fluence $\geq 10^{17}$ n/cm² ($E < 1.0$ MeV), and as input to the reactor vessel (RV) integrity evaluations in support of current plant operations and SLR.

A summary of the Point Beach Units 1 and 2 RVI TLAAs follows. Based on the results presented herein, it is concluded that the Point Beach Units 1 and 2 RPVs will continue to meet RPV integrity regulatory requirements through SLR.

Fluence

The RV beltline neutron fluence values applicable to a postulated 20-year license renewal period were calculated for the Point Beach Units 1 and 2 materials. The analysis methodologies used to calculate the Point Beach Units 1 and 2 vessel fluence values satisfy the requirements set forth in Regulatory Guide 1.190. See Section 2 for more details.

Pressurized Thermal Shock

The RT_{PTS} values of all of the beltline materials in the Point Beach Units 1 and 2 RPV are below the RT_{PTS} screening criteria of 270°F for base metal and/or longitudinal welds, and 300°F for circumferentially oriented welds (per 10 CFR 50.61), through SLR (72 EFPY).

Determination of Adjusted Reference Temperatures and Pressure-Temperature Limit Curve Applicability

Adjusted reference temperatures (ARTs) are calculated at 50 EFPY and 72 EFPY. The ART values are used to perform an applicability check on the Point Beach Units 1 and 2 50 EFPY pressure-temperature (P-T) limit curves currently implemented in the Pressure Temperature Limits Report (PTLR). With the consideration of the Point Beach Units 1 and 2 updated fluence projections and revised Position 2.1 CF value, the existing EOLE P-T limit curves continue to remain valid through at least EOLE (50 EFPY). More precisely, the current P-T limit curves could be extended to 52 EFPY. This conclusion considers the reactor vessel inlet/outlet/safety injection nozzles, as required by Regulatory Issue Summary (RIS) 2014-11. See Section 7 for more details.

Surveillance Capsule Withdrawal Schedule

With consideration of a 20-year license renewal to 80 years of operation (72 EFPY), a change to the capsule withdrawal schedule is recommended for Point Beach Units 1 and 2. The only capsule which contains the limiting weld materials of both Point Beach Units 1 and 2 is the supplemental capsule currently residing in Point Beach Unit 2. In order to support SLR, this capsule should be delayed till a refueling outage after the supplemental capsule reaches a fluence equivalent to the maximum Point Beach Units 1 and 2 reactor vessel fluence at 80 years, which will be achieved when Point Beach Unit 2 reaches 51 EFPY. See Section 8 for more details.

In addition to the RV integrity TLAA evaluations, the Point Beach Units 1 and 2 surveillance data credibility evaluation is contained in Appendix A of this report.

Revision 0 of this report presented the Point Beach Unit 2 vessel fluence values based on preliminary, unverified results. Revision 1 of this report incorporates verified Unit 2 fluence values into the results. The preliminary Unit 2 reactor vessel and surveillance capsule fluence values reported in Revision 0 have been verified to be greater than or equal to the verified values; therefore, all previous results are conservative.

1 TIME-LIMITED AGING ANALYSIS

Time-limited aging analyses (TLAAs) are those licensee calculations that:

1. Consider the effects of aging
2. Involve time-limited assumptions defined by the current operating term (e.g., 60 years)
3. Involve structures, systems, and components (SSCs) within the scope of license renewal
4. Involve conclusions or provide the basis for conclusions related to the capability of the SSCs to perform its intended functions
5. Were determined to be relevant by the licensee in making a safety determination
6. Are contained or incorporated by reference in the current licensing basis (CLB)

The potential TLAAs for the RPV for SLR are identified in Table 1-1 along with indication of whether or not they meet the six criteria of 10 CFR 54.3 [Ref. 1] for TLAAs. The purpose of this report is to evaluate beltline materials with respect to RVI TLAAs.

Table 1-1 Evaluation of Time-Limited Aging Analyses Per the Criteria of 10 CFR 54.3

Time-Limited Aging Analysis	Calculated Fluence	Pressurized Thermal Shock	Upper-Shelf Energy^(a)	Pressure-Temperature Limits for Heatup and Cooldown
Considers the Effects of Aging	YES	YES	YES	YES
Involves Time-Limited Assumptions Defined by the Current Operating Term	YES	YES	YES	YES
Involves SSC Within the Scope of License Renewal	YES	YES	YES	YES
Involves Conclusions or Provides the Basis for Conclusions Related to the Capability of SSC to Perform Its Intended Function	YES	YES	YES	YES
Determined to be Relevant by the Licensee in Making a Safety Determination	YES	YES	YES	YES
Contained or Incorporated by Reference in the CLB	YES	YES	YES	YES

Note:

(a) The upper-shelf energy (USE) analysis is outside the scope of this report.

2 CALCULATED NEUTRON FLUENCE FOR POINT BEACH UNITS 1 AND 2

2.1 INTRODUCTION

This section describes a discrete ordinates (S_n) transport analysis performed for the Point Beach Units 1 and 2 reactor to determine the neutron radiation environment within the reactor pressure vessel and surveillance capsules. In this analysis, fast neutron exposure parameters in terms of fast neutron ($E > 1.0$ MeV) fluence and iron atom displacements (dpa) were established on a fuel-cycle-specific basis. Comparisons of the results from the dosimetry evaluations with the analytical predictions served to validate the plant-specific neutron transport calculations. These validated calculations subsequently form the basis for projections of the neutron exposure of the reactor pressure vessel for operating periods extending to 72 EFPY.

The use of fast neutron ($E > 1.0$ MeV) fluence to correlate measured material property changes to the neutron exposure of the material has traditionally been accepted for the development of damage trend curves as well as for the implementation of trend curve data to assess the condition of the vessel. However, it has been suggested that an exposure model that accounts for differences in neutron energy spectra between surveillance capsule locations and positions within the vessel wall could lead to an improvement in the uncertainties associated with damage trend curves and improved accuracy in the evaluation of damage gradients through the reactor vessel wall.

Because of this potential shift away from a threshold fluence toward an energy-dependent damage function for data correlation, ASTM Standard Practice E853-18, "Standard Practice for Analysis and Interpretation of Light-Water Reactor Surveillance Neutron Exposure Results" [Ref. 2] recommends reporting displacements per iron atom along with fluence ($E > 1.0$ MeV) to provide a database for future reference. The energy-dependent dpa function to be used for this evaluation is specified in ASTM Standard Practice E693-94, "Standard Practice for Characterizing Neutron Exposures in Iron and Low Alloy Steels in Terms of Displacements per Atom" [Ref. 3]. The application of the dpa parameter to the assessment of embrittlement gradients through the thickness of the reactor vessel wall has been promulgated in Revision 2 to RG 1.99, "Radiation Embrittlement of Reactor Vessel Materials" [Ref. 4].

All the calculations and dosimetry evaluations described in this section were based on nuclear cross-section data derived from ENDF/B-VI. Furthermore, the neutron transport and dosimetry evaluation methodologies follow the guidance of Regulatory Guide 1.190 [Ref. 5]. Additionally, the methods used to develop the calculated pressure vessel fluence are consistent with the NRC-approved methodology described in WCAP-18124-NP-A [Ref. 6].

2.2 DISCRETE ORDINATES ANALYSIS

Discrete ordinates transport calculations were performed on a fuel-cycle-specific basis to determine the neutron and gamma ray environment within the reactor geometry. The specific methods applied are consistent with those described in WCAP-18124-NP-A [Ref. 6].

All the transport calculations were carried out using the three-dimensional discrete ordinates code RAPTOR-M3G and the BUGLE-96 cross-section library. The BUGLE-96 library provides a 67-group coupled neutron-gamma ray cross-section data set produced specifically for light water reactor applications.

In these analyses, anisotropic scattering was treated with a P_5 Legendre expansion and the angular discretization was modeled with an S_{16} order of angular quadrature. Energy- and space-dependent core power distributions, as well as system operating temperatures, were treated on a fuel-cycle-specific basis.

A top view of the RAPTOR-M3G model at the core midplane is shown in Figure 2-1. In this figure, a single quadrant is depicted. A top view of the RAPTOR-M3G model through the nozzle centerline is shown in Figure 2-3. Side views of the RAPTOR-M3G model of the reactor are shown in Figure 2-4 through Figure 2-6. The model extends radially from the centerline of the reactor core out to a location interior to the concrete bioshield, and over an axial span from an elevation nine feet below the active fuel to eight feet above the active fuel.

In addition to the core, reactor vessel internals, RPV, and concrete bioshield, the RAPTOR-M3G model developed for this quadrant geometry includes explicit representations of the surveillance capsules, RPV cladding, and the insulation located external to the RPV. The RPV supports extending through the bioshield, and various cut-outs in the bioshield, are included as well.

From a neutronic standpoint, the inclusion of the surveillance capsules and associated support structure in the analytical model is significant. Since the presence of the capsules and structure has a marked impact on the magnitude of the neutron flux as well as on the relative neutron and gamma ray spectra at dosimetry locations within the capsules, a meaningful evaluation of the radiation environment internal to the capsules can be made only when these perturbation effects are properly accounted for in the analysis.

In developing the RAPTOR-M3G model of the reactor geometry shown in Figure 2-1 through Figure 2-6, nominal design dimensions were employed for the various structural components. Coolant above the active core assumed the same density as the core outlet conditions, and coolant below the active core assumed the same density as the core inlet conditions. These coolant temperatures were varied on a cycle-specific basis. The reactor core itself was treated as a homogeneous mixture of fuel, cladding, water, and miscellaneous core structures.

The RAPTOR-M3G model consisted of 256 radial by 214 azimuthal by 377 axial intervals. Mesh sizes were chosen to assure that proper convergence of the inner iterations was achieved on a pointwise basis. The pointwise inner iteration flux convergence criterion utilized in the calculations was set at a value of 0.001. A review of the results indicates that all the neutron and gamma groups fully converged for all cycles.

For Point Beach Unit 1, neutron exposure data pertinent to the RPV clad/base metal interface are given in Tables 2.4-1 and 2.4-2 for neutron fluence rate ($E > 1.0$ MeV) and fluence ($E > 1.0$ MeV), respectively, and in Tables 2.4-3 and 2.4-4 for dpa/s and dpa, respectively. In each case, the data are provided for each operating cycle of the Point Beach Unit 1 reactor. Neutron fluence ($E > 1.0$ MeV) and dpa are also projected to future operating times extending to 72 EFPY. The projections use Cycle 37 as the basis for future projections with a 10% positive bias on peripheral assembly power. The RPV exposure data are presented in terms of the maximum exposure experienced by the pressure vessel at azimuthal angles of 0° , 15° , 30° , 45° , 60° , 75° , and 90° , and at the azimuthal location providing the maximum exposure relative to the core cardinal axes.

For Point Beach Unit 2, neutron exposure data pertinent to the RPV clad/base metal interface are given in Tables 2.5-1 and 2.5-2 for neutron fluence rate ($E > 1.0$ MeV) and fluence ($E > 1.0$ MeV), respectively, and in Tables 2.5-3 and 2.5-4 for dpa/s and dpa, respectively. In each case, the data are provided for each operating cycle of the Point Beach Unit 2 reactor. Neutron fluence ($E > 1.0$ MeV) and dpa are also projected to future operating times extending to 72 EFPY. The projections use Cycle 38 as the basis for future projections with a 10% positive bias on peripheral assembly power. The RPV exposure data are presented in terms of the maximum exposure experienced by the pressure vessel at azimuthal angles of 0° , 15° , 30° , 45° , 60° , 75° , and 90° , and at the azimuthal location providing the maximum exposure relative to the core cardinal axes.

The maximum projected fast neutron fluence ($E > 1.0$ MeV) and dpa of the various RPV materials are given Tables 2.4-5 and 2.4-6, respectively, for Point Beach Unit 1. Similarly, the maximum projected fast neutron fluence ($E > 1.0$ MeV) and dpa of the various RPV materials are given Tables 2.5-5 and 2.5-6, respectively, for Point Beach Unit 2. These neutron exposure data are the maximum values at either the RPV clad/base metal interface or the RPV outer surface. Note that for regions and materials above and below the core (e.g., inlet nozzle to nozzle belt forging weld and lower shell to lower head ring circumferential weld), the neutron exposure values at the RPV outer surface can be greater than those at the clad/base metal interface [Ref. 7].

Results of the discrete ordinates transport analyses pertinent to the surveillance capsule evaluations are provided in Tables 2.4-7 through 2.4-11 for Point Beach Unit 1, and Tables 2.5-7 through 2.5-11 for Point Beach Unit 2. In Tables 2.4-7 and 2.5-7 the calculated fast neutron fluence rate ($E > 1.0$ MeV) is provided at the geometric center of capsule locations as a function of irradiation time for Point Beach Units 1 and 2, respectively. In Tables 2.4-8 and 2.5-8 the calculated fast neutron fluence ($E > 1.0$ MeV) is provided for the individual capsules for Point Beach Units 1 and 2, respectively. Similar data presented in terms of iron atom displacement rate and integrated iron atom displacements are given in Tables 2.4-9 and 2.4-10, respectively, for Unit 1, and Tables 2.5-9 and 2.5-10, respectively, for Unit 2.

In Tables 2.4-11 and 2.5-11, lead factors associated with surveillance capsules are provided as a function of operating time for Point Beach Units 1 and 2, respectively. The lead factor is defined as the ratio of the neutron fluence ($E > 1.0$ MeV) at the geometric center of the surveillance capsule to the maximum neutron fluence ($E > 1.0$ MeV) at the RPV clad/base metal interface.

2.3 DOSIMETRY COMPARISONS

Six in-vessel surveillance capsules attached to the thermal shield were included in the Point Beach Units 1 and 2 reactor designs. The capsules were located at azimuthal angles of 77° and 257° (13° from the core cardinal axis), 67° and 247° (23° from the core cardinal axis), and 57° and 237° (33° from the core cardinal axis).

To supplement the neutron dosimetry provided by the sensor sets contained in the in-vessel surveillance capsules, multiple foil sensors were installed at several locations in the annular region located between the RPV thermal insulation and the concrete bioshield. These multiple foil sets were designed to provide measured reaction rate data sufficient to characterize the neutron spectra at these measurement locations. The ex-vessel neutron dosimetry (EVND) was installed at azimuthal locations of 0° , 15° , 30° , and 45° relative to the core cardinal axis prior to Unit 1 Cycle 17 and Unit 2 Cycle 15. A summary of the EVND

capsules irradiated during Unit 1 Cycles 17 through 24 and Unit 2 Cycles 15 through 20 are given in Table 2.4-12 and Table 2.5-12.

Comparisons of the measurement results from each of the in-vessel surveillance capsules withdrawn and tested to-date, and the ex-vessel sensor set irradiations with corresponding analytical predictions were used to demonstrate compliance with the requirements of Regulatory Guide 1.190 [Ref. 5] as well as to support the uncertainty estimates associated with the calculated exposure levels. These comparisons were examined on two levels. In the first instance, calculations of individual sensor reaction rates were compared directly with the measurement data from the counting laboratory. This level of comparison was not impacted by the least-squares evaluations of the sensor sets. In the second case, calculated values of neutron exposure rates in terms of fast neutron fluence rate ($E > 1.0$ MeV) and iron atom displacement rate were compared with the best-estimate exposure rates obtained from the least-squares evaluation.

In Table 2.4-13 and Table 2.5-13, comparisons of measurement-to-calculation (M/C) ratios are listed for the threshold sensors contained in the in-vessel surveillance capsules. From Table 2.4-13, it is noted that for the Unit 1 threshold reaction foils, the average of all M/C ratios for each reaction ranges from 0.85 to 1.11 with an overall average of 0.99 and an associated standard deviation of 10.8%. From Table 2.5-13, it is noted that for the Unit 2 threshold reaction foils, the average of all M/C ratios for each reaction ranges from 0.96 to 1.08 with an overall average of 1.01 and an associated standard deviation of 5.9%.

In Table 2.4-14 and Table 2.5-14, similar comparisons are provided for the sensor sets withdrawn from the midplane axial elevation measurement locations in the reactor cavity. From Table 2.4-14, it is noted that for the Unit 1 threshold reaction foils, the average of all M/C ratios for each reaction ranges from 0.82 to 0.88 with an overall average of 0.85 and an associated standard deviation of 4.1%. From Table 2.5-14, it is noted that for the Unit 2 threshold reaction foils, the average of all M/C ratios for each reaction ranges from 0.86 to 1.06 with an overall average of 0.90 and an associated standard deviation of 6.8%. The overall average was based on an equal weighting of the sensor types with no account taken of the spectral coverage of the individual sensors. Comparisons of the M/C ratios for the sensor sets withdrawn from the off-midplane measurement locations in the reactor cavity are provided in Table 2.4-15 and Table 2.5-15 for Units 1 and 2, respectively.

For Unit 1, in Table 2.4-16 and Table 2.4-17, best-estimate-to-calculation (BE/C) ratios for fast neutron fluence rate ($E > 1.0$ MeV) and iron atom displacement rate resulting from the least-squares evaluation of each sensor set are provided for both the in-vessel and midplane ex-vessel irradiations. For the in-vessel capsules, the average BE/C ratio is seen to be 0.95 with an associated standard deviation of 14.0% for fast neutron fluence rate ($E > 1.0$ MeV) and 0.98 with an associated standard deviation of 10.8% for iron atom displacement rate. The corresponding average BE/C ratios from the midplane ex-vessel irradiations are 0.82 with a standard deviation of 10.8% for fast neutron fluence rate ($E > 1.0$ MeV) and 0.83 with a standard deviation of 9.2% for iron atom displacement rate.

For Unit 2, in Table 2.5-16 and Table 2.5-17, best-estimate-to-calculation (BE/C) ratios for fast neutron fluence rate ($E > 1.0$ MeV) and iron atom displacement rate resulting from the least-squares evaluation of each sensor set are provided for both the in-vessel and midplane ex-vessel irradiations. For the in-vessel capsules, the average BE/C ratio is seen to be 1.01 with an associated standard deviation of 1.2% for fast neutron fluence rate ($E > 1.0$ MeV) and 1.02 with an associated standard deviation of 1.3% for iron atom displacement rate. The corresponding average BE/C ratios from the midplane ex-vessel irradiations are

0.87 with a standard deviation of 4.4% for fast neutron fluence rate ($E > 1.0$ MeV) and 0.89 with a standard deviation of 4.8% for iron atom displacement rate.

The data sets listed in Table 2.4-13 through Table 2.4-17 for Unit 1, and Table 2.5-13 through Table 2.5-17 for Unit 2, provide a validation of the results of the plant-specific neutron transport calculations. These data comparisons show that for the in-vessel locations, the measurements and calculations agree within the 20% criterion specified in Regulatory Guide 1.190. For the ex-vessel locations, the measurements and calculations agree well within the 30% criterion specified in Regulatory Guide 1.190.

The total database summary of the M/C comparisons based on the individual sensor reactions without recourse to the least-squares adjustment procedure is provided in Table 2.4-18 for Unit 1 and Table 2.5-18 for Unit 2. A similar comparison for exposure rates expressed in terms of fast neutron fluence rate ($E > 1.0$ MeV) and iron atom displacement rate is provided in Table 2.4-19 for Unit 1 and Table 2.5-19 for Unit 2.

For Unit 1, these data comparisons show similar results with the linear average M/C ratio of 0.92 in good agreement with the resultant least-squares BE/C ratios of 0.89 for fast neutron fluence rate ($E > 1.0$ MeV) and 0.91 for iron atom displacement rate. For Unit 2, these data comparisons show similar results with the linear average M/C ratio of 0.96 in good agreement with the resultant least-squares BE/C ratios of 0.94 for fast neutron fluence rate ($E > 1.0$ MeV) and 0.96 for iron atom displacement rate. The comparisons show that the $\pm 20\%$ (1σ) agreement between calculation and measurement required by Regulatory Guide 1.190 is met.

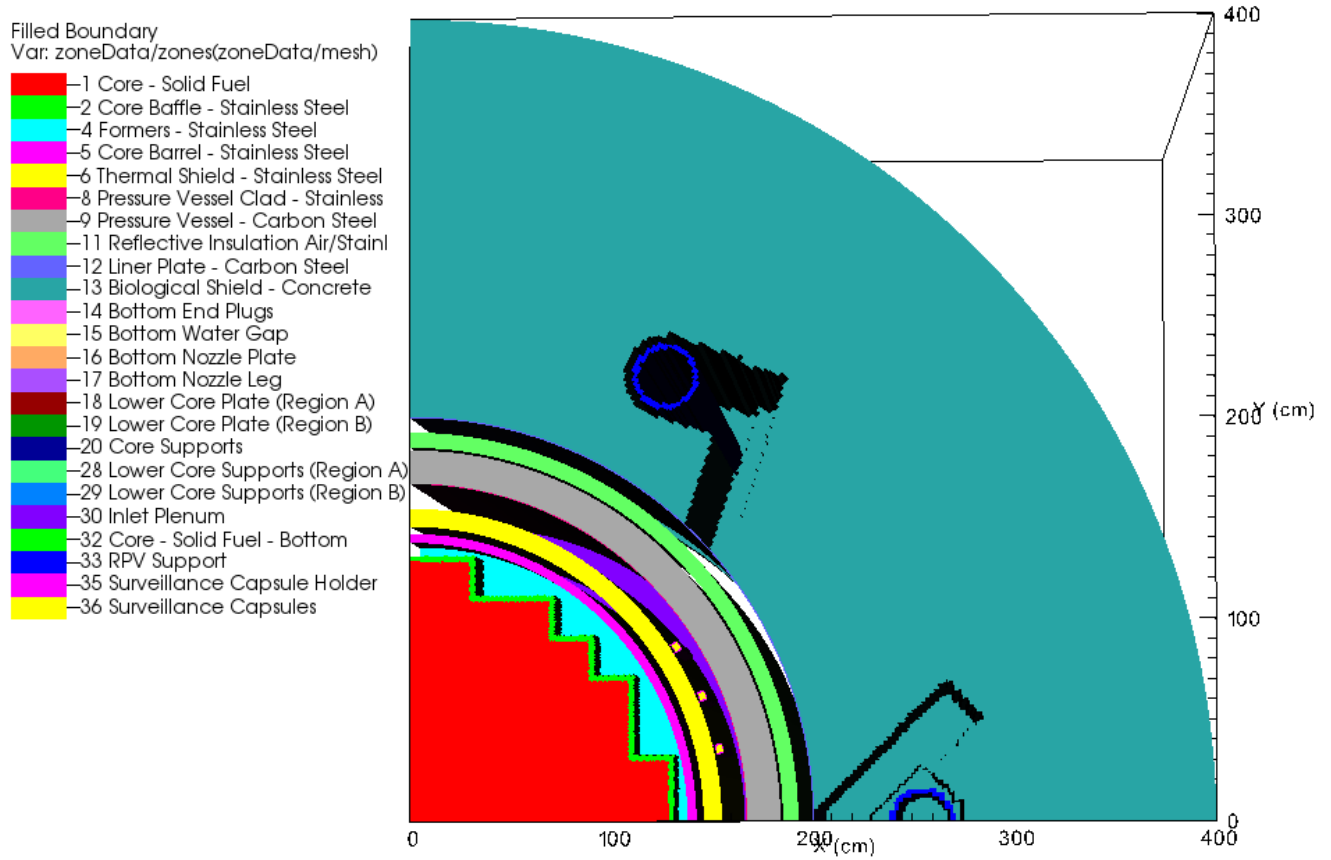


Figure 2-1 Top View of RAPTOR-M3G Model – Core Midplane (Z = 0 cm)

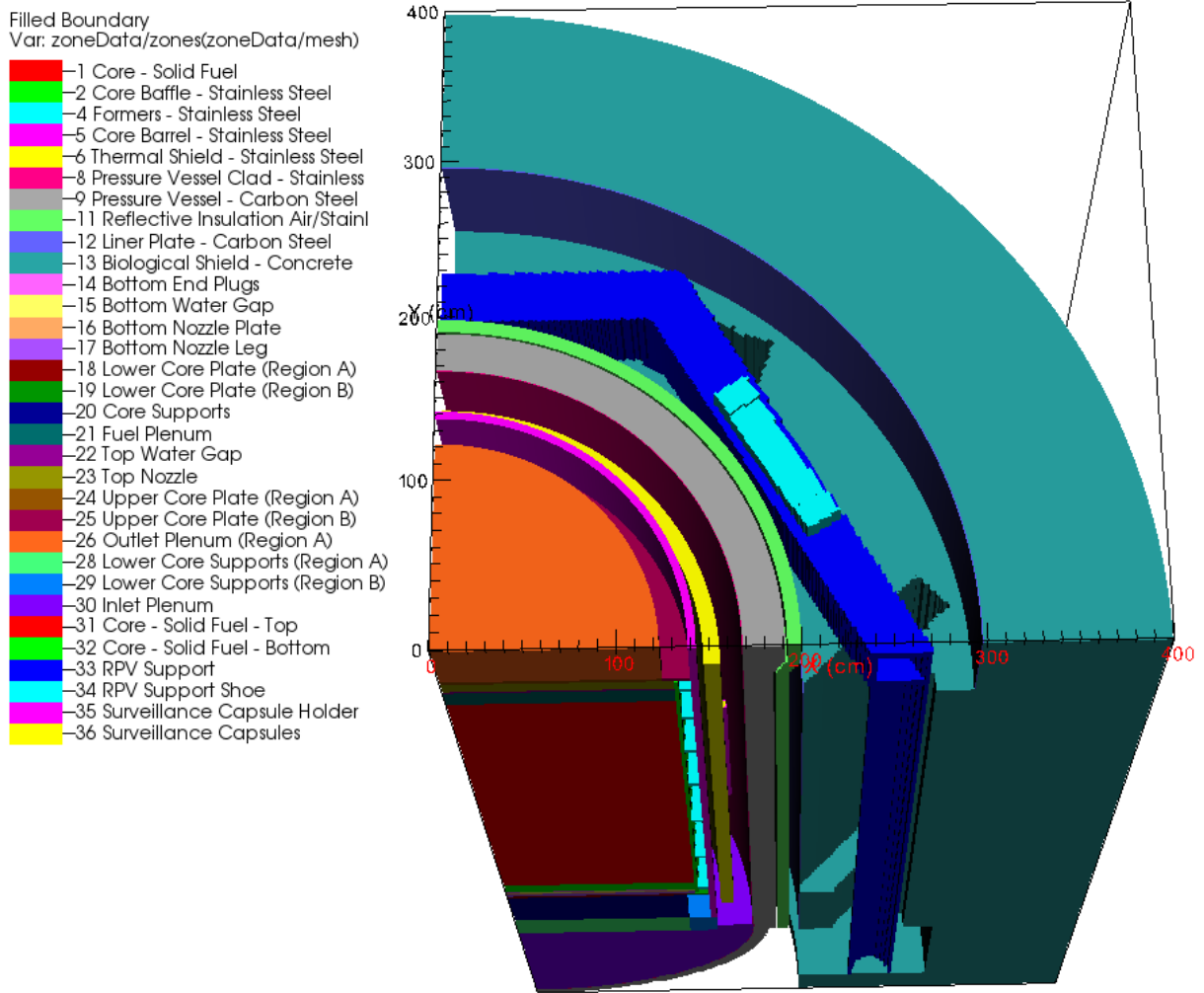


Figure 2-2 Top View of RAPTOR-M3G Model Above Ring Girder (Z = 264 cm)

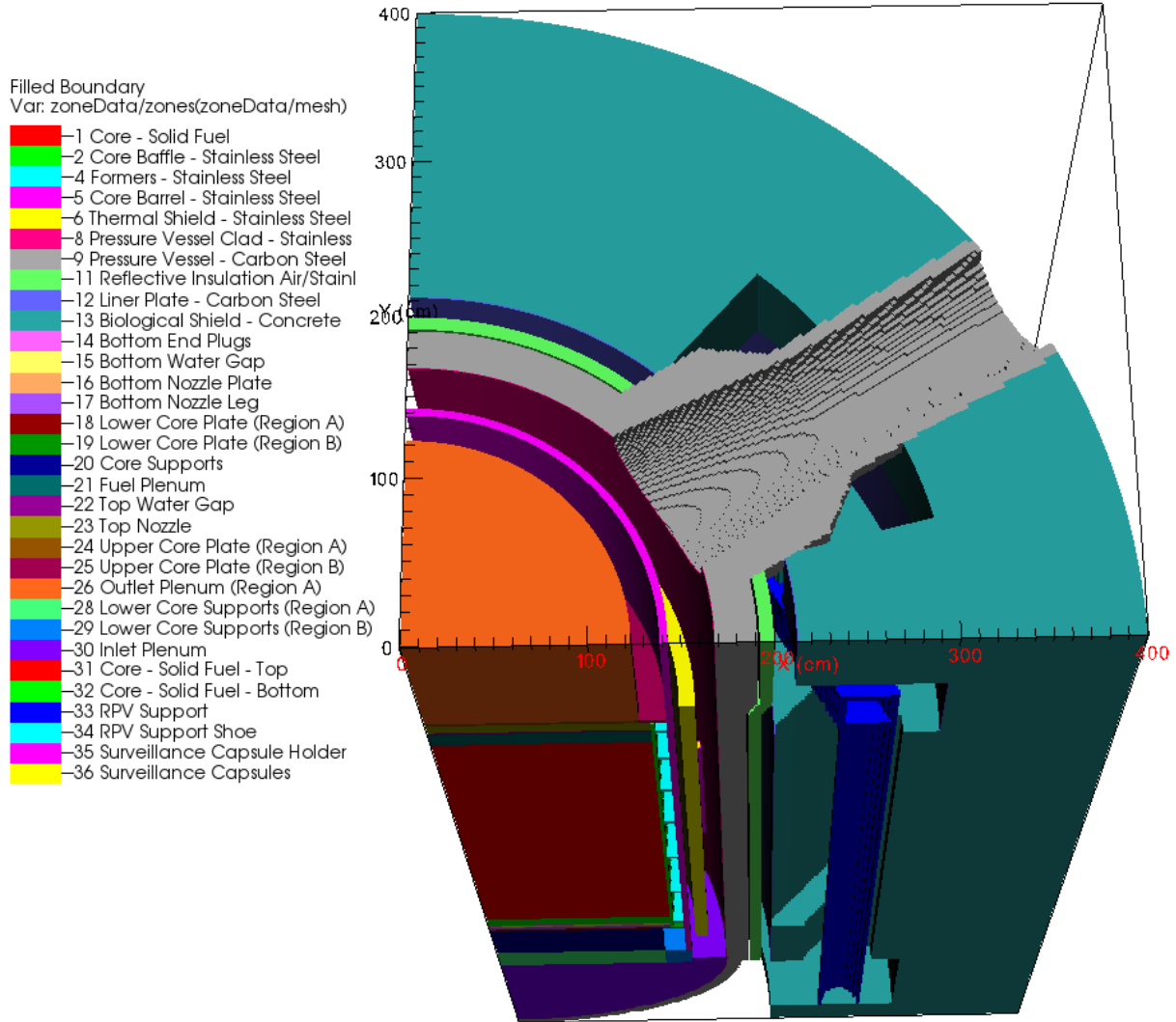


Figure 2-3 Top View of RAPTOR-M3G Model Through Nozzle Centerline (Z = 332 cm)

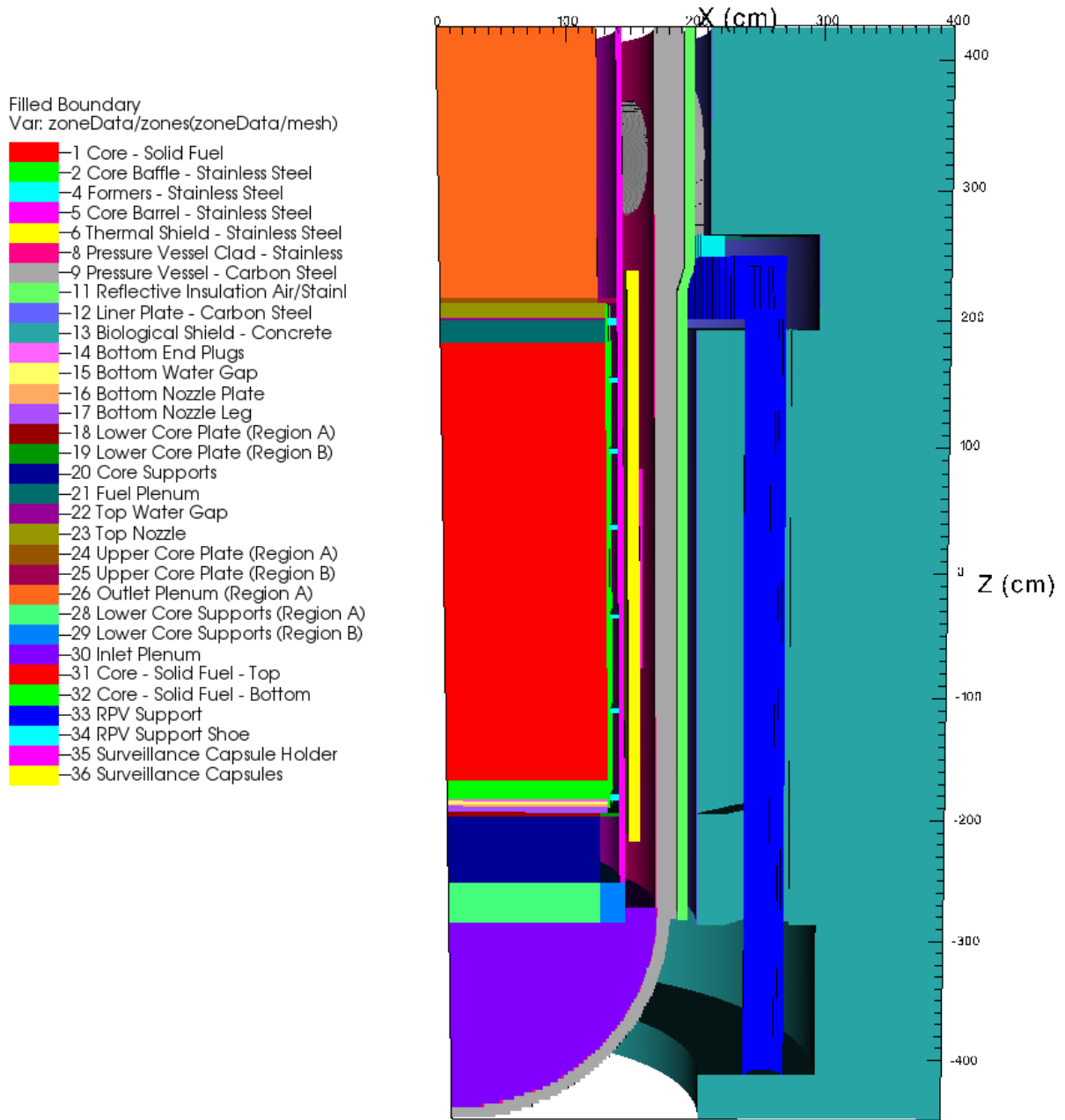


Figure 2-4 Side View of RAPTOR-M3G Model Through Support Column ($\theta = 0^\circ$)

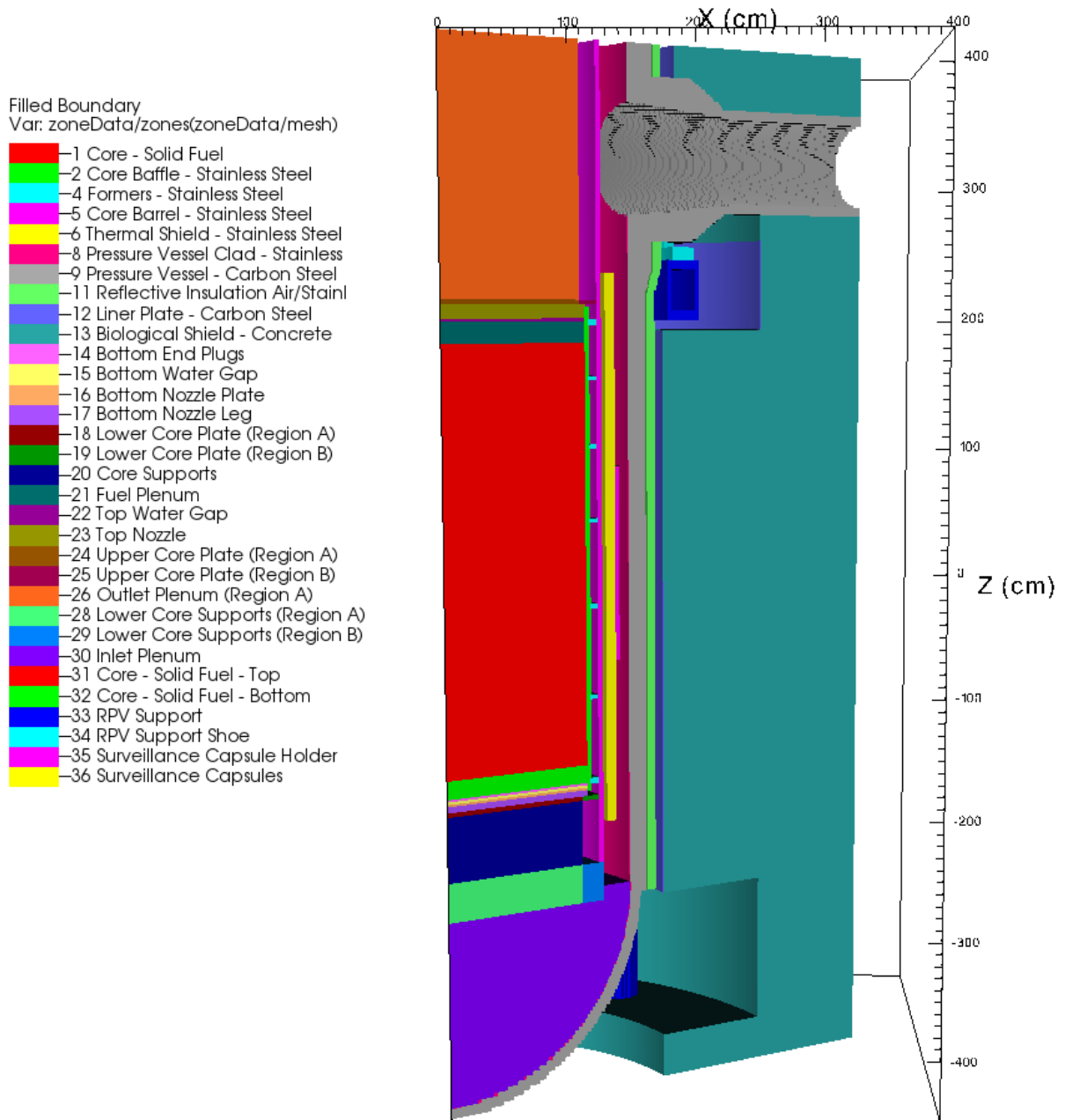


Figure 2-5 Side View of RAPTOR-M3G Model Through Support Column ($\theta = 31.5^\circ$)

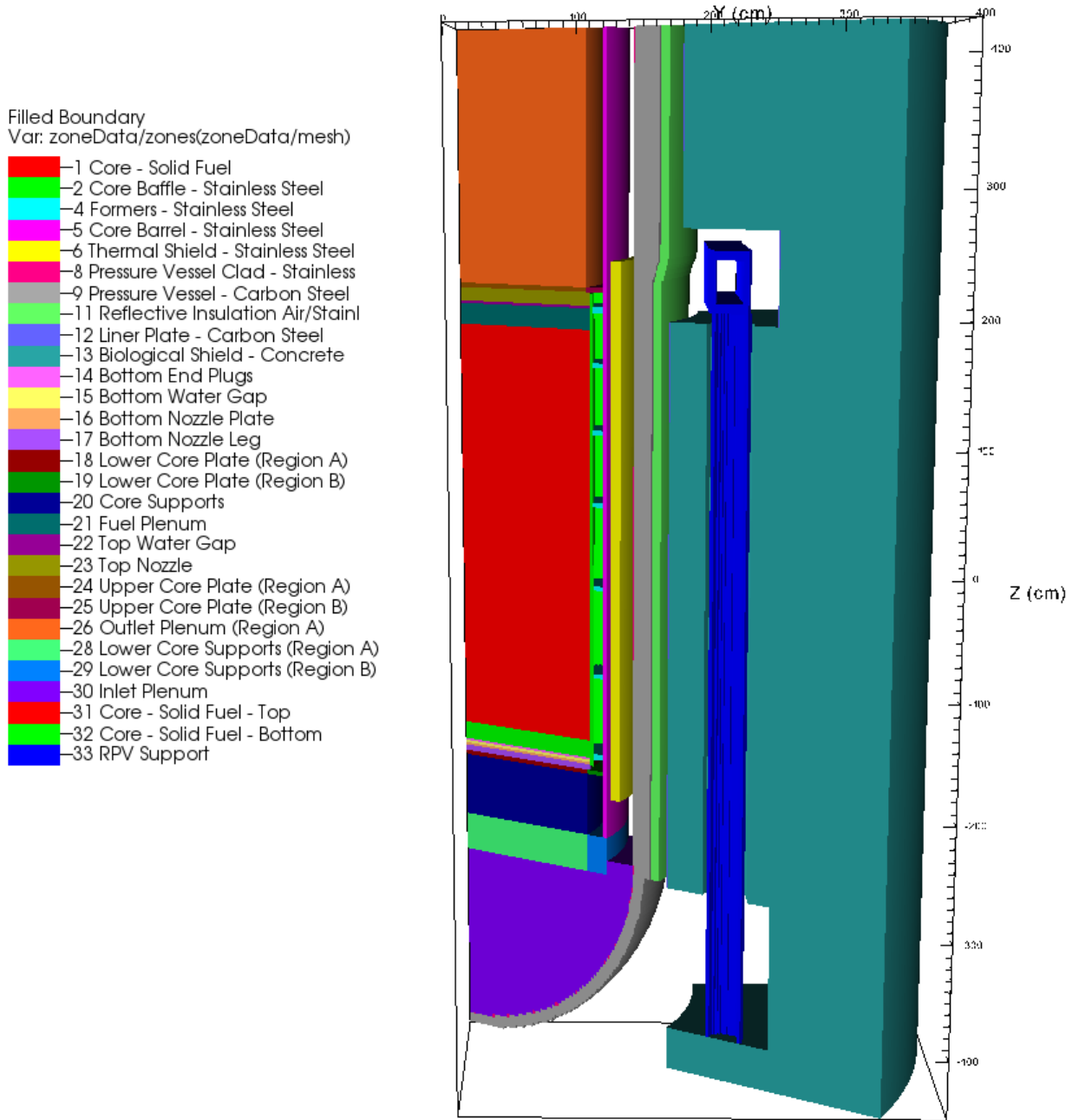


Figure 2-6 Side View of RAPTOR-M3G Model Through Support Column ($\theta = 60^\circ$)

2.4 POINT BEACH UNIT 1 NEUTRON FLUENCE DATA TABLES

Table 2.4-1 Point Beach Unit 1 Calculated Maximum Fast Neutron Fluence Rate ($E > 1.0$ MeV) at the RPV Clad/Base Metal Interface

Cycle	Cycle Length (EFPY)	Total Time (EFPY)	Fluence Rate (n/cm ² -s)								Elevation of Max. (cm)
			0°	15°	30°	45°	60°	75°	90°	Maximum ^(a)	
1	1.49	1.49	4.53E+10	2.62E+10	1.76E+10	1.54E+10	1.77E+10	2.69E+10	4.53E+10	4.53E+10	1.0
2	0.92	2.40	4.16E+10	2.46E+10	1.67E+10	1.44E+10	1.69E+10	2.48E+10	4.07E+10	4.16E+10	67.0
3	1.21	3.61	4.27E+10	2.52E+10	1.75E+10	1.50E+10	1.76E+10	2.58E+10	4.27E+10	4.27E+10	-3.0
4	0.70	4.31	4.73E+10	2.77E+10	1.94E+10	1.68E+10	1.95E+10	2.81E+10	4.71E+10	4.73E+10	-1.0
5	0.79	5.10	4.53E+10	2.75E+10	1.95E+10	1.70E+10	1.96E+10	2.79E+10	4.59E+10	4.59E+10	-73.0
6	0.81	5.91	4.24E+10	2.54E+10	1.89E+10	1.68E+10	1.89E+10	2.58E+10	4.26E+10	4.26E+10	-1.0
7	0.87	6.78	4.35E+10	2.53E+10	1.76E+10	1.50E+10	1.77E+10	2.58E+10	4.35E+10	4.35E+10	1.0
8	0.64	7.42	3.58E+10	2.08E+10	1.53E+10	1.45E+10	1.54E+10	2.11E+10	3.55E+10	3.58E+10	-1.0
9	0.60	8.02	3.22E+10	1.96E+10	1.48E+10	1.42E+10	1.50E+10	1.99E+10	3.25E+10	3.25E+10	-77.0
10	0.65	8.67	2.82E+10	1.85E+10	1.46E+10	1.43E+10	1.46E+10	1.85E+10	2.81E+10	2.82E+10	-81.0
11	0.61	9.28	3.08E+10	1.79E+10	1.23E+10	1.03E+10	1.23E+10	1.81E+10	3.08E+10	3.08E+10	-69.0
12	0.96	10.24	2.89E+10	1.89E+10	1.41E+10	1.22E+10	1.39E+10	1.85E+10	2.80E+10	2.89E+10	-67.0
13	0.79	11.03	2.94E+10	1.98E+10	1.50E+10	1.25E+10	1.51E+10	2.04E+10	2.96E+10	2.96E+10	65.0
14	0.84	11.88	2.80E+10	1.92E+10	1.48E+10	1.22E+10	1.48E+10	1.96E+10	2.81E+10	2.81E+10	1.0
15	0.84	12.72	2.81E+10	1.90E+10	1.41E+10	1.15E+10	1.42E+10	1.94E+10	2.81E+10	2.81E+10	5.0
16	0.85	13.57	2.90E+10	1.95E+10	1.47E+10	1.19E+10	1.48E+10	1.99E+10	2.89E+10	2.90E+10	3.0
17	0.83	14.40	2.96E+10	1.82E+10	1.29E+10	1.22E+10	1.30E+10	1.86E+10	2.96E+10	2.96E+10	65.0
18	0.83	15.23	2.74E+10	1.68E+10	1.16E+10	1.05E+10	1.17E+10	1.73E+10	2.74E+10	2.74E+10	65.0
19	0.86	16.08	2.63E+10	1.70E+10	1.26E+10	1.16E+10	1.27E+10	1.73E+10	2.62E+10	2.63E+10	65.0
20	0.79	16.88	3.06E+10	1.88E+10	1.29E+10	1.13E+10	1.32E+10	1.93E+10	3.06E+10	3.06E+10	65.0
21	0.89	17.77	2.67E+10	1.65E+10	1.29E+10	1.24E+10	1.30E+10	1.70E+10	2.68E+10	2.68E+10	65.0
22	0.85	18.62	2.83E+10	1.71E+10	1.27E+10	1.21E+10	1.28E+10	1.75E+10	2.83E+10	2.83E+10	65.0
23	0.87	19.49	2.71E+10	1.66E+10	1.24E+10	1.19E+10	1.26E+10	1.71E+10	2.72E+10	2.72E+10	65.0
24	0.98	20.47	2.65E+10	1.64E+10	1.21E+10	1.12E+10	1.22E+10	1.70E+10	2.66E+10	2.66E+10	65.0
25	1.21	21.67	2.81E+10	1.79E+10	1.36E+10	1.21E+10	1.40E+10	1.86E+10	2.82E+10	2.82E+10	65.0
26	1.25	22.93	2.59E+10	1.63E+10	1.21E+10	1.11E+10	1.23E+10	1.67E+10	2.57E+10	2.59E+10	65.0
27	1.28	24.20	2.93E+10	1.79E+10	1.30E+10	1.17E+10	1.29E+10	1.79E+10	2.88E+10	2.93E+10	65.0
28	1.42	25.62	2.79E+10	1.68E+10	1.32E+10	1.28E+10	1.33E+10	1.72E+10	2.79E+10	2.79E+10	65.0

Table 2.4-1 Point Beach Unit 1 Calculated Maximum Fast Neutron Fluence Rate ($E > 1.0$ MeV) at the RPV Clad/Base Metal Interface (Continued)

Cycle	Cycle Length (EFPY)	Total Time (EFPY)	Fluence Rate (n/cm ² -s)								Elevation of Max. (cm)
			0°	15°	30°	45°	60°	75°	90°	Maximum ^(a)	
29	1.29	26.91	3.11E+10	1.86E+10	1.31E+10	1.23E+10	1.32E+10	1.89E+10	3.09E+10	3.11E+10	65.0
30	1.33	28.24	2.91E+10	1.74E+10	1.16E+10	1.03E+10	1.17E+10	1.79E+10	2.91E+10	2.91E+10	65.0
31	1.32	29.56	2.28E+10	1.42E+10	1.18E+10	1.20E+10	1.20E+10	1.49E+10	2.32E+10	2.32E+10	65.0
32	1.27	30.83	2.56E+10	1.63E+10	1.29E+10	1.22E+10	1.30E+10	1.64E+10	2.55E+10	2.56E+10	-73.0
33	1.48	32.31	2.33E+10	1.57E+10	1.30E+10	1.23E+10	1.31E+10	1.58E+10	2.32E+10	2.33E+10	-73.0
34	1.22	33.53	3.28E+10	2.03E+10	1.46E+10	1.38E+10	1.50E+10	2.06E+10	3.28E+10	3.28E+10	-73.0
35	1.43	34.96	3.27E+10	2.11E+10	1.60E+10	1.44E+10	1.61E+10	2.13E+10	3.28E+10	3.28E+10	-73.0
36	1.34	36.30	3.48E+10	2.23E+10	1.52E+10	1.35E+10	1.53E+10	2.25E+10	3.48E+10	3.48E+10	-73.0
37	1.50	37.80	3.50E+10	2.04E+10	1.39E+10	1.29E+10	1.39E+10	2.06E+10	3.49E+10	3.50E+10	-73.0
38	1.37	39.17	3.29E+10	2.10E+10	1.54E+10	1.44E+10	1.57E+10	2.13E+10	3.29E+10	3.29E+10	-73.0
39	1.46	40.63	3.26E+10	2.08E+10	1.51E+10	1.37E+10	1.52E+10	2.10E+10	3.26E+10	3.26E+10	-73.0

Note:

(a) Maximum occurs at an azimuthal angle of 0°, or the octant symmetric angle, 90°.

Table 2.4-2 Point Beach Unit 1 Calculated Maximum Fast Neutron Fluence ($E > 1.0$ MeV) at the RPV Clad/Base Metal Interface

Cycle	Cycle Length (EFPY)	Total Time (EFPY)	Fluence (n/cm ²)								Elevation of Max. (cm)
			0°	15°	30°	45°	60°	75°	90°	Maximum ^(a)	
1	1.49	1.49	2.12E+18	1.23E+18	8.24E+17	7.21E+17	8.30E+17	1.26E+18	2.12E+18	2.12E+18	1.0
2	0.92	2.40	3.32E+18	1.93E+18	1.31E+18	1.14E+18	1.32E+18	1.97E+18	3.30E+18	3.32E+18	3.0
3	1.21	3.61	4.95E+18	2.89E+18	1.97E+18	1.71E+18	1.99E+18	2.96E+18	4.92E+18	4.95E+18	-1.0
4	0.70	4.31	5.99E+18	3.50E+18	2.40E+18	2.08E+18	2.42E+18	3.58E+18	5.96E+18	5.99E+18	-1.0
5	0.79	5.10	7.10E+18	4.16E+18	2.87E+18	2.50E+18	2.89E+18	4.26E+18	7.08E+18	7.10E+18	-1.0
6	0.81	5.91	8.19E+18	4.81E+18	3.36E+18	2.93E+18	3.38E+18	4.92E+18	8.18E+18	8.19E+18	-1.0
7	0.87	6.78	9.38E+18	5.50E+18	3.84E+18	3.34E+18	3.87E+18	5.63E+18	9.37E+18	9.38E+18	-1.0
8	0.64	7.42	1.01E+19	5.92E+18	4.16E+18	3.64E+18	4.18E+18	6.06E+18	1.01E+19	1.01E+19	-1.0
9	0.60	8.02	1.07E+19	6.27E+18	4.43E+18	3.90E+18	4.45E+18	6.42E+18	1.07E+19	1.07E+19	-1.0
10	0.65	8.67	1.12E+19	6.62E+18	4.70E+18	4.17E+18	4.73E+18	6.77E+18	1.12E+19	1.12E+19	-1.0
11	0.61	9.28	1.18E+19	6.96E+18	4.94E+18	4.37E+18	4.97E+18	7.12E+18	1.18E+19	1.18E+19	-1.0
12	0.96	10.24	1.27E+19	7.54E+18	5.36E+18	4.73E+18	5.38E+18	7.67E+18	1.27E+19	1.27E+19	-1.0
13	0.79	11.03	1.34E+19	8.02E+18	5.73E+18	5.04E+18	5.76E+18	8.18E+18	1.34E+19	1.34E+19	-1.0
14	0.84	11.88	1.42E+19	8.52E+18	6.12E+18	5.36E+18	6.15E+18	8.70E+18	1.41E+19	1.42E+19	-1.0
15	0.84	12.72	1.49E+19	9.02E+18	6.50E+18	5.67E+18	6.53E+18	9.22E+18	1.49E+19	1.49E+19	-1.0
16	0.85	13.57	1.57E+19	9.55E+18	6.89E+18	5.99E+18	6.93E+18	9.75E+18	1.57E+19	1.57E+19	-1.0
17	0.83	14.40	1.63E+19	9.97E+18	7.22E+18	6.30E+18	7.26E+18	1.02E+19	1.63E+19	1.63E+19	3.0
18	0.83	15.23	1.69E+19	1.04E+19	7.53E+18	6.58E+18	7.57E+18	1.06E+19	1.69E+19	1.69E+19	5.0
19	0.86	16.08	1.76E+19	1.08E+19	7.87E+18	6.89E+18	7.91E+18	1.10E+19	1.75E+19	1.76E+19	7.0
20	0.79	16.88	1.82E+19	1.12E+19	8.19E+18	7.18E+18	8.24E+18	1.14E+19	1.82E+19	1.82E+19	11.0
21	0.89	17.77	1.89E+19	1.16E+19	8.55E+18	7.53E+18	8.60E+18	1.19E+19	1.89E+19	1.89E+19	61.0
22	0.85	18.62	1.97E+19	1.20E+19	8.89E+18	7.85E+18	8.94E+18	1.23E+19	1.97E+19	1.97E+19	61.0
23	0.87	19.49	2.04E+19	1.25E+19	9.23E+18	8.18E+18	9.29E+18	1.27E+19	2.04E+19	2.04E+19	61.0
24	0.98	20.47	2.13E+19	1.30E+19	9.60E+18	8.52E+18	9.67E+18	1.33E+19	2.12E+19	2.13E+19	61.0
25	1.21	21.67	2.23E+19	1.37E+19	1.01E+19	8.98E+18	1.02E+19	1.40E+19	2.23E+19	2.23E+19	61.0
26	1.25	22.93	2.34E+19	1.43E+19	1.06E+19	9.42E+18	1.07E+19	1.46E+19	2.33E+19	2.34E+19	61.0
27	1.28	24.20	2.45E+19	1.50E+19	1.11E+19	9.89E+18	1.12E+19	1.54E+19	2.45E+19	2.45E+19	61.0
28	1.42	25.62	2.58E+19	1.58E+19	1.17E+19	1.05E+19	1.18E+19	1.61E+19	2.57E+19	2.58E+19	61.0
29	1.29	26.91	2.70E+19	1.65E+19	1.22E+19	1.10E+19	1.23E+19	1.69E+19	2.70E+19	2.70E+19	61.0
30	1.33	28.24	2.83E+19	1.73E+19	1.27E+19	1.14E+19	1.28E+19	1.76E+19	2.82E+19	2.83E+19	61.0

Table 2.4-2 Point Beach Unit 1 Calculated Maximum Fast Neutron Fluence ($E > 1.0$ MeV) at the RPV Clad/Base Metal Interface (Continued)

Cycle	Cycle Length (EFPY)	Total Time (EFPY)	Fluence (n/cm ²)								Elevation of Max. (cm)
			0°	15°	30°	45°	60°	75°	90°	Maximum ^(a)	
31	1.32	29.56	2.92E+19	1.78E+19	1.32E+19	1.19E+19	1.33E+19	1.83E+19	2.92E+19	2.92E+19	63.0
32	1.27	30.83	3.02E+19	1.85E+19	1.37E+19	1.24E+19	1.38E+19	1.89E+19	3.02E+19	3.02E+19	63.0
33	1.48	32.31	3.13E+19	1.92E+19	1.43E+19	1.29E+19	1.44E+19	1.96E+19	3.12E+19	3.13E+19	63.0
34	1.22	33.53	3.25E+19	1.99E+19	1.49E+19	1.35E+19	1.50E+19	2.04E+19	3.24E+19	3.25E+19	63.0
35	1.43	34.96	3.39E+19	2.08E+19	1.56E+19	1.41E+19	1.57E+19	2.13E+19	3.39E+19	3.39E+19	63.0
36	1.34	36.30	3.53E+19	2.17E+19	1.62E+19	1.47E+19	1.63E+19	2.22E+19	3.53E+19	3.53E+19	63.0
37	1.50	37.80	3.69E+19	2.26E+19	1.69E+19	1.53E+19	1.70E+19	2.32E+19	3.69E+19	3.69E+19	63.0
38	1.37	39.17	3.83E+19	2.35E+19	1.75E+19	1.59E+19	1.77E+19	2.40E+19	3.82E+19	3.83E+19	63.0
39	1.46	40.63	3.97E+19	2.44E+19	1.82E+19	1.65E+19	1.83E+19	2.50E+19	3.97E+19	3.97E+19	63.0
		42 ^(b)	4.13E+19	2.53E+19	1.88E+19	1.71E+19	1.90E+19	2.59E+19	4.13E+19	4.13E+19	63.0
		48 ^(b)	4.83E+19	2.93E+19	2.17E+19	1.97E+19	2.18E+19	3.00E+19	4.83E+19	4.83E+19	63.0
		54 ^(b)	5.53E+19	3.33E+19	2.45E+19	2.24E+19	2.47E+19	3.41E+19	5.53E+19	5.53E+19	65.0
		60 ^(b)	6.24E+19	3.74E+19	2.73E+19	2.50E+19	2.75E+19	3.83E+19	6.23E+19	6.24E+19	65.0
		66 ^(b)	6.94E+19	4.14E+19	3.02E+19	2.77E+19	3.04E+19	4.24E+19	6.93E+19	6.94E+19	65.0
		72 ^(b)	7.64E+19	4.54E+19	3.31E+19	3.04E+19	3.33E+19	4.65E+19	7.63E+19	7.64E+19	65.0

Notes:

- (a) Maximum occurs at an azimuthal angle of 0°.
- (b) The projections use Cycle 37 as the basis for future projections with a 10% positive bias on peripheral assembly power.

Table 2.4-3 Point Beach Unit 1 Calculated Maximum Iron Atom Displacement Rate at the RPV Clad/Base Metal Interface

Cycle	Cycle Length (EFPY)	Total Time (EFPY)	Displacement Rate (dpa/s)								Elevation of Max. (cm)
			0°	15°	30°	45°	60°	75°	90°	Maximum ^(a)	
1	1.49	1.49	7.42E-11	4.46E-11	2.91E-11	2.50E-11	2.89E-11	4.45E-11	7.42E-11	7.42E-11	1.0
2	0.92	2.40	6.79E-11	4.14E-11	2.75E-11	2.35E-11	2.75E-11	4.09E-11	6.67E-11	6.79E-11	67.0
3	1.21	3.61	6.97E-11	4.27E-11	2.88E-11	2.44E-11	2.86E-11	4.26E-11	6.98E-11	6.98E-11	-5.0
4	0.70	4.31	7.72E-11	4.66E-11	3.20E-11	2.73E-11	3.17E-11	4.64E-11	7.71E-11	7.72E-11	-1.0
5	0.79	5.10	7.40E-11	4.59E-11	3.21E-11	2.76E-11	3.19E-11	4.60E-11	7.50E-11	7.50E-11	-73.0
6	0.81	5.91	6.93E-11	4.28E-11	3.12E-11	2.72E-11	3.09E-11	4.26E-11	6.96E-11	6.96E-11	-1.0
7	0.87	6.78	7.10E-11	4.28E-11	2.91E-11	2.44E-11	2.88E-11	4.26E-11	7.12E-11	7.12E-11	1.0
8	0.64	7.42	5.84E-11	3.50E-11	2.53E-11	2.35E-11	2.51E-11	3.48E-11	5.79E-11	5.84E-11	-3.0
9	0.60	8.02	5.26E-11	3.25E-11	2.43E-11	2.30E-11	2.44E-11	3.29E-11	5.31E-11	5.31E-11	-79.0
10	0.65	8.67	4.57E-11	3.05E-11	2.38E-11	2.31E-11	2.36E-11	3.03E-11	4.56E-11	4.57E-11	-83.0
11	0.61	9.28	4.99E-11	2.97E-11	2.01E-11	1.67E-11	2.00E-11	2.96E-11	5.00E-11	5.00E-11	-1.0
12	0.96	10.24	4.71E-11	3.17E-11	2.32E-11	1.97E-11	2.26E-11	3.04E-11	4.57E-11	4.71E-11	-65.0
13	0.79	11.03	4.80E-11	3.34E-11	2.47E-11	2.02E-11	2.45E-11	3.35E-11	4.85E-11	4.85E-11	65.0
14	0.84	11.88	4.57E-11	3.23E-11	2.43E-11	1.98E-11	2.42E-11	3.23E-11	4.59E-11	4.59E-11	1.0
15	0.84	12.72	4.58E-11	3.20E-11	2.32E-11	1.87E-11	2.31E-11	3.19E-11	4.59E-11	4.59E-11	5.0
16	0.85	13.57	4.73E-11	3.28E-11	2.42E-11	1.93E-11	2.41E-11	3.27E-11	4.73E-11	4.73E-11	3.0
17	0.83	14.40	4.83E-11	3.07E-11	2.12E-11	1.98E-11	2.11E-11	3.07E-11	4.84E-11	4.84E-11	65.0
18	0.83	15.23	4.46E-11	2.84E-11	1.91E-11	1.71E-11	1.90E-11	2.84E-11	4.47E-11	4.47E-11	65.0
19	0.86	16.08	4.29E-11	2.86E-11	2.07E-11	1.88E-11	2.06E-11	2.85E-11	4.28E-11	4.29E-11	65.0
20	0.79	16.88	4.99E-11	3.17E-11	2.13E-11	1.84E-11	2.15E-11	3.17E-11	5.00E-11	5.00E-11	65.0
21	0.89	17.77	4.36E-11	2.79E-11	2.13E-11	2.01E-11	2.11E-11	2.79E-11	4.37E-11	4.37E-11	65.0
22	0.85	18.62	4.62E-11	2.88E-11	2.09E-11	1.96E-11	2.08E-11	2.88E-11	4.63E-11	4.63E-11	63.0
23	0.87	19.49	4.42E-11	2.81E-11	2.05E-11	1.93E-11	2.05E-11	2.82E-11	4.43E-11	4.43E-11	63.0
24	0.98	20.47	4.31E-11	2.78E-11	1.99E-11	1.81E-11	1.99E-11	2.79E-11	4.34E-11	4.34E-11	63.0
25	1.21	21.67	4.58E-11	3.02E-11	2.23E-11	1.97E-11	2.27E-11	3.06E-11	4.61E-11	4.61E-11	65.0
26	1.25	22.93	4.22E-11	2.76E-11	1.99E-11	1.81E-11	2.00E-11	2.74E-11	4.20E-11	4.22E-11	65.0
27	1.28	24.20	4.78E-11	3.02E-11	2.14E-11	1.89E-11	2.09E-11	2.95E-11	4.71E-11	4.78E-11	65.0
28	1.42	25.62	4.54E-11	2.83E-11	2.17E-11	2.07E-11	2.16E-11	2.83E-11	4.55E-11	4.55E-11	63.0
29	1.29	26.91	5.07E-11	3.14E-11	2.15E-11	1.99E-11	2.14E-11	3.11E-11	5.04E-11	5.07E-11	63.0
30	1.33	28.24	4.74E-11	2.94E-11	1.91E-11	1.68E-11	1.90E-11	2.94E-11	4.75E-11	4.75E-11	63.0

Table 2.4-3 Point Beach Unit 1 Calculated Maximum Iron Atom Displacement Rate at the RPV Clad/Base Metal Interface (Continued)

Cycle	Cycle Length (EFPY)	Total Time (EFPY)	Displacement Rate (dpa/s)								Elevation of Max. (cm)
			0°	15°	30°	45°	60°	75°	90°	Maximum ^(a)	
31	1.32	29.56	3.71E-11	2.40E-11	1.95E-11	1.94E-11	1.95E-11	2.46E-11	3.79E-11	3.79E-11	65.0
32	1.27	30.83	4.16E-11	2.71E-11	2.13E-11	1.98E-11	2.11E-11	2.70E-11	4.16E-11	4.16E-11	-73.0
33	1.48	32.31	3.79E-11	2.60E-11	2.13E-11	1.99E-11	2.12E-11	2.59E-11	3.79E-11	3.79E-11	-71.0
34	1.22	33.53	5.34E-11	3.37E-11	2.40E-11	2.23E-11	2.44E-11	3.39E-11	5.35E-11	5.35E-11	-73.0
35	1.43	34.96	5.34E-11	3.50E-11	2.63E-11	2.33E-11	2.62E-11	3.51E-11	5.35E-11	5.35E-11	-73.0
36	1.34	36.30	5.68E-11	3.70E-11	2.50E-11	2.18E-11	2.49E-11	3.70E-11	5.68E-11	5.68E-11	-73.0
37	1.50	37.80	5.69E-11	3.39E-11	2.30E-11	2.09E-11	2.27E-11	3.39E-11	5.70E-11	5.70E-11	-73.0
38	1.37	39.17	5.36E-11	3.49E-11	2.54E-11	2.33E-11	2.55E-11	3.50E-11	5.36E-11	5.36E-11	-73.0
39	1.46	40.63	5.31E-11	3.45E-11	2.49E-11	2.23E-11	2.48E-11	3.46E-11	5.32E-11	5.32E-11	-73.0

Note:

(a) Maximum occurs at an azimuthal angle of 0°, or the octant symmetric angle, 90°.

Table 2.4-4 Point Beach Unit 1 Calculated Maximum Iron Atom Displacements at the RPV Clad/Base Metal Interface

Cycle	Cycle Length (EFPY)	Total Time (EFPY)	Displacements (dpa)								Elevation of Max. (cm)
			0°	15°	30°	45°	60°	75°	90°	Maximum ^(a)	
1	1.49	1.49	3.48E-03	2.09E-03	1.37E-03	1.17E-03	1.36E-03	2.09E-03	3.48E-03	3.48E-03	1.0
2	0.92	2.40	5.43E-03	3.28E-03	2.16E-03	1.85E-03	2.15E-03	3.26E-03	5.40E-03	5.43E-03	3.0
3	1.21	3.61	8.09E-03	4.91E-03	3.26E-03	2.78E-03	3.24E-03	4.89E-03	8.06E-03	8.09E-03	-1.0
4	0.70	4.31	9.79E-03	5.94E-03	3.97E-03	3.39E-03	3.94E-03	5.91E-03	9.75E-03	9.79E-03	-1.0
5	0.79	5.10	1.16E-02	7.06E-03	4.75E-03	4.06E-03	4.72E-03	7.03E-03	1.16E-02	1.16E-02	-1.0
6	0.81	5.91	1.34E-02	8.16E-03	5.55E-03	4.76E-03	5.52E-03	8.13E-03	1.34E-02	1.34E-02	-1.0
7	0.87	6.78	1.53E-02	9.34E-03	6.35E-03	5.43E-03	6.31E-03	9.30E-03	1.53E-02	1.53E-02	-1.0
8	0.64	7.42	1.65E-02	1.01E-02	6.87E-03	5.91E-03	6.82E-03	1.00E-02	1.65E-02	1.65E-02	-1.0
9	0.60	8.02	1.75E-02	1.06E-02	7.31E-03	6.33E-03	7.26E-03	1.06E-02	1.75E-02	1.75E-02	-1.0
10	0.65	8.67	1.83E-02	1.12E-02	7.76E-03	6.77E-03	7.71E-03	1.12E-02	1.83E-02	1.83E-02	-1.0
11	0.61	9.28	1.93E-02	1.18E-02	8.15E-03	7.09E-03	8.10E-03	1.18E-02	1.93E-02	1.93E-02	-1.0
12	0.96	10.24	2.07E-02	1.27E-02	8.85E-03	7.68E-03	8.77E-03	1.27E-02	2.07E-02	2.07E-02	-3.0
13	0.79	11.03	2.19E-02	1.36E-02	9.46E-03	8.18E-03	9.38E-03	1.35E-02	2.19E-02	2.19E-02	-1.0
14	0.84	11.88	2.31E-02	1.44E-02	1.01E-02	8.71E-03	1.00E-02	1.44E-02	2.31E-02	2.31E-02	-1.0
15	0.84	12.72	2.43E-02	1.53E-02	1.07E-02	9.20E-03	1.06E-02	1.52E-02	2.43E-02	2.43E-02	-1.0
16	0.85	13.57	2.56E-02	1.62E-02	1.14E-02	9.72E-03	1.13E-02	1.61E-02	2.56E-02	2.56E-02	-1.0
17	0.83	14.40	2.67E-02	1.69E-02	1.19E-02	1.02E-02	1.18E-02	1.68E-02	2.66E-02	2.67E-02	3.0
18	0.83	15.23	2.77E-02	1.75E-02	1.24E-02	1.07E-02	1.23E-02	1.75E-02	2.77E-02	2.77E-02	7.0
19	0.86	16.08	2.87E-02	1.82E-02	1.30E-02	1.12E-02	1.29E-02	1.82E-02	2.87E-02	2.87E-02	9.0
20	0.79	16.88	2.98E-02	1.90E-02	1.35E-02	1.17E-02	1.34E-02	1.89E-02	2.98E-02	2.98E-02	13.0
21	0.89	17.77	3.09E-02	1.97E-02	1.41E-02	1.22E-02	1.40E-02	1.96E-02	3.09E-02	3.09E-02	59.0
22	0.85	18.62	3.22E-02	2.04E-02	1.47E-02	1.27E-02	1.46E-02	2.03E-02	3.22E-02	3.22E-02	59.0
23	0.87	19.49	3.34E-02	2.11E-02	1.52E-02	1.33E-02	1.51E-02	2.10E-02	3.34E-02	3.34E-02	59.0
24	0.98	20.47	3.47E-02	2.20E-02	1.58E-02	1.38E-02	1.57E-02	2.19E-02	3.47E-02	3.47E-02	59.0
25	1.21	21.67	3.65E-02	2.31E-02	1.67E-02	1.46E-02	1.66E-02	2.30E-02	3.65E-02	3.65E-02	61.0
26	1.25	22.93	3.81E-02	2.42E-02	1.75E-02	1.53E-02	1.74E-02	2.41E-02	3.81E-02	3.81E-02	61.0
27	1.28	24.20	4.01E-02	2.54E-02	1.83E-02	1.61E-02	1.82E-02	2.53E-02	4.00E-02	4.01E-02	61.0
28	1.42	25.62	4.21E-02	2.67E-02	1.93E-02	1.70E-02	1.92E-02	2.66E-02	4.21E-02	4.21E-02	61.0
29	1.29	26.91	4.41E-02	2.80E-02	2.02E-02	1.78E-02	2.01E-02	2.78E-02	4.41E-02	4.41E-02	61.0
30	1.33	28.24	4.61E-02	2.92E-02	2.10E-02	1.85E-02	2.09E-02	2.91E-02	4.61E-02	4.61E-02	61.0

Table 2.4-4 Point Beach Unit 1 Calculated Maximum Iron Atom Displacements at the RPV Clad/Base Metal Interface (Continued)

Cycle	Cycle Length (EFPY)	Total Time (EFPY)	Displacements (dpa)								Elevation of Max. (cm)
			0°	15°	30°	45°	60°	75°	90°	Maximum ^(a)	
31	1.32	29.56	4.77E-02	3.02E-02	2.18E-02	1.93E-02	2.17E-02	3.01E-02	4.77E-02	4.77E-02	61.0
32	1.27	30.83	4.93E-02	3.12E-02	2.26E-02	2.01E-02	2.25E-02	3.12E-02	4.93E-02	4.93E-02	61.0
33	1.48	32.31	5.10E-02	3.24E-02	2.36E-02	2.10E-02	2.35E-02	3.23E-02	5.10E-02	5.10E-02	61.0
34	1.22	33.53	5.30E-02	3.37E-02	2.45E-02	2.18E-02	2.44E-02	3.36E-02	5.30E-02	5.30E-02	61.0
35	1.43	34.96	5.53E-02	3.52E-02	2.57E-02	2.29E-02	2.56E-02	3.51E-02	5.53E-02	5.53E-02	61.0
36	1.34	36.30	5.76E-02	3.67E-02	2.67E-02	2.38E-02	2.66E-02	3.66E-02	5.76E-02	5.76E-02	61.0
37	1.50	37.80	6.02E-02	3.83E-02	2.78E-02	2.47E-02	2.77E-02	3.82E-02	6.03E-02	6.03E-02	61.0
38	1.37	39.17	6.25E-02	3.97E-02	2.89E-02	2.57E-02	2.87E-02	3.96E-02	6.25E-02	6.25E-02	61.0
39	1.46	40.63	6.48E-02	4.12E-02	3.00E-02	2.67E-02	2.99E-02	4.11E-02	6.49E-02	6.49E-02	61.0
		42 ^(b)	6.75E-02	4.28E-02	3.11E-02	2.77E-02	3.09E-02	4.27E-02	6.75E-02	6.75E-02	61.0
		48 ^(b)	7.89E-02	4.96E-02	3.58E-02	3.20E-02	3.55E-02	4.95E-02	7.89E-02	7.89E-02	63.0
		54 ^(b)	9.03E-02	5.64E-02	4.04E-02	3.63E-02	4.02E-02	5.63E-02	9.03E-02	9.03E-02	63.0
		60 ^(b)	1.02E-01	6.32E-02	4.51E-02	4.06E-02	4.48E-02	6.31E-02	1.02E-01	1.02E-01	63.0
		66 ^(b)	1.13E-01	7.00E-02	4.98E-02	4.49E-02	4.94E-02	6.98E-02	1.13E-01	1.13E-01	63.0
		72 ^(b)	1.25E-01	7.68E-02	5.45E-02	4.92E-02	5.41E-02	7.66E-02	1.25E-01	1.25E-01	63.0

Notes:

- (a) Maximum occurs at an azimuthal angle of 0°, or the octant symmetric angle, 90°.
- (b) The projections use Cycle 37 as the basis for future projections with a 10% positive bias on peripheral assembly power.

Table 2.4-5 Point Beach Unit 1 Calculated Maximum Fast Neutron Fluence ($E > 1.0$ MeV) at RPV Welds and Shells^(a)

Material	Fluence (n/cm ²)			
	40.63 EFPY	42 EFPY	48 EFPY	54 EFPY
Inlet Nozzle to Nozzle Belt Forging Weld (lowest extent) ^(b)	3.50E+16	3.63E+16	4.18E+16	4.73E+16
Nozzle Belt Forging (lowest extent) [122P237]	2.56E+18	2.66E+18	3.09E+18	3.52E+18
Nozzle Belt Forging to Intermediate Shell Circumferential Weld [SA-1426]	2.95E+18	3.06E+18	3.56E+18	4.05E+18
Intermediate Shell Longitudinal Weld [SA-775/SA-812]	2.44E+19	2.53E+19	2.93E+19	3.33E+19
Intermediate Shell Plate [A9811-1]	3.97E+19	4.13E+19	4.83E+19	5.53E+19
Intermediate Shell to Lower Shell Circumferential Weld [SA-1101]	3.53E+19	3.69E+19	4.39E+19	5.09E+19
Lower Shell Longitudinal Weld [SA-847]	2.28E+19	2.37E+19	2.79E+19	3.22E+19
Lower Shell Plate [C1423-1]	3.55E+19	3.71E+19	4.43E+19	5.15E+19
Lower Shell to Lower Head Ring Circumferential Weld	2.37E+16	2.47E+16	2.91E+16	3.36E+16

Material	Fluence (n/cm ²)			
	60 EFPY	66 EFPY	72 EFPY	
Inlet Nozzle to Nozzle Belt Forging Weld (lowest extent) ^(b)	5.28E+16	5.83E+16	6.38E+16	
Nozzle Belt Forging (lowest extent) [122P237]	3.95E+18	4.38E+18	4.81E+18	
Nozzle Belt Forging to Intermediate Shell Circumferential Weld [SA-1426]	4.55E+18	5.05E+18	5.54E+18	
Intermediate Shell Longitudinal Weld [SA-775/SA-812]	3.74E+19	4.14E+19	4.54E+19	
Intermediate Shell Plate [A9811-1]	6.23E+19	6.94E+19	7.64E+19	
Intermediate Shell to Lower Shell Circumferential Weld [SA-1101]	5.79E+19	6.49E+19	7.19E+19	
Lower Shell Longitudinal Weld [SA-847]	3.64E+19	4.06E+19	4.48E+19	
Lower Shell Plate [C1423-1]	5.87E+19	6.59E+19	7.31E+19	
Lower Shell to Lower Head Ring Circumferential Weld	3.80E+16	4.24E+16	4.68E+16	

Notes:

- (a) The projections use Cycle 37 as the basis for future projections with a 10% positive bias on peripheral assembly power.
- (b) Also applicable to outlet nozzle/nozzle belt forging weld and safety injection nozzle/nozzle belt forging weld.

Table 2.4-6 Point Beach Unit 1 Calculated Maximum Iron Atom Displacements at RPV Welds and Shells^(a)

Material	Displacements (dpa)			
	40.63 EFPY	42 EFPY	48 EFPY	54 EFPY
Inlet Nozzle to Nozzle Belt Forging Weld (lowest extent) ^(b)	2.91E-04	3.02E-04	3.48E-04	3.94E-04
Nozzle Belt Forging (lowest extent) [122P237]	4.40E-03	4.57E-03	5.32E-03	6.06E-03
Nozzle Belt Forging to Intermediate Shell Circumferential Weld [SA-1426]	5.04E-03	5.23E-03	6.09E-03	6.94E-03
Intermediate Shell Longitudinal Weld [SA-775/SA-812]	4.12E-02	4.28E-02	4.96E-02	5.64E-02
Intermediate Shell Plate [A9811-1]	6.49E-02	6.75E-02	7.89E-02	9.03E-02
Intermediate Shell to Lower Shell Circumferential Weld [SA-1101]	5.80E-02	6.07E-02	7.21E-02	8.36E-02
Lower Shell Longitudinal Weld [SA-847]	3.83E-02	3.99E-02	4.69E-02	5.39E-02
Lower Shell Plate [C1423-1]	5.79E-02	6.06E-02	7.23E-02	8.40E-02
Lower Shell to Lower Head Ring Circumferential Weld	1.09E-04	1.14E-04	1.34E-04	1.54E-04

Material	Displacements (dpa)			
	60 EFPY	66 EFPY	72 EFPY	
Inlet Nozzle to Nozzle Belt Forging Weld (lowest extent) ^(b)	4.40E-04	4.87E-04	5.33E-04	
Nozzle Belt Forging (lowest extent) [122P237]	6.80E-03	7.54E-03	8.29E-03	
Nozzle Belt Forging to Intermediate Shell Circumferential Weld [SA-1426]	7.79E-03	8.64E-03	9.49E-03	
Intermediate Shell Longitudinal Weld [SA-775/SA-812]	6.32E-02	7.00E-02	7.68E-02	
Intermediate Shell Plate [A9811-1]	1.02E-01	1.13E-01	1.25E-01	
Intermediate Shell to Lower Shell Circumferential Weld [SA-1101]	9.51E-02	1.07E-01	1.18E-01	
Lower Shell Longitudinal Weld [SA-847]	6.09E-02	6.79E-02	7.49E-02	
Lower Shell Plate [C1423-1]	9.58E-02	1.08E-01	1.19E-01	
Lower Shell to Lower Head Ring Circumferential Weld	1.74E-04	1.95E-04	2.15E-04	

Notes:

- (a) The projections use Cycle 37 as the basis for future projections with a 10% positive bias on peripheral assembly power.
- (b) Also applicable to outlet nozzle/nozzle belt forging weld and safety injection nozzle/nozzle belt forging weld.

**Table 2.4-7 Point Beach Unit 1 Calculated Fast Neutron Fluence Rate ($E > 1.0$ MeV)
at Surveillance Capsule Locations**

Cycle	Cycle Length (EFPY)	Total Time (EFPY)	Fluence (n/cm ² -s)					
			V	S	R	T	P	N
1	1.49	1.49	1.33E+11	7.18E+10	1.33E+11	7.61E+10	7.61E+10	7.18E+10
2	0.92	2.40		6.89E+10	1.25E+11	7.31E+10	7.31E+10	6.89E+10
3	1.21	3.61		7.25E+10	1.29E+11	7.64E+10	7.64E+10	7.25E+10
4	0.70	4.31			1.41E+11	8.34E+10	8.34E+10	8.10E+10
5	0.79	5.10			1.37E+11	8.24E+10	8.24E+10	8.03E+10
6	0.81	5.91				7.97E+10	7.97E+10	7.94E+10
7	0.87	6.78				7.66E+10	7.66E+10	7.31E+10
8	0.64	7.42				6.58E+10	6.58E+10	6.38E+10
9	0.60	8.02				6.11E+10	6.11E+10	5.94E+10
10	0.65	8.67				5.79E+10	5.79E+10	5.74E+10
11	0.61	9.28				5.71E+10	5.71E+10	5.16E+10
12	0.96	10.24					6.10E+10	5.57E+10
13	0.79	11.03					6.68E+10	5.97E+10
14	0.84	11.88					6.58E+10	5.89E+10
15	0.84	12.72					6.38E+10	5.58E+10
16	0.85	13.57					6.61E+10	5.83E+10
17	0.83	14.40					5.37E+10	5.26E+10
18	0.83	15.23					4.98E+10	4.69E+10
19	0.86	16.08					5.33E+10	5.14E+10
20	0.79	16.88					5.56E+10	5.20E+10
21	0.89	17.77					5.24E+10	5.38E+10
22	0.85	18.62						5.28E+10
23	0.87	19.49						5.15E+10
24	0.98	20.47						4.97E+10
25	1.21	21.67						5.55E+10
26	1.25	22.93						4.96E+10
27	1.28	24.20						5.36E+10
28	1.42	25.62						5.56E+10
29	1.29	26.91						5.43E+10
30	1.33	28.24						4.73E+10
31	1.32	29.56						5.02E+10
32	1.27	30.83						5.32E+10
33	1.48	32.31						5.36E+10
34	1.22	33.53						5.89E+10
35	1.43	34.96						6.44E+10
36	1.34	36.30						6.04E+10
37	1.50	37.80						5.63E+10
38	1.37	39.17						6.23E+10
39	1.46	40.63						6.06E+10

**Table 2.4-8 Point Beach Unit 1 Calculated Fast Neutron Fluence (E > 1.0 MeV)
at Surveillance Capsules**

Cycle	Cycle Length (EFPY)	Total Time (EFPY)	Fluence (n/cm ²)					
			V	S	R	T	P	N
1	1.49	1.49	6.23E+18	3.37E+18	6.23E+18	3.57E+18	3.57E+18	3.37E+18
2	0.92	2.40		5.36E+18	9.84E+18	5.68E+18	5.68E+18	5.36E+18
3	1.21	3.61		8.13E+18	1.48E+19	8.60E+18	8.60E+18	8.13E+18
4	0.70	4.31			1.79E+19	1.04E+19	1.04E+19	9.91E+18
5	0.79	5.10			2.13E+19	1.25E+19	1.25E+19	1.19E+19
6	0.81	5.91				1.45E+19	1.45E+19	1.39E+19
7	0.87	6.78				1.66E+19	1.66E+19	1.60E+19
8	0.64	7.42				1.80E+19	1.80E+19	1.72E+19
9	0.60	8.02				1.91E+19	1.91E+19	1.84E+19
10	0.65	8.67				2.03E+19	2.03E+19	1.95E+19
11	0.61	9.28				2.14E+19	2.14E+19	2.05E+19
12	0.96	10.24					2.33E+19	2.22E+19
13	0.79	11.03					2.49E+19	2.37E+19
14	0.84	11.88					2.67E+19	2.53E+19
15	0.84	12.72					2.84E+19	2.68E+19
16	0.85	13.57					3.01E+19	2.83E+19
17	0.83	14.40					3.15E+19	2.97E+19
18	0.83	15.23					3.28E+19	3.09E+19
19	0.86	16.08					3.43E+19	3.23E+19
20	0.79	16.88					3.57E+19	3.36E+19
21	0.89	17.77					3.72E+19	3.51E+19
22	0.85	18.62						3.66E+19
23	0.87	19.49						3.80E+19
24	0.98	20.47						3.95E+19
25	1.21	21.67						4.16E+19
26	1.25	22.93						4.36E+19
27	1.28	24.20						4.57E+19
28	1.42	25.62						4.82E+19
29	1.29	26.91						5.04E+19
30	1.33	28.24						5.24E+19
31	1.32	29.56						5.45E+19
32	1.27	30.83						5.66E+19
33	1.48	32.31						5.91E+19
34	1.22	33.53						6.14E+19
35	1.43	34.96						6.43E+19
36	1.34	36.30						6.69E+19
37	1.50	37.80						6.95E+19
38	1.37	39.17						7.22E+19
39	1.46	40.63						7.50E+19
		42 ^(a)						7.77E+19
		48 ^(a)						8.94E+19
		54 ^(a)						1.01E+20
		60 ^(a)						1.13E+20
		66 ^(a)						1.24E+20
		72 ^(a)						1.36E+20

Note:

(a) The projections use Cycle 37 as the basis for future projections with a 10% positive bias on peripheral assembly power.

Table 2.4-9 Point Beach Unit 1 Calculated Iron Atom Displacement Rate at Surveillance Capsule Locations

Cycle	Cycle Length (EFPY)	Total Time (EFPY)	Displacement Rate (dpa/s)					
			V	S	R	T	P	N
1	1.49	1.49	2.44E-10	1.27E-10	2.44E-10	1.34E-10	1.34E-10	1.27E-10
2	0.92	2.40		1.22E-10	2.29E-10	1.28E-10	1.28E-10	1.22E-10
3	1.21	3.61		1.28E-10	2.36E-10	1.34E-10	1.34E-10	1.28E-10
4	0.70	4.31			2.59E-10	1.46E-10	1.46E-10	1.43E-10
5	0.79	5.10			2.51E-10	1.45E-10	1.45E-10	1.42E-10
6	0.81	5.91				1.40E-10	1.40E-10	1.41E-10
7	0.87	6.78				1.34E-10	1.34E-10	1.29E-10
8	0.64	7.42				1.15E-10	1.15E-10	1.12E-10
9	0.60	8.02				1.07E-10	1.07E-10	1.05E-10
10	0.65	8.67				1.01E-10	1.01E-10	1.01E-10
11	0.61	9.28				9.91E-11	9.91E-11	9.04E-11
12	0.96	10.24					1.06E-10	9.81E-11
13	0.79	11.03					1.16E-10	1.05E-10
14	0.84	11.88					1.15E-10	1.04E-10
15	0.84	12.72					1.11E-10	9.83E-11
16	0.85	13.57					1.15E-10	1.03E-10
17	0.83	14.40					9.36E-11	9.26E-11
18	0.83	15.23					8.67E-11	8.26E-11
19	0.86	16.08					9.26E-11	9.05E-11
20	0.79	16.88					9.67E-11	9.15E-11
21	0.89	17.77					9.12E-11	9.46E-11
22	0.85	18.62						9.29E-11
23	0.87	19.49						9.06E-11
24	0.98	20.47						8.74E-11
25	1.21	21.67						9.78E-11
26	1.25	22.93						8.72E-11
27	1.28	24.20						9.45E-11
28	1.42	25.62						9.78E-11
29	1.29	26.91						9.56E-11
30	1.33	28.24						8.32E-11
31	1.32	29.56						8.83E-11
32	1.27	30.83						9.36E-11
33	1.48	32.31						9.43E-11
34	1.22	33.53						1.04E-10
35	1.43	34.96						1.14E-10
36	1.34	36.30						1.06E-10
37	1.50	37.80						9.92E-11
38	1.37	39.17						1.10E-10
39	1.46	40.63						1.07E-10

Table 2.4-10 Point Beach Unit 1 Calculated Iron Atom Displacements at Surveillance Capsules

Cycle	Cycle Length (EFPY)	Total Time (EFPY)	Displacements (dpa)					
			V	S	R	T	P	N
1	1.49	1.49	1.14E-02	5.97E-03	1.14E-02	6.28E-03	6.28E-03	5.97E-03
2	0.92	2.40		9.50E-03	1.81E-02	9.99E-03	9.99E-03	9.50E-03
3	1.21	3.61		1.44E-02	2.71E-02	1.51E-02	1.51E-02	1.44E-02
4	0.70	4.31			3.28E-02	1.83E-02	1.83E-02	1.75E-02
5	0.79	5.10			3.90E-02	2.19E-02	2.19E-02	2.11E-02
6	0.81	5.91				2.55E-02	2.55E-02	2.47E-02
7	0.87	6.78				2.92E-02	2.92E-02	2.82E-02
8	0.64	7.42				3.15E-02	3.15E-02	3.05E-02
9	0.60	8.02				3.35E-02	3.35E-02	3.25E-02
10	0.65	8.67				3.56E-02	3.56E-02	3.46E-02
11	0.61	9.28				3.75E-02	3.75E-02	3.63E-02
12	0.96	10.24					4.07E-02	3.93E-02
13	0.79	11.03					4.36E-02	4.19E-02
14	0.84	11.88					4.67E-02	4.47E-02
15	0.84	12.72					4.96E-02	4.73E-02
16	0.85	13.57					5.27E-02	5.00E-02
17	0.83	14.40					5.52E-02	5.25E-02
18	0.83	15.23					5.74E-02	5.46E-02
19	0.86	16.08					6.00E-02	5.71E-02
20	0.79	16.88					6.24E-02	5.94E-02
21	0.89	17.77					6.49E-02	6.20E-02
22	0.85	18.62						6.45E-02
23	0.87	19.49						6.70E-02
24	0.98	20.47						6.97E-02
25	1.21	21.67						7.34E-02
26	1.25	22.93						7.69E-02
27	1.28	24.20						8.07E-02
28	1.42	25.62						8.51E-02
29	1.29	26.91						8.90E-02
30	1.33	28.24						9.24E-02
31	1.32	29.56						9.61E-02
32	1.27	30.83						9.99E-02
33	1.48	32.31						1.04E-01
34	1.22	33.53						1.08E-01
35	1.43	34.96						1.13E-01
36	1.34	36.30						1.18E-01
37	1.50	37.80						1.23E-01
38	1.37	39.17						1.27E-01
39	1.46	40.63						1.32E-01
		42 ^(a)						1.37E-01
		48 ^(a)						1.58E-01
		54 ^(a)						1.78E-01
		60 ^(a)						1.99E-01
		66 ^(a)						2.19E-01
		72 ^(a)						2.40E-01

Note:

(a) The projections use Cycle 37 as the basis for future projections with a 10% positive bias on peripheral assembly power.

Table 2.4-11 Point Beach Unit 1 Calculated Surveillance Capsule Lead Factors

Cycle	Cycle Length (EFPY)	Total Time (EFPY)	Lead Factor					
			V	S	R	T	P	N
1	1.49	1.49	2.93	1.58	2.93	1.68	1.68	1.58
2	0.92	2.40		1.61	2.96	1.71	1.71	1.61
3	1.21	3.61		1.64	2.98	1.74	1.74	1.64
4	0.70	4.31			2.98	1.74	1.74	1.65
5	0.79	5.10			3.00	1.76	1.76	1.68
6	0.81	5.91				1.77	1.77	1.70
7	0.87	6.78				1.77	1.77	1.70
8	0.64	7.42				1.78	1.78	1.71
9	0.60	8.02				1.79	1.79	1.72
10	0.65	8.67				1.81	1.81	1.74
11	0.61	9.28				1.81	1.81	1.74
12	0.96	10.24					1.83	1.75
13	0.79	11.03					1.86	1.77
14	0.84	11.88					1.88	1.78
15	0.84	12.72					1.90	1.80
16	0.85	13.57					1.92	1.81
17	0.83	14.40					1.93	1.82
18	0.83	15.23					1.94	1.83
19	0.86	16.08					1.95	1.84
20	0.79	16.88					1.96	1.84
21	0.89	17.77					1.96	1.86
22	0.85	18.62						1.86
23	0.87	19.49						1.86
24	0.98	20.47						1.86
25	1.21	21.67						1.86
26	1.25	22.93						1.87
27	1.28	24.20						1.86
28	1.42	25.62						1.87
29	1.29	26.91						1.87
30	1.33	28.24						1.85
31	1.32	29.56						1.87
32	1.27	30.83						1.88
33	1.48	32.31						1.89
34	1.22	33.53						1.89
35	1.43	34.96						1.90
36	1.34	36.30						1.89
37	1.50	37.80						1.88
38	1.37	39.17						1.89
39	1.46	40.63						1.89
		42 ^(a)						1.88
		48 ^(a)						1.85
		54 ^(a)						1.83
		60 ^(a)						1.81
		66 ^(a)						1.79
		72 ^(a)						1.78

Note:

(a) The projections use Cycle 37 as the basis for future projections with a 10% positive bias on peripheral assembly power.

Table 2.4-12 Point Beach Unit 1 Ex-Vessel Neutron Dosimetry Summary

Azimuth (degrees)	Capsule Identification - Cycle 17 Irradiation		
	Core Top	Core Midplane	Core Bottom
0	A	B	C
15		D	
30		E	
45		F	

Azimuth (degrees)	Capsule Identification - Cycle 18 Irradiation		
	Core Top	Core Midplane	Core Bottom
0	S	T	U
15		V	
30		W	
45		X	

Azimuth (degrees)	Capsule Identification - Cycle 19 Irradiation		
	Core Top	Core Midplane	Core Bottom
0	GG	HH	II
15		JJ	
30		KK	
45		LL	

Azimuth (degrees)	Capsule Identification - Cycles 20-22 Irradiation		
	Core Top	Core Midplane	Core Bottom
0	SS	TT	UU
15		VV	
30		WW	
45		XX	

Azimuth (degrees)	Capsule Identification – Cycles 23-24 Irradiation		
	Core Top	Core Midplane	Core Bottom
0	I	H	G
15		J	
30		K	
45		L	

Table 2.4-13 Point Beach Unit 1 Comparison of Measured to Calculated Threshold Reaction Rates–In-Vessel Capsules

Capsule	Reaction				
	$^{63}\text{Cu (n,\alpha)}$	$^{54}\text{Fe (n,p)}$	$^{58}\text{Ni (n,p)}$	$^{238}\text{U (n,f)}$	$^{237}\text{Np (n,f)}$
V	1.18	0.79	0.66	0.79	1.04
S	1.02	0.99	0.87	0.92	1.08
R	1.06	1.04	1.03	1.07	1.11
T	1.10	1.02	-	1.03	1.20
Average	1.09	0.96	0.85	0.95	1.11
% std dev	6.2	12.2	21.8	13.4	6.1

Reaction	Average M/C	% Standard Deviation
$^{63}\text{Cu (n,\alpha)}$	1.09	6.2
$^{54}\text{Fe (n,p)}$	0.96	12.2
$^{58}\text{Ni (n,p)}$	0.85	21.8
$^{238}\text{U (n,f)}$	0.95	13.4
$^{237}\text{Np (n,f)}$	1.11	6.1
Linear Average	0.99	10.8

Table 2.4-14 Point Beach Unit 1 Comparison of Measured to Calculated Threshold Reaction Rates – Ex-Vessel Midplane Capsules

Capsule	Reaction				
	⁶³ Cu (n,α)	⁴⁶ Ti (n,p)	⁵⁴ Fe (n,p)	⁵⁸ Ni (n,p)	²³⁸ U (n,f)
B	0.74	0.76	0.71	0.69	0.66
D	0.86	0.85	0.76	0.76	0.71
E	0.93	0.92	0.84	0.83	0.80
F	0.93	0.93	0.86	0.87	0.87
T	0.71	0.73	0.69	0.70	0.68
V	0.86	0.89	0.80	0.80	0.79
W	0.97	0.98	0.89	0.92	0.88
X	0.97	0.99	0.91	0.93	0.92
HH	0.74	0.75	0.70	0.69	0.70
JJ	0.89	0.87	0.80	0.78	0.77
KK	1.00	0.98	0.89	0.89	0.90
LL	0.97	0.97	0.91	0.90	0.91
TT	0.75	0.77	0.71	0.71	0.70
VV	0.86	0.86	0.76	0.78	0.74
WW	0.95	0.96	0.91	0.89	0.89
XX	0.99	0.97	0.91	0.92	0.92
H	0.69	0.67	0.67	0.66	0.71
J	0.87	0.88	0.80	0.81	0.88
K	0.95	0.99	0.92	0.88	1.00
L	0.98	0.95	0.92	0.94	1.06
Average	0.88	0.88	0.82	0.82	0.82
% std dev	11.5	11.3	10.8	11.4	13.8

Reaction	Average M/C	% Standard Deviation
⁶³ Cu (n,α)	0.88	11.5
⁵⁴ Fe (n,p)	0.88	11.3
⁵⁸ Ni (n,p)	0.82	10.8
²³⁸ U (n,f)	0.82	11.4
²³⁷ Np (n,f)	0.82	13.8
Linear Average	0.85	4.1

Table 2.4-15 Point Beach Unit 1 Comparison of Measured to Calculated Threshold Reaction Rates – Ex-Vessel Off-Midplane Capsules

Capsule	Reaction				
	$^{63}\text{Cu (n,\alpha)}$	$^{46}\text{Ti (n,p)}$	$^{54}\text{Fe (n,p)}$	$^{58}\text{Ni (n,p)}$	$^{238}\text{U (n,f)}$
A	0.97	1.07	0.90	1.00	1.05
C	1.00	1.04	1.01	0.98	1.01
S	1.31	1.40	1.23	1.36	1.34
U	0.72	0.79	0.75	0.77	0.87
GG	1.05	1.19	1.01	1.10	1.16
II	0.80	0.89	0.83	0.82	0.89
SS	0.92	0.90	0.88	0.97	1.05
UU	0.85	0.90	0.85	0.84	0.89
I	1.91	2.33	1.92	2.07	2.34
G	0.71	0.91	0.73	0.89	1.03

Table 2.4-16 Point Beach Unit 1 Comparison of Best-Estimate to Calculated Exposure Rates – In-Vessel Capsules

Capsule	Neutron Fluence Rate (E > 1.0 MeV)		Iron Displacement Rate	
	BE/C	% std dev	BE/C	% std dev
V	0.77	6	0.83	7
S	0.95	6	0.97	7
R	1.05	6	1.05	7
T	1.05	6	1.06	7
Average	0.95	14.0	0.98	10.8

Table 2.4-17 Point Beach Unit 1 Comparison of Best-Estimate to Calculated Exposure Rates – Ex-Vessel Midplane Capsules

Capsule	Neutron Fluence Rate (E > 1.0 MeV)		Iron Displacement Rate	
	BE/C	% std dev	BE/C	% std dev
B	0.70	7	0.73	10
D	0.74	7	0.76	11
E	0.81	7	0.83	11
F	0.86	7	0.87	10
T	0.71	7	0.74	10
V	0.79	7	0.81	11
W	0.89	7	0.89	10
X	0.91	7	0.92	10
HH	0.71	7	0.74	10
JJ	0.78	7	0.80	11
KK	0.88	7	0.88	10
LL	0.90	7	0.90	10
TT	0.72	7	0.75	10
VV	0.76	7	0.78	11
WW	0.88	7	0.89	10
XX	0.91	7	0.91	10
H	0.70	7	0.74	10
J	0.83	7	0.85	11
K	0.92	7	0.93	10
L	0.97	7	0.97	10
Average	0.82	10.8	0.83	9.2

Table 2.4-18 Point Beach Unit 1 Total Database Summary (M/C Reaction Rate Ratios)

Reaction	In-Vessel Database		Midplane Ex-Vessel Database		Combined Database	
	Average M/C	% Unc. (1 σ)	Average M/C	% Unc. (1 σ)	Average M/C	% Unc. (1 σ)
⁶³ Cu (n, α)	1.09	6.2	0.88	11.5	0.99	6.2
⁴⁶ Ti (n,p)	-	-	0.88	11.3	-	-
⁵⁴ Fe (n,p)	0.96	12.2	0.82	10.8	0.89	8.3
⁵⁸ Ni (n,p)	0.85	21.8	0.82	11.4	0.83	12.4
²³⁸ U (n,f)	0.95	13.4	0.82	13.8	0.89	9.6
²³⁷ Np (n,f)	1.11	6.1	-	-	-	-
Linear Average	0.99	10.8	0.85	4.1	0.92	6.1

Table 2.4-19 Point Beach Unit 1 Total Database Summary (Integral Exposure Rate Ratios)

Parameter	In-Vessel Database		Midplane Ex-Vessel Database		Combined Database	
	Average BE/C	% Unc. (1 σ)	Average BE/C	% Unc. (1 σ)	Average BE/C	% Unc. (1 σ)
Fluence Rate (E > 1.0 MeV)	0.95	14.0	0.82	10.8	0.89	9.0
dpa/s	0.98	10.8	0.83	9.2	0.91	7.2

2.5 POINT BEACH UNIT 2 NEUTRON FLUENCE DATA TABLES

Table 2.5-1 Point Beach Unit 2 Calculated Maximum Fast Neutron Fluence Rate ($E > 1.0$ MeV) at the RPV Clad/Base Metal Interface

Cycle	Cycle Length (EFPY)	Total Time (EFPY)	Fluence Rate (n/cm ² -s)								Elevation of Max. (cm)
			0°	15°	30°	45°	60°	75°	90°	Maximum ^(a)	
1	1.52	1.52	4.66E+10	2.70E+10	1.82E+10	1.59E+10	1.83E+10	2.77E+10	4.66E+10	4.66E+10	1.0
2	1.05	2.57	4.60E+10	2.70E+10	1.90E+10	1.69E+10	1.92E+10	2.74E+10	4.60E+10	4.60E+10	-65.0
3	0.87	3.44	4.53E+10	2.62E+10	1.85E+10	1.65E+10	1.86E+10	2.65E+10	4.52E+10	4.53E+10	-67.0
4	0.87	4.31	4.20E+10	2.44E+10	1.75E+10	1.54E+10	1.76E+10	2.50E+10	4.19E+10	4.20E+10	1.0
5	0.89	5.20	4.25E+10	2.57E+10	1.78E+10	1.43E+10	1.78E+10	2.58E+10	4.17E+10	4.25E+10	1.0
6	0.87	6.06	3.20E+10	2.09E+10	1.83E+10	1.52E+10	1.86E+10	2.16E+10	3.22E+10	3.22E+10	1.0
7	0.89	6.96	3.53E+10	2.05E+10	1.53E+10	1.47E+10	1.53E+10	2.06E+10	3.47E+10	3.53E+10	1.0
8	0.86	7.81	3.69E+10	2.08E+10	1.48E+10	1.42E+10	1.50E+10	2.16E+10	3.74E+10	3.74E+10	-1.0
9	0.79	8.60	3.76E+10	2.13E+10	1.49E+10	1.43E+10	1.51E+10	2.19E+10	3.76E+10	3.76E+10	1.0
10	1.20	9.80	3.32E+10	1.95E+10	1.51E+10	1.43E+10	1.53E+10	2.02E+10	3.35E+10	3.35E+10	-1.0
11	0.85	10.65	2.69E+10	1.89E+10	1.51E+10	1.30E+10	1.51E+10	1.88E+10	2.58E+10	2.69E+10	-1.0
12	0.80	11.45	2.94E+10	1.94E+10	1.43E+10	1.19E+10	1.46E+10	1.99E+10	2.94E+10	2.94E+10	3.0
13	0.81	12.25	2.68E+10	1.79E+10	1.37E+10	1.15E+10	1.38E+10	1.85E+10	2.70E+10	2.70E+10	5.0
14	0.86	13.12	2.74E+10	1.87E+10	1.48E+10	1.36E+10	1.49E+10	1.93E+10	2.75E+10	2.75E+10	1.0
15	0.80	13.92	2.69E+10	1.83E+10	1.38E+10	1.12E+10	1.40E+10	1.86E+10	2.67E+10	2.69E+10	7.0
16	0.85	14.78	2.64E+10	1.64E+10	1.17E+10	1.05E+10	1.18E+10	1.67E+10	2.64E+10	2.64E+10	71.0
17	0.84	15.62	2.66E+10	1.65E+10	1.20E+10	1.13E+10	1.21E+10	1.68E+10	2.66E+10	2.66E+10	71.0
18	0.85	16.46	2.56E+10	1.64E+10	1.25E+10	1.16E+10	1.26E+10	1.66E+10	2.55E+10	2.56E+10	71.0
19	0.83	17.29	2.60E+10	1.63E+10	1.23E+10	1.14E+10	1.24E+10	1.62E+10	2.55E+10	2.60E+10	71.0
20	0.88	18.18	2.63E+10	1.64E+10	1.27E+10	1.21E+10	1.28E+10	1.67E+10	2.63E+10	2.63E+10	71.0
21	0.90	19.08	2.51E+10	1.58E+10	1.20E+10	1.14E+10	1.23E+10	1.63E+10	2.53E+10	2.53E+10	71.0
22	0.75	19.82	2.39E+10	1.58E+10	1.45E+10	1.57E+10	1.47E+10	1.61E+10	2.38E+10	2.39E+10	71.0
23	0.92	20.74	2.44E+10	1.52E+10	1.17E+10	1.14E+10	1.18E+10	1.56E+10	2.44E+10	2.44E+10	71.0
24	1.57	22.31	2.54E+10	1.62E+10	1.24E+10	1.13E+10	1.24E+10	1.65E+10	2.54E+10	2.54E+10	71.0
25	1.27	23.58	2.48E+10	1.56E+10	1.31E+10	1.30E+10	1.32E+10	1.67E+10	2.57E+10	2.57E+10	71.0
26	1.35	24.93	2.76E+10	1.76E+10	1.39E+10	1.29E+10	1.38E+10	1.76E+10	2.72E+10	2.76E+10	71.0
27	1.33	26.27	2.56E+10	1.56E+10	1.10E+10	9.92E+09	1.11E+10	1.59E+10	2.56E+10	2.56E+10	71.0
28	1.25	27.52	2.67E+10	1.68E+10	1.27E+10	1.18E+10	1.28E+10	1.71E+10	2.67E+10	2.67E+10	71.0

Table 2.5-1 Point Beach Unit 2 Calculated Maximum Fast Neutron Fluence Rate ($E > 1.0$ MeV) at the RPV Clad/Base Metal Interface (Continued)

Cycle	Cycle Length (EFPY)	Total Time (EFPY)	Fluence Rate (n/cm ² -s)								Elevation of Max. (cm)
			0°	15°	30°	45°	60°	75°	90°	Maximum ^(a)	
29	1.37	28.89	2.67E+10	1.66E+10	1.25E+10	1.16E+10	1.26E+10	1.70E+10	2.67E+10	2.67E+10	71.0
30	1.42	30.31	2.21E+10	1.45E+10	1.32E+10	1.26E+10	1.33E+10	1.48E+10	2.21E+10	2.21E+10	71.0
31	1.19	31.50	2.65E+10	1.59E+10	9.88E+09	8.24E+09	9.97E+09	1.66E+10	2.70E+10	2.70E+10	71.0
32	1.33	32.83	3.02E+10	1.90E+10	1.55E+10	1.49E+10	1.58E+10	1.92E+10	2.98E+10	3.02E+10	71.0
33	1.28	34.11	3.55E+10	2.04E+10	1.42E+10	1.32E+10	1.43E+10	2.07E+10	3.55E+10	3.55E+10	71.0
34	1.45	35.56	3.34E+10	2.14E+10	1.63E+10	1.48E+10	1.65E+10	2.13E+10	3.28E+10	3.34E+10	71.0
35	1.37	36.93	3.72E+10	2.19E+10	1.49E+10	1.37E+10	1.50E+10	2.24E+10	3.76E+10	3.76E+10	-73.0
36	1.46	38.40	3.75E+10	2.17E+10	1.44E+10	1.35E+10	1.46E+10	2.18E+10	3.73E+10	3.75E+10	-73.0
37	1.40	39.80	3.39E+10	2.05E+10	1.48E+10	1.44E+10	1.48E+10	2.07E+10	3.38E+10	3.39E+10	-73.0
38	1.52	41.32	3.70E+10	2.15E+10	1.45E+10	1.37E+10	1.46E+10	2.17E+10	3.70E+10	3.70E+10	-73.0

Note:

(a) Maximum occurs at an azimuthal angle of 0°, or the octant symmetric angle, 90°.

Table 2.5-2 Point Beach Unit 2 Calculated Maximum Fast Neutron Fluence ($E > 1.0$ MeV) at the RPV Clad/Base Metal Interface

Cycle	Cycle Length (EFPY)	Total Time (EFPY)	Fluence (n/cm ²)								Elevation of Max. (cm)
			0°	15°	30°	45°	60°	75°	90°	Maximum ^(a)	
1	1.52	1.52	2.24E+18	1.30E+18	8.74E+17	7.63E+17	8.80E+17	1.33E+18	2.24E+18	2.24E+18	1.0
2	1.05	2.57	3.75E+18	2.18E+18	1.50E+18	1.32E+18	1.51E+18	2.23E+18	3.75E+18	3.75E+18	-1.0
3	0.87	3.44	4.99E+18	2.89E+18	2.00E+18	1.77E+18	2.02E+18	2.96E+18	4.98E+18	4.99E+18	-3.0
4	0.87	4.31	6.14E+18	3.56E+18	2.48E+18	2.19E+18	2.50E+18	3.64E+18	6.13E+18	6.14E+18	-1.0
5	0.89	5.20	7.32E+18	4.28E+18	2.98E+18	2.59E+18	3.00E+18	4.36E+18	7.30E+18	7.32E+18	-1.0
6	0.87	6.06	8.20E+18	4.85E+18	3.48E+18	3.00E+18	3.50E+18	4.95E+18	8.18E+18	8.20E+18	-1.0
7	0.89	6.96	9.19E+18	5.42E+18	3.91E+18	3.42E+18	3.94E+18	5.53E+18	9.16E+18	9.19E+18	-1.0
8	0.86	7.81	1.02E+19	5.99E+18	4.31E+18	3.80E+18	4.34E+18	6.11E+18	1.02E+19	1.02E+19	-1.0
9	0.79	8.60	1.11E+19	6.52E+18	4.68E+18	4.16E+18	4.72E+18	6.66E+18	1.11E+19	1.11E+19	-1.0
10	1.20	9.80	1.24E+19	7.25E+18	5.25E+18	4.70E+18	5.29E+18	7.42E+18	1.24E+19	1.24E+19	-1.0
11	0.85	10.65	1.31E+19	7.76E+18	5.66E+18	5.05E+18	5.70E+18	7.93E+18	1.31E+19	1.31E+19	-1.0
12	0.80	11.45	1.38E+19	8.24E+18	6.02E+18	5.34E+18	6.07E+18	8.43E+18	1.38E+19	1.38E+19	-1.0
13	0.81	12.25	1.45E+19	8.69E+18	6.37E+18	5.64E+18	6.42E+18	8.90E+18	1.45E+19	1.45E+19	-1.0
14	0.86	13.12	1.53E+19	9.19E+18	6.77E+18	6.01E+18	6.83E+18	9.43E+18	1.52E+19	1.53E+19	-1.0
15	0.80	13.92	1.60E+19	9.65E+18	7.12E+18	6.29E+18	7.18E+18	9.90E+18	1.59E+19	1.60E+19	-1.0
16	0.85	14.78	1.65E+19	1.00E+19	7.43E+18	6.57E+18	7.49E+18	1.03E+19	1.65E+19	1.65E+19	3.0
17	0.84	15.62	1.71E+19	1.04E+19	7.75E+18	6.87E+18	7.81E+18	1.07E+19	1.71E+19	1.71E+19	5.0
18	0.85	16.46	1.76E+19	1.08E+19	8.08E+18	7.18E+18	8.15E+18	1.11E+19	1.76E+19	1.76E+19	7.0
19	0.83	17.29	1.83E+19	1.12E+19	8.40E+18	7.48E+18	8.47E+18	1.14E+19	1.83E+19	1.83E+19	63.0
20	0.88	18.18	1.90E+19	1.16E+19	8.76E+18	7.82E+18	8.83E+18	1.19E+19	1.90E+19	1.90E+19	63.0
21	0.90	19.08	1.97E+19	1.20E+19	9.10E+18	8.14E+18	9.18E+18	1.23E+19	1.97E+19	1.97E+19	63.0
22	0.75	19.82	2.03E+19	1.24E+19	9.44E+18	8.51E+18	9.52E+18	1.27E+19	2.03E+19	2.03E+19	63.0
23	0.92	20.74	2.10E+19	1.28E+19	9.78E+18	8.84E+18	9.86E+18	1.31E+19	2.10E+19	2.10E+19	65.0
24	1.57	22.31	2.23E+19	1.36E+19	1.04E+19	9.40E+18	1.05E+19	1.40E+19	2.22E+19	2.23E+19	65.0
25	1.27	23.58	2.33E+19	1.43E+19	1.09E+19	9.92E+18	1.10E+19	1.46E+19	2.32E+19	2.33E+19	65.0
26	1.35	24.93	2.44E+19	1.50E+19	1.15E+19	1.05E+19	1.16E+19	1.54E+19	2.44E+19	2.44E+19	65.0
27	1.33	26.27	2.55E+19	1.57E+19	1.20E+19	1.09E+19	1.21E+19	1.60E+19	2.55E+19	2.55E+19	65.0
28	1.25	27.52	2.66E+19	1.63E+19	1.25E+19	1.14E+19	1.26E+19	1.67E+19	2.65E+19	2.66E+19	65.0
29	1.37	28.89	2.77E+19	1.70E+19	1.30E+19	1.19E+19	1.31E+19	1.75E+19	2.77E+19	2.77E+19	65.0
30	1.42	30.31	2.87E+19	1.77E+19	1.36E+19	1.24E+19	1.37E+19	1.81E+19	2.87E+19	2.87E+19	67.0

Table 2.5-2 Point Beach Unit 2 Calculated Maximum Fast Neutron Fluence ($E > 1.0$ MeV) at the RPV Clad/Base Metal Interface (Continued)

Cycle	Cycle Length (EFPY)	Total Time (EFPY)	Fluence (n/cm ²)								Elevation of Max. (cm)
			0°	15°	30°	45°	60°	75°	90°	Maximum ^(a)	
31	1.19	31.50	2.97E+19	1.83E+19	1.40E+19	1.27E+19	1.41E+19	1.87E+19	2.97E+19	2.97E+19	67.0
32	1.33	32.83	3.10E+19	1.91E+19	1.46E+19	1.33E+19	1.47E+19	1.95E+19	3.09E+19	3.10E+19	67.0
33	1.28	34.11	3.24E+19	1.99E+19	1.52E+19	1.39E+19	1.53E+19	2.04E+19	3.24E+19	3.24E+19	67.0
34	1.45	35.56	3.39E+19	2.08E+19	1.59E+19	1.45E+19	1.60E+19	2.14E+19	3.39E+19	3.39E+19	67.0
35	1.37	36.93	3.55E+19	2.17E+19	1.65E+19	1.51E+19	1.67E+19	2.23E+19	3.54E+19	3.55E+19	67.0
36	1.46	38.40	3.71E+19	2.27E+19	1.72E+19	1.57E+19	1.73E+19	2.33E+19	3.71E+19	3.71E+19	67.0
37	1.40	39.80	3.86E+19	2.36E+19	1.78E+19	1.63E+19	1.80E+19	2.41E+19	3.86E+19	3.86E+19	67.0
38	1.52	41.32	4.03E+19	2.45E+19	1.85E+19	1.70E+19	1.86E+19	2.51E+19	4.03E+19	4.03E+19	67.0
		42 ^(b)	4.11E+19	2.50E+19	1.88E+19	1.73E+19	1.90E+19	2.56E+19	4.11E+19	4.11E+19	67.0
		48 ^(b)	4.85E+19	2.92E+19	2.18E+19	2.01E+19	2.20E+19	2.99E+19	4.85E+19	4.85E+19	67.0
		54 ^(b)	5.59E+19	3.36E+19	2.48E+19	2.29E+19	2.50E+19	3.42E+19	5.58E+19	5.59E+19	67.0
		60 ^(b)	6.33E+19	3.81E+19	2.78E+19	2.57E+19	2.80E+19	3.86E+19	6.32E+19	6.33E+19	67.0
		66 ^(b)	7.06E+19	4.25E+19	3.08E+19	2.86E+19	3.11E+19	4.29E+19	7.06E+19	7.06E+19	67.0
		72 ^(b)	7.80E+19	4.69E+19	3.38E+19	3.14E+19	3.41E+19	4.72E+19	7.80E+19	7.80E+19	67.0

Notes:

- (a) Maximum occurs at an azimuthal angle of 0°.
- (b) The projections use Cycle 38 as the basis for future projections with a 10% positive bias on peripheral assembly power.

Table 2.5-3 Point Beach Unit 2 Calculated Maximum Iron Atom Displacement Rate at the RPV Clad/Base Metal Interface

Cycle	Cycle Length (EFPY)	Total Time (EFPY)	Displacement Rate (dpa/s)								Elevation of Max. (cm)
			0°	15°	30°	45°	60°	75°	90°	Maximum ^(a)	
1	1.52	1.52	7.64E-11	4.60E-11	3.02E-11	2.59E-11	3.00E-11	4.59E-11	7.64E-11	7.64E-11	1.0
2	1.05	2.57	7.52E-11	4.53E-11	3.14E-11	2.74E-11	3.13E-11	4.53E-11	7.52E-11	7.52E-11	-63.0
3	0.87	3.44	7.39E-11	4.39E-11	3.05E-11	2.68E-11	3.03E-11	4.38E-11	7.39E-11	7.39E-11	-65.0
4	0.87	4.31	6.85E-11	4.13E-11	2.89E-11	2.50E-11	2.87E-11	4.12E-11	6.85E-11	6.85E-11	1.0
5	0.89	5.20	6.94E-11	4.33E-11	2.93E-11	2.33E-11	2.90E-11	4.25E-11	6.83E-11	6.94E-11	-1.0
6	0.87	6.06	5.23E-11	3.52E-11	3.02E-11	2.47E-11	3.03E-11	3.56E-11	5.27E-11	5.27E-11	1.0
7	0.89	6.96	5.75E-11	3.47E-11	2.53E-11	2.39E-11	2.50E-11	3.39E-11	5.67E-11	5.75E-11	1.0
8	0.86	7.81	6.01E-11	3.50E-11	2.45E-11	2.30E-11	2.44E-11	3.57E-11	6.11E-11	6.11E-11	-3.0
9	0.79	8.60	6.13E-11	3.61E-11	2.46E-11	2.31E-11	2.46E-11	3.61E-11	6.15E-11	6.15E-11	1.0
10	1.20	9.80	5.42E-11	3.29E-11	2.50E-11	2.32E-11	2.49E-11	3.33E-11	5.48E-11	5.48E-11	-1.0
11	0.85	10.65	4.40E-11	3.16E-11	2.49E-11	2.11E-11	2.46E-11	3.10E-11	4.22E-11	4.40E-11	-3.0
12	0.80	11.45	4.80E-11	3.28E-11	2.35E-11	1.93E-11	2.38E-11	3.28E-11	4.80E-11	4.80E-11	3.0
13	0.81	12.25	4.37E-11	3.02E-11	2.26E-11	1.86E-11	2.25E-11	3.04E-11	4.42E-11	4.42E-11	5.0
14	0.86	13.12	4.47E-11	3.16E-11	2.44E-11	2.21E-11	2.43E-11	3.17E-11	4.49E-11	4.49E-11	1.0
15	0.80	13.92	4.39E-11	3.09E-11	2.28E-11	1.83E-11	2.27E-11	3.06E-11	4.36E-11	4.39E-11	65.0
16	0.85	14.78	4.30E-11	2.75E-11	1.92E-11	1.71E-11	1.92E-11	2.75E-11	4.30E-11	4.30E-11	73.0
17	0.84	15.62	4.33E-11	2.76E-11	1.98E-11	1.82E-11	1.97E-11	2.77E-11	4.34E-11	4.34E-11	71.0
18	0.85	16.46	4.17E-11	2.75E-11	2.06E-11	1.88E-11	2.05E-11	2.74E-11	4.16E-11	4.17E-11	71.0
19	0.83	17.29	4.24E-11	2.73E-11	2.02E-11	1.85E-11	2.01E-11	2.67E-11	4.16E-11	4.24E-11	71.0
20	0.88	18.18	4.29E-11	2.76E-11	2.09E-11	1.97E-11	2.08E-11	2.75E-11	4.29E-11	4.29E-11	71.0
21	0.90	19.08	4.09E-11	2.65E-11	1.98E-11	1.85E-11	1.99E-11	2.68E-11	4.12E-11	4.12E-11	71.0
22	0.75	19.82	3.89E-11	2.67E-11	2.39E-11	2.54E-11	2.38E-11	2.65E-11	3.89E-11	3.89E-11	71.0
23	0.92	20.74	3.97E-11	2.56E-11	1.93E-11	1.84E-11	1.91E-11	2.56E-11	3.98E-11	3.98E-11	71.0
24	1.57	22.31	4.13E-11	2.72E-11	2.04E-11	1.83E-11	2.02E-11	2.72E-11	4.15E-11	4.15E-11	71.0
25	1.27	23.58	4.04E-11	2.62E-11	2.15E-11	2.10E-11	2.15E-11	2.74E-11	4.20E-11	4.20E-11	73.0
26	1.35	24.93	4.50E-11	2.96E-11	2.28E-11	2.09E-11	2.24E-11	2.89E-11	4.44E-11	4.50E-11	71.0
27	1.33	26.27	4.17E-11	2.62E-11	1.80E-11	1.61E-11	1.80E-11	2.62E-11	4.17E-11	4.17E-11	71.0
28	1.25	27.52	4.35E-11	2.81E-11	2.10E-11	1.91E-11	2.09E-11	2.81E-11	4.36E-11	4.36E-11	71.0
29	1.37	28.89	4.36E-11	2.79E-11	2.05E-11	1.88E-11	2.04E-11	2.79E-11	4.36E-11	4.36E-11	71.0
30	1.42	30.31	3.60E-11	2.43E-11	2.16E-11	2.04E-11	2.16E-11	2.43E-11	3.61E-11	3.61E-11	73.0

Table 2.5-3 Point Beach Unit 2 Calculated Maximum Iron Atom Displacement Rate at the RPV Clad/Base Metal Interface (Continued)

Cycle	Cycle Length (EFPY)	Total Time (EFPY)	Displacement Rate (dpa/s)								Elevation of Max. (cm)
			0°	15°	30°	45°	60°	75°	90°	Maximum ^(a)	
31	1.19	31.50	4.32E-11	2.67E-11	1.62E-11	1.34E-11	1.62E-11	2.73E-11	4.41E-11	4.41E-11	71.0
32	1.33	32.83	4.92E-11	3.19E-11	2.54E-11	2.41E-11	2.57E-11	3.16E-11	4.87E-11	4.92E-11	71.0
33	1.28	34.11	5.79E-11	3.42E-11	2.34E-11	2.15E-11	2.32E-11	3.42E-11	5.80E-11	5.80E-11	71.0
34	1.45	35.56	5.45E-11	3.58E-11	2.68E-11	2.41E-11	2.68E-11	3.51E-11	5.36E-11	5.45E-11	73.0
35	1.37	36.93	6.07E-11	3.64E-11	2.45E-11	2.23E-11	2.45E-11	3.70E-11	6.14E-11	6.14E-11	-71.0
36	1.46	38.40	6.10E-11	3.60E-11	2.37E-11	2.18E-11	2.38E-11	3.60E-11	6.09E-11	6.10E-11	-73.0
37	1.40	39.80	5.51E-11	3.40E-11	2.44E-11	2.34E-11	2.41E-11	3.40E-11	5.52E-11	5.52E-11	-73.0
38	1.52	41.32	6.03E-11	3.57E-11	2.39E-11	2.21E-11	2.38E-11	3.57E-11	6.04E-11	6.04E-11	-73.0

Note:

(a) Maximum occurs at an azimuthal angle of 0°, or the octant symmetric angle, 90°.

Table 2.5-4 Point Beach Unit 2 Calculated Maximum Iron Atom Displacements at the RPV Clad/Base Metal Interface

Cycle	Cycle Length (EFPY)	Total Time (EFPY)	Displacements (dpa)								Elevation of Max. (cm)
			0°	15°	30°	45°	60°	75°	90°	Maximum ^(a)	
1	1.52	1.52	3.67E-03	2.21E-03	1.45E-03	1.24E-03	1.44E-03	2.21E-03	3.67E-03	3.67E-03	1.0
2	1.05	2.57	6.14E-03	3.70E-03	2.48E-03	2.15E-03	2.47E-03	3.70E-03	6.15E-03	6.15E-03	-3.0
3	0.87	3.44	8.16E-03	4.90E-03	3.31E-03	2.88E-03	3.29E-03	4.89E-03	8.16E-03	8.16E-03	-3.0
4	0.87	4.31	1.00E-02	6.03E-03	4.10E-03	3.56E-03	4.08E-03	6.02E-03	1.00E-02	1.00E-02	-3.0
5	0.89	5.20	1.20E-02	7.24E-03	4.92E-03	4.21E-03	4.89E-03	7.21E-03	1.19E-02	1.20E-02	-3.0
6	0.87	6.06	1.34E-02	8.20E-03	5.75E-03	4.88E-03	5.71E-03	8.18E-03	1.34E-02	1.34E-02	-3.0
7	0.89	6.96	1.50E-02	9.18E-03	6.46E-03	5.56E-03	6.42E-03	9.13E-03	1.50E-02	1.50E-02	-1.0
8	0.86	7.81	1.66E-02	1.01E-02	7.12E-03	6.18E-03	7.08E-03	1.01E-02	1.66E-02	1.66E-02	-1.0
9	0.79	8.60	1.82E-02	1.10E-02	7.74E-03	6.76E-03	7.69E-03	1.10E-02	1.82E-02	1.82E-02	-1.0
10	1.20	9.80	2.02E-02	1.23E-02	8.68E-03	7.63E-03	8.63E-03	1.23E-02	2.02E-02	2.02E-02	-1.0
11	0.85	10.65	2.14E-02	1.31E-02	9.35E-03	8.20E-03	9.29E-03	1.31E-02	2.14E-02	2.14E-02	-1.0
12	0.80	11.45	2.26E-02	1.39E-02	9.94E-03	8.68E-03	9.89E-03	1.39E-02	2.26E-02	2.26E-02	-1.0
13	0.81	12.25	2.37E-02	1.47E-02	1.05E-02	9.16E-03	1.05E-02	1.47E-02	2.37E-02	2.37E-02	-1.0
14	0.86	13.12	2.49E-02	1.56E-02	1.12E-02	9.76E-03	1.11E-02	1.55E-02	2.49E-02	2.49E-02	-1.0
15	0.80	13.92	2.61E-02	1.64E-02	1.18E-02	1.02E-02	1.17E-02	1.63E-02	2.60E-02	2.61E-02	-1.0
16	0.85	14.78	2.70E-02	1.70E-02	1.23E-02	1.07E-02	1.22E-02	1.70E-02	2.70E-02	2.70E-02	3.0
17	0.84	15.62	2.79E-02	1.76E-02	1.28E-02	1.12E-02	1.27E-02	1.76E-02	2.79E-02	2.79E-02	7.0
18	0.85	16.46	2.88E-02	1.83E-02	1.33E-02	1.17E-02	1.33E-02	1.82E-02	2.88E-02	2.88E-02	7.0
19	0.83	17.29	2.99E-02	1.89E-02	1.39E-02	1.22E-02	1.38E-02	1.89E-02	2.99E-02	2.99E-02	61.0
20	0.88	18.18	3.11E-02	1.96E-02	1.45E-02	1.27E-02	1.44E-02	1.95E-02	3.11E-02	3.11E-02	61.0
21	0.90	19.08	3.23E-02	2.03E-02	1.50E-02	1.32E-02	1.50E-02	2.03E-02	3.22E-02	3.23E-02	61.0
22	0.75	19.82	3.32E-02	2.10E-02	1.56E-02	1.38E-02	1.55E-02	2.09E-02	3.31E-02	3.32E-02	63.0
23	0.92	20.74	3.43E-02	2.17E-02	1.61E-02	1.44E-02	1.61E-02	2.17E-02	3.43E-02	3.43E-02	63.0
24	1.57	22.31	3.64E-02	2.31E-02	1.71E-02	1.53E-02	1.71E-02	2.30E-02	3.63E-02	3.64E-02	63.0
25	1.27	23.58	3.80E-02	2.41E-02	1.80E-02	1.61E-02	1.79E-02	2.41E-02	3.80E-02	3.80E-02	65.0
26	1.35	24.93	3.99E-02	2.54E-02	1.90E-02	1.70E-02	1.89E-02	2.53E-02	3.99E-02	3.99E-02	65.0
27	1.33	26.27	4.16E-02	2.65E-02	1.97E-02	1.77E-02	1.96E-02	2.64E-02	4.16E-02	4.16E-02	65.0
28	1.25	27.52	4.33E-02	2.76E-02	2.06E-02	1.84E-02	2.05E-02	2.76E-02	4.34E-02	4.34E-02	65.0
29	1.37	28.89	4.52E-02	2.88E-02	2.15E-02	1.92E-02	2.13E-02	2.88E-02	4.52E-02	4.52E-02	65.0
30	1.42	30.31	4.68E-02	2.99E-02	2.24E-02	2.01E-02	2.23E-02	2.98E-02	4.69E-02	4.69E-02	65.0

Table 2.5-4 Point Beach Unit 2 Calculated Maximum Iron Atom Displacements at the RPV Clad/Base Metal Interface (Continued)

Cycle	Cycle Length (EFPY)	Total Time (EFPY)	Displacements (dpa)								Elevation of Max. (cm)
			0°	15°	30°	45°	60°	75°	90°	Maximum ^(a)	
31	1.19	31.50	4.85E-02	3.09E-02	2.30E-02	2.06E-02	2.29E-02	3.09E-02	4.85E-02	4.85E-02	65.0
32	1.33	32.83	5.05E-02	3.22E-02	2.41E-02	2.16E-02	2.39E-02	3.22E-02	5.05E-02	5.05E-02	67.0
33	1.28	34.11	5.29E-02	3.36E-02	2.50E-02	2.25E-02	2.49E-02	3.36E-02	5.29E-02	5.29E-02	67.0
34	1.45	35.56	5.53E-02	3.52E-02	2.62E-02	2.36E-02	2.61E-02	3.52E-02	5.53E-02	5.53E-02	67.0
35	1.37	36.93	5.79E-02	3.67E-02	2.72E-02	2.45E-02	2.71E-02	3.67E-02	5.79E-02	5.79E-02	67.0
36	1.46	38.40	6.06E-02	3.84E-02	2.83E-02	2.55E-02	2.82E-02	3.83E-02	6.06E-02	6.06E-02	67.0
37	1.40	39.80	6.30E-02	3.98E-02	2.94E-02	2.65E-02	2.92E-02	3.98E-02	6.30E-02	6.30E-02	67.0
38	1.52	41.32	6.58E-02	4.15E-02	3.05E-02	2.75E-02	3.04E-02	4.14E-02	6.58E-02	6.58E-02	67.0
		42 ^(b)	6.71E-02	4.23E-02	3.10E-02	2.81E-02	3.09E-02	4.22E-02	6.71E-02	6.71E-02	67.0
		48 ^(b)	7.91E-02	4.94E-02	3.59E-02	3.25E-02	3.57E-02	4.93E-02	7.92E-02	7.92E-02	67.0
		54 ^(b)	9.12E-02	5.65E-02	4.08E-02	3.71E-02	4.07E-02	5.65E-02	9.12E-02	9.12E-02	67.0
		60 ^(b)	1.03E-01	6.36E-02	4.57E-02	4.17E-02	4.56E-02	6.36E-02	1.03E-01	1.03E-01	67.0
		66 ^(b)	1.15E-01	7.07E-02	5.06E-02	4.63E-02	5.05E-02	7.07E-02	1.15E-01	1.15E-01	67.0
		72 ^(b)	1.27E-01	7.78E-02	5.56E-02	5.09E-02	5.55E-02	7.78E-02	1.27E-01	1.27E-01	67.0

Notes:

- (a) Maximum occurs at an azimuthal angle of 0°, or the octant symmetric angle, 90°.
- (b) The projections use Cycle 38 as the basis for future projections with a 10% positive bias on peripheral assembly power.

Table 2.5-5 Point Beach Unit 2 Pressure Vessel Maximum Fast Neutron Fluence^(a)

Material	Fluence (n/cm ²)			
	41.32 EFPY	42 EFPY	48 EFPY	54 EFPY
Inlet Nozzle to Nozzle Belt Forging Weld (lowest extent) ^(b)	3.64E+16	3.70E+16	4.28E+16	4.86E+16
Nozzle Belt Forging (lowest extent) [123V352]	3.53E+18	3.59E+18	4.16E+18	4.74E+18
Nozzle Belt Forging to Intermediate Shell Circumferential Weld [21935]	4.01E+18	4.08E+18	4.74E+18	5.39E+18
Intermediate Shell Forging [123V500]	4.03E+19	4.11E+19	4.85E+19	5.59E+19
Intermediate Shell to Lower Shell Circumferential Weld [SA-1484]	3.55E+19	3.63E+19	4.37E+19	5.11E+19
Lower Shell Forging [122W195]	3.83E+19	3.92E+19	4.67E+19	5.43E+19
Lower Shell to Lower Head Ring Circumferential Weld	2.69E+16	2.75E+16	3.21E+16	3.68E+16

Material	Fluence (n/cm ²)			
	60 EFPY	66 EFPY	72 EFPY	
Inlet Nozzle to Nozzle Belt Forging Weld (lowest extent) ^(b)	5.45E+16	6.03E+16	6.61E+16	
Nozzle Belt Forging (lowest extent) [123V352]	5.31E+18	5.89E+18	6.46E+18	
Nozzle Belt Forging to Intermediate Shell Circumferential Weld [21935]	6.04E+18	6.70E+18	7.35E+18	
Intermediate Shell Forging [123V500]	6.33E+19	7.06E+19	7.80E+19	
Intermediate Shell to Lower Shell Circumferential Weld [SA-1484]	5.85E+19	6.60E+19	7.34E+19	
Lower Shell Forging [122W195]	6.19E+19	6.95E+19	7.71E+19	
Lower Shell to Lower Head Ring Circumferential Weld	4.15E+16	4.62E+16	5.08E+16	

Notes:

- (a) The projections use Cycle 38 as the basis for future projections with a 10% positive bias on peripheral assembly power.
- (b) Also applicable to outlet nozzle/nozzle belt forging weld and safety injection nozzle/nozzle belt forging weld.

Table 2.5-6 Point Beach Unit 2 Calculated Maximum Iron Atom Displacements at RPV Welds and Shells^(a)

Material	Displacements (dpa)			
	41.32 EFPY	42 EFPY	48 EFPY	54 EFPY
Inlet Nozzle to Nozzle Belt Forging Weld (lowest extent) ^(b)	3.01E-04	3.07E-04	3.56E-04	4.04E-04
Nozzle Belt Forging (lowest extent) [123V352]	6.00E-03	6.11E-03	7.09E-03	8.07E-03
Nozzle Belt Forging to Intermediate Shell Circumferential Weld [21935]	6.77E-03	6.90E-03	8.01E-03	9.12E-03
Intermediate Shell Forging [123V500]	6.58E-02	6.71E-02	7.92E-02	9.12E-02
Intermediate Shell to Lower Shell Circumferential Weld [SA-1484]	5.83E-02	5.96E-02	7.18E-02	8.40E-02
Lower Shell Forging [122W195]	6.26E-02	6.40E-02	7.63E-02	8.87E-02
Lower Shell to Lower Head Ring Circumferential Weld	1.24E-04	1.26E-04	1.48E-04	1.69E-04

Material	Fluence (n/cm ²)			
	60 EFPY	66 EFPY	72 EFPY	
Inlet Nozzle to Nozzle Belt Forging Weld (lowest extent) ^(b)	4.53E-04	5.01E-04	5.50E-04	
Nozzle Belt Forging (lowest extent) [123V352]	9.06E-03	1.00E-02	1.10E-02	
Nozzle Belt Forging to Intermediate Shell Circumferential Weld [21935]	1.02E-02	1.13E-02	1.24E-02	
Intermediate Shell Forging [123V500]	1.03E-01	1.15E-01	1.27E-01	
Intermediate Shell to Lower Shell Circumferential Weld [SA-1484]	9.62E-02	1.08E-01	1.20E-01	
Lower Shell Forging [122W195]	1.01E-01	1.13E-01	1.26E-01	
Lower Shell to Lower Head Ring Circumferential Weld	1.91E-04	2.12E-04	2.34E-04	

Notes:

- (a) The projections use Cycle 38 as the basis for future projections with a 10% positive bias on peripheral assembly power.
- (b) Also applicable to outlet nozzle/nozzle belt forging weld and safety injection nozzle/nozzle belt forging weld.

**Table 2.5-7 Point Beach Unit 2 Calculated Fast Neutron Fluence Rate ($E > 1.0$ MeV)
at Surveillance Capsule Locations**

Cycle	Cycle Length (EFPY)	Total Time (EFPY)	Fluence (n/cm ² -s)						A ^(a)
			V	T	R	S	P	N	
1	1.52	1.52	1.36E+11	7.85E+10	1.36E+11	7.40E+10	7.85E+10	7.40E+10	
2	1.05	2.57		8.06E+10	1.36E+11	7.88E+10	8.06E+10	7.88E+10	
3	0.87	3.44		7.77E+10	1.32E+11	7.69E+10	7.77E+10	7.69E+10	
4	0.87	4.31			1.25E+11	7.32E+10	7.49E+10	7.32E+10	
5	0.89	5.20			1.31E+11	7.30E+10	7.83E+10	7.30E+10	
6	0.87	6.06				7.62E+10	7.52E+10	7.62E+10	
7	0.89	6.96				6.36E+10	6.54E+10	6.36E+10	
8	0.86	7.81				6.09E+10	6.45E+10	6.09E+10	
9	0.79	8.60				6.13E+10	6.52E+10	6.13E+10	
10	1.20	9.80				6.28E+10	6.39E+10	6.28E+10	
11	0.85	10.65				6.11E+10	6.58E+10	6.11E+10	
12	0.80	11.45				5.68E+10	6.44E+10	5.68E+10	
13	0.81	12.25				5.47E+10	6.11E+10	5.47E+10	
14	0.86	13.12				6.04E+10	6.43E+10	6.04E+10	
15	0.80	13.92				5.49E+10	6.23E+10	5.49E+10	
16	0.85	14.78				4.74E+10	4.87E+10	4.74E+10	
17	0.84	15.62					5.03E+10	4.94E+10	
18	0.85	16.46					5.16E+10	5.13E+10	
19	0.83	17.29					5.07E+10	5.06E+10	
20	0.88	18.18					5.15E+10	5.28E+10	
21	0.90	19.08					4.94E+10	4.99E+10	
22	0.75	19.82					5.55E+10	6.24E+10	
23	0.92	20.74						4.89E+10	
24	1.57	22.31						5.09E+10	
25	1.27	23.58						5.52E+10	
26	1.35	24.93						5.80E+10	7.18E+10
27	1.33	26.27						4.49E+10	6.41E+10
28	1.25	27.52						5.31E+10	6.80E+10
29	1.37	28.89						5.18E+10	6.76E+10
30	1.42	30.31						5.50E+10	5.95E+10
31	1.19	31.50						3.85E+10	6.63E+10
32	1.33	32.83						6.29E+10	7.90E+10
33	1.28	34.11						5.75E+10	8.43E+10
34	1.45	35.56						6.59E+10	8.84E+10
35	1.37	36.93						5.95E+10	1.06E+11
36	1.46	38.40						5.79E+10	1.05E+11
37	1.40	39.80						6.05E+10	9.85E+10
38	1.52	41.32						5.84E+10	1.04E+11

Note:

(a) Supplemental Capsule A also identified as Supplemental Capsule W in some documents.

Table 2.5-8 Point Beach Unit 2 Calculated Neutron Fluence ($E > 1.0$ MeV) at the Surveillance Capsule Center

Cycle	Cycle Length (EFPY)	Total Time (EFPY)	Fluence (n/cm ²)						
			V	T	R	S	P	N	A ^(a)
1	1.52	1.52	6.54E+18	3.77E+18	6.54E+18	3.55E+18	3.77E+18	3.55E+18	
2	1.05	2.57		6.44E+18	1.10E+19	6.17E+18	6.44E+18	6.17E+18	
3	0.87	3.44		8.58E+18	1.47E+19	8.28E+18	8.58E+18	8.28E+18	
4	0.87	4.31			1.81E+19	1.03E+19	1.06E+19	1.03E+19	
5	0.89	5.20			2.17E+19	1.23E+19	1.28E+19	1.23E+19	
6	0.87	6.06				1.44E+19	1.49E+19	1.44E+19	
7	0.89	6.96				1.62E+19	1.67E+19	1.62E+19	
8	0.86	7.81				1.78E+19	1.85E+19	1.78E+19	
9	0.79	8.60				1.94E+19	2.01E+19	1.94E+19	
10	1.20	9.80				2.17E+19	2.25E+19	2.17E+19	
11	0.85	10.65				2.34E+19	2.43E+19	2.34E+19	
12	0.80	11.45				2.48E+19	2.59E+19	2.48E+19	
13	0.81	12.25				2.62E+19	2.74E+19	2.62E+19	
14	0.86	13.12				2.78E+19	2.92E+19	2.78E+19	
15	0.80	13.92				2.92E+19	3.08E+19	2.92E+19	
16	0.85	14.78				3.05E+19	3.21E+19	3.05E+19	
17	0.84	15.62					3.34E+19	3.18E+19	
18	0.85	16.46					3.48E+19	3.32E+19	
19	0.83	17.29					3.61E+19	3.45E+19	
20	0.88	18.18					3.76E+19	3.60E+19	
21	0.90	19.08					3.90E+19	3.74E+19	
22	0.75	19.82					4.03E+19	3.89E+19	
23	0.92	20.74						4.03E+19	
24	1.57	22.31						4.28E+19	
25	1.27	23.58						4.50E+19	
26	1.35	24.93						4.75E+19	3.06E+18
27	1.33	26.27						4.94E+19	5.76E+18
28	1.25	27.52						5.15E+19	8.44E+18
29	1.37	28.89						5.37E+19	1.14E+19
30	1.42	30.31						5.62E+19	1.40E+19
31	1.19	31.50						5.76E+19	1.65E+19
32	1.33	32.83						6.03E+19	1.98E+19
33	1.28	34.11						6.26E+19	2.33E+19
34	1.45	35.56						6.56E+19	2.73E+19
35	1.37	36.93						6.82E+19	3.19E+19
36	1.46	38.40						7.09E+19	3.68E+19
37	1.40	39.80						7.36E+19	4.11E+19
38	1.52	41.32						7.64E+19	4.61E+19
		42 ^(b)						7.77E+19	4.85E+19
		48 ^(b)						8.98E+19	7.00E+19
		54 ^(b)						1.02E+20	9.15E+19
		60 ^(b)						1.14E+20	1.13E+20
		66 ^(b)						1.26E+20	1.35E+20
		72 ^(b)						1.38E+20	1.56E+20

Notes:

(a) Supplemental Capsule A also identified as Supplemental Capsule W in some documents.

(b) The projections use Cycle 38 as the basis for future projections with a 10% positive bias on peripheral assembly power.

Table 2.5-9 Point Beach Unit 2 Calculated Iron Atom Displacement Rate at Surveillance Capsule Locations

Cycle	Cycle Length (EFPY)	Total Time (EFPY)	Displacement Rate (dpa/s)						A ^(a)
			V	T	R	S	P	N	
1	1.52	1.52	2.51E-10	1.38E-10	2.51E-10	1.31E-10	1.38E-10	1.31E-10	
2	1.05	2.57		1.42E-10	2.49E-10	1.40E-10	1.42E-10	1.40E-10	
3	0.87	3.44		1.37E-10	2.42E-10	1.36E-10	1.37E-10	1.36E-10	
4	0.87	4.31			2.28E-10	1.30E-10	1.31E-10	1.30E-10	
5	0.89	5.20			2.39E-10	1.29E-10	1.37E-10	1.29E-10	
6	0.87	6.06				1.35E-10	1.32E-10	1.35E-10	
7	0.89	6.96				1.12E-10	1.14E-10	1.12E-10	
8	0.86	7.81				1.07E-10	1.13E-10	1.07E-10	
9	0.79	8.60				1.08E-10	1.14E-10	1.08E-10	
10	1.20	9.80				1.11E-10	1.12E-10	1.11E-10	
11	0.85	10.65				1.08E-10	1.15E-10	1.08E-10	
12	0.80	11.45				1.00E-10	1.12E-10	1.00E-10	
13	0.81	12.25				9.64E-11	1.06E-10	9.64E-11	
14	0.86	13.12				1.06E-10	1.12E-10	1.06E-10	
15	0.80	13.92				9.68E-11	1.08E-10	9.68E-11	
16	0.85	14.78				8.33E-11	8.47E-11	8.33E-11	
17	0.84	15.62					8.75E-11	8.69E-11	
18	0.85	16.46					8.96E-11	9.02E-11	
19	0.83	17.29					8.81E-11	8.90E-11	
20	0.88	18.18					8.96E-11	9.28E-11	
21	0.90	19.08					8.59E-11	8.77E-11	
22	0.75	19.82					9.65E-11	1.10E-10	
23	0.92	20.74						8.60E-11	
24	1.57	22.31						8.95E-11	
25	1.27	23.58						9.73E-11	
26	1.35	24.93						1.02E-10	1.30E-10
27	1.33	26.27						7.90E-11	1.16E-10
28	1.25	27.52						9.35E-11	1.23E-10
29	1.37	28.89						9.12E-11	1.23E-10
30	1.42	30.31						9.68E-11	1.08E-10
31	1.19	31.50						6.78E-11	1.20E-10
32	1.33	32.83						1.11E-10	1.43E-10
33	1.28	34.11						1.01E-10	1.53E-10
34	1.45	35.56						1.16E-10	1.61E-10
35	1.37	36.93						1.05E-10	1.93E-10
36	1.46	38.40						1.02E-10	1.92E-10
37	1.40	39.80						1.07E-10	1.79E-10
38	1.52	41.32						1.03E-10	1.89E-10

Note:

(a) Supplemental Capsule A also identified as Supplemental Capsule W in some documents.

Table 2.5-10 Point Beach Unit 2 Calculated Iron Atom Displacements at Surveillance Capsules

Cycle	Cycle Length (EFPY)	Total Time (EFPY)	Displacements (dpa)						
			V	T	R	S	P	N	A ^(a)
1	1.52	1.52	1.20E-02	6.63E-03	1.20E-02	6.31E-03	6.63E-03	6.31E-03	
2	1.05	2.57		1.13E-02	2.03E-02	1.09E-02	1.13E-02	1.09E-02	
3	0.87	3.44		1.51E-02	2.69E-02	1.47E-02	1.51E-02	1.47E-02	
4	0.87	4.31			3.32E-02	1.82E-02	1.87E-02	1.82E-02	
5	0.89	5.20			3.99E-02	2.18E-02	2.25E-02	2.18E-02	
6	0.87	6.06				2.55E-02	2.61E-02	2.55E-02	
7	0.89	6.96				2.87E-02	2.93E-02	2.87E-02	
8	0.86	7.81				3.16E-02	3.24E-02	3.16E-02	
9	0.79	8.60				3.43E-02	3.52E-02	3.43E-02	
10	1.20	9.80				3.85E-02	3.94E-02	3.85E-02	
11	0.85	10.65				4.13E-02	4.25E-02	4.13E-02	
12	0.80	11.45				4.39E-02	4.53E-02	4.39E-02	
13	0.81	12.25				4.63E-02	4.80E-02	4.63E-02	
14	0.86	13.12				4.92E-02	5.11E-02	4.92E-02	
15	0.80	13.92				5.17E-02	5.38E-02	5.17E-02	
16	0.85	14.78				5.39E-02	5.61E-02	5.39E-02	
17	0.84	15.62					5.84E-02	5.62E-02	
18	0.85	16.46					6.08E-02	5.86E-02	
19	0.83	17.29					6.31E-02	6.10E-02	
20	0.88	18.18					6.56E-02	6.36E-02	
21	0.90	19.08					6.81E-02	6.61E-02	
22	0.75	19.82					7.04E-02	6.87E-02	
23	0.92	20.74						7.11E-02	
24	1.57	22.31						7.56E-02	
25	1.27	23.58						7.95E-02	
26	1.35	24.93						8.38E-02	5.55E-03
27	1.33	26.27						8.72E-02	1.04E-02
28	1.25	27.52						9.08E-02	1.53E-02
29	1.37	28.89						9.48E-02	2.06E-02
30	1.42	30.31						9.91E-02	2.54E-02
31	1.19	31.50						1.02E-01	2.99E-02
32	1.33	32.83						1.06E-01	3.60E-02
33	1.28	34.11						1.10E-01	4.22E-02
34	1.45	35.56						1.16E-01	4.95E-02
35	1.37	36.93						1.20E-01	5.79E-02
36	1.46	38.40						1.25E-01	6.68E-02
37	1.40	39.80						1.30E-01	7.47E-02
38	1.52	41.32						1.35E-01	8.38E-02
		42 ^(b)						1.37E-01	8.82E-02
		48 ^(b)						1.58E-01	1.27E-01
		54 ^(b)						1.80E-01	1.67E-01
		60 ^(b)						2.01E-01	2.06E-01
		66 ^(b)						2.22E-01	2.45E-01
		72 ^(b)						2.44E-01	2.84E-01

Notes:

(a) Supplemental Capsule A also identified as Supplemental Capsule W in some documents.

(b) The projections use Cycle 38 as the basis for future projections with a 10% positive bias on peripheral assembly power.

Table 2.5-11 Point Beach Unit 2 Calculated Surveillance Capsule Lead Factors

Cycle	Cycle Length (EFPY)	Total Time (EFPY)	Lead Factor						A ^(a)
			V	T	R	S	P	N	
1	1.52	1.52	2.92	1.68	2.92	1.59	1.68	1.59	
2	1.05	2.57		1.72	2.94	1.64	1.72	1.64	
3	0.87	3.44		1.72	2.94	1.66	1.72	1.66	
4	0.87	4.31			2.95	1.68	1.73	1.68	
5	0.89	5.20			2.97	1.68	1.75	1.68	
6	0.87	6.06				1.76	1.81	1.76	
7	0.89	6.96				1.76	1.82	1.76	
8	0.86	7.81				1.75	1.81	1.75	
9	0.79	8.60				1.74	1.81	1.74	
10	1.20	9.80				1.76	1.82	1.76	
11	0.85	10.65				1.78	1.85	1.78	
12	0.80	11.45				1.79	1.87	1.79	
13	0.81	12.25				1.80	1.89	1.80	
14	0.86	13.12				1.82	1.91	1.82	
15	0.80	13.92				1.83	1.93	1.83	
16	0.85	14.78				1.85	1.94	1.85	
17	0.84	15.62					1.96	1.86	
18	0.85	16.46					1.97	1.88	
19	0.83	17.29					1.97	1.89	
20	0.88	18.18					1.97	1.89	
21	0.90	19.08					1.97	1.89	
22	0.75	19.82					1.98	1.92	
23	0.92	20.74						1.92	
24	1.57	22.31						1.92	
25	1.27	23.58						1.94	
26	1.35	24.93						1.95	0.13
27	1.33	26.27						1.94	0.23
28	1.25	27.52						1.94	0.32
29	1.37	28.89						1.94	0.41
30	1.42	30.31						1.96	0.49
31	1.19	31.50						1.94	0.56
32	1.33	32.83						1.95	0.64
33	1.28	34.11						1.93	0.72
34	1.45	35.56						1.94	0.80
35	1.37	36.93						1.92	0.90
36	1.46	38.40						1.91	0.99
37	1.40	39.80						1.91	1.07
38	1.52	41.32						1.89	1.14
		42 ^(b)						1.89	1.18
		48 ^(b)						1.85	1.44
		54 ^(b)						1.82	1.64
		60 ^(b)						1.80	1.79
		66 ^(b)						1.79	1.90
		72 ^(b)						1.77	2.00

Notes:

(a) Supplemental Capsule A also identified as Supplemental Capsule W in some documents.

(b) The projections use Cycle 38 as the basis for future projections with a 10% positive bias on peripheral assembly power.

Table 2.5-12 Point Beach Unit 2 Ex-Vessel Neutron Dosimetry Summary

Cycle 15 Irradiation Capsule Set 2 Identification				
Azimuth (degrees)	Vessel Support	Core Top	Core Midplane	Core Bottom
0	XX	G	H	I
15			J	
30			K	
45			L	
Cycle 16 Irradiation Capsule Set 3 Identification				
Azimuth (degrees)	Vessel Support	Core Top	Core Midplane	Core Bottom
0		M	N	O
15			P	
30			Q	
45			R	
Cycle 17 Irradiation Capsule Set 5 Identification				
Azimuth (degrees)	Vessel Support	Core Top	Core Midplane	Core Bottom
0		AA	BB	CC
15			DD	
30			EE	
45			FF	
Cycles 18–20 Irradiation Capsule Set 7 Identification				
Azimuth (degrees)	Vessel Support	Core Top	Core Midplane	Core Bottom
0		MM	NN	OO
15			PP	
30			QQ	
45			RR	

Table 2.5-13 Point Beach Unit 2 Comparison of Measured to Calculated Threshold Reaction Rates – In-Vessel Capsules

Capsule	Reaction					
	⁶³ Cu (n,α)	⁵⁴ Fe (n,p) Rear	⁵⁴ Fe (n,p) Front	⁵⁸ Ni (n,p)	²³⁸ U (n,f)	²³⁷ Np (n,f)
V	0.92	0.95	0.89		1.09	1.07
T	0.97	1.02	1.01	0.99	0.99	1.08
R	1.03	0.98	0.98	1.01	1.04	1.09
S	1.07			0.94	1.10	1.07
Average	1.00	0.99	0.96	0.98	1.05	1.08
% std dev	6.4	3.5	6.7	3.6	4.8	0.9

Reaction	Average M/C	% Standard Deviation
⁶³ Cu (n,α)	1.00	6.4
⁵⁴ Fe (n,p) Rear	0.99	3.5
⁵⁴ Fe (n,p) Front	0.96	6.7
⁵⁸ Ni (n,p)	0.98	3.6
²³⁸ U (n,f)	1.05	4.8
²³⁷ Np (n,f)	1.08	0.9
Linear Average	1.01	5.9

Table 2.5-14 Point Beach Unit 2 Comparison of Measured to Calculated Threshold Reaction Rates – Ex-Vessel Midplane Capsules

Capsule	Reaction						
	$^{63}\text{Cu (n,\alpha)}$	$^{46}\text{Ti (n,p)}$	$^{54}\text{Fe (n,p)}$	$^{54}\text{Fe (n,p)}$ (Cd)	$^{58}\text{Ni (n,p)}$	$^{238}\text{U (n,f)}$	$^{237}\text{Np (n,f)}$
H	0.86	0.89	0.82	0.84	0.85	0.84	1.00
J	0.98	1.01	0.91	0.89	0.90	0.90	1.07
K	0.92	0.96	0.94	0.87	0.88	0.88	1.00
L	0.98	1.03	0.90	0.88	0.93	0.96	1.16
N	0.84	0.86	0.82	0.79	0.82	0.82	
P	0.91	0.91	0.86	0.82	0.86	0.86	
Q	0.97	0.96	0.89	0.91	0.90	0.87	
R	0.99	0.97	0.94	0.92	0.94	0.91	
BB	0.87	0.87	0.85	0.82	0.83	0.81	
DD	0.96	0.95	0.89	0.88	0.88	0.87	
EE	0.94	0.96	0.88	0.88	0.88	0.90	
FF	0.98	0.97	0.91	0.90	0.91	0.89	
NN	0.88	0.89	0.83	0.81	0.83	0.84	
PP	0.95	0.93	0.83	0.85	0.85	0.88	
QQ	0.95	0.95	0.85	0.84	0.86	0.86	
RR	0.95	0.92	0.84	0.85	0.87	0.90	
Average	0.93	0.94	0.87	0.86	0.87	0.87	1.06
% std dev	5.0	5.1	4.7	4.4	4.0	4.2	7.4

Reaction	Average M/C	% Standard Deviation
$^{63}\text{Cu (n,\alpha)}$	0.93	5.0
$^{46}\text{Ti (n,p)}$	0.94	5.1
$^{54}\text{Fe (n,p)}$	0.87	4.7
$^{54}\text{Fe (n,p) Cd}$	0.86	4.4
$^{58}\text{Ni (n,p)}$	0.87	4.0
$^{238}\text{U (n,f)}$	0.87	4.2
$^{237}\text{Np (n,f)}$	1.06	7.4
Linear Average	0.90	6.8

Table 2.5-15 Point Beach Unit 2 Comparison of Measured to Calculated Threshold Reaction Rates – Ex-Vessel Off-Midplane Capsules

Capsule	Reaction						
	$^{63}\text{Cu} (n,\alpha)$	$^{46}\text{Ti} (n,p)$	$^{54}\text{Fe} (n,p)$	$^{54}\text{Fe} (n,p)$ Cd	$^{58}\text{Ni} (n,p)$	$^{238}\text{U} (n,f)$	$^{237}\text{Np} (n,f)$
G	0.76	0.87	0.71	0.81	0.81	0.86	0.97
I	0.79	0.89	0.77	0.77	0.82	0.88	1.03
XX	0.77	0.82	0.71	0.74	0.72	0.95	1.04
M	0.94	1.00	0.93	0.92	0.97	1.03	
O	0.87	0.94	0.87	0.85	0.92	0.98	
AA	0.99	1.05	0.96	0.96	1.02	1.09	
CC	0.92	0.99	0.90	0.88	0.95	0.98	
MM	0.86	0.95	0.82	0.83	0.91	0.94	
OO	0.79	0.94	0.81	0.80	0.87	0.92	

Table 2.5-16 Point Beach Unit 2 Comparison of Best-Estimate to Calculated Exposure Rates – In-Vessel Capsules

Capsule	Neutron Fluence Rate (E > 1.0 MeV)		Iron Displacement Rate	
	BE/C	% std dev	BE/C	% std dev
V	0.99	6	1.00	7
T	1.02	6	1.02	7
R	1.02	6	1.03	7
S	1.01	6	1.02	7
Average	1.01	1.2	1.02	1.3

Table 2.5-17 Point Beach Unit 2 Comparison of Best-Estimate to Calculated Exposure Rates – Ex-Vessel Midplane Capsules

Capsule	Neutron Fluence Rate (E > 1.0 MeV)		Iron Displacement Rate	
	BE/C	% std dev	BE/C	% std dev
H	0.87	6	0.91	9
J	0.92	6	0.95	9
K	0.91	6	0.93	9
L	0.95	6	0.99	9
N	0.82	7	0.84	10
P	0.84	7	0.86	11
Q	0.88	7	0.89	10
R	0.91	7	0.91	10
BB	0.83	7	0.84	10
DD	0.86	7	0.88	11
EE	0.88	7	0.89	10
FF	0.89	7	0.89	10
NN	0.83	7	0.85	10
PP	0.84	7	0.86	11
QQ	0.84	7	0.86	11
RR	0.86	7	0.87	10
Average	0.87	4.4	0.89	4.8

Table 2.5-18 Point Beach Unit 2 Total Database Summary (M/C Reaction Rate Ratios)

Reaction	In-Vessel Database		Midplane Ex-Vessel Database		Combined Database	
	Average M/C	% Unc. (1 σ)	Average M/C	% Unc. (1 σ)	Average M/C	% Unc. (1 σ)
⁶³ Cu (n, α)	1.00	6.4	0.93	5.0	0.97	4.1
⁴⁶ Ti (n,p)	-	-	0.94	5.1	-	-
⁵⁴ Fe (n,p)	0.97	5.0	0.87	4.5	0.92	3.4
⁵⁸ Ni (n,p)	0.98	3.6	0.87	4.0	0.93	2.7
²³⁸ U (n,f)	1.05	4.8	0.87	4.2	0.96	3.2
²³⁷ Np (n,f)	1.08	0.9	1.06	7.4	1.07	3.7
Linear Average	1.01	5.9	0.90	6.8	0.96	4.3

Table 2.5-19 Point Beach Unit 2 Total Database Summary (Integral Exposure Rate Ratios)

Parameter	In-Vessel Database		Midplane Ex-Vessel Database		Combined Database	
	Average BE/C	% Unc. (1 σ)	Average BE/C	% Unc. (1 σ)	Average BE/C	% Unc. (1 σ)
Fluence Rate (E > 1.0 MeV)	1.01	1.2	0.87	4.4	0.94	2.3
dpa/s	1.02	1.3	0.89	4.8	0.96	2.5

3 FRACTURE TOUGHNESS PROPERTIES

The requirements for RVI are specified in 10 CFR 50, Appendix G [Ref. 8] and 10 CFR 50.61 [Ref. 9]. The beltline region of the reactor vessel is defined as the following in 10 CFR 50, Appendix G:

... the region of the reactor vessel (shell material including welds, heat affected zones and plates or forgings) that directly surrounds the effective height of the active core and adjacent regions of the reactor vessel that are predicted to experience sufficient neutron radiation damage to be considered in the selection of the most limiting material with regard to radiation damage.

As described in NRC Regulatory Issue Summary (RIS) 2014-11 [Ref. 10], any reactor vessel materials that are predicted to experience a neutron fluence exposure greater than 1.0×10^{17} n/cm² ($E > 1.0$ MeV) at the end of the licensed operating period should be considered to experience neutron embrittlement. The materials that exceed this fluence threshold are referred to as the “beltline” materials herein and are evaluated to ensure that the applicable neutron embrittlement effects are considered.

As seen from Tables 2.4-5 and 2.5-5, the beltline materials include the nozzle belt forging, the intermediate shell, the lower shell, and the longitudinal and circumferential welds connecting these components. (Note that for reactor vessel welds, the terms “girth” and “circumferential” are used interchangeably; herein, these welds shall be referred to as circumferential welds.) The fluence for the safety injection/inlet/outlet nozzle to nozzle belt forging welds are less than 1.0×10^{17} n/cm² ($E > 1.0$ MeV) at 72 EFPY. Therefore, the materials of the safety injection/inlet/outlet nozzle forgings and the associated welds to the nozzle belt forging do not need to be considered in the beltline. Figure 3-1 provides a schematic of the RPV which identifies the beltline region.

Although the reactor vessel nozzles are not a part of the extended beltline, per NRC RIS 2014-11, the nozzle materials must be evaluated for their potential effect on P-T limit curves due to the higher stresses in the nozzle corner region. These higher stresses can potentially result in more restrictive P-T limits, even if the RT_{NDT} for these components are not as high as those of the reactor vessel beltline shell materials that have simpler geometries. The effect of these higher stresses is addressed in Section 7.2.

A summary of the best-estimate copper (Cu) and nickel (Ni) contents in units of weight percent (wt. %), as well as initial RT_{NDT} and σ_I for the Point Beach Units 1 and 2 reactor vessel beltline materials are provided in Table 3-1.

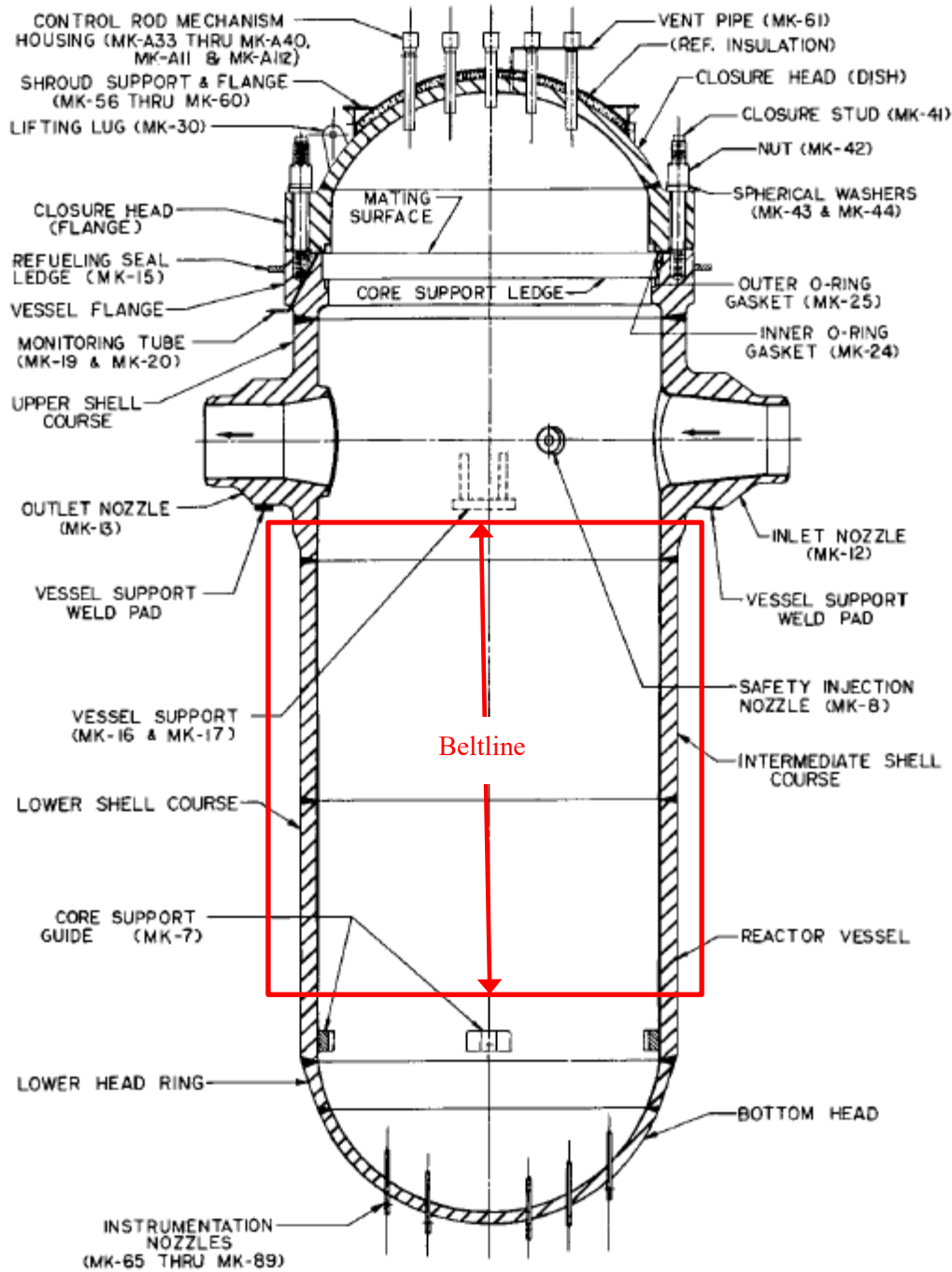


Figure 3-1 RPV Base Metal Material Identifications for Point Beach Units 1 and 2

Note: Beltline region is approximate and meant for illustrational purposes only. Additionally, the closure head is representative of the original closure head. This figure specifically represents Unit 1; however, the general layout of the Unit 2 RPV is the same as for Unit 1.

Table 3-1 Point Beach Units 1 and 2 Reactor Vessel Beltline and Surveillance Material Properties and Chemistry^(a)

Material Description	Heat Number	Flux Type (Lot) ^(b)	Wt. % Cu	Wt. % Ni	RT _{NDT(U)} (°F)	σ_I ^(c) (°F)
Unit 1						
Nozzle Belt (NB) Forging	122P237	-	0.11 ^(d)	0.82	50	0
Intermediate Shell (IS) Plate	A9811-1	-	0.20	0.06	1	26.9 ^(e)
Lower Shell (LS) Plate	C1423-1	-	0.12	0.07	1	26.9 ^(e)
NB to IS Circ. Weld (100%)	8T1762 (SA-1426)	Linde 80 (8553)	0.19	0.57	-48.6 ^(f)	18.0 ^(f)
IS Long. Weld (Inner Diameter [ID] 27%)	1P0815 (SA-812)	Linde 80 (8350)	0.17	0.52	-48.6 ^(f)	18.0 ^(f)
IS Long. Weld (Outer Diameter [OD] 73%)	1P0661 (SA-775)	Linde 80 (8304)	0.17	0.64	-48.6 ^(f)	18.0 ^(f)
IS to LS Circ. Weld (100%)	71249 (SA-1101)	Linde 80 (8445)	0.23	0.59	-53.5 ^(f)	12.8 ^(f)
LS Long. Weld (100%)	61782 (SA-847)	Linde 80 (8350)	0.23	0.52	-58.5 ^(f)	15.4 ^(f)
Unit 1 Surveillance Weld ^(g)	72445 (SA-1263)	Linde 80 (8504)	0.23	0.62	-	-
Unit 2						
Nozzle Belt Forging	123V352	-	0.11 ^(d)	0.73	40	0
Intermediate Shell Forging	123V500	-	0.09	0.70	40	0
Lower Shell Forging	122W195	-	0.05	0.72	40	0
NB to IS Circ. Weld	21935	Linde 1092 (3869)	0.18	0.70	-56 ^(h)	17 ^(h)
IS to LS Circ. Weld	72442 (SA-1484)	Linde 80 (8579)	0.26	0.60	-33.2 ^(f)	12.2 ^(f)
Unit 2 Surveillance Weld ^(g)	406L44 (WF-193)	Linde 80 (8773)	0.25	0.59	-	-

Notes:

- (a) Information extracted from WCAP-16669-NP [Ref. 11] and/or Pressure Temperature Limits Report (PTLR) [Ref. 12], unless otherwise noted.
- (b) Lot # taken from BAW-2325, Revision 1 [Ref. 13] for the Linde 80 welds and MISC-PENG-ER-019 [Ref. 14] for the Linde 1092 weld.
- (c) All RT_{NDT(U)} values are based on measured data with a $\sigma_I = 0^\circ\text{F}$, unless otherwise noted.
- (d) Value confirmed to be a conservative estimate in LTR-SDA-20-039 [Ref. 15].
- (e) σ_I is set equal to 26.9°F to be consistent with the analysis of record (AOR), AREVA Calculation 32-9019240-000 [Ref. 16].
- (f) RT_{NDT(U)} and σ_I updated per BAW-2308, Revision 2-A [Ref. 17].
- (g) The reactor vessel surveillance programs are described in WCAP-7513 [Ref. 18] and WCAP-7712 [Ref. 19] for Units 1 and 2, respectively. The chemistry and heat/lot of the surveillance welds are identified in BAW-2325. Note that the heats are not used in the Point Beach Units 1 and 2 RVs; hence, the surveillance results are not directly applicable to and not used in this report.
- (h) Generic RT_{NDT(U)} and σ_I value for Linde 1092 per 10 CFR 50.61 [Ref. 9].

4 SURVEILLANCE DATA

Per Regulatory Guide 1.99, Revision 2 [Ref. 4], calculation of Position 2.1 chemistry factors (CFs) requires data from the plant-specific surveillance program. In addition to the plant-specific surveillance data, data from surveillance programs at other plants which include a Point Beach Units 1 and 2 reactor vessel beltline material may also need to be considered when calculating Position 2.1 CFs. Data from a surveillance program at another plant is often called 'sister plant' data.

The Point Beach Unit 1 surveillance capsules contain shell material from intermediate and lower shell plates. Table 4-1 summarizes the surveillance data available from the Point Beach Unit 1 reactor vessel surveillance program that will be used in the calculation of the Position 2.1 CF values. Per Appendix A, the surveillance plate data are deemed credible for Point Beach Unit 1; therefore, a reduced margin term will be utilized in the PTS and ART calculations contained in Sections 6 and 7. The surveillance weld material is not used in the Point Beach Unit 1 RVs; hence, the surveillance weld results are not applicable and not included herein.

The Point Beach Unit 2 surveillance capsules contain shell material from intermediate and lower shell forgings. Table 4-2 summarizes the surveillance data available from the Point Beach Unit 2 reactor vessel surveillance program that will be used in the calculation of the Position 2.1 CF values. Per Appendix A, the surveillance forging data are deemed credible for Point Beach Unit 2; therefore, a reduced margin term will be utilized in the PTS and ART calculations contained in Sections 6 and 7. The surveillance weld material is not used in the Point Beach Unit 2 RVs; hence, the surveillance weld results are not applicable and not included herein.

There exists surveillance weld data available from sister plants for weld Heat #s 61782, 71249, and 72442 which are used in the Point Beach Units 1 and 2 RVs. However; AREVA Calculation 32-9019240-000 [Ref. 16] determined that the generic Table 1 CFs in Regulatory Guide 1.99, Revision 2, are conservative with respect to the measured data. Since this conclusion is based solely on sister plant data, it is unchanged when considering SLR for Point Beach Units 1 and 2. It is noted that Ginna Capsule N test results, documented in WCAP-17036-NP [Ref. 20], were not available when AREVA Calculation 32-9019240-000 was performed. However, since the testing for Heat # 61782 in WCAP-17036-NP showed measured data less than the Position 1.1 prediction, the additional test data is not expected to impact the Heat # 61782 conclusion. Furthermore, these sister plant welds are Linde 80 welds which use the initial RT_{NDT} from BAW-2308 [Ref. 17]. BAW-2308 requires a minimum CF of 167°F. Therefore, these welds use the maximum CF between the Position 1.1 CF or the minimum CF required by BAW-2308 (167°F).

Table 4-1 Point Beach Unit 1 Surveillance Program Results

Material	Capsule	Withdrawal (EOC)	Fluence ^(a) (n/cm ² , E > 1.0 MeV)	Measured $\Delta RT_{NDT}^{(b)}$ (°F)	Irradiation Temperature (°F)
Unit 1 Surveillance Plate; Intermediate Shell Plate (Heat # A9811-1)	V	1	6.23E+18	81	553
	S	3	8.13E+18	87	547
	R	5	2.13E+19	93	546
	T	11	2.14E+19	82	541
Unit 1 Surveillance Plate; Lower Shell Plate (Heat # C1423-1)	V	1	6.23E+18	41	553
	S	3	8.13E+18	43	547
	R	5	2.13E+19	28	546
	T	11	2.14E+19	45	541

Notes:

- (a) The fluence values are taken from Table 2.4-8.
- (b) Information is extracted from BAW-2325 [Ref. 13]. All specimens are in the longitudinal (LT) direction.

Table 4-2 Point Beach Unit 2 Surveillance Program Results

Material	Capsule	Withdrawal (End-of-cycle [EOC])	Fluence ^(a) (n/cm ² , E > 1.0 MeV)	Measured $\Delta RT_{NDT}^{(b)}$ (°F)	Irradiation Temperature (°F)
Unit 2 Surveillance Forging; Intermediate Shell Forging (Heat # 123V500)	V	1	6.54E+18	39	553
	T	3	8.58E+18	62	547
	R	5	2.17E+19	88	546
	S	16	3.05E+19	101	544
Unit 2 Surveillance Forging; Lower Shell Forging (Heat # 122W195)	V	1	6.54E+18	39	553
	T	3	8.58E+18	35	547
	R	5	2.17E+19	50	546
	S	16	3.05E+19	61	544

Notes

- (a) The fluence values are taken from Table 2.5-8 of this report.
- (b) Information is extracted from BAW-2325 [Ref. 13]. All specimens are in the tangential direction.

5 CHEMISTRY FACTORS

The chemistry factors (CFs) were calculated using Regulatory Guide 1.99, Revision 2, Positions 1.1 and 2.1. Position 1.1 CFs for each reactor vessel material are calculated using the best-estimate copper and nickel weight percent of the material and Tables 1 and 2 of Regulatory Guide 1.99, Revision 2. However, a minimum CF of 167°F is utilized for materials which use initial RT_{NDT} values from BAW-2308 [Ref.17]. The best-estimate copper and nickel weight percent values for the Point Beach Units 1 and 2 reactor vessel materials are provided in Table 3-1.

The Position 2.1 CFs are calculated for the materials that have available surveillance data from the plant-specific surveillance program. The Position 2.1 CF calculation is performed using the method described in Regulatory Guide 1.99, Revision 2. The Point Beach Units 1 and 2 surveillance data are summarized in Section 4 and will be utilized in the Position 2.1 CF calculations in this section. The Position 2.1 CF calculations are presented in Table 5-1 for the Point Beach Unit 1 surveillance materials. The Position 2.1 CF calculations are presented in Table 5-2 for the Point Beach Unit 2 surveillance materials. No adjustments of the measured ΔRT_{NDT} values are required due to chemistry and/or temperature differences since all data is from the plant-specific program.

The Position 1.1 and Position 2.1 CFs are summarized in Table 5-3 for Point Beach Units 1 and 2.

Table 5-1 Calculation of Chemistry Factors Using Point Beach Unit 1 Surveillance Capsule Data

Material	Capsule	Capsule Fluence ^(a) (x 10 ¹⁹ n/cm ² , E > 1.0 MeV)	FF ^(b)	Measured ΔRT_{NDT} ^(a) (°F)	FF * ΔRT_{NDT} (°F)	FF ²	
Unit 1 Surveillance Plate; Intermediate Shell Plate (Heat # A9811-1)	V	0.623	0.867	81	70.26	0.752	
	S	0.813	0.942	87	81.95	0.887	
	R	2.13	1.205	93	112.11	1.453	
	T	2.14	1.207	82	98.95	1.456	
	SUM:					363.27	4.549
	$CF_{A9811-1} = \Sigma(FF * \Delta RT_{NDT}) \div \Sigma(FF^2) = (363.27) \div (4.549) = 79.9^{\circ}F$						
Unit 1 Surveillance Plate; Lower Shell Plate (Heat # C1423-1)	V	0.623	0.867	41	35.56	0.752	
	S	0.813	0.942	43	40.50	0.887	
	R	2.13	1.205	28	33.75	1.453	
	T	2.14	1.207	45	54.30	1.456	
	SUM:					164.12	4.549
	$CF_{C1423-1} = \Sigma(FF * \Delta RT_{NDT}) \div \Sigma(FF^2) = (164.12) \div (4.549) = 36.1^{\circ}F$						

Notes:(a) The fluence and ΔRT_{NDT} values are taken from Table 4-1.(b) FF = fluence factor = $f^{(0.28 - 0.10 * \log(f))}$.

Table 5-2 Calculation of Chemistry Factors Using Point Beach Unit 2 Surveillance Capsule Data

Material	Capsule	Capsule Fluence ^(a) (x 10 ¹⁹ n/cm ² , E > 1.0 MeV)	FF ^(b)	Measured ΔRT_{NDT} ^(a) (°F)	FF * ΔRT_{NDT} (°F)	FF ²	
Unit 2 Surveillance Forging; Intermediate Shell Forging (Heat # 123V500)	V	0.654	0.881	39	34.36	0.776	
	T	0.858	0.957	62	59.34	0.916	
	R	2.17	1.210	88	106.51	1.465	
	S	3.05	1.295	101	130.76	1.676	
	SUM:					330.96	4.833
	$CF_{123V500} = \Sigma(FF * \Delta RT_{NDT}) \div \Sigma(FF^2) = (330.96) \div (4.833) = 68.5^{\circ}F$						
Unit 2 Surveillance Forging; Lower Shell Forging (Heat # 122W195)	V	0.654	0.881	39	34.36	0.776	
	T	0.858	0.957	35	33.50	0.916	
	R	2.17	1.210	50	60.51	1.465	
	S	3.05	1.295	61	78.97	1.676	
	SUM:					207.34	4.833
	$CF_{122W195} = \Sigma(FF * \Delta RT_{NDT}) \div \Sigma(FF^2) = (207.34) \div (4.833) = 42.9^{\circ}F$						

Notes:(a) The fluence and ΔRT_{NDT} values are taken from Table 4-2.(b) FF = fluence factor = $f^{(0.28 - 0.10 * \log(f))}$.

Table 5-3 Position 1.1 and 2.1 Chemistry Factors for Point Beach Units 1 and 2

Material Description	Chemistry Factor	
	Position 1.1 ^(a) (°F)	Position 2.1 ^(b) (°F)
<i>Unit 1</i>		
Nozzle Belt Forging	77.0	-
Intermediate Shell Plate	88.0	79.9
Lower Shell Plate	55.3	36.1
NB To IS Circ. Weld (100%)	167.0	-
IS Long. Weld (ID 27%)	167.0	-
IS Long. Weld (OD 73%)	167.0	-
IS to LS Circ. Weld (100%)	167.6	-
LS Long. Weld (100%)	167.0	-
<i>Unit 2</i>		
Nozzle Belt Forging	76.0	-
Intermediate Shell Forging	58.0	68.5
Lower Shell Forging	31.0	42.9
NB to IS Circ. Weld	170.5	-
IS to LS Circ. Weld	180.0	-

Notes:

- (a) All values are based on Tables 1 and 2 of Regulatory Guide 1.99, Revision 2 (Position 1.1) using the Cu and Ni weight percent values given in Table 3-1. However, for Linde 80 weld materials implementing BAW-2308, a minimum CF of 167°F is required.
- (b) Values are from Tables 5-1 and 5-2.

6 PRESSURIZED THERMAL SHOCK EVALUATION

Pressurized thermal shock (PTS) may occur during a severe system transient such as a loss-of-coolant accident (LOCA) or steam line break. Such transients may challenge the integrity of the RPV under the following conditions: severe overcooling of the inside surface of the vessel wall followed by high pressurization, significant degradation of vessel material toughness caused by radiation embrittlement, and the presence of a critical-size defect anywhere within the vessel wall.

In 1985, the U.S. NRC issued a formal ruling on PTS (10 CFR 50.61 [Ref. 9]) that established screening criteria on pressurized water reactor (PWR) vessel embrittlement, as measured by the maximum reference nil-ductility transition temperature in the limiting beltline component at the end of license, termed RT_{PTS} . RT_{PTS} screening values were set by the U.S. NRC for beltline axial welds, forgings or plates, and for beltline circumferential weld seams for plant operation to the end of plant license. All domestic PWR vessels have been required to evaluate vessel embrittlement in accordance with the criteria through the end of license. The U.S. NRC revised 10 CFR 50.61 in 1991 and 1995 to change the procedure for calculating radiation embrittlement. These revisions make the procedure for calculating the reference temperature for pressurized thermal shock (RT_{PTS}) values consistent with the methods given in Regulatory Guide 1.99, Revision 2 [Ref. 4].

These accepted methods were used with the clad/base metal interface fluence values of Sections 2 and 1.1 to calculate the following RT_{PTS} values for the Point Beach Units 1 and 2 RPV materials at 72 EFPY (SLR). The RT_{PTS} calculations are summarized in Table 6-1.

PTS Conclusion

All of the beltline reactor vessel materials for Point Beach Units 1 and 2 are projected to remain below the RT_{PTS} screening criteria values of 270°F for plates, forgings, and longitudinal welds, and 300°F for circumferentially oriented welds (per 10 CFR 50.61) at SLR.

Table 6-1 RT_{PTS} Calculations for Point Beach Units 1 and 2 Reactor Vessel Beltline Materials

Material	Heat #	CF ^(a)	Surface Fluence ^(b) (x 10 ¹⁹ n/cm ² , E > 1.0 MeV)	Surf. FF ^(c)	RT _{NDT(U)} ^(d) (°F)	Predicted ΔRT _{NDT} (°F)	σ _U (°F)	σ _Δ ^(e) (°F)	M (°F)	RT _{PTS} (°F)
<i>Unit 1</i>										
Nozzle Belt Forging	122P237	77.0	0.481	0.796	50	61.3	0	17	34.0	145.3
Intermediate Shell Plate	A9811-1	88.0	7.64	1.477	1	129.9	26.9	17	63.6	194.6
IS with credible surveillance data ^(f)		79.9	7.64	1.477	1	118.0	26.9	8.5	56.4	175.4
Lower Shell Plate	C1423-1	55.3	7.31	1.470	1	81.3	26.9	17	63.6	145.9
LS with credible surveillance data ^(f)		36.1	7.31	1.470	1	53.1	26.9	8.5	56.4	110.5
NB to IS Circ. Weld (100%)	8T1762 (SA-1426)	167.0	0.554	0.835	-48.6	139.4	18.0	28	66.6	157.4
IS Long. Weld (ID 27%)	1P0815 (SA-812)	167.0	4.54	1.383	-48.6	231.0	18.0	28	66.6	248.9
IS Long. Weld (OD 73%) ^(g)	1P0661 (SA-775)	167.0	4.54	1.383	-48.6	231.0	18.0	28	66.6	248.9
IS to LS Circ. Weld (100%)	71249 (SA-1101)	167.6	7.19	1.467	-53.5	245.9	12.8	28	61.6	254.0
LS Long. Weld (100%)	61782 (SA-847)	167.0	4.48	1.380	-58.5	230.5	15.4	28	63.9	235.9
<i>Unit 2</i>										
Nozzle Belt Forging	123V352	76.0	0.646	0.878	40	66.7	0	17	34.0	140.7
Intermediate Shell Forging	123V500	58.0	7.80	1.480	40	85.8	0	17	34.0	159.8
IS with credible surveillance data ^(f)		68.5	7.80	1.480	40	101.4	0	8.5	17.0	158.4
Lower Shell Forging	122W195	31.0	7.71	1.478	40	45.8	0	17	34.0	119.8
LS with credible surveillance data ^(f)		42.9	7.71	1.478	40	63.4	0	8.5	17.0	120.4
NB to IS Circ. Weld	21935	170.5	0.735	0.914	-56	155.8	17	28	65.5	165.3
IS to LS Circ. Weld	72442 (SA-1484)	180.0	7.34	1.470	-33.2	264.7	12.2	28	61.1	292.6

Notes contained on the following page.

Notes:

- (a) Chemistry factors are taken from Table 5-3.
- (b) The 72 EFPY surface fluence values for the reactor vessel materials were taken from Tables 2.4-5 and 2.5-5.
- (c) $FF = \text{fluence factor} = f^{(0.28 - 0.10 * \log(f))}$.
- (d) $RT_{NDT(U)}$ values taken from Table 3-1.
- (e) Per 10 CFR 50.61, the base metal $\sigma_{\Delta} = 17^{\circ}\text{F}$ when surveillance data is non-credible or not used to determine the CF, and the base metal $\sigma_{\Delta} = 8.5^{\circ}\text{F}$ when credible surveillance data is used to determine the CF. Also, per 10 CFR 50.61, the weld metal $\sigma_{\Delta} = 28^{\circ}\text{F}$ when surveillance data is non-credible or not used to determine the CF, and the weld metal $\sigma_{\Delta} = 14^{\circ}\text{F}$ when credible surveillance data is used to determine the CF. However, σ_{Δ} need not exceed $0.5 * \Delta RT_{NDT}$.
- (f) The credibility evaluation for the Point Beach Units 1 and 2 surveillance data in Appendix A of this calculation determined that the Point Beach Unit 1 surveillance data for the plate materials are deemed credible. Point Beach Unit 2 surveillance forging data for the forging materials are deemed credible. Therefore, the Position 2.1 CF can be used with a reduced margin term in lieu of the Position 1.1 CF.
- (g) This material is not present at the inner surface of the RV; however, the calculation is shown for information.

7 HEATUP AND COOLDOWN PRESSURE-TEMPERATURE LIMIT CURVES

Heatup and cooldown limit curves, also known as pressure-temperature (P-T) limit curves, are calculated using the most limiting value of RT_{NDT} (reference nil-ductility transition temperature) corresponding to the limiting material in the RPV. The most limiting RT_{NDT} of the material in the RPV is determined by using the unirradiated RPV material fracture toughness properties and estimating the irradiation-induced shift (ΔRT_{NDT}) per RG 1.99 [Ref. 4].

7.1 ADJUSTED REFERENCE TEMPERATURES CALCULATION

RT_{NDT} increases as the material is exposed to fast-neutron irradiation; therefore, to find the most limiting RT_{NDT} at any time period in the reactor's life, ΔRT_{NDT} due to the radiation exposure associated with that time period must be added to the original unirradiated RT_{NDT} . Using the adjusted reference temperature (ART) values, P-T limit curves are determined in accordance with the requirements of 10 CFR Part 50, Appendix G [Ref. 8], as augmented by Appendix G to Section XI of the ASME Boiler and Pressure Vessel Code [Ref. 21].

P-T limit curves for SLR (72 EFPY) do not need to be submitted as part of the Point Beach Units 1 and 2 SLR application since P-T limit curves are available as a part of the current license. However, new P-T limit curve development or an extension of the applicability of the current curves must be completed prior to the expiration of the current curves as specified in the Point Beach Units 1 and 2 licensing basis.

P-T limit curves for normal heatup and cooldown of the primary reactor coolant system for Point Beach Units 1 and 2 were developed in WCAP-16669-NP [Ref. 11] assuming operation with hafnium rods for 53 EFPY. This term was reduced to 50 EFPY when implemented into the PTLR [Ref. 12] to accommodate the extended power uprate (EPU) [Ref. 22]. As a result of updated fluence data for SLR, an applicability check of the current 50 EFPY P-T limit curves is appropriate.

To confirm the EOLE P-T limit curves developed in WCAP-16669-NP without hafnium rods, the updated reactor vessel ART values from the beltline materials must be shown to be less than or equal to the limiting beltline material ART values used in the P-T limits analysis. The Regulatory Guide 1.99, Revision 2 [Ref. 4] methodology was used along with the fluence values of Sections 2 and 1.1 to calculate ART values for the Point Beach Units 1 and 2 reactor vessel materials at EOLE (50 EFPY) and SLR (72 EFPY).

Tables 7-1 and 7-2 provide the surface, 1/4T, and 3/4T fluence and fluence factor (FF) values for Point Beach Units 1 and 2 at 50 EFPY and 72 EFPY which are needed to calculate ART values. The ART calculations for EOLE are summarized in Table 7-3 for 1/4T and Table 7-4 for 3/4T. The ART calculations for SLR are summarized in Table 7-5 for 1/4T and Table 7-6 for 3/4T.

Table 7-1 Point Beach Units 1 and 2 Fluence and Fluence Factor Values for the Surface, 1/4T, and 3/4T Locations at 50 EFPY

Material	Surface Fluence ^(a) (x 10 ¹⁹ n/cm ² , E > 1.0 MeV)	1/4T Fluence ^(b) (x 10 ¹⁹ n/cm ² , E > 1.0 MeV)	1/4T FF ^(c)	3/4T Fluence ^(b) (x 10 ¹⁹ n/cm ² , E > 1.0 MeV)	3/4T FF ^(c)
Unit 1					
Nozzle Belt Forging	0.323	0.219	0.591	0.100	0.418
Intermediate Shell Plate	5.06	3.43	1.322	1.57	1.125
Lower Shell Plate	4.67	3.16	1.303	1.45	1.103
NB to IS Circ. Weld	0.372	0.252	0.626	0.116	0.446
IS Long. Weld	3.06	2.07	1.199	0.951	0.986
IS to LS Circ. Weld	4.62	3.13	1.301	1.43	1.100
LS Long. Weld	2.93	1.99	1.187	0.910	0.974
Unit 2					
Nozzle Belt Forging	0.435	0.295	0.666	0.135	0.480
Intermediate Shell Forging	5.10	3.45	1.323	1.58	1.127
Lower Shell Forging	4.92	3.33	1.315	1.53	1.117
NB to IS Circ. Weld	0.496	0.336	0.699	0.154	0.509
IS to LS Circ. Weld	4.62	3.13	1.300	1.43	1.100

Notes:

- (a) The 50 EFPY surface fluence values for the reactor vessel materials were determined by interpolating between the values in Tables 2.4-5 and 2.5-5.
- (b) 1/4T and 3/4T fluence values were calculated from the surface fluence, the reactor vessel beltline thickness (6.5 inches) and equation $f = f_{\text{surf}} * e^{-0.24(x)}$ from Regulatory Guide 1.99, Revision 2, where x = the depth into the vessel wall (inches).
- (c) FF = fluence factor = $f^{(0.28 - 0.10 * \log(f))}$.

Table 7-2 Point Beach Units 1 and 2 Fluence and Fluence Factor Values for the Surface, 1/4T, and 3/4T Locations at 72 EFPY

Material	Surface Fluence ^(a) (x 10 ¹⁹ n/cm ² , E > 1.0 MeV)	1/4T Fluence ^(b) (x 10 ¹⁹ n/cm ² , E > 1.0 MeV)	1/4T FF ^(c)	3/4T Fluence ^(b) (x 10 ¹⁹ n/cm ² , E > 1.0 MeV)	3/4T FF ^(c)
Unit 1					
Nozzle Belt Forging	0.481	0.326	0.692	0.149	0.502
Intermediate Shell Plate	7.64	5.17	1.409	2.37	1.233
Lower Shell Plate	7.31	4.95	1.400	2.27	1.222
NB to IS Circ. Weld	0.554	0.375	0.729	0.172	0.534
IS Long. Weld	4.54	3.07	1.296	1.41	1.095
IS to LS Circ. Weld	7.19	4.87	1.397	2.23	1.217
LS Long. Weld	4.48	3.03	1.293	1.39	1.092
Unit 2					
Nozzle Belt Forging	0.646	0.437	0.770	0.200	0.570
Intermediate Shell Forging	7.80	5.28	1.413	2.42	1.238
Lower Shell Forging	7.71	5.22	1.411	2.39	1.235
NB to IS Circ. Weld	0.735	0.498	0.805	0.228	0.601
IS to LS Circ. Weld	7.34	4.97	1.401	2.28	1.223

Notes:

- (a) The 72 EFPY surface fluence values for the reactor vessel materials were taken from Tables 2.4-5 and 2.5-5.
- (b) 1/4T and 3/4T fluence values were calculated from the surface fluence, the reactor vessel beltline thickness (6.5 inches) and equation $f = f_{\text{surf}} * e^{-0.24(x)}$ from Regulatory Guide 1.99, Revision 2, where x = the depth into the vessel wall (inches).
- (c) FF = fluence factor = $f^{(0.28 - 0.10 * \log(f))}$.

Table 7-3 Calculation of the Point Beach Units 1 and 2 ART Values at the 1/4T Location for the Reactor Vessel Beltline Materials at EOLE (50 EFPY)

Material	Heat #	R.G. 1.99, Rev. 2 Position	CF ^(a)	1/4T Fluence ^(b) (x 10 ¹⁹ n/cm ² , E > 1.0 MeV)	1/4T FF ^(b)	RT _{NDT(U)} ^(c) (°F)	Predicted ΔRT _{NDT} (°F)	σ _I (°F)	σ _Δ ^(d) (°F)	M (°F)	ART (°F)
<i>Unit 1</i>											
Nozzle Belt Forging	122P237	1.1	77.0	0.219	0.591	50	45.5	0	17	34.0	129.5
Intermediate Shell Plate	A9811-1	1.1	88.0	3.43	1.322	1	116.3	26.9	17	63.6	181.0
IS with credible surveillance data ^(e)		2.1	79.9	3.43	1.322	1	105.6	26.9	8.5	56.4	163.0
Lower Shell Plate	C1423-1	1.1	55.3	3.16	1.303	1	72.1	26.9	17	63.6	136.7
LS with credible surveillance data ^(e)		2.1	36.1	3.16	1.303	1	47.0	26.9	8.5	56.4	104.5
NB to IS Circ. Weld (100%)	8T1762 (SA-1426)	1.1	167.0	0.252	0.626	-48.6	104.6	18.0	28	66.6	122.5
IS Long. Weld (ID 27%)	1P0815 (SA-812)	1.1	167.0	2.07	1.199	-48.6	200.2	18.0	28	66.6	218.1
IS Long. Weld (OD 73%)	1P0661 (SA-775)	1.1	167.0	N/A	N/A	N/A	N/A	N/A	N/A	N/A	N/A
IS to LS Circ. Weld (100%)	71249 (SA-1101)	1.1	167.6	3.13	1.301	-53.5	217.9	12.8	28	61.6	226.1
LS Long. Weld (100%)	61782 (SA-847)	1.1	167.0	1.99	1.187	-58.5	198.3	15.4	28	63.9	203.7
<i>Unit 2</i>											
Nozzle Belt Forging	123V352	1.1	76.0	0.295	0.666	40	50.6	0	17	34.0	124.6
Intermediate Shell Forging	123V500	1.1	58.0	3.45	1.323	40	76.8	0	17	34.0	150.8
IS with credible surveillance data ^(e)		2.1	68.5	3.45	1.323	40	90.7	0	8.5	17.0	147.7
Lower Shell Forging	122W195	1.1	31.0	3.33	1.315	40	40.8	0	17	34.0	114.8
LS with credible surveillance data ^(e)		2.1	42.9	3.33	1.315	40	56.4	0	8.5	17.0	113.4
NB to IS Circ. Weld	21935	1.1	170.5	0.336	0.699	-56	119.3	17	28	65.5	128.8
IS to LS Circ. Weld	72442 (SA-1484)	1.1	180.0	3.13	1.300	-33.2	234.1	12.2	28	61.1	262.0

Notes contained on following page.

Notes:

- (a) Chemistry factors are taken from Table 5-3.
- (b) Fluence and Fluence Factors taken from Table 7-1.
- (c) $RT_{NDT(U)}$ values taken from Table 3-1.
- (d) Per the guidance of Regulatory Guide 1.99, Revision 2 [Ref. 4], the base metal $\sigma_{\Delta} = 17^{\circ}\text{F}$ for Position 1.1 and Position 2.1 with non-credible surveillance data, and the base metal $\sigma_{\Delta} = 8.5^{\circ}\text{F}$ for Position 2.1 with credible surveillance data. Also, per Regulatory Guide 1.99, Revision 2, the weld metal $\sigma_{\Delta} = 28^{\circ}\text{F}$ for Position 1.1 and Position 2.1 with non-credible surveillance data, and the weld metal $\sigma_{\Delta} = 14^{\circ}\text{F}$ for Position 2.1 with credible surveillance data. However, σ_{Δ} need not exceed $0.5 * \Delta RT_{NDT}$ for either base metals or welds, with or without surveillance data.
- (e) The credibility evaluation for the Point Beach Units 1 and 2 surveillance data in Appendix A of this calculation determined that the Point Beach Unit 1 surveillance data for the plate materials are deemed credible. Point Beach Unit 2 surveillance forging data for the forging materials are deemed credible. Therefore, the Position 2.1 CF can be used with a reduced margin term in lieu of the Position 1.1 CF.

Table 7-4 Calculation of the Point Beach Units 1 and 2 ART Values at the 3/4T Location for the Reactor Vessel Beltline Materials at EOLE (50 EFPY)

Material	Heat #	R.G. 1.99, Rev. 2 Position	CF ^(a)	3/4T Fluence ^(b) (x 10 ¹⁹ n/cm ² , E > 1.0 MeV)	3/4T FF ^(b)	RT _{NDT(U)} ^(c) (°F)	Predicted ΔRT _{NDT} (°F)	σ _I (°F)	σ _Δ ^(d) (°F)	M (°F)	ART (°F)
<i>Unit 1</i>											
Nozzle Belt Forging	122P237	1.1	77.0	0.100	0.418	50	32.2	0	16.1	32.2	114.3
Intermediate Shell Plate	A9811-1	1.1	88.0	1.57	1.125	1	99.0	26.9	17	63.6	163.6
IS with credible surveillance data ^(e)		2.1	79.9	1.57	1.125	1	89.9	26.9	8.5	56.4	147.3
Lower Shell Plate	C1423-1	1.1	55.3	1.45	1.103	1	61.0	26.9	17	63.6	125.6
LS with credible surveillance data ^(e)		2.1	36.1	1.45	1.103	1	39.8	26.9	8.5	56.4	97.2
NB to IS Circ. Weld (100%)	8T1762 (SA-1426)	1.1	167.0	0.116	0.446	-48.6	74.6	18.0	28	66.6	92.5
IS Long. Weld (ID 27%)	1P0815 (SA-812)	1.1	167.0	N/A	N/A	N/A	N/A	N/A	N/A	N/A	N/A
IS Long. Weld (OD 73%)	1P0661 (SA-775)	1.1	167.0	0.951	0.986	-48.6	164.6	18.0	28	66.6	182.6
IS to LS Circ. Weld (100%)	71249 (SA-1101)	1.1	167.6	1.43	1.100	-53.5	184.4	12.8	28	61.6	192.5
LS Long. Weld (100%)	61782 (SA-847)	1.1	167.0	0.910	0.974	-58.5	162.6	15.4	28	63.9	168.0
<i>Unit 2</i>											
Nozzle Belt Forging	123V352	1.1	76.0	0.135	0.480	40	36.5	0	17	34.0	110.5
Intermediate Shell Forging	123V500	1.1	58.0	1.58	1.127	40	65.3	0	17	34.0	139.3
IS with credible surveillance data ^(e)		2.1	68.5	1.58	1.127	40	77.2	0	8.5	17.0	134.2
Lower Shell Forging	122W195	1.1	31.0	1.53	1.117	40	34.6	0	17	34.0	108.6
LS with credible surveillance data ^(e)		2.1	42.9	1.53	1.117	40	47.9	0	8.5	17.0	104.9
NB to IS Circ. Weld	21935	1.1	170.5	0.154	0.509	-56	86.7	17	28	65.5	96.2
IS to LS Circ. Weld	72442 (SA-1484)	1.1	180.0	1.43	1.100	-33.2	198.0	12.2	28	61.1	225.8

Note contained on following page.

Notes:

- (a) Chemistry factors are taken from Table 5-3.
- (b) Fluence and Fluence Factors taken from Table 7-1.
- (c) $RT_{NDT(U)}$ values taken from Table 3-1.
- (d) Per the guidance of Regulatory Guide 1.99, Revision 2 [Ref. 4], the base metal $\sigma_{\Delta} = 17^{\circ}\text{F}$ for Position 1.1 and Position 2.1 with non-credible surveillance data, and the base metal $\sigma_{\Delta} = 8.5^{\circ}\text{F}$ for Position 2.1 with credible surveillance data. Also, per Regulatory Guide 1.99, Revision 2, the weld metal $\sigma_{\Delta} = 28^{\circ}\text{F}$ for Position 1.1 and Position 2.1 with non-credible surveillance data, and the weld metal $\sigma_{\Delta} = 14^{\circ}\text{F}$ for Position 2.1 with credible surveillance data. However, σ_{Δ} need not exceed $0.5 * \Delta RT_{NDT}$ for either base metals or welds, with or without surveillance data.
- (e) The credibility evaluation for the Point Beach Units 1 and 2 surveillance data in Appendix A of this calculation determined that the Point Beach Unit 1 surveillance data for the plate materials are deemed credible. Point Beach Unit 2 surveillance forging data for the forging materials are deemed credible. Therefore, the Position 2.1 CF can be used with a reduced margin term in lieu of the Position 1.1 CF.

Table 7-5 Calculation of the Point Beach Units 1 and 2 ART Values at the 1/4T Location for the Reactor Vessel Beltline Materials at SLR (72 EFPY)

Material	Heat #	R.G. 1.99, Rev. 2 Position	CF ^(a)	1/4T Fluence ^(b) (x 10 ¹⁹ n/cm ² , E > 1.0 MeV)	1/4T FF ^(b)	RT _{NDT(U)} ^(c) (°F)	Predicted ΔRT _{NDT} (°F)	σ _I (°F)	σ _Δ ^(d) (°F)	M (°F)	ART (°F)
<i>Unit 1</i>											
Nozzle Belt Forging	122P237	1.1	77.0	0.326	0.692	50	53.3	0	17	34.0	137.3
Intermediate Shell Plate	A9811-1	1.1	88.0	5.17	1.409	1	124.0	26.9	17	63.6	188.6
IS with credible surveillance data ^(e)		2.1	79.9	5.17	1.409	1	112.6	26.9	8.5	56.4	170.0
Lower Shell Plate	C1423-1	1.1	55.3	4.95	1.400	1	77.4	26.9	17	63.6	142.1
LS with credible surveillance data ^(e)		2.1	36.1	4.95	1.400	1	50.6	26.9	8.5	56.4	108.0
NB to IS Circ. Weld (100%)	8T1762 (SA-1426)	1.1	167.0	0.375	0.729	-48.6	121.7	18.0	28	66.6	139.7
IS Long. Weld (ID 27%)	1P0815 (SA-812)	1.1	167.0	3.07	1.296	-48.6	216.5	18.0	28	66.6	234.5
IS Long. Weld (OD 73%)	1P0661 (SA-775)	1.1	167.0	N/A	N/A	N/A	N/A	N/A	N/A	N/A	N/A
IS to LS Circ. Weld (100%)	71249 (SA-1101)	1.1	167.6	4.87	1.397	-53.5	234.1	12.8	28	61.6	242.2
LS Long. Weld (100%)	61782 (SA-847)	1.1	167.0	3.03	1.293	-58.5	216.0	15.4	28	63.9	221.4
<i>Unit 2</i>											
Nozzle Belt Forging	123V352	1.1	76.0	0.437	0.770	40	58.5	0	17	34.0	132.5
Intermediate Shell Forging	123V500	1.1	58.0	5.28	1.413	40	82.0	0	17	34.0	156.0
IS with credible surveillance data ^(e)		2.1	68.5	5.28	1.413	40	96.8	0	8.5	17.0	153.8
Lower Shell Forging	122W195	1.1	31.0	5.22	1.411	40	43.7	0	17	34.0	117.7
LS with credible surveillance data ^(e)		2.1	42.9	5.22	1.411	40	60.5	0	8.5	17.0	117.5
NB to IS Circ. Weld	21935	1.1	170.5	0.498	0.805	-56	137.3	17	28	65.5	146.8
IS to LS Circ. Weld	72442 (SA-1484)	1.1	180.0	4.97	1.401	-33.2	252.2	12.2	28	61.1	280.1

Note contained on following page.

Notes:

- (a) Chemistry factors are taken from Table 5-3.
- (b) Fluence and Fluence Factors taken from Table 7-2.
- (c) $RT_{NDT(U)}$ values taken from Table 3-1.
- (d) Per the guidance of Regulatory Guide 1.99, Revision 2 [Ref. 4], the base metal $\sigma_{\Delta} = 17^{\circ}\text{F}$ for Position 1.1 and Position 2.1 with non-credible surveillance data, and the base metal $\sigma_{\Delta} = 8.5^{\circ}\text{F}$ for Position 2.1 with credible surveillance data. Also, per Regulatory Guide 1.99, Revision 2, the weld metal $\sigma_{\Delta} = 28^{\circ}\text{F}$ for Position 1.1 and Position 2.1 with non-credible surveillance data, and the weld metal $\sigma_{\Delta} = 14^{\circ}\text{F}$ for Position 2.1 with credible surveillance data. However, σ_{Δ} need not exceed $0.5 * \Delta RT_{NDT}$ for either base metals or welds, with or without surveillance data.
- (e) The credibility evaluation for the Point Beach Units 1 and 2 surveillance data in Appendix A of this calculation determined that the Point Beach Unit 1 surveillance data for the plate materials are deemed credible. Point Beach Unit 2 surveillance forging data for the forging materials are deemed credible. Therefore, the Position 2.1 CF can be used with a reduced margin term in lieu of the Position 1.1 CF.

Table 7-6 Calculation of the Point Beach Units 1 and 2 ART Values at the 3/4T Location for the Reactor Vessel Beltline Materials at SLR (72 EFPY)

Material	Heat #	R.G. 1.99, Rev. 2 Position	CF ^(a)	3/4T Fluence ^(b) (x 10 ¹⁹ n/cm ² , E > 1.0 MeV)	3/4T FF ^(b)	RT _{NDT(U)} ^(c) (°F)	Predicted ΔRT _{NDT} (°F)	σ _I (°F)	σ _Δ ^(d) (°F)	M (°F)	ART (°F)
<i>Unit 1</i>											
Nozzle Belt Forging	122P237	1.1	77.0	0.149	0.502	50	38.6	0	17	34.0	122.6
Intermediate Shell Plate	A9811-1	1.1	88.0	2.37	1.233	1	108.5	26.9	17	63.6	173.1
IS with credible surveillance data ^(e)		2.1	79.9	2.37	1.233	1	98.5	26.9	8.5	56.4	155.9
Lower Shell Plate	C1423-1	1.1	55.3	2.27	1.222	1	67.6	26.9	17	63.6	132.2
LS with credible surveillance data ^(e)		2.1	36.1	2.27	1.222	1	44.1	26.9	8.5	56.4	101.5
NB to IS Circ. Weld (100%)	8T1762 (SA-1426)	1.1	167.0	0.172	0.534	-48.6	89.2	18.0	28	66.6	107.1
IS Long. Weld (ID 27%)	1P0815 (SA-812)	1.1	167.0	N/A	N/A	N/A	N/A	N/A	N/A	N/A	N/A
IS Long. Weld (OD 73%)	1P0661 (SA-775)	1.1	167.0	1.41	1.095	-48.6	182.9	18.0	28	66.6	200.9
IS to LS Circ. Weld (100%)	71249 (SA-1101)	1.1	167.6	2.23	1.217	-53.5	204.0	12.8	28	61.6	212.1
LS Long. Weld (100%)	61782 (SA-847)	1.1	167.0	1.39	1.092	-58.5	182.3	15.4	28	63.9	187.7
<i>Unit 2</i>											
Nozzle Belt Forging	123V352	1.1	76.0	0.200	0.570	40	43.3	0	17	34.0	117.3
Intermediate Shell Forging	123V500	1.1	58.0	2.42	1.238	40	71.8	0	17	34.0	145.8
IS with credible surveillance data ^(e)		2.1	68.5	2.42	1.238	40	84.8	0	8.5	17.0	141.8
Lower Shell Forging	122W195	1.1	31.0	2.39	1.235	40	38.3	0	17	34.0	112.3
LS with credible surveillance data ^(e)		2.1	42.9	2.39	1.235	40	53.0	0	8.5	17.0	110.0
NB to IS Circ. Weld	21935	1.1	170.5	0.228	0.601	-56	102.5	17	28	65.5	112.0
IS to LS Circ. Weld	72442 (SA-1484)	1.1	180.0	2.28	1.223	-33.2	220.1	12.2	28	61.1	248.0

Note contained on following page.

Notes:

- (a) Chemistry factors are taken from Table 5-3.
- (b) Fluence and Fluence Factors taken from Table 7-2.
- (c) $RT_{NDT(U)}$ values taken from Table 3-1.
- (d) Per the guidance of Regulatory Guide 1.99, Revision 2 [Ref. 4], the base metal $\sigma_{\Delta} = 17^{\circ}\text{F}$ for Position 1.1 and Position 2.1 with non-credible surveillance data, and the base metal $\sigma_{\Delta} = 8.5^{\circ}\text{F}$ for Position 2.1 with credible surveillance data. Also, per Regulatory Guide 1.99, Revision 2, the weld metal $\sigma_{\Delta} = 28^{\circ}\text{F}$ for Position 1.1 and Position 2.1 with non-credible surveillance data, and the weld metal $\sigma_{\Delta} = 14^{\circ}\text{F}$ for Position 2.1 with credible surveillance data. However, σ_{Δ} need not exceed $0.5 * \Delta RT_{NDT}$ for either base metals or welds, with or without surveillance data.
- (e) The credibility evaluation for the Point Beach Units 1 and 2 surveillance data in Appendix A of this calculation determined that the Point Beach Unit 1 surveillance data for the plate materials are deemed credible. Point Beach Unit 2 surveillance forging data for the forging materials are deemed credible. Therefore, the Position 2.1 CF can be used with a reduced margin term in lieu of the Position 1.1 CF.

7.2 P-T LIMIT CURVES APPLICABILITY

This section determines the applicability term of the current EOLE P-T limit curves by comparing the ART values contained in the analysis of record (AOR) with the ART values calculated using the updated fluence projections and materials information contained herein. If the ART values used in the previous analysis are *higher* or *equal* to the ART values calculated using the updated fluence, then the applicability term of the current curves will remain unchanged or possibly can be extended. If the ART values used in the previous analysis are *lower* than the ART values calculated using the updated fluence, then the applicability term of the current curves may need to be shortened. This new period of applicability can be calculated based on a comparison of the ART values and linear interpolation using the fluence projections. Tables 7-3 through 7-6 calculate the beltline 1/4T and 3/4T ART calculations for Point Beach Units 1 and 2 at EOLE (50 EFPY) and SLR (72 EFPY).

Table 7-7 compares the TLAA limiting ART values at EOLE and SLR to the limiting ART values used in development of the existing EOLE P-T limit curves implemented in the PTLR [Ref. 12] which are based on the 53 EFPY P-T limit curves without hafnium rods in WCAP-16669-NP [Ref. 11].

Table 7-7 Summary of the Limiting ART Values

Assumed Flaw Orientation	1/4T Limiting ART (°F)			3/4T Limiting ART (°F)		
	P-T Limit Curves AOR ^(a)	EOLE (50 EFPY)	SLR (72 EFPY)	P-T Limit Curves AOR ^(a)	EOLE (50 EFPY)	SLR (72 EFPY)
Axial	220.0 (Unit 1 IS Long. Weld)	218.1 (Unit 1 IS Long. Weld)	234.5 (Unit 1 IS Long. Weld)	184.6 (Unit 1 IS Long. Weld)	182.6 (Unit 1 IS Long. Weld)	200.9 (Unit 1 IS Long. Weld)
Circumferential	265.2 (Unit 2 IS to LS Circ. Weld)	262.0 (Unit 2 IS to LS Circ. Weld)	280.1 (Unit 2 IS to LS Circ. Weld)	229.2 (Unit 2 IS to LS Circ. Weld)	225.8 (Unit 2 IS to LS Circ. Weld)	248.0 (Unit 2 IS to LS Circ. Weld)

Note:

- (a) Limiting 1/4T and 3/4T ART values for the 53 EFPY P-T limit curves without hafnium rods from WCAP-16669-NP [Ref. 11]. AOR = analysis of record.

P-T Limit Curves Applicability Conclusion

The results show that the existing EOLE P-T limit curves continue to remain valid through at least EOLE (50 EFPY) for the beltline materials. More precisely, the limiting axial flow ART values in WCAP-16669-NP will be reached when the fluence on the Unit 1 intermediate shell longitudinal weld is 3.20×10^{19} n/cm², which corresponds to approximately 52 EFPY. Therefore, new curves will need to be implemented prior to exceeding the 50 EFPY period of applicability (or 52 EFPY if the PTLR applicability term is updated).

As noted in WCAP-16669-NP, the P-T limit curves are based on the limiting material with an axial flow. Because the methodology to evaluate material with an assumed circumferential flow (i.e., circ weld, is less severe than those for axial flows) P-T limit curves with a postulated “axial flow” and the limiting axial weld ART values bound those generated using the “circumferential flow” methodology with the limiting circumferential weld ART values despite the circumferential flow ART being higher.

Nozzle P-T Limit Curves

NRC Regulatory Issue Summary (RIS) 2014-11 [Ref. 10] requires that the P-T limit curves account for the higher stresses in the nozzle corner region due to the potential for more restrictive P-T limits, even if the RT_{NDT} for these components are not as high as those of the reactor vessel beltline shell materials that have simpler geometries.

MCOE-LTR-13-115 [Ref. 24] contains an evaluation of the Point Beach Units 1 and 2 nozzle materials effect on P-T limit curves in WCAP-16669-NP, consistent with RIS 2014-11 [Ref. 10], and determined the nozzle materials are not limiting. The nozzle projected fluence values are less than 1.0×10^{17} n/cm² ($E > 1.0$ MeV) at 72 EFPY; therefore, the embrittlement effects on the nozzles need not be considered in the evaluation, and the conclusion of MCOE-LTR-13-115 concerning the nozzles' effect on the P-T curves is not affected by the new fluence analysis.

In addition, PWROG-15109-NP-A [Ref. 25] addresses this concern generically for the U.S. pressurized water reactor (PWR) operating fleet. The results of PWROG-15109-NP-A demonstrate that P-T limit curves developed with current NRC-approved methods (e.g., WCAP-14040-A [Ref. 23]) bound the generic nozzle P-T limit curves. This document has been approved by the NRC as an acceptable means to address the concerns of RIS 2014-11. The results and conclusions of PWROG-15109-NP-A are applicable as long as the plant-specific Point Beach Units 1 and 2 fluence at the nozzle corners remain less than the screening criterion of 4.28×10^{17} n/cm², as described in PWROG-15109-NP-A. Sections 2 and 1.1 demonstrate Point Beach Units 1 and 2 adherence to this screening criterion. Thus PWROG-15109-NP-A is applicable, and nozzle P-T limit curves need no further consideration.

PWROG-15109-NP-A only addresses the inlet/outlet nozzles. However, the hoop stresses for the safety injection nozzle at the inside corner are compressive or very small, as demonstrated by PVP2012-78119 [Ref. 31]. Therefore, any stress intensity factor in the safety injection nozzle will be bounded by those of the reactor vessel beltline and extended beltline, and the beltline P-T limit curves will remain bounding.

Low Temperature Overpressure Protection System (LTOPS) Applicability Conclusion

An evaluation was performed to validate that the current Low Temperature Overpressure Protection System (LTOPS) analysis in Reference 30 remains valid through EOLE and reconcile any changes to the applicability term. The current LTOPS analysis was performed using the Reference 23 methodology to develop the LTOPS pressurizer Power Operated Relief Valve (PORV) setpoint and other operational requirements necessary to protect the steady state isothermal P-T limits. This evaluation determined that there have been no changes to the key input parameters used in the analysis. Therefore, similar to the P-T limits, the current LTOPS requirements remain valid and bounding through the current 50 EFPY applicability term and could be extended to 52 EFPY. Specifically, the maximum allowable LTOPS pressurizer PORV setpoint of 420 psig (includes uncertainty) remains valid with a limitation that only one RCP can be running at indicated RCS temperatures $\leq 197.8^\circ\text{F}$ (includes uncertainty). The LTOPS enable temperature of 285°F [Ref. 30] also remains valid since it is based on an ART value that bounds operation through 52 EFPY. The LTOPS requirements will need to be updated when new P-T curves are generated through the end of SLR and/or if plant changes are made that affect the LTOPS transients or mitigation capabilities.

8 SURVEILLANCE CAPSULE WITHDRAWAL SCHEDULES

This section provides recommended capsule withdrawal schedules for Point Beach Units 1 and 2 in order to ensure compliance with 10 CFR 50, Appendix H [Ref. 26] and consideration of NUREG-1801, Revision 2 (GALL) [Ref. 27] and NUREG-2191 (GALL-SLR) [Ref. 28].

10 CFR 50, Appendix H [Ref. 26] states:

The design of the surveillance program and the withdrawal schedule must meet the requirements of the edition of ASTM E 185 that is current on the issue date of the ASME Code to which the reactor vessel was purchased. Later editions of ASTM E 185 may be used, but including only those editions through 1982. For each capsule withdrawal, the test procedures and reporting requirements must meet the requirements of ASTM E 185-82 to the extent practicable for the configuration of the specimens in the capsule.

The original Point Beach Unit 1 reactor vessel was designed and constructed to ASME Section III, 1965 Edition through Summer 1965 Addenda. The original Point Beach Unit 2 reactor vessel was designed and constructed to ASME Section III, 1968 Edition through Winter 1968 Addenda. Thus, per 10 CFR 50, Appendix H, the Point Beach Units 1 and 2 surveillance program withdrawal schedules may meet the requirements of any version of the ASTM E185 standard from the 1962 version for Unit 1 or the 1966 version for Unit 2 (the versions which were current on the issue date of the ASME Codes to which the reactor vessels were purchased) through the 1982 version. Per WCAP-7513 [Ref. 18] and WCAP-7712 [Ref. 19], the Point Beach Units 1 and 2 surveillance capsule programs were designed to the ASTM E185-66 standard, which was the version active at that time. Therefore, the requirements of 10 CFR 50, Appendix H were met at the time of the design of the reactor vessel surveillance program.

Since that time, Point Beach has implemented the capsule withdrawal schedules in PTLR [Ref. 12] to support license renewal to 60 years. Per the license renewal SER [Ref. 29], the only remaining capsule currently required to be withdrawn and tested for Units 1 and 2 is the Supplement Capsule A. This supplemental capsule was inserted into Unit 2 in 2002 and includes the limiting circumferential flaw material from Units 1 and 2 as well as other materials of interest. The supplemental capsule was inserted because the capsules from the original surveillance programs do not contain specimens from the limiting material. To support license renewal, it was committed to withdraw and test the supplemental capsule during an outage at which it accumulates a fluence equivalent to the 60 calendar-year vessel fluence.

Since the supplemental capsule is the only capsule which contains specimens from Point Beach Units 1 and 2 limiting materials, it is recommended that the withdrawal of this capsule be delayed to support subsequent license renewal. The GALL-SLR stipulates that at least one capsule is withdrawn and tested with a fluence of between one and two times the 80-year peak reactor vessel wall neutron fluence. The Supplemental Capsule A will satisfy the 80-year fluence for both Point Beach Units 1 and 2 at approximately 51 EFPY. The timing of this withdrawal of the supplemental capsule will also satisfy the GALL requirement that at least one capsule is withdrawn and tested with a fluence of between one and two times the 60-year peak reactor vessel wall neutron fluence, since the 80-year fluence is less than twice the 60-year fluence. It is noted that the GALL-SLR also stipulates that it is not acceptable to re-direct a 60-year capsule to also fulfill this requirement. However, since only one capsule contains the materials of interest, it is recommended that the use of this 60-year capsule to support SLR is submitted for approval by the NRC. In order to implement this recommended schedule, a change to the existing license renewal

commitment must be requested and an exception to GALL-SLR Reactor Vessel Surveillance aging management program must be identified.

Surveillance Capsule Withdrawal Schedule Conclusion

The supplemental surveillance capsule, currently inserted in Point Beach Unit 2 with the limiting materials from the Point Beach Units 1 and 2, should be withdrawn and tested at a fluence of between one and two times the 80-year peak reactor vessel wall neutron fluence. The latest recommended surveillance capsule withdrawal schedules, which include a future capsule withdrawal to support the proposed 80-year operating licenses, are provided in Tables 8-1 and 8-2, respectively. The schedules are in accordance with 10 CFR 50, Appendix H [Ref. 26] and consider the guidance contained in the GALL [Ref. 27] and GALL-SLR [Ref. 28]. It is noted that the capsule fluence should be used to determine when the capsule is withdrawn, and the EFPY is an approximation. The capsule should be withdrawn at the outage nearest to, but following, when the capsule fluence is met.

Table 8-1 Point Beach Unit 1 Recommended Surveillance Capsule Withdrawal Schedule

Capsule ID	Withdrawal EOC (Year)	Withdrawal EFPY	Capsule Fluence (n/cm ² , E > 1.0 MeV)
V	EOC-1 (Sept 1972)	1.49	6.23 x 10 ¹⁸
S	EOC-3 (Dec 1975)	3.61	8.13 x 10 ¹⁸
R	EOC-5 (Oct 1977)	5.10	2.13 x 10 ¹⁹
T	EOC-11 (Mar 1984)	9.28	2.14 x 10 ¹⁹
p ^(a)	EOC-21 ^(a) (April 1994)	17.77	3.72 x 10 ¹⁹
N	Standby ^(b)	-	-

Note:

- (a) Stored in the Spent Fuel Pool.
(b) Standby capsule is currently in the reactor vessel.

Table 8-2 Point Beach Unit 2 Recommended Surveillance Capsule Withdrawal Schedule

Capsule ID	Withdrawal EOC (Year)	Withdrawal EFPY	Capsule Fluence (n/cm ² , E > 1.0 MeV)
V	EOC-1 (Nov 1974)	1.52	6.54E+18
T	EOC-3 (Mar 1977)	3.44	8.58E+18
R	EOC-5 (April 1979)	5.20	2.17E+19
S	EOC-16 (Oct 1990)	14.78	3.05E+19
p ^(a)	EOC-22 ^(a) (June 1997)	19.82	4.03E+19
N	Standby ^(b)	-	-
A	-	51 ^(c)	7.95E+19

Note:

- (a) Stored in the Spent Fuel Pool.
(b) Standby capsule is currently in the reactor vessel.
(c) Capsule should be removed at the first refueling outage that meets or exceeds 51 EFPY.

9 REFERENCES

1. Code of Federal Regulations, 10 CFR Part 54.3, "Definitions," U.S. Nuclear Regulatory Commission, Washington, D.C., Federal Register, Volume 72, dated August 28, 2007.
2. ASTM E853-18, "Standard Practice for Analysis and Interpretation of Light-Water Reactor Surveillance Neutron Exposure Results," 2018.
3. ASTM E693-94, "Standard Practice for Characterizing Neutron Exposures in Iron and Low Alloy Steels in Terms of Displacements Per Atom (DPA), E706 (ID)," 1994.
4. U.S. Nuclear Regulatory Commission, Office of Nuclear Regulatory Research, Regulatory Guide 1.99, Revision 2, "Radiation Embrittlement of Reactor Vessel Materials," May 1988. [*Agencywide Documents Access and Management System (ADAMS) Accession Number ML003740284*]
5. U.S. Nuclear Regulatory Commission, Office of Nuclear Regulatory Research, Regulatory Guide 1.190, Revision 0, "Calculational and Dosimetry Methods for Determining Pressure Vessel Neutron Fluence," March 2001. [*ADAMS Accession Number ML010890301*]
6. Westinghouse Report WCAP-18124-NP-A, Revision 0, "Fluence Determination with RAPTOR-M3G and FERRET," July 2018. [*ADAMS Accession Number ML18204A010*]
7. Westinghouse InfoGram IG-13-2, "Fluence Attenuation Profile in Reactor Pressure Vessel Shell and Inlet/Outlet Nozzle Regions," July 2013.
8. U.S. Nuclear Regulatory Commission, Federal Register, Code of Federal Regulations, 10 CFR Part 50, Appendix G, "Fracture Toughness Requirements," November 29, 2019.
9. U.S. Nuclear Regulatory Commission, Federal Register, Code of Federal Regulations 10 CFR 50.61, "Fracture Toughness Requirements for Protection Against Pressurized Thermal Shock Events," November 29, 2019.
10. U.S. Nuclear Regulatory Commission, Regulatory Issue Summary 2014-11, "Information on Licensing Applications for Fracture Toughness Requirements for Ferritic Reactor Coolant Pressure Boundary Components," October 2014. [*ADAMS Accession Number ML14149A165*]
11. Westinghouse Report WCAP-16669-NP, Revision 1, "Point Beach Units 1 and 2 Heatup and Cooldown Limit Curves for Normal Operation," January 2009.
12. Point Beach Technical Requirements Manual (TRM) 2.2, Revision 11, "Pressure Temperature Limits Report (PTLR)," December 2019. [*ADAMS Accession Numbers ML20009E096*]
13. AREVA Report BAW-2325, Revision 1 "Response to Request for Additional Information (RAI), Regarding Reactor Pressure Vessel Integrity, B&W Owners Group - Reactor Vessel Working Group," January 1999 [*ADAMS Accession Number ML14162A108*]
14. Westinghouse Report MISC-PENG-ER-019, Revision 0, "The Reactor Vessel Group Records Evaluation Program Phase II Final Report for the Point Beach 2 Reactor Pressure Vessel Plates, Forgings, Welds and Cladding." October 1995.
15. Westinghouse Letter LTR-SDA-20-039, Revision 0, "Database of Large Ring Forgings Produced by Bethlehem Steel to Support a Generic Copper Value for Point Beach Units 1 and 2 Subsequent License Renewal (SLR)," June 2020.
16. AREVA Calculation Note 32-9019240-000, "ART Values for Point Beach Unit 1 and Unit 2," June 2006. [*ADAMS Accession Number ML13113A008*]

17. AREVA Report BAW-2308, Revisions 1-A and 2-A, “Initial RT_{NDT} of Linde 80 Weld Materials,” August 2005 and March 2008 [*ADAMS Accession Numbers ML052070408 and ML081270388, respectively*].
18. Westinghouse Report WCAP-7513, Revision 0, “Wisconsin Michigan Power Co. Point Beach Unit No. 1 Reactor Vessel Radiation Surveillance Program,” June 1970.
19. Westinghouse Report WCAP-7712, Revision 0, “Wisconsin Michigan Power Co. and the Wisconsin Electric Power Co. Point Beach Unit No. 2 Reactor Vessel Radiation Surveillance Program,” June 1971.
20. Westinghouse Report WCAP-17036-NP, Revision 1, “Analysis of Capsule N from the R.E. Ginna Reactor Vessel Radiation Surveillance Program,” September 2010.
21. Appendix G to the 1998 through the 2000 Addenda Edition of the ASME Boiler and Pressure Vessel (B&PV) Code, Section XI, Division 1, “Fracture Toughness Criteria for Protection Against Failure.”
22. NRC Letter, “Point Beach Nuclear Plant, Units 1 and 2 - Issuance of Amendment Regarding Change to Technical Specification 5.6.5, ‘Reactor Coolant System (RCS) Pressure and Temperature Limits Report (PTLR)’ (TAC Nos. MF0532 and MF0533),” and NRC Letter, “Point Beach Nuclear Plant (Point Beach), Units 1 and 2 - Exemption From the Requirements of 10 CFR Section 50.61 and Appendix G to 10 CFR Part 50 (TAC Nos. MF0534 and MF0535),” dated June 30, 2014. [*ADAMS Accession Numbers ML14126A594, ML14126A378, and ML14126A612*]
23. Westinghouse Report WCAP-14040-A, Revision 4, “Methodology Used to Develop Cold Overpressure Mitigating System Setpoints and RCS Heatup and Cooldown Limit Curves,” May 2004.
24. Westinghouse Letter MCOE-LTR-13-115, Revision 0, “Point Beach Units 1 and 2 Pressure-Temperature Limits License Amendment Request: NRC Request for Additional Information Response,” February 2014.
25. PWROG Report PWROG-15109-NP-A, Revision 0, “PWR Pressure Vessel Nozzle Appendix G Evaluation,” January 2020. [*ADAMS Accession Number ML20024E573*]
26. U.S. Nuclear Regulatory Commission, Federal Register, Code of Federal Regulations 10 CFR 50, Appendix H, “Reactor Vessel Material Surveillance Program Requirements,” November 29, 2019.
27. U.S. Nuclear Regulatory Commission Report NUREG-1801, Revision 2, “Generic Aging Lessons Learned (GALL) Report,” December 2010. [*ADAMS Accession Number ML103490041*]
28. U.S. Nuclear Regulatory Commission Report NUREG-2191, Volume 2, “Generic Aging Lessons Learned for Subsequent License Renewal (GALL-SLR) Report,” July 2017. [*ADAMS Accession Number ML17187A204*]
29. U.S. Nuclear Regulatory Commission Report NUREG-1839, “Safety Evaluation Report Related to the License Renewal of the Point Beach Nuclear Plant, Units 1 and 2” December 2005. [*ADAMS Accession Number ML053420134 and ML053420137*]
30. Westinghouse Calculation Note CN-SCS-06-68, Revision 1, “LTOPS Setpoint Analysis for Point Beach Units 1 and 2,” December 2008.
31. ASME PVP2012-78119, “Supplemental Stress and Fracture Mechanics Analyses of Pressurized Water Reactor Pressure Vessel Nozzles.”

APPENDIX A POINT BEACH UNITS 1 AND 2 SURVEILLANCE PROGRAM CREDIBILITY EVALUATION

A.1 INTRODUCTION

Regulatory Guide 1.99, Revision 2 [Ref. A-1] describes general procedures acceptable to the NRC staff for calculating the effects of neutron radiation embrittlement of the low-alloy steels currently used for light-water-cooled reactor vessels. Position 2.1 of Regulatory Guide 1.99, Revision 2, describe the method for calculating the adjusted reference temperature of reactor vessel beltline materials using surveillance capsule data. The methods of Position 2.1 can only be applied when two or more credible surveillance data sets become available from the reactor in question.

To date, there have been four surveillance capsules removed and tested from each of the Point Beach Units 1 and 2 reactor vessels. In accordance with Regulatory Guide 1.99, Revision 2, the credibility of the surveillance data will be judged based on five criteria.

Table A-1 reviews the five criteria in Regulatory Guide 1.99, Revision 2. The following subsections evaluate each of these five criteria for Point Beach Units 1 and 2 in order to determine the credibility of the surveillance data for use in neutron radiation embrittlement calculations.

Table A-1 Regulatory Guide 1.99, Revision 2, Credibility Criteria

Criterion No.	Description
1	Materials in the capsules should be those judged most likely to be controlling with regard to radiation embrittlement.
2	Scatter in the plots of Charpy energy versus temperature for the irradiated and unirradiated conditions should be small enough to permit the determination of the 30 ft-lb temperature and upper-shelf energy unambiguously.
3	When there are two or more sets of surveillance data from one reactor, the scatter of ΔRT_{NDT} values about a best-fit line drawn as described in Regulatory Position 2.1 normally should be less than 28°F for welds and 17°F for base metal. Even if the fluence range is large (two or more orders of magnitude), the scatter should not exceed twice those values. Even if the data fail this criterion for use in shift calculations, they may be credible for determining decrease in upper-shelf energy if the upper shelf can be clearly determined, following the definition given in ASTM E185-82.
4	The irradiation temperature of the Charpy specimens in the capsule should match the vessel wall temperature at the cladding/base metal interface within +/- 25°F.
5	The surveillance data for the correlation monitor material in the capsule should fall within the scatter band of the database for that material.

A.2 POINT BEACH UNIT 1 CREDIBILITY EVALUATION

Criterion 1: Materials in the capsules should be those judged most likely to be controlling with regard to radiation embrittlement.

The beltline region of the reactor vessel is defined in Appendix G to 10 CFR Part 50, “Fracture Toughness Requirements” [Ref. A-2], as follows:

“the region of the reactor vessel (shell material including welds, heat affected zones, and plates or forgings) that directly surrounds the effective height of the active core and adjacent regions of the reactor vessel that are predicted to experience sufficient neutron radiation damage to be considered in the selection of the most limiting material with regard to radiation damage.”

The Point Beach Unit 1 reactor vessel consists of the following beltline region materials:

- Nozzle belt forging, Heat # 122P237
- Intermediate shell plate, Heat # A9811-1
- Lower shell plate, Heat # C1423-1
- Intermediate shell longitudinal weld (ID 27%)
Heat # 1P0815, Flux Type Linde 80, & Flux Lot 8350
- Intermediate shell longitudinal weld (OD 73%)
Heat # 1P0661, Flux Type Linde 80, & Flux Lot 8304
- Lower shell longitudinal weld
Heat # 61782, Flux Type Linde 80, & Flux Lot 8350
- Nozzle belt to intermediate shell circumferential weld
Heat # 8T1762, Flux Type Linde 80, & Flux Lot 8553
- Intermediate shell to lower shell circumferential weld
Heat # 71249, Flux Type Linde 80, & Flux Lot 8445

At the time the Point Beach Unit 1 surveillance program was designed and licensed the program most likely would have considered only the lower shell plate and intermediate shell plate as potentially limiting base metal material with regard to radiation embrittlement. These materials remain the limiting base metal materials with respect to Regulatory Guide 1.99, Revision 2 Position 1.1. Both of these materials are included in the surveillance capsules.

The surveillance weld was fabricated with weld wire Heat # 72445 and Linde 80 flux, Lot # 8504. This heat is considered similar to the Point Beach Unit 1 vessel welds but was not used in the Point Beach Unit 1 reactor vessel. However, the Point Beach Unit 1 surveillance program is supplemented with data from a capsule described in WCAP-15856 [Ref. A-3]. The supplemental capsule was inserted into Point Beach Unit 2 and includes a surveillance weld fabricated with weld wire Heat # 71249 and Linde 80 flux, Lot # 8445 utilizing the same fabrication practice as that used to fabricate the actual vessel beltline welds. This surveillance weld is made of the same heat with the same type flux & lot utilized in the Point Beach Unit 1 intermediate to lower shell circumferential weld. This material is the limiting weld in the Point Beach Unit 1 reactor vessel with respect to the ΔRT_{NDT} and RT_{NDT} experienced at the clad/base metal interface and the 1/4T & 3/4T locations. The supplemental capsule also includes specimens of the Point Beach Unit 1 intermediate shell plate, Heat # A9811-1.

Based on the previous discussion, Criterion 1 is met for the Point Beach Unit 1 surveillance program.

Criterion 2: Scatter in the plots of Charpy energy versus temperature for the irradiated and unirradiated conditions should be small enough to permit the determination of the 30 ft-lb temperature and upper-shelf energy unambiguously.

Based on engineering judgment, the scatter in the data presented in these plots, as documented in BMI-0673 [Ref. A-4], WCAP-8739 [Ref. A-5], WCAP-9357 [Ref. A-6], and WCAP-10736 [Ref. A-7], is small enough to permit the determination of the 30 ft-lb temperature and the upper-shelf energy of the Point Beach Unit 1 surveillance materials unambiguously.

Hence, the Point Beach Unit 1 surveillance program meets Criterion 2.

Criterion 3: When there are two or more sets of surveillance data from one reactor, the scatter of ΔRT_{NDT} values about a best-fit line drawn as described in Regulatory Position 2.1 normally should be less than 28°F for welds and 17°F for base metal. Even if the fluence range is large (two or more orders of magnitude), the scatter should not exceed twice those values. Even if the data fail this criterion for use in shift calculations, they may be credible for determining decrease in upper-shelf energy if the upper shelf can be clearly determined, following the definition given in ASTM E185-82.

The functional form of the least squares method as described in Regulatory Position 2.1 will be utilized to determine a best-fit line for this data and to determine if the scatter of these ΔRT_{NDT} values about this line is less than 28°F for welds and less than 17°F for plates or forgings.

Following is the calculation of the best-fit line as described in Regulatory Position 2.1 of Regulatory Guide 1.99, Revision 2. In addition, the recommended NRC methods for determining credibility will be followed. The NRC methods were presented to the industry at a meeting held by the NRC on February 12 and 13, 1998 [Ref. A-8]. At this meeting the NRC presented five cases. Of the five cases, Case 1 (“Surveillance Data Available from Plant but No Other Source”) most closely represents the situation for the Point Beach Unit 1 surveillance plate materials. Since the surveillance weld is not representative of weld material in the Point Beach Unit 1 reactor vessel, it is not evaluated.

Surveillance data are available for weld Heat #s 61782 and 71249 from other various surveillance programs. However, AREVA Calculation 32-9019240-000 [Ref. A-9] determined that the generic table CFs of Regulatory Guide 1.99, Revision 2, are conservative with respect to the measured data. The new Point Beach Unit 1 specific evaluations do not affect these conclusions and they will not be readdressed here.

Evaluation of Point Beach Unit 1 Data Only (Case 1)

Following the NRC Case 1 guidelines, the Point Beach Unit 1 surveillance plates will be evaluated using the Point Beach Unit 1 data. Table A-2 provides the calculation of the interim CF for Point Beach Unit 1.

Table A-2 Calculation of Interim Chemistry Factors for the Credibility Evaluation Using Point Beach Unit 1 Surveillance Capsule Data Only

Material	Capsule	Capsule Fluence ^(a) (x 10 ¹⁹ n/cm ² , E > 1.0 MeV)	FF ^(b)	Measured ΔRT_{NDT} ^(c) (°F)	FF * ΔRT_{NDT} (°F)	FF ²	
Intermediate Shell Plate Heat # A9811-1 (Longitudinal)	V	0.623	0.867	81	70.26	0.752	
	S	0.813	0.942	87	81.95	0.887	
	R	2.13	1.205	93	112.11	1.453	
	T	2.14	1.207	82	98.95	1.456	
	SUM:					363.27	4.549
	$CF_{A9811-1} = \Sigma(FF * \Delta RT_{NDT}) \div \Sigma(FF^2) = (363.27) \div (4.549) = 79.9^{\circ}F$						
Lower Shell Plate Heat # C1423-1 (Longitudinal)	V	0.623	0.867	41	35.56	0.752	
	S	0.813	0.942	43	40.50	0.887	
	R	2.13	1.205	28	33.75	1.453	
	T	2.14	1.207	45	54.30	1.456	
	SUM:					164.12	4.549
	$CF_{C1423-1} = \Sigma(FF * \Delta RT_{NDT}) \div \Sigma(FF^2) = (164.12) \div (4.549) = 36.1^{\circ}F$						

Notes:

- (a) Fluence taken from Table 2.4-8.
 (b) FF = fluence factor = $f^{0.28 - 0.10 * \log(f)}$.
 (c) Measured ΔRT_{NDT} taken from Table 4-1.

The scatter of ΔRT_{NDT} values about the functional form of a best-fit line drawn as described in Regulatory Position 2.1 is presented in Table A-3.

Table A-3 Point Beach Unit 1 Surveillance Capsule Data Scatter about the Best-Fit Line

Material	Capsule	CF ^(a) (Slope _{best-fit}) (°F)	Capsule Fluence ^(b) (x 10 ¹⁹ n/cm ²)	FF ^(c)	Measured ΔRT_{NDT} ^(d) (°F)	Predicted ΔRT_{NDT} ^(e) (°F)	Scatter ΔRT_{NDT} ^(f) (°F)	<17°F (Plate)
Unit 1 Surveillance Plate Intermediate Shell Plate (Heat # A9811-1)	V	79.9	0.623	0.867	81	69.3	11.7	Yes
	S	79.9	0.813	0.942	87	75.3	11.7	Yes
	R	79.9	2.13	1.205	93	96.3	3.3	Yes
	T	79.9	2.14	1.207	82	96.4	14.4	Yes
Unit 1 Surveillance Plate Lower Shell Plate (Heat # C1423-1)	V	36.1	0.623	0.867	41	31.3	9.7	Yes
	S	36.1	0.813	0.942	43	34.0	9.0	Yes
	R	36.1	2.13	1.205	28	43.5	15.5	Yes
	T	36.1	2.14	1.207	45	43.6	1.4	Yes

Notes:

- (a) CF calculated in Table A-2.
- (b) Fluence taken from Table 2.4-8.
- (c) $FF = \text{fluence factor} = f^{(0.28 - 0.10 * \log(f))}$.
- (d) Measured ΔRT_{NDT} taken from Table 4-1.
- (e) Predicted $\Delta RT_{NDT} = CF \times FF$
- (f) Scatter $\Delta RT_{NDT} = \text{Absolute Value} [\text{Predicted } \Delta RT_{NDT} - \text{Measured } \Delta RT_{NDT}]$.

Table A-3 indicates that, for both the intermediate and lower shell plates, four of the four surveillance data points fall inside the +/- 1 σ of 17°F scatter band for surveillance plate materials. 100% of the data are bounded; therefore, the surveillance plates data are deemed “credible” per the third criterion.

Criterion 4: The irradiation temperature of the Charpy specimens in the capsule should match the vessel wall temperature at the cladding/base metal interface within +/- 25°F.

The capsule specimens are located in the reactor between the thermal shield and the vessel wall and are positioned opposite the center of the core. The test capsules are contained in baskets attached to the thermal shield. The location of the specimens with respect to the reactor vessel beltline provides assurance that the reactor vessel wall and the specimens experience equivalent operating conditions such that the temperatures will not differ by more than 25°F. Hence, this criterion is met.

Criterion 4 is met for the Point Beach Unit 1 surveillance program.

Criterion 5: The surveillance data for the correlation monitor material in the capsule should fall within the scatter band of the database for that material.

The Point Beach Unit 1 surveillance program contains A302B correlation monitor material as shown in NUREG/CR-6413, ORNL/TM-13133 [Ref. A-10]. Figure 10 of NUREG/CR-6413, ORNL/TM-13133 contains a plot of residual versus fast fluence for the correlation monitor material. This figure shows a 2σ uncertainty of 50°F. The data used in Figure 10 is contained in Table 13 of NUREG/CR-6413 (identified as product SRM). Standard Reference Material (SRM) was contained in the four surveillance capsules that have been removed and tested from Point Beach Unit 1; however, the fluence values have been updated. Table A-4 contains an updated calculation of the residual versus fast fluence.

Table A-4 Calculation of Residual versus Fast Fluence

Capsule	Capsule Fluence ^(a) ($\times 10^{19}$ n/cm ² , E > 1.0 MeV)	FF	Measured Shift ^(b) (°F)	RG 1.99 Shift (CF * FF) ^(c) (°F)	Residual Measured Shift (°F)
V	0.623	0.867	95	86.7	8.3
S	0.813	0.942	95	94.2	0.8
R	2.13	1.205	110	120.5	10.5
T	2.14	1.207	120	120.7	0.7

Notes:

(a) Values taken from Table 4-1.

(b) Values taken from NUREG/CR-6413 [Ref. A-10] Table 13.

(c) Per NUREG/CR-6413 [Ref. A-10] Table 13, the Cu and Ni weight percent values for the Point Beach Unit 1 correlation monitor material are 0.20 Cu and 0.18 Ni. This equates to a CF of 100.0°F from Regulatory Guide 1.99, Revision 2.

Table A-4 shows a 2σ uncertainty of less than 50°F, which is the allowable scatter in Figure 10 of NUREG/CR-6413. Hence, this criterion is met.

Criterion 5 is met for the Point Beach Unit 1 surveillance program.

Conclusion

Based on the preceding responses to the five criteria of Regulatory Guide 1.99, Revision 2, Section B, the Point Beach Unit 1 surveillance data for the plate materials are deemed credible. The plant-specific surveillance weld data is not evaluated since it is not used in the Unit 1 reactor vessel.

A.3 POINT BEACH UNIT 2 CREDIBILITY EVALUATION

Criterion 1: Materials in the capsules should be those judged most likely to be controlling with regard to radiation embrittlement.

The beltline region of the reactor vessel is defined in Appendix G to 10 CFR Part 50, “Fracture Toughness Requirements” [Ref. A-2], as follows:

“the region of the reactor vessel (shell material including welds, heat affected zones, and plates or forgings) that directly surrounds the effective height of the active core and adjacent regions of the reactor vessel that are predicted to experience sufficient neutron radiation damage to be considered in the selection of the most limiting material with regard to radiation damage.”

The Point Beach Unit 2 reactor vessel consists of the following beltline region materials:

- Nozzle belt forging, Heat # 123V352
- Intermediate shell forging, Heat # 123V500
- Lower shell forging, Heat # 122W195
- Nozzle belt to intermediate shell circumferential weld
Heat # 21935, Flux Type Linde 1092, & Flux Lot 3869,
- Intermediate shell to lower shell circumferential weld
Heat # 72442, Flux Type Linde 80, & Flux Lot 8579

At the time the Point Beach Unit 2 surveillance program was designed and licensed the program most likely would have considered only the lower shell forging and intermediate shell forging as potentially limiting base metal material with regard to radiation embrittlement. Both of these materials are included in the surveillance capsules, and the intermediate shell forging remains the limiting base metal material.

The surveillance weld was fabricated with weld wire Heat # 406L44 and Linde 80 flux, Lot # 8773. This heat is considered similar to the intermediate to lower shell girth weld but was not used in the Point Beach Unit 2 reactor vessel. However, the Point Beach Unit 2 surveillance program is supplemented with data from a capsule described in WCAP-15856 [Ref. A-3]. The supplemental capsule was inserted into Point Beach Unit 2 and includes a surveillance weld fabricated with weld wire Heat # 72442 and Linde 80 flux, Lot # 8579 utilizing the same fabrication practice as that used to fabricate the actual vessel beltline welds. This surveillance weld was made of the same heat with the same type flux & lot as was used in the Point Beach Unit 2 intermediate to lower shell circumferential weld. This material is the limiting weld in Point Beach Unit 2 with respect to the ΔRT_{NDT} and RT_{NDT} experienced at the clad/base metal interface and the 1/4T & 3/4T locations.

Based on the discussion, Criterion 1 is met for the Point Beach Unit 2 surveillance program.

Criterion 2: Scatter in the plots of Charpy energy versus temperature for the irradiated and unirradiated conditions should be small enough to permit the determination of the 30 ft-lb temperature and upper-shelf energy unambiguously.

Based on engineering judgment, the scatter in the data presented in these plots, as documented in BMI-0675 [Ref. A-11], WCAP-9331 [Ref. A-12], WCAP-9635 [Ref. A-13], BAW-2140 [Ref. A-14], is small enough to permit the determination of the 30 ft-lb temperature and the upper-shelf energy of the Point Beach Unit 2 surveillance materials unambiguously.

Hence, Criterion 2 is met for the Point Beach Unit 2 surveillance program.

Criterion 3: When there are two or more sets of surveillance data from one reactor, the scatter of ΔRT_{NDT} values about a best-fit line drawn as described in Regulatory Position 2.1 normally should be less than 28°F for welds and 17°F for base metal. Even if the fluence range is large (two or more orders of magnitude), the scatter should not exceed twice those values. Even if the data fail this criterion for use in shift calculations, they may be credible for determining decrease in upper-shelf energy if the upper shelf can be clearly determined, following the definition given in ASTM E185-82.

The functional form of the least squares method as described in Regulatory Position 2.1 will be utilized to determine a best-fit line for this data and to determine if the scatter of these ΔRT_{NDT} values about this line is less than 28°F for welds and less than 17°F for plates or forgings.

Following is the calculation of the best-fit line as described in Regulatory Position 2.1 of Regulatory Guide 1.99, Revision 2. In addition, the recommended NRC methods for determining credibility will be followed. The NRC methods were presented to the industry at a meeting held by the NRC on February 12 and 13, 1998 [Ref. A-8]. At this meeting the NRC presented five cases. Of the five cases, Case 1 (“Surveillance Data Available from Plant but No Other Source”) most closely represents the situation for the Point Beach Unit 2 surveillance forging materials. Since the surveillance weld is not representative of weld material in the Point Beach Unit 2 reactor vessel, it is not evaluated.

Surveillance data are available for weld Heat # 72442 from other various surveillance programs. However, AREVA Calculation 32-9019240-000 [Ref. A-9] determined that the generic table CFs of Regulatory Guide 1.99, Revision 2, are conservative with respect to the measured data. The new Point Beach Unit 2 specific evaluations do not affect these conclusions and they will not be readdressed here.

Evaluation of Point Beach Unit 2 Data Only (Case 1)

Following the NRC Case 1 guidelines, the Point Beach Unit 2 surveillance forgings will be evaluated using the Point Beach Unit 2 data. Table A-5 provides the calculation of the interim CF for Point Beach Unit 2.

Table A-5 Calculation of Interim Chemistry Factors for the Credibility Evaluation Using Point Beach Unit 2 Surveillance Capsule Data Only

Material	Capsule	Capsule Fluence ^(a) (x 10 ¹⁹ n/cm ² , E > 1.0 MeV)	FF ^(b)	Measured ΔRT_{NDT} ^(c) (°F)	FF * ΔRT_{NDT} (°F)	FF ²
Intermediate Shell Forging Heat # 123V500 (Tangential)	V	0.654	0.881	39	34.36	0.776
	T	0.858	0.957	62	59.34	0.916
	R	2.17	1.210	88	106.51	1.465
	S	3.05	1.295	101	130.76	1.676
	SUM:					330.96
CF _{123V500} = $\Sigma(\text{FF} * \Delta RT_{NDT}) \div \Sigma(\text{FF}^2) = (330.96) \div (4.833) = 68.5^\circ\text{F}$						
Intermediate Shell Forging Heat # 122W195 (Tangential)	V	0.654	0.881	39	34.36	0.776
	T	0.858	0.957	35	33.50	0.916
	R	2.17	1.210	50	60.51	1.465
	S	3.05	1.295	61	78.97	1.676
	SUM:					207.34
CF _{122W195} = $\Sigma(\text{FF} * \Delta RT_{NDT}) \div \Sigma(\text{FF}^2) = (207.34) \div (4.833) = 42.9^\circ\text{F}$						

Notes:

- (a) Fluence taken from Table 2.5-8.
- (b) FF = fluence factor = $f^{(0.28 - 0.10 * \log(f))}$.
- (c) Measured ΔRT_{NDT} taken from Table 4-2.

The scatter of ΔRT_{NDT} values about the functional form of a best-fit line drawn as described in Regulatory Position 2.1 is presented in Table A-6.

Table A-6 Point Beach Unit 2 Surveillance Capsule Data Scatter about the Best-Fit Line Using All Available Surveillance Data

Material	Capsule	CF ^(a) (Slope _{best-fit}) (°F)	Capsule Fluence ^(b) (x 10 ¹⁹ n/cm ²)	FF ^(c)	Measured ΔRT_{NDT} ^(d) (°F)	Predicted ΔRT_{NDT} ^(e) (°F)	Scatter ΔRT_{NDT} ^(f) (°F)	<17°F (Forging)
Unit 2 Surveillance Forging Intermediate Shell Forging (Heat # 123V500)	V	68.5	0.654	0.881	39	60.3	21.3	No
	T	68.5	0.858	0.957	62	65.6	3.6	Yes
	R	68.5	2.17	1.210	88	82.9	5.1	Yes
	S	68.5	3.05	1.295	101	88.7	12.3	Yes
Unit 2 Surveillance Forging Lower Shell Forging (Heat # 122W195)	V	42.9	0.654	0.881	39	37.8	1.2	Yes
	T	42.9	0.858	0.957	35	41.1	6.1	Yes
	R	42.9	2.17	1.210	50	51.9	1.9	Yes
	S	42.9	3.05	1.295	61	55.5	5.5	Yes

Notes:

- (a) CF calculated in Table A-5.
- (b) Fluence taken from Table 2.5-8.
- (c) FF = fluence factor = $f^{0.28 - 0.10 * \log(f)}$.
- (d) Measured ΔRT_{NDT} taken from Table 4-2.
- (e) Predicted $\Delta RT_{NDT} = CF \times FF$
- (f) Scatter $\Delta RT_{NDT} = \text{Absolute Value} [\text{Predicted } \Delta RT_{NDT} - \text{Measured } \Delta RT_{NDT}]$.

Table A-6 indicates that, for the IS forging, three of the four surveillance data points fall inside the +/- 1 σ of 17°F scatter band for surveillance forging materials (75% of the data are bounded). Table A-6 indicates that, for the LS forging, four of the four surveillance data points fall inside the +/- 1 σ of 17°F scatter band for surveillance forging materials (100% of the data are bounded).

Therefore, the surveillance forging data is deemed “credible” per the third criterion for both forging materials.

Criterion 4: The irradiation temperature of the Charpy specimens in the capsule should match the vessel wall temperature at the cladding/base metal interface within +/- 25°F.

The capsule specimens are located in the reactor between the thermal shield and the vessel wall and are positioned opposite the center of the core. The test capsules are contained in baskets attached to the thermal shield. The location of the specimens with respect to the reactor vessel beltline provides assurance that the reactor vessel wall and the specimens experience equivalent operating conditions such that the temperatures will not differ by more than 25°F. Hence, this criterion is met.

Criterion 4 is met for the Point Beach Unit 2 surveillance program.

Criterion 5: The surveillance data for the correlation monitor material in the capsule should fall within the scatter band of the database for that material.

The Point Beach Unit 2 surveillance program contains A533B-1 correlation monitor material (Heavy Section Steel Technology [HSST] Plate 02) as shown in NUREG/CR-6413, ORNL/TM-13133 [Ref. A-10]. Figure 11 of NUREG/CR-6413, ORNL/TM-13133 contains a plot of residual versus fast fluence for the correlation monitor material. This figure shows a 2σ uncertainty of 50°F. The data used in Figure 11 is contained in Table 15 of NUREG/CR-6413 (identified as product SRM). Standard reference material (SRM) was contained in the four surveillance capsules that have been removed and tested from Point Beach Unit 2; however, the fluence values have been updated. Table A-7 contains an updated calculation of the residual versus fast fluence.

Table A-7 Calculation of Residual versus Fast Fluence

Capsule	Capsule Fluence^(a) ($\times 10^{19}$ n/cm², E > 1.0 MeV)	FF	Measured Shift^(b) (°F)	RG 1.99 Shift (CF * FF)^(c) (°F)	Residual Measured Shift (°F)
V	0.654	0.881	95	112.8	17.8
T	0.858	0.957	105	122.5	17.5
R	2.17	1.210	151	154.9	3.9
S	3.05	1.295	145	165.7	20.7

Notes:

(a) Values taken from Table 4-2.

(b) Values taken from NUREG/CR-6413 [Ref. A-10] Table 15.

(c) Per NUREG/CR-6413 [Ref. A-10] Table 15, the Cu and Ni weight percent values for the Point Beach Unit 1 correlation monitor material are 0.17 Cu and 0.64 Ni. This equates to a CF of 128.0°F from Regulatory Guide 1.99, Revision 2.

Table A-7 shows a 2σ uncertainty of less than 50°F, which is the allowable scatter in Figure 11 of NUREG/CR-6413. Hence, this criterion is met.

Criterion 5 is met for the Point Beach Unit 2 surveillance program.

Conclusion

Based on the preceding responses to the five criteria of Regulatory Guide 1.99, Revision 2, Section B, the Point Beach Unit 2 surveillance forging data for the forging materials are deemed credible. The plant-specific surveillance weld data is not evaluated since it is not used in the Unit 2 reactor vessel.

A.4 REFERENCES

- A-1. U.S. Nuclear Regulatory Commission, Office of Nuclear Regulatory Research, Regulatory Guide 1.99, Revision 2, "Radiation Embrittlement of Reactor Vessel Materials," May 1988. [ADAMS Accession Number ML003740284]
- A-2. U.S. Nuclear Regulatory Commission, Federal Register, Code of Federal Regulations, 10 CFR Part 50, Appendix G, "Fracture Toughness Requirements," November 29, 2019.
- A-3. Westinghouse Report WCAP-15856, Revision 0, "Supplemental Reactor Vessel Surveillance Capsule 'A' for the Point Beach Units 1 and 2 Reactor Vessel Installed in the Point Beach Unit 2 Reactor Vessel," May 2002.
- A-4. BMI Report BMI-0673, Revision 0, "Point Beach Nuclear Plant Unit No. 1 Pressure Vessel Surveillance Program: Evaluation of Capsule V," June 1973.
- A-5. Westinghouse Report WCAP-8739, Revision 0, "Analysis of Capsule S from the Wisconsin Electric Power Company and the Wisconsin Michigan Power Company Point Beach Nuclear Plant Unit No. 1 Reactor Vessel Radiation Surveillance Program," November 1976.
- A-6. Westinghouse Report WCAP-9357, Revision 0, "Analysis of Capsule R from the Wisconsin Electric Power Company Point Beach Nuclear Plant Unit No. 1 Reactor Vessel Radiation Surveillance Program," August 1978.
- A-7. Westinghouse Report WCAP-10736, Revision 0, "Analysis of Capsule T from the Wisconsin Electric Power Company Point Beach Nuclear Plant Unit No. 1 Reactor Vessel Radiation Surveillance Program," December 1984.
- A-8. K. Wichman, M. Mitchell, and A. Hiser, USNRC, Generic Letter 92-01 and RPV Integrity Workshop Handouts, "NRC/Industry Workshop on RPV Integrity Issues," February 1998. [ADAMS Accession Number ML110070570].
- A-9. AREVA Calculation Note 32-9019240-000, "ART Values for Point Beach Unit 1 and Unit 2," June 2006. [ADAMS Accession Number ML13113A008]
- A-10. NUREG/CR-6413, ORNL/TM-13133, "Analysis of the Irradiation Data for A302B and A533B Correlation Monitor Materials," April 1996.
- A-11. BMI Report BMI-0675, Revision 0, "Point Beach Nuclear Plant Unit No. 2 Pressure Vessel Surveillance Program: Evaluation of Capsule V," June 1975.
- A-12. Westinghouse Report WCAP-9331, Revision 0, "Analysis of Capsule T from the Wisconsin Electric Power Company Point Beach Nuclear Plant Unit No. 2 Reactor Vessel Radiation Surveillance Program," August 1978.
- A-13. Westinghouse Report WCAP-9635, Revision 0, "Analysis of Capsule R from the Wisconsin Electric Power Company Point Beach Nuclear Plant Unit No. 2 Reactor Vessel Radiation Surveillance Program EPRI Research Project 1021-3 Topical Report," December 1979.
- A-14. BAW Report BAW-2140, Revision 0, "Analysis of Capsule S Wisconsin Electric Power Company Point Beach Nuclear Plant Unit No. 2," August 1991.

This page was added to the quality record by the PRIME system upon its validation and shall not be considered in the page numbering of this document.

Approval Information

Author Approval Lynch Donald Aug-31-2020 08:57:31

Reviewer Approval Mays Benjamin E Aug-31-2020 11:21:47

Reviewer Approval Hawk Andrew E Aug-31-2020 14:13:21

Approver Approval Patterson Lynn Aug-31-2020 14:22:02

Approver Approval Houssay Laurent Aug-31-2020 15:55:36

Hold to Release Approval Lynch Donald Aug-31-2020 16:06:52

Files approved on Aug-31-2020

*** This record was final approved on 8/31/2020 4:06:52 PM. (This statement was added by the PRIME system upon its validation)

Point Beach Nuclear Plant Units 1 and 2
Dockets 50-266 and 50-301
NRC 2020-0032 Enclosure 4, Attachment 4

Enclosure 4

**Non-proprietary Reference Documents and
Redacted Versions of Proprietary Reference
Documents**

(Public Version)

Attachment 4

**Framatome Topical Report BAW-2192, Revision 0,
Supplement 3NP, Revision 0, “Low Upper-Shelf
Toughness Fracture Mechanics Analysis of Reactor
Vessels of B&W Owners Reactor Vessel Working
Group for Levels A & B Service Loads,” October 2020**

(51 Total Pages, including cover sheets)

**Low Upper-Shelf Toughness
Fracture Mechanics Analysis of
Reactor Vessels of B&W Owners
Reactor Vessel Working Group for
Levels A & B Service Loads**

BAW-2192
Revision 0
Supplement 3NP
Revision 0

Topical Report

October 2020

(c) 2020 Framatome Inc.

Copyright © 2020

**Framatome Inc.
All Rights Reserved**

Nature of Changes

Item	Section(s) or Page(s)	Description and Justification
1	All	Initial Issue

Contents

		<u>Page</u>
1.0	INTRODUCTION	1-1
1.1	Equivalent Margins Analysis—Analysis of Record	1-3
2.0	REGULATORY REQUIREMENTS	2-1
2.1	Regulatory Requirements	2-1
2.2	Compliance with 10 CFR 50 Appendix G and Acceptance Criteria	2-2
2.2.1	Acceptance Criteria Levels A and B	2-2
3.0	DESCRIPTION OF PBN UNIT 1 AND 2 REACTOR VESSELS & 80-YEAR FLUENCE PROJECTIONS	3-1
4.0	MATERIAL PROPERTIES.....	4-1
4.1	J-Integral Resistance Model	4-1
4.2	Mechanical Properties of Weld Metals.....	4-2
4.2.1	Mechanical Properties for the Point Beach Reactor Vessels	4-3
5.0	FRACTURE MECHANICS ANALYSIS	5-1
5.1	Methodology	5-1
5.2	Procedure for Evaluating Levels A and B Service Loadings.....	5-2
5.3	Evaluation for Flaw Extension.....	5-5
5.3.1	Reactor Vessel Units 1 and 2 Shell Welds	5-6
5.3.2	Reactor Vessel Shell Welds Near RV Upper Transition Region	5-7
5.3.3	Reactor Vessel Unit 1 RV Nozzle Welds	5-8
5.4	Evaluation for Flaw Stability.....	5-8
5.4.1	Reactor Vessel Units 1 and 2 Shell Welds	5-9
5.4.2	Reactor Vessel Unit 1 Nozzle Welds	5-9
6.0	SUMMARY AND CONCLUSIONS	6-1
6.1	Reactor Vessel Shell Welds-Units 1 and 2	6-1
6.2	Reactor Vessel Nozzle Welds-Unit 1	6-1
7.0	REFERENCES	7-1
8.0	CERTIFICATION	8-1
	APPENDIX A.....	A-1

List of Tables

Table 3-1	Copper Content and 80-Year (72 EFPY) Fluence ($E > 1.0$ MeV) for PBN Unit 1 Reactor Vessel Linde 80 Weld Locations	3-2
Table 4-1	Parameters in Jd Model 6B	4-4
Table 4-2	Mechanical Properties of PBN Unit 1 RV Shell Materials	4-5
Table 4-3	Mechanical Properties of Point Beach Unit 2 RV Shell Materials	4-6
Table 5-1	Reactor Vessel Shell Dimensions and Operating Conditions	5-10
Table 5-2	PBN Unit 1 and Unit 2 Flaw Evaluation Summary for RV Shell Regions	5-11
Table 5-3	J-Integral (FEA) Versus Flaw Extension for Point Beach Unit 1, Weld SA-1426 (Levels A & B Service Loadings)	5-12
Table 5-4	J-Integral (FEA) Versus Flaw Extension for Point Beach Unit 1, Weld SA-812/SA-775 (Levels A & B Service Loadings)	5-13
Table 5-5	Reactor Vessel Nozzle Belt Dimensions	5-14
Table 5-6	Flaw Evaluation Summary of PBN Unit 1 RV Nozzle-to-NBF Margins (Levels A & B Service Loadings)	5-14
Table A-1	Model 6B, Range of Test Data	A-2

List of Figures

Figure 3-1	Reactor Vessel—PBN Unit 1	3-4
Figure 3-2	Reactor Vessel—Point Beach Unit 2	3-5
Figure 5-1	J-Integral Versus Flaw Extension for Point Beach Controlling Reactor Vessel Shell Weld SA-812/SA-775	5-15
Figure 5-2	J-Integral versus Flaw Extension for Point Beach RV Outlet Nozzle	5-16

Nomenclature

Acronym	Definition
B&W	Babcock and Wilcox
B&WOG	Babcock and Wilcox Owners Group
CE	Combustion Engineering
CvUSE	Charpy Upper Shelf Energy
EFPY	Effective Full Power Years
EMA	Equivalent Margins Analysis
INF	Inlet Nozzle Forging
Jd	J deformation
J-R	J-integral Resistance
LAR	License Amendment Request
ONF	Outlet Nozzle Forging
PBN	Point Beach Nuclear
RV	Reactor Vessel
RVWG	Reactor Vessel Working Group
SLR	Subsequent License Renewal
SRP	Standard Review Plan
Sy	Yield Strength
TSs	Technical Specifications
USE	Upper Shelf Energy

ABSTRACT

This Supplement 3 to BAW-2192PA reports an equivalent margins analysis (EMA) considering Levels A and B service loads for high copper Linde 80 weld metals and using fluence values expected at 80-years (subsequent license renewal-SLR). This supplement to BAW-2192 applies to the following Westinghouse-designed reactor vessels: PBN Unit 1 fabricated by Babcock & Wilcox (B&W), and PBN Unit 2 fabricated by B&W and Combustion Engineering (CE).

The analytical procedure used in this supplement is in accordance with ASME Section XI, 2017 Edition, Appendix K, Subarticle K-1200. EMA results are reported for all reactor vessel Linde 80 weld locations with 80-year fluence projections that exceed $1.0 \text{ E}+17 \text{ n/cm}^2$ ($E > 1.0 \text{ MeV}$) and for Unit 1 Linde 80 welds that connect the RV inlet and outlet nozzles to the nozzle belt forging. The ASME Section XI acceptance criteria for Levels A & B Service Loads for all reactor vessel shell welds are satisfied. The acceptance criteria for Levels A & B Service Loads for RV nozzle welds are also satisfied.

The EMA utilizes the B&WOG J-integral resistance (J-R) Model 6B reported in NRC Staff approved Topical Report BAW-2192, Revision 0, Supplement 1P-A, Revision 0, Appendix A. Model 6B was developed based on fracture toughness test data obtained through 2020, with specimen fluence that ranges from 0.0 to $5.80\text{E}+19 \text{ n/cm}^2$. The copper content of the PBN Linde 80 welds and $\frac{1}{4}$ T fluence are within the range of explanatory variables used to develop Model 6B, as reported in Appendix A of this supplement.

1.0 INTRODUCTION

The purpose of Supplement 3 to BAW-2192PA , Revision 0 [1] is to report an equivalent margins analysis (EMA) considering Levels A and B service loads for high copper Linde 80 welds using fluence values expected at 80-years (subsequent license renewal-SLR). This supplement to BAW-2192 applies to the following Westinghouse-designed reactor vessels: PBN Unit 1 fabricated by B&W, and PBN Unit 2 fabricated by B&W and CE.

Equivalent margins analyses for the plants within the scope of this report are reported for all reactor vessel weld locations with 80-year fluence projections that exceed $1.0 \text{ E}+17 \text{ n/cm}^2$ ($E > 1.0 \text{ MeV}$) [2], and are conservatively completed for the reactor vessel nozzle to nozzle-belt forging Linde 80 welds for PBN Unit 1. PBN Unit 2 nozzle to nozzle-belt forging welds are not fabricated from Linde 80 welds. Plants that reference this report must calculate 80-year neutron fluence at reactor vessel weld locations in accordance with NUREG-2192 [3], Standard Review Plan for Review of Subsequent License Renewal Applications, to demonstrate that the fluence estimates provided in Section 3.0 are applicable to their reactor vessels. Upper shelf energy evaluations at reactor vessel base metal locations with 80-year fluence projections greater than $1.0 \text{ E}+17 \text{ n/cm}^2$ are not within the scope of this report.

The EMA utilizes the B&WOG J-integral resistance (J-R) Model 6B reported in BAW-2192, Revision 0, Supplement 1P-A, Revision 0, Appendix A [4]. The following groups are used for the Linde 80 welds within the scope of this report:

- Reactor Vessel Shell Welds-circumferential and longitudinal Linde 80 welds (if applicable) within the intermediate shell (IS) and lower shell (LS) courses for PBN Units 1 and 2, and the circumferential weld that connects the nozzle belt forging (NBF) to the intermediate shell course for PBN Unit 1. There are no geometric discontinuities at these weld locations and all reactor vessel shell welds surround the effective height of the active core. These locations have historically been considered “beltline” or “beltline region” as defined by 10 CFR 50, Appendix G.
- RV Nozzle Welds-Linde 80 welds for PBN Unit 1 that connect the RV inlet and outlet nozzle forgings to the nozzle belt forging. These welds are projected to receive fluence levels less than $1.0E+17$ n/cm² at 80-years but are conservatively evaluated herein at an inside surface fluence of $1.0E+18$ n/cm². The equivalent welds for PBN Unit 2 are made from non-Linde 80 welds, by Combustion Engineering, and are projected to receive fluence levels less than $1.0E+17$ n/cm² at 80-years and are not within the scope of this report.

The 60-year EMA analysis of record for PBN Units 1 and 2 Linde 80 welds is reported in Section 1.1. Section 2.0 provides the current NRC regulatory requirements for the EMA. Section 3.0 provides a description of the reactor vessel Linde 80 welds within the scope of this report, with illustrations of reactor vessel Linde 80 welds that are evaluated for equivalent margins in Figure 3-1 and Figure 3-2. Section 4.0 provides the material properties that are required for the EMA, and Section 5.0 presents the results of the EMA. Section 6.0 provides the summary and conclusions, Section 7.0 lists all references and Appendix A provides the technical basis for the use of B&WOG J-R Model 6B for the EMA reported herein.

1.1 ***Equivalent Margins Analysis—Analysis of Record***

BAW-2192PA, Revision 00 [1] provided the EMA analysis of record for Levels A and B service loads for PBN Units 1 and 2 for 40 years. For 60 years, PBN Units 1 and 2 reported plant-specific evaluations in BAW-2467P, Revision 01 [5]. The summary reports for EMA analyses of record are as follows.

Point Beach Units 1 and 2

The PBN Units 1 and 2 current licensing basis equivalent margins analysis at 53 EFPY is summarized in Section 2.1.2 of NRC document “POINT BEACH NUCLEAR PLANTS, UNIT 1 AND 2- EXTENDED POWER UPRATE AMENDMENT (TAC NOS. ME1044 AND ME1045),” ADAMS Accession number ML110450159 [6]. NRC acceptance of the Point Beach EMA at 53 EFPY for EPU is based on the following documentation:

- Point Beach Nuclear Plant, Units 1 and 2-Issuance of Amendments Regarding Review of Reactor Vessel Fracture Mechanics Analysis (TAC NOS. MD2359 AND MD2360), ADAMS Accession Number ML071300623 [7].

2.0 REGULATORY REQUIREMENTS

2.1 *Regulatory Requirements*

In accordance with 10 CFR 50 Appendix G [8], IV, A, 1., Reactor Vessel Upper Shelf Energy Requirements are as follows:

- a. Reactor vessel beltline materials must have Charpy upper-shelf energy in the transverse direction for base material and along the weld for weld material according to the ASME Code, of no less than 75 ft-lb (102 J) initially and must maintain Charpy upper-shelf energy throughout the life of the vessel of no less than 50 ft-lb (68 J), unless it is demonstrated in a manner approved by the Director, Office of Nuclear Reactor Regulation or Director, Office of New Reactors, as appropriate, that lower values of Charpy upper-shelf energy will provide margins of safety against fracture equivalent to those required by Appendix G of Section XI of the ASME Code. This analysis must use the latest edition and addenda of the ASME Code incorporated by reference into 10 CFR 50.55a (b)(2) at the time the analysis is submitted.
- b. Additional evidence of the fracture toughness of the beltline materials after exposure to neutron irradiation may be obtained from results of supplemental fracture toughness tests for use in the analysis specified in section IV.A.1.a.
- c. The analysis for satisfying the requirements of section IV.A.1 of this appendix must be submitted, as specified in § 50.4, for review and approval on an individual case basis at least three years prior to the date when the predicted Charpy upper-shelf energy will no longer satisfy the requirements of section IV.A.1 of this appendix, or on a schedule approved by the Director, Office of Nuclear Reactor Regulation.

When the reactor vessels within the scope of this report were fabricated, Charpy V-notch testing of the reactor vessel welds were in accordance with the original construction code, which did not specifically require Charpy V-notch tests on the upper shelf.

Applicable construction codes are as follows:

- PBN Unit 1, ASME Section III 1965 Edition, by Babcock & Wilcox
- PBN Unit 2, ASME Section III 1965 Edition, by Babcock & Wilcox and Combustion Engineering

In accordance with NRC Regulatory Guide 1.161 [9], the NRC has determined that the analytical methods described in ASME Section XI, Appendix K, provide acceptable guidance for evaluating reactor pressure vessels when the Charpy upper-shelf energy falls below the 50 ft-lb limit of Appendix G to 10 CFR Part 50. However, the staff noted that Appendix K does not provide information on the selection of transients and gives very little detail on the selection of material properties. Selection of the limiting design transient (i.e., cooldown at 100 F/h) is consistent with BAW-2192PA, Revision 0 [1], Section 5.3. Section 4.1 of this report includes a summary of the B&WOG J-integral resistance model, and Section 4.2 provides mechanical properties of weld metals.

2.2 Compliance with 10 CFR 50 Appendix G and Acceptance Criteria

The analyses reported herein are performed in accordance with the 2017 Edition [10] of Section XI of the ASME Code, Appendix K. The current edition of ASME Section XI listed in 10 CFR 50.55a is the 2017 Edition [10]. The material properties used in this analysis are based on ASME Section II, Part D, 2017 Edition.

2.2.1 Acceptance Criteria Levels A and B

ASME Section XI [10], Subarticle K-2200, provides the following acceptance criteria for Levels A and B Service Conditions:

- a. When analytically evaluating adequacy of the upper shelf toughness for the weld material for Levels A and B Service Loadings, an interior semi-elliptical surface flaw with a depth one-quarter of the wall thickness and a length six times the depth shall be postulated, with the flaw's major axis oriented along the weld of concern, and the flaw plane oriented in the radial direction. When analytically evaluating adequacy of the upper shelf toughness for the base material, both interior axial and circumferential flaws with depths one quarter of the wall thickness and lengths six times the depth shall be postulated, and toughness properties for the corresponding orientation shall be used. Smaller flaw sizes may be used when justified. Two criteria shall be satisfied:
- 1) The applied J-integral analytically evaluated at a pressure 1.15 times the accumulation pressure as defined in the plant specific Overpressure Protection Report, with a structural factor of 1 on thermal loading for the plant specific heatup and cooldown conditions, shall be less than the J-integral of the material at a ductile flaw extension of 0.1 in. (2.5 mm).
 - 2) Flaw extensions at pressures up to 1.25 times the accumulation pressure of 1) shall be ductile and stable, using a structural factor of 1 on thermal loading for the plant specific heatup and cooldown conditions.
- b. The J-integral resistance versus flaw extension curve shall be a conservative representation for the vessel material under analytical evaluation.

3.0 DESCRIPTION OF PBN UNIT 1 AND 2 REACTOR VESSELS & 80-YEAR FLUENCE PROJECTIONS

The PBN Units 1 and 2 reactor vessels and applicable Linde 80 weld locations are shown in Figure 3-1 and Figure 3-2. All weld locations evaluated for equivalent margins in this report are identified by an asterisk (*) in each figure. Plant-specific welds copper and nickel content and 80-year fluence projections data needed for the equivalent margins analysis are provided in Table 3-1. The fluence projections are reported for all reactor vessel Linde 80 weld locations that are expected to exceed $1.0E+17$ n/cm² at 80 years. Note that PBN Unit 2 weld 21935 (nozzle belt forging to intermediate shell weld), although having a projected fluence $> 1.0E+17$ n/cm² at 80-years, is not a Linde 80 weld, does not fall below 50 ft-lbs, and is not within the scope of this report. All 80-year fluence values are at the clad/base metal interface. Copper and nickel content of the reactor vessel shell welds is consistent with EMA analyses of record reported in Section 1.1; the copper and nickel content for RV shell welds and RV nozzle-to-nozzle belt forging welds reported in Table 3-1 were obtained from either the EMA analysis of record or a search of PBN reactor vessel fabrication reports.

**Table 3-1 Copper Content and 80-Year (72 EFPY) Fluence (E > 1.0 MeV) for PBN Unit 1
 Reactor Vessel Linde 80 Weld Locations**

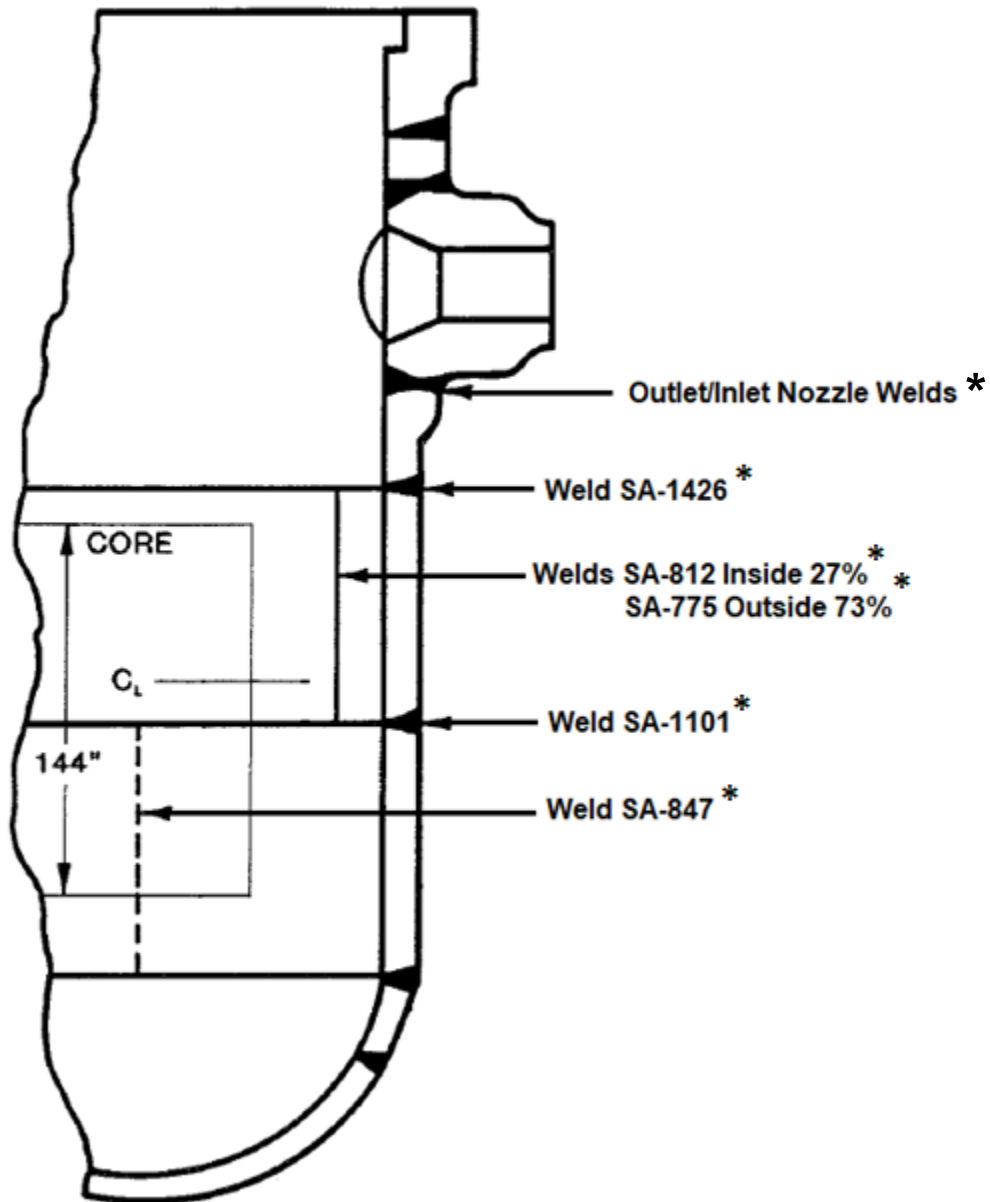
Reactor Vessel Location	Weld ID	Cu, wt%	Ni, wt%	Clad/Base Metal Interface Surface Fluence (E > 1.0 MeV), n/cm ²
PBN Unit 1, 80-Year Fluence (E > 1.0 MeV)				
Nozzle belt forging to bottom of outlet nozzle forging welds	Linde 80	[]	[]	6.51E+16 Use 1.0E+18 (Note 1)
Nozzle belt forging to bottom of inlet nozzle forging Welds	Linde 80	[]	[]	6.51E+16 Use 1.0E+18 (Note 1)
Nozzle belt forging to intermediate shell circumferential weld.	SA-1426	0.19	0.57	5.66E+18
Intermediate shell longitudinal weld	SA-812 (27% inside)	0.17	0.52	4.64E+19
	SA-775 (73% outside)	0.17	0.64	4.64E+19
Intermediate shell to lower shell circumferential weld.	SA-1101	0.23	0.59	7.36E+19
Lower shell longitudinal weld	SA-847	0.23	0.52	4.58E+19

Reactor Vessel Location	Weld ID	Cu, wt%	Ni, wt%	Clad/Base Metal Interface Surface Fluence (E > 1.0 MeV), n/cm ²
Lower shell to lower head ring circumferential weld	Linde 80	N/A	N/A	4.79E+16 (Note 2)
PBN Unit 2, 80-Year Fluence (E > 1.0 MeV)				
Intermediate shell course to lower shell course circumferential weld	SA-1484	0.26	0.60	7.65E+19

Notes:

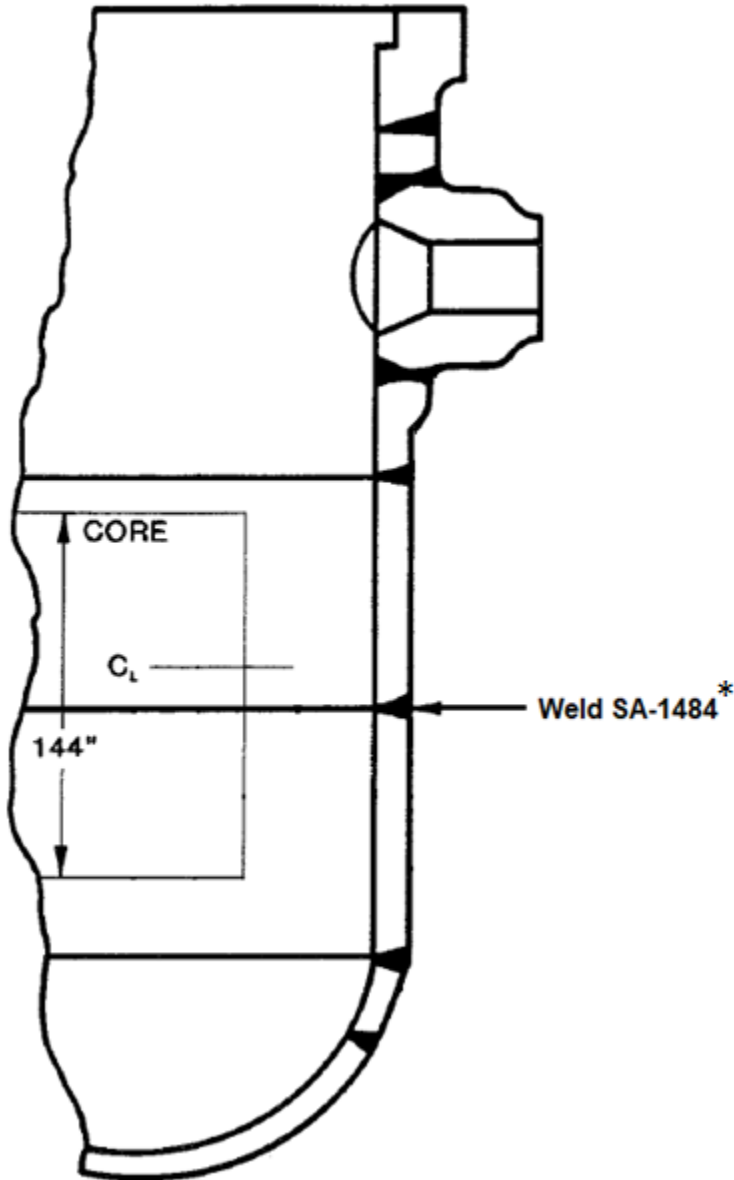
- 1: EMA not required since fluence is less than 1.0E+17 n/cm²; however, EMA of this weld is conservatively included herein. Conservative/bounding fluence of 1.0E+18 n/cm² to be used for EMA analyses only. This may be assumed to be a wetted surface value, applicable at any postulated flaw depth.
- 2: EMA not required as fluence is less than 1.0E+17 n/cm².

Figure 3-1
Reactor Vessel—PBN Unit 1



* EMA performed for specified weld and reported herein.

Figure 3-2
Reactor Vessel—Point Beach Unit 2



* EMA performed for weld and reported herein

4.0 MATERIAL PROPERTIES

4.1 *J-Integral Resistance Model*

The J-integral resistance model for Mn-Mo-Ni/Linde 80 welds in the reactor vessels of the B&WOG RVWG plants were developed using a large J-integral resistance data base. A detailed description of Model 6B, which was developed to support subsequent license renewal, is provided in BAW-2192PA, Supplement 1P-A, Revision 0, Appendix A [4], and is applicable to the Oconee Nuclear Station, Surry Units 1 and 2, and Turkey Point Units 3 and 4. Appendix A of this report provides justification for the use of Model 6B for PBN Units 1 and 2.

The coefficients a , d , and C_4 are provided in Table 4-1. As required by ASME Section XI, ASME K-3300, when evaluating the vessel for Levels A, B, and C Service Loadings, the J-integral resistance versus crack-extension curve (J-R curve) shall be a conservative representation of the toughness of the controlling beltline material at upper shelf temperatures in the operating range. As such, the Jd correlation minus 2 standard errors is used for evaluation of Levels A & B service loadings (i.e., equation (1) multiplied by []).

As discussed in Appendix B to BAW-2192PA, the J-R curve was generated from a J-integral database obtained from the same class of material with the same orientation as the applicable reactor vessel materials using correlations for the effects of temperature, chemical composition, and fluence level. Crack extension was by ductile tearing with no cleavage. This complies with the ASME Code, Section XI, K-3300.

4.2 *Mechanical Properties of Weld Metals*

The following subsections provide representative properties for the PBN Units 1 and 2 reactor vessels. The temperature dependent mechanical properties are developed from the 2017 Edition of the ASME Code (Section II, Part D) [11] for the reactor base metal and cladding (the ASME Code does not provide separate mechanical properties for base and weld metal). Both ASME Code minimum and representative irradiated yield strengths are also provided. The mechanical properties such as weld metal yield strengths typically used were the irradiated properties but in some cases the ASME Code minimum properties were conservatively considered.

4.2.1 Mechanical Properties for the Point Beach Reactor Vessels

PBN Unit 1 reactor vessel intermediate and lower shell courses are fabricated from SA-302, Grade B low alloy steel. The PBN Unit 2 reactor vessel intermediate and lower shell courses are fabricated from SA-508, Grade 2, Class 1 low alloy steel. Table 4-2 and Table 4-3 provide the Young's modulus (E), the mean coefficient of thermal expansion (α), and the yield strength (S_y) for the RV shell regions. Available weld metal yield strength is irradiated data obtained from PBN capsule reports.

For the Point Beach reactor vessel shell regions, the normal operating steady state condition cold leg temperature value is [] (Table 5-1). The yield strength values for these weld metals at []

Table 4-1 Parameters in Jd Model 6B

A large, empty rectangular frame with a thin black border, centered on the page. It is intended to contain the data for Table 4-1, but the content is missing.

Table 4-2 Mechanical Properties of PBN Unit 1 RV Shell Materials

Temp. (°F)	RV Base Metal, A-302B			Weld Metals Yield Strength, Sy	
	E (ksi)	α (in/in/°F)	Sy (ksi)	SA-847 (ksi)	SA-1101 (ksi)
100	28885	6.47E-06	50.00	[]	[]
200	28500	6.70E-06	47.00	[]	[]
300	28000	6.90E-06	45.50	[]	[]
400	27600	7.10E-06	44.20	[]	[]
500	27000	7.30E-06	43.20	[]	[]
549.3	26665	7.35E-06	42.66	[]	[]
550	26650	7.35E-06	42.65	[]	[]
600	26300	7.40E-06	42.10	[]	[]

Table 4-3 Mechanical Properties of Point Beach Unit 2 RV Shell Materials

Temp. (°F)	RV Base Metal, A508 Grade 2			Weld Metals Yield Strength, Sy
	E (ksi)	α (in/in/°F)	Sy (ksi)	SA-1484 (ksi)
100	27638	6.47E-06	50.00	[]
200	27100	6.70E-06	47.00	[]
300	26700	6.90E-06	45.50	[]
400	26200	7.10E-06	44.20	[]
500	25700	7.30E-06	43.20	[]
549.3	25416	7.35E-06	42.66	[]
580	25264	7.38E-06	42.32	[]
600	25100	7.40E-06	42.10	[]

5.0 FRACTURE MECHANICS ANALYSIS

5.1 *Methodology*

In accordance with ASME Section XI, Appendix K [10], Subarticle K-1200, the following analytical procedure was used for Levels A & B Service Loads.

- a. The postulated flaws in the reactor vessel shell welds and RV nozzle-to-shell welds were postulated in accordance with the acceptance criteria of Subarticle K-2200.
- b. Loading conditions at the locations of the postulated flaws were determined for Levels A and B Service Loadings. For Levels A and B Service loadings the equations to calculate the stress intensity factor (SIF) due to pressure and thermal gradients for a given pressure and cooldown rate are given in Article K-4210. Consistent with Section 5 of BAW-2192PA, Revision 0 [1], the accumulation pressure is taken as ten percent above the design pressure and the maximum cooldown rate is 100°F/hr. In the area of the nozzle-to-shell weld, applied loadings consist of pressure, thermal, and attached piping reactions.
- c. Material properties, including E , α , σ_y , and the J-integral resistance curve (J-R curve), were determined at the locations of the postulated flaws. Young's modulus, mean coefficient of thermal expansion and yield strength are addressed in Section 4.2. The J-R curve is discussed in Section 4.1.

- d. The postulated flaws were evaluated in accordance with the acceptance criteria of Article K-2000. Requirements for evaluating the applied J-integral are provided in Subarticle K-3200, and for determining flaw stability in Subarticle K-3400. Subarticle K-3500(a) invokes the procedure provided in Subarticle K-4200 (K-4220) for evaluating the applied J-integral for a specified amount of ductile flaw extension. Three permissible evaluation methods to address flaw stability are described in Subarticle K-3500(b). The evaluation method selected herein is the J-R curve crack driving force diagram procedure described in Subarticle K-4310.

5.2 Procedure for Evaluating Levels A and B Service Loadings

For RV shell regions remote from structural discontinuities, the applied J-integral is calculated in accordance with Appendix K, Subarticle K-4210, using an effective flaw depth to account for small scale yielding at the crack tip, and evaluated per K-4220 for upper-shelf toughness and per K-4310 for flaw stability, as outlined below.

1. For an axial flaw of depth a , the stress intensity factor due to internal pressure is calculated with a structural factor (SF) on pressure using the following:

$$K_{I_p} = (SF)p \left(1 + \frac{R_i}{t} \right) (\pi a)^{0.5} F_1$$

where

$$F_1 = 0.982 + 1.006 \left(\frac{a}{t} \right)^2, \quad 0.20 \leq \left(\frac{a}{t} \right) \leq 0.50$$

2. For a circumferential flaw of depth a , the stress intensity factor due to internal pressure is calculated with a structural factor (SF) on pressure using the following:

$$K_{I_p} = (SF)p \left(1 + \frac{R_i}{2t} \right) (\pi a)^{0.5} F_2$$

where

$$F_2 = 0.885 + 0.233\left(\frac{a}{t}\right) + 0.345\left(\frac{a}{t}\right)^2, \quad 0.20 \leq \left(\frac{a}{t}\right) \leq 0.50$$

3. For an axial or circumferential flaw of depth a , the stress intensity factor due to radial thermal gradients are calculated using the following:

$$K_{It} = C_m (CR) t^{2.5} F_3, \quad 0 \leq (CR) \leq 100 \text{ }^\circ\text{F/hr}$$

where

for SA-508, Class 2 or SA-302 Grade B steels, the material coefficient C_m is defined as:

$$C_m = \frac{E\alpha}{(1-\nu)d} = 0.0051,$$

CR = cooldown rate ($^\circ\text{F/hr}$), and

$$F_3 = 0.1181 + 0.5353\left(\frac{a}{t}\right) - 1.273\left(\frac{a}{t}\right)^2 + 0.6046\left(\frac{a}{t}\right)^3, \quad 0.20 \leq \left(\frac{a}{t}\right) \leq 0.50$$

4. The effective flaw depth for small scale yielding, a_e , is calculated using the following:

$$a_e = a + \left(\frac{1}{6\pi}\right) \left[\frac{K_{Ip} + K_{It}}{\sigma_y} \right]^2$$

5. For an axial flaw of depth a_e , the stress intensity factor due to internal pressure is:

$$K'_{Ip} = (SF)p \left(1 + \frac{R_i}{t}\right) (\pi a_e)^{0.5} F'_1$$

where

$$F'_1 = 0.982 + 1.006\left(\frac{a_e}{t}\right)^2, \quad 0.20 \leq \left(\frac{a_e}{t}\right) \leq 0.50$$

6. For a circumferential flaw of depth a_e , the stress intensity factor due to internal pressure is:

$$K'_{Ip} = (SF)p \left(1 + \frac{R_i}{2t} \right) (\pi a_e)^{0.5} F'_2$$

where

$$F'_2 = 0.885 + 0.233 \left(\frac{a_e}{t} \right) + 0.345 \left(\frac{a_e}{t} \right)^2, \quad 0.20 \leq \left(\frac{a_e}{t} \right) \leq 0.50$$

7. For an axial or circumferential flaw of depth a_e , the stress intensity factor due to radial thermal gradients is:

$$K'_{It} = C_m (CR) t^{2.5} F'_3, \quad 0 \leq (CR) \leq 100 \text{ } ^\circ\text{F/hr}$$

where

$$F'_3 = 0.1181 + 0.5353 \left(\frac{a_e}{t} \right) - 1.273 \left(\frac{a_e}{t} \right)^2 + 0.6046 \left(\frac{a_e}{t} \right)^3, \quad 0.20 \leq \left(\frac{a_e}{t} \right) \leq 0.50$$

8. The J -integral due to applied loads for small scale yielding is calculated using the following:

$$J_1 = 1000 \frac{(K'_{Ip} + K'_{It})^2}{E'}$$

where

$$E' = \frac{E}{1 - \nu^2}$$

9. Evaluation of upper-shelf toughness at a flaw extension of 0.10 in. is performed for a flaw depth,

$$a = 0.25t + 0.10 \text{ in.},$$

using

$$SF = 1.15$$

$$p = P_a$$

where

P_a is the accumulation pressure for Levels A and B Service Loadings, such that

$$J_1 < J_{0.1}$$

where

J_1 = the applied J -integral for a safety factor of 1.15 on pressure, and a safety factor of 1.0 on thermal loading

$J_{0.1}$ = the lower bound J -integral resistance at a ductile flaw extension of 0.10 in.

10. Evaluation of flaw stability is performed through use of a crack driving force diagram procedure, by comparing the slopes of the applied J -integral curve and the lower bound J - R curve. The applied J -integral is calculated for a series of flaw depths corresponding to increasing amounts of ductile flaw extension. The applied pressure is the accumulation pressure for Levels A and B Service Loadings, P_a , and the safety factor (SF) on pressure is 1.25. Flaw stability at a given applied load is verified when the slope of the applied J -integral curve is less than the slope of the J - R curve at the point on the J - R curve where the two curves intersect.

Additionally, for the PBN Unit 1 reactor vessel, the applied J -integrals at the nozzle-to-nozzle belt forging welds and the nozzle belt forging to intermediate shell circumferential and axial welds were determined using stresses from a detailed three-dimensional finite element analysis. Path line stresses were used to determine applied J -integrals that included a plastic zone correction to account for small scale yielding.

5.3 Evaluation for Flaw Extension

The applied J -integrals for the PBN Unit 1 and Unit 2 RV shell welds, and the Unit 1 RV nozzle welds are calculated as discussed in Section 5.2.

5.3.1 Reactor Vessel Units 1 and 2 Shell Welds

The basic reactor vessel shell geometry and design pressure along with operating condition temperature information for the PBN reactor vessels is provided in Table 5-1. Initial flaw depths equal to $\frac{1}{4}$ of the vessel wall thickness are analyzed for Levels A and B service loadings, and which do not consider any contribution due to external nozzle loads, following the procedure in accordance with ASME Section XI, Subarticle K-4210 utilizing a cooldown rate of 100 F/h and accumulation pressure of 2734 psig as outlined in Section 5.2, and are evaluated for acceptance based on values for the J-integral resistance of the material from the Linde 80 J-R Model 6B discussed in Section 4.1. For PBN Unit 1, calculations are initially carried out to identify the most limiting and therefore the controlling welds. PBN Unit 2 has only one Linde 80 weld, SA-1484.

The results of flaw evaluations for each of the RV shell welds of the PBN reactor vessels are presented in Table 5-2. The controlling welds are determined by noting the minimum ratio of the material J-resistance ($J_{0.1}$), at 549.3 °F, to the applied J-integral (J_1) (also referred to as “margin”) for each reactor vessel. As reported in Table 5-2, the minimum ratios of material J-resistance to applied J-integral ($J_{0.1}/J_1$) are [] for Unit 1 weld SA-812/SA-775, and [] for Unit 1 weld SA-847. Since the applied J-integral for weld SA-812/SA-775 does not include consideration of stresses due to nozzle loads, the impact of nozzle loads on the margin for Levels A and B service loadings for this weld must be considered. Nozzle loads will be well attenuated for Linde 80 welds SA-1101 and SA-847 and need not be considered for these locations. In addition, nozzle loads need not be considered for Unit 2 Linde 80 weld SA-1484 owing to its location remote from the nozzles (similar to SA-1101) and it also has a significant margin ($J_{0.1}/J_1$) []

5.3.2 Reactor Vessel Shell Welds Near RV Upper Transition Region

The Unit 1 nozzle belt forging to intermediate shell circumferential weld, SA-1426, and axial weld SA-812/SA-775 that intersects weld SA-1426 are both located under the upper transition section of the reactor vessel as reflected in Figure 3-1. As a result, both of these welds are subjected to additional stresses due to mechanical loads (piping and support load combinations). The applied J-integral (J_1) $1/4t$ values with flaw extensions up to 0.5-inches are obtained from the results of a detailed Finite Element Analysis (FEA) to account for the additional nozzle loads. The methods described in ASME Section XI, A-3200, including crack face pressure, with an actual FEA pressure stress profile, were used to develop Stress Intensity Factors (SIFs) at path-line locations applicable to welds SA-1426 and SA-812/SA-775.

The applied J_1 value with a crack extension of 0.1-inch with an applied safety factor of 1.15 is then compared against the corresponding lower bound $J(0.1)$ value of the material for both the circumferential (SA-1426) and axial weld (SA-812/SA-775) in Table 5-3 and Table 5-4, respectively. The lower bound $J(0.1)$ values are obtained by calculating the material properties at the temperatures specified in Table 5-3 and Table 5-4. The minimum ratio of material J-resistance ($J_{0.1}$) to applied J-integral (J_1) is [] for weld SA-812/SA-775. Therefore, comparing the results for weld SA-812/SA-775 reported in Section 5.3.1, it is concluded that consideration of nozzle loads does reduce the available margin and weld SA-812/SA-775 of PBN Unit 1 is the controlling Linde 80 weld amongst all the Linde 80 reactor vessel shell welds of PBN Unit 1 and PBN Unit 2.

5.3.3 Reactor Vessel Unit 1 RV Nozzle Welds

The PBN Unit 1 reactor vessel nozzle welds are located in the substantially thicker cylindrical shell section (reinforced to account for the inlet/outlet RV nozzle openings and typically referred to as the nozzle belt), located above the reactor vessel shell welds. The applied J-integral (J_1) $1/4t$ values with flaw extensions up to 0.5-inches are obtained from the results of a detailed Finite Element Analysis (FEA). The methods described in ASME Section XI, A-3200, utilizing crack face pressure from the actual FEA pressure stress profile were used to develop Stress Intensity Factors (SIFs) for the Unit 1 RV inlet and outlet nozzle welds. The reactor vessel nozzle belt dimensions are reported in Table 5-5. For the PBN Unit 1 reactor vessel nozzle welds, the J-applied results with safety factor of 1.15 on applied pressure is compared against the lower bound J-integral resistance at a ductile flaw extension of 0.1 inches ($J_{0.1}$) in Table 5-6. The limiting item is the RV outlet nozzle with a margin of []

5.4 Evaluation for Flaw Stability

The flaw stability analysis is performed by calculating the applied J-integrals for various amounts of flaw extension with a safety factor (on pressure) of 1.25. The resulting applied J-integral curve can then be compared against the lower bound J-R curve for the weld metal.

5.4.1 Reactor Vessel Units 1 and 2 Shell Welds

For the controlling weld material (SA-812/SA-775) of Point Beach Units 1 and 2, the applied J-integral values are calculated and reported in Table 5-4. The resulting J-applied curves are then compared against the lower bound J-R curve for this material in Figure 5-1. An evaluation line at a flaw extension of 0.1 inch is included to confirm the results of Table 5-4 by showing the margin between the applied J-integral with the safety factor of 1.25 and the lower bound J-integral resistance of the material. The requirement for ductile and stable crack growth is demonstrated by Figure 5-1 since the slope of the applied J-integral curve for a safety factor of 1.25 is less than slope of the lower bound *J-R* curve at the point where the two curves intersect.

5.4.2 Reactor Vessel Unit 1 Nozzle Welds

As discussed in Section 5.3.3 and reported in Table 5-6, the limiting location for the PBN Unit 1 reactor vessel nozzle welds is the outlet nozzle with a margin of []

The applied J-integral for the outlet nozzle weld with a safety factor of 1.25 on pressure at various flaw extensions is plotted with the lower bound J-resistance curve in Figure 5-2. The slope of the applied J-integral is less than the slope of the lower bound J-resistance curve at the point of intersection, which demonstrates that the flaw is stable as required by ASME Section XI, Appendix K.

**Table 5-1 Reactor Vessel Shell Dimensions and Operating
Conditions**

A large, empty rectangular frame with a thin black border, positioned centrally on the page. It is intended to contain the data for Table 5-1, but the content is currently blank.

Table 5-2
PBN Unit 1 and Unit 2 Flaw Evaluation Summary for RV Shell Regions

A large, empty rectangular frame with a thin black border, positioned centrally on the page. It is intended to contain the data for Table 5-2, but the content is currently blank.

**Table 5-3 J-Integral (FEA) Versus Flaw Extension for Point Beach Unit 1, Weld SA-1426
(Levels A & B Service Loadings)**

A large, empty rectangular frame with a thin black border, positioned centrally on the page. It is intended to contain the data for Table 5-3, but the content is currently blank.

**Table 5-4 J-Integral (FEA) Versus Flaw Extension for Point Beach Unit 1, Weld SA-812/SA-775
(Levels A & B Service Loadings)**

A large, empty rectangular frame with a thin black border, positioned centrally on the page. It is intended to contain the data for Table 5-4, but the content is currently blank.

Table 5-5 Reactor Vessel Nozzle Belt Dimensions



**Table 5-6 Flaw Evaluation Summary of PBN Unit 1 RV Nozzle-to-NBF Margins
(Levels A & B Service Loadings)**



**Figure 5-1 J-Integral Versus Flaw Extension for Point Beach
Controlling Reactor Vessel Shell Weld SA-812/SA-775**



**Figure 5-2 J-Integral versus Flaw Extension for Point Beach RV
Outlet Nozzle**



6.0 SUMMARY AND CONCLUSIONS

6.1 *Reactor Vessel Shell Welds-Units 1 and 2*

The ASME Section XI, acceptance criteria for Levels A & B Service Loads for all reactor vessel shell welds are satisfied. The results of the limiting welds for Point Beach Units 1 and 2 are reported below.

Point Beach Units 1 and 2

- The limiting RV shell weld is PBN Unit 1 axial weld SA-812/SA-775. With factors of safety of 1.15 on pressure and 1.0 on thermal loading, the applied J-integral (J_1) is less than the J-integral of the material at a ductile flaw extension of 0.10 in. ($J_{0.1}$). The ratio $J_{0.1}/J_1 = [\quad]$ is greater than the required value of 1.0.
- With a factor of safety of 1.25 on pressure and 1.0 on thermal loading, flaw extensions are ductile and stable since the slope of the applied J-integral curve is less than the slope of the lower bound J-R curve at the point where the two curves intersect (Figure 5-1).

6.2 *Reactor Vessel Nozzle Welds-Unit 1*

The acceptance criteria for Levels A & B Service Loads for the Unit 1 RV nozzle welds are satisfied. The results of the limiting weld considering RV nozzle welds (inlet and outlet) for Point Beach Unit 1 are reported below.

Point Beach Unit 1

- The limiting weld for PBN Unit 1 RV nozzle welds is the RV outlet-to-NBF weld. With factors of safety of 1.15 on pressure and 1.0 on thermal loading, the applied J-integral (J_1) is less than the J-integral of the material at a ductile flaw extension of 0.10 in. ($J_{0.1}$). The ratio $J_{0.1}/J_1 = [\quad]$ is greater than the required value of 1.0.

- With a factor of safety of 1.25 on pressure and 1.0 on thermal loading, flaw extensions are ductile and stable since the slope of the applied J-integral curve is less than the slope of the lower bound J-R curve at the point where the two curves intersect (Figure 5-2).

7.0 REFERENCES

1. BAW-2192PA, Revision 00, "Low Upper Shelf Toughness Fracture Analysis of Reactor Vessels of B&W Owners Group Reactor Vessel Working Group for Levels A and B Conditions," April 1994, ADAMS Accession (Legacy) 9406240261 (P), 9312220294 (NP).
2. NRC Regulatory Issue Summary 2014-11, Information on Licensing Applications for Fracture Toughness Requirements for Ferritic Reactor Coolant Pressure Boundary Components.
3. NUREG-2192, Standard Review Plan for Review of Subsequent License Renewal Applications for Nuclear Power Plants, ADAMS Accession Number ML17188A158.
4. Framatome Document BAW-2192, Revision 0, Supplement 1P-A, Revision 0, "Low Upper Shelf Toughness Fracture Mechanics Analysis of Reactor Vessels of B&W Owners Reactor Vessel Working Group for Level A & B Service Loads".
5. BAW-2467P, Revision 1, Low Upper-Shelf Toughness Fracture Mechanics Analysis of Reactor Vessel of Point Beach Units 1 and 2 for Extended Life through 53 Effective Full Power Years.
6. Point Beach Nuclear Plant, Units 1 and 2 - Extended Power Uprate Amendment (TAC Nos. ME1044 and ME1045). ADAMS Accession numbers ML110450159, May 3, 2011, ML 111170513, SER- ML110450159.
7. Point Beach Nuclear Plant, Units 1 and 2-Issuance of Amendments Regarding Review of Reactor Vessel Fracture Mechanics Analysis (TAC NOS. MD2359 AND MD2360), ADAMS Accession Number ML071300623, May 10, 2007.


8. Code of Federal Regulations, Title 10, Part 50 – Domestic Licensing of Production and Utilization Facilities, Appendix G – Fracture Toughness Requirements, Federal Register Vol. 84, Page 65644, November 29, 2019.
9. NRC Regulatory Guide 1.161, Evaluation of Reactor Pressure Vessels With Charpy Upper Shelf Energy Less Than 50 ft-lb.
10. ASME Boiler & Pressure Vessel Code, Section XI, Rules for Inservice Inspection of Nuclear power Plant Components, Appendix K, 2017 Edition.
11. ASME Boiler & Pressure Vessel Code, Section II, Materials, Part D, Properties (Customary), 2017 Edition.

8.0 CERTIFICATION


This report is an accurate description of the low upper-shelf toughness fracture analysis of Point Beach Units 1 and 2 vessels.


Mark A. Rinckel
Mechanical Unit

This report has been reviewed and is an accurate description of the low upper-shelf toughness fracture analysis of reactor vessels of Point Beach Units 1 and 2.


Ashok D. Nana
Component Analysis and Fracture
Mechanics Unit

Verification of independent review.


David R. Cofflin
Component Analysis and Fracture
Mechanics Unit

This report is approved for release.


Danielle Page Blair
NSSS Project Management

APPENDIX A
B&W J-R MODEL DATA ANALYSIS AND EMPIRICAL MODEL
DEVELOPMENT

A.1 BACKGROUND



Table A-1 Model 6B, Range of Test Data

**A.2 APPLICABILITY OF B&WOG MODEL 6-B TO PBN UNITS 1 AND 2 LINDE
80 WELDS**



A.3 SUMMARY AND CONCLUSIONS



Point Beach Nuclear Plant Units 1 and 2
Dockets 50-266 and 50-301
NRC 2020-0032 Enclosure 4, Attachment 5

Enclosure 4

**Non-proprietary Reference Documents and
Redacted Versions of Proprietary Reference
Documents**

(Public Version)

Attachment 5

**Framatome Topical Report BAW-2178, Revision 0,
Supplement 2NP, Revision 0, “Low Upper-Shelf
Toughness Fracture Mechanics Analysis of Reactor
Vessels of B&W Owners Reactor Vessel Working
Group for Levels C & D Service Loads,” October 2020**

(55 Total Pages, including cover sheets)

**Low Upper-Shelf Toughness
Fracture Mechanics Analysis of
Reactor Vessels of B&W Owners
Reactor Vessel Working Group for
Levels C & D Service Loads**

BAW-2178
Revision 0
Supplement 2NP
Revision 0

Topical Report

October 2020

(c) 2020 Framatome Inc.

Copyright © 2020

**Framatome Inc.
All Rights Reserved**

Nature of Changes

Item	Section(s) or Page(s)	Description and Justification
1	All	Initial Issue

Contents

		<u>Page</u>
1.0	INTRODUCTION	1-1
1.1	Equivalent Margins Analysis—Analysis of Record	1-3
2.0	REGULATORY REQUIREMENTS	2-1
2.1	Regulatory Requirements	2-1
2.2	Compliance with 10 CFR 50 Appendix G and Acceptance Criteria	2-2
2.2.1	Acceptance Criteria Levels C and D	2-2
3.0	DESCRIPTION OF PBN REACTOR VESSELS	3-1
4.0	MATERIAL PROPERTIES AND LEVELS C&D SERVICE LOADINGS	4-1
4.1	J-Integral Resistance Model	4-1
4.2	Mechanical Properties of Weld Metals	4-2
4.3	Levels C and D Service Loadings	4-3
5.0	FRACTURE MECHANICS ANALYSIS	5-1
5.1	Methodology	5-1
5.2	Procedure for Evaluating Levels C and D Service Loadings	5-2
5.2.1	Processing of Transient Time-History Data	5-3
5.2.2	Temperature Range for Upper Shelf Fracture Toughness Evaluations	5-3
5.2.3	Cladding Effects	5-4
5.3	Evaluation for Levels C and D Service Loadings	5-7
5.3.1	Reactor Vessel Shell Welds	5-8
5.3.2	PBN Unit 1 RV Nozzle Welds	5-11
6.0	SUMMARY AND CONCLUSIONS	6-1
6.1	Reactor Vessel Shell Welds	6-1
6.1.1	PBN Units 1 and 2	6-1
6.2	RV Nozzle Welds	6-2
6.2.1	PBN Units 1 and 2	6-2
7.0	REFERENCES	7-1
8.0	CERTIFICATION	8-1

List of Tables

Table 3-1	Copper and Nickel Content and 80-Year (72 EFPY) Fluence (E > 1.0 MeV) for PBN Unit 1 and Unit 2 Reactor Vessel Linde 80 Weld Locations	3-2
Table 3-2	Reactor Vessel Shell Dimensions.....	3-4
Table 3-3	Reactor Vessel Nozzle Belt Dimensions	3-4
Table 4-1	Parameters in Jd Model 6B	4-5
Table 4-2	Mechanical Properties of PBN Unit 1 RV Shell Materials	4-6
Table 4-3	Mechanical Properties of PBN Unit 2 RV Shell Materials	4-7
Table 5-1	PBN Axial Weld SA-812/SA-775 J-Integral versus Flaw Extension for Levels C & D Service Loadings	5-12
Table 5-2	PBN-Levels C & D Results for Unit 1 Inlet and Outlet Nozzle-to-NBF Welds	5-13

List of Figures

Figure 3-1	Reactor Vessel—PBN Unit 1	3-5
Figure 3-2	Reactor Vessel—PBN Unit 2	3-6
Figure 4-1	PBN Units 1 and 2 ASME III Equipment Specification Steam Line Break Transient	4-8
Figure 4-2	PBN Units 1 and 2 FSAR SLB Without Offsite Power, RCS Temperature	4-9
Figure 4-3	PBN Units 1 and 2 FSAR SLB Without Offsite Power, RCS Pressure ...	4-10
Figure 5-1	PBN Axial Weld SA-812/SA-775--K1c, KJc (mean and lower bound), and Applied KI for all Levels C and D transients	5-14
Figure 5-2	PBN Axial Weld SA-812/SA-775-J-Integral Versus Flaw Extension for Levels C & D Service Loadings	5-15
Figure 5-3	PBN Unit 1- Level C & D Applied J Integral vs Crack Tip Temperature for the RV Outlet Nozzle to NBF Weld.....	5-16
Figure 5-4	PBN Unit 1-Levels C & D Applied J Integral vs Crack Extension for the Outlet Nozzle to NBF Weld.....	5-17

Nomenclature

Acronym	Definition
B&W	Babcock and Wilcox
CE	Combustion Engineering
B&WOG	Babcock and Wilcox Owners Group
CvUSE	Charpy Upper Shelf Energy
EFPY	Effective Full Power Years
EMA	Equivalent Margins Analysis
E-Spec	Equipment Specification
FSAR	Final Safety Analysis Report
INF	Inlet Nozzle Forging
IS	Intermediate Shell
Jd	J deformation
J-R	J-integral Resistance
LBB	Leak-Before-Break
LOCA	Loss of Coolant Accident
LS	Lower Shell
NBF	Nozzle Belt Forging
ONF	Outlet Nozzle Forging
PBN	Point Beach Nuclear
RV	Reactor Vessel
RVWG	Reactor Vessel Working Group
SLB	Steam Line Break
SLR	Subsequent License Renewal
Sy	Yield Strength
TSs	Technical Specifications
USE	Upper Shelf Energy

ABSTRACT

Supplement 2 to BAW-2178PA, Revision 0, reports an equivalent margins analysis (EMA) considering Levels C and D service loads for high copper Linde 80 weld metals using fluence values expected at 80-years (subsequent license renewal--SLR). This supplement to BAW-2178 applies to the following Westinghouse-designed reactor vessels fabricated by Babcock & Wilcox and Combustion Engineering (B&W/CE): Point Beach Nuclear (PBN) Unit 1 fabricated by Babcock & Wilcox (B&W), and PBN Unit 2 fabricated by B&W and Combustion Engineering (CE).

The analytical procedure used in this supplement is in accordance with ASME Section XI, 2017 Edition, Appendix K, Subarticle K-1200, with selection of design transients based on the guidance in Regulatory Guide 1.161, Section 4.0. EMA results are reported for all reactor vessel Linde 80 weld locations with 80-year fluence projections that exceed $1.0 \text{ E}+17 \text{ n/cm}^2$ ($E > 1.0 \text{ MeV}$) and for the RV inlet and outlet nozzle-to-nozzle belt forging Linde 80 welds for Unit 1. The ASME Section XI, acceptance criteria for Levels C & D Service Loads for all reactor vessel shell welds are satisfied. The acceptance criteria for Levels C & D Service Loads for RV nozzle welds are also satisfied. The EMA reported herein utilizes J-integral resistance B&WOG Model 6B; demonstration that B&WOG Model 6B is applicable to PBNP Units 1 and 2 is provided in BAW-2192, Supplement 3, Revision 0, Appendix A.

The EMA utilizes the B&WOG J-integral resistance (J-R) Model 6B reported in NRC Staff approved Topical Report BAW-2192, Revision 0, Supplement 1P-A, Revision 0, Appendix A. Model 6B was developed based on fracture toughness test data obtained through 2020, with specimen fluence that ranges from 0.0 to 5.80E+19 n/cm². The copper content of all PBN Linde 80 welds and ¼ T fluence are within the range of explanatory variables used to develop Model 6B, as reported in Appendix A of BAW-2192, Supplement 3, Revision 0. In addition, the 80-year PBN RV fluence at the t/10 location for Unit 1 limiting weld SA-812/SA-775 is less than 5.80E19 n/cm², and within the fluence range of explanatory variables used to develop Model 6B.

1.0 INTRODUCTION

The purpose of Supplement 2 to BAW-2178PA, Revision 0 [1], is to report an equivalent margins analysis (EMA) considering Levels C and D service loads for high copper Linde 80 weld using fluence values expected at 80-years (subsequent license renewal--SLR). This supplement to BAW-2178PA, Revision 0, applies to the following Westinghouse-designed reactor vessels fabricated by B&W/Combustion Engineering: Point Beach Nuclear (PBN) Unit 1 fabricated by B&W, and PBN Unit 2 fabricated by B&W and CE.

Equivalent margins analyses for the plants within the scope of this report are reported for all reactor vessel shell weld locations with 80-year fluence projections that exceed $1.0 \text{ E}+17 \text{ n/cm}^2$ ($E > 1.0 \text{ MeV}$) [2] and are conservatively completed for the reactor vessel nozzle to nozzle-belt forging Linde 80 welds for PBN Unit 1. PBN Unit 2 nozzle-to nozzle-belt forging welds are not fabricated from Linde 80 welds. Plants that reference this report must calculate 80-year neutron fluence at reactor vessel weld locations in accordance with NUREG-2192 [3], Standard Review Plan for Review of Subsequent License Renewal Applications, to demonstrate that the fluence estimates provided in Section 3.0 are applicable to their plants. Upper shelf energy evaluations at reactor vessel base metal locations with 80-year fluence projections greater than $1.0 \text{ E}+17 \text{ n/cm}^2$, if needed, are not within the scope of this report.

The EMA utilizes the B&WOG J-integral resistance (J-R) Model 6B reported in BAW-2192, Supplement 1P-A, Revision 0 [4]. Justification for use of Model 6B for PBNP Units 1 and 2 is addressed in BAW-2192, Supplement 3P, Revision 0, Appendix A [5].

The following groups are used for the welds within the scope of this report.

- Reactor Vessel Shell Welds - circumferential and longitudinal Linde 80 welds (if applicable) within the intermediate shell (IS) and lower shell (LS) courses for PBN Units 1 and 2, and the circumferential weld that connects the nozzle belt forging (NBF) to the intermediate shell course for PBN Unit 1. There are no geometric discontinuities at these weld locations and all reactor vessel shell welds surround the effective height of the active core. These locations have historically been considered “beltline” or “beltline region” as defined by 10 CFR 50, Appendix G.
- RV Nozzle Welds - Linde 80 welds for PBN Unit 1 that connect the RV inlet and outlet nozzle forgings to the nozzle belt forging. These welds are projected to receive fluence levels less than $1.0E+17$ n/cm² at 80-years but are conservatively evaluated herein at an inside surface fluence of $1.0E+18$ n/cm². The equivalent welds for PBN Unit 2 are made from non-Linde 80 welds, by Combustion Engineering, and are projected to receive fluence levels less than $1.0E+17$ n/cm² at 80-years and are not within the scope of this report.

The 60-year EMA summary reports for PBN Units 1 and 2 are reported in Section 1.1. Section 2.0 provides the current NRC regulatory requirements for the EMA. Section 3.0 provides a description of all reactor vessel Linde 80 welds within the scope of this report, with illustrations of applicable reactor vessel Linde 80 welds in Figure 3-1 and Figure 3-2. Section 4.0 provides the material properties that are required for the EMA, and Section 5.0 presents the results of the EMA. Section 6.0 provides the summary and conclusions, and Section 7.0 lists all references. BAW-2192, Revision 0, Supplement 3P, Revision 0, Appendix A [5], provides the technical justification for the use of B&WOG J-R Model 6B for the EMA reported herein.

1.1 ***Equivalent Margins Analysis—Analysis of Record***

BAW-2178PA, Revision 0 [1], provided the EMA analysis of record for Levels C and D Point Units 1 and 2 for 40 years. For 60 years, PBN Units 1 and 2 reported plant-specific evaluations in BAW-2467P, Revision 01 [6]. NRC approval of the 60-year EMA analysis of record is provided in the following NRC documents.

Point Beach Units 1 and 2

The Point Beach Units 1 and 2 current licensing basis equivalent margins analysis at 53 EFPY is summarized in Section 2.1.2 of NRC document “POINT BEACH NUCLEAR PLANTS, UNIT 1 AND 2- EXTENDED POWER UPRATE AMENDMENT (TAC NOS. ME1044 AND ME1045),” ADAMS Accession number ML110450159 [7]. NRC acceptance of the Point Beach EMA at 53 EFPY for EPU is based on the following documentation:

- Point Beach Nuclear Plant, Units 1 and 2-Issuance of Amendments Regarding Review of Reactor Vessel Fracture Mechanics Analysis (TAC NOS. MD2359 AND MD2360), ADAMS Accession Number ML071300623 [8].

2.0 REGULATORY REQUIREMENTS

2.1 *Regulatory Requirements*

In accordance with 10 CFR 50 Appendix G [9], IV, A, 1., Reactor vessel Upper Shelf Energy Requirements are as follows.

- a. Reactor vessel beltline materials must have Charpy upper-shelf energy in the transverse direction for base material and along the weld for weld material according to the ASME Code, of no less than 75 ft-lb (102 J) initially and must maintain Charpy upper-shelf energy throughout the life of the vessel of no less than 50 ft-lb (68 J), unless it is demonstrated in a manner approved by the Director, Office of Nuclear Reactor Regulation or Director, Office of New Reactors, as appropriate, that lower values of Charpy upper-shelf energy will provide margins of safety against fracture equivalent to those required by Appendix G of Section XI of the ASME Code. This analysis must use the latest edition and addenda of the ASME Code incorporated by reference into 10 CFR 50.55a (b)(2) at the time the analysis is submitted.
- b. Additional evidence of the fracture toughness of the beltline materials after exposure to neutron irradiation may be obtained from results of supplemental fracture toughness tests for use in the analysis specified in section IV.A.1.a.
- c. The analysis for satisfying the requirements of section IV.A.1 of this appendix must be submitted, as specified in § 50.4, for review and approval on an individual case basis at least three years prior to the date when the predicted Charpy upper-shelf energy will no longer satisfy the requirements of section IV.A.1 of this appendix, or on a schedule approved by the Director, Office of Nuclear Reactor Regulation.

When the reactor vessels within the scope of this report were fabricated, Charpy V-notch testing of the reactor vessel welds were in accordance with the original construction code, which did not specifically require Charpy V-notch tests on the upper shelf. Applicable construction codes are as follows:

- PBN Unit 1, ASME Section III 1965 Edition, by Babcock & Wilcox
- PBN Unit 2, ASME Section III 1965 Edition, by Babcock & Wilcox and Combustion Engineering

In accordance with NRC Regulatory Guide 1.161 [10], the NRC has determined that the analytical methods described in ASME Section XI, Appendix K, provide acceptable guidance for evaluating reactor pressure vessels when the Charpy upper-shelf energy falls below the 50 ft-lb limit of Appendix G to 10 CFR Part 50. However, the staff noted that Appendix K does not provide information on the selection of transients and gives very little detail on the selection of material properties. Selection of material properties and selection of design transients are addressed in Sections 4.2 and 4.3, respectively.

2.2 Compliance with 10 CFR 50 Appendix G and Acceptance Criteria

The analyses reported herein are performed in accordance with the 2017 Edition [11] of Section XI of the ASME Code, Appendix K. The current edition of ASME Section XI listed in 10 CFR 50.55a is the 2017 Edition. The material properties used in this analysis are based on ASME Section II, Part D, 2017, Edition [12].

2.2.1 Acceptance Criteria Levels C and D

ASME Section XI [11], Subarticles K-2300 and K-2400, provide acceptance criteria for Levels C and D Service Conditions, respectively. Consistent with BAW-2178PA, Revision 0 [1], the evaluations reported herein utilize acceptance criteria applicable to Level C Service Loadings as summarized below.

- a. When analytically evaluating adequacy of the upper shelf toughness for the weld material for Level C Service Loadings, interior semi-elliptical surface flaws with depths up to 1/10 of the base metal wall thickness, plus the cladding thickness, with total depths not exceeding 1 in. (25 mm), and a surface length 6 times the depth, shall be postulated, with the flaw's major axis oriented along the weld of concern, and the flaw plane oriented in the radial direction. When analytically evaluating adequacy of the upper shelf toughness for the base material, both interior axial and circumferential flaws shall be postulated, and toughness properties for the corresponding orientation shall be used. Flaws of various depths, ranging up to the maximum postulated depth, shall be analyzed to determine the most limiting flaw depth. Smaller maximum flaw sizes may be used when justified. Two criteria shall be satisfied:
- 1) The applied J-integral shall be less than the J-integral of the material at a ductile flaw extension of 0.10 in. (2.5 mm), using a structural factor of 1 on loading.
 - 2) Flaw extensions shall be ductile and stable, using a structural factor of 1 on loading.
- b. The J-integral resistance versus flaw extension curve shall be a conservative representation for the vessel material under analytical evaluation.

For the Level C and D transients defined in Section 4.3 for PBN, the evaluations reported herein will conservatively utilize the Level C acceptance criteria given above as a means to treat the transients as a combined Levels C & D event category. The above Level C acceptance criteria will be conservatively imposed on the Level D transients, whose acceptance criteria are given below. This approach is conservative since PBN Units 1 and 2 have no Level C design transients defined within the ASME Section III Design Specifications for either vessel.

- a. When evaluating adequacy of the upper shelf toughness for Level D Service Loadings, flaws as specified for Level C Service Loadings shall be postulated, and toughness properties for the corresponding orientation shall be used. Flaws of various depths, ranging up to the maximum postulated depth, shall be analyzed to determine the most limiting flaw depth. Flaw extensions shall be ductile and stable, using a structural factor of 1 on loading.
- b. The J-integral resistance versus flaw extension curve shall be a best estimate representation for the vessel material under evaluation.
- c. The extent of stable flaw extension shall be less than or equal to 75% of the vessel wall thickness, and the remaining ligament shall not be subject to tensile instability.

3.0 DESCRIPTION OF PBN REACTOR VESSELS

The PBN reactor vessels with applicable weld locations are shown in Figure 3-1 and Figure 3-2. All weld locations evaluated for equivalent margins in this report are identified by an asterisk (*). Unit-specific weld copper and nickel content and 80-year fluence projections data needed for the equivalent margins analysis are provided in Table 3-1. The fluence projections are reported for the reactor vessel Linde 80 weld locations that are expected to exceed $1.0E+17$ n/cm² at 80 years. Note that PBN Unit 2 weld 21935 (nozzle belt forging to intermediate shell weld), although having a projected fluence $> 1.0E+17$ n/cm² at 80-years, is not a Linde 80 weld, does not fall below 50 ft-lbs, and is not within the scope of this report. All fluence values are at the clad/base metal interface.

Copper and nickel content of the reactor vessel shell welds is consistent with EMA analyses of record reported in Section 1.1. The copper and nickel content for RV shell welds and RV nozzle-to-nozzle belt forging welds reported in Table 3-1 were obtained from either the EMA analysis of record or a search of PBN reactor vessel fabrication reports. The dimensions of the reactor vessel shell geometry for the PBN reactor vessels are provided in Table 3-2. Similarly, the dimensions for the reactor vessel nozzle belt region located above the reactor vessel intermediate shell course for each of these reactor vessels are given in Table 3-3.

Table 3-1 Copper and Nickel Content and 80-Year (72 EFPY) Fluence (E > 1.0 MeV) for PBN Unit 1 and Unit 2 Reactor Vessel Linde 80 Weld Locations

Reactor Vessel Location	Weld ID	Cu, wt%	Ni, wt%	Clad/Base Metal Interface Surface Fluence (E > 1.0 MeV), n/cm ²
Point Beach Unit 1, 80-Year Fluence (E > 1.0 MeV)				
Nozzle belt forging to bottom of outlet nozzle forging welds	Linde 80	[]	[]	6.51E+16 Use 1.0E+18 (Note 1)
Nozzle belt forging to bottom of inlet nozzle forging Welds	Linde 80	[]	[]	6.51E+16 Use 1.0E+18 (Note 1)
Nozzle belt forging to intermediate shell circumferential weld.	SA-1426	0.19	0.57	5.66E+18
Intermediate shell longitudinal weld	SA-812 (27% inside)	0.17	0.52	4.64E+19
	SA-775 (73% outside)	0.17	0.64	4.64E+19
Intermediate shell to lower shell circumferential weld.	SA-1101	0.23	0.59	7.36E+19
Lower shell longitudinal weld	SA-847	0.23	0.52	4.58E+19
Lower shell to lower head ring circumferential weld	Linde 80			4.79E+16 (Note 2)

Reactor Vessel Location	Weld ID	Cu, wt%	Ni, wt%	Clad/Base Metal Interface Surface Fluence (E > 1.0 MeV), n/cm ²
Point Beach Unit 2, 80-Year Fluence (E > 1.0 MeV)				
Intermediate shell course to lower shell course circumferential weld	SA-1484	0.26	0.60	7.65E+19

Notes: 1: Conservative/bounding fluence of 1.0E+18 n/cm² to be used for EMA analyses only. This may be assumed to be a wetted surface value, applicable at any postulated flaw depth, for consistency with previous EMA analyses.

2: EMA not required as fluence is less than 1.0E+17 n/cm².

Table 3-2 Reactor Vessel Shell Dimensions

Plant	Ri (in)	Ro (in)	t (in)	Design Pressure (psi)	100% Power Cold Leg Temperature (F)
PBN Unit 1	66.00	72.656	6.50	2485	549.3
PBN Unit 2	66.00	72.656	6.50	2485	549.3

Table 3-3 Reactor Vessel Nozzle Belt Dimensions

--

Figure 3-1
Reactor Vessel—PBN Unit 1

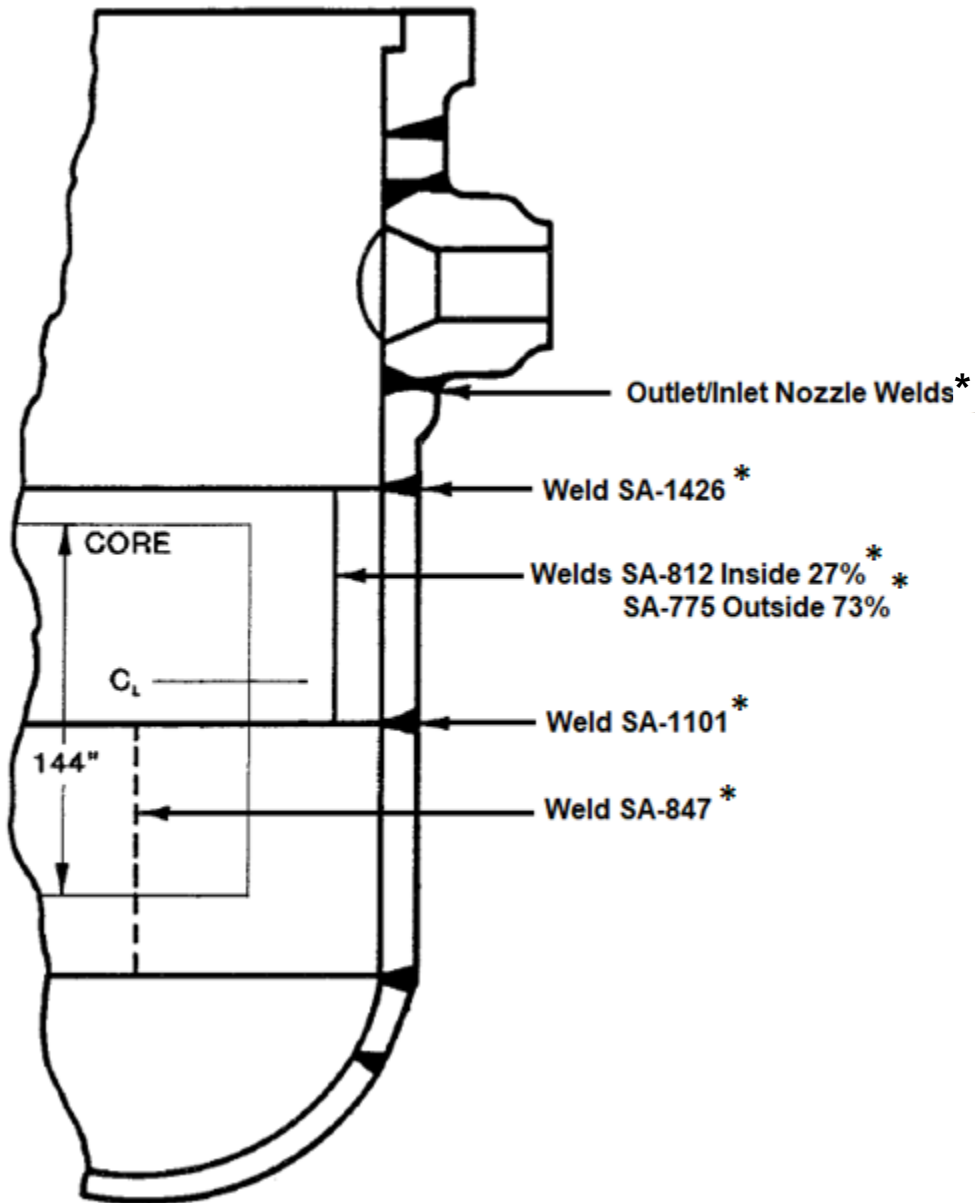
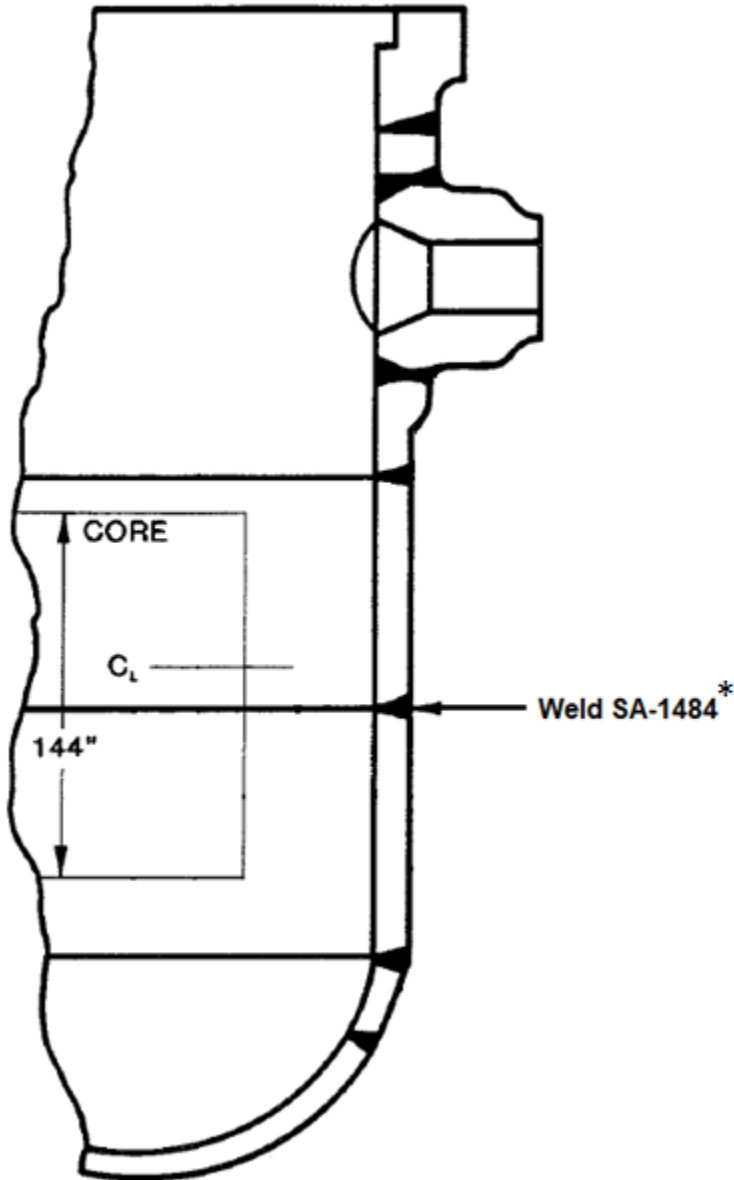


Figure 3-2
Reactor Vessel—PBN Unit 2



4.0 MATERIAL PROPERTIES AND LEVELS C&D SERVICE LOADINGS

4.1 *J-Integral Resistance Model*

The J-integral resistance model for Mn-Mo-Ni/Linde 80 welds in the reactor vessels of the B&WOG RVWG plants were developed using a large J-resistance model (J-R model) data base. A detailed description of this model is provided in BAW-2192PA, Supplement 1P-A, Revision 0, Appendix A [4]. This model was developed using specimens irradiated to $5.8E+19$ n/cm² and is used for the EMA of PBN Linde 80 welds.



The coefficients, a , d , and C_4 are provided in Table 4-1. As required by ASME Section XI, ASME K-3300, when evaluating the vessel for Levels A, B, and C Service Loadings, the J-integral resistance versus crack-extension curve (J-R curve) shall be a conservative representation of the toughness of the controlling beltline material at upper shelf temperatures in the operating range. When evaluating the vessel for Level D Service Loadings, the J-R curve shall be a best estimate representation of the toughness of the controlling beltline material at upper shelf temperatures in the operating range. As such, the J_d correlation minus 2 standard errors is used for evaluation of Level C Service Loadings (i.e., equation (1) multiplied by []) while the unaltered J_d correlation would be used to evaluate Level D Service Loadings. However, for PBN the J_d correlation minus 2 standard errors is conservatively used for level D Service Loadings evaluated herein.

As discussed in Appendix B to BAW-2192PA [1], the J-R curve was generated from a J-integral database obtained from the same class of material with the same orientation using correlations for effects of temperature, chemical composition, and fluence level. Crack extension was by ductile tearing with no cleavage. This complies with ASME Section XI, K-3300.

4.2 *Mechanical Properties of Weld Metals*

The following subsections provide representative properties for the PBN reactor vessels. The temperature dependent mechanical properties are developed from the 2017 Edition of the ASME Code (Section II) for the reactor base metal and cladding (the ASME Code does not provide separate mechanical properties for base and weld metal).

Both ASME Code minimum and representative irradiated yield strengths are also provided. The mechanical properties such as weld metal yield strengths typically used were the irradiated properties but in some cases the ASME Code minimum properties were conservatively considered.

PBN Unit 1 reactor vessel was fabricated using SA-302, Grade B low alloy steel. PBN Unit 2 reactor vessel was fabricated using SA-508, Grade 2, Class 1 low alloy steel. Table 4-2 and Table 4-3 provide the Young's modulus (E), the mean coefficient of thermal expansion (α), and the yield strength (S_y) for the RV shell regions. For PBN Unit 1 and 2 reactor vessel shell and Unit 1 RV nozzle regions, the normal operating steady state condition cold leg temperature value is []

4.3 *Levels C and D Service Loadings*

PBN has no Level C design transients defined in the reactor vessel ASME Section III Equipment Specification for either unit. As discussed in Section 4.2 of the 60-year EMA analysis of record (Reference [6]) three Level D transients are specified for the PBN Units. The original Westinghouse equipment specification includes a Steam Line Break (SLB) transient and a Reactor Coolant Line Break (Large Break LOCA) transient. The Point Beach FSAR (June 2003) contains a Steam Line Break without Offsite Power. These three transients were analyzed in the PBN EMA for 60-years as reported in Reference [6]. The most limiting of the three transients for the EMA was determined to be the Large Break LOCA transient. However, with operation to 80-years and consideration of extended beltline materials, the approach used to select design transients for the EMA at 60-years may be overly conservatively with respect to evaluating the Large Break LOCA transient and thus Level D design transient selection is revisited for 80-years.

PBN Units 1 and 2 were approved for Leak-Before-Break (LBB) for large primary loop piping [13, 14]. For subsequent license renewal, the LBB analysis for the large primary loop has recently been re-evaluated for 80-years. The results demonstrate that the required LBB margins continue to be met for the 80-year service life. The pressurizer surge line break was eliminated from the structural design basis for PBN Units 1 and 2. In addition, NextEra performed a LBB reconciliation for selected auxiliary lines connected to the reactor coolant system for the 80-year service period, which will be reported in the PBN subsequent license renewal application. Therefore, the ASME Section III Equipment Specification large primary loop LOCA may be removed from consideration as a Level D transient for the 80-year EMA.

In addition, it was determined that the FSAR (2003) and Equipment Specification SLB (E-Spec SLB) transients evaluated for 60-years may have been updated for Extended Power Uprate (EPU). As such, the most recent SLB transient based on the PBN Units 1 and 2 Reactor Vessel ASME Section III Equipment Specification was identified and is reproduced as Figure 4-1 below. The ASME Section III Equipment Specification SLB transient is the same between both the units. The Equipment Specification SLB event is initiated from no-load condition of 547 °F and offsite power is assumed to be available with RC pumps energized throughout the event. The ASME Section III Equipment Specification provides the design basis transients for the reactor vessel and is appropriate to consider for the equivalent margins analysis for 80-years. With regard to the FSAR SLB event, the current version of the PBN FSAR (FSAR 2019) has redefined the SLB without offsite power and this transient is reproduced as Figure 4-2 and Figure 4-3.

Table 4-1 Parameters in Jd Model 6B

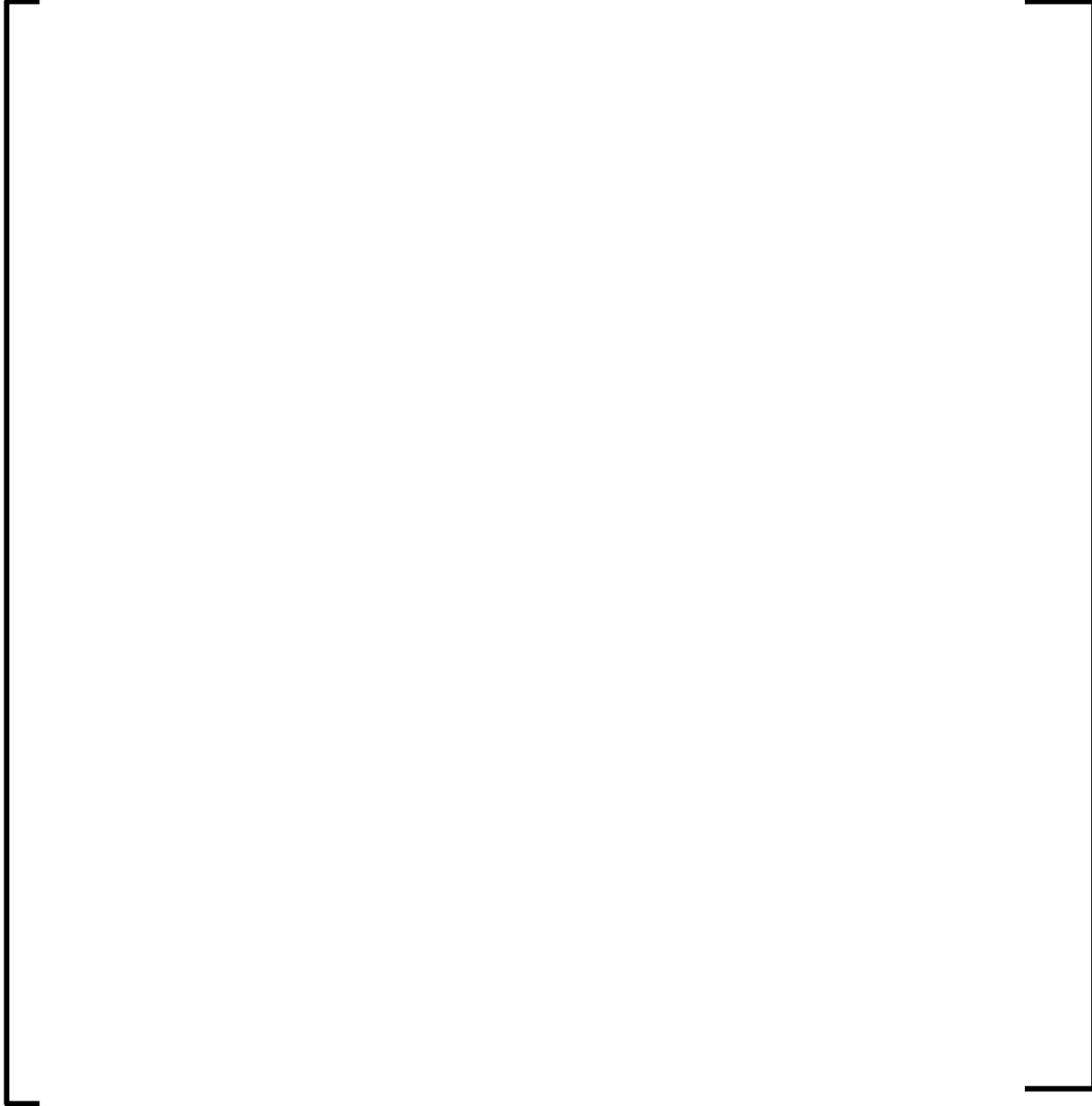
A large, empty rectangular frame with a thin black border, centered on the page. It appears to be a placeholder for a table that is not present in this version of the document.

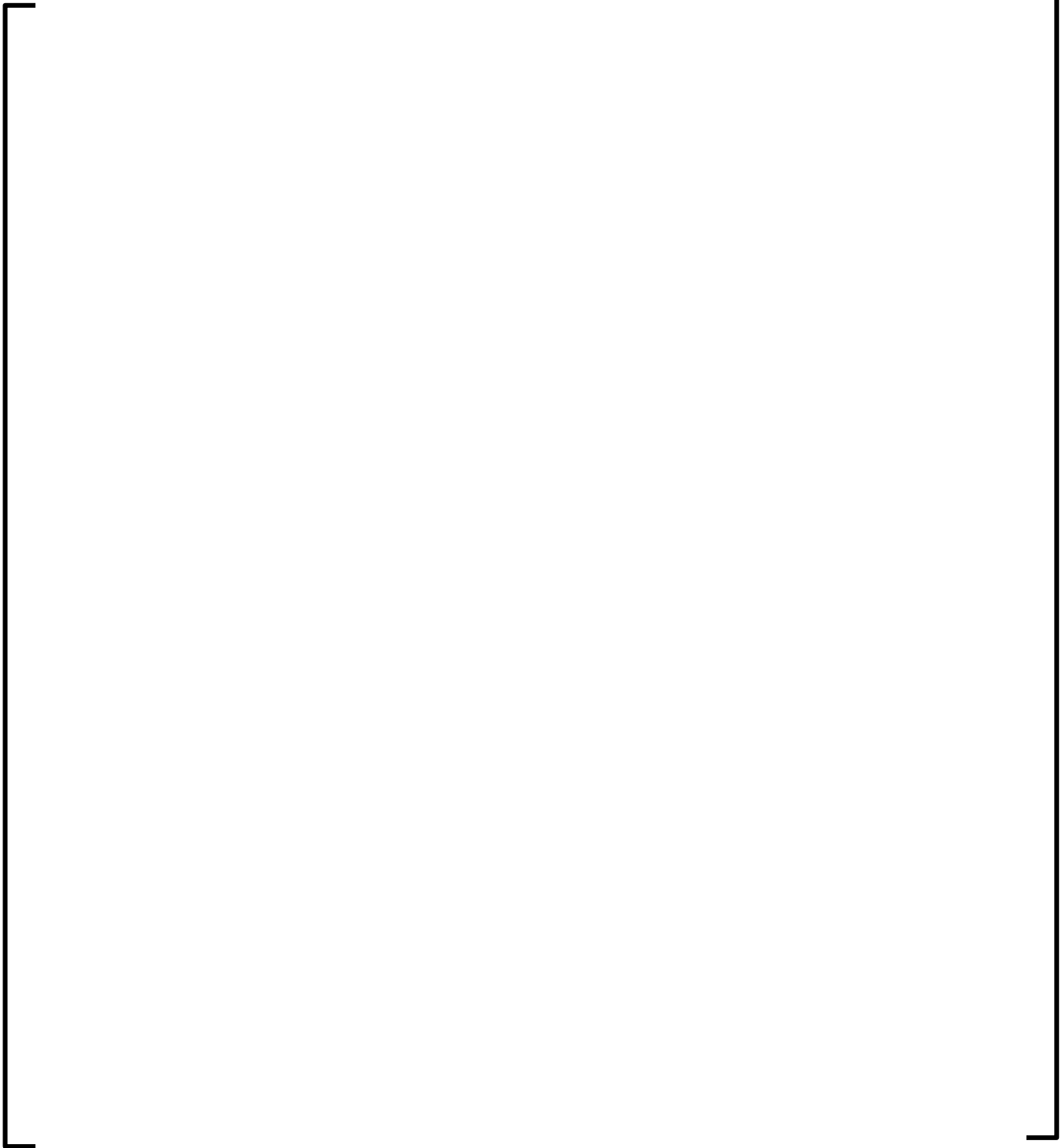
Table 4-2 Mechanical Properties of PBN Unit 1 RV Shell Materials

Temp. (°F)	RV Base Metal, A-302B			Weld Metals Yield Strength, Sy	
	E (ksi)	α (in/in/°F)	Sy (ksi)	SA-847 (ksi)	SA-1101 (ksi)
100	28885	6.47E-06	50.00	[]	[]
200	28500	6.70E-06	47.00	[]	[]
300	28000	6.90E-06	45.50	[]	[]
400	27600	7.10E-06	44.20	[]	[]
500	27000	7.30E-06	43.20	[]	[]
550	26650	7.35E-06	42.65	[]	[]
600	26300	7.40E-06	42.10	[]	[]

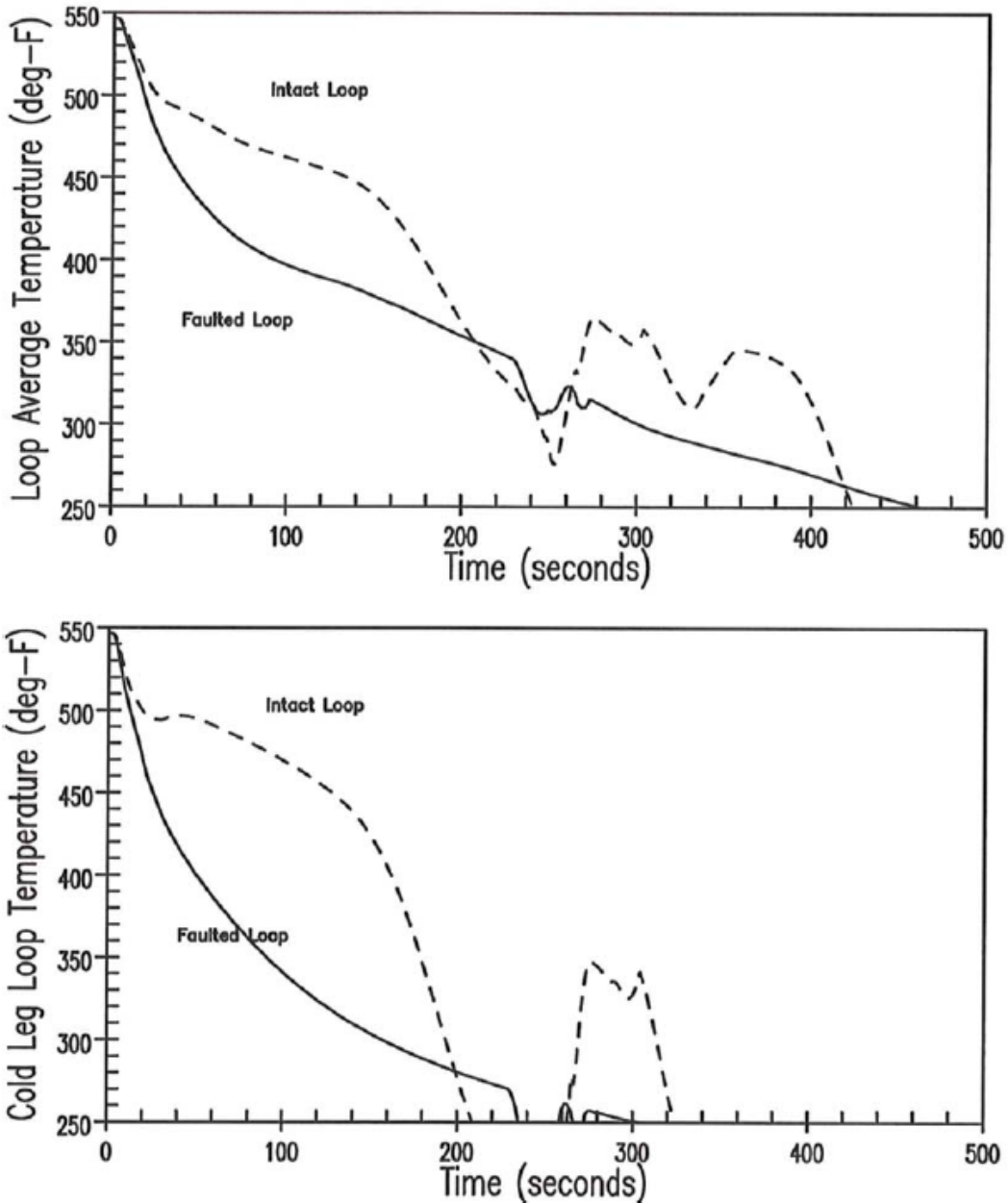
Table 4-3 Mechanical Properties of PBN Unit 2 RV Shell Materials

Temp. (°F)	RV Base Metal, A508 Grade 2			Weld Metals Yield Strength, Sy
	E (ksi)	α (in/in/°F)	Sy (ksi)	SA-1484 (ksi)
100	27638	6.47E-06	50.00	[]
200	27100	6.70E-06	47.00	[]
300	26700	6.90E-06	45.50	[]
400	26200	7.10E-06	44.20	[]
500	25700	7.30E-06	43.20	[]
580	25220	7.38E-06	42.32	[]
600	25100	7.40E-06	42.10	[]

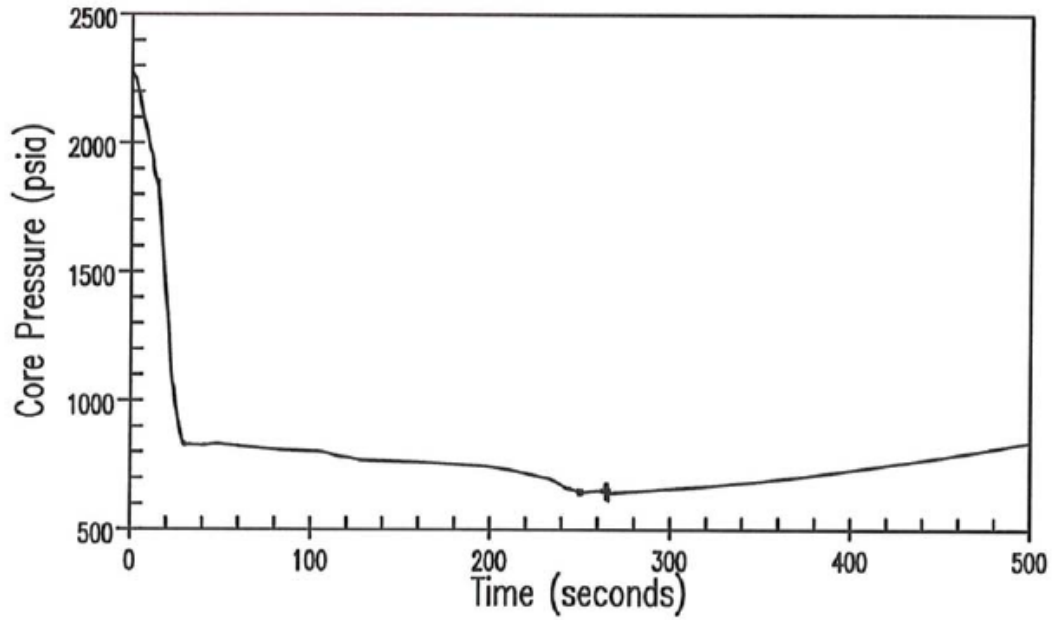
**Figure 4-1 PBN Units 1 and 2 ASME III Equipment Specification
Steam Line Break Transient**



**Figure 4-2 PBN Units 1 and 2 FSAR SLB Without Offsite Power,
RCS Temperature**



**Figure 4-3 PBN Units 1 and 2 FSAR SLB Without Offsite Power,
RCS Pressure**



5.0 FRACTURE MECHANICS ANALYSIS

5.1 *Methodology*

In accordance with ASME Section XI, Appendix K [11], Subarticle K-1200, the following analytical procedure was used for Levels C & D Service Loadings:

- a. Flaws in the reactor vessel shell welds and the RV nozzle-to-shell welds were postulated in accordance with the acceptance criteria of Subarticles K-2300 and K-2400.
- b. Loading conditions at the locations of the postulated flaws were determined for Levels C and D Service Loadings.
- c. Material properties, including E , α , σ_y , and the J-integral resistance curve (J-R curve), were determined at the locations of the postulated flaws. Young's modulus, mean coefficient of thermal expansion and yield strength are addressed in Section 4.2. The J-R curve is discussed in Section 4.1.
- d. The postulated flaws were evaluated in accordance with the acceptance criteria of Article K-2000 by calculating the applied J-integral according to the procedure provided by Subarticle K-5210. The applied J-integral was then evaluated to satisfy the criteria for flaw extension in Subarticle K-5220 and flaw stability in Subarticle K-5300.

5.2 Procedure for Evaluating Levels C and D Service Loadings

The evaluation for the Levels C and D service loadings is performed as follows:

1. For each transient described in Section 4.3, calculate stress intensity factors for a semi-elliptical flaw of depth up to $1/10$ of the base metal wall thickness, as a function of time, due to internal pressure and radial thermal gradients with a structural factor of 1 on loading. The applied stress intensity factor, K_I , calculated for each of these transients is compared to the K_{Jc} upper-shelf toughness curve of the weld material. The transient for which the applied K_I most closely approaches the K_{Jc} curve is chosen as the limiting transient, and the critical time in the limiting transient selected for further evaluation occurs at the point where K_I most closely approaches the K_{Jc} curve.
2. At the critical transient time, develop a crack driving force diagram with the applied J -integral and J - R curves plotted as a function of flaw extension. The adequacy of the upper-shelf toughness is evaluated by comparing the applied J -integral with the J - R curve at a flaw extension of 0.10 in. Flaw stability is assessed by examining the slopes of the applied J -integral and J - R curves at the points of intersection.
3. Verify that the extent of stable flaw extension is no greater than 75% of the vessel wall thickness by determining when the applied J -integral curve intersects the mean J - R curve.
4. Verify that the remaining ligament is not subject to tensile instability. The internal pressure p shall be less than P_I , where P_I is the internal pressure at tensile instability of the remaining ligament. The pressure at instability, P_I , is given in K-5300, Appendix K of ASME Section XI for both axial and circumferential flaws.

5.2.1 Processing of Transient Time-History Data

The applied J-integrals at the Unit 1 nozzle-to-nozzle belt forging welds were determined from three-dimensional finite element analysis. The through-thickness path line stresses were subsequently used to calculate stress intensity factors and the applied J-integrals were determined based on consideration of small scale yielding.

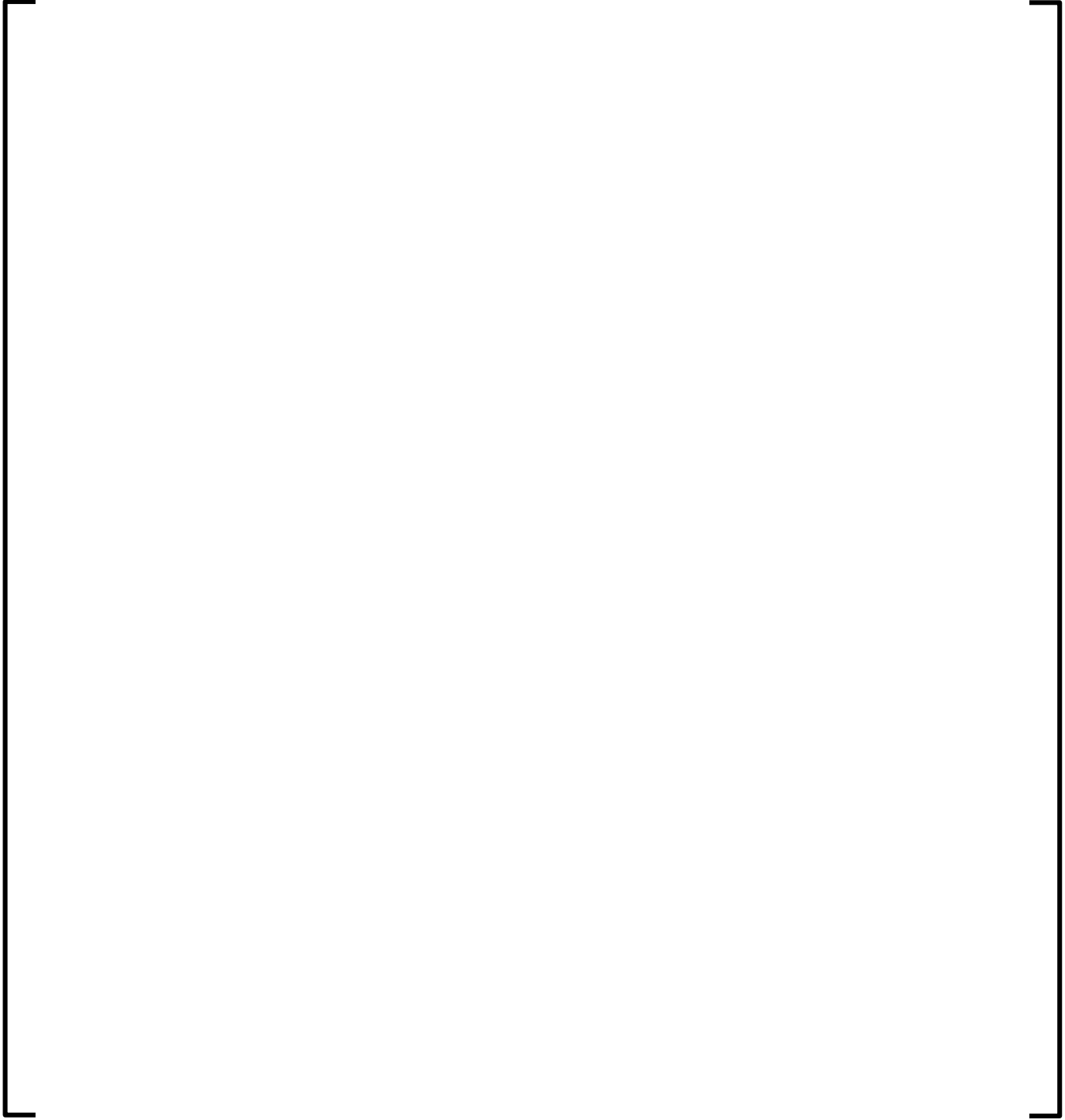
For the controlling reactor vessel shell weld SA-812/SA-775, stress intensity factors were calculated using the one-dimensional, finite element thermal and closed form stress models and linear elastic fracture mechanics methodology of the PCRIT computer code.

5.2.2 Temperature Range for Upper Shelf Fracture Toughness Evaluations

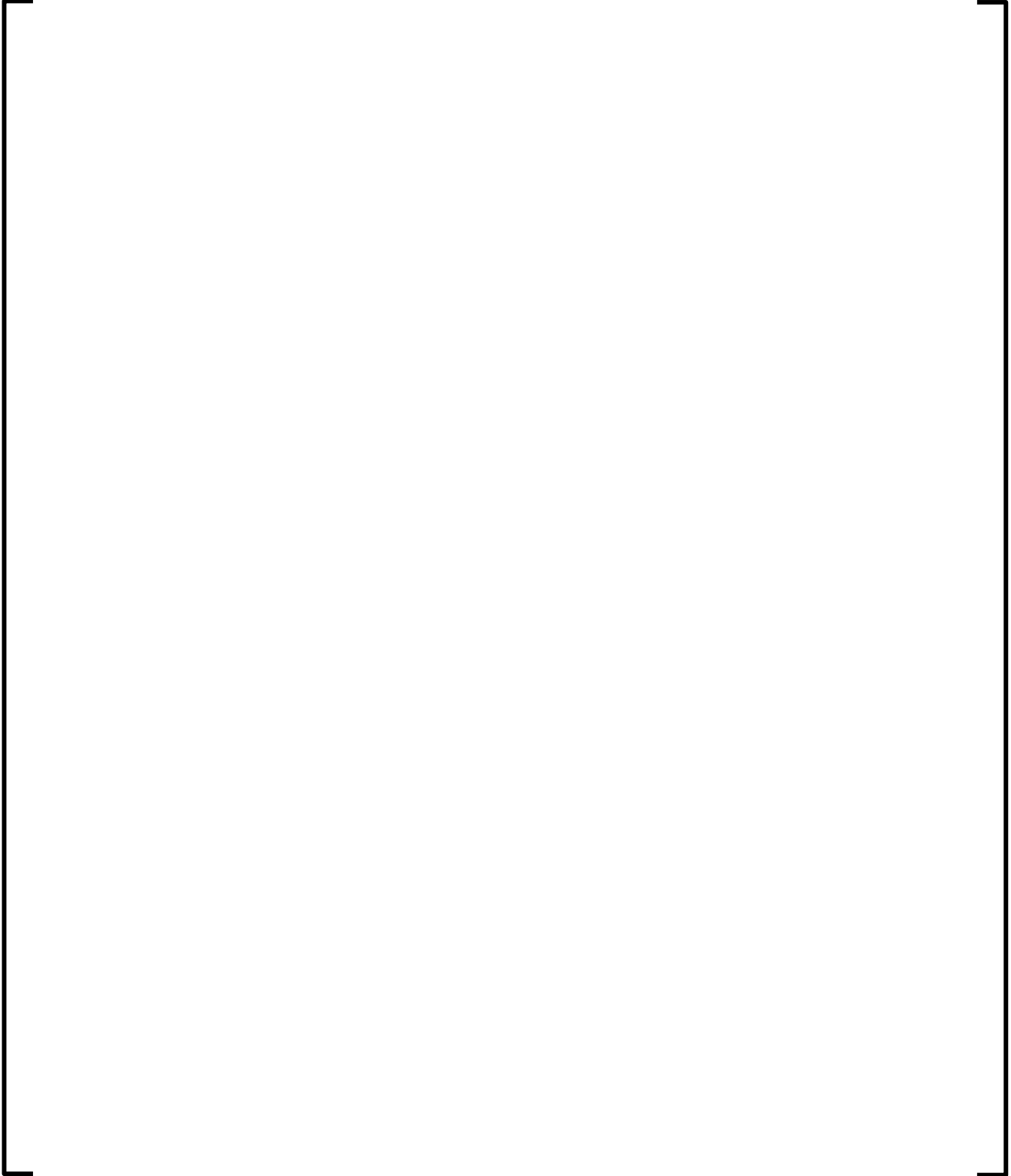
Upper-shelf fracture toughness is determined through use of Charpy V-notch impact energy versus temperature plots by noting the temperature above which the Charpy energy remains on a plateau, maintaining a relatively high constant energy level. Similarly, fracture toughness can be addressed in three different regions on the temperature scale, i.e., a lower-shelf toughness region, a transition region, and an upper-shelf toughness region.

Fracture toughness of reactor vessel steel and associated weld metals are conservatively predicted by the ASME initiation toughness curve, K_{Ic} , in the lower-shelf and transition regions. In the upper-shelf region, the upper-shelf toughness curve, K_{Jc} , is derived from the upper-shelf J -integral resistance model described in Section 4.1. The upper-shelf toughness then becomes a function of fluence, copper content, temperature, and fracture specimen size. When upper-shelf toughness is plotted versus temperature, a plateau-like curve develops that decreases slightly with increasing temperature. Since the present analysis addresses the low upper-shelf fracture toughness issue, only the upper-shelf temperature range, which begins at the intersection of K_{Ic} and the upper-shelf toughness curves, K_{Jc} , is considered.

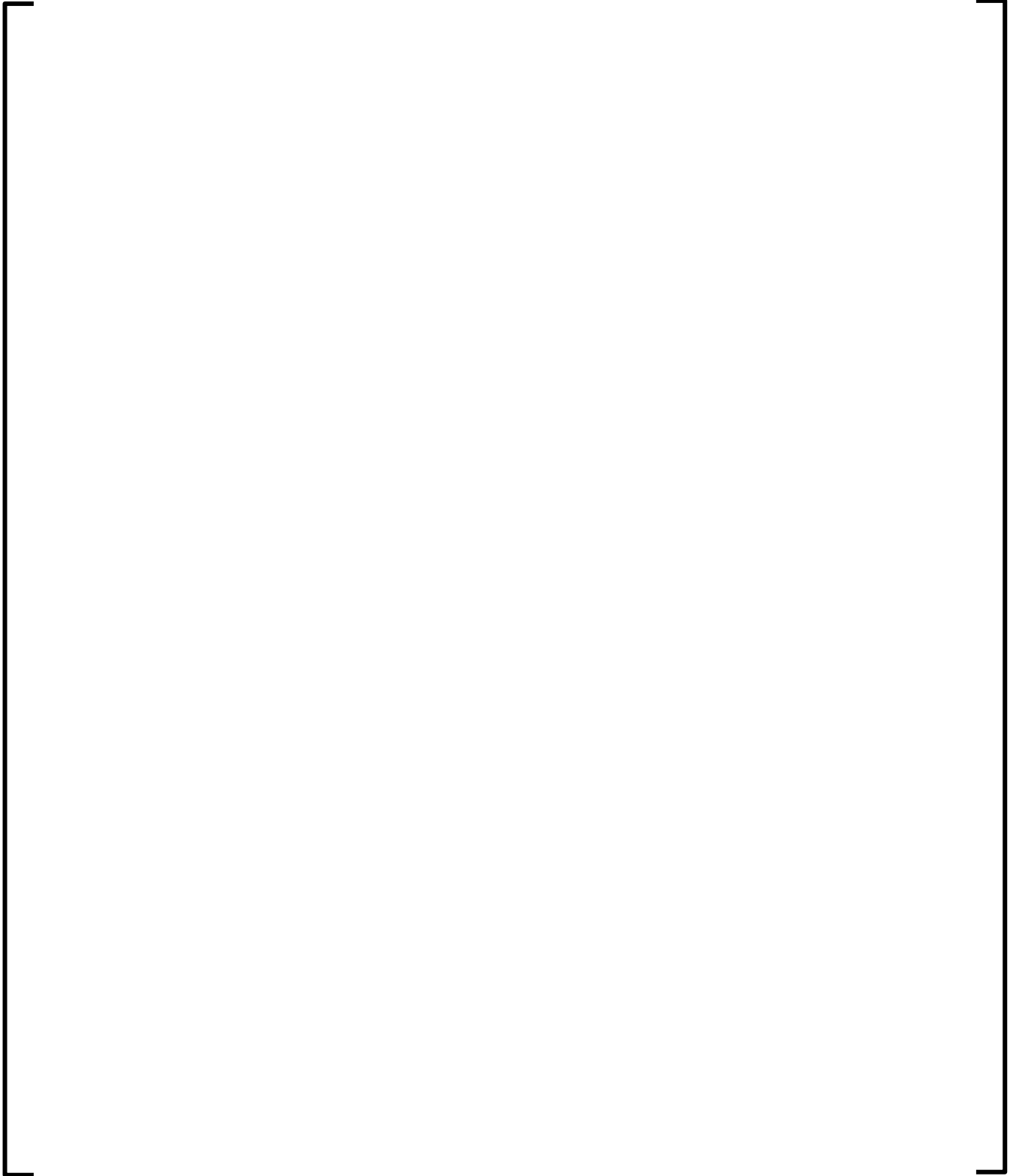
5.2.3 Cladding Effects



Low Upper-Shelf Toughness Fracture Mechanics Analysis of Reactor Vessels of
B&W Owners Reactor Vessel Working Group for Levels C & D Service Loads
Topical Report



Low Upper-Shelf Toughness Fracture Mechanics Analysis of Reactor Vessels of
B&W Owners Reactor Vessel Working Group for Levels C & D Service Loads
Topical Report



[
]

5.3 Evaluation for Levels C and D Service Loadings

The type of analysis models and computer code used to evaluate the RV shell welds and the Unit 1 RV nozzle welds for Levels C & D service loads are addressed in Section 5.2.1. Section 4.3 addresses the specific types of transient events analyzed for the PBN reactor vessels. The applied J-integral for the RV shell welds and the Unit 1 RV nozzle welds, due to these Levels C & D transients, is calculated and evaluated as discussed in Section 5.2.

The transition region toughness and upper shelf toughness are discussed in Section 5.2.2. Transition region toughness is obtained from the ASME Section XI equation for crack initiation,

$$K_{Ic} = 33.2 + 20.734 \exp[0.02(T - RT_{NDT})]$$

using the applicable RTNDT value for a flaw depth of 1/10th the wall thickness, where:

$$K_{Ic} = \text{transition region toughness, ksi}\sqrt{\text{in}}$$

$$T = \text{crack tip temperature, } ^\circ\text{F}$$

Upper shelf toughness K_{Jc} is derived from the J-integral resistance model of Section 4.1 for a flaw depth of 1/10th the wall thickness, a crack extension of 0.10 inch, and the applicable fluence value at the crack tip:

$$K_{Jc} = \sqrt{\frac{J_{0.1}E}{1000(1 - \nu^2)}}$$

where

$$K_{Jc} = \text{upper-shelf region toughness, ksi}\sqrt{\text{in}}$$

$$J_{0.1} = \text{J-integral resistance at } \Delta a = 0.1 \text{ in.}$$

Using the above equations, the transition and upper shelf toughness values as a function of temperature are determined for the controlling weld and Levels C and D service loading conditions.

5.3.1 Reactor Vessel Shell Welds

For the PBN Unit 1 and Unit 2 reactor vessels, the controlling weld was identified to be Unit 1 axial weld SA-812/SA-775 based on the results of Levels A and B Service Loadings [5]. This controlling weld is evaluated at a flaw depth of 1/10 the base metal thickness for Levels C and D Service Loadings. The copper content of SA-812/SA-775 is conservatively assumed to be 0.23%, which is the copper content of axial weld SA-847. The two main steam line break transients identified in Section 4.3 and illustrated in Figure 4-1, Figure 4-2, and Figure 4-3 are evaluated. The analysis is performed using the PCRIT Code.

Figure 5-1 reports the variation of the applied stress intensity factor, K_I , for these two transient cases as a function of the crack tip temperature. This figure also shows the transition region toughness K_{Ic} curve and the mean and lower bound upper-shelf toughness K_{Jc} curves with crack tip temperature. The K_{Ic} curve is conservatively determined (to maximize the upper shelf temperature range) using the Adjusted Reference Temperature (ART) value at 1/10th of the wall thickness for weld SA-847, which at 80-years is [] The symbols on the K_I curves for each of the two transient cases indicate points in time at which PCRIT solutions are available. The E-spec SLB is identified as the limiting transient since it most closely approaches the K_{Jc} limit of the weld. All subsequent analyses were based on evaluation of this transient case with the FSAR SLB reported for information. In the upper-shelf toughness range, the E-spec SLB K_I curve is closest to the lower bound K_{Jc} curve at [] minutes into the transient. This time is selected as the critical time in the transient at which to perform the flaw evaluation for Levels C and D Service Loadings.

The additional stress intensity factor attributable to the cladding, $K_{I_{clad}}$, at [] minutes (limiting time point) into the E-spec SLB transient is determined to be [] at a flaw depth corresponding to $1/10^{\text{th}}$ of the wall thickness. Applied J-Integrals are calculated for the controlling weld for various flaw depths in Table 5-1 using stress intensity factors from PCRIT for the E-spec SLB and adding [] to account for cladding effects. Stress intensity factors are converted to J -integrals by the previously reported plane strain relationship.

Since the RV shell weld for the PBN reactor vessels is [] inch thick as given in Table 3-2, the initial flaw depth of $1/10$ of the wall thickness is [] inches. The flaw extension is calculated by subtracting this depth from the built-in PCRIT flaw depths. The results along with the mean and lower bound J-R curves are plotted in Figure 5-2. An evaluation line is used at a flaw extension of 0.10 in. to show that the applied J -integral is less than the lower bound J -integral of the material, as required by Appendix K.

The applied J -integral at a flaw extension of 0.1 inch is determined to be [] as reported at the base of Table 5-1. The associated material J -resistance ($J_{0.1}$) to the applied J -integral (J_1) ratio can be determined using the lower bound J-R curve value of [] for Levels C and D conditions, using a fluence of $4.64E+19$ n/cm², Cu = 0.23%, and T of 324 °F. The margin for Level C and D Service Loading is []

The requirements for ductile and stable crack growth are demonstrated by Figure 5-2 since the slope of the applied J -integral curve is less than the slopes of both the lower bound and mean J-R curves at the points of intersection.

Referring to Figure 5-2, the Level D Service Loading requirement that the extent of stable flaw extension be no greater than 75% of the vessel wall thickness is easily satisfied since the applied J -integral curve intersects the mean J - R curve at a flaw extension that is only a small fraction of the wall thickness (less than 1%).

The last requirement for Level D Conditions is that the internal pressure p shall be less than P_l , the internal pressure at tensile instability of the remaining ligament. The calculations for P_l were determined for a circumferential flaw. An additional check is performed for circumferential flaws to ensure that internal pressure does not exceed the pressure at tensile instability caused by the applied hoop stress acting over the nominal wall thickness of the vessel. This validity limit on pressure is satisfied by

$$P_{\text{instability}} \leq 1.07 \sigma_o \frac{t}{R_i}.$$

To demonstrate that the remaining ligament does not exceed the pressure at instability a conservative flaw depth equal to 1/10th of the wall thickness plus 0.1 inch is used.

Although the internal pressure at tensile instability is calculated to be [] ksi, the validity check on hoop stress requires that the internal pressure not exceed [] ksi, which is still much greater than any anticipated accident condition pressure. Therefore, the remaining ligament is not subject to tensile instability.

5.3.2 PBN Unit 1 RV Nozzle Welds

The Unit 1 RV nozzle welds are located above the upper transition weld in the substantially thicker cylindrical NBF section (reinforced to account for the inlet/outlet RV nozzle openings). The reactor vessel nozzle belt dimensions are reported in Table 3-3. For the PBN Unit 1 reactor vessel, the applied J-integrals for the RV inlet and outlet nozzle-to-NBF welds were evaluated for Levels C and D Service Loadings. Both transients shown in Figure 4-1 through Figure 4-3 are evaluated. The bounding results with structural factor of 1 on the applied pressure are compared with the lower bound J-integral resistance at a ductile flaw extension of 0.1 inches in Table 5-2. The outlet nozzle is seen to be limiting and has a margin of []

The applied J-integral vs. crack tip temperature for each transient, Equipment Specification SLB and FSAR SLB, is plotted in Figure 5-3 for the Unit 1 RV outlet nozzle weld, along with the temperature dependent mean and lower bound $J_{0.1}$ curves. All points of the transient remain below the lower bound $J_{0.1}$. Additionally, Figure 5-3 shows the K_{Ic} fracture toughness using an RT_{NDT} of [] converted to an equivalent J using $K_{Ic}^2/(E/(1-\nu^2))$; the intersection of this curve with the $J_{0.1}$ curves establishes the upper shelf temperature range. The applied J-integral at the limiting time point at various flaw extensions is plotted with the lower bound J-resistance curve in Figure 5-4; the slope of the applied J-integral is less than the slope of the lower bound J-resistance curve at the point of intersection, which demonstrates that the flaw is stable as required by ASME Section XI, Appendix K.

**Table 5-1 PBN Axial Weld SA-812/SA-775 J-Integral versus Flaw
Extension for Levels C & D Service Loadings**

A large, empty rectangular frame with a thin black border, positioned centrally on the page. It is intended to contain the data for Table 5-1, but the content is currently blank.

**Table 5-2 PBN-Levels C & D Results for Unit 1 Inlet and Outlet
Nozzle-to-NBF Welds**

A large, empty rectangular frame with a thin black border, positioned centrally on the page. It is intended to contain the data for Table 5-2, but the content is missing.

Figure 5-1 PBN Axial Weld SA-812/SA-775--K_{Ic}, K_{Jc} (mean and lower bound), and Applied K_I for all Levels C and D transients



**Figure 5-2 PBN Axial Weld SA-812/SA-775-J-Integral Versus Flaw
Extension for Levels C & D Service Loadings**



**Figure 5-3 PBN Unit 1- Level C & D Applied J Integral vs Crack Tip
Temperature for the RV Outlet Nozzle to NBF Weld**



**Figure 5-4 PBN Unit 1-Levels C & D Applied J Integral vs Crack
Extension for the Outlet Nozzle to NBF Weld**



6.0 SUMMARY AND CONCLUSIONS

6.1 *Reactor Vessel Shell Welds*

The ASME Section XI, acceptance criteria for Levels C & D Service Loads for all reactor vessel shell welds are satisfied. ASME Section XI, Appendix K, Level C acceptance criteria (Subarticle K-2300), relative to the ratio of applied J-integral to J-integral of the material and use of the lower bound J-integral resistance curve, were conservatively imposed on the Level D transients evaluated in Section 5.0, although ASME Section XI, Subarticle K-2400(b) permits use of a best estimate J-integral resistance curve for Level D Service Loadings. The result of the limiting weld for PBN Units 1 and 2 is reported below.

6.1.1 PBN Units 1 and 2

The limiting weld among the Point Beach reactor vessel shell welds is Point Beach Unit 1 axial weld SA-812/SA-775. The limiting transient for Level C & D service loads is the E-Spec SLB.

- With a structural factor of 1 on loading, the applied J-integral (J_1) for the limiting reactor vessel shell weld (SA-812/SA-775) is less than the lower bound J-integral of the material at a ductile flaw extension of 0.10 inch ($J_{0.1}$) with a ratio $J_{0.1}/J_1 = [\quad]$ which is greater than the required value of 1.
- With a structural factor of 1 on loading, flaw extensions are ductile and stable for the limiting reactor vessel shell weld SA-812/SA-775 since the slope of the applied J-integral curve is less than the slopes of both the lower bound and mean J-R curves at the points of intersection.
- For weld SA-812/SA-775, it was demonstrated that flaw growth is stable at much less than 75% of the vessel wall thickness. It has also been shown that the remaining ligament is sufficient to preclude tensile instability.

6.2 *RV Nozzle Welds*

The ASME Section XI, acceptance criteria for Levels C & D Service Loads for PBN Unit 1 reactor vessel nozzle welds are satisfied. ASME Section XI, Appendix K, Level C acceptance criteria (Subarticle K-2300), relative to the ratio of applied J-integral to J-integral of the material and use of the lower bound J-integral resistance curve, were conservatively imposed on the Level D transients evaluated in Section 5.0, although ASME Section XI, Subarticle K-2400(b) permits use of a best estimate J-integral resistance curve for Level D Service Loadings. The results for PBN Unit 1 are reported below.

6.2.1 **PBN Units 1 and 2**

The RV inlet and outlet nozzle-to-shell welds were evaluated for Levels C and D Service Loadings. The limiting transient for Level C & D service loads is the E-Spec SLB.

- With a structural factor of 1 on loading, the applied J-integral (J_1) for the RV nozzle-to-shell welds are less than the lower bound J-integral of the material at a ductile flaw extension of 0.10 inch ($J_{0.1}$) with the following ratios for $J_{0.1}/J_1$: [] for the RV outlet nozzle-to-shell weld and [] for the RV inlet nozzle-to-shell weld.
- With a structural factor of 1 on loading, flaw extensions are ductile and stable for the limiting RV outlet nozzle-to-shell weld (i.e., limiting location considering RV nozzle-to-shell welds and upper transition weld).

For the RV outlet nozzle-to-shell weld it was demonstrated that flaw growth is stable at much less than 75% of the vessel wall thickness. Tensile instability was not explicitly calculated but because this section of the reactor vessel is thicker compared to the RV shell welds, it is considered to be bounded by the RV shell location.

7.0 REFERENCES

1. BAW-2178PA, Revision 0, "Low Upper Shelf Toughness Fracture Analysis of Reactor Vessels of B&W Owners Group Reactor Vessel Working Group for Level C and D Conditions," April 1994, ADAMS Accession (Legacy) 9406290288 (P).
2. NRC Regulatory Issue Summary 2014-11, Information on Licensing Applications for Fracture Toughness Requirements for Ferritic Reactor Coolant Pressure Boundary Components.
3. NUREG-2192, Standard Review Plan for Review of Subsequent License Renewal Applications for Nuclear Power Plants, ADAMS Accession Number ML17188A158.
4. BAW-2192, Supplement 1P-A, Revision 0, "Low Upper Shelf Toughness Fracture Mechanics Analysis of Reactor Vessels of B&W Owners Reactor Vessel Working Group for Level A & B Service Loads.
5. BAW-2192, Supplement 3P, Revision 0, "Low Upper Shelf Toughness Fracture Mechanics Analysis of Reactor Vessels of B&W Owners Reactor Vessel Working Group for Level A & B Service Loads.
6. BAW-2467P, Revision 1, Low Upper-Shelf Toughness Fracture Mechanics Analysis of Reactor Vessel of Point Beach Units 1 and 2 for Extended Life through 53 Effective Full Power Years.
7. Point Beach Nuclear Plant, Units 1 and 2 - Extended Power Uprate Amendment (TAC Nos. ME1044 and ME1045). ADAMS Accession numbers ML110450159, May 3, 2011, ML 111170513, SER-ML110450159.

8. Point Beach Nuclear Plant, Units 1 and 2-Issuance of Amendments Regarding Review of Reactor Vessel Fracture Mechanics Analysis (TAC NOS. MD2359 AND MD2360), ADAMS Accession Number ML071300623, May 10, 2007.
9. Code of Federal Regulations, Title 10, Part 50 – Domestic Licensing of Production and Utilization Facilities, Appendix G – Fracture Toughness Requirements, Federal Register Vol. 60. No. 243, December 19, 1995.
10. NRC Regulatory Guide 1.161, Evaluation of Reactor Pressure Vessels With Charpy Upper Shelf Energy Less Than 50 ft-lb.
11. 2017 Edition ASME & Boiler Pressure Vessel Code, Section XI, Rules for Inservice Inspection of Nuclear power Plant Components, Appendix K.
12. 2017 Edition ASME & Boiler Pressure Vessel Code, Section II, Materials, Part D.
13. Generic Letter 84-04, Safety Evaluation of Westinghouse Topical Reports Dealing with Elimination of Postulated Pipe Breaks in PWR Primary Main Loops, February 1, 1984.
14. Point Beach, Units 1 and 2, Issuance of Amendments Re: Leak-Before-Break Evaluation for the Primary Loop Piping. ADAMS Accession Number-ML043360295.

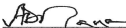
8.0 CERTIFICATION

This report is an accurate description of the low upper-shelf toughness fracture analysis of PBN Units 1 and 2 vessels.



Mark A. Rinckel
Mechanical Unit

This report has been reviewed and is an accurate description of the low upper-shelf toughness fracture analysis of reactor vessels of PBN Units 1 and 2.



Ashok D. Narla
Component Analysis & Fracture
Mechanics Unit

Verification of independent review.



Thomas S. Beckham
Mechanical Unit

This report is approved for release.



Danielle Page Blair
NSSS Project Management

Point Beach Nuclear Plant Units 1 and 2
Dockets 50-266 and 50-301
NRC 2020-0032 Enclosure 4, Attachment 6

Enclosure 4

**Non-proprietary Reference Documents and
Redacted Versions of Proprietary Reference
Documents**

(Public Version)

Attachment 6

**Framatome Technical Report ANP-3886NP, Revision
0, PWROG-20043-NP, "PWROG – PBN Unit 1 IS Plate
A9811-1 Equivalent Margins Analysis for SLR,"
October 2020**

(48 Total Pages, including cover sheets)



PWROG-20043-NP
Revision 0

Framatome Doc. No. ANP-3886NP-000

FRAMATOME INC. NON-PROPRIETARY

PBN Unit 1 IS Plate A9811-1

Equivalent Margins Analysis for SLR

Materials Committee

PA-MSC-1481, Revision 7

October 2020

PWROG-20043-NP
Revision 0

PBN Unit 1 IS Plate A9811-1 Equivalent Margins Analysis for SLR

PA-MS-C-1481, Revision 7

Mark A. Rinckel*, Advisory Engineer
Mechanical Unit-Subsequent License Renewal

October 2020

Reviewer: Ashok Nana*, Advisory Engineer
Component Analysis & Fracture Mechanics

Approved: Scott Beckham*, Supervisor
Mechanical Unit-Subsequent License Renewal

Approved: Danielle Page Blair*, Program Director
PWR Owners Group PMO

Framatome Inc.
3315 Old Forest Road
Lynchburg, VA 24501, USA

ACKNOWLEDGEMENTS

This report was developed and funded by the PWR Owners Group under the leadership of the participating utility representatives of the Materials Committee. The author would like to thank the following people and/or organizations for their valuable contributions to this report:

- Gordon Hall, Westinghouse Electric Company
- Scott Boggs, NextEra Energy
- Steve Franzone, NextEra Energy
- Bill Maher, NextEra Energy
- Luziana Matte, Contract Engineer, Framatome Inc.
- Silvester Noronha, Contract Engineer, Framatome Inc.

LEGAL NOTICE

This report was prepared as an account of work performed by Framatome Inc. Framatome Inc. nor its affiliates, nor any person acting on its behalf:

1. Makes any warranty or representation, express or implied including the warranties of fitness for a particular purpose or merchantability, with respect to the accuracy, completeness, or usefulness of the information contained in this report, or that the use of any information, apparatus, method, or process disclosed in this report may not infringe privately owned rights; or
2. Assumes any liabilities with respect to the use of, or for damages resulting from the use of, any information, apparatus, method, or process disclosed in this report.

COPYRIGHT NOTICE

This report has been prepared by Framatome Inc. and bears a Framatome copyright notice. As a member of the PWR Owners Group, you are permitted to copy and redistribute all or portions of the report within your organization; however all copies made by you must include the copyright notice in all instances.

DISTRIBUTION NOTICE

This report was prepared for the PWR Owners Group. This Distribution Notice is intended to establish guidance for access to this information. This report (including proprietary and non-proprietary versions) is not to be provided to any individual or organization outside of the PWR Owners Group program participants without prior written approval of the PWR Owners Group Program Management Office. However, prior written approval is not required for program participants to provide copies of Class 3 Non-Proprietary reports to third parties that are supporting implementation at their plant, and for submittals to the NRC.

**PWR Owners Group
United States Member Participation* for PA-MS-C-1481, Revision 7**

Utility Member	Plant Site(s)	Participant	
		Yes	No
Ameren Missouri	Callaway (W)		X
American Electric Power	D.C. Cook 1 & 2 (W)		X
Arizona Public Service	Palo Verde Unit 1, 2, & 3 (CE)		X
Dominion Energy	Millstone 2 (CE)		X
	Millstone 3 (W)		X
	North Anna 1 & 2 (W)		X
	Surry 1 & 2 (W)		X
	V.C. Summer (W)		X
Duke Energy Carolinas	Catawba 1 & 2 (W)		X
	McGuire 1 & 2 (W)		X
	Oconee 1, 2, & 3 (B&W)		X
Duke Energy Progress	Robinson 2 (W)		X
	Shearon Harris (W)		X
Entergy Palisades	Palisades (CE)		X
Entergy Nuclear Northeast	Indian Point 2 & 3 (W)		X
Entergy Operations South	Arkansas 1 (B&W)		X
	Arkansas 2 (CE)		X
	Waterford 3 (CE)		X
Exelon Generation Co. LLC	Braidwood 1 & 2 (W)		X
	Byron 1 & 2 (W)		X
	Calvert Cliffs 1 & 2 (CE)		X
	Ginna (W)		X
FirstEnergy Nuclear Operating Co.	Beaver Valley 1 & 2 (W)		X
	Davis-Besse (B&W)		X
Florida Power & Light \ NextEra	St. Lucie 1 & 2 (CE)		X
	Turkey Point 3 & 4 (W)		X
	Seabrook (W)		X
	Pt. Beach 1 & 2 (W)	X	
Luminant Power	Comanche Peak 1 & 2 (W)		X
Pacific Gas & Electric	Diablo Canyon 1 & 2 (W)		X
PSEG – Nuclear	Salem 1 & 2 (W)		X

**PWR Owners Group
United States Member Participation* for PA-MS-C-1481, Revision 7**

Utility Member	Plant Site(s)	Participant	
		Yes	No
So. Texas Project Nuclear Operating Co.	South Texas Project 1 & 2 (W)		X
Southern Nuclear Operating Co.	Farley 1 & 2 (W)		X
	Vogtle 1 & 2 (W)		X
Tennessee Valley Authority	Sequoyah 1 & 2 (W)		X
	Watts Bar 1 & 2 (W)		X
Wolf Creek Nuclear Operating Co.	Wolf Creek (W)		X
Xcel Energy	Prairie Island 1 & 2 (W)		X

* Project participants as of the date the final deliverable was completed. On occasion, additional members will join a project. Please contact the PWR Owners Group Program Management Office to verify participation before sending this document to participants not listed above.

**PWR Owners Group
International Member Participation* for PA-MS-1481, Revision 7**

Utility Member	Plant Site(s)	Participant	
		Yes	No
Asociación Nuclear Ascó-Vandellòs	Asco 1 & 2 (W)		X
	Vandellos 2 (W)		X
Centrales Nucleares Almaraz-Trillo	Almaraz 1 & 2 (W)		X
EDF Energy	Sizewell B (W)		X
Electrabel	Doel 1, 2 & 4 (W)		X
	Tihange 1 & 3 (W)		X
Electricite de France	58 Units		X
Elektricitets Produktiemaatschappij Zuid-Nederland	Borssele 1 (Siemens)		X
Eletronuclear-Elektrobras	Angra 1 (W)		X
Emirates Nuclear Energy Corporation	Barakah 1 & 2		X
Hokkaido	Tomari 1, 2 & 3 (MHI)		X
Japan Atomic Power Company	Tsuruga 2 (MHI)		X
Kansai Electric Co., LTD	Mihama 3 (W)		X
	Ohi 1, 2, 3 & 4 (W & MHI)		X
	Takahama 1, 2, 3 & 4 (W & MHI)		X
Korea Hydro & Nuclear Power Corp.	Kori 1, 2, 3 & 4 (W)		X
	Hanbit 1 & 2 (W)		X
	Hanbit 3, 4, 5 & 6 (CE)		X
	Hanul 3, 4, 5 & 6 (CE)		X
Kyushu	Genkai 2, 3 & 4 (MHI)		X
	Sendai 1 & 2 (MHI)		X
Nuklearna Elektrarna KRSKO	Krsko (W)		X
Ringhals AB	Ringhals 2, 3 & 4 (W)		X
Shikoku	Ikata 2 & 3 (MHI)		X
Taiwan Power Co.	Maanshan 1 & 2 (W)		X

* **Project participants as of the date the final deliverable was completed. On occasion, additional members will join a project. Please contact the PWR Owners Group Program Management Office to verify participation before sending this document to participants not listed above.**

TABLE OF CONTENTS

1	INTRODUCTION.....	1-1
2	REGULATORY REQUIREMENTS.....	2-1
	2.1 10 CFR 50 Appendix G.....	2-1
	2.2 Compliance with 10 CFR 50 Appendix G and Acceptance Criteria.....	2-2
3	DESCRIPTION OF PBN IS PLATE A9811-1.....	3-1
	3.1 72 EFPY Fluence.....	3-1
	3.2 Charpy V-Notch Initial Upper Shelf Energy.....	3-1
	3.3 Charpy V-Notch Upper Shelf Energy at 72 EFPY.....	3-2
	3.3.1 72 EFPY CVN at or Near Bottom of Plate.....	3-2
	3.3.2 72 EFPY CVN at or Near Top of Plate.....	3-2
4	MATERIAL PROPERTIES.....	4-1
	4.1 J-Integral Resistance Model.....	4-1
	4.1.1 Selection of the J-Integral Resistance (J-R) Model.....	4-1
	4.1.2 NUREG/CR-5265 Lower Bound J-R Curve Data Selection.....	4-2
	4.1.3 J-R Curve Adjustment Estimation.....	4-5
	4.1.4 Statistical Uncertainty Factor (SF) Determination.....	4-8
	4.1.5 IS Plate A9811-1 CVN-Review of RVID2.....	4-11
	4.1.6 Final J-R Model for IS Plate A9811-1.....	4-11
	4.2 Mechanical Properties of IS Plate A9811-1.....	4-15
	4.3 Selection of Limiting Design Transients--Levels A-D Service Loadings.....	4-15
	4.3.1 Levels A and B Service Loadings.....	4-15
	4.3.2 Levels C and D Service Loading.....	4-15
5	FRACTURE MECHANICS ANALYSIS.....	5-1
	5.1 Methodology.....	5-1
	5.2 Evaluation for Flaw Extension.....	5-1
	5.2.1 Levels A and B Service Loadings.....	5-1
	5.2.2 Levels C and D Service Loadings.....	5-5
6	SUMMARY AND CONCLUSIONS.....	6-1
7	REFERENCES.....	7-1

LIST OF TABLES

Table 4-1: Unirradiated USE RVID Database for Plate A-302-B Material	4-11
Table 5-1: Flaw Evaluation for Levels A & B Service Loadings	5-2
Table 5-2: Applied J-Integral versus Flaw Extension for Levels A & B Service Loadings for IS Plate A9811-1 Limiting Axial and Circumferential Flaws (SF = 1.25)	5-2
Table 5-3: Material J-Resistance versus Flaw Extension for IS Plate A9811-1 Limiting Axial and Circumferential Flaws.....	5-3
Table 5-4: Flaw Evaluation for Levels C & D Service Loadings	5-7
Table 5-5: Applied J-Integral versus Flaw Extension for Levels C & D Service Loadings for IS Plate A9811-1 Limiting Axial and Circumferential Flaws (SF = 1.0)	5-8
Table 5-6: Material J-Resistance versus Flaw Extension for IS Plate A9811-1 Limiting Axial and Circumferential Flaws (T = 324°F).....	5-9
Table 5-7: Tensile Instability Check for Levels C & D Service Loadings	5-12

LIST OF FIGURES

Figure 4-1: NUREG/CR-5265, Comparison of all J -R Curves for Tests of Plate A-302-B.....	4-3
Figure 4-2: Normalized Charpy Prediction Relative to Measured Test Data (MRP-439)	4-4
Figure 4-3: Normalized Charpy Prediction Relative to NUREG/CR-5625 6T Test Data	4-5
Figure 4-4: Hiser’s Power Law Fit Eq. (2) Relative to NUREG/CR-5625 6T Test Data	4-7
Figure 4-5: Least-Square Fit (Mean) and (Mean - 2 S _e) Lines, A-302-B Plate, L-T and T-L directions, 400 to 550°F.....	4-8
Figure 4-6: Statistical Uncertainty Factor (SF) vs Charpy V-notch (CVN) Distribution	4-10
Figure 4-7: IS plate A9811-1 J-R Model, T-L (Weak) Direction Top and Bottom of Plate, 100°F to 600°F.....	4-12
Figure 4-8: IS plate A9811-1 J-R Model, L-T (Strong) Direction, Bottom of Plate, 100°F to 600°F.....	4-13
Figure 4-9: IS plate A9811-1 J-R Model, L-T (Strong) Direction, Top of Plate, 100°F to 600°F.....	4-14
Figure 5-1: J-Integral versus Flaw Extension for Levels A & B Service Loadings for IS Plate A9811-1 – Limiting Axial Flaw	5-4
Figure 5-2: J-Integral versus Flaw Extension for Levels A & B Service Loadings for IS Plate A9811-1 – Limiting Circumferential Flaw	5-5
Figure 5-3: J-Integral versus Flaw Extension for Levels C & D Service Loadings for IS Plate A9811-1 – Limiting Axial Flaw	5-10
Figure 5-4: J-Integral versus Flaw Extension for Levels C & D Service Loadings for IS Plate A9811-1 – Limiting Circumferential Flaw	5-11

1 INTRODUCTION

Point Beach Nuclear (PBN) Unit 1 intermediate shell (IS) plate (heat A9811-1) has a predicted 80-year (72 EFPY) USE value that is just below 50 ft-lbs at 80-years; all remaining beltline and extended beltline plate and forging materials for Units 1 and 2 are above 50 ft-lbs at 72 EFPY. Therefore, a 72 EFPY EMA is required for IS plate A9811-1 to demonstrate that lower values of Charpy USE will provide margins of safety against fracture equivalent to those required by Appendix G of Section XI of the ASME Code. The purpose of this document to report an equivalent margins analysis for PBN Unit1 IS plate A9811-1 using methodology that complies with ASME Section XI, Appendix K, 2017 Edition [1] and a J-integral resistance model that complies with Regulatory Guide 1.161 [2], Section 3.3.2.

The methodology for calculation of applied J-integrals for postulated circumferential and axial flaws in IS plate A9811-1 is consistent with the methodologies for calculation of applied J-integrals for Linde 80 welds for subsequent license renewal reported in PBN-specific supplements to topical reports BAW-2178 and BAW-2192, References [3 and 4]. Since the sulfur content of IS plate A9811-1 exceeds 0.018%, the base metal J-R models reported in NUREG/CR-5729 [5] may not be used for the IS plate EMA. The J-integral resistance model used for the EMA of IS plate A9811-1 is based on NUREG/CR-5265 [6], specimen V50-101, 6T, and the guidance provided for use of this specimen to develop a J-integral resistance model for A302B plate material is provided in Reference [7].

2 REGULATORY REQUIREMENTS

2.1 10 CFR 50 APPENDIX G

In accordance with 10 CFR 50 Appendix G [8], IV, A, 1., Reactor Vessel Upper Shelf Energy Requirements are as follows:

- Reactor vessel beltline materials must have Charpy upper-shelf energy in the transverse direction for base material and along the weld for weld material according to the ASME Code, of no less than 75 ft-lb (102 J) initially and must maintain Charpy upper-shelf energy throughout the life of the vessel of no less than 50 ft-lb (68 J), unless it is demonstrated in a manner approved by the Director, Office of Nuclear Reactor Regulation or Director, Office of New Reactors, as appropriate, that lower values of Charpy upper-shelf energy will provide margins of safety against fracture equivalent to those required by Appendix G of Section XI of the ASME Code. This analysis must use the latest edition and addenda of the ASME Code incorporated by reference into 10 CFR 50.55a (b)(2) at the time the analysis is submitted.
- Additional evidence of the fracture toughness of the beltline materials after exposure to neutron irradiation may be obtained from results of supplemental fracture toughness tests for use in the analysis specified in section IV.A.1.a.
- The analysis for satisfying the requirements of section IV.A.1 of this appendix must be submitted, as specified in § 50.4, for review and approval on an individual case basis at least three years prior to the date when the predicted Charpy upper-shelf energy will no longer satisfy the requirements of section IV.A.1 of this appendix, or on a schedule approved by the Director, Office of Nuclear Reactor Regulation or Director, Office of New Reactors, as appropriate.

When the reactor vessels within the scope of this report were fabricated, Charpy V-notch (CVN) testing of the reactor vessel welds in accordance with the original construction code, which did not specifically require Charpy V-notch tests on the upper shelf. Applicable construction codes are as follows:

- PBN Unit 1, ASME Section III 1965 Edition, by Babcock & Wilcox
- PBN Unit 2, ASME Section III 1965 Edition, by Babcock & Wilcox and Combustion Engineering

In accordance with NRC Regulatory Guide 1.161 [2], the NRC has determined that the analytical methods described in ASME Section XI, Appendix K, provide acceptable guidance for evaluating reactor pressure vessels when the Charpy upper-shelf energy falls below the 50 ft-lb limit of Appendix G to 10 CFR Part 50. However, the staff noted that Appendix K does not provide information on the selection of transients and gives very little detail on the selection of material properties. Section 4.1 of this report includes a summary of the J-integral resistance

model, Section 4.2 provides mechanical properties of IS plate A9811-1, and Section 4.3 discusses selection of limiting design transients.

2.2 COMPLIANCE WITH 10 CFR 50 APPENDIX G AND ACCEPTANCE CRITERIA

The current edition of ASME Section XI listed in 10 CFR 50.55a is the 2017 Edition. Therefore, the analyses reported herein are performed in accordance with the 2017 Edition [1] of Section XI of the ASME Code, Appendix K. The material properties used in this analysis are based on ASME Section II, Part D, 2017, Edition [9].

3 DESCRIPTION OF PBN IS PLATE A9811-1

PBN Intermediate Shell plate A9811-1 is made from ASTM 302 Grade B plate procured from Lukens Steel Company. Intermediate shell plate A9811-1 mill test report chemical analyses are reported below. "T" refers to top of the plate or leading end and "B" refers to the plate bottom or trailing end. F.G.P. refers to fine grain practice, which at Lukens meant that the steel was silicon-killed and aluminum treated. Chemical analyses were usually performed twice. The first analysis was the ladle or heat analysis which refers to the final analysis of the heat of steel. Samples were usually taken during the pouring of the ingots. The second analysis was the check or product analysis that was taken from the plate itself to produce fine grain material. The sulfur content is 0.02%. The nickel content of IS plate is 0.056% [11].

CONSIGNEE <i>MR G FRIESE</i> <i>N43P BWL</i>		LUKENS STEEL COMPANY PHYSICAL TESTING LABORATORY COATESVILLE, PA. TEST CERTIFICATE		DATE 1-3-65 FILE NO 602 CTF NO RM 12965 ME										
PURCHASER 7 Babcock & Wilcox Co. Attn: Pur. Dept.		CARRIER 12-23-65 NYC 715913 LAM 170611		PLG., STRUCT. & HULL QUAL.: BENDING TESTS: FIRE BOX QUALITIES: BENDING TESTS: O.K. HOMOGENEITY TESTS: O.K.										
CHEMICAL ANALYSIS														
MELT NO.	C	Mn	P	S	CU	S	Ni	Cr	Mo	V	Ti	Al	B	
A9811	20	1.42	010	022		24			48					Ladle F.G.P.
" Slab 1 T	19	1.42	010	020		25			48					Check
" Slab 1 B	20	1.42	011	020		25			49					Check
A9799	19	1.24	006	020		16			47					Ladle F.G.P.
" Slab 1 T	20	1.26	010	016		18			47					Check
" Slab 1 B	20	1.26	010	019		20			50					Check
PHYSICAL PROPERTIES														
MILL ORDER & CUSTOMER P.O.	SPECIFICATIONS	MELT NO.	SURF. FIN.	PLATE THICKNESS	TENSILE	YIELD	ELONG.	REDUCED	DESCRIPTION					

3.1 72 EFPY FLUENCE

The peak 72 EFPY fluence for IS plate A9811-1 is $7.81E+19$ n/cm² (E> 1.0MeV) at the clad/base metal interface. The specific location is at or near the bottom of the plate. The peak 72 EFPY fluence at the top of IS plate A 9811-1 is assumed to be equivalent to the peak fluence at the Unit 1 nozzle belt forging to IS circumferential weld SA-1426 of $5.66E+18$ n/cm² (E> 1.0MeV) [3].

3.2 CHARPY V-NOTCH INITIAL UPPER SHELF ENERGY

Initial upper shelf energy (USE) for IS plate A9811-1 was established at 70 ft-lbs through the PBN response to GL 92-01 [10, 11]. The method of establishing unirradiated USE is reported as the 65% (indirect) method. Initial upper shelf energy is obtained from WCAP-7513 [12], wherein Charpy V-notch upper shelf energy was established based on 7 data points on the upper shelf (111.0, 115.0, 114.0, 110.0, 103.0, 95.0, and 104.5 ft-lbs), providing a mean value of 107.5 ft-lbs in the longitudinal (strong) direction and 0.65* 107.5 of 69.9 or 70 ft-lbs in the transverse (weak) direction. The basis for use of 65% is in accordance with MTEB 5-2, now BTP 5-3 [13], which states that test results from longitudinally-oriented specimens are reduced to 65 percent of their value to provide conservative estimates of values expected from transversely oriented specimens. Justification for the use of 65% for high sulfur A302B plate material is provided by the NRC memo "Ratio of Transverse to Longitudinal Orientation Charpy

Upper Shelf Energy [14],” wherein reference is made to a plot (Figure 2) of the transverse to longitudinal upper shelf energy ratio versus sulfur content for A-302B and 533B plate materials. This plot does not suggest a discernible trend with increasing sulfur and concludes there is no significant distinction between A-302B and A-533B materials.

3.3 CHАРPY V-NOTCH UPPER SHELF ENERGY AT 72 EFPY

Since IS plate A9811-1 will experience variation in neutron exposure (higher at the bottom of the plate than at the top) and stress intensity factor (higher at the top of the plate than at the bottom due to effects of external nozzle loads) as a function of axial elevation, both circumferential and axial orientation flaws are postulated at both the bottom and the top of the plate. As such, Charpy V-Notch upper shelf energies are required in both the weak and strong directions at the top and bottom of the plate.

3.3.1 72 EFPY CVN at or Near Bottom of Plate

CVN values at or near the bottom of plate A9811-1 used to adjust Specimen V-50-101, 6T, are based on RG 1.99, Revision 2, Position 2.2, as follows:

- 1/4T fluence is $7.81E+19 \text{ (n/cm}^2\text{)} * e^{(-0.24*6.5/4)} = 5.29E19 \text{ n/cm}^2$
- Strong direction $107.5*(1-.2016(5.29E19/1.0E19)^{0.2368}) = 75.35 \text{ ft-lbs}$ in the strong direction (for axial flaws).
- Weak direction $75.35 \text{ ft-lbs} * 0.65 = 49 \text{ ft-lbs}$ (for circumferential flaws)

3.3.2 72 EFPY CVN at or Near Top of Plate

CVN values at or near the top of IS plate A9811-1 used to adjust Specimen V-50-101, 6T, are based on RG 1.99, Revision 2, Position 2.2, as follows.

- 1/4T fluence is $5.66E+18 \text{ (n/cm}^2\text{)} * e^{(-0.24*6.5/4)} = 3.83E18 \text{ n/cm}^2$
- Strong direction $107.5*(1-.2016(3.83E18/1.0E19)^{0.2368}) = 90.23 \text{ ft-lbs}$ in the strong direction (for axial flaws).
- Weak direction, a value of 49 ft-lbs is conservatively selected to equal the value at the bottom of the plate.

4 MATERIAL PROPERTIES

4.1 J-INTEGRAL RESISTANCE MODEL

The J-integral resistance model for IS plate A9811-1 is from NUREG/CR-5265, Specimen V-50-101, 6T, [6] adjusted for temperature in accordance with Regulatory Guide 1.161 [2], Equations (26)-(29) and for CVN in accordance with Reference [7]. This is consistent with the J-integral resistance methodology used for Palisades reported in WCAP-17651-NP [15] and with the Oak Ridge National Laboratory evaluation of Nine Mile Point EMA reported in Reference [7]. Temperatures used to adjust the NUREG/CR-5265 J-R Specimen V-50-101, 6T, data are consistent with the temperatures defined in Section 4.3 herein for Service Levels A-D.

4.1.1 Selection of the J-Integral Resistance (J-R) Model

In accordance with Section K-3300 of ASME Section XI, 2017 Edition, Reference [1], when analytically evaluating the vessel for Levels A, B, C, and D Service Loadings, the J-integral resistance versus crack extension curve (J-R curve) shall be a conservative or a best estimate representation of the toughness of the controlling beltline material at the upper shelf temperatures in the operating range. One of the following options shall be used to determine the J-R curve.

1. A J-R curve shall be generated for the material by following accepted test procedures. The J-R curve shall be based on the proper combination of crack orientation, temperature, and fluence level.
2. A J-R curve shall be generated from a J-integral database obtained from the same class of material with the same orientation using correlations for effects of temperature, chemical composition, and fluence level.
3. When (a) or (b) cannot be used, an indirect method of estimating the J-R curve shall be used provided the method is justified for the material

As reported in Section 3, the chemical composition of IS Plate A9811-1 indicates that the sulfur content is 0.020 wt.% and the nickel content is 0.056 wt.%. In accordance with Section 3.3 of the Regulatory Guide 1.161, Reference [2], since the sulfur content of the IS plate A9811-1 exceeds 0.018 wt. %, the base metal J-R models reported in NUREG/CR-5729, Reference [5], may not be suitable for use for the IS plate A9811-1 EMA.

Following the guidelines of Section 3.3.2 of RG 1.161, Reference [2], for analyses addressing materials with sulfur content greater than 0.018 wt. %, the limited J-R curve data for a 6-inch-thick specimen (ASTM 6T CT at 180°F temperature) from an high sulfur A-302-B plate in the T-L (weak) orientation is available in NUREG/CR-5265, Reference [6], and may be used with adjustments for the specimen plate temperatures at which the maximum J-integral from the applied loads are determined for Service Levels A through D and with adjustments for the Charpy V-notch (CVN) values. Section 3.3.2 of Reference [2] also indicates that for analyses addressing Service Levels A, B, and C, a lower bound (mean - 2 standard deviations)

representation of the J-R curve should be used and for analyses addressing Service Level D, the mean value of the J-R curve should be used.

The lower bound representation of the J-R curve data from NUREG/CR-5265, Reference [6], will be conservatively selected in this document for the development of the IS Plate A9811-1 J-R model and applied for Service Levels A, B, C, and D.

4.1.2 NUREG/CR-5265 Lower Bound J-R Curve Data Selection

The J-R curve data from NUREG/CR-5265, Reference [6], is available on A-302-B plate specimens (V50) ranging in size from 0.5T to 6T with a reported sulfur content of 0.021 and 0.025 wt. %, and with the low toughness orientation for the plates in the T-L (weak) orientation.

The deformation theory J-integral data (i.e., J_D) for specimens 0.5T to 6T is shown in Figure 4-1. As shown in Figure 4-1, the T-L (weak) orientation J-R curves for A-302-B steel exhibit reverse size effects, with the J-R curves falling as specimen size increases. In accordance with Reference [6], the high content of manganese-sulfide (MnS) inclusions and/or the banded regions of microstructure are believed to be the causes of this unusual specimen size effect. An independent study by Framatome (formerly B&W) in 1993 concluded that there is uncertainty whether the manufacturing practices used to produce the V50 plate are representative of those used on RPV plates and that the presence of MnS inclusions clusters can lead to large size effects on J-R curves.

NUREG/CR-6426, Reference [16], developed a ductile fracture toughness data in the form of J-R curves for modified A-302 Grade B plate materials typical of those used in fabricating reactor pressure vessels. None of the results observed in Reference [16] showed size effects of any consequence on the J-R curve behavior indicating that the reverse size effects observed in NUREG/CR-5265, Reference [6], are unique to the V50 plate specimens and are not a generic characteristic for all heats of A-302-B steels. The necessity for conservatism requires that the lowest J-R curve be selected as the basis for estimating J-R curves for A-302-B steel. The lowest curve in Figure 4-1 is from specimen V50-101, a 6T specimen tested at 180°F and this curve will be selected for the development of the J-R model for the IS Plate A9811-1.

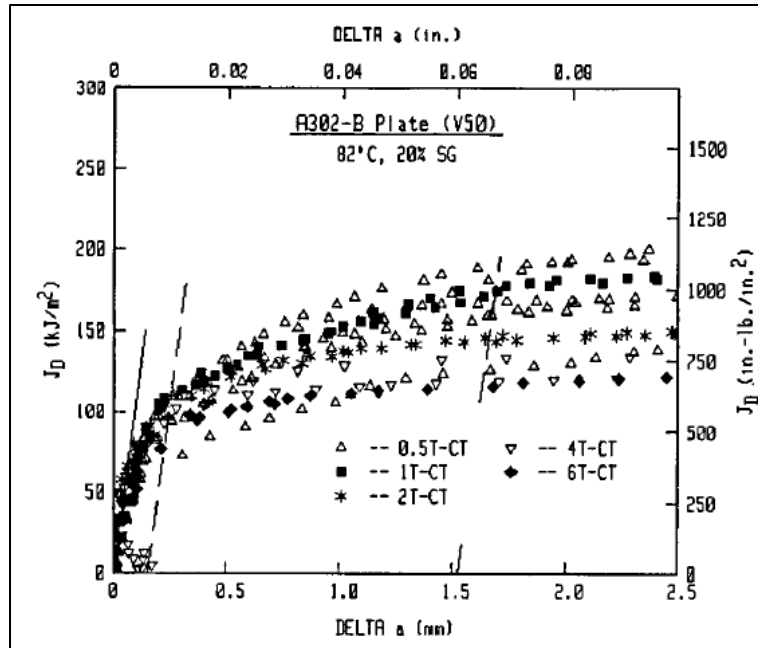


Figure 4-1: NUREG/CR-5265, Comparison of all J-R Curves for Tests of Plate A-302-B

Clearly, the 6T specimen J-R curve is not a mean minus 2 standard error ($-2 S_e$) curve because of its reliance on a single specimen value of J_D . Recent fracture test results presented in Reference [17] from San Onofre Unit 1 on a potentially more representative A-302-B plate indicate vastly superior properties to those reported in NUREG/CR-5265.

In accordance with Reference [17], two J-R tests were conducted on a single A-302 Grade B plate, heat A3099, from San Onofre Unit 1, with a sulfur content of 0.0195 wt.% (specimens ID YB18-1 and YB18-2). As shown in Figure 4-2, one normalized test result was above the NUREG/CR-5729, Reference [5], Charpy base metal prediction lower bound curve ($-2 S_e$), while the second fell between the ($-2 S_e$) and ($-3 S_e$) lower bound curves. Following the same methodology described in Section 3.0 of Reference [17], the measured 6T specimen data from NUREG/CR-5265, is normalized and compared to the calculated J-R curve using the Charpy model at standard conditions. A comparison of the normalized 6T specimen data from NUREG/CR-5265 with the NUREG/CR-5729 Charpy base metal prediction curves (mean, mean $-2 S_e$, and mean $-3 S_e$) is provided in Figure 4-3. As shown in Figure 4-3, at the normalized J_D value at 0.10 inches of crack extension ($J_{D(0.1)}$), the NUREG/CR-5729 Charpy base metal prediction lower bound curve ($-3 S_e$) is a little more than 2 times the normalized $J_{D(0.1)}$ value of the NUREG/CR-5265 6T specimen.

In addition, Framatome performed an independent evaluation of the NUREG/CR-5265 test results in September 1993 and concluded the following.

- There is uncertainty whether manufacturing practices used to produce the V-50 plate are representative of those regularly used on early RPV plates. Ingot size and cross rolling ratios are known differences which could affect directionally sensitive properties.

- J-R fracture toughness tests on large V-50 compact tension specimens may not be valid because of delamination occurring during testing.
- Tests on other RPV plates show that the presence of MnS inclusion clusters can lead to large size effects on J-R curves. The role of constraint or specimen geometry may also lead to large size effects on J-R curves.

This further validates that the V50 plate from NUREG/CR-5265, Reference [6], was an anomaly and the V50-101 6T specimen may be considered a very conservative lower bound of the available high-sulfur A-302 B plate J-R data.



Figure 4-2: Normalized Charpy Prediction Relative to Measured Test Data (MRP-439)

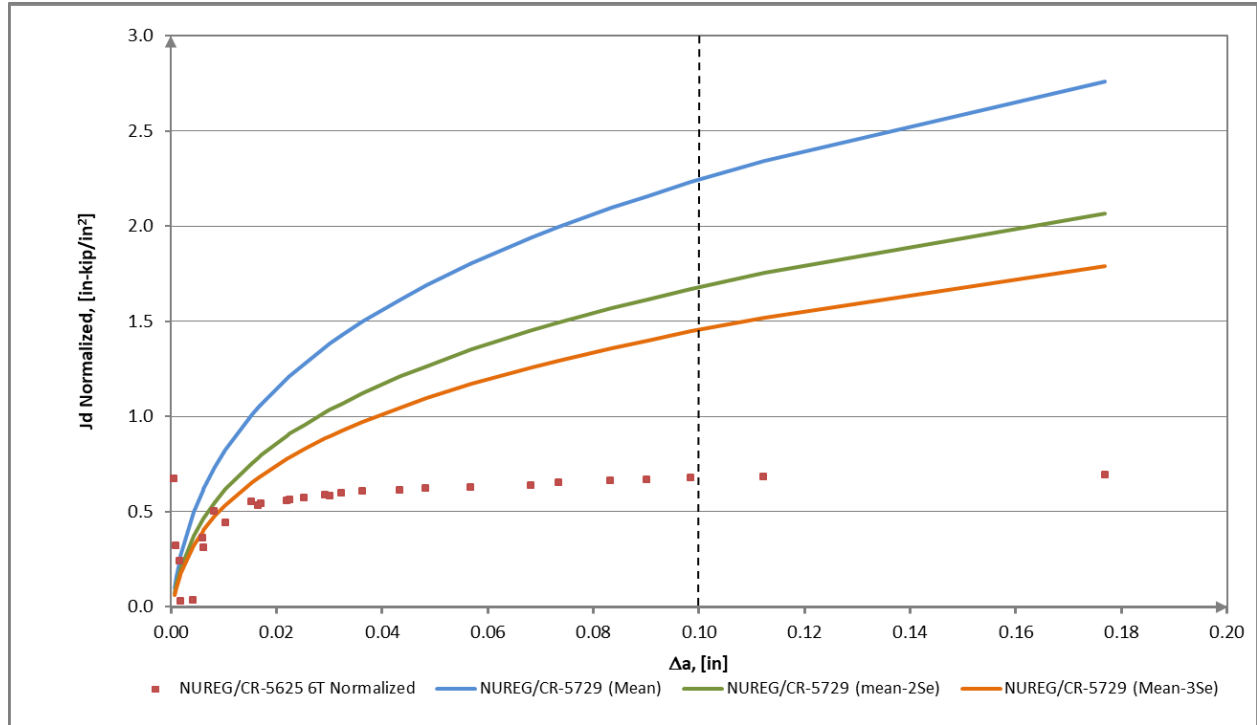


Figure 4-3: Normalized Charpy Prediction Relative to NUREG/CR-5625 6T Test Data

4.1.3 J-R Curve Adjustment Estimation

With the selection of specimen V50-101 from NUREG/CR-5265, Reference [6], the development of the J-R curve estimating procedure for the A9811-1 steel plate requires a formulation for adjusting the curve to account for variations in Charpy V-notch (*CVN*) values and temperature, plus accounting for random variability.

A procedure for estimating the J-R curve for relatively high sulfur (> 0.018 wt. %) and low upper-shelf energy steels has been developed and is described in Reference [7]. The J-R curve estimating equation described in Reference [7] has the following form:

$$J = (SF) \cdot C_1(\Delta a)^{C_2} \cdot [f(CVN)] \cdot [g(T, \Delta a)] \quad \text{Eq. (1)}$$

Where *SF* is a statistical uncertainty factor, $C_1(\Delta a)^{C_2}$ is Hiser's power law fit to specimen V50-101 data, $f(CVN)$ is a mean correlation between $J_{0.1}$ and *CVN* based on Hiser's analysis of available A-302-B data, normalized to *CVN* = 50 *ft-lbs*, and $g(T, \Delta a)$ is a temperature variation factor obtained from the Eason's correlations in NUREG/CR-5729. The equations for these factors are:

$$C_1(\Delta a)^{C_2} = 946.82 \cdot (\Delta a)^{0.1334} \quad \text{Eq. (2)}$$

$$f(CVN) = \frac{11.75 \cdot CVN + 108}{695.5} \quad \text{Eq. (3)}$$

$$g(T, \Delta a) = \exp\{-0.00277 \cdot (T - 180) \cdot [1 + 0.116 \cdot \ln(\Delta a) - 0.0092 \cdot (\Delta a)^{-0.409}]\} \quad \text{Eq. (4)}$$

In accordance with Reference [7], the fit using Hiser's power law fit Equation (2) [$C_1(\Delta a)^{C_2}$] to the V50-101 data for $\Delta a \leq 0.10$ in is very good, as illustrated in Figure 4-4. However, there is a sudden decrease in slope of the measured J-R curve at $\Delta a = 0.10$ in, causing the power law fit to become "un-conservative" for crack extensions $\Delta a > 0.10$ in. This decrease in slope is not considered realistic behavior of the material and, for the purpose of this EMA, Eq. (1) will be used for evaluating the margins at the ductile flaw extension $\Delta a = 0.10$ in, and the flaw stability will be evaluated [

]. This is considered typical of the A-302-B plate material plant test data as shown in Figure 4-2.

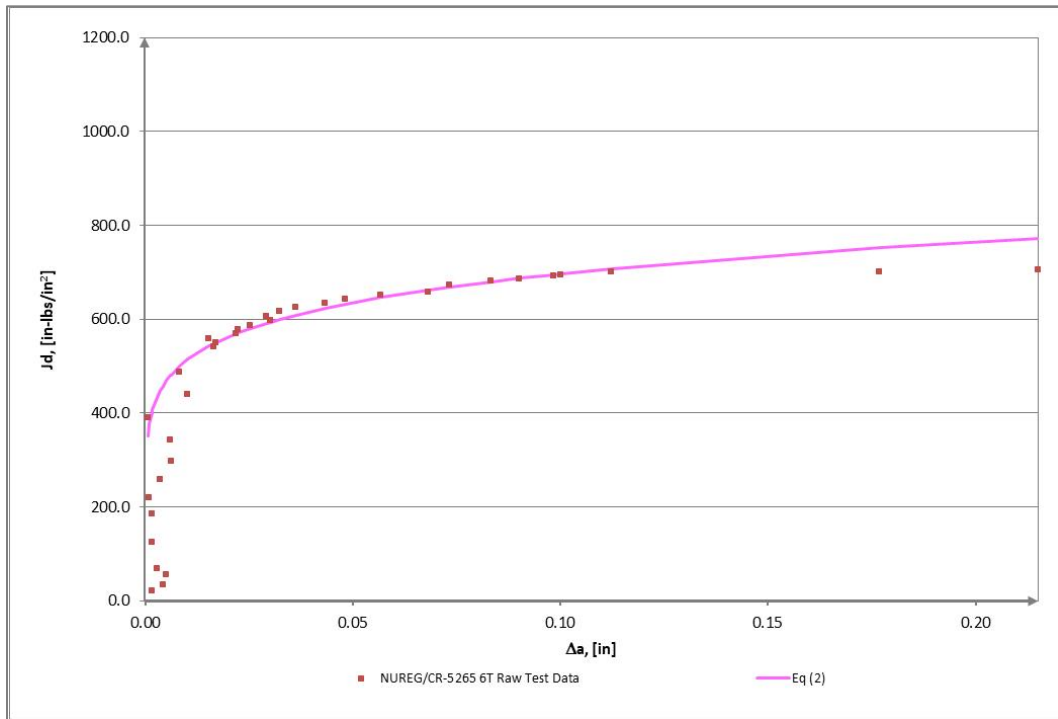
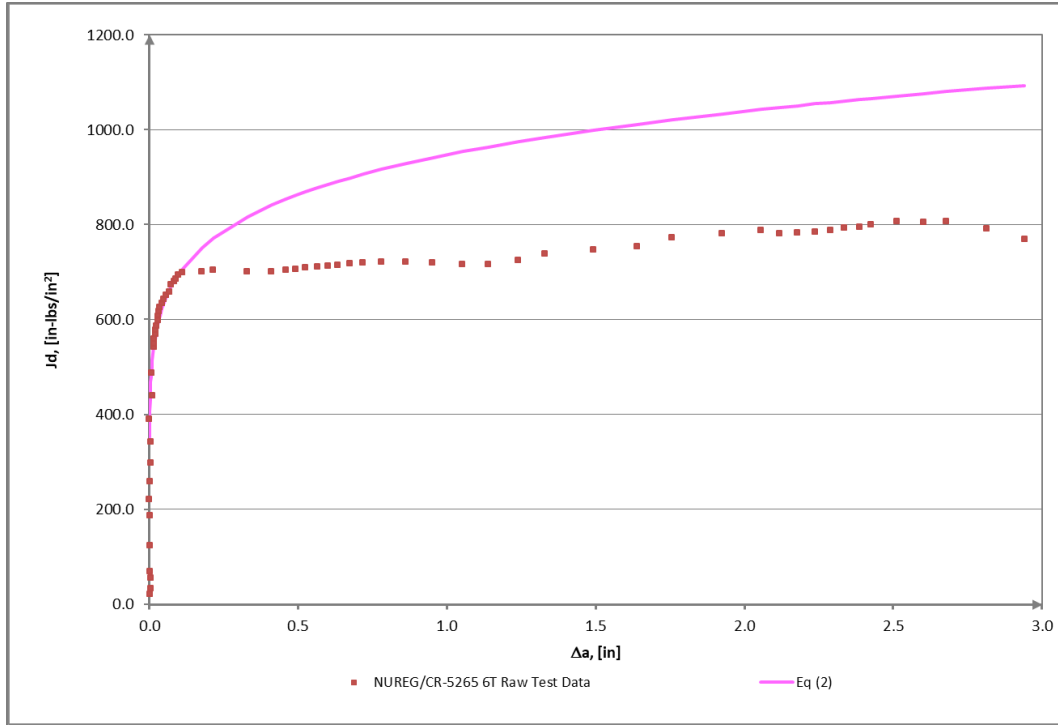


Figure 4-4: Hiser’s Power Law Fit Eq. (2) Relative to NUREG/CR-5265 6T Test Data

4.1.4 Statistical Uncertainty Factor (SF) Determination

The statistical uncertainty factor, Equation (1) above, cannot be determined directly as there are no statistical estimates of the statistical uncertainty factor (*SF*) for A302-B steel plate and a single specimen test. In accordance with Reference [7], the $f(CVN)$ factor that is a part of the J-R curve estimation equation (Eq. (1) and Eq. (3) of Section 4.1.3) is the mean correlation between $J_{0.1}$ and *CVN* based on Hiser's analysis of available A-302-B data, normalized to *CVN* = 50 ft-lbs. In Reference [18], Hiser developed the mean and the mean -2*S_e* correlations between $J_{0.1}$, corresponding to $\Delta a = 0.10$ in and *CVN*, and these correlations are shown in Figure C.6 of Reference [19] and reproduced in Figure 4-5 below. The correlations in Figure 4-5 have the following equations:

$$J_{0.1}(\text{mean}) = 108 + 11.75 \text{ CVN} \quad \text{Eq. (5)}$$

$$J_{0.1}(\text{mean}-2S_e) = -162 + 11.75 \text{ CVN} \quad \text{Eq. (6)}$$

Where $J_{0.1}$ is in in-lb/in² and *CVN* is in ft-lb.

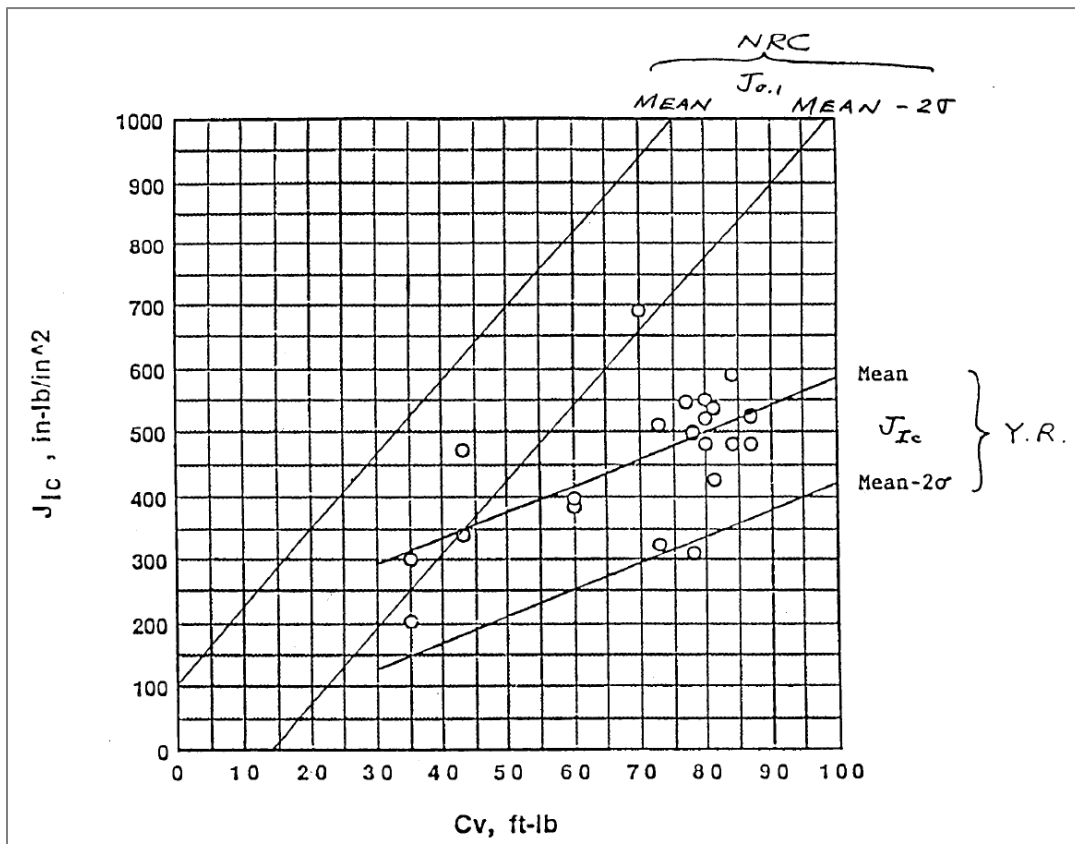


Figure 4-5: Least-Square Fit (Mean) and (Mean - 2 *S_e*) Lines, A-302-B Plate, L-T and T-L directions, 400 to 550°F

The $f(CVN)$ factor was obtained in Reference [7] by normalizing Eq. (5) to $J_{0.1(mean)}$ at $CVN = 50$ ft-lbs (see Figure 4-5) (i.e., $J_{0.1(mean)} = 108 + 11.75 \times 50$ ft-lbs = 695.5 in-lb/in²) to obtain the mean correlation $f(CVN)_{(mean)} = (11.75CVN + 108) / (695.5)$. Following this similar methodology, the mean $-2S_e$ $f(CVN)$ correlation can be calculated as $f(CVN)_{(mean-2Se)} = (11.75CVN - 162) / (11.75 \times 50$ ft-lbs - 162) = $(11.75CVN - 162) / (425.5)$. The only factor in Eq. (1) of Section 4.1.3 that involves statistical variability is $f(CVN)$. Therefore; for a given J-R curve, it is possible to write:

$$(SF) \times f(CVN)_{(mean)} = f(CVN)_{(mean-2Se)} \quad \text{Eq. (7)}$$

And solving Eq. (7) for (SF) gives:

$$(SF) = f(CVN)_{(mean-2Se)} / f(CVN)_{(mean)} = [(11.75CVN - 162) / (425.5)] / [(11.75CVN + 108) / (695.5)] \quad \text{Eq. (8)}$$

A plot of Eq. (8) (i.e., SF vs CVN), as presented in Figure 4-6, shows that SF values are less than 1.0 only for CVN values less than 50 ft-lbs. As reported in Section 3.3, the CVN values used for the development of the J-R Model of the PBNP Unit 1 IS Plate A9811-1 are 49 ft-lbs in the weak (T-L) direction and, 75.35 ft-lbs in the strong (L-T) direction. The CVN values in the strong direction are 75.35 ft-lbs and 90.23 ft-lbs at the bottom and top of the IS plate,

[

]

[

]



Figure 4-6: Statistical Uncertainty Factor (*SF*) vs Charpy V-notch (*CVM*) Distribution

4.1.5 IS Plate A9811-1 CVN-Review of RVID2

The NRC Reactor Vessel Integrity Database (RVID), Reference [20], summarizes the properties of the reactor vessel beltline materials for each operating U.S. commercial nuclear power plant. Table 4-1 lists the unirradiated *USE* (initial *CvUSE*) available in Reference [20] obtained for A-302-B base metal specimens through the direct method, which uses actual test data instead of other scaling methods such as the 65% method. The calculated *mean* – $2S_e$ value of the initial *CvUSE* is equal to *70.2 ft-lbs*, which is greater than *69.9 ft-lbs*. Therefore, the *CVN* value of *49 ft-lbs* (see Section 3.3.1) in the weak direction (circumferential flaws), is considered appropriate.

Table 4-1: Unirradiated USE RVID Database for Plate A-302-B Material			
Plant	Heat ID	Base Metal	Unirradiated USE (ft-lbs)
BIG ROCK POINT	19246-1	A-302-B	82
BIG ROCK POINT	19246-3	A-302-B	82
BIG ROCK POINT	19246-2	A-302-B	82
BIG ROCK POINT	19246-4	A-302-B	82
HADDAM NECK	A5887	A-302-B	105
HADDAM NECK	B0716	A-302-B	90
BIG ROCK POINT	19246-1	A-302-B	82
Mean =			87.2
Standard Deviation (S_e) =			8.5
Mean - 2(S_e) =			70.2

4.1.6 Final J-R Model for IS Plate A9811-1

Following the methodology outlined above, the IS Plate A9811-1 J-R curve (J-integral J_D vs crack extension Δa) is developed for a range of temperatures that fall within the applicable Service Levels A, B, C, and D transient temperatures (i.e., 100°F to 600°F) and are plotted in Figure 4-7, Figure 4-8 and Figure 4-9 for *CVN* values in the T-L (weak) and L-T (strong) directions, respectively.

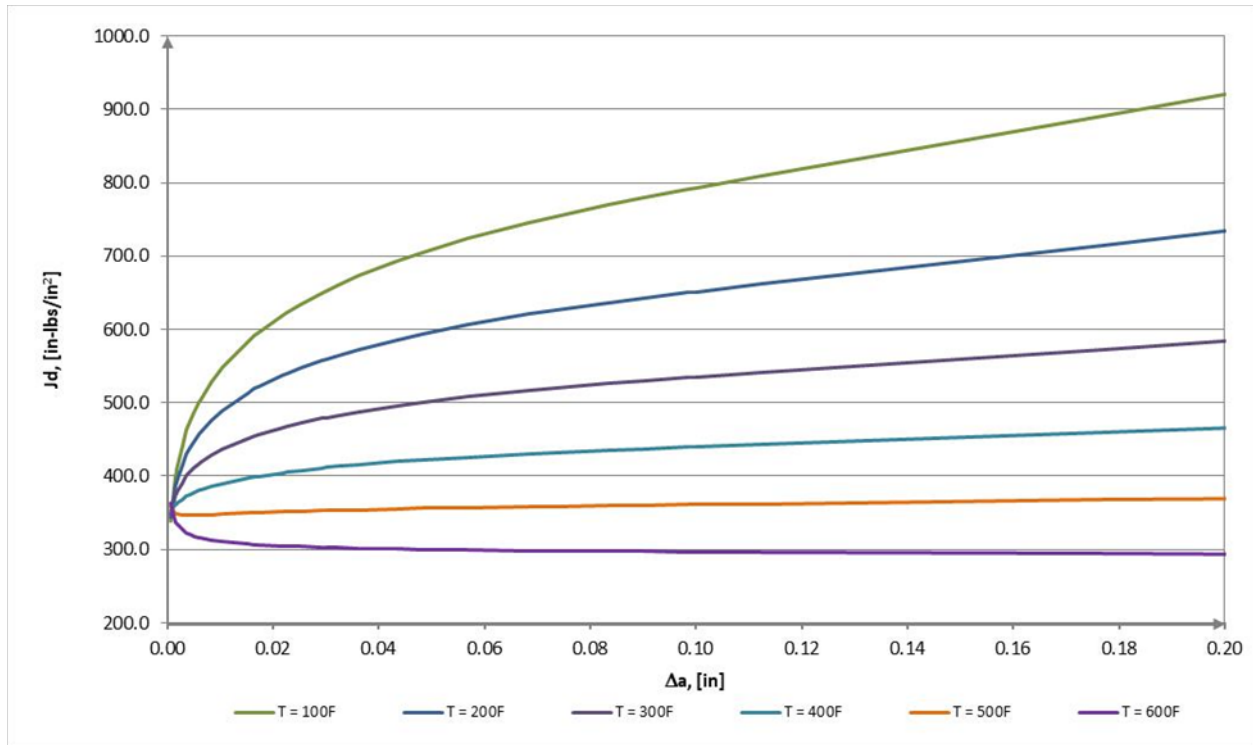


Figure 4-7: IS plate A9811-1 J-R Model, T-L (Weak) Direction Top and Bottom of Plate, 100°F to 600°F

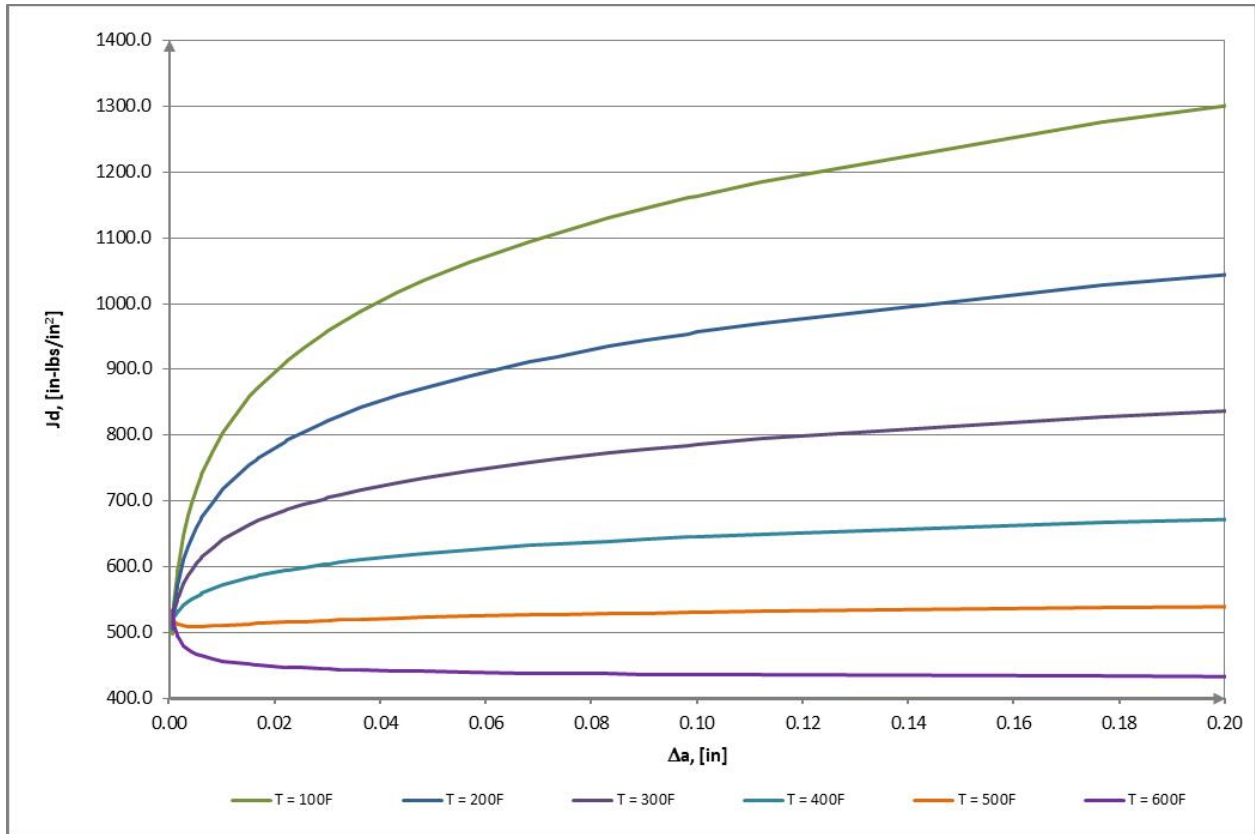


Figure 4-8: IS plate A9811-1 J-R Model, L-T (Strong) Direction, Bottom of Plate, 100°F to 600°F

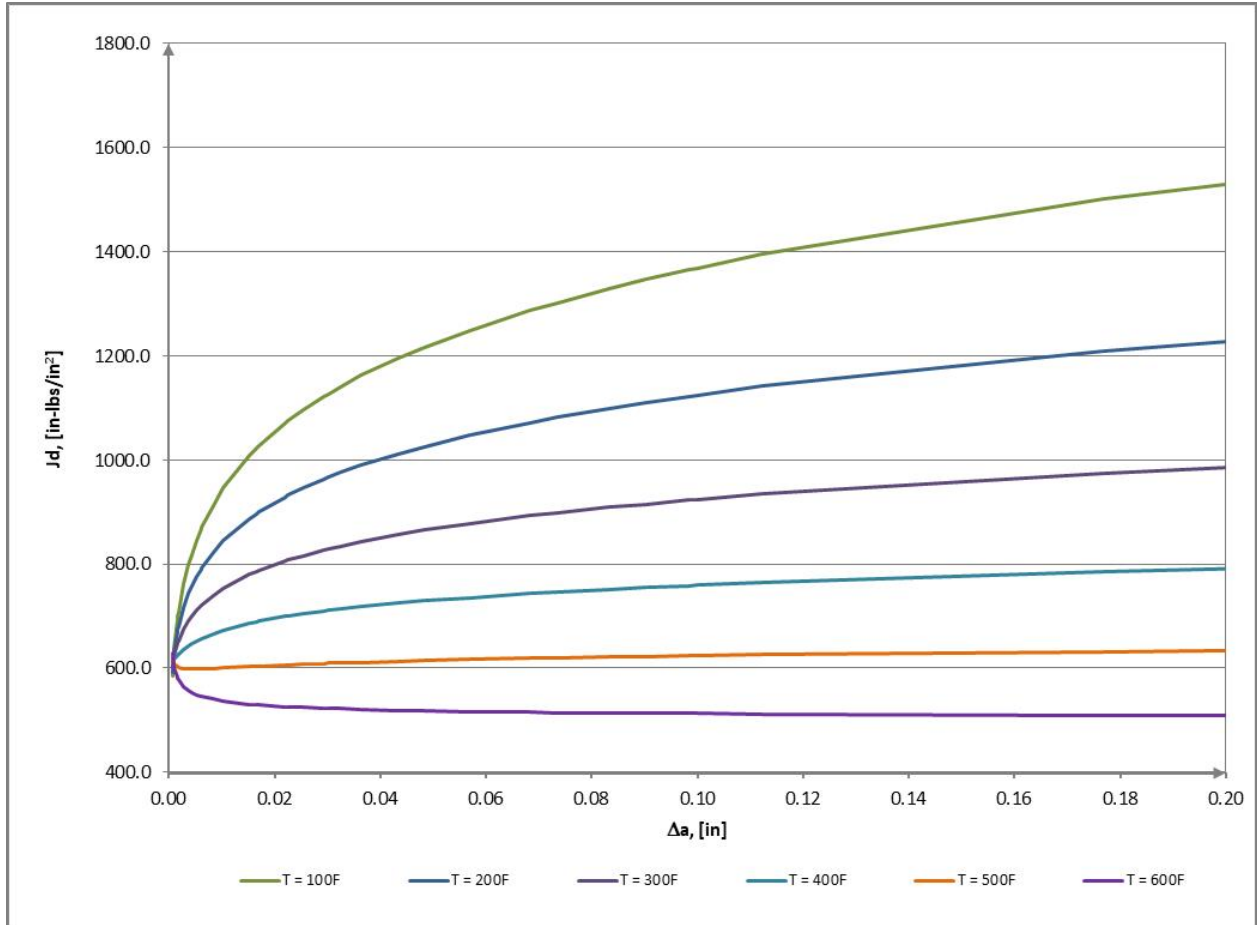


Figure 4-9: IS plate A9811-1 J-R Model, L-T (Strong) Direction, Top of Plate, 100°F to 600°F

4.2 MECHANICAL PROPERTIES OF IS PLATE A9811-1

As reported in Section 3.0, the material designation of the IS Plate A9811-1 is A-302 Class B (Mn-1/2Mo) and its chemical composition indicates that the sulfur content is 0.020 wt.%. The nickel content of the IS plate is 0.056%.

The values of yield strength (σ_y) and ultimate strength (σ_{ult}) of the IS Plate A9811-1 material used to calculate the flow stress for the tensile stability are obtained from Reference [21] at a conservative temperature of $650^\circ F$ and are listed below:

4.3 SELECTION OF LIMITING DESIGN TRANSIENTS--LEVELS A-D SERVICE LOADINGS

4.3.1 Levels A and B Service Loadings

Selection of the limiting design transients for Levels A and B Service Loadings is consistent with the PBN-specific supplement to BAW-2192, Revision 0, Supplement 3P, Revision 0 [3], Section 2.0, and is a cooldown from hot zero power at $100^\circ F/h$, which is consistent with ASME Section XI, Appendix K.

4.3.2 Levels C and D Service Loading

Selection of the limiting design transients for Levels C and D Service Loadings is consistent with the PBN-specific supplement to BAW-2178, Revision 0, Supplement 2P, Revision 0 [4], Section 4.3, i.e., the Equipment Specification (E-Spec) Steam Line Break (SLB) and FSAR SLB without offsite power.

5 FRACTURE MECHANICS ANALYSIS

5.1 METHODOLOGY

The methodologies and acceptance criteria for evaluation of postulated circumferential and axial flaws in IS plate A9811-1 is consistent with the following PBN-specific topical reports, with the exception that the J-integral resistance model described in Section 4.1 above is used for IS plate A9811-1.

For Level A and B Service Loads-BAW-2192, Revision 0, Supplement 3P, Revision 0, Sections 2.2.1, 5.1 and 5.2 [3]

For Level C and D Service Loads-BAW-2178, Revision 0, Supplement 2P, Revision 0, Sections 2.2.1, 5.1 and 5.2 [4]

5.2 EVALUATION FOR FLAW EXTENSION

5.2.1 Levels A and B Service Loadings

Initial flaw depth equal to 1/4 of the plate wall thickness is analyzed for service levels A and B loading conditions following methodology reported in Section 5.1 and values for the J-integral resistance of the material developed in Section 4.1. The results of the flaw evaluation for service levels A and B loading conditions, with an applied structural factor on pressure of 1.15, are presented in Table 5-1, where it is seen that the minimum ratio of material J-resistance ($J_{0.1}$) to applied J-integral (J_1) is [] for the limiting axial flaw and [] for the limiting circumferential flaw on the top of the IS plate A9811-1, which is greater than the minimum acceptable value of 1.0.

For the limiting axial and circumferential, the applied J-integral (J_1) with a structural factor of 1.25, at the reactor coolant temperature of [], and the results of the material lower bound J-integral resistance curve as a function of the flaw extension (J-R curve) developed in Section 4.1 are reported in Table 5-2 and Table 5-3 and plotted in Figure 5-1 and Figure 5-2. An evaluation line at a flaw extension 0.10 inch is used in Figure 5-1 and Figure 5-2 to confirm the results of Table 5-1 by showing that the applied J-integral values for a structural factor of 1.15 are less than the lower bound J-integral resistance values of the material at the limiting reactor coolant temperature of [] for the axial and circumferential flaws.

The requirement for ductile and stable crack growth is also demonstrated in Table 5-2 and Table 5-3 since the calculated slopes of the applied J-integral curve for a structural factor of 1.25 at a flaw extension 0.10 inch are less than the calculated slopes of the lower bound J-R curves at flaw extensions up to 0.10 inch at the corresponding reactor coolant temperature of []. Note that the applied J-integral (J_1) curves with a structural factor of 1.25 for the limiting circumferential and axial flaws are only available at the reactor coolant temperature of [].

Table 5-1: Flaw Evaluation for Levels A & B Service Loadings

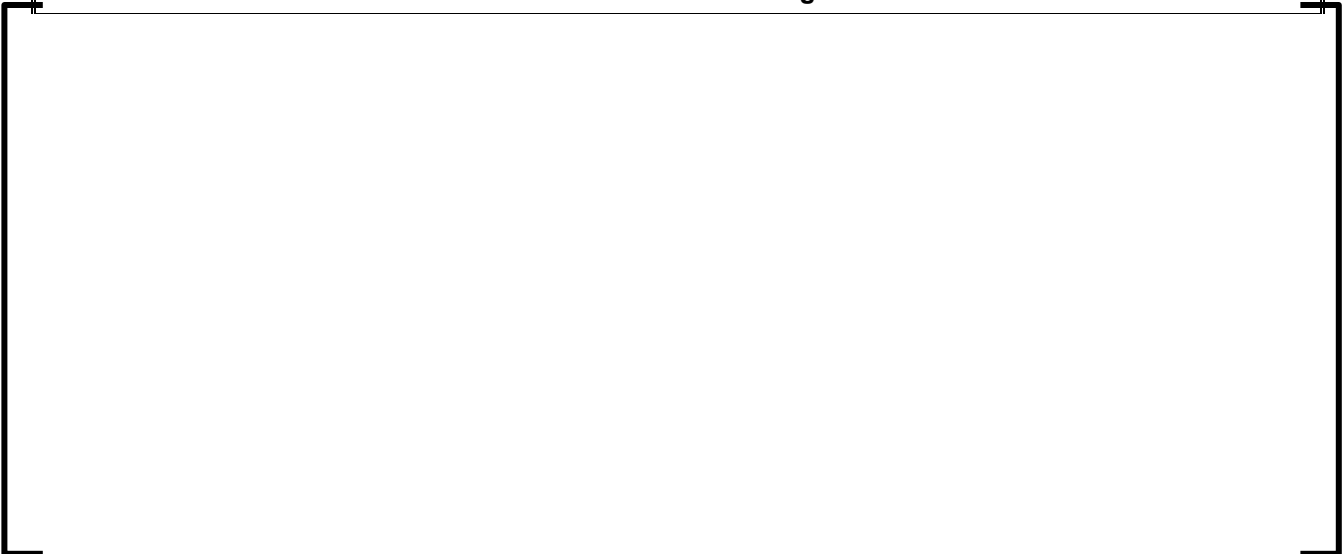


Table 5-2: Applied J-Integral versus Flaw Extension for Levels A & B Service Loadings for IS Plate A9811-1 Limiting Axial and Circumferential Flaws (SF = 1.25)

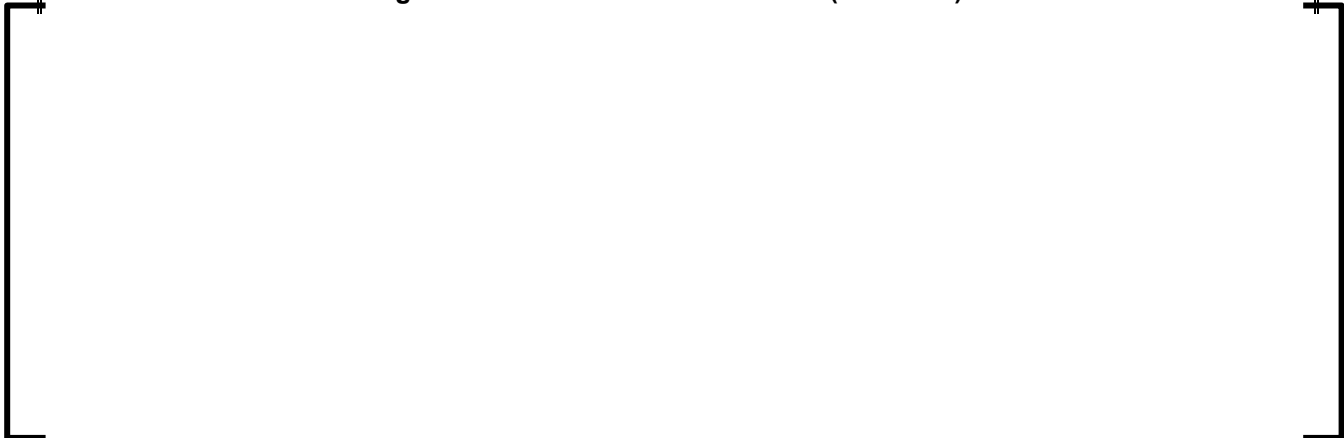


Table 5-3: Material J-Resistance versus Flaw Extension for IS Plate A9811-1 Limiting Axial and Circumferential Flaws

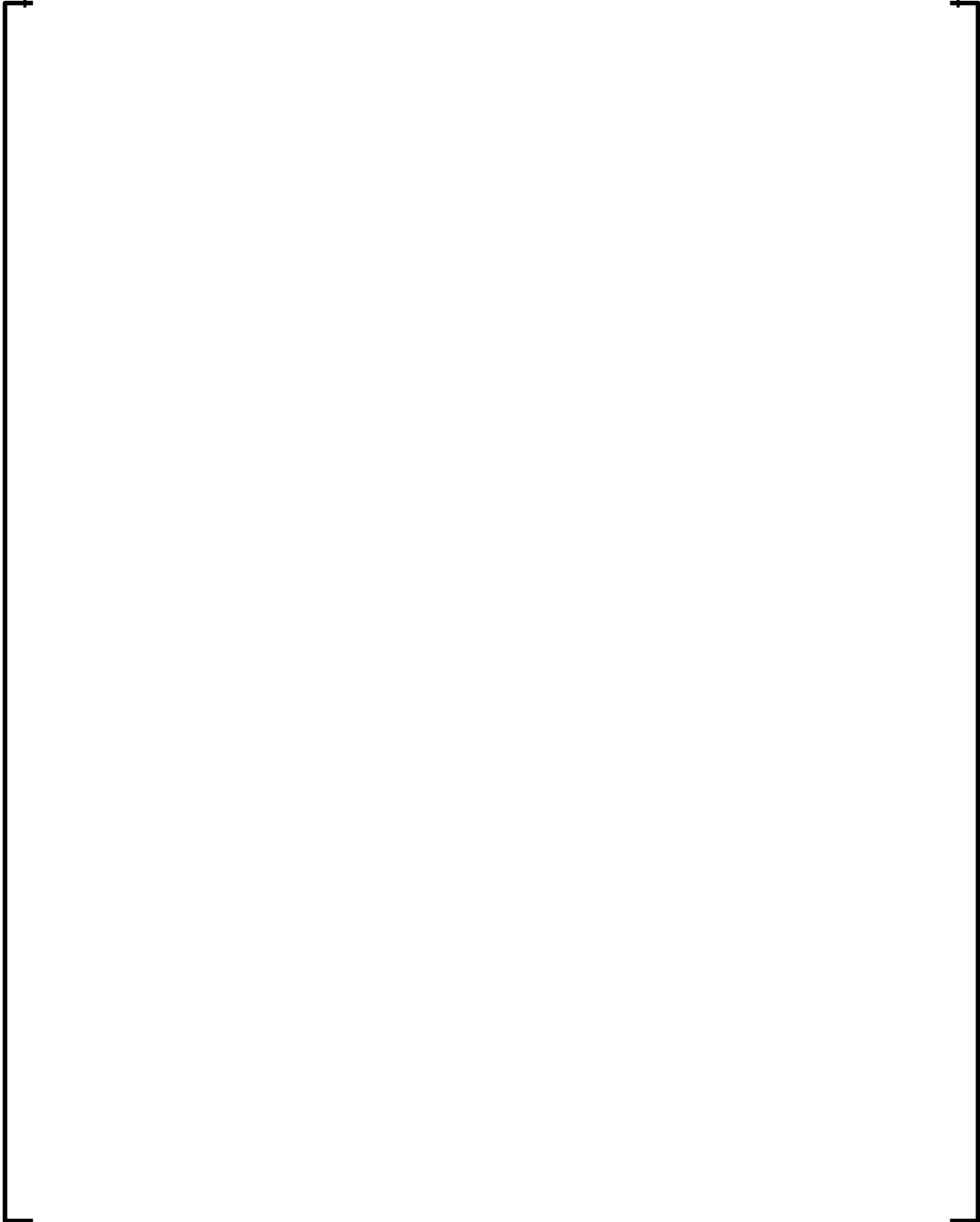




Figure 5-1: J-Integral versus Flaw Extension for Levels A & B Service Loadings for IS Plate A9811-1 – Limiting Axial Flaw



Figure 5-2: J-Integral versus Flaw Extension for Levels A & B Service Loadings for IS Plate A9811-1 – Limiting Circumferential Flaw

5.2.2 Levels C and D Service Loadings

Initial flaw depth equal to 1/10 of the plate wall thickness is analyzed for service levels C and D loading conditions following the methodology in Section 5.1 and values for the J-integral resistance of the material developed in Section 4.1. The results of the flaw evaluation for service levels C and D loading conditions, with an applied structural factor on loading of 1.0, are presented in Table 5-4 where it is seen that the minimum ratio of material J-resistance ($J_{0.1}$) to applied J-integral (J_I) is [] for the limiting axial flaw and [] for the limiting circumferential flaw of the IS plate A9811-1, which is greater than the minimum acceptable value of 1.0.

For the limiting axial and circumferential flaws, the applied J-integral (J_I) with a structural factor on loadings of 1.0, and the results of the material lower bound J-integral resistance curve as a function of the flaw extension (J-R curve) developed in Section 4.1 are reported in Table 5-5 and Table 5-6, and plotted in Figure 5-3 and Figure 5-4 at the applicable reactor coolant temperature of 324°F. An evaluation line at a flaw extension 0.10 inch is used in Figure 5-3 and Figure 5-4 to

confirm the results of Table 5-4 by showing that the applied J-integral values for a structural factor of 1.0 are less than the lower bound J-integral resistance values of the material at the limiting reactor coolant temperature as required by Appendix K of Section XI.

The requirements for ductile and stable crack growth (Article K-3400) are also demonstrated in Table 5-5 and Table 5-6 since the calculated slopes of the applied J-integral curve at a flaw extension 0.10 inch are less than the calculated slopes of the lower bound J-R curve at flaw extensions up to 0.10 inch at the corresponding reactor coolant temperature of 324°F.

In addition, per Article K-5300(b), for Level D Service Loadings, the total flaw depth after stable flaw extension shall be less than or equal to 75% of the vessel wall thickness, and the remaining ligament shall not be subject to tensile instability. The first part of the requirements established in K-5300(b) is satisfied since the applied J-integral curve intersects the J-R curve at calculated flaw extensions of 12% of the wall thickness for both the limiting axial and circumferential flaws.

Article K-5300(b) also requires that the remaining ligament is not subject to tensile instability. This requirement is satisfied by showing that the internal pressure, p , is less than the internal pressure at tensile instability of the remaining ligament, which for a circumferential and axial flaws are defined as,

$$P_{i,circ} = 1.07\sigma_0 \left[\frac{\left(1 - \frac{A_c}{A}\right)}{\left(\frac{R_i^2}{2R_m t}\right) + \frac{A_c}{A}} \right] \text{ (circumferential flaws)}$$

$$P_{i,axial} = 1.07\sigma_0 \left[\frac{\left(1 - \frac{A_c}{A}\right)}{\left(\frac{R_i}{t}\right) + \frac{A_c}{A}} \right] \text{ (axial flaws)}$$

where

σ_0 = flow stress = $(\sigma_y + \sigma_{ult}) / 0.2$ (σ_y and σ_{ult} are defined in Section 4.2)

A = area parameter = $t(l + t)$

A_c = area of the flaw = $\pi a l / 4$

R_i = inner radius of the vessel

R_m = mean radius of the vessel

t = wall thickness of the vessel

a = flaw depth

l = flaw length

An additional check is performed for circumferential flaws to ensure that internal pressure does not exceed the pressure at tensile instability caused by the applied hoop stress acting over the nominal wall thickness of the vessel. This validity limit on pressure is satisfied by

$$P_{i,circ} \leq 1.07\sigma_0 \frac{t}{R_i}$$

Table 5-7 presents the necessary calculations to demonstrate the remaining ligament is not subject to tensile instability using flaw depths ranging from 1% to 25% of the wall thickness. The internal pressures at tensile instability are calculated to be 11,570 *psi* for circumferential flaws and 5,583 *psi* for axial flaws at flaws with depth of 25% of the wall thickness. Additionally, the validity check on hoop stress requires that, for circumferential flaws, the internal pressure not exceed 6,402 *psi*, which is still much greater than any anticipated faulted condition pressure. Therefore, the flaw stability criteria established in Article K-5300(b) are met.

Table 5-4: Flaw Evaluation for Levels C & D Service Loadings

Table 5-5: Applied J-Integral versus Flaw Extension for Levels C & D Service Loadings for IS Plate A9811-1 Limiting Axial and Circumferential Flaws (SF = 1.0)

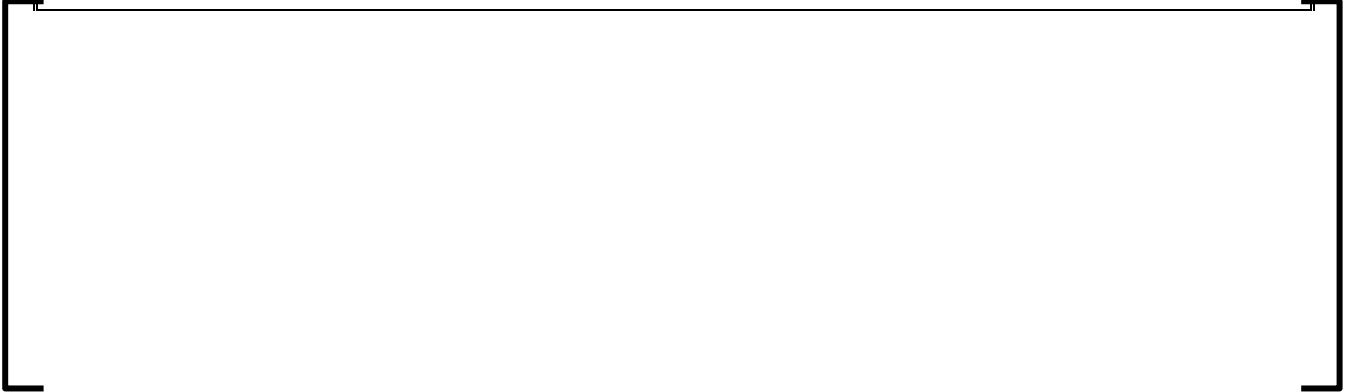


Table 5-6: Material J-Resistance versus Flaw Extension for IS Plate A9811-1 Limiting Axial and Circumferential Flaws (T = 324°F)

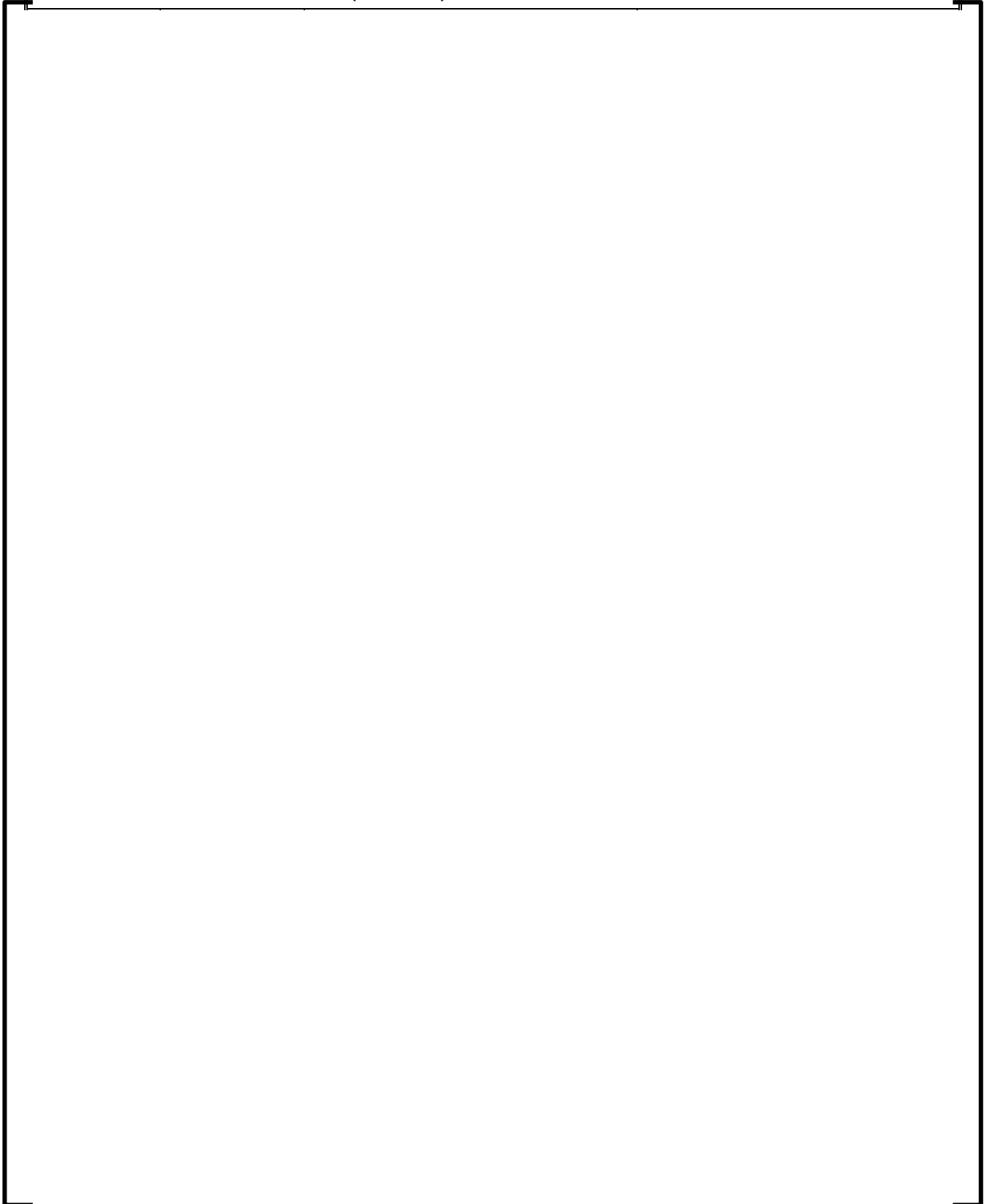




Figure 5-3: J-Integral versus Flaw Extension for Levels C & D Service Loadings for IS Plate A9811-1 – Limiting Axial Flaw

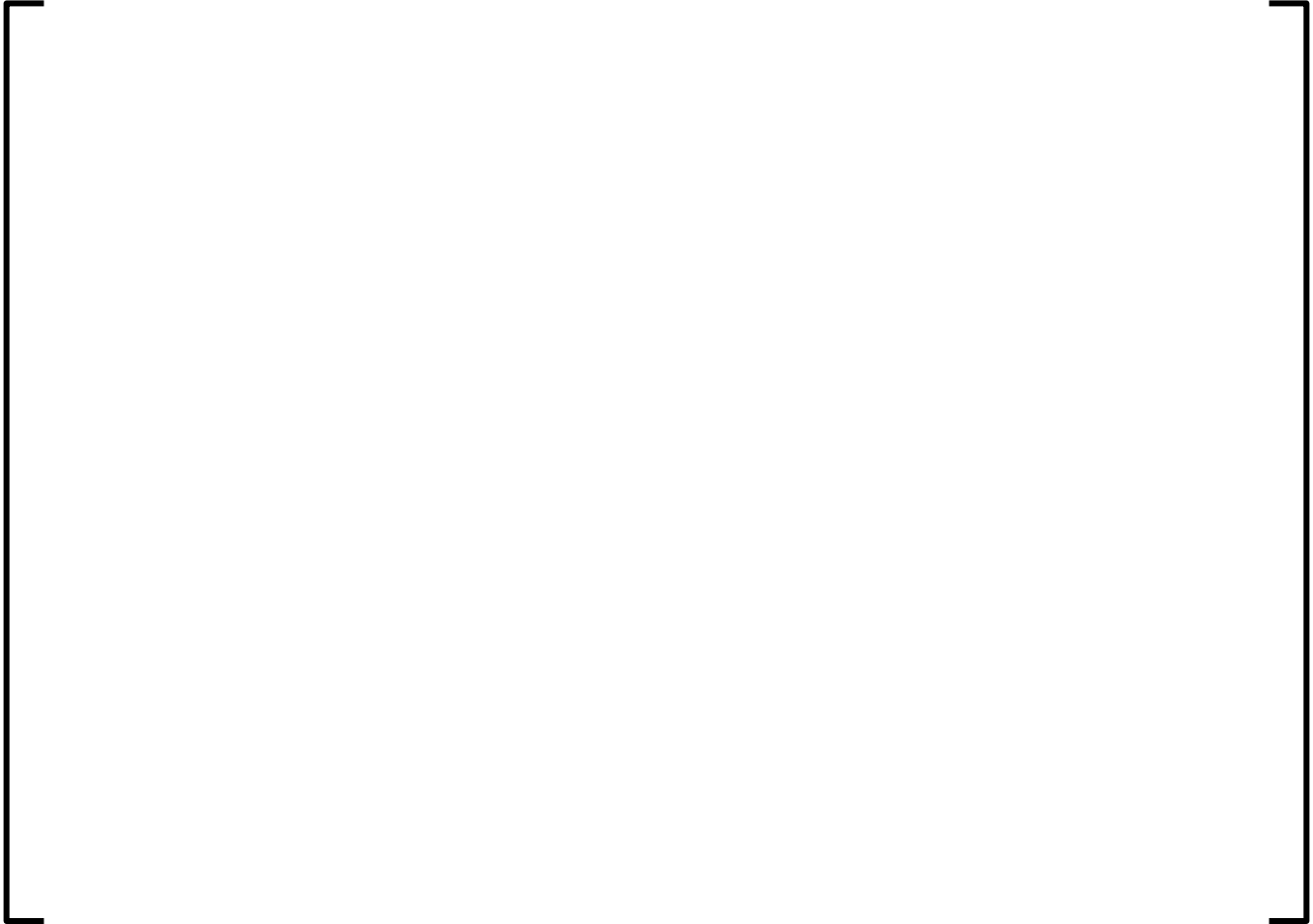
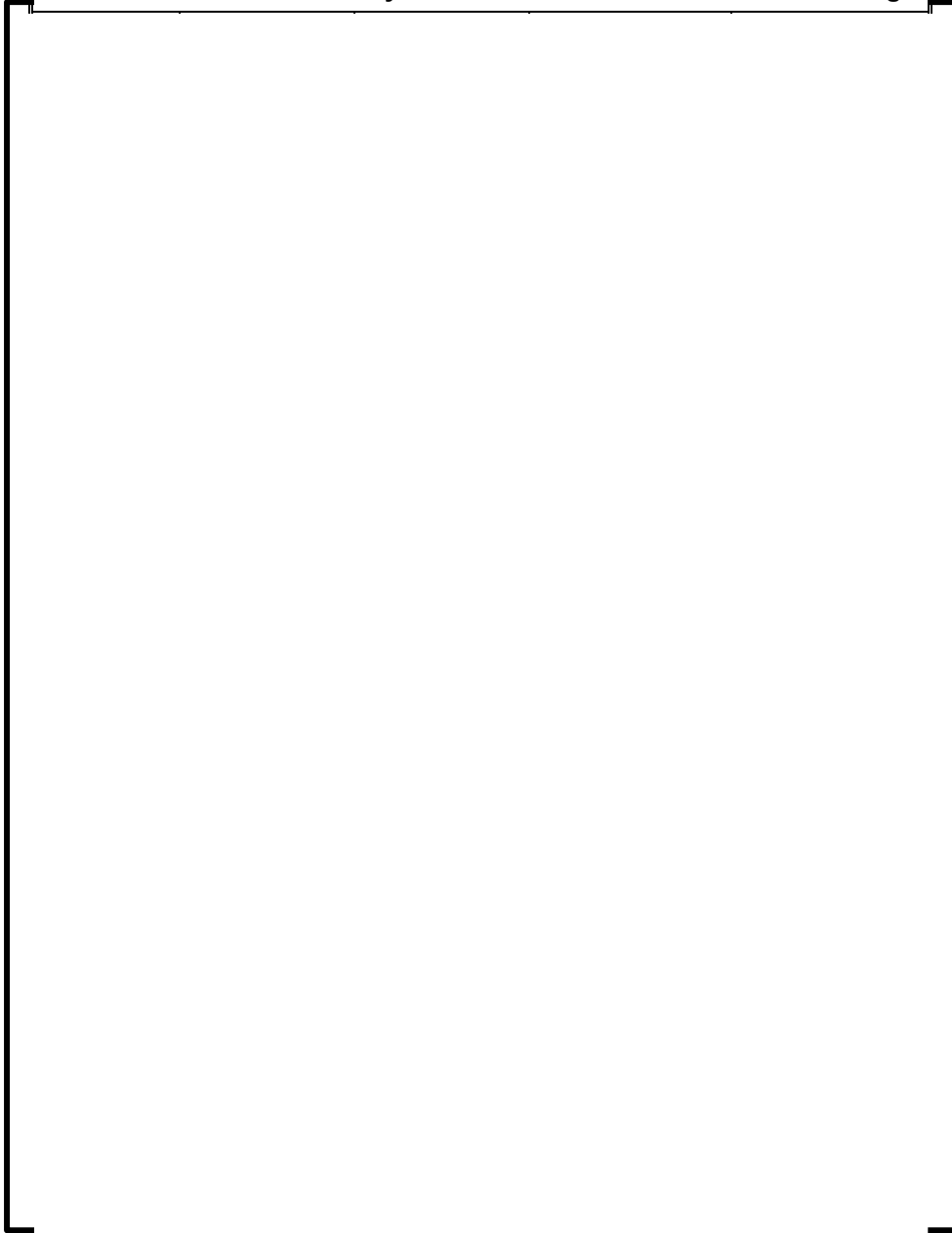


Figure 5-4: J-Integral versus Flaw Extension for Levels C & D Service Loadings for IS Plate A9811-1 – Limiting Circumferential Flaw

Table 5-7: Tensile Instability Check for Levels C & D Service Loadings



6 SUMMARY AND CONCLUSIONS

As reported in Section 1.0, PBN Unit 1 IS plate (heat A9811-1) has a predicted 72 EFPY USE value that is just below 50 ft-lbs at 80-years; all remaining beltline and extended beltline plate and forging materials for Units 1 and 2 are above 50 ft-lbs at 72 EFPY. IS plate A9811-1 is made from A302B plate material with sulfur content of 0.02% and nickel content of 0.056%. In addition, it was confirmed that IS plate A9811-1 has a predicted USE greater than 50 ft-lbs at 53 EFPY (60-years) using Regulatory Guide 1.99 Revision 2, Position 2.2. Therefore, a 72 EFPY EMA is required for IS plate A9811-1 to demonstrate compliance with 10 CFR 50, Appendix G, for subsequent license renewal.

The analytical procedure used for the 72 EFPY equivalent margins analysis of PBN Unit 1 IS plate A9811-1 is in accordance with ASME Section XI, Appendix K, 2017 Edition, with selection of design transients based on the guidance in Regulatory Guide 1.161. The methodology for calculation of J_{applied} for IS plate A9811-1 is consistent with the methodology used to calculate J_{applied} for Linde 80 welds [3, 4]; both axial and circumferential flaws are postulated in IS plate A9811-1. The J-integral resistance model used for IS plate A9811-11 is from NUREG/CR-5265, Specimen V-50-101, 6T, adjusted for temperature and use of the CVN model in accordance with Reference [7]. Regulatory Guide 1.161 [2], Equations (26)-(29), are used to develop the temperature and crack extension indexing reported in Reference [7].

Temperatures used to adjust NUREG/CR-5265 J-R Specimen V-50-101 data are consistent with the temperatures reported in BAW-2192, Supplement 3P, Revision 0 [3], for Levels A and B Service Loads, and in BAW-2178, Supplement 2P, Revision 0 [4], for Levels C and D Service Loads. CVN values used to adjust Specimen V-50-101, 6T, are 49 ft-lbs in the weak direction (for circumferential flaws) and 75.35 ft-lbs in the strong direction (for axial flaws). A statistical uncertainty factor applied to the temperature/CVN indexing of J-R specimen V50-101 of 1.0 was selected based on comparison of recent 302B plate J-R test data for a San Onofre high sulfur A302B plate, heat A0399 [17] with sulfur content of 0.0195%, irradiated to a fluence of $3.85E+19$ n/cm², to CVN values obtained using Regulatory Guide 1.161, Equations (26)-(29). Results of the EMA for Unit 1 IS plate A9811-1 are summarized below.

Levels A & B Service Loads

- The applied J-integral values for the assumed 1/4-thickness inside-surface for axial and circumferential flaws in IS plate (A9811-1) with a safety margin of 1.15 on pressure loading is within the material fracture toughness J-resistance at 0.1-inch crack extension. The limiting ratios $J_{0.1}/J_1$ are [] for an axial flaw and [] for a circumferential flaw, which are greater than the required value of 1.0.
- With a structural factor of 1.25 on pressure and 1 on thermal loading, flaw extensions are ductile and stable since the slope of the applied J-integral curve is less than the slope of the lower bound J-R curve at the point where the two curves intersect.

Levels C & D Service Loads

- With a structural factor of 1 on loading, the applied J-integral (J_1) for the IS plate (A9811-1) postulated circumferential and axial flaws are less than the lower bound J-integral of the material at a ductile flaw extension of 0.10 inch ($J_{0.1}$) with a limiting ratio $J_{0.1}/J_1$ is [] for an axial flaw, which is greater than the required value of 1.0.
- With a structural factor of 1 on loading, flaw extensions are ductile and stable for the IS plate (A9811-1) postulated circumferential and axial flaws since the slope of the applied J-integral curve is less than the slopes of both the lower bound and mean J-R curves at the points of intersection.
- For the postulated circumferential and axial flaws in IS plate (A9811-1), are stable at much less than 75% of the vessel wall thickness. Also, the remaining ligament is sufficient to preclude tensile instability by a large margin.

The margins ($J_{0.1}/J_1$) at 72 EFPY for PBN Unit 1 IS plate A9811-1 for Service Loads A-B are approximately similar (Linde 80 Weld SA-812 at [] versus [] for IS Plate A9811-1). The margins ($J_{0.1}/J_1$) at 72 EFPY for PBN Unit 1 IS plate A9811-1 for Service Loads C-D are approximately similar (Linde 80 Weld SA-812 at [] versus [] for IS Plate A9811-1).

7 REFERENCES

1. 2017 Edition ASME & Boiler Pressure Vessel Code, Section XI, Rules for Inservice Inspection of Nuclear power Plant Components, Appendix K.
2. Regulatory Guide 1.161, Evaluation of Reactor Pressure Vessels with Charpy Upper-Shelf Energy Less Than 50 ft-lbs.
3. Framatome document BAW-2192, Revision 0, Supplement 3P, Revision 0.
4. Framatome document BAW-2178, Revision 0, Supplement 2P, Revision 0.
5. Eason, E. D., J. E. Wright, and E. E. Nelson, "Multivariable Modeling of Pressure Vessel and Piping J-R Data," NUREG/CR-5729, MCS 910401, RF, R5, May 1991.
6. A. L. Hiser and J. B. Terrell, "Size Effects on J-R Curves for A 302-B Plate," NUREG/CR-5265, MEA-2320, RF, R5, Jan. 1989.
7. TECHNICAL EVALUATION REPORT (TER): REVIEW OF NMPC PROJECT 03-9425 REPORTS, "ELASTIC-PLASTIC FRACTURE MECHANICS ASSESSMENT OF NINE MILE POINT UNIT 1 BELTLINE PLATES FOR SERVICE LEVEL A AND B LOADINGS (MPM-USE-129215) AND SERVICE LEVEL C AND D LOADINGS (MPM-USE-293216)", ADAMS Accession number ML17059A282.
8. Code of Federal Regulations, Title 10, Part 50 – Domestic Licensing of Production and Utilization Facilities, Appendix G – Fracture Toughness Requirements, Federal Register Vol. 60. No. 243, December 19, 1995.
9. 2017 Edition ASME & Boiler Pressure Vessel Code, Section II, Materials, Part D.
10. Dockets 50-266 and 50-301, Generic Letter 92-01, Revision 1, Reactor Vessel Structural Integrity, Point Beach Nuclear Plant, Units 1 and 2, June 27, 1994, ADAMS Accession Number ML20070C816.
11. BAW-2222, Reactor Vessel Working Group Response to Closure Letters to NRC Generic Letter 92-01, Revision 1, ADAMS Accession (Legacy) Number 9407060101 and 9407010286.
12. WCAP-7513, S. E. Yanichko, "Wisconsin Michigan Power Co. Point Beach Unit 1 Reactor Vessel Radiation Surveillance Program," June, 1970.
13. Branch Technical Position 5-3, Fracture Toughness Requirement, draft Revision 3-July 2018.
14. NRC memo from C.Z. Serpan to C.Y. Cheng, Ratio of Transverse to Longitudinal Orientation Charpy Upper Shelf Energy, ADAMS Accession Number ML14324A919.
15. WCAP-17651-NP, Palisades Nuclear Power Plant Reactor Vessel Equivalent Margins Analysis, ADAMS Accession Number 13295A541.

-
16. D. E. McCabe, E. T. Manneschildt, and R. L., Swain, "Ductile Fracture Toughness of Modified A 302 Grade B Plate Materials," US NRC NUREG/CR-6426, Volumes 1 and 2, January and February 1997.
 17. Materials Reliability Program: Upper-Shelf Fracture Toughness of Irradiated Reactor Pressure Vessel Steel (MRP-439), Report No.: 3002016010, December, 2019.
 18. A. L. Hiser, NRC, "Summary of Fracture Toughness Estimates for Irradiated Yankee Rowe Vessel Materials," letter to C. Y. Cheng, NRC, with attachment, August 30, 1990.
 19. R. D. Cheverton, T. L. Dickson, J. G. Merkle, R. K. Nanstad, "Review of Reactor Pressure Vessel Evaluation Report for Yankee Rowe Nuclear Power Station (YAEC No. 1735)," US NRC NUREG/CR-5799, March 1992.
 20. NRC Reactor Vessel Integrity Database Version 2.0.1, distributed as a Microsoft Excel spreadsheet at <https://www.nrc.gov/reactors/operating/ops-experience/reactor-vessel-integrity/database-overview.html> (This database includes updates from June 1999 to July 2000).
 21. ASME Boiler and Pressure Vessel Code, Section II, Materials, Part D, Properties (Customary), 2017 Edition.

Point Beach Nuclear Plant Units 1 and 2
Dockets 50-266 and 50-301
NRC 2020-0032 Enclosure 4, Attachment 7

Enclosure 4
Non-proprietary Reference Documents and
Redacted Versions of Proprietary Reference
Documents
(Public Version)
Attachment 7

**Structural Integrity Associates, Inc. Report
No.2000088.401, Revision 2, “Cycle Counts and
Fatigue Projections for 80 Years of Plant Operation
for Point Beach Nuclear Units 1 and 2,” October 19,
2020**

(13 Total Pages, including cover sheets)



REPORT NO. 2000088.401
REVISION: 2
PROJECT NO. 2000088.00
October 2020

Cycle Counts and Fatigue Projections for 80 Years of Plant Operation for Point Beach Nuclear Units 1 and 2

Prepared For:

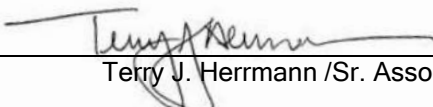
NextEra Point Beach, LLC
Point Beach Nuclear Units 1 and 2
Two Rivers, WI

Contract No. 02410780

Prepared By:


Structural Integrity Associates, Inc.
San Jose, CA

Prepared by:


Terry J. Herrmann / Sr. Associate

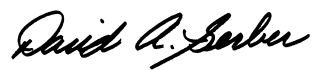
Date: 10/19/2020

Reviewed by:


David A. Gerber / Sr. Associate

Date: 10/19/2020

Approved by:


David A. Gerber / Sr. Associate

Date: 10/19/2020

REVISION CONTROL SHEET

Report Number: 2000088.401

Title: Cycle Counts and Fatigue Projections for 80 Years of Plant Operation for Point Beach Nuclear Units 1 and 2

Client: NextEra Point Beach, LLC

SI Project Number: 2000088.00

Quality Program: Nuclear Commercial

SECTION	PAGES	REVISION	DATE	COMMENTS
All	All	0	5/15/2020	Initial Issue
1 2 3	1-1 2-2, 2-3, 2-6 & 2-7 3-1	1	8/18/2020	Revised to address Pressurizer Spray Piping (see CAR-20-020)
3	2-7 3-1	2	10/19/2020	Revise TLAA Disposition for Pressurizer Spray Piping. Revision number unchanged for 10/19/2020 editorial update to 10/1/2020 version to correct TLAA disposition from (i) to (iii) on page 2-7).



TABLE OF CONTENTS

1	INTRODUCTION	1-1
2	METAL FATIGUE	2-1
2.1	Metal Fatigue of Class 1 Piping Components	2-1
3	REFERENCES	3-1

LIST OF TABLES

Table 2.1-1.	60-Year Cumulative Fatigue Usage.....	2-2
Table 2.1-2.	80-Year Projection Parameters	2-4
Table 2.1-3.	80-Year Projected Cumulative Fatigue Usage.....	2-7
Table 2.1-3.	80-Year Projected Cycles - PBN Units 1 and 2	2-5



1 INTRODUCTION

NextEra Point Beach, LLC (NEPB) is in the process of developing and submitting a subsequent license renewal (SLR) application that would extend plant operations at Point Beach Units 1 and 2 from 60 to 80 years. The preparation includes the development and submittal of an SLR application (SLRA), and subsequent NRC review concluding in a renewed operating license for both units.

The SLR process follows a similar process as the first Point Beach (PBN) license renewal application (LRA) submitted in 2004. As a result of the first LRA submittal, the NRC issued operating licenses in June 2005 to operate an additional 20 years beyond the original 40 year operating licenses.

Starting from previous cycle count and fatigue usage work performed by SI, plant instrument data is analyzed to achieve a cycle count as of December 2019 for currently configured transients and components monitored by FatiguePro. These are then projected for the 80-year subsequent period of extended operation (SPEO).

This report provides information for inclusion in the SLRA related to transient cycle counts and cumulative usage factors (CUFs) based on engineering calculations and evaluations associated with metal fatigue of Class 1 piping Time-Limited Aging Analyses (TLAAs).

Note: SI's scope of work is limited to Class 1 piping having fatigue analyses. Piping and components designed in accordance with ANSI B31.1 design rules which are not required to have an explicit analysis of cumulative fatigue usage are not included. Reactor vessels, reactor vessel internals, pressurizers, steam generators and reactor coolant pumps must be addressed separately.

The pressurizer spray piping is an additional piping location included in Revision 1 of this report per SI CAR-20-020 [9]. Fatigue usage of the spray piping was calculated to evaluate the effect of thermal stratification for piping evaluated in response to NRC Bulletin 88-08 [10, 11]. This location was identified as the limiting location for PBN in [12, Section 4.3.8].



2 METAL FATIGUE

The thermal and mechanical fatigue analyses of plant mechanical components have been identified as time-limited aging analyses for PBN. Specific components have been designed considering transient cycle assumptions, as listed in vendor specifications and the PBN UFSAR.

Fatigue analyses are considered TLAA's for Class 1 and non-Class 1 mechanical components. Fatigue is an age-related degradation mechanism caused by cyclic stressing of a component by either mechanical or thermal stresses.

The aging management reviews in SLRA Section 3 will identify mechanical components that are within the scope of license renewal and are subject to aging management review. This section evaluates the piping-related fatigue analyses for those components where the tables in SLRA Section 3 identify "TLAA - Metal Fatigue" as the aging management program. Evaluation of the TLAA per 10 CFR 54.21(c)(1) [1] determines whether

- (i) the analyses remain valid for the SPEO,
- (ii) the analyses have been projected to the end of the SPEO, or
- (iii) the effects of aging on the intended function(s) will be adequately managed for the SPEO.

Documentation of the evaluation of Class 1 piping component fatigue analyses is provided in Section 2.1 (for inclusion in SLRA Section 4.3.1 along with input from others for other Class 1 component locations).

Note: Evaluation of environmentally assisted fatigue (EAF) is documented in a separate report.

2.1 Metal Fatigue of Class 1 Piping Components

TLAA Description

The Class 1 piping component fatigue analyses for PBN have been performed in accordance with the requirements of the ASME Boiler and Pressure Vessel Code, Section III, Class 1. The ASME Boiler and Pressure Vessel Code, Section III, Class 1 requires a design analysis to address fatigue and establish limits such that initiation of fatigue cracks is precluded.

Fatigue analyses were prepared for these components to determine the effects of cyclic loadings resulting from changes in system temperature, pressure, and seismic loading cycles. These ASME Section III, Class 1 fatigue analyses are based upon explicit numbers and amplitudes of thermal and pressure transients described in the design specifications. The intent of the design basis transient cycle definitions is to bound a wide range of possible events with varying ranges of severity in temperature, pressure, and flow. The fatigue analyses were required to demonstrate that the cumulative usage factor (CUF) will not exceed the design allowable limit of 1.0 when the equipment is exposed to all of the postulated transients. Considering the calculation of fatigue usage factors is part of the current licensing basis and is



used to support safety determinations, and the number of occurrences of each transient type was based upon 60-year assumptions, these Class 1 fatigue analyses have been identified as TLAAs requiring evaluation for the SPEO.

TLAA Evaluation

Where fatigue usage calculations were performed for Class 1 piping components, they were performed in accordance with the requirements of the ASME Boiler and Pressure Vessel Code, Section III, Class 1.

The Electric Power Research Institute (EPRI) FatiguePro software program, part of the Fatigue Monitoring Program described in the PBN License Renewal Application [2, Appendix B] is used to obtain cycle count and fatigue usage information for selected Class 1 piping component locations. Fatigue usage is calculated using either a cycle-based fatigue (CBF) or stress-based fatigue (SBF) approach. The CBF approach populates a previously-developed design fatigue table with counted transient cycles. The SBF approach uses algorithms developed from a detailed finite element analysis where actual plant data is used to determine a stress response and calculate actual fatigue usage.

The current 60-year fatigue CUFs for the PBN Units 1 and 2 Class 1 piping component locations are presented in Table 2.1-1 (most limiting CUF from Unit 1 or 2). This table was prepared using the CUF values for the Class 1 piping component locations from Reference [3, Table 10] and [10].

Table 2.1-1. 60-Year Cumulative Fatigue Usage

Location	CUF (60 yr)
Pressurizer Surge Line	0.0383
Charging Nozzle	0.1182
Safety Injection Nozzle	0.0072
RHR / SI Tee	0.0142
Pressurizer Spray Piping	0.277

Design Cycles

The design cycles were intended to be conservative and bounding for all foreseeable plant operational conditions. The design cycles were utilized in the design stress reports for various Class 1 piping components satisfying ASME fatigue usage design requirements. Design cycles are identified in UFSAR Table 4.1-8 [4] and the Class 1 piping fatigue analyses.

Experience has shown that actual plant operation is conservatively represented by these design cycles. The use of actual operating history data allows the quantification of these conservatisms in the existing fatigue analyses. To demonstrate that the Class 1 component fatigue analyses

remain valid for the SPEO, the design cycles applicable to the Class 1 components from the UFSAR were reviewed.

The actual frequency of occurrence for the design cycles was determined and projections of the number of design cycles for both PBN units to 80 years of operation were made as a function of the average accumulation rate to-date and a shorter-term average accumulation rate. Because the accumulation behavior of more recent plant operations is expected to be a better predictor of future operation, it is generally weighted more heavily than the average accumulation rate. The following combinations of LTW/STW/Short Term Period parameters are used in the projections, as given in Table 2.1-2. The reasons for these combinations are described below.

1/0/12: this is the linear projection over all years. This category is for “random” accident events; they have a low number of current cycles, and are mostly independent from changing plant operation, so there is no rationale to emphasize the recent history.

1/1/12: this is the most used combination; standard weights—gives some emphasis to recent events presuming (a) the automatic cycle counting algorithms are more rigorous, and (b) operation procedures change slowly over time, so recent history is more predictive of the future.

1/2/12: this is used for Loss of Charging Flow and Loss of Letdown Flow to give extra emphasis to the period counted with FP3, because the counting before implementation of the FatiguePro software was less accurate.

2/1/12: this is used for a single transient where the projection line was too flat using the default 1/0/12 parameters, because no events were identified in the 12-year update, so additional LTW was included to increase the projected numbers.

3/1/12: this weighting is used for 2 leak test transients because these events are still expected to occur although they did not occur in the past 12-year period. This circumstance was accommodated by increasing the LTW to de-emphasize the STW.

The 80-year cycle projections are presented in Table 2.1-3 for Units 1 and 2. The bounding value for each unit is shown. These values are presented in the column entitled “Projection Upper Bound”. The column labeled “Suggested Allowable Cycles” provides values of cycles that would form a reasonable basis for a maximum set of transients for analysis and which provides margin to account for potential increased rate later in the SPEO.

In the case of transient cycles monitored by the FatiguePro program (transients 1 through 25), the future projected cycles to 80 years are added to the cycle counts through December 2019 and compared to the design cycles. Details of the evaluation of projected cycles for PBN Units 1 and 2 for 80 years are documented in Reference [5].

In the case of cycles used in the analysis of the pressurizer spray piping, stratification cycles are conservatively projected based on thermocouple data with a leaking spray control valve that is assumed to continue to leak throughout 80 years of plant operation [10, Section 7].



Table 2.1-2. 80-Year Projection Parameters

Row	Transient	Projection Parameters
1	10% Step Load Decrease	1 / 1 / 12
2	10% Step Load Increase	1 / 1 / 12
3	50% Step Load Decrease	1 / 1 / 12
4	Accumulator Safety Injection	1 / 0 / 12
5	Auxiliary Spray Actuation	1 / 1 / 12
6	HPSI Injection	1 / 0 / 12
7	Inadv. ACC Blowdown	1 / 0 / 12
8	Inadv. RCS Depressurization	1 / 0 / 12
9	Loss of Charging Flow	1 / 2 / 12
10	Loss of Letdown Flow	1 / 2 / 12
11	PZR Cooldown	1 / 1 / 12
12	PZR Heatup	1 / 1 / 12
13	Primary Side Hydrostatic Test	1 / 0 / 12
14	Primary Side Leak Test	1 / 1 / 12
15	Primary to Secondary Leak Test	3 / 1 / 12
16	RCS Cooldown	1 / 1 / 12
17	RCS Heatup	1 / 1 / 12
18	RPV Safety Injection	1 / 0 / 12
19	Reactor Trip	1 / 1 / 12
20	Refueling	1 / 1 / 12
21	Relief Valve Actuation	2 / 1 / 12
22	Secondary to Primary Leak Test	3 / 1 / 12
23	Trip Due to Loss of RC Pump	1 / 0 / 12
24	Unit Loading 5%/min	1 / 1 / 12
25	Unit Unloading 5%/min	1 / 1 / 12

Footnote:

Projection Parameters = LTW/STW/Short Term Years

In all cases for transients 1 through 25, the number of projected and suggested allowable cycles through 80 years of operation are below the number of design basis cycles. None of the projection upper bound values for transients 1 through 25 exceeds 61% of the design allowable cycles apart from refueling cycles, which are a function of the length of the fuel cycles and not plant operation.

Therefore, for transients 26 through 34, which are not counted by the FatiguePro software, there is reasonable assurance that the number of cycles for 80 years will not exceed the design basis allowable cycles.



Table 2.1-3. 80-Year Projected Cycles - PBN Units 1 and 2

Row	Transient	Current Cycles as of YE 2019		Projection Upper Bound	Design Allowable Cycles	Suggested Allowable Cycles
		Unit 1	Unit 2			
1	10% Step Load Decrease	25	30	44	2000	100
2	10% Step Load Increase	0	1	2	2000	20
3	50% Step Load Decrease	46	20	66	200	100
4	Accumulator Safety Injection	4	1	7	89	8
5	Auxiliary Spray Actuation	0	0	0	10	2
6	HPSI Injection	2	0	4	89	4
7	Inadv. ACC Blowdown	0	0	0	4	2
8	Inadv. RCS Depressurization	0	0	0	20	2
9	Loss of Charging Flow	16	17	34	60	50
10	Loss of Letdown Flow	20	17	46	200	75
11	PZR Cooldown	78	61	115	200	120
12	PZR Heatup	79	62	116	200	120
13	Primary Side Hydrostatic Test	1	2	3	5	3
14	Primary Side Leak Test	36	38	57	94	60
15	Primary to Secondary Leak Test	2	9	14	27	15
16	RCS Cooldown	79	62	118	200	120
17	RCS Heatup	80	63	119	200	120
18	RPV Safety Injection	0	0	0	89	2
19	Reactor Trip	68	52	107	300	120
20	Refueling	49	46	77	80	80
21	Relief Valve Actuation	1	3	7	100	8
22	Secondary to Primary Leak Test	38	33	57	128	60
23	Trip Due to Loss of RC Pump	1	2	4	100	4
24	Unit Loading 5%/min	1691	1806	2478	11600	8000
25	Unit Unloading 5%/min	1544	1670	2295	11600	8000
26	FW Cycling at Hot Standby	NC	NC	N/A	2000	Not provided
27	Boron Concentration Eq.	NC	NC	N/A	23360	Not provided
28	Loss of Load (Trip)	NC	NC	N/A	80	80
29	Loss of Power (Trip)	NC	NC	N/A	40	40
30	Loss of Flow (Trip)	NC	NC	N/A	80	80
31	Turbine Roll Test	NC	NC	N/A	10	10
32	Control Rod Drop	NC	NC	N/A	N/A	80
33	Excessive FW Flow	NC	NC	N/A	N/A	30
34	OBE	NC	NC	N/A	N/A	10

Footnotes:

Italicized font in the Design Allowable Cycles column indicates a value from the FSAR.

NC = Not Counted by FatiguePro

N/A = Not applicable - there is no basis for computing the upper bound.

UFSAR Transient 'Steady State Fluctuations' omitted; small fluctuations do not cause fatigue usage.

Transients 19 & 23 constitute the 400 Reactor Trip Transients in the UFSAR

UFSAR Transient 16 'Reactor Coolant Pipe Break' is a Faulted Event, which is not counted.

UFSAR Transient 17 'Steam Line Break' is a Faulted Event, which is not counted.

Transient Severity

The PBN license renewal application [2, Section 4.3] notes that the severity (temperature and pressure ranges and rates) of the original PBN design transients bound actual plant operation and that the Fatigue Monitoring Program includes monitoring for the number and severity of plant design transients with on-going fatigue analysis of a sampling of component locations whose level of metal fatigue is expected to be most adversely impacted, including each of the component locations identified in NUREG/CR-6260 for older vintage Westinghouse plants. As noted in [7], only the NUREG/CR-6260 Class 1 piping locations are monitored.

In addition, the PBN EPU licensing report [8, Sections 2.2.2 and 2.2.6] provide further evidence that transient parameter severity at extended power uprate conditions is generally less than that assumed for design transients (e.g., pressurizer insurge-outsurg transients, reactor coolant system average temperature).

In the case of the pressurizer spray piping, transient severity is based on data collected specifically for the purpose of assessing thermal stratification [10, Section 2].

Fatigue Usage

Since PBN design cycle projections indicate the 40-year design cycles will not be exceeded during the SPEO, there is reasonable assurance that fatigue usage will remain less than the ASME Code CUF criterion of 1.0.

However, in some instances, plant-specific analyses were performed based on use of monitored plant instruments. To validate that fatigue usage for 80 years of operation for the PBN Class 1 piping components will remain acceptable, both CBF and SBF projections were performed using the FatiguePro software and are provided in Table 2.1-4.

CBF usage (CUF) projections were performed like cycle projections were performed except that CUF projections are performed using LTW/STW/NY parameters of 1/1/12 for all monitored CBF locations [5]. This is reasonable and appropriate since they provide a linear projection of the most recent 12 years of collected data and the results show good agreement to the previously calculated 60-year CUF values for the RHR / SI Tee (the SI nozzle used an updated CBF method), as expected. In addition, there is significant margin to the ASME Code CUF criterion of 1.0.

SBF usage projections were performed based on the monitored CUF history calculated in FatiguePro (representing the period from 1/1/2005 through 12/31/2019) and then projected forward linearly to the end of the SPEO [6]. Although fewer years were used in the SBF projections, this is also reasonable and appropriate since the most recent data is used, it represents nearly 10 years of operation and also shows good agreement with the 60-year CUF values. The SBF projections show considerable margin to the ASME Code CUF criterion of 1.0.

In the case of the pressurizer spray piping, stratification cycles are conservatively projected based on thermocouple data with a leaking spray control valve that is assumed to continue to leak throughout 80 years of plant operation.



Table 2.1-4 shows some 80-year projected CUF values that are less than 60-year CUF values (i.e., Pressurizer Surge Line (Hot Leg Nozzle) and RHR / SI Tee). This is because the 60-year CUF values are from a design analysis and 80-year CUF values are projected based on the monitoring system.

Table 2.1-4. 80-Year Projected Cumulative Fatigue Usage

Location	CUF (60 yr)	CUF (80 yr - Projected)
Pressurizer Surge Line (Hot Leg Nozzle) ⁽²⁾	0.0383	0.0235
Charging Nozzle ⁽²⁾	0.1182	0.1274
Safety Injection Nozzle ^(1,3)	0.0072	0.3050
RHR / SI Tee ⁽¹⁾	0.0142	0.0047
Pressurizer Spray Piping ⁽⁴⁾	0.277	0.369

Notes:

1. Cycle-based fatigue (CBF) was used to establish this value for 80 years of operation.
2. Stress-based fatigue (SBF) was used to establish this value for 80 years of operation.
3. The CBF method used to calculate usage was updated with a more accurate one than that used for initial license renewal. Use of the earlier method resulted in an 80-year projected usage of 0.0003 [5, Table 7].
4. The values were conservatively established by the Generic Letter 88-08 analysis [10].

TLAA Disposition: 10 CFR 54.21(c)(1)(iii)

The current licensing basis ASME Boiler and Pressure Vessel Code, Section III, Class 1 piping fatigue calculations remain valid for the SPEO. The results demonstrate that the number of assumed design cycles will not be exceeded in 80 years of plant operation. PBN will monitor design cycles using the Fatigue Monitoring AMP described in SLRA Section Appendix B. If actual cycles approach 80 percent of their analyzed numbers during the SPEO, the AMP ensures that appropriate corrective action will be taken. Monitoring of design cycles can be performed using manual counting methods or by software, such as FatiguePro, Version 3.

TLAA Disposition: 10 CFR 54.21(c)(1)(ii)

In the case of the pressurizer spray piping, the analysis has been projected to the end of the period of extended operation. Stratification cycles are conservatively projected based on thermocouple data with a leaking spray control valve that is assumed to leak throughout 80 years of plant operation. Due to the conservatism applied to this analysis, cycle monitoring is not required.

3 REFERENCES

1. 10 CFR Part 54, Requirements for Renewal of Operating Licenses for Nuclear Power Plants.
2. Point Beach Nuclear Plant Units 1 & 2 Application for Renewed Operating Licenses, <https://www.nrc.gov/reactors/operating/licensing/renewal/applications/point-beach/lra.pdf>
3. SI Calculation No. NMC-03Q-301, Rev. 5, "Environmental Fatigue Calculations," January 2007.
4. Point Beach UFSAR, ADAMS ML16251A154, Table 4.1-8. SI File No. 2000088.201.
5. SI Calculation No. 2000088.301, Rev. 2, "Development of 80-Year Projected Cycles for Point Beach Nuclear Plant Units 1 and 2," May 2020.
6. SI Calculation No. 2000088.303, Rev. 0, "Plant Monitoring CUF Update for Point Beach Nuclear Plant Units 1 and 2," April 2020.
7. SI Calculation No. 2000088.305, Rev. 1, "Environmentally Assisted Fatigue (EAF) Screening of Class 1 Piping Locations for Point Beach," August 2020.
8. Point Beach Units 1 and 2 EPU Licensing Report, April 2009, ADAMS Accession No. ML091250566.
9. SI CAR-20-020, Point Beach Fatigue Usage Not Evaluated in EAF Screening Calculation, July 2020.
10. SI Calculation PBCH-03Q-301, Revision 3, Evaluation of Thermal Stratification Due to Valve Leakage, September 2020.
11. US NRC Bulletin 88-08, *Thermal Stresses in Piping Connected to Reactor Coolant Systems*.
12. Safety Evaluation Report Related to the License Renewal of the Point Beach Nuclear Plant, Units 1 and 2, NUREG-1839 Volume 2, December 2005, ADAMS Accession No. ML053420137.

Point Beach Nuclear Plant Units 1 and 2
Dockets 50-266 and 50-301
NRC 2020-0032 Enclosure 4, Attachment 8

Enclosure 4

**Non-proprietary Reference Documents and
Redacted Versions of Proprietary Reference
Documents**

(Public Version)

Attachment 8

**Westinghouse LTR-SDA-II-20-05-NP, Revision 2,
“Environmentally Assisted Fatigue Screening Results
for Point Beach Unit 1 and Unit 2 Safety Class 1
Primary Equipment,” June 30, 2020**

(6 Total Pages, including cover sheets)



1000 Westinghouse Drive
Cranberry Twp., PA 16066

To: John T. Ahearn
cc: Gregory M. Imbrogno
From: RV/CV Design and Analysis
Ext: 412-374-4377
Fax: 724-940-8565

Date: June 30, 2020

Our ref: LTR-SDA-II-20-05-NP, Rev. 2

Subject: Environmentally Assisted Fatigue Screening Results for Point Beach Unit 1 and Unit 2 Safety Class 1 Primary Equipment

References:

1. Westinghouse Offer Letter LTR-AMER-MKG-20-97, Rev. 0, "Westinghouse Offer for Subsequent License Renewal for Point Beach."
2. Westinghouse Calculation, CN-SDA-II-20-005, Rev. 1, "Environmentally Assisted Fatigue Screening of the Primary Equipment for Point Beach Unit 1 and Unit 2."
3. NUREG/CR-6909, Rev. 1, "Effect of LWR Water Environments on the Fatigue Life of Reactor Materials."
4. NUREG/CR-6260, "Application of NUREG/CR-5999 Interim Fatigue Curves to Selected Nuclear Power Plant Components."
5. Technical Specification for Point Beach Units 1 and 2, Rev. 17, September 3, 2019.
6. Point Beach Nuclear Plant, Units 1 and 2, "Application for Renewed Operating Licenses."
7. "License Renewal Environmental Fatigue Screening Application," C. T. Kupper, M. A. Gray, PVP2014-29093, ASME 2014 (stored as document number "WAAP-8748 Final" in PRIME).
8. Westinghouse Report WCAP-16983-P, Rev. 1, "Point Beach Units 1 and 2 Extended Power Uprate (EPU) Engineering Report." (Including WCAP-16983-P-R1-ASMT-1)
9. Point Beach Nuclear Plant, Units 1 and 2, "Application for Renewed Operating Licenses."

This document may contain technical data subject to the export control laws of the United States. In the event that this document does contain such information, the Recipient's acceptance of this document constitutes agreement that this information in document form (or any other medium), including any attachments and exhibits hereto, shall not be exported, released or disclosed to foreign persons whether in the United States or abroad by recipient except in compliance with all U.S. export control regulations. Recipient shall include this notice with any reproduced or excerpted portion of this document or any document derived from, based on, incorporating, using or relying on the information contained in this document.

© 2020 Westinghouse Electric Company LLC
All Rights Reserved



Foreword:

This document contains Westinghouse Electric Company LLC proprietary information and data which has been identified in brackets. Coding ^(a,c,e) associated with the brackets sets forth the basis on which information is considered proprietary. These code letters are listed with their meanings in BMS-LGL-84, and are defined as follows:

- a. The information reveals the distinguishing aspects of a process (or component, structure, tool, method, etc.) where the prevention of its use by any of Westinghouse's competitors without license from Westinghouse constitutes a competitive economic advantage over other companies.
- c. The information, if used by a competitor, would reduce the competitor's expenditure of resources or improve the competitor's advantage in the design, manufacture, shipment, installation, assurance of quality, or licensing of a similar product.
- e. The information reveals aspects of past, present, or future Westinghouse or customer funded development plans and programs of potential commercial value to Westinghouse.

The proprietary information and data contained within the brackets of this document were obtained at considerable Westinghouse expense and its release could seriously affect our competitive position. This information is to be withheld from public disclosure in accordance with the Rules of Practice 10CFR2.390 and the information presented herein be safeguarded in accordance with 10CFR2.390. Withholding of this information does not affect the public interest.

This information has been provided for your internal use only and should not be released to persons or organizations outside the Directorate of Regulation and the ACRS (Advisory Committee on Reactor Safeguards) without the express written approval of Westinghouse Electric Company LLC. Should it become necessary to release this information to such persons as part of the review procedure, please contact Westinghouse Electric Company LLC, which will make the necessary arrangements required to protect the Company's proprietary interests.

The proprietary information in brackets has been deleted in this non-proprietary version. The deleted information is provided in the proprietary version of this report (LTR-SDA-II-20-05-P).

The purpose of this letter is to provide results from the Environmentally Assisted Fatigue (EAF) screening evaluation performed for the Point Beach Unit 1 and 2 Class 1 primary equipment based on the scope discussed in [1]. The primary objective of the EAF screening evaluation is to compare components within a common system to determine the sentinel locations with respect to EAF using the Westinghouse screening methodology as described in [7]. Components within each system are compared on the bases of common transients and common stress analysis methods to determine the most limiting location. Revision 1 of this letter addresses editorial comments that are attached to this letter electronically as *LTR-SDA-II-20-005 Rev 0 DCRF Rev C.pdf*. Revision 2 of this letter addresses a correction to the material type for the PZR Spray Nozzle location from carbon steel to stainless steel per IR-2020-6418. This change affects the screening CUF_{en} for this location, but the overall conclusion of the EAF screening evaluation remains the same.

Table 1 summarizes the cumulative usage factors (CUF) considering environmental effects (CUF_{en}) from [2] applicable for 80 years of operation. The screening CUF_{en} was determined conservatively by applying the appropriate environmental fatigue correction factor (F_{en}) for the material calculated using the methods from [3] considering the pressurized water reactor (PWR) environment. Note that a given transient section in Table 1 may not list a sentinel location for each material type. In these cases, the CUF_{en} values for the locations of this material type were less than unity or the transient section does not contain the material type.

Table 1: Summary of Sentinel Locations for the Safety Class 1 Primary Equipment

Line/System	Component/Location	Material Category	CUF	$F_{adj}^{(1)}$	F_{en}	Screening CUF_{en}
Reactor Vessel	CRDM Nozzle	Ni-Cr-Fe Alloy	[] ^{a,c,e}	[] ^{a,c,e}	[] ^{a,c,e}	6.492
	Vessel Flange	Low-Alloy Steel	0.992	[] ^{a,c,e}	[] ^{a,c,e}	6.226
	Inlet Nozzle Support Pad ⁽³⁾	Low-Alloy Steel	0.155 (Unit 1) 0.038 (Unit 2)	[] ^{a,c,e}	[] ^{a,c,e}	0.973 (Unit 1) 0.238 (Unit 2)
	Outlet Nozzle Support Pad ⁽³⁾	Low-Alloy Steel	0.122	[] ^{a,c,e}	[] ^{a,c,e}	0.766
	Inlet Nozzle ⁽³⁾	Low-Alloy Steel	0.039	[] ^{a,c,e}	[] ^{a,c,e}	0.245
	Outlet Nozzle ⁽³⁾	Low-Alloy Steel	0.028	[] ^{a,c,e}	[] ^{a,c,e}	0.176
CRDM	Upper Latch Housing	Stainless Steel	0.364	[] ^{a,c,e}	[] ^{a,c,e}	46.628
PZR Upper Head/Shell ⁽²⁾	Spray Nozzle ⁽⁴⁾	Stainless Steel	0.871	[] ^{a,c,e}	[] ^{a,c,e}	111.575
	Upper Head ⁽⁴⁾	Carbon Steel	[] ^{a,c,e}	[] ^{a,c,e}	[] ^{a,c,e}	0.778
	Safety and Relief Nozzle ⁽⁴⁾	Carbon Steel	0.484	[] ^{a,c,e}	[] ^{a,c,e}	3.038
	Instrument Nozzle ⁽⁴⁾⁽⁷⁾	Stainless Steel	[] ^{a,c,e}	[] ^{a,c,e}	[] ^{a,c,e}	0.320
PZR Lower Head ⁽²⁾	Surge Nozzle ⁽³⁾⁽⁴⁾	Carbon Steel	0.584	[] ^{a,c,e}	[] ^{a,c,e}	3.665
	Instrument Nozzle ⁽⁴⁾⁽⁷⁾	Stainless Steel	[] ^{a,c,e}	[] ^{a,c,e}	[] ^{a,c,e}	0.320
	Heater Well ⁽⁴⁾	Stainless Steel	[] ^{a,c,e}	[] ^{a,c,e}	[] ^{a,c,e}	0.000
SG	Tubes ⁽⁸⁾	Ni-Cr-Fe Alloy	0.948 (Unit 1) 0.233 (Unit 2)	[] ^{a,c,e}	[] ^{a,c,e}	35.512 (Unit 1) 8.728 (Unit 2)
	Primary Chamber, Tubesheet, and Stub Barrel Complex (Unit 2)	Low-Alloy Steel	0.463	[] ^{a,c,e}	[] ^{a,c,e}	2.906

Notes:

- (1) The F_{adj} factor documented in this table accounts for the differences between the fatigue curves used in the analyses of record (AOR) (Section III Appendix I of the ASME Code prior to the 2007 Edition through 2009 addenda) and the fatigue curves in [3]. []^{a,c,e}

[

] ^{a,c,e} For certain locations, the appropriate fatigue curves from [3] were applied to the fatigue usage calculation and therefore, an F_{adj} factor is not utilized.

- (2) During operation, the pressurizer upper head is subject to transients which are greatly influenced by the pressurizer steam temperature as well as the spray temperature. Whereas, the pressurizer lower head region is influenced by pressurizer fluid temperatures as well as hot leg insurge or outsurge fluid temperatures. Therefore, the pressurizer is divided into two transient sections for the EAF screening herein.
- (3) NUREG/CR-6260 [4] location within the scope outlined in [1]. In some cases these locations have screened out, with a screening $CUF_{en} < 1.0$, but are provided here for completeness.
- (4) These locations were evaluated for EAF for first license renewal per [6]. In some cases these locations have screened out, with a screening $CUF_{en} < 1.0$, but are provided here for completeness.

(5) [

] ^{a,c,e}

(6) [

] ^{a,c,e}

- (7) The bounding fatigue usage value for the PZR Upper and Lower Instrument Nozzle locations was used to represent the locations in both transient sections.
- (8) Point Beach currently inspects the SG Tubes under the SG Tube Integrity aging management plan discussed in [5]. Therefore, this inspection program could potentially be used by the plant to disposition this location.
- (9) The evaluations included in [8] do not include consideration of insurge/outsurge transient effects in the PZR Lower Head. Per Section 4.3.5 of [9], insurge/outsurge evaluations were completed by other vendors.

If you have any questions, please contact the undersigned.

Author: Jamie L. Oakman*
Reactor Vessel/Containment
Vessel Design & Analysis

Verifier: Gregory M. Imbrogno*
Reactor Vessel/Containment Vessel
Design & Analysis

Manager: Lynn A. Patterson*
Reactor Vessel/Containment Vessel
Design & Analysis

****Electronically approved records are authenticated in the electronic document management system.***

This page was added to the quality record by the PRIME system upon its validation and shall not be considered in the page numbering of this document.

Approval Information

Author Approval Oakman Jamie L Jun-30-2020 12:26:36

Verifier Approval Imbrogno Greg M Jul-01-2020 12:59:39

Manager Approval Patterson Lynn Jul-01-2020 13:38:54

Files approved on Jul-01-2020

*** This record was final approved on 7/1/2020 1:38:54 PM. (This statement was added by the PRIME system upon its validation)

Point Beach Nuclear Plant Units 1 and 2
Dockets 50-266 and 50-301
NRC 2020-0032 Enclosure 4, Attachment 9

Enclosure 4

**Non-proprietary Reference Documents and
Redacted Versions of Proprietary Reference
Documents**

(Public Version)

Attachment 9

**Structural Integrity Associates, Inc. Report No.
2000088.402, Revision 1, “Environmentally-Assisted
Fatigue Evaluation for 80 Years of Plant Operation for
Point Beach Nuclear Units 1 and 2,” September 25,
2020**

(12 Total Pages, including cover sheets)



REPORT NO. 2000088.402
REVISION: 1
PROJECT NO. 2000088.00
September 2020

Environmentally-Assisted Fatigue Evaluation for 80 Years of Plant Operation for Point Beach Nuclear Units 1 and 2

Prepared For:

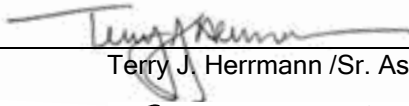
NextEra Energy Point Beach, LLC
Point Beach Nuclear Units 1 and 2
Two Rivers, WI

Contract No. 02410780

Prepared By:

Structural Integrity Associates, Inc.
San Jose, CA

Prepared by:


Terry J. Herrmann / Sr. Associate

Date: 09/25/2020

Reviewed by:


David A. Gerber / Sr. Associate

Date: 09/25/2020

Approved by:


David A. Gerber / Sr. Associate

Date: 09/25/2020



REVISION CONTROL SHEET

Report Number: 2000088.402

Title: Environmentally-Assisted Fatigue Evaluation for 80 Years of Plant Operation for Point Beach Nuclear Units 1 and 2

Client: NextEra Energy Point Beach, LLC

SI Project Number: 2000088.00

Quality Program: Nuclear Commercial

SECTION	PAGES	REVISION	DATE	COMMENTS
-- 1.0 2.0 3.0	i - iii 1-1 2-1 - 2-5 3-1	0	5/27/2020	Initial Issue
1.0 2.0 3.0	1-1 2-2 - 2-5 3-1 - 3-2	1	9/25/2020	Revised to address Pressurizer Spray Piping (see CAR-20-020).



TABLE OF CONTENTS

1	INTRODUCTION	1-1
2	METAL FATIGUE	2-1
2.1	Environmentally Assisted Fatigue	2-1
3	REFERENCES	3-1

LIST OF TABLES

Table 2.1-1.	EAF Screening Results with Bounding CUF_{en} Values	2-4
Table 2.1-2.	80-Year EAF Usage Values.....	2-5



1 INTRODUCTION

NextEra Energy Point Beach, LLC is in the process of developing and submitting a subsequent license renewal (SLR) application that would extend plant operations at Point Beach Units 1 and 2 (PBN) from 60 to 80 years. The preparation includes the development and submittal of an SLR application (SLRA), and subsequent NRC review, concluding in a renewed operating license for both units.

The SLR process follows a similar process as the first Point Beach (PBN) license renewal application (LRA) submitted in 2004. As a result of the first LRA submittal, the NRC issued operating licenses in June 2005 to operate an additional 20 years beyond the original 40 year operating licenses.

Starting from previous fatigue analyses performed by SI, a review was performed to identify Class 1 piping locations that are part of the reactor coolant pressure boundary (RCPB) and are wetted by reactor coolant, in order to assess the effects of environmentally assisted fatigue (EAF).

This report provides information for inclusion in the SLRA related to Environmentally-Assisted Fatigue (EAF), based on engineering calculations and evaluations associated with metal fatigue of Class 1 piping Time-Limited Aging Analyses (TLAAs) for which environmental effects must be addressed.

Note: SI's scope of work is limited to Class 1 piping having fatigue analyses. In the case of PBN, where the Class 1 piping was designed to the B31.1 Power Piping Code, explicit fatigue analyses were not performed. However, for initial License Renewal, Class 1 fatigue analyses were performed for selected piping locations and an implicit fatigue analysis performed for the pressurizer spray piping. An evaluation was performed that established these same Class 1 locations as limiting for SLR. Reactor vessels, reactor vessel internals, pressurizers, steam generators and reactor coolant pumps must be addressed separately.

The pressurizer spray piping is an additional piping location included in Revision 1 of this report per SI CAR-20-020 [16]. The implicit fatigue analysis of the pressurizer spray piping, updated for 80 years of operation, is also evaluated for EAF [17].

2 METAL FATIGUE

The thermal and mechanical fatigue analyses of plant mechanical components have been identified as time-limited aging analyses for PBN. Specific components have been designed, considering transient cycle assumptions, as listed in vendor specifications and the PBN UFSAR.

Fatigue analyses are considered TLAA's for Class 1 and non-Class 1 mechanical components. Fatigue is an age-related degradation mechanism caused by cyclic stressing of a component by either mechanical or thermal stresses.

The aging management reviews in SLRA Section 3 will identify mechanical components that are within the scope of license renewal and are subject to aging management review. This section evaluates the piping-related fatigue analyses for those components where the tables in SLRA Section 3 identify "TLAA - Metal Fatigue" as the aging management program and EAF applies. Evaluation of the TLAA per 10 CFR 54.21(c)(1) [1] determines whether

- (i) the analyses remain valid for the SPEO,
- (ii) the analyses have been projected to the end of the SPEO, or
- (iii) the effects of aging on the intended function(s) will be adequately managed for the SPEO.

Documentation of the evaluation of Class 1 piping component environmentally-assisted fatigue analyses is provided in Section 2.1 (for inclusion in SLRA Section 4.3.3 along with input from others for other Class 1 component locations).

2.1 Environmentally-Assisted Fatigue

TLAA Description

The current PBN approach to environmentally-assisted fatigue (EAF) is described in the PBN License Renewal Application [2, Section 4.3.10] and UFSAR Section 15.4.2 [3].

As outlined in Section X.M1 of NUREG-2191 [4], the effects of the reactor water environment on cumulative usage factor (CUF) must be examined for a set of sample critical components for the plant. This sample set includes the locations identified in NUREG/CR-6260, "Application of NUREG/CR-5999 Interim Fatigue Curves to Selected Nuclear Power Plant Components" [5] and additional plant-specific component locations in the reactor coolant pressure boundary if they may be more limiting than those considered in NUREG/CR-6260.

These additional limiting locations are identified through an environmentally-assisted fatigue screening evaluation. The EAF screening evaluation reviewed the CLB fatigue evaluations for all Class 1 piping pressure boundary components, including the NUREG/CR-6260 locations, to determine the lead indicator (also referred to as sentinel) locations for EAF.



As noted in NUREG-2191 [7, p. 3-26 and 4-12, also Section 4.3.9] the Code of record for PBN piping is B31.1, which uses a stress range reduction factor and does not calculate fatigue usage values for this piping. However, as noted in [7, Section 4.3.10] fatigue analyses and environmental fatigue calculations were performed for NUREG/CR-6260 locations.

Other than the NUREG/CR-6260 Class 1 piping locations and the pressurizer spray piping, remaining piping does not have fatigue usage calculations and there is no requirement in NUREG-2191 to calculate fatigue usage for these locations. Therefore, another means was applied to evaluate whether these other locations may be more limiting.

The plants most similar in design to PBN are other Westinghouse 2-Loop (W 2-loop) pressurized water reactors (PWRs). Similar W 2-loop plants are:

- Kewaunee
- R. E. Ginna
- Prairie Island

Since the guidance for considering locations that may be more limiting was not issued until after these plants submitted their License Renewal Applications (LRAs), none of these plants performed such an evaluation in support of their respective LRAs.

Following issuance of NUREG-2191, the Surry Power Station (SPS) applied for Subsequent License Renewal (SLR) [14]. In support of the Surry application, SI performed EAF screening using a Common Basis Stress Evaluation (CBSE) approach [14, Section 4.3.4] that considered all other Class 1 piping. Although Surry is a W 3-loop plant design, the Code of record for its Class 1 piping is also B31.1. EAF screening for Surry identified that the applicable NUREG/CR-6260 locations and the pressurizer spray piping were the sentinel locations [14, Table 4.3.4-1].

In addition, the Safety Evaluation Report (SER) for Turkey Point [15, Section 4.3.3] noted that the assessment performed to identify any locations that may be more limiting than those in NUREG/CR-6260 consisted of components with ASME Section III cumulative usage factor (CUF) values calculated as part of the design basis.

This provides reasonable assurance that the NUREG/CR-6260 locations and the pressurizer spray piping constitute the piping sentinel locations for PBN.

Demonstrating that reactor coolant pressure boundary components have an environmentally-assisted CUF (CUF_{en}) less than or equal to a limit of 1.0 is an acceptable option for managing environmentally-assisted fatigue (EAF) for the reactor coolant pressure boundary. Considering the calculation of fatigue usage factors is part of the CLB and is used to support safety determinations, and the number of occurrences of each transient type was based upon 60-year assumptions, these Class 1 fatigue analyses have been identified as TLAAs requiring evaluation for the SPEO.



TLAA Evaluation

NUREG-2192, [6], provides a recommendation for evaluating the effects of the reactor water environment on the fatigue life of ASME Section III Class 1 components that contact reactor coolant. NUREG-2192 indicates that applicants should include CUF_{en} calculations for the limiting reactor coolant pressure boundary component locations exposed to the reactor water environment. This sample set includes the locations identified in NUREG/CR-6260 [5] and additional plant-specific component locations in the reactor coolant pressure boundary if they may be more limiting than those considered in NUREG/CR-6260. Plant-specific justification can be provided to demonstrate that calculations for the NUREG/CR-6260 locations do not need to be included.

The NUREG/CR-6260 Class 1 piping locations for PBN consist of the following locations [7, Section 4.3.10]:

- Residual Heat Removal to Safety Injection tee ("RHR / SI Tee")
- Charging nozzle
- Accumulator Safety Injection (SI) nozzle
- Pressurizer surge line

For the aforementioned NUREG/CR-6260 Class 1 piping locations and the pressurizer spray piping, the PBN EAF assessment for SLR [9] was performed using the applicable guidance from NUREG-2192 [6]. Section 4.3.2.1.2.1, "10 CFR 54.21(c)(1)(i)," of NUREG-2192 for components evaluated for CUF_{en} states the following:

The existing CUF_{en} calculations remain valid for the subsequent period of extended operation because the number of accumulated cycles, the assumed severity of the cyclic loadings, and the assumed water chemistry conditions evaluated in the calculations are not projected to exceed the limits evaluated for these parameters. The revised projections for the number of accumulated cycles are verified to be consistent with historical plant operating characteristics and anticipated future operation.

A plant-specific justification can be provided to demonstrate that existing CUF_{en} calculations performed using guidance in Section 4.3.2.1.3 of NUREG-1800, Revision 2 will remain valid for the subsequent period of extended operation and are sufficiently conservative when compared to those CUF_{en} calculations that would be generated using the guidance in RG 1.207, Revision 1, or in NUREG/CR-6909, Revision 0 (with "average temperature" used consistent with the clarification that was added to NUREG/CR-6909, Revision 1).

Based on the foregoing discussion, the updated SLR EAF assessment for PBN was performed as follows:

- The plant-specific NUREG/CR-6260 Class 1 piping locations were reevaluated for SLR.
- To ensure that any locations that may be more limiting than the NUREG/CR- 6260 locations were addressed, the reactor coolant pressure boundary Class 1 piping components were evaluated for EAF for SLR.
- The pressurizer spray piping was evaluated for EAF for SLR.



- The revised plant-specific EAF multipliers applicable for SLR were calculated based on the latest F_{en} methods using the guidance in NUREG/CR-6909, Revision 1 [8].

The EAF screening assessment did not identify any additional plant-specific component locations that may be more limiting than the NUREG/CR-6260 locations and the pressurizer spray piping [9]. Bounding CUF_{en} values are obtained using 60-year CUF values and maximum F_{en} multipliers based on a conservative service temperature of 325°C and applying the most conservative strain rate. The results of the EAF screening is presented in Table 2.1-1.

Table 2.1-1. EAF Screening Results with Bounding CUF_{en} Values

Location	Material	CUF (60 yr)	F_{en}	CUF_{en} Screening
Pressurizer Surge Line	Stainless Steel	0.0383	12.807	0.491
Charging Nozzle	Stainless Steel	0.11815	12.807	1.513
Accumulator Safety Injection Nozzle	Stainless Steel	0.0072	12.807	0.092
RHR / SI Tee	Stainless Steel	0.0142	12.807	0.182
Pressurizer Spray Piping	Stainless Steel	0.277	12.807	3.548

The above approach used CUF values calculated with the ASME Code fatigue curve for stainless steel, which is generally less conservative than the one used in NUREG/CR-6909, Revision 1 [8]. Thus, for stainless steel material it is necessary to use the revised fatigue curve from NUREG/CR-6909, Revision 1 for SLR.

On April 7, 2009 FPL Energy Point Beach, LLC applied for an Extended Power Uprate (EPU) license to operate at a core thermal power of 1800 MWt [10]. On May 3, 2011, the NRC approved the application [11].

The EPU changed numerous core thermal parameters pertinent to fatigue analyses of the piping and, therefore, further analysis was performed for each of these locations to confirm the 80-year CUF_{en} values will remain acceptable ($CUF_{en} < 1.0$) during the SPEO [12]. The results of this analysis are presented in Table 2.1-2.



Table 2.1-2. 80-Year EAF Usage Values

Location	CUF (80 yr)	Effective F_{en}	80-year CUF_{en}
Pressurizer Surge Line ^(3, 4)	0.1487	6.51	0.9685
Charging Nozzle ^(1, 2)	0.1619	4.41	0.7149
Accumulator Safety Injection Nozzle ^(1, 2)	0.0173	5.39	0.0930
RHR / SI Tee ^(1, 2)	0.0332	2.28	0.0758
Pressurizer Spray Piping ^(4, 5)	0.154	4.83	0.744

Notes:

1. Design cycles were conservatively used.
2. F_{en} values are conservatively based on maximum load pair temperature.
3. For some load pairs, analyzed cycles are less than design cycles.
4. Detailed F_{en} values for each load pair were calculated.
5. The analysis method used to obtain estimated fatigue usage for 80 years due to thermal stratification [17] is that of the Current Licensing Basis [7, Section 4.3.8] updated to reflect the subsequent period of extended operation and application of NUREG/CR-6909 [8].

As described above, the calculated environmentally assisted CUF values (CUF_{en} values) are maintained less than 1.0 for all applicable reactor coolant pressure boundary piping components based on conservative F_{en} values and number of analyzed cycles. In all cases, the number of analyzed cycles for 80 years are equal to or greater than the suggested allowable of cycles in [13, Table 6].

TLAA Disposition: 10 CFR 54.21(c)(1)(iii)

For the Class 1 pressure boundary piping components, the environmentally assisted fatigue analyses will be managed using the Fatigue Monitoring AMP (SLRA Section B.2.2.1). The Fatigue Monitoring AMP will assure that corrective action specified in the program is taken prior to any of the relevant fatigue parameter values exceeding the limits established in the fatigue analyses. Monitoring of design cycles can be performed using manual counting methods or by software, such as FatiguePro, Version 3.

TLAA Disposition: 10 CFR 54.21(c)(1)(ii)

In the case of the pressurizer spray piping, the analysis has been projected to the end of the period of extended operation. Stratification cycles are conservatively projected based on thermocouple data with a leaking spray control valve that is assumed to leak throughout 80 years of plant operation. Due to the conservatism applied to this analysis, cycle monitoring is not required.

3 REFERENCES

1. 10 CFR Part 54, Requirements for Renewal of Operating Licenses for Nuclear Power Plants.
2. Point Beach Nuclear Plant Units 1 & 2 Application for Renewed Operating Licenses, <https://www.nrc.gov/reactors/operating/licensing/renewal/applications/point-beach/lra.pdf>
3. Point Beach Nuclear Plant Units 1 & 2 Final Safety Analysis Report, 2010, SI File No. 1101239.213.
4. NUREG-2191, Generic Aging Lessons Learned for Subsequent License Renewal (GALL-SLR) Report, Final Report, Volume 2, ADAMS Accession No. ML17187A204.
5. NUREG/CR-6260 (INEL-95/0045), Application of NUREG/CR-5999 Interim Fatigue Curves to Selected Nuclear Power Plant Components, March 1995, ADAMS Accession No. ML031480219.
6. NUREG-2192, Standard Review Plan for Review of Subsequent License Renewal Applications for Nuclear Power Plants, Final Report, ADAMS Accession No. ML17188A158.
7. Safety Evaluation Report Related to the License Renewal of the Point Beach Nuclear Plant, Units 1 and 2, NUREG-1839 Volume 2, December 2005, ADAMS Accession No. ML053420137.
8. NUREG/CR-6909, Revision 1, Effect of LWR Water Environments on the Fatigue Life of Reactor Materials Final Report, May 2018.
9. SI Calculation No. 2000088.305, Rev. 1, "Environmentally Assisted Fatigue (EAF) Screening of Class 1 Piping Locations for Point Beach," August 2020.
10. FPL Energy Point Beach, LLC, License Amendment Request 261, Extended Power Uprate, dated April 7, 2009. <https://www.nrc.gov/docs/ML1107/ML110750120.html>
11. NRC Letter, POINT BEACH NUCLEAR PLANT (PBNP), UNITS 1 AND 2 - ISSUANCE OF LICENSE AMENDMENTS REGARDING EXTENDED POWER UPRATE (TAC NOS. ME1044 AND ME1045), Dated May 3, 2011. <https://www.nrc.gov/docs/ML1111/ML111170513.html>
12. SI Calculation No. 2000088.310P, Rev. 1, "EAF Refined Analyses (Charging Nozzle, Hot Leg Surge Nozzle, SI Nozzle, SI/RHR Tee)," August 2020.
13. SI Calculation No. 2000088.301, Rev. 1, "Development of 80-Year Projected Cycles for Point Beach Nuclear Plant Units 1 and 2," April 2020.
14. Surry Power Station, Units 1 and 2 Application for Subsequent License Renewal, October 2018, ADAMS Accession No. ML18291A828.
15. Safety Evaluation Report Related to the Subsequent License Renewal of Turkey Point Generating Units 3 and 4, July 2019, ADAMS Accession No. ML19191A057.
16. SI CAR-20-020, Point Beach Fatigue Usage Not Evaluated in EAF Screening Calculation, July 2020.

17. SI Calculation PBCH-03Q-301, Revision 3, Evaluation of Thermal Stratification Due to Valve Leakage, September 2020.



Point Beach Nuclear Plant Units 1 and 2
Dockets 50-266 and 50-301
NRC 2020-0032 Enclosure 4, Attachment 10

Enclosure 4

**Non-proprietary Reference Documents and
Redacted Versions of Proprietary Reference
Documents**

(Public Version)

Attachment 10

**Westinghouse LTR-SDA-II-20-08-NP, Revision 1,
“Environmentally Assisted Fatigue Evaluation
Results for the Point Beach Unit 1 and Unit 2 Primary
Equipment Sentinel Locations for Subsequent
License Renewal,” July 15, 2020**

(16 Total Pages, including cover sheets)



1000 Westinghouse Drive
Cranberry Twp., PA 16066

To: John T. Ahearn
cc:

Date: July 15, 2020

From: RV/CV Design and Analysis
Ext: 412-374-4474
Fax: 724-940-8565

Ref: LTR-SDA-II-20-08-NP Rev. 1

Subject: Environmentally Assisted Fatigue Evaluation Results for the Point Beach Unit 1 and Unit 2 Primary Equipment Sentinel Locations for Subsequent License Renewal

To support the Point Beach Unit 1 and Unit 2 Subsequent License Renewal (SLR) program, environmentally assisted fatigue (EAF) evaluations were performed for the following primary equipment locations in accordance with the work scope described in [1] and [2]:

- Reactor vessel closure head (RVCH) control rod drive mechanism (CRDM) nozzle
- Reactor vessel (RV) flange
- CRDM upper latch housing (ULH)
- Steam generator (SG) primary chamber, tubesheet, and stub barrel complex (Unit 2)
- Pressurizer (PZR) safety and relief nozzle
- PZR surge nozzle (excluding insurge and outsurge transient effects)

This letter report summarizes the results of these EAF evaluations. This report does not include the American Society of Mechanical Engineers (ASME) Section XI Appendix L flaw tolerance evaluation for the PZR spray nozzle described in [2] or the EAF evaluations for the controlling PZR lower head locations including insurge and outsurge transient effects described in [3]. These evaluations will be addressed in a separate report. Revision 1 of this letter report addresses the comments in the attached "LTR-SDA-II-20-08-NP Rev 0- DCRF Rev C Signed.pdf" file. All changes from Revision 0 to Revision 1 are denoted by revision bars in the left margin.

Author: Eric J. Matthews*
Reactor Vessel/Containment Vessel Design and Analysis

Verifier: Gregory M. Imbrogno*
Reactor Vessel/Containment Vessel Design and Analysis

Manager: Lynn A. Patterson*
Reactor Vessel/Containment Vessel Design and Analysis

This document may contain technical data subject to the export control laws of the United States. In the event that this document does contain such information, the Recipient's acceptance of this document constitutes agreement that this information in document form (or any other medium), including any attachments and exhibits hereto, shall not be exported, released or disclosed to foreign persons whether in the United States or abroad by recipient except in compliance with all U.S. export control regulations. Recipient shall include this notice with any reproduced or excerpted portion of this document or any document derived from, based on, incorporating, using or relying on the information contained in this document.

© 2020 Westinghouse Electric Company LLC
All Rights Reserved

***Electronically approved records are authenticated in the Process, Records, and Information Management Environment.**

Foreword:

This document contains Westinghouse Electric Company LLC proprietary information and data which has been identified in brackets. Coding ^(a,c,e) associated with the brackets sets forth the basis on which information is considered proprietary. These code letters are listed with their meanings in BMS-LGL-84, and are defined as follows:

- a. The information reveals the distinguishing aspects of a process (or component, structure, tool, method, etc.) where the prevention of its use by any of Westinghouse's competitors without license from Westinghouse constitutes a competitive economic advantage over other companies.
- c. The information, if used by a competitor, would reduce the competitor's expenditure of resources or improve the competitor's advantage in the design, manufacture, shipment, installation, assurance of quality, or licensing of a similar product.
- e. The information reveals aspects of past, present, or future Westinghouse or customer funded development plans and programs of potential commercial value to Westinghouse.

The proprietary information and data contained within the brackets of this document were obtained at considerable Westinghouse expense and its release could seriously affect our competitive position. This information is to be withheld from public disclosure in accordance with the Rules of Practice 10 CFR 2.390 and the information presented herein is to be safeguarded in accordance with 10 CFR 2.390. Withholding of this information does not affect the public interest.

This information has been provided for your internal use only and should not be released to persons or organizations outside the Directorate of Regulation and the ACRS (Advisory Committee on Reactor Safeguards) without the express written approval of Westinghouse Electric Company LLC. Should it become necessary to release this information to such persons as part of the review procedure, please contact Westinghouse Electric Company LLC, which will make the necessary arrangements required to protect the Company's proprietary interests.

The proprietary information in brackets has been deleted in this non-proprietary version. The deleted information is provided in the proprietary version of this report (LTR-SDA-II-20-08-P).

1.0 Introduction and Summary of Results

As outlined in [1] and [2], the Point Beach Unit 1 and Unit 2 SLR program is intended to extend the operation license of these plants from 60 years to 80 years. Nuclear Regulatory Commission (NRC) guidance on the content of SLR applications is provided in [4.1] and [4.2]. Per subsection 4.3.2.1 of [4.2], pursuant to 10 CFR 54.21(c)(1)(i) through (iii), each metal fatigue time-limited aging analysis must demonstrate compliance with one of the following:

- i. The analyses remain valid for the period of extended operation (PEO);
- ii. The analyses have been projected to the end of the PEO; or
- iii. The effects of aging on the intended function(s) will be adequately managed for the PEO.

In addition, per subsection 4.3.2.1.2 of [4.2], EAF evaluations should be performed for the limiting component locations exposed to the reactor water environment. A screening of Class 1 reactor coolant pressure boundary primary equipment was performed in [5] to determine sentinel (limiting) locations to be considered in subsequent EAF evaluations. The sentinel locations identified for the primary equipment include the following:

- RVCH CRDM nozzle
- RV flange
- CRDM ULH
- SG primary chamber, tubesheet, and stub barrel complex (Unit 2)
- PZR safety and relief nozzle
- PZR surge nozzle (excluding insurge and outsurge transient effects)

Per Task 4b of [1] and 4c of [2], this letter report summarizes the results of EAF evaluations performed in [6] for these sentinel locations for the PEO. The results of the EAF evaluations are summarized in Table 1-1, and a more detailed summary of the results is presented in Table 3-1. The EAF evaluations were performed using the guidelines in [4.3] and the EAF penalty factor (F_{en}) equations in [4.4]. The transient cycles considered in the EAF evaluations are bounding for an 80-year period of operation. The cumulative usage factor including reactor water environmental effects (CUF_{en}) for each sentinel location is less than the ASME Boiler and Pressure Vessel (BPV) Code limit of 1.0 and is therefore acceptable.

The transient cycles considered in the EAF evaluations were reduced from those considered in the analysis of record (AOR) for some locations. Changes to plant documents (such as cycle counting procedures, final safety analysis report (FSAR), etc.) may be required to address the reduced transient cycles considered in these EAF evaluations to support the SLR program.

This report does not include the ASME Section XI Appendix L flaw tolerance evaluation for the PZR spray nozzle described in [2] or the EAF evaluations for the controlling PZR lower head locations including insurge and outsurge transient effects described in [3]. These evaluations will be addressed in a separate report.

Table 1-1: Summary of EAF Results for Primary Equipment Sentinel Locations

Line / System	Component / Location	Material Category	CUF _{en}
RV	CRDM Nozzle	Ni-Cr-Fe Alloy	0.946
	Vessel Flange	Low Alloy Steel (LAS)	0.985
CRDM	ULH	Stainless Steel (SS)	0.713
SG	Primary Chamber, Tubesheet, and Stub Barrel Complex (Unit 2)	LAS	0.967
PZR Upper Head / Shell	Safety and Relief Nozzle	Carbon Steel (CS)	0.953
PZR Lower Head	Surge Nozzle (excluding insurge and outsurge transient effects)	CS	0.542

2.0 Environmentally Assisted Fatigue Evaluation Methodology

The EAF evaluations were performed using the guidelines in [4.3] and the F_{en} equations in [4.4]. These evaluations utilized the AORs and design fatigue curves in Section A.2.1 of [4.4] to derive a cumulative usage factor (CUF), and then utilized the F_{en} equations in Section A.2 of [4.4] to derive a CUF_{en} . The applicable F_{en} equations from [4.4] are presented in Section 2.1. The goal of the EAF evaluations was to calculate a CUF_{en} below 1.0 through typical linear elastic fatigue analysis techniques. Conservatism in the stress and fatigue analyses in the AORs were identified and removed if possible in the CUF calculations. The conservatism reduction methods implemented for each sentinel location are discussed in Section 3.0. For sentinel locations with low CUFs, the CUF_{en} was calculated by applying the maximum F_{en} , calculated per Section 2.2, to the CUF. For sentinel locations that could not accept this conservative method, strain rate dependent F_{en} values were calculated for significant fatigue pairs using the modified rate approach, which is described in Section 4.4 of [4.4] and summarized in Section 2.3. In general, the EAF evaluations of the sentinel locations can be categorized into two groups:

1. Simplified EAF Evaluations

The AOR CUF was reduced by applying the design fatigue curves in Section A.2.1 of [4.4] and implementing reduced cycles for specific transients. The CUF_{en} was calculated by applying the maximum F_{en} to the CUF.

2. Detailed EAF Evaluations

The AOR CUF was recalculated by applying the design fatigue curves in Section A.2.1 of [4.4], implementing reduced cycles for specific transients, and implementing additional refinements related to the identification of stress cycles and application of more appropriate fatigue strength reduction factors (FSRFs). The CUF_{en} was calculated by applying the maximum F_{en} to the CUF or using the modified rate approach.

2.1 F_{en} Equations

The materials for the sentinel locations in the EAF evaluations include CS, LAS, SS, and Ni-Cr-Fe alloy. The F_{en} for each of these materials was calculated using the equations in Section A.2 of [4.4], which are presented in Equation 2-1 to Equation 2-3.

CS and LAS:

$$F_{en} = \exp((0.003 - 0.031 \dot{\epsilon}^*) S^* T^* O^*) \quad 2-1$$

Where:

$$S^* = 2.0 + 98 S$$

$$S \leq 0.015 \text{ wt. \%}$$

$$S^* = 3.47$$

$$S > 0.015 \text{ wt. \%}$$

S = Sulfur Content (wt. %)

$$T^* = 0.395$$

$$T < 150^\circ\text{C} (302^\circ\text{F})$$

$$T^* = (T - 75)/190$$

$$150^\circ\text{C} (302^\circ\text{F}) \leq T \leq 325^\circ\text{C} (617^\circ\text{F})$$

T = Service Temperature (°C)

for calculation of T*

$$O^* = 1.49$$

$$\text{DO} < 0.04 \text{ ppm}$$

$$O^* = \ln(\text{DO}/0.009)$$

$$0.04 \text{ ppm} \leq \text{DO} \leq 0.5 \text{ ppm}$$

$$O^* = 4.02$$

$$\text{DO} > 0.5 \text{ ppm}$$

DO = Dissolved Oxygen Content (ppm)

$$\dot{\epsilon}^* = 0$$

$$\dot{\epsilon} > 2.2 \text{ \%}/\text{s}$$

$$\dot{\epsilon}^* = \ln(\dot{\epsilon}/2.2)$$

$$0.0004 \text{ \%}/\text{s} \leq \dot{\epsilon} \leq 2.2 \text{ \%}/\text{s}$$

$$\dot{\epsilon}^* = \ln(0.0004/2.2)$$

$$\dot{\epsilon} < 0.0004 \text{ \%}/\text{s}$$

 $\dot{\epsilon}$ = Strain Rate (%/s)**SS:**

$$F_{en} = \exp(- T^* \dot{\epsilon}^* O^*) \quad 2-2$$

Where:

$$T^* = 0$$

$$T < 100^\circ\text{C} (212^\circ\text{F})$$

$$T^* = (T - 100)/250$$

$$100^\circ\text{C} (212^\circ\text{F}) \leq T \leq 325^\circ\text{C} (617^\circ\text{F})$$

T = Service Temperature (°C)

$$\dot{\epsilon}^* = 0$$

$$\dot{\epsilon} > 7.0 \text{ \%}/\text{s}$$

$$\dot{\epsilon}^* = \ln(\dot{\epsilon}/7.0)$$

$$0.0004 \text{ \%}/\text{s} \leq \dot{\epsilon} \leq 7.0 \text{ \%}/\text{s}$$

$$\dot{\epsilon}^* = \ln(0.0004/7.0)$$

$$\dot{\epsilon} < 0.0004 \text{ \%}/\text{s}$$

 $\dot{\epsilon}$ = Strain Rate (%/s)

SS:

$$F_{en} = \exp(-T^* \dot{\epsilon}^* O^*)$$

2-2

All wrought and cast SSs and heat treatments and SS weld metals:

$$O^* = 0.29 \quad DO < 0.1 \text{ ppm}$$

Sensitized high-carbon wrought and cast SSs:

$$O^* = 0.29 \quad DO \geq 0.1 \text{ ppm}$$

All wrought SSs except sensitized high-carbon SSs:

$$O^* = 0.14 \quad DO \geq 0.1 \text{ ppm}$$

DO = Dissolved Oxygen Content
(ppm)**Ni-Cr-Fe Alloys (except Inconel 718):**

$$F_{en} = \exp(-T^* \dot{\epsilon}^* O^*)$$

2-3

Where:

$$T^* = 0 \quad T < 50^\circ\text{C} (122^\circ\text{F})$$

$$T^* = (T - 50)/275 \quad 50^\circ\text{C} (122^\circ\text{F}) \leq T \leq 325^\circ\text{C} (617^\circ\text{F})$$

$$T = \text{Service Temperature } (^\circ\text{C})$$

$$\dot{\epsilon}^* = 0 \quad \dot{\epsilon} > 5.0 \text{ \%}/\text{s}$$

$$\dot{\epsilon}^* = \ln(\dot{\epsilon}/5.0) \quad 0.0004 \text{ \%}/\text{s} \leq \dot{\epsilon} \leq 5.0 \text{ \%}/\text{s}$$

$$\dot{\epsilon}^* = \ln(0.0004/5.0) \quad \dot{\epsilon} < 0.0004 \text{ \%}/\text{s}$$

$$\dot{\epsilon} = \text{Strain Rate } (\text{\%/s})$$

$$O^* = 0.06 \quad \text{NWC BWR water (i.e., DO} \geq 0.1 \text{ ppm)}$$

$$O^* = 0.14 \quad \text{PWR or HWC BWR water (i.e., DO} < 0.1 \text{ ppm)}$$

$$\text{DO} = \text{Dissolved Oxygen Content (ppm)}$$

2.2 Maximum F_{en} Values

[

] a,c,e

| [

] ^{a,c,e}

2.3 Modified Rate Approach

The modified rate approach described in Section 4.4 of [4.4] is a method to calculate the F_{en} under transient conditions. This approach calculates the F_{en} at many points over the strain range during intervals of increasing strain, and then calculates the overall F_{en} for a fatigue pair by integrating over the entire strain range. The modified rate approach is presented in Equation 2-4.

$$F_{en} = \frac{\sum F_{en,i} \Delta \epsilon_i}{\sum \Delta \epsilon_i} \quad 2-4$$

Where:

F_{en} = overall F_{en} for the fatigue pair

$F_{en,i}$ = F_{en} computed for interval from time i to time $i-1$ based on $\dot{\epsilon}_i$ and the transformed parameters S^* , T^* , O^* , and $\hat{\epsilon}^*$

$$\dot{\epsilon}_i = \frac{\Delta \epsilon_i}{\Delta t_i}$$

$\Delta \epsilon_i$ = strain range from time i to time $i-1$

Δt_i = change in time from time i to time $i-1$

2.4 Strain Amplitude Threshold Values

Threshold strain and stress amplitude values are defined in Section A.2 of [4.4], below which environmental effects on the fatigue lives may not occur (i.e., $F_{en} = 1.0$). These threshold values are as follows for each component material:

- CS and LAS: 0.07% (strain amplitude), 21.0 ksi (stress amplitude)
- SS: 0.10% (strain amplitude), 28.3 ksi (stress amplitude)
- Ni-Cr-Fe Alloy: 0.10% (strain amplitude), 28.3 ksi (stress amplitude)

2.5 Dissolved Oxygen Content

Per [7.1], the reactor coolant system (RCS) DO content is controlled using [8.1], [8.2], and [8.3]. When the RCS temperature is above 250°F, the DO content in the RCS is maintained below 5 ppb (0.005 ppm) as discussed in [7.1] and supported by data from 2012 to 2020 (contained in the RCS Oxygen.xlsx spreadsheet attached to [7.1]). When the RCS temperature is below 250°F, the DO content may exceed 5 ppb (0.005 ppm). Specifically, the DO content is elevated in Mode 5 during the introduction of hydrogen peroxide to dissolve transient corrosion product layers in the RCS. Therefore, the following assumptions regarding the DO content were made in the EAF evaluations:

[

] ^{a,c,e}

2.6 Maximum Temperature for F_{en} Equations

Per Section A.2 of [4.4], a maximum temperature limit of 325°C (617°F) is specified for the F_{en} equations as a reasonable bound to cover most anticipated light water reactor operating conditions when considering the use of average temperature. In cases where transient temperatures exceed 325°C (617°F), the guidelines in [4.4] state that the analyst shall document the exceedance and justify its use in the F_{en} equations. The EAF evaluations assumed that [

] ^{a,c,e}

2.7 Impact of Design Transient Rates on Environmental Fatigue Usage

Design basis fatigue evaluations typically consider thermal transients that are characterized by high rates of temperature change with respect to the transients that occur in actual plant operation to maximize stress response and corresponding air fatigue usage values. However, transients with slower rates could generally produce higher F_{en} values that could potentially result in higher environmental fatigue usage values than transients with identical temperature changes and faster rates. The generic parametric study in [9] concluded that environmental fatigue usage maximizes at a smaller but nonzero ramp time, which implies that the effect of ramp rate on stress and resulting air fatigue usage generally dominates over its effect on the F_{en} in the environmental fatigue usage. Therefore, the EAF evaluations assumed that [

] a,c,e

3.0 Environmentally Assisted Fatigue Evaluation Results

EAF evaluations were performed for the following Point Beach Units 1 and 2 primary equipment sentinel locations using the guidelines in [4.3] and F_{en} equations in [4.4]:

- RVCH CRDM nozzle
- RV flange
- CRDM ULH
- SG primary chamber, tubesheet, and stub barrel complex (Unit 2)
- PZR safety and relief nozzle
- PZR surge nozzle (excluding insurge and outsurge transient effects)

The results of the EAF evaluations are presented in Table 3-1. The EAF evaluations were performed using the guidelines in [4.3] and the F_{en} equations in [4.4]. The transient cycles considered in the EAF evaluations are bounding for an 80-year period of operation. The CUF_{en} for each sentinel location is less than the ASME BPV Code limit of 1.0 and is therefore acceptable.

The transient cycles considered in the EAF evaluations were reduced from those considered in the AOR for some locations. Changes to plant documents (such as cycle counting procedures, FSAR, etc.) may be required to address the reduced transient cycles considered in these EAF evaluations to support the SLR program.

This report does not include the ASME Section XI Appendix L flaw tolerance evaluation for the PZR spray nozzle described in [2] or the EAF evaluations for the controlling PZR lower head locations including insurge and outsurge transient effects described in [3]. These evaluations will be addressed in a separate report.

Table 3-1: EAF Results for Primary Equipment Sentinel Locations

Line / System	Component / Location	Material Category	CUF		F_{en}	CUF_{en}	EAF Evaluation Group	SLR CUF Conservatism Reduction Summary
			AOR ⁽¹⁾	SLR				
RV	CRDM Nozzle	Ni-Cr-Fe Alloy	[] ^{a,c,e}	[] ^{a,c,e}	[] ^{a,c,e}	0.946	[] ^{a,c,e}	<p>The Ni-Cr-Fe alloy design fatigue curve in Section A.2.1 of [4.4] was applied. Refinements were made regarding the identification of stress cycles and application of more appropriate FSRFs. The cycles were reduced for the following transients:</p> <ul style="list-style-type: none"> • Unit Loading 5%/min: 2,700 cycles • Unit Unloading 5%/min: 2,700 cycles <p>The design cycles from the AOR were considered for all other transients.</p>
	Vessel Flange	LAS	[] ^{a,c,e}	[] ^{a,c,e}	[] ^{a,c,e}	0.985	[] ^{a,c,e}	<p>The LAS design fatigue curve in Section A.2.1 of [4.4] was applied. The cycles were reduced for the following transients:</p> <ul style="list-style-type: none"> • Unit Loading 5%/min: 5,000 cycles • Unit Unloading 5%/min: 5,000 cycles <p>The design cycles from the AOR were considered for all other transients.</p>
CRDM	ULH	SS	[] ^{a,c,e}	[] ^{a,c,e}	[] ^{a,c,e}	0.713	[] ^{a,c,e}	<p>The SS design fatigue curve in Section A.2.1 of [4.4] was applied. Refinements were made regarding the identification of stress cycles</p>

Line / System	Component / Location	Material Category	CUF		F _{en}	CUF _{en}	EAF Evaluation Group	SLR CUF Conservatism Reduction Summary
			AOR ⁽¹⁾	SLR				
								and application of more appropriate FSRFs. The design cycles from the AOR were considered for all transients.
SG	Primary Chamber, Tubesheet, and Stub Barrel Complex (Unit 2)	LAS	[] ^{a,c,e}	[] ^{a,c,e}	[] ^{a,c,e}	0.967	[] ^{a,c,e}	The LAS design fatigue curve in Section A.2.1 of [4.4] was applied. The cycles were reduced for the following transients: <ul style="list-style-type: none"> • Unit Loading 5%/min: 10,015 cycles • Feedwater Cycling at Hot Standby: 24,815 cycles The design cycles from the AOR were considered for all other transients.
PZR Upper Head / Shell	Safety and Relief Nozzle	CS	[] ^{a,c,e}	[] ^{a,c,e}	[] ^{a,c,e}	0.953	[] ^{a,c,e}	The CS design fatigue curve in Section A.2.1 of [4.4] was applied. The design cycles from the AOR were considered for all transients.
PZR Lower Head	Surge Nozzle (excluding insurge and outsurge transient effects)	CS	[] ^{a,c,e}	[] ^{a,c,e}	[] ^{a,c,e}	0.542	[] ^{a,c,e}	The CS design fatigue curve in Section A.2.1 of [4.4] was applied. The design cycles from the AOR were considered for all transients.

Notes:

(1) The AOR CUFs are listed in Table 2-1 of [5].

(2) The original AOR CUF for the CRDM nozzle is []^{a,c,e}. This CUF was adjusted in the EAF screening evaluation in [5] by applying the appropriate design fatigue curve from [4.4].

4.0 References

1. Westinghouse Letter, LTR-AMER-MKG-20-585, Revision 0, “Westinghouse Offer for Additional Scope for Subsequent License Renewal for Point Beach Units 1&2.”
2. Westinghouse Letter, LTR-AMER-MKG-20-847, Revision 0, “Westinghouse Offer for Additional EAF Evaluations and Appendix L Evaluation Scope for Subsequent License Renewal for Point Beach Units 1&2.”
3. Westinghouse Letter, LTR-AMER-MKG-20-923, Revision 0, “Westinghouse Offer for Additional EAF Evaluations (Pressurizer Lower Head including In-Surge / Out-Surge Transient Effects) Scope for Subsequent License Renewal for Point Beach Units 1&2.”
4. NRC Documents:
 - 4.1. NRC Document, NUREG-2191, Volumes 1 and 2, “Generic Aging Lessons Learned for Subsequent License Renewal (GALL-SLR) Report,” July 2017 (Agencywide Documents Access and Management System (ADAMS) Accession Nos. ML17187A031 and ML17187A204).
 - 4.2. NRC Document, NUREG-2192, “Standard Review Plan for Review of Subsequent License Renewal Applications for Nuclear Power Plants,” July 2017 (ADAMS Accession No. ML17188A158).
 - 4.3. NRC Regulatory Guide, 1.207, Revision 1, “Guidelines for Evaluating the Effects of Light-Water Reactor Water Environments in Fatigue Analyses of Metal Components,” (ADAMS Accession No. ML16315A130).
 - 4.4. NRC Document, NUREG/CR-6909, Revision 1, “Effect of LWR Water Environments on the Fatigue Life of Reactor Materials,” (ADAMS Accession No. ML16319A004).
5. Westinghouse Calculation Note, CN-SDA-II-20-005, Revision 1, “Environmentally Assisted Fatigue Screening of the Primary Equipment for Point Beach Unit 1 and Unit 2.”
6. Westinghouse Calculation Note, CN-SDA-II-20-006, Revision 0, “Environmentally Assisted Fatigue Evaluation of the Point Beach Unit 1 and Unit 2 Primary Equipment Sentinel Locations for Subsequent License Renewal.”
7. Design Input Transmittals:
 - 7.1. NextEra Energy Letter, NPL 2020-0010, Revision 0, “Input Request for Environmentally Assisted Fatigue Screening of Equipment.”
 - 7.2. NextEra Energy Letter, PBNWEC-20-0020, Revision 1, “Response to WEC-NEE-PB-SLR-20-002.”
8. Point Beach Procedures:
 - 8.1. NP 3.2.2, Revision 28, “Primary Water Chemistry Monitoring Program,” (electronically attached to [7.1]).

- 8.2. CAMP 101, Revision 73, “Daily Routine Sampling Schedule for Operating, Refueling, or Shutdown Units,” (electronically attached to [7.1]).
- 8.3. CAMP 112, Revision 22, “Addition of Hydrazine to the Primary System,” (electronically attached to [7.1]).
9. Materials Reliability Program: Evaluation of Controlling Transient Ramp Times Using Piping Methodologies When Considering Environmental Fatigue (Fen) Effects (MRP-218). EPRI, Palo Alto, CA: 2007. 1015014.

This page was added to the quality record by the PRIME system upon its validation and shall not be considered in the page numbering of this document.

Approval Information

Author Approval Matthews Eric J Jul-16-2020 14:14:01

Verifier Approval Imbrogno Greg M Jul-16-2020 15:30:41

Manager Approval Patterson Lynn Jul-16-2020 15:32:49

Files approved on Jul-16-2020

*** This record was final approved on 7/16/2020 3:32:49 PM. (This statement was added by the PRIME system upon its validation)

Point Beach Nuclear Plant Units 1 and 2
Dockets 50-266 and 50-301
NRC 2020-0032 Enclosure 4, Attachment 11

Enclosure 4

Non-proprietary Reference Documents and
Redacted Versions of Proprietary Reference
Documents

(Public Version)

Attachment 11

**Westinghouse LTR-SDA-II-20-13-NP, Revision 2,
“Environmentally Assisted Fatigue Evaluation
Results for the Point Beach Unit 1 and Unit 2
Pressurizer Lower Head for Subsequent License
Renewal,” September 23, 2020**

(29 Total Pages, including cover sheets)



1000 Westinghouse Drive
Cranberry Twp., PA 16066

To: John T. Ahearn
cc:

Date: September 23, 2020

From: RV/CV Design and Analysis
Ext: 412-374-4377
Fax: 724-940-8565

Ref: LTR-SDA-II-20-13-NP Rev. 2

Subject: Environmentally Assisted Fatigue Evaluation Results for the Point Beach Unit 1 and Unit 2 Pressurizer Lower Head for Subsequent License Renewal

To support the Point Beach Unit 1 and Unit 2 Subsequent License Renewal (SLR) program, environmentally assisted fatigue (EAF) evaluations were performed for the Pressurizer (PZR) lower head in accordance with the work scope described in [1]. Per Task 4D of [1], this letter report summarizes the EAF evaluation, including insurge/outsurge (I/O) transient effects, for the limiting PZR lower head locations to demonstrate adequate structural integrity for an 80-year operating period. Revision 1 of this letter addresses customer comments that are attached electronically in PRIME. Revision 2 of this letter includes a minor editorial revision in Section 4.0. Revision bars in the left-hand margin denote any changes from Revision 1 to Revision 2.

Author: Jamie L. Oakman*
Reactor Vessel/Containment Vessel Design and Analysis

Verifier: Gregory M. Imbrogno*
Reactor Vessel/Containment Vessel Design and Analysis

Manager: Lynn A. Patterson*
Reactor Vessel/Containment Vessel Design and Analysis

Trademark Notes:

WESTEMS is a trademark of Westinghouse Electric Company, LLC, its affiliates and/or its subsidiaries in the United States of America and may be registered in other countries throughout the world. All rights reserved. Unauthorized use is strictly prohibited. Other names may be trademarks of their respective owners.

This document may contain technical data subject to the export control laws of the United States. In the event that this document does contain such information, the Recipient's acceptance of this document constitutes agreement that this information in document form (or any other medium), including any attachments and exhibits hereto, shall not be exported, released or disclosed to foreign persons whether in the United States or abroad by recipient except in compliance with all U.S. export control regulations. Recipient shall include this notice with any reproduced or excerpted portion of this document or any document derived from, based on, incorporating, using or relying on the information contained in this document.

© 2020 Westinghouse Electric Company LLC
All Rights Reserved

***Electronically approved records are authenticated in the Process, Records, and Information Management Environment.**

Foreword:

This document contains Westinghouse Electric Company LLC proprietary information and data which has been identified in brackets. Coding ^(a,c,e) associated with the brackets sets forth the basis on which information is considered proprietary. These code letters are listed with their meanings in BMS-LGL-84, and are defined as follows:

- a. The information reveals the distinguishing aspects of a process (or component, structure, tool, method, etc.) where the prevention of its use by any of Westinghouse's competitors without license from Westinghouse constitutes a competitive economic advantage over other companies.
- c. The information, if used by a competitor, would reduce the competitor's expenditure of resources or improve the competitor's advantage in the design, manufacture, shipment, installation, assurance of quality, or licensing of a similar product.
- e. The information reveals aspects of past, present, or future Westinghouse or customer funded development plans and programs of potential commercial value to Westinghouse.

The proprietary information and data contained within the brackets of this document were obtained at considerable Westinghouse expense and its release could seriously affect our competitive position. This information is to be withheld from public disclosure in accordance with the Rules of Practice 10 CFR 2.390 and the information presented herein is to be safeguarded in accordance with 10 CFR 2.390. Withholding of this information does not affect the public interest.

This information has been provided for your internal use only and should not be released to persons or organizations outside the Directorate of Regulation and the ACRS (Advisory Committee on Reactor Safeguards) without the express written approval of Westinghouse Electric Company LLC. Should it become necessary to release this information to such persons as part of the review procedure, please contact Westinghouse Electric Company LLC, which will make the necessary arrangements required to protect the Company's proprietary interests.

The proprietary information in brackets can be viewed in the proprietary version of this report (LTR-SDA-II-20-13-P).

1.0 Introduction

As outlined in [1], the Point Beach Unit 1 and Unit 2 subsequent license renewal (SLR) program is intended to extend the operation license of these plants from 60 years to 80 years. Nuclear Regulatory Commission (NRC) guidance on the content of SLR applications is provided in [2.1] and [2.2]. Per subsection 4.3.2.1 of [2.2], pursuant to 10 CFR 54.21(c)(1)(i) through (iii), each metal fatigue time-limited aging analysis must demonstrate compliance with one of the following:

- i. The analyses remain valid for the period of extended operation (PEO);
- ii. The analyses have been projected to the end of the PEO; or
- iii. The effects of aging on the intended function(s) will be adequately managed for the PEO.

In addition, per subsection 4.3.2.1.2 of [2.2], environmentally assisted fatigue (EAF) evaluations should be performed for the limiting component locations exposed to the reactor water environment. A screening of Class 1 reactor coolant pressure boundary primary equipment was performed in [3] to determine sentinel (limiting) locations to be considered in subsequent EAF evaluations. The sentinel locations identified for the primary equipment include the following:

- Reactor Vessel Closure Head (RVCH) Control Rod Drive Mechanism (CRDM) nozzle
- Reactor Vessel (RV) flange
- CRDM Upper Latch Housing (ULH)
- Steam Generator (SG) primary chamber, tubesheet, and stub barrel complex (Unit 2)
- Pressurizer (PZR) safety and relief nozzle
- PZR surge nozzle (excluding insurge and outsurge transient effects)

The EAF results for the sentinel locations listed above are summarized in [4], but did not contain an evaluation of the PZR lower head locations including insurge/outsurge (I/O) transient effects. A fatigue analysis including I/O transient effects was performed for the PZR lower head locations for first license renewal and is applicable for 60 years of operation. The results of that evaluation are reported in Table 4.3.5-1 of [12] and the evaluation is considered the analysis of record (AOR) for the PZR lower head locations, consider I/O transient effects. Per Task 4D of [1], this letter report summarizes the results of EAF evaluation performed in [5] for the PZR lower head, including insurge and outsurge transient effects, for the PEO, applicable for 80 years of operation. These I/O transient events, which occur during heatup and cooldown cycles (i.e., sub-transients), were not specifically considered in the original pressurizer design analyses. The I/O transient events were used to re-evaluate the structural integrity of the pressurizers based on methods recommended by the Westinghouse Owners Group (WOG) in [8].

2.0 Methodology

This calculation note performs an EAF evaluation, including I/O transient effects, for the limiting PZR lower head locations using the guidelines in [2.3] and the EAF penalty factor (F_{en}) equations in [2.4]. The goal of this evaluation is to demonstrate that the PZR lower head EAF results for a reference plant are applicable to Point Beach Units 1 and 2. To accomplish this, a comparative evaluation is performed for the applicable inputs required for an EAF evaluation of the PZR lower head (i.e., transients and piping loads). The method to identify the reference plant evaluation and compare the applicable inputs is further discussed in subsections 2.1 to 2.2.

2.1 Identification of Reference Plant Evaluation

Generic finite element models were developed in [8] to represent the PZR lower head designs of operating WOG plants. Transfer function databases, which represent thermal and mechanical stress responses due to unit loads for an analysis section number (ASN), for these models were compiled in [9]. The reference plant evaluation (RPE) is identified as an evaluation that utilizes the generic PZR lower head finite element model that is applicable to Point Beach Units 1 and 2. Therefore, the geometry, materials, and boundary conditions utilized in the RPE are applicable to Point Beach Units 1 and 2.

2.2 Piping Load Comparative Analysis

To demonstrate that the piping loads from the reference plant evaluation are applicable for Point Beach, the Point Beach piping moment loads are compared to those for the reference plant evaluation. If the reference plant moment loads are not able to be shown to bound the Point Beach moment loads, simplified fatigue calculations are performed to justify that the difference in moment loads has a negligible impact on the fatigue evaluation.

2.3 Reactor Coolant System Transient Comparative Analysis

To demonstrate that the reactor coolant system (RCS) transients from the reference plant evaluation are applicable for Point Beach, the cycles and time history temperatures and pressures for the Point Beach EPU transients are compared to those for the reference plant evaluation. If the transient cycles and time history temperatures and pressures for the reference plant are not able to be shown to bound Point Beach, simplified fatigue calculations are performed to justify that the differences have a negligible impact on the fatigue evaluation.

2.4 Insurge and Outsurge Transient Comparative Analysis

Point Beach plant data electronically attached to [6.1] and/or heatup/cooldown procedures [7] are reviewed to determine the number of I/O events that occur during each heatup and cooldown transient, as

well as the severity of event. To demonstrate that the I/O transients from the reference plant evaluation are applicable for Point Beach, the cycles and severity of the I/O transients identified for Point Beach are compared to those for the reference plant evaluation. The I/O transient details are identified for three separate periods of operation: past, current, and future. The past period of operation is assumed to be the period of operations before the modified operation procedures (MOPs) recommended in [13] were applied, while the current and future periods of operation are associated with post-MOP operations.

2.5 Reference Plant Fatigue EAF Analysis

The EAF evaluations were performed using the guidelines in [2.3] and the F_{en} equations in Revision 0 [2.5] and draft Revision 1 [2.6] of NUREG/CR-6909 because the final version of NUREG/CR-6909, Revision 1 was not yet released. These evaluations utilized the RPE AORs, which consider I/O transient effects and design fatigue curves in Revision 0 [2.5] and draft Revision 1 [2.6] to derive a cumulative usage factor (CUF), and then utilized the bounding F_{en} equations from Revision 0 [2.5] and draft Revision 1 [2.6] for each location to derive a cumulative usage factor considering the effects of environmental fatigue (CUF_{en}). For carbon steel (CS) locations, the bounding F_{en} is achieved using the equations in Revision 0 [2.5]. For stainless steel (SS), the bounding F_{en} is achieved using the equations in draft Revision 1 [2.6]. For Point Beach, the applicable F_{en} equations from Revision 1 [2.4] are presented in Section 2.5.1. The F_{en} equations for carbon steel from Revision 1 [2.4] are the same as the equations in draft Revision 1 [2.6]. The F_{en} equations for stainless steel from Revision 1 [2.4] are bounded by the equations in draft Revision 1 [2.6]. Therefore, the RPE EAF results are bounding of the results that would be produced using Revision 1 [2.4].

The goal of the RPE was to calculate a CUF_{en} below 1.0 through typical linear elastic fatigue analysis techniques. For sentinel locations with low CUFs, the CUF_{en} was calculated by applying the maximum F_{en} , calculated per Section 2.5.2, to the CUF. For sentinel locations that could not accept this conservative method, strain rate dependent F_{en} values were calculated for significant fatigue pairs using the modified rate approach, which is described in [2.4] and summarized in Section 2.5.3.

2.5.1 F_{en} Equations

The materials for the sentinel locations in the EAF evaluations include CS and SS. The F_{en} for each of these materials was calculated using the equations in Section A.2 of [2.4], which are presented in Equation 2-1 and Equation 2-2.

CS:

$$F_{en} = \exp((0.003 - 0.031 \dot{\epsilon}^*) S^* T^* O^*) \quad 2-1$$

Where:

$$S^* = 2.0 + 98S$$

$$S \leq 0.015 \text{ wt. \%}$$

$$S^* = 3.47$$

$$S > 0.015 \text{ wt. \%}$$

S = Sulfur Content (wt. %)

$$T^* = 0.395$$

$$T < 150^\circ\text{C} (302^\circ\text{F})$$

$$T^* = (T - 75)/190$$

$$150^\circ\text{C} (302^\circ\text{F}) \leq T \leq 325^\circ\text{C} (617^\circ\text{F})$$

T = Service Temperature ($^\circ\text{C}$)

for calculation of T^*

$$O^* = 1.49$$

$$\text{DO} < 0.04 \text{ ppm}$$

$$O^* = \ln(\text{DO}/0.009)$$

$$0.04 \text{ ppm} \leq \text{DO} \leq 0.5 \text{ ppm}$$

$$O^* = 4.02$$

$$\text{DO} > 0.5 \text{ ppm}$$

DO = Dissolved Oxygen Content (ppm)

$$\dot{\epsilon}^* = 0$$

$$\dot{\epsilon} > 2.2 \text{ \%}/\text{s}$$

$$\dot{\epsilon}^* = \ln(\dot{\epsilon}/2.2)$$

$$0.0004 \text{ \%}/\text{s} \leq \dot{\epsilon} \leq 2.2 \text{ \%}/\text{s}$$

$$\dot{\epsilon}^* = \ln(0.0004/2.2)$$

$$\dot{\epsilon} < 0.0004 \text{ \%}/\text{s}$$

$\dot{\epsilon}$ = Strain Rate (\%/s)

SS:

$$F_{en} = \exp(- T^* \dot{\epsilon}^* O^*) \quad 2-2$$

Where:

$$T^* = 0$$

$$T < 100^\circ\text{C} (212^\circ\text{F})$$

$$T^* = (T - 100)/250$$

$$100^\circ\text{C} (212^\circ\text{F}) \leq T \leq 325^\circ\text{C} (617^\circ\text{F})$$

T = Service Temperature ($^\circ\text{C}$)

$$\dot{\epsilon}^* = 0$$

$$\dot{\epsilon} > 7.0 \text{ \%}/\text{s}$$

$$\dot{\epsilon}^* = \ln(\dot{\epsilon}/7.0)$$

$$0.0004 \text{ \%}/\text{s} \leq \dot{\epsilon} \leq 7.0 \text{ \%}/\text{s}$$

$$\dot{\epsilon}^* = \ln(0.0004/7.0)$$

$$\dot{\epsilon} < 0.0004 \text{ \%}/\text{s}$$

$\dot{\epsilon}$ = Strain Rate (\%/s)

$$O^* = 0.29$$

$$\text{DO} < 0.1 \text{ ppm (PWR or BWR HWC water)}$$

DO = Dissolved Oxygen Content (ppm)

2.5.2 Maximum F_{en} Values

[

] ^{a,c,e}

[

] ^{a,c,e}

2.5.3 Modified Rate Approach

The modified rate approach described in Section 4.4 of [2.4] is a method to calculate the F_{en} under transient conditions. This approach calculates the F_{en} at many points over the strain range during intervals of increasing strain, and then calculates the overall F_{en} for a fatigue pair by integrating over the entire strain range. The modified rate approach is presented in Equation 2-3.

$$F_{en} = \frac{\sum F_{en,i} \Delta \epsilon_i}{\sum \Delta \epsilon_i} \quad 2-3$$

Where:

F_{en} = overall F_{en} for the fatigue pair

$F_{en,i}$ = F_{en} computed for interval from time i to time i-1 based on $\dot{\epsilon}_i$ and the transformed parameters S^* , T^* , O^* , and $\dot{\epsilon}^*$

$$\dot{\epsilon}_i = \frac{\Delta \epsilon_i}{\Delta t_i}$$

$\Delta \epsilon_i$ = strain range from time i to time i-1

Δt_i = change in time from time i to time i-1

2.5.4 Strain Amplitude Threshold Values

Threshold strain and stress amplitude values are defined in Section A.2 of [2.4], below which environmental effects on the fatigue lives may not occur (i.e., $F_{en} = 1.0$). These threshold values are as follows for each component material:

- CS: 0.07% (strain amplitude), 21.0 ksi (stress amplitude)
- SS: 0.10% (strain amplitude), 28.3 ksi (stress amplitude)

2.5.5 Dissolved Oxygen Content

For most operating conditions, the DO is extremely low ($DO < 0.04$ ppm), to the point that a threshold F_{en} could be applied if only normal full power operation was considered because $O^* = 0$. A value of 0.005 ppm is used for the DO content, which is typical of the PWR environment [10]. Per [6.4], the RCS DO content is controlled using [7.3], [7.4], and [7.5]. When the RCS temperature is above 250°F, the DO content in the RCS is maintained below 5 ppb (0.005 ppm) as discussed in [6.4] and supported by data from 2012 to 2020 (contained in the RCS Oxygen.xlsx spreadsheet attached to [6.4]). During early and relatively short periods of HU where $DO < 0.04$ ppm may not always be verifiable, the service temperature (T) will be low ($< 150^\circ\text{C}$) making $T^* = 0$. And the transformed strain rate term in the applicable F_{en} equation reduces to zero anyway.

2.5.6 Maximum Temperature for F_{en} Equations

Per Section A.2 of [2.4], a maximum temperature limit of 325°C (617°F) is specified for the F_{en} equations as a reasonable bound to cover most anticipated light water reactor operating conditions when considering the use of average temperature. In cases where transient temperatures exceed 325°C (617°F), the guidelines in [2.4] state that the analyst shall document the exceedance and justify its use in the F_{en} equations. The EAF evaluations assumed that [

] ^{a,c,e}

3.0 Comparative Analysis

3.1 Identification of Reference Plant Evaluation

Per [5], the following PZR lower head finite element model is applicable to Point Beach Units 1 and 2:

- Model Designator: Cast 14s140
- PZR: Series 84
- Lower Head Material: Cast SA-216 WCC
- Surge Nozzle Size: 14 in
- Surge Nozzle Schedule: 140

The “Cast 14s140” model was also used to perform the reference plant PZR lower head EAF evaluations. Therefore, the reference plant EAF evaluation was identified as the RPE to be compared to Point Beach Units 1 and 2.

3.2 ASME BPV Code Reconciliation

Based on [11] the original American Society of Mechanical Engineers (ASME) Boiler and Pressure Vessel (BPV) Construction Code is the 1965 Edition with Addenda through Summer 1966 for the Point Beach PZR. Per the response to Q4 in [6.2], the current ASME Section XI Code year for Point Beach Unit 1 and Unit 2 is the 2007 Edition through 2008 Addenda. The RPE was performed to the 1989 Edition of the ASME Code for the material property input and the WESTEMS program that is used to calculate fatigue usage in the RPE uses the 2010 Edition of the ASME Code for the calculations. There is no substantial difference in the basic design requirements of NB-3200 between versions 1965 Edition, 1989 Edition, 2007 Edition, and 2010 Edition. Additionally, the changes to material properties between editions are typically small and therefore have insignificant effect on the results of this evaluation. Therefore, per [5], the ASME Code year considered in the RPE is demonstrated to be applicable to Point Beach for the purposes of this evaluation.

3.3 Piping Load Comparative Analysis

Since fatigue usage is calculated based on stress ranges between transient states, this comparison considers moment load ranges instead of the moment loads at individual transient states. The moment load ranges between Point Beach and the RPE for a representative set of transient states are compared to determine if the RPE moment load ranges bound the Point Beach moment load ranges. In general, the Point Beach moment load ranges were similar but greater than the RPE moment load ranges, however, it is noted that the RPE calculated the Poisson correction factor in NB-3227.6 in accordance with ASME Code editions prior to the 2010 Edition. Prior to the 2010 Edition, the equation for the Poisson correction factor in NB-3227.6 was based on a fictitious alternating stress, which was obtained from the design fatigue curve at the number of cycles for the transient pair. In the 2010 Edition, this fictitious alternating

stress was replaced with the actual alternating stress prior to the elastic modulus adjustment in NB-3222.4(e)(4). This change is considered an improvement in analysis methods and has the effect of reducing the Poisson correction factor. An assessment done in [5] demonstrates that the Poisson correction factor in the 2010 Edition of the ASME Code offsets the differences in moment loads between Point Beach and the RPE as well as the differences in pressure loads discussed in Section 3.4. Therefore, the RPE remains applicable for the Point Beach piping moment loads.

3.4 Reactor Coolant System Transient Comparative Analysis

A comparison of the reactor coolant system transients is required to determine if the RPE adequately bounds the Point Beach evaluation. To accomplish this, the pressure variations, temperature variations, and cycles for each transient are compared in [5]. The majority of the transient cycles that were analyzed for the RPE were higher than the design cycles for Point Beach. Per [6.3], the design allowable cycles are bounding of the 80 year projected cycles and therefore apply for 80 years of operation. In general, the thermal transients for the RPE are bounding of the transients for Point Beach because the temperature variations in the RPE transients are generally much larger than those for Point Beach. While the pressure transients for the RPE are comparable to those for Point Beach, the loss of load transient has a higher maximum pressure for Point Beach than for the RPE. An assessment done in [5] demonstrates that the Poisson correction factor in later ASME Code editions (see Section 3.2) offsets the differences in both the piping moment loads and pressure loads between Point Beach and the RPE, as discussed in Section 3.3. Therefore, the RPE remains applicable for the Point Beach RCS transients.

3.5 Insurge and Outsurge Transient Comparative Analysis

In order to perform a comparative analysis of the I/O transients for Point Beach, the plant operating period is divided into three main periods, as follows:

- Past operation (pre-1993)
- Current operation (1993-2017)
- Future operation (post-2017)

3.5.1 Past Operation

The past operation time period is defined as the period from plant start up through the year 1993 because the Westinghouse report that documents operational strategies for mitigating or eliminating PZR I/O transients during heatup and cooldown operations [13] was released in 1993. It is expected that after the release of this documentation, the Point Beach plant operation would follow the recommendations within [13]. Detailed plant data is not readily available for the past operation period for Point Beach Unit 1 or Unit 2. However, the surge line thermal stratification analysis [18] provides a list of heatup and cooldown events and the corresponding system temperature difference (ΔT) values from the beginning of operation through the early 1990s. Additionally, documentation on plant operation from the surge line

thermal stratification evaluation [18] and the comparison of plant procedures from the past and present provide a justification to extrapolate the current operation period data to the past operation for the number of I/O events.

3.5.1.1 Heatup/Cooldown System ΔT

The Point Beach Unit 1 and Unit 2 PZR surge line was evaluated for the effects of thermal stratification in [14]. To support the surge line evaluation, operator interviews were conducted and historical plan records were reviewed and summarized in [14]. The maximum system ΔT for each heatup and cooldown event at both units was determined as part of the PZR surge line thermal stratification evaluation. [

] ^{a,c,e} This assumption is justified by reviewing the dates for the heatups and cooldowns that are known for the early years of operation for both units, as well as the cycles through 2019 in [6.3].

To account for the number of heatup (HU) and cooldown (CD) events for which information is not known, the distribution for the known events is applied to the unknown events as shown in Table 3-1 and Table 3-2 for Unit 1 and Table 3-3 and Table 3-4 for Unit 2. For ease of later comparison to the RPE, the same system ΔT distribution is used herein.

Table 3-1: Point Beach Unit 1 Past Operation Period Maximum System ΔT Distribution - Heatup

Known HU	[] ^{a,c,e}				
Unknown HU	[] ^{a,c,e}				
Total HU	[] ^{a,c,e}				
System ΔT (°F)	Known Count	Known Distribution	Distributed Unknown Count	Rounded Unknown Count	Final Total Count
[] ^{a,c,e}	[] ^{a,c,e}	[] ^{a,c,e}	[] ^{a,c,e}	[] ^{a,c,e}	[] ^{a,c,e}
[] ^{a,c,e}	[] ^{a,c,e}	[] ^{a,c,e}	[] ^{a,c,e}	[] ^{a,c,e}	[] ^{a,c,e}
[] ^{a,c,e}	[] ^{a,c,e}	[] ^{a,c,e}	[] ^{a,c,e}	[] ^{a,c,e}	[] ^{a,c,e}
[] ^{a,c,e}	[] ^{a,c,e}	[] ^{a,c,e}	[] ^{a,c,e}	[] ^{a,c,e}	[] ^{a,c,e}
[] ^{a,c,e}	[] ^{a,c,e}	[] ^{a,c,e}	[] ^{a,c,e}	[] ^{a,c,e}	[] ^{a,c,e}
[] ^{a,c,e}	[] ^{a,c,e}	[] ^{a,c,e}	[] ^{a,c,e}	[] ^{a,c,e}	[] ^{a,c,e}
[] ^{a,c,e}	[] ^{a,c,e}	[] ^{a,c,e}	[] ^{a,c,e}	[] ^{a,c,e}	[] ^{a,c,e}
[] ^{a,c,e}	[] ^{a,c,e}	[] ^{a,c,e}	[] ^{a,c,e}	[] ^{a,c,e}	[] ^{a,c,e}
[] ^{a,c,e}	[] ^{a,c,e}	[] ^{a,c,e}	[] ^{a,c,e}	[] ^{a,c,e}	[] ^{a,c,e}
Totals	[] ^{a,c,e}	[] ^{a,c,e}	[] ^{a,c,e}	[] ^{a,c,e}	[] ^{a,c,e}

Table 3-2: Point Beach Unit 1 Past Operation Period Maximum System ΔT Distribution - Cooldown

Known CD	[] ^{a,c,e}				
Unknown CD	[] ^{a,c,e}				
Total CD	[] ^{a,c,e}				
System ΔT (°F)	Known Count	Known Distribution	Distributed Unknown Count	Rounded Unknown Count	Final Total Count
[] ^{a,c,e}	[] ^{a,c,e}	[] ^{a,c,e}	[] ^{a,c,e}	[] ^{a,c,e}	[] ^{a,c,e}
[] ^{a,c,e}	[] ^{a,c,e}	[] ^{a,c,e}	[] ^{a,c,e}	[] ^{a,c,e}	[] ^{a,c,e}
[] ^{a,c,e}	[] ^{a,c,e}	[] ^{a,c,e}	[] ^{a,c,e}	[] ^{a,c,e}	[] ^{a,c,e}
[] ^{a,c,e}	[] ^{a,c,e}	[] ^{a,c,e}	[] ^{a,c,e}	[] ^{a,c,e}	[] ^{a,c,e}
[] ^{a,c,e}	[] ^{a,c,e}	[] ^{a,c,e}	[] ^{a,c,e}	[] ^{a,c,e}	[] ^{a,c,e}
[] ^{a,c,e}	[] ^{a,c,e}	[] ^{a,c,e}	[] ^{a,c,e}	[] ^{a,c,e}	[] ^{a,c,e}
[] ^{a,c,e}	[] ^{a,c,e}	[] ^{a,c,e}	[] ^{a,c,e}	[] ^{a,c,e}	[] ^{a,c,e}
[] ^{a,c,e}	[] ^{a,c,e}	[] ^{a,c,e}	[] ^{a,c,e}	[] ^{a,c,e}	[] ^{a,c,e}
[] ^{a,c,e}	[] ^{a,c,e}	[] ^{a,c,e}	[] ^{a,c,e}	[] ^{a,c,e}	[] ^{a,c,e}
Totals	[] ^{a,c,e}	[] ^{a,c,e}	[] ^{a,c,e}	[] ^{a,c,e}	[] ^{a,c,e}

Table 3-3: Point Beach Unit 2 Past Operation Period Maximum System ΔT Distribution - Heatup

Known HU	[] ^{a,c,e}				
Unknown HU	[] ^{a,c,e}				
Total HU	[] ^{a,c,e}				
System ΔT (°F)	Known Count	Known Distribution	Distributed Unknown Count	Rounded Unknown Count	Final Total Count
[] ^{a,c,e}	[] ^{a,c,e}	[] ^{a,c,e}	[] ^{a,c,e}	[] ^{a,c,e}	[] ^{a,c,e}
[] ^{a,c,e}	[] ^{a,c,e}	[] ^{a,c,e}	[] ^{a,c,e}	[] ^{a,c,e}	[] ^{a,c,e}
[] ^{a,c,e}	[] ^{a,c,e}	[] ^{a,c,e}	[] ^{a,c,e}	[] ^{a,c,e}	[] ^{a,c,e}
[] ^{a,c,e}	[] ^{a,c,e}	[] ^{a,c,e}	[] ^{a,c,e}	[] ^{a,c,e}	[] ^{a,c,e}
[] ^{a,c,e}	[] ^{a,c,e}	[] ^{a,c,e}	[] ^{a,c,e}	[] ^{a,c,e}	[] ^{a,c,e}
[] ^{a,c,e}	[] ^{a,c,e}	[] ^{a,c,e}	[] ^{a,c,e}	[] ^{a,c,e}	[] ^{a,c,e}
[] ^{a,c,e}	[] ^{a,c,e}	[] ^{a,c,e}	[] ^{a,c,e}	[] ^{a,c,e}	[] ^{a,c,e}
[] ^{a,c,e}	[] ^{a,c,e}	[] ^{a,c,e}	[] ^{a,c,e}	[] ^{a,c,e}	[] ^{a,c,e}
Totals	[] ^{a,c,e}	[] ^{a,c,e}	[] ^{a,c,e}	[] ^{a,c,e}	[] ^{a,c,e}

Table 3-4: Point Beach Unit 2 Past Operation Period Maximum System ΔT Distribution - Cooldown

Known CD	[] ^{a,c,e}				
Unknown CD	[] ^{a,c,e}				
Total CD	[] ^{a,c,e}				
System ΔT (°F)	Known Count	Known Distribution	Distributed Unknown Count	Rounded Unknown Count	Final Total Count
[] ^{a,c,e}	[] ^{a,c,e}	[] ^{a,c,e}	[] ^{a,c,e}	[] ^{a,c,e}	[] ^{a,c,e}
[] ^{a,c,e}	[] ^{a,c,e}	[] ^{a,c,e}	[] ^{a,c,e}	[] ^{a,c,e}	[] ^{a,c,e}
[] ^{a,c,e}	[] ^{a,c,e}	[] ^{a,c,e}	[] ^{a,c,e}	[] ^{a,c,e}	[] ^{a,c,e}
[] ^{a,c,e}	[] ^{a,c,e}	[] ^{a,c,e}	[] ^{a,c,e}	[] ^{a,c,e}	[] ^{a,c,e}
[] ^{a,c,e}	[] ^{a,c,e}	[] ^{a,c,e}	[] ^{a,c,e}	[] ^{a,c,e}	[] ^{a,c,e}
[] ^{a,c,e}	[] ^{a,c,e}	[] ^{a,c,e}	[] ^{a,c,e}	[] ^{a,c,e}	[] ^{a,c,e}
[] ^{a,c,e}	[] ^{a,c,e}	[] ^{a,c,e}	[] ^{a,c,e}	[] ^{a,c,e}	[] ^{a,c,e}
[] ^{a,c,e}	[] ^{a,c,e}	[] ^{a,c,e}	[] ^{a,c,e}	[] ^{a,c,e}	[] ^{a,c,e}
Totals	[] ^{a,c,e}	[] ^{a,c,e}	[] ^{a,c,e}	[] ^{a,c,e}	[] ^{a,c,e}

3.5.1.2 I/O Events

Per Section 2.4.2 of [14], the general heatup and cooldown processes were categorized with plants using the “water-solid” approach as recommended to mitigate the effects of PZR I/O transients during these events. Plant operating records were reviewed and it was found that there were heatup and cooldown events in the history of both units where the system ΔT exceeded the 210°F limit assumed in the WOG generic PZR surge line thermal stratification analysis [15]. In some instances, this was due to a pressure test being performed with a steam bubble in the pressurizer. Although the general plant heatup procedure was a water-solid approach, there were a substantial number of events with a system ΔT higher than 210°F. No events were recorded for which the system ΔT exceeded the administrative limit of 320°F. For future operation, (post-1993 at the time of this report), Wisconsin Electric had committed to revise their operation procedures to limit the system ΔT to 210°F.

When comparing the major steps in the heatup operating procedure from 1984 [7.2] to their current version [7.1], it can be said that the procedures are essentially the same. Therefore, it would be valid to extrapolate the I/O event data from the current operation period (discussed in detail in Section 3.5.2.3) to the past operation period, which is []^{a,c,e} I/O events per heatup/cooldown cycle at maximum system ΔT and assumed to insurge into the PZR.

3.5.1.3 Comparison to RPE Pre-MOP I/O Transients

The system ΔT and cycles for the Point Beach past operation period are compared to the RPE system ΔT and cycles for the RPE non-MOP period in Table 3-5 and Table 3-6 for heatup and cooldown events, respectively.

Table 3-5: Point Beach Past Operation Period Maximum System ΔT Distribution Comparison - Heatup

System ΔT (°F)	Point Beach Unit 1 Final Total Count	Point Beach Unit 2 Final Total Count	RPE Final Total Count
[] ^{a,c,e}	[] ^{a,c,e}	[] ^{a,c,e}	[] ^{a,c,e}
[] ^{a,c,e}	[] ^{a,c,e}	[] ^{a,c,e}	[] ^{a,c,e}
[] ^{a,c,e}	[] ^{a,c,e}	[] ^{a,c,e}	[] ^{a,c,e}
[] ^{a,c,e}	[] ^{a,c,e}	[] ^{a,c,e}	[] ^{a,c,e}
[] ^{a,c,e}	[] ^{a,c,e}	[] ^{a,c,e}	[] ^{a,c,e}
[] ^{a,c,e}	[] ^{a,c,e}	[] ^{a,c,e}	[] ^{a,c,e}
[] ^{a,c,e}	[] ^{a,c,e}	[] ^{a,c,e}	[] ^{a,c,e}
[] ^{a,c,e}	[] ^{a,c,e}	[] ^{a,c,e}	[] ^{a,c,e}
Totals	[] ^{a,c,e}	[] ^{a,c,e}	[] ^{a,c,e}

Table 3-6: Point Beach Past Operation Period Maximum System ΔT Distribution Comparison - Cooldown

System ΔT ($^{\circ}F$)	Point Beach Unit 1 Final Total Count	Point Beach Unit 2 Final Total Count	RPE Final Total Count
[] ^{a,c,e}	[] ^{a,c,e}	[] ^{a,c,e}	[] ^{a,c,e}
[] ^{a,c,e}	[] ^{a,c,e}	[] ^{a,c,e}	[] ^{a,c,e}
[] ^{a,c,e}	[] ^{a,c,e}	[] ^{a,c,e}	[] ^{a,c,e}
[] ^{a,c,e}	[] ^{a,c,e}	[] ^{a,c,e}	[] ^{a,c,e}
[] ^{a,c,e}	[] ^{a,c,e}	[] ^{a,c,e}	[] ^{a,c,e}
[] ^{a,c,e}	[] ^{a,c,e}	[] ^{a,c,e}	[] ^{a,c,e}
[] ^{a,c,e}	[] ^{a,c,e}	[] ^{a,c,e}	[] ^{a,c,e}
[] ^{a,c,e}	[] ^{a,c,e}	[] ^{a,c,e}	[] ^{a,c,e}
Totals	[] ^{a,c,e}	[] ^{a,c,e}	[] ^{a,c,e}

As shown in Table 3-5 and Table 3-6, the RPE non-MOP heatup and cooldown transients bound both the Point Beach Unit 1 and Unit 2 transients both in terms of overall cycles and system ΔT distribution. The RPE system ΔT distribution includes more cycles at higher system ΔT values than the Point Beach units.

The RPE I/O events for non-MOP heatup and cooldown transients are [

]^{a,c,e} As discussed in Section 3.5.1.2, the number of I/O events for Point Beach Unit 1 and Unit 2 is []^{a,c,e} I/O cycles per heatup or cooldown cycle, assumed at full system ΔT . This is much lower than the []^{a,c,e} number of events for the RPE. Based on the comparison of the heatup/cooldown event maximum system ΔT and the number of I/O cycles per heatup/cooldown, it is concluded that the RPE non-MOP I/O transients are bounding of the Point Beach Unit 1 and Unit 2 past operation time period.

3.5.2 Current and Future Operation

The current operation time period is defined as the period from 1993 when operational strategies for mitigating PZR I/O transients were published, through 2017 when the most current plant data is available from Point Beach. During this time period, it is expected that Point Beach plant operations would follow the recommendations from [13] regarding procedures for heatup and cooldown events to mitigate PZR I/O transient events. Note that additional plant data was provided through 2019 for both units, however this data is not included in the evaluation documented in this section. The additional data is analyzed in Appendix C of [5] and it is determined that the additional two years of data have a negligible impact on the current and future I/O transient comparison evaluation and conclusion documented herein.

The future operation time period is defined as the period from 2020 to the end of plant life for each unit. Because no plant data is available for the future operation period, the current operation period is assumed to be representative of the future operation period at Point Beach. Therefore, both the current and future operation time periods are addressed in this section.

3.5.2.1 Plant Data Review

Detailed plant data from Point Beach Unit 1 and Unit 2 is electronically attached to [6.1] for 3/31/2002 through 11/8/2017 for each unit. The procedure for reviewing these plant data files to identify I/O events is as follows:

1. [
- 2.
- 3.
- 4.

]a,c,e

Table 3-7 and Table 3-8 document the results of Steps 1-4 above for Unit 1 and Unit 2, respectively. The average number of I/O events per heatup or cooldown transient is reported in each table.

Table 3-7: Point Beach Unit 1 Plant Data Review Results for Current Operation Period

Start Date	End Date	Transient	Maximum System ΔT ($^{\circ}F$)	Number of I/O Events	Event ΔT ($^{\circ}F$)
9/11/2002	9/17/2002	Cooldown	[] ^{a,c,e}	[] ^{a,c,e}	[] ^{a,c,e}
10/8/2002	10/22/2002	Heatup	[] ^{a,c,e}	[] ^{a,c,e}	[] ^{a,c,e}
3/31/2004	4/9/2004	Cooldown	[] ^{a,c,e}	[] ^{a,c,e}	[] ^{a,c,e}
5/27/2004	6/16/2004	Heatup	[] ^{a,c,e}	[] ^{a,c,e}	[] ^{a,c,e}
9/22/2005	9/30/2005	Cooldown	[] ^{a,c,e}	[] ^{a,c,e}	[] ^{a,c,e}
10/27/2005	11/9/2005	Heatup	[] ^{a,c,e}	[] ^{a,c,e}	[] ^{a,c,e}
11/9/2005	11/13/2005	Cooldown	[] ^{a,c,e}	[] ^{a,c,e}	[] ^{a,c,e}
11/19/2005	11/29/2005	Heatup	[] ^{a,c,e}	[] ^{a,c,e}	[] ^{a,c,e}
3/29/2007	4/5/2007	Cooldown	[] ^{a,c,e}	[] ^{a,c,e}	[] ^{a,c,e}
4/24/2007	5/12/2007	Heatup	[] ^{a,c,e}	[] ^{a,c,e}	[] ^{a,c,e}
6/12/2007	6/17/2007	Cooldown	[] ^{a,c,e}	[] ^{a,c,e}	[] ^{a,c,e}
6/17/2007	6/25/2007	Heatup	[] ^{a,c,e}	[] ^{a,c,e}	[] ^{a,c,e}

Start Date	End Date	Transient	Maximum System ΔT ($^{\circ}F$)	Number of I/O Events	Event ΔT ($^{\circ}F$)
1/15/2008	1/19/2008	Cooldown	[] ^{a,c,e}	[] ^{a,c,e}	[] ^{a,c,e}
2/1/2008	2/6/2008	Heatup	[] ^{a,c,e}	[] ^{a,c,e}	[] ^{a,c,e}
10/2/2008	10/11/2008	Cooldown	[] ^{a,c,e}	[] ^{a,c,e}	[] ^{a,c,e}
11/5/2008	11/20/2008	Heatup	[] ^{a,c,e}	[] ^{a,c,e}	[] ^{a,c,e}
2/28/2010	3/6/2010	Cooldown	[] ^{a,c,e}	[] ^{a,c,e}	[] ^{a,c,e}
3/26/2010	4/8/2010	Heatup	[] ^{a,c,e}	[] ^{a,c,e}	[] ^{a,c,e}
9/30/2011	10/13/2011	Cooldown	[] ^{a,c,e}	[] ^{a,c,e}	[] ^{a,c,e}
11/27/2011	12/30/2011	Heatup	[] ^{a,c,e}	[] ^{a,c,e}	[] ^{a,c,e}
3/16/2013	3/22/2013	Cooldown	[] ^{a,c,e}	[] ^{a,c,e}	[] ^{a,c,e}
4/10/2013	4/23/2013	Heatup	[] ^{a,c,e}	[] ^{a,c,e}	[] ^{a,c,e}
10/2/2014	10/7/2014	Cooldown	[] ^{a,c,e}	[] ^{a,c,e}	[] ^{a,c,e}
10/24/2014	11/4/2014	Heatup	[] ^{a,c,e}	[] ^{a,c,e}	[] ^{a,c,e}
3/10/2016	3/16/2016	Cooldown	[] ^{a,c,e}	[] ^{a,c,e}	[] ^{a,c,e}
3/31/2016	4/13/2016	Heatup	[] ^{a,c,e}	[] ^{a,c,e}	[] ^{a,c,e}
10/4/2017	10/11/2017	Cooldown	[] ^{a,c,e}	[] ^{a,c,e}	[] ^{a,c,e}
10/25/2017	11/4/2017	Heatup	[] ^{a,c,e}	[] ^{a,c,e}	[] ^{a,c,e}
		Average:	[] ^{a,c,e}	[] ^{a,c,e}	

Table 3-8: Point Beach Unit 2 Plant Data Review Results for Current Operation Period

Start Date	End Date	Transient	Maximum System ΔT ($^{\circ}F$)	Number of I/O Events	Event ΔT ($^{\circ}F$)
4/11/2002	4/16/2002	Cooldown	[] ^{a,c,e}	[] ^{a,c,e}	[] ^{a,c,e}
5/5/2002	5/17/2002	Heatup	[] ^{a,c,e}	[] ^{a,c,e}	[] ^{a,c,e}
10/2/2003	10/6/2003	Cooldown	[] ^{a,c,e}	[] ^{a,c,e}	[] ^{a,c,e}
10/30/2003	11/24/2003	Heatup	[] ^{a,c,e}	[] ^{a,c,e}	[] ^{a,c,e}
11/19/2004	11/21/2004	Cooldown	[] ^{a,c,e}	[] ^{a,c,e}	[] ^{a,c,e}
11/22/2004	11/26/2004	Heatup	[] ^{a,c,e}	[] ^{a,c,e}	[] ^{a,c,e}
3/29/2005	4/7/2005	Cooldown	[] ^{a,c,e}	[] ^{a,c,e}	[] ^{a,c,e}
6/27/2005	7/18/2005	Heatup	[] ^{a,c,e}	[] ^{a,c,e}	[] ^{a,c,e}
10/13/2006	10/17/2006	Cooldown	[] ^{a,c,e}	[] ^{a,c,e}	[] ^{a,c,e}
11/7/2006	11/20/2006	Heatup	[] ^{a,c,e}	[] ^{a,c,e}	[] ^{a,c,e}
4/4/2008	4/8/2008	Cooldown	[] ^{a,c,e}	[] ^{a,c,e}	[] ^{a,c,e}
5/3/2008	5/17/2008	Heatup	[] ^{a,c,e}	[] ^{a,c,e}	[] ^{a,c,e}
10/12/2009	10/18/2009	Cooldown	[] ^{a,c,e}	[] ^{a,c,e}	[] ^{a,c,e}
11/28/2009	12/13/2009	Heatup	[] ^{a,c,e}	[] ^{a,c,e}	[] ^{a,c,e}
2/26/2011	3/5/2011	Cooldown	[] ^{a,c,e}	[] ^{a,c,e}	[] ^{a,c,e}
5/26/2011	6/30/2011	Heatup	[] ^{a,c,e}	[] ^{a,c,e}	[] ^{a,c,e}
6/27/2012	6/30/2012	Cooldown	[] ^{a,c,e}	[] ^{a,c,e}	[] ^{a,c,e}

Start Date	End Date	Transient	Maximum System ΔT ($^{\circ}F$)	Number of I/O Events	Event ΔT ($^{\circ}F$)
6/30/2012	7/5/2012	Heatup	[] ^{a,c,e}	[] ^{a,c,e}	[] ^{a,c,e}
10/30/2012	11/4/2012	Cooldown	[] ^{a,c,e}	[] ^{a,c,e}	[] ^{a,c,e}
11/24/2012	12/5/2012	Heatup	[] ^{a,c,e}	[] ^{a,c,e}	[] ^{a,c,e}
3/15/2014	3/20/2014	Cooldown	[] ^{a,c,e}	[] ^{a,c,e}	[] ^{a,c,e}
4/9/2014	4/22/2014	Heatup	[] ^{a,c,e}	[] ^{a,c,e}	[] ^{a,c,e}
10/1/2015	10/6/2015	Cooldown	[] ^{a,c,e}	[] ^{a,c,e}	[] ^{a,c,e}
10/22/2015	11/3/2015	Heatup	[] ^{a,c,e}	[] ^{a,c,e}	[] ^{a,c,e}
3/16/2017	3/20/2017	Cooldown	[] ^{a,c,e}	[] ^{a,c,e}	[] ^{a,c,e}
4/7/2017	4/24/2017	Heatup	[] ^{a,c,e}	[] ^{a,c,e}	[] ^{a,c,e}
		Average:	[] ^{a,c,e}	[] ^{a,c,e}	

3.5.2.2 Heatup/Cooldown Cycles and System ΔT

To account for the number of heatup and cooldown events for which information is not known, the distribution for the known events is applied to the unknown events as shown in Table 3-9 and Table 3-10 for Unit 1 and Table 3-11 and Table 3-12 for Unit 2. For ease of later comparison to the RPE, the same system ΔT distribution is used herein.

Table 3-9: Point Beach Unit 1 Current & Future Operation Period Maximum System ΔT Distribution - Heatup

Known HU	[] ^{a,c,e}				
Unknown HU	[] ^{a,c,e}				
Total HU	[] ^{a,c,e}				
System ΔT (°F)	Known Count	Known Distribution	Distributed Unknown Count	Rounded Unknown Count	Final Total Count
[] ^{a,c,e}	[] ^{a,c,e}	[] ^{a,c,e}	[] ^{a,c,e}	[] ^{a,c,e}	[] ^{a,c,e}
[] ^{a,c,e}	[] ^{a,c,e}	[] ^{a,c,e}	[] ^{a,c,e}	[] ^{a,c,e}	[] ^{a,c,e}
[] ^{a,c,e}	[] ^{a,c,e}	[] ^{a,c,e}	[] ^{a,c,e}	[] ^{a,c,e}	[] ^{a,c,e}
[] ^{a,c,e}	[] ^{a,c,e}	[] ^{a,c,e}	[] ^{a,c,e}	[] ^{a,c,e}	[] ^{a,c,e}
[] ^{a,c,e}	[] ^{a,c,e}	[] ^{a,c,e}	[] ^{a,c,e}	[] ^{a,c,e}	[] ^{a,c,e}
[] ^{a,c,e}	[] ^{a,c,e}	[] ^{a,c,e}	[] ^{a,c,e}	[] ^{a,c,e}	[] ^{a,c,e}
[] ^{a,c,e}	[] ^{a,c,e}	[] ^{a,c,e}	[] ^{a,c,e}	[] ^{a,c,e}	[] ^{a,c,e}
[] ^{a,c,e}	[] ^{a,c,e}	[] ^{a,c,e}	[] ^{a,c,e}	[] ^{a,c,e}	[] ^{a,c,e}
[] ^{a,c,e}	[] ^{a,c,e}	[] ^{a,c,e}	[] ^{a,c,e}	[] ^{a,c,e}	[] ^{a,c,e}
Totals	[] ^{a,c,e}	[] ^{a,c,e}	[] ^{a,c,e}	[] ^{a,c,e}	[] ^{a,c,e}

Table 3-10: Point Beach Unit 1 Current Operation Period Maximum System ΔT Distribution - Cooldown

Known CD	[] ^{a,c,e}				
Unknown CD	[] ^{a,c,e}				
Total CD	[] ^{a,c,e}				
System ΔT (°F)	Known Count	Known Distribution	Distributed Unknown Count	Rounded Unknown Count	Final Total Count
[] ^{a,c,e}	[] ^{a,c,e}	[] ^{a,c,e}	[] ^{a,c,e}	[] ^{a,c,e}	[] ^{a,c,e}
[] ^{a,c,e}	[] ^{a,c,e}	[] ^{a,c,e}	[] ^{a,c,e}	[] ^{a,c,e}	[] ^{a,c,e}
[] ^{a,c,e}	[] ^{a,c,e}	[] ^{a,c,e}	[] ^{a,c,e}	[] ^{a,c,e}	[] ^{a,c,e}
[] ^{a,c,e}	[] ^{a,c,e}	[] ^{a,c,e}	[] ^{a,c,e}	[] ^{a,c,e}	[] ^{a,c,e}
[] ^{a,c,e}	[] ^{a,c,e}	[] ^{a,c,e}	[] ^{a,c,e}	[] ^{a,c,e}	[] ^{a,c,e}
[] ^{a,c,e}	[] ^{a,c,e}	[] ^{a,c,e}	[] ^{a,c,e}	[] ^{a,c,e}	[] ^{a,c,e}
[] ^{a,c,e}	[] ^{a,c,e}	[] ^{a,c,e}	[] ^{a,c,e}	[] ^{a,c,e}	[] ^{a,c,e}
[] ^{a,c,e}	[] ^{a,c,e}	[] ^{a,c,e}	[] ^{a,c,e}	[] ^{a,c,e}	[] ^{a,c,e}
[] ^{a,c,e}	[] ^{a,c,e}	[] ^{a,c,e}	[] ^{a,c,e}	[] ^{a,c,e}	[] ^{a,c,e}
Totals	[] ^{a,c,e}	[] ^{a,c,e}	[] ^{a,c,e}	[] ^{a,c,e}	[] ^{a,c,e}

Table 3-11: Point Beach Unit 2 Current Operation Period Maximum System ΔT Distribution - Heatup

Known HU	[] ^{a,c,e}				
Unknown HU	[] ^{a,c,e}				
Total HU	[] ^{a,c,e}				
System ΔT (°F)	Known Count	Known Distribution	Distributed Unknown Count	Rounded Unknown Count	Final Total Count
[] ^{a,c,e}	[] ^{a,c,e}	[] ^{a,c,e}	[] ^{a,c,e}	[] ^{a,c,e}	[] ^{a,c,e}
[] ^{a,c,e}	[] ^{a,c,e}	[] ^{a,c,e}	[] ^{a,c,e}	[] ^{a,c,e}	[] ^{a,c,e}
[] ^{a,c,e}	[] ^{a,c,e}	[] ^{a,c,e}	[] ^{a,c,e}	[] ^{a,c,e}	[] ^{a,c,e}
[] ^{a,c,e}	[] ^{a,c,e}	[] ^{a,c,e}	[] ^{a,c,e}	[] ^{a,c,e}	[] ^{a,c,e}
[] ^{a,c,e}	[] ^{a,c,e}	[] ^{a,c,e}	[] ^{a,c,e}	[] ^{a,c,e}	[] ^{a,c,e}
[] ^{a,c,e}	[] ^{a,c,e}	[] ^{a,c,e}	[] ^{a,c,e}	[] ^{a,c,e}	[] ^{a,c,e}
[] ^{a,c,e}	[] ^{a,c,e}	[] ^{a,c,e}	[] ^{a,c,e}	[] ^{a,c,e}	[] ^{a,c,e}
[] ^{a,c,e}	[] ^{a,c,e}	[] ^{a,c,e}	[] ^{a,c,e}	[] ^{a,c,e}	[] ^{a,c,e}
[] ^{a,c,e}	[] ^{a,c,e}	[] ^{a,c,e}	[] ^{a,c,e}	[] ^{a,c,e}	[] ^{a,c,e}
Totals	[] ^{a,c,e}	[] ^{a,c,e}	[] ^{a,c,e}	[] ^{a,c,e}	[] ^{a,c,e}

Table 3-12: Point Beach Unit 2 Current Operation Period Maximum System ΔT Distribution - Cooldown

Known CD	[] ^{a,c,e}				
Unknown CD	[] ^{a,c,e}				
Total CD	[] ^{a,c,e}				
System ΔT (°F)	Known Count	Known Distribution	Distributed Unknown Count	Rounded Unknown Count	Final Total Count
[] ^{a,c,e}	[] ^{a,c,e}	[] ^{a,c,e}	[] ^{a,c,e}	[] ^{a,c,e}	[] ^{a,c,e}
[] ^{a,c,e}	[] ^{a,c,e}	[] ^{a,c,e}	[] ^{a,c,e}	[] ^{a,c,e}	[] ^{a,c,e}
[] ^{a,c,e}	[] ^{a,c,e}	[] ^{a,c,e}	[] ^{a,c,e}	[] ^{a,c,e}	[] ^{a,c,e}
[] ^{a,c,e}	[] ^{a,c,e}	[] ^{a,c,e}	[] ^{a,c,e}	[] ^{a,c,e}	[] ^{a,c,e}
[] ^{a,c,e}	[] ^{a,c,e}	[] ^{a,c,e}	[] ^{a,c,e}	[] ^{a,c,e}	[] ^{a,c,e}
[] ^{a,c,e}	[] ^{a,c,e}	[] ^{a,c,e}	[] ^{a,c,e}	[] ^{a,c,e}	[] ^{a,c,e}
[] ^{a,c,e}	[] ^{a,c,e}	[] ^{a,c,e}	[] ^{a,c,e}	[] ^{a,c,e}	[] ^{a,c,e}
[] ^{a,c,e}	[] ^{a,c,e}	[] ^{a,c,e}	[] ^{a,c,e}	[] ^{a,c,e}	[] ^{a,c,e}
[] ^{a,c,e}	[] ^{a,c,e}	[] ^{a,c,e}	[] ^{a,c,e}	[] ^{a,c,e}	[] ^{a,c,e}
Totals	[] ^{a,c,e}	[] ^{a,c,e}	[] ^{a,c,e}	[] ^{a,c,e}	[] ^{a,c,e}

3.5.2.3 I/O Events

Per Table 3-7 and Table 3-8, the average I/O events per heatup/cooldown transient for each unit are nearly identical with the bounding value (for Unit 1) being []^{a,c,e} I/O events per heatup/cooldown. Therefore, []^{a,c,e} events per heatup/cooldown transient are conservatively applied for the current operation time period. The []^{a,c,e} events are conservatively applied at the maximum system ΔT and assumed to penetrate into the PZR.

3.5.2.4 Comparison to RPE Pre-MOP I/O Transients

The system ΔT and cycles from Section 3.5.2.2 for the Point Beach current operation period are compared to the RPE system ΔT and cycles for the RPE MOP and future period in Table 3-13 and Table 3-14 for heatup and cooldown events, respectively.

Table 3-13: Point Beach Current Operation Period Maximum System ΔT Distribution Comparison - Heatup

System ΔT (°F)	Point Beach Unit 1 Final Total Count	Point Beach Unit 2 Final Total Count	RPE Final Total Count
[] ^{a,c,e}	[] ^{a,c,e}	[] ^{a,c,e}	[] ^{a,c,e}
[] ^{a,c,e}	[] ^{a,c,e}	[] ^{a,c,e}	[] ^{a,c,e}
[] ^{a,c,e}	[] ^{a,c,e}	[] ^{a,c,e}	[] ^{a,c,e}
[] ^{a,c,e}	[] ^{a,c,e}	[] ^{a,c,e}	[] ^{a,c,e}
[] ^{a,c,e}	[] ^{a,c,e}	[] ^{a,c,e}	[] ^{a,c,e}
[] ^{a,c,e}	[] ^{a,c,e}	[] ^{a,c,e}	[] ^{a,c,e}
[] ^{a,c,e}	[] ^{a,c,e}	[] ^{a,c,e}	[] ^{a,c,e}
[] ^{a,c,e}	[] ^{a,c,e}	[] ^{a,c,e}	[] ^{a,c,e}
Totals	[] ^{a,c,e}	[] ^{a,c,e}	[] ^{a,c,e}

Table 3-14: Point Beach Current Operation Period Maximum System ΔT Distribution Comparison - Cooldown

System ΔT (°F)	Point Beach Unit 1 Final Total Count	Point Beach Unit 2 Final Total Count	RPE Final Total Count
[] ^{a,c,e}	[] ^{a,c,e}	[] ^{a,c,e}	[] ^{a,c,e}
[] ^{a,c,e}	[] ^{a,c,e}	[] ^{a,c,e}	[] ^{a,c,e}
[] ^{a,c,e}	[] ^{a,c,e}	[] ^{a,c,e}	[] ^{a,c,e}
[] ^{a,c,e}	[] ^{a,c,e}	[] ^{a,c,e}	[] ^{a,c,e}

System ΔT (°F)	Point Beach Unit 1 Final Total Count	Point Beach Unit 2 Final Total Count	RPE Final Total Count
[] ^{a,c,e}	[] ^{a,c,e}	[] ^{a,c,e}	[] ^{a,c,e}
[] ^{a,c,e}	[] ^{a,c,e}	[] ^{a,c,e}	[] ^{a,c,e}
[] ^{a,c,e}	[] ^{a,c,e}	[] ^{a,c,e}	[] ^{a,c,e}
[] ^{a,c,e}	[] ^{a,c,e}	[] ^{a,c,e}	[] ^{a,c,e}
Totals	[] ^{a,c,e}	[] ^{a,c,e}	[] ^{a,c,e}

As shown in Table 3-13 and Table 3-14, the RPE MOP heatup and cooldown transients bound both the Point Beach Unit 1 and Unit 2 transients in system ΔT distribution. The RPE system ΔT distribution includes more cycles at higher system ΔT values than the Point Beach units, but less cycles overall. This is due to the RPE analysis having more cycles of non-MOP heatups and cooldowns than Point Beach and both units have a total number of design cycles for the heatup and cooldown transients of 200 cycles each. The cycles of non-MOP operations from RPE are far more conservative than the cycles of MOP operations. Therefore, it is conservative that RPE analyzed more cycles of non-MOP cycles than MOP cycles.

[]^{a,c,e}
This is consistent with what is conservatively assumed for Point Beach in Section 3.5.2.3.

Based on the comparison of the heatup/cooldown event maximum system ΔT and the number of I/O cycles per heatup/cooldown for the “pre-MOP” period and the “post-MOP” period, it is concluded that the RPE I/O transients are bounding of the Point Beach Unit 1 and Unit 2 I/O transients. It should also be noted that per [6.3], the number of HU/CD cycles projected for 80 years of operation is less than the 200 design cycles considered in the RPE. Therefore, this assessment is applicable to 80 years of operation for Point Beach Unit 1 and Unit 2.

4.0 EAF Evaluation Results

The results of the RPE are summarized in Table 4-1. See Figure 4-1 for a visual depiction of the ASN locations considered in this evaluation. The three leading locations (ASNs 2, 5, and 6) were selected to be included in the scope of the EAF evaluation. Note that ASN 5 is located right on the nozzle to safe end dissimilar weld between carbon and stainless steel materials. Therefore, evaluations based on both sets of material properties were performed in this calculation. The PZR instrumentation penetration location is not modeled in the RPE because it was not identified as a leading location; however, the application for first license renewal [12] includes EAF results for this location so it is reported here for consistency with the [12].

The CUF_{en} for each sentinel location is less than the ASME BPV Code limit of 1.0 and is therefore acceptable. These results are applicable to 80 years of operation at Point Beach Unit 1 and Unit 2. As stated in Section X.M1 of NUREG-2191, the AMP for a given plant may include monitoring and tracking the number of occurrences and severity of each of the critical thermal and pressure transients for the selected components. These transients of interest are determined from those used in the TLAA evaluations, including fatigue evaluations, flaw tolerance evaluations, and/or crack growth evaluations; therefore, monitoring the fatigue sensitive transients verifies that the results (fatigue usage or inspection frequencies) remain valid or effective. Per [6.3], the 80 year projected cycles for the transients being tracked at Point Beach Units 1 and 2 are bounded by the design allowable cycles. Per the RPE, no projected cycles were used in the EAF evaluation of the PZR lower head locations. No changes or enhancements are necessary to the current cycle counting program at Point Beach Units 1 and 2 described in [6.3] in order to assure the EAF evaluation herein remains valid.

Table 4-1: Summary of EAF Results for the PZR Lower Head

ASN	Description	Material Type	CUF		Overall Effective F_{en}	CUF_{en}	SLR CUF Conservatism Reduction Summary
			AOR ⁽⁴⁾	SLR			
2	Lower Head at Heater Penetration	Carbon Steel	0.057	[] ^{a,c,e}	[] ^{a,c,e}	0.5284	An ASME NB-3200 analysis was performed for SLR. The Insurge/Outsurge transient event distribution was refined by incorporating plant specific data and operational trends.
N/A	Instrumentation Penetration ⁽²⁾	Stainless Steel	0.012	[] ^{a,c,e}	[] ^{a,c,e}	< 0.9648	
5	Nozzle to Safe End Weld	Carbon Steel	N/A ⁽⁵⁾	[] ^{a,c,e}	[] ^{a,c,e}	0.6577	
5	Nozzle to Safe End Weld	Stainless Steel	5.0E-7	[] ^{a,c,e}	[] ^{a,c,e}	0.9648	
6	Safe End to Pipe Weld	Stainless Steel	N/A ⁽⁵⁾	[] ^{a,c,e}	[] ^{a,c,e}	0.9534	

Notes:

1. []^{a,c,e}
2. The PZR instrumentation penetration location is not evaluated explicitly in the RPE because it was not identified as a leading location; however, the application for first license renewal [12] includes EAF results for this location. To provide EAF results for the instrumentation penetration location, the results reported for the PZR surge nozzle, which are bounding of the instrumentation nozzle, are reported.
3. []^{a,c,e}
4. The fatigue AOR for the PZR lower head locations, including I/O transient effects, was completed for first license renewal and the fatigue usage results are summarized in [12].
5. No fatigue usage result for this location is reported in [12].

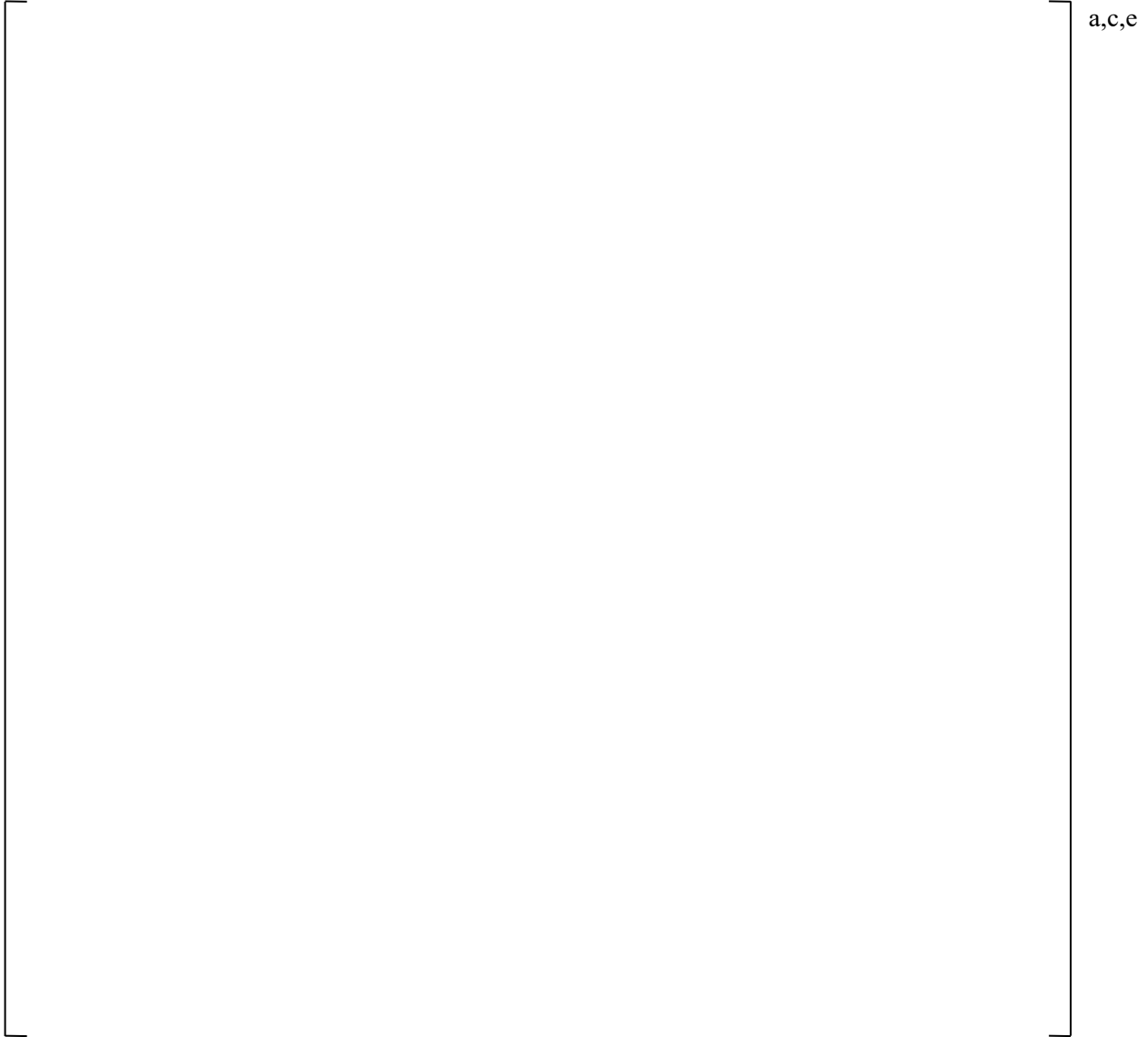


Figure 4-1: ASN Locations

5.0 References

1. Westinghouse Letter, LTR-AMER-MKG-20-923, Revision 0, “Westinghouse Offer for Additional EAF Evaluations (Pressurizer Lower Head including In-Surge / Out-Surge Transient Effects) Scope for Subsequent License Renewal for Point Beach Units 1&2.”
2. NRC Documents:
 - 2.1. NRC Document, NUREG-2191, Volumes 1 and 2, “Generic Aging Lessons Learned for Subsequent License Renewal (GALL-SLR) Report,” July 2017.
 - 2.2. NRC Document, NUREG-2192, “Standard Review Plan for Review of Subsequent License Renewal Applications for Nuclear Power Plants,” July 2017.
 - 2.3. NRC Regulatory Guide, 1.207, Revision 1, “Guidelines for Evaluating the Effects of Light-Water Reactor Water Environments in Fatigue Analyses of Metal Component.
 - 2.4. NRC Document, NUREG/CR-6909, Revision 1, “Effect of LWR Coolant Environments on the Fatigue Life of Reactor Materials.”
 - 2.5. NRC Document, NUREG/CR-6909, Revision 0, “Effect of LWR Water Environments on the Fatigue Life of Reactor Materials.”
 - 2.6. NRC Document, NUREG/CR-6909, Revision 1, Draft Report for Comment, “Effect of LWR Coolant Environments on the Fatigue Life of Reactor Materials,” March 2014.
3. Westinghouse Calculation Note, CN-SDA-II-20-005, Revision 1, “Environmentally Assisted Fatigue Screening of the Primary Equipment for Point Beach Unit 1 and Unit 2.”
4. Westinghouse Letter, LTR-SDA-II-20-08-P, Revision 1, Environmentally Assisted Fatigue Evaluation Results for the Point Beach Unit 1 and Unit 2 Primary Equipment Sentinel Locations for Subsequent License Renewal.”
5. Westinghouse Calculation Note, CN-SDA-II-20-011, Revision 0, “Environmentally Assisted Fatigue Evaluation of the Point Beach Unit 1 and Unit 2 Pressurizer Lower Head.”
6. Design Input Transmittals:
 - 6.1. NextEra Energy Letter, PNBWEC-20-0046, Revision 0, “Response to Westinghouse Letters WEC-NEE-PB-SLR-20-022, NEXT-20-85 and WEC-NEE-PB-SLR-20-033, NEXT-20-103.”
 - 6.2. Nextera Energy Letter, PBNWEC-20-0024, Revision 0, “Response to Westinghouse Letter WEC-NEE-PB-SLR-20-007, NEXT-20-37.”
 - 6.3. Nextera Energy Letter, PBNWEC-20-0020, Revision 1, “Response to WEC-NEE-PB-SLR-20-002.”
 - 6.4. NextEra Energy Letter, NPL 2020-0010, Revision 0, “Input Request for Environmentally Assisted Fatigue Screening of Equipment.”
7. Point Beach Procedures:
 - 7.1. OP 1A, Revision 18, “Cold Shutdown to Hot Standby Unit 1.” (electronically attached to [6.1])

- 7.2. WMTP 11.29, Revision 0, “Major – Cold Shutdown to Low Power Operation, Modified for Reactor Coolant System Hydrostatic Test.” (electronically attached to [6.1])
- 7.3. NP 3.2.2, Revision 28, “Primary Water Chemistry Monitoring Program,” (electronically attached to [6.4]).
- 7.4. CAMP 101, Revision 73, “Daily Routine Sampling Schedule for Operating, Refueling, or Shutdown Units,” (electronically attached to [6.4]).
- 7.5. CAMP 112, Revision 22, “Addition of Hydrazine to the Primary System,” (electronically attached to [6.4]).
8. Westinghouse Report, WCAP-14950, Revision 0, “Mitigation and Evaluation of Pressurizer Insurge/Outsurge Transients.”
9. Westinghouse Calculation Note, W-SMT-96-052, Revision 0, “WOG PZR Insurge Analyses – Transfer Function Databases.”
10. *Pressurized Water Reactor Primary Water Chemistry Guidelines: Revision 7, Volume 1*. EPRI, Palo Alto, CA: 2014.3002000505.
11. Westinghouse Calculation Note, CN-SGDA-08-27, Revision 0, “Evaluation of Pressurizer for EPU Uprate at Point Beach Units 1 and 2.”
12. Point Beach Nuclear Plant, Units 1 and 2, “Application for Renewed Operating Licenses.”
13. Westinghouse Report, WCAP-13588, Revision 0, “Operating Strategies for Mitigating Pressurizer Insurge and Outsurge Transients.”
14. Westinghouse Report, WCAP-13509, Revision 0, “Structural Evaluation of the Point Beach Units 1 & 2 Pressurizer Surge Lines, Considering the Effects of Thermal Stratification.”
15. Westinghouse Report, WCAP-12639, Revision 0, “Westinghouse Owners Group Pressurizer Surge Line Thermal Stratification Generic Detailed Analysis Program MUHP-1091 Summary Report.”
16. Westinghouse Letter, LTR-PAFM-17-20, Revision 1, “Software Release Letter for WESTEMS Version 4.5.7.1 on Windows 7 and Windows 10 System States.”
17. WESTEMS History File Tool User’s Manual, Revision 5. (electronically attached to [16])
18. WEP-964/12, WEP/WIS – POINT BEACH SURGE LINE STRATIFICATION CMS/TFATIK TRANSIENT & STRESS FILES DEVELOPMENT – Data Package for Surge Line Stratification Transient File for Point Beach Units 1 and 2 Horizontal Piping – File Incorporated Plant Specific Historical Data”

This page was added to the quality record by the PRIME system upon its validation and shall not be considered in the page numbering of this document.

Approval Information

Author Approval Oakman Jamie L Sep-23-2020 11:06:09

Verifier Approval Imbrogno Greg M Sep-23-2020 11:48:45

Manager Approval McNutt Don for Patterson Lynn Sep-23-2020 12:40:02

Files approved on Sep-23-2020

*** This record was final approved on 9/23/2020 12:40:02 PM. (This statement was added by the PRIME system upon its validation)

Point Beach Nuclear Plant Units 1 and 2
Dockets 50-266 and 50-301
NRC 2020-0032 Enclosure 4, Attachment 12

Enclosure 4
Non-proprietary Reference Documents and
Redacted Versions of Proprietary Reference
Documents
(Public Version)
Attachment 12

**Structural Integrity Associates, Inc. File No.
200088.310P – REDACTED, Revision 1, “EAF
Refined Analyses (Charging Nozzle, Hot Leg Surge
Nozzle, SI Nozzle, SI/RHR Tee),” August 14, 2020**

(29 Total Pages, including cover sheets)



File No.: 2000088.310P - REDACTED

Project No.: 2000088

Quality Program Type: Nuclear Commercial

CALCULATION PACKAGE

PROJECT NAME:

Point Beach- 1/2 SLR Fatigue TLAA

CONTRACT NO.:

02410780

CLIENT:

NextEra Energy Point Beach, LLC

PLANT:

Point Beach Units 1 and 2

CALCULATION TITLE:

EAF Refined Analyses (Charging Nozzle, Hot Leg Surge Nozzle, SI Nozzle, SI/RHR Tee)

Document Revision	Affected Pages	Revision Description	Project Manager Approval Signature & Date	Preparer(s) & Checker(s) Signatures & Date
0	1 - 28	Initial Issue	Dave A. Gerber 5/27/20	Preparer: Timothy D. Gilman 5/27/20 Checkers: Terry J. Herrmann 5/27/20 Charles J. Fourcade 5/27/20
1	1,12,15,17-20,24-25	Revised to produce PROPRIETARY & REDACTED versions	 Dave A. Gerber 8/14/20	Preparer: Timothy D. Gilman 8/14/20 Checker: Terry J. Herrmann 8/14/20

PROPRIETARY INFORMATION

This document previously contained proprietary information, which has been redacted.

PROPRIETARY INFORMATION NOTICE

THIS DOCUMENT CONTAINED PROPRIETARY INFORMATION WHICH HAS BEEN REDACTED.

This entire document is therefore not considered Proprietary. Proprietary information previously used in the document is "Bracketed" ({}).

File No.: 2000088.310P - REDACTED Revision: 1

Page 2 of 28
F0306-01R4

This document previously contained proprietary information, which has been redacted.



Structural Integrity
Associates, Inc.

info@structint.com



1-877-4SI-POWER



structint.com



Table of Contents

1.0	OBJECTIVE	5
2.0	METHODOLOGY	5
2.1	Cumulative Environmental Fatigue Usage Factor	5
2.2	F_{en} Formulation for Austenitic Stainless Steel Materials	5
	<i>2.2.1 Dynamic Effects</i>	<i>8</i>
3.0	INPUTS AND ASSUMPTIONS	9
3.1	80-Year Cycle Projections	9
3.2	Fatigue Analyses	10
3.3	Power Uprate Effects	11
	<i>3.3.1 RCS Cold Leg Branch Nozzles (Charging Nozzle and ACC SI Nozzle)</i>	<i>12</i>
	<i>3.3.2 Hot Leg Surge Nozzle</i>	<i>12</i>
	<i>3.3.3 RHR Tee</i>	<i>12</i>
3.4	Assumptions	12
4.0	CALCULATIONS	13
4.1	Charging Inlet Nozzle	13
4.2	Hot Leg Surge Nozzle	16
4.3	RHR Tee and ACC SI Nozzle	20
5.0	CONCLUSIONS	26
6.0	REFERENCES	27

List of Tables

Table 1: 80-Year Projected Cycles	9
Table 2: Inputs for Component Evaluations	10
Table 3: NSSS Design Parameters for PBNP Units 1 and 2 Extended Power Uprate	11
Table 4: Cycles Used in Charging Nozzle Analysis	14
Table 5: CUF _{en} for Charging Inlet Nozzle, PATH5	15
Table 6: Cycles Used in Hot Leg Surge Nozzle Analysis	17
Table 7: Number of Cycles for RCS Group Lumped Transient	18
Table 8: CUF _{en} for Hot Leg Surge Nozzle, PATH4	19
Table 9: Cycles Used in RHR Tee and ACC SI Nozzle Analyses	23
Table 10: CUF _{en} for RHR Tee, Node 36	24
Table 11: CUF _{en} for ACC SI Nozzle, Node 110	25
Table 12: Summary of EAF Usage Factors	26

List of Figures

Figure 1: Charging Nozzle Path Locations Evaluated for EAF	13
Figure 2: Hot Leg Surge Nozzle Path Locations Evaluated for EAF	16
Figure 3: RHR / Safety Injection Piping Model	21
Figure 4: RHR / Safety Injection System Sketch	22

1.0 OBJECTIVE

The objective of this calculation is to determine the 80-year environmentally-assisted fatigue usage for the following Point Beach (PBNP) components:

- Charging inlet nozzle
- Hot leg surge nozzle
- Residual heat removal (RHR) to safety injection (SI) piping tee
- Accumulator (ACC) safety injection nozzle

The calculations will be performed using guidance from NUREG/CR-6909, Revision 1 [1], which is an NRC accepted method for 80-year subsequent license renewal (SLR) applications per the GALL SLR report [2].

2.0 METHODOLOGY

2.1 Cumulative Environmental Fatigue Usage Factor

The cumulative fatigue (CUF) effect of stress cycles is calculated using a linear damage relationship (Miner's Rule). That is:

$$CUF = \sum_{i=1}^n \frac{1}{N_i} \leq 1.0$$

where:

n	=	Number of stress cycles in the loading spectrum (i.e., the number of load pairs)
N_i	=	Fatigue life at $S_{alt,i}$ computed using applicable S-N fatigue curve [1, Appendix A] and logarithmic interpolation of the values
$S_{alt,i}$	=	Alternating stress intensity of stress cycle i
U_i	=	$1/N_i$ = Partial usage factor for the i^{th} stress cycle
CUF	=	Cumulative usage factor

Environmental effects are incorporated by multiplying the partial usage factors for each stress cycle by an appropriate F_{en} correction factor. For example, given n different stress cycles, the cumulative environmental fatigue usage factor (CUF_{en}) is:

$$CUF_{en} = U_1 \cdot F_{en,1} + U_2 \cdot F_{en,2} + U_3 \cdot F_{en,3} + U_i \cdot F_{en,i} \dots + U_n \cdot F_{en,n} \quad [1, \text{Eq. A.20}]$$

where:

U_i	=	computed fatigue usage using the air fatigue curve for the "i th " stress cycle
$F_{en,i}$	=	computed F_{en} for the "i th " stress cycle

2.2 F_{en} Formulation for Austenitic Stainless Steel Materials

NUREG/CR-6909, Revision 1 [1] defines the F_{en} fatigue correction factor as the ratio of fatigue life in air at room temperature ($N_{air,RT}$ = allowable number of stress cycles in air) to that in water at the service temperature (N_{water} = allowable number of stress cycles in the reactor water environment). Since fatigue

usage for one stress cycle (or “load pair”) is the inverse of its allowable number of cycles (1/N), the F_{en} factor is an adjustment to the calculated air usage using an air fatigue curve, as follows.

$$F_{en} = N_{air,RT} / N_{water} \quad [1, \text{Eq. A.1}]$$

NUREG/CR-6909 Revision 1 [1] provides an environmental fatigue correction factor (F_{en}) for austenitic stainless steel materials.

$$F_{en} = \exp(-T^* \varepsilon^* O^*) \quad [1, \text{Eq. A.8}]$$

T^* , ε^* , O^* are transformed temperature, strain rate, and dissolved oxygen (DO) level, respectively. These terms are defined as follows.

$$T^* = (T - 100) / 250 \quad (100^\circ\text{C} \leq T \leq 325^\circ\text{C})$$

where:

$$T = \text{service temperature } (^\circ\text{C})$$

$$\varepsilon^* = 0 \quad (\dot{\varepsilon} > 7\%/s)$$

$$\varepsilon^* = \ln(\dot{\varepsilon}/7) \quad (0.0004\%/s \leq \dot{\varepsilon} \leq 7\%/s)$$

$$\varepsilon^* = \ln(0.0004/7) \quad (\dot{\varepsilon} < 0.0004\%/s)$$

where:

$$\dot{\varepsilon} = \text{strain rate } (\%/s)$$

For DO less than 0.1 ppm (pressurized water reactor environment), $O^* = 0.29$ for all wrought and cast ss and weld metals.

For wrought and cast austenitic stainless steels, a threshold value of 0.10% for strain amplitude (one-half the strain range for the cycle) is defined, below which environmental effects on the fatigue life of these steels do not occur. Since the elastic modulus of the fatigue curve (E_c) is 28,300 ksi, this strain threshold corresponds to 28.3 ksi alternating stress intensity from the fatigue analysis. That is, if $S_{alt} \leq 28.3$ ksi then $F_{en} = 1.0$. Thus,

$$F_{en} = 1 \text{ for strain amplitude, } \varepsilon_a \leq 0.10\% \text{ or } S_{alt} \leq (E_c)(0.10\%)/(100\%) = 28.3 \text{ ksi}$$

As a first step, it is conservative to select the maximum service temperature of the load pair and assume a zero-strain rate. If necessary, the Modified Rate Approach [1, Section 4.4] is used to compute F_{en} for each stress cycle. F_{en} for an increasingly tensile portion of a stress cycle is given as:

$$F_{en} = \frac{\sum_{i=2}^n F_{en,i} \Delta \varepsilon_i}{\sum_{i=2}^n \Delta \varepsilon_i}$$

where:

- $F_{en,i}$ = F_{en} computed at Point $i = \text{fn}(\dot{\varepsilon}_i, T^*_i)$.
 n = Number of time points in the stress cycle.
 i = The time step
 $\dot{\varepsilon}_i$ = Strain rate at Point i , %/sec
 = $\Delta \varepsilon_i / \Delta t \cdot 100\%$
 Δt = Change in time at Point i , sec
 = $t_i - t_{i-1}$
 $\Delta \varepsilon_i$ = Change in strain at Point i , mm/mm.

$\Delta \varepsilon_i$, based on all six components of the stress tensor, is computed by performing the following procedure.

First, the principal stress ranges and stress intensity range from Point $i-1$ to Point i are computed per ASME NB-3216.2 [3a, 3b, 3c], which uses all six stress components and considers the possibility of varying principal stress directions. Total P+Q+F stresses are used in the calculation of strain rate.

$$= \frac{\begin{matrix} \sigma_{x,i} & \sigma_{y,i} & \sigma_{z,i} & \sigma_{xy,i} & \sigma_{yz,i} & \sigma_{xz,i} \\ \sigma_{x,i-1} & \sigma_{y,i-1} & \sigma_{z,i-1} & \sigma_{xy,i-1} & \sigma_{yz,i-1} & \sigma_{xz,i-1} \end{matrix}}{\begin{matrix} \sigma'_x & \sigma'_y & \sigma'_z & \sigma'_{xy} & \sigma'_{yz} & \sigma'_{xz} \end{matrix}}$$

From σ'_x , σ'_y , etc. the principal stress ranges (σ'_1 , σ'_2 , σ'_3) and stress intensity range σ'_I are computed. Per convention, σ'_1 , σ'_2 , and σ'_3 are reordered so that $\sigma'_1 \geq \sigma'_2 \geq \sigma'_3$.

The sign of the principal total stress range from Point $i-1$ to i with the largest absolute value determines whether the strain increment is primarily increasingly tensile or increasingly compressive in nature.

The increasingly tensile change in strain, or the strain increment, $\Delta \varepsilon_i$, is computed as follows.

$$\Delta \varepsilon_i = \begin{cases} \frac{\sigma'_I}{E_c}, & \text{if } Sgn = 1 \\ 0, & \text{Otherwise} \end{cases}$$

where:

$$Sgn = \begin{cases} sgn(\sigma_1), & \text{if } |\sigma_1| \geq |\sigma_3| \\ sgn(\sigma_3), & \text{Otherwise} \end{cases}$$

$\text{sgn}(\sigma)$ = The sign (-1 or +1) of σ .

E_c = Elastic modulus of the fatigue curve.

2.2.1 Dynamic Effects

When Operating Basis Earthquake (OBE) loads are present for a load pair, guidance from Reference [5] is used to determine the effective F_{en} , or $F_{en,efftv}$ as follows.

$$F_{en,efftv} = (1 - R_{dyn})F_{en} + R_{dyn} \text{ [5. Eq. 3-15]}$$

where:

$F_{en,efftv}$ = F_{en} multiplier to be applied to load pair consisting partially of dynamic loading

R_{dyn} = Fraction of S_{alt} that is based on dynamic loading

$$= (S_{alt,dyn} - S_{alt,no-dyn})/S_{alt,dyn}$$

F_{en} = F_{en} multiplier

$S_{alt,dyn}$ = S_{alt} of fatigue pair including dynamic load amplitude

$S_{alt,no-dyn}$ = S_{alt} of fatigue pair without including dynamic load amplitude



3.0 INPUTS AND ASSUMPTIONS

3.1 80-Year Cycle Projections

80-year cycle projections [6] are shown in Table 1. "Projection Upper Bound" represents an upper bound projection that is conservative for both units.

Table 1: 80-Year Projected Cycles

Row	Transient	Current Cycles as of YE 2019		Projection Upper Bound	Design Allowable Cycles	Suggested Allowable Cycles
		Unit 1	Unit 2			
1	10% Step Load Decrease	25	30	44	2000	100
2	10% Step Load Increase	0	1	2	2000	20
3	50% Step Load Decrease	46	20	66	200	100
4	Accumulator Safety Injection	4	1	7	89	8
5	Auxiliary Spray Actuation	0	0	0	10	2
6	HPSI Injection	2	0	4	89	4
7	Inadv. ACC Blowdown	0	0	0	4	2
8	Inadv. RCS Depressurization	0	0	0	20	2
9	Loss of Charging Flow	16	17	34	60	50
10	Loss of Letdown Flow	20	17	46	200	75
11	PZR Cooldown	78	61	115	200	120
12	PZR Heatup	79	62	116	200	120
13	Primary Side Hydrostatic Test	1	2	3	5	3
14	Primary Side Leak Test	36	38	57	94	60
15	Primary to Secondary Leak Test	2	9	14	27	15
16	RCS Cooldown	79	62	118	200	120
17	RCS Heatup	80	63	119	200	120
18	RPV Safety Injection	0	0	0	89	2
19	Reactor Trip	68	52	107	300	120
20	Refueling	49	46	77	80	80
21	Relief Valve Actuation	1	3	7	100	8
22	Secondary to Primary Leak Test	38	33	57	128	60
23	Trip Due to Loss of RC Pump	1	2	4	100	4
24	Unit Loading 5%/min	1691	1806	2478	11600	8000
25	Unit Unloading 5%/min	1544	1670	2295	11600	8000
26	FW Cycling at Hot Standby	NC	NC	N/A	2000	Not provided
27	Boron Concentration Eq.	NC	NC	N/A	23360	Not provided
28	Loss of Load (Trip)	NC	NC	N/A	80	80
29	Loss of Power (Trip)	NC	NC	N/A	40	40
30	Loss of Flow (Trip)	NC	NC	N/A	80	80
31	Turbine Roll Test	NC	NC	N/A	10	10
32	Control Rod Drop	NC	NC	N/A	N/A	80
33	Excessive FW Flow	NC	NC	N/A	N/A	30
34	OBE	NC	NC	N/A	N/A	10

Footnotes:

Italicized font in the Design Allowable Cycles column indicates a value from the FSAR.

NC = Not Counted by FatiguePro

N/A = Not applicable - there is no basis for computing the upper bound.

UFSAR Transient 'Steady State Fluctuations' omitted; small fluctuations do not cause fatigue usage.

Transients 19 & 23 constitute the 400 Reactor Trip Transients in the UFSAR

UFSAR Transient 16 'Reactor Coolant Pipe Break' is a Faulted Event, which is not counted.

UFSAR Transient 17 'Steam Line Break' is a Faulted Event, which is not counted.

3.2 Fatigue Analyses

Previously performed analyses used for 60-year license renewal are used as inputs to the calculations for SLR here. Table 2 summarizes the calculations. These series of calculations provide the transient loads, component materials, evaluated locations, and fatigue analysis results used as input the analyses in this calculation package.

Table 2: Inputs for Component Evaluations

Component	Calculation	Ref.
Charging Nozzle	Loads for Charging Nozzles	[7]
	Thermal and Mechanical Stress Analysis of the Charging Nozzle	[8]
	Charging Nozzle Fatigue Analysis	[9]
	Charging Nozzle Environmentally-Assisted Fatigue (EAF) Analysis	[10]
Hot Leg Surge Nozzle	Hot Leg Surge Nozzle Loads	[11]
	Thermal and Mechanical Stress Analysis of Hot Leg Surge Nozzle,	[12]
	Hot Leg Surge Nozzle Fatigue Analysis	[13]
	Hot Leg Surge Nozzle Environmentally-Assisted Fatigue Analysis Calculation	[14]
	Hot Leg Surge Nozzle Environmentally-Assisted Fatigue (EAF) Analysis Using 60-Year Projected Number of Cycles	[15]
RHR Tee and ACC SI Nozzle	Point Beach Safety Injection Piping Fatigue Evaluation	[16]

3.3 Power Uprate Effects

On April 7, 2009 FPL Energy Point Beach, LLC applied for an Extended Power Uprate (EPU) license to operate at a core thermal power of 1800 MWt [17]. On May 3, 2011, the NRC approved the application [18].

The input analyses referenced in Section 3.2 were each performed before the NRC approved implementation of the EPU, so it is important to reconcile the previous calculations to EPU conditions.

The EPU License Amendment Request (LAR) [17, Attachment 5 “Licensing Report”, p. 1.0-2] states that the reactor coolant average temperature at 1800 MWt core power will be increased from 570°F to 576°F. This is the result of increasing the reactor outlet temperature (T_{hot}) and simultaneously decreasing the reactor inlet temperature (T_{cold}). Thermal parameters for EPU condition [17, Attachment 5, Table 1-1, p. 1.1-4] are shown in Table 3.

PBNP evaluated the impact of the EPU on the fatigue evaluations performed in support of 60-year license renewal and stated that the 40-year design transient set is bounding for a 60-year operating term. Therefore, the fatigue analyses performed to support license renewal were concluded to be bounding and remain valid for EPU conditions [17, Attachment 5, p. 2.2.2-11].

Table 3: NSSS Design Parameters for PBNP Units 1 and 2 Extended Power Uprate

Thermal Design Parameters	Extended Power Uprate			
	Case 1	Case 2	Case 3	Case 4
NSSS Power, MWt	1806	1806	1806	1806
10 ⁶ Btu/hr	6162	6162	6162	6162
Reactor Power, MWt	1800	1800	1800	1800
10 ⁶ Btu/hr	6142	6142	6142	6142
Thermal Design Flow, loop gpm	89,000	89,000	89,000	89,000
Reactor 10 ⁶ lb/hr	69.3	69.3	67.6	67.6
Reactor Coolant Pressure, psia	2250	2250	2250	2250
Core Bypass, %	6.5 (a,b)	6.5 (a,b)	6.5 (a,c)	6.5 (a,c)
Reactor Coolant Temperature, °F				
Core Outlet	597.3 (b)	597.3 (b)	615.3 (c)	615.3 (c)
Vessel Outlet T_{hot}	592.9	592.9	611.1	611.1
Core Average	561.8 (b)	561.8 (b)	581.0 (c)	581.0 (c)
Vessel Average	558.0	558.0	577.0	577.0
Vessel/Core Inlet T_{cold}	523.1 (f)	523.1 (f)	542.9	542.9
Steam Generator Outlet	522.9 (f)	522.9 (f)	542.7	542.7
Steam Generator				
Steam Outlet Temperature, °F	490.8	486.3	511.6 (d)	507.3
Steam Outlet Pressure, psia	626	601	755 (d)	727
Steam Outlet Flow, 10 ⁶ lb/hr total	7.36/8.08 (e)	7.36/8.08 (e)	7.39/8.12 (d,e)	7.39/8.11 (e)
Feed Temperature, °F	390.0/458.0	390.0/458.0	390.0/458.0	390.0/458.0
Steam Outlet Moisture, % max.	0.25	0.25	0.25	0.25
Tube Plugging Level, %	0	10	0	10
Zero Load Temperature, °F	547	547	547	547

The EPU, therefore, has no significant, adverse impact on fatigue of PBNP components. Additional justification for the specific components analyzed herein are as follows.

3.3.1 RCS Cold Leg Branch Nozzles (Charging Nozzle and ACC SI Nozzle)

Design transients for the Reactor Coolant System (RCS) cold leg branch nozzles conservatively postulate a normal operating cold leg temperature of { }°F [7][16], which is expected to bound the actual cold leg temperature. A higher assumed temperature produces a larger temperature difference during cold injection events, which are the principal drivers of fatigue at the cold leg branch nozzles. As shown in Table 3, the maximum core inlet temperature (T_{cold}) is less than 550°F in all cases. Since the EPU has the effect of decreasing the original reactor inlet temperature, the temperature differences remain bounded by the design transient definitions.

3.3.2 Hot Leg Surge Nozzle

For the surge line, thermal fatigue is driven primarily by insurge, outsurge, and stratification cycling. The magnitude of alternating stresses during these events is based primarily by the temperature difference between the pressurizer and the RCS hot leg during plant heatup and cooldown conditions, which are not impacted by EPU. For insurge/outsurge events that occur during normal operating conditions the EPU increases the hot leg temperature while keeping the pressurizer at essentially the same temperature as pre-EPU conditions. The EPU operating conditions therefore have the effect of primarily decreasing the severity of events in the surge line during normal operating conditions. Therefore, the design transients for pre-EPU are valid and conservative for post-EPU conditions. This is recognized, as discussed in the LAR [17, Attachment 5, p. 2.2.2-7]:

“For the pressurizer surge line, the impact of the design transients with respect to the thermal stratification and fatigue analysis is controlled by ΔT between the pressurizer temperature and the hot-leg temperature. The controlling ΔT s for the pressurizer surge line are associated primarily with the plant heatup and cooldown events which are not affected by the EPU program. It has been reviewed and shown that the temperatures and the design transients affected by the EPU have an insignificant effect on the pressurizer surge line analysis, including the effects of thermal stratification. Therefore, the EPU has no adverse impact on either the thermal stratification or the fatigue analysis for the pressurizer surge line..”

3.3.3 RHR Tee

The RHR tee is upstream of the RCS cold leg and is not impacted by changes in system design parameters. The LAR states that the design basis Accumulator and RHR lines' loads and results remain applicable for the EPU [17, Attachment 5, p. 2.1.6-5]. The component's fatigue is driven chiefly by RHR operation, which is initiated at a set point temperature of approximately 350°F, and injection events associated with the safety injection system.

3.4 Assumptions

Some design events used in the fatigue analyses and not listed in Table 1 are not currently counted. When these counts are not available, it is assumed that 80-year projected cycles will be similarly bounded by the numbers of cycles assumed for the 40-year design basis (i.e., “40 = 80”). PBNP will validate these assumptions. If not able to be validated by PBNP, Cycle-Based Fatigue algorithms can be used to adequately manage these components, using the results from this calculation package as input.

4.0 CALCULATIONS

4.1 Charging Inlet Nozzle

An EAF analysis for 60 years was previously performed [10] using the ASME fatigue curve [3c], design numbers of cycles, and F_{en} formulations provided in NUREG/CR-5704 [4]. Locations analyzed are shown in Figure 1. The maximum U_{en} was determined to be 0.3784 at the PATH5 nozzle to piping girth butt field weld [10, Figure 1].

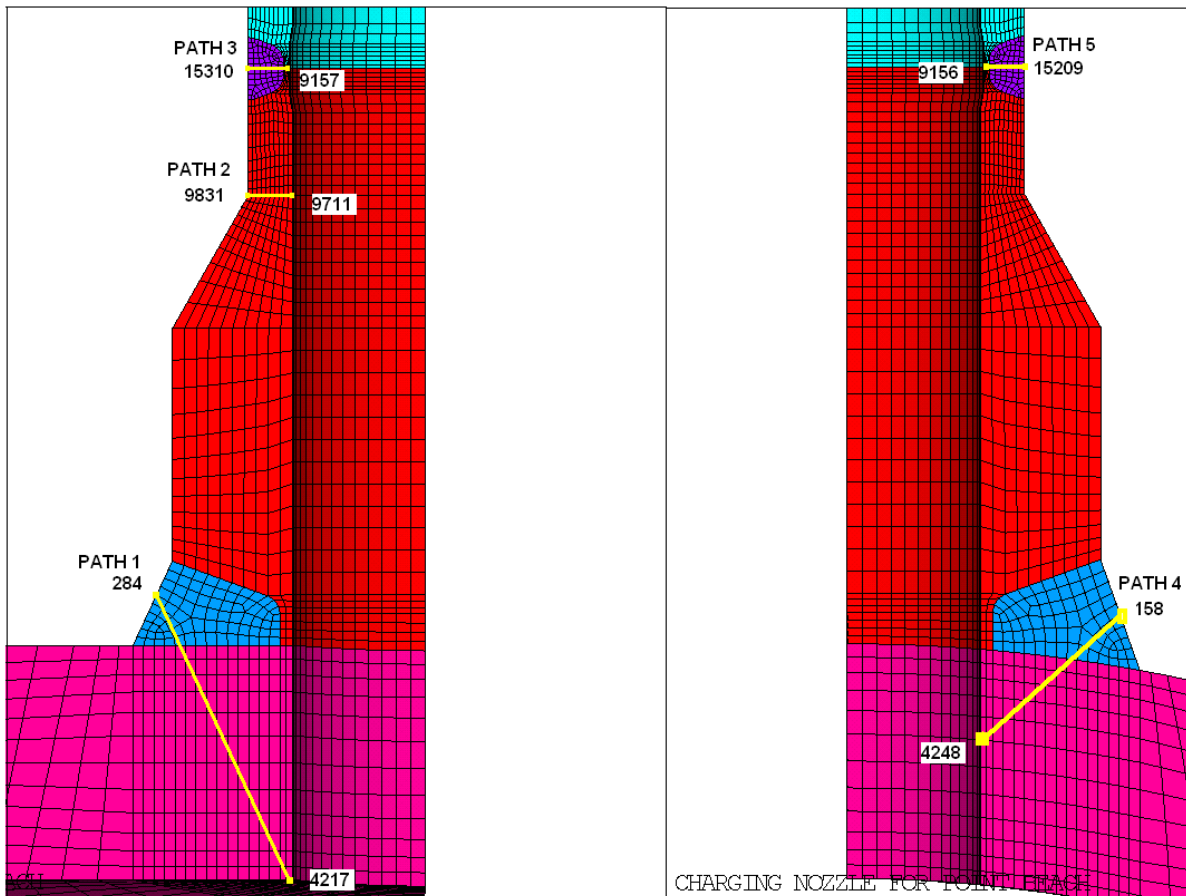


Figure 1: Charging Nozzle Path Locations Evaluated for EAF
(PATH5 is Limiting)

Cycles used for the charging inlet nozzle fatigue analysis are taken from Reference [7, Table 1] and shown in Table 4. For cycles currently being counted, the counts used in this analysis are each greater than or equal to the 80-year projections in Table 1 and, therefore, conservative.

Table 4: Cycles Used in Charging Nozzle Analysis

Transient	Design Cycles
<u>Auxiliary Transients</u>	
Charging and letdown flow shutoff and return to service	60
Letdown flow shutoff with prompt return to service	200
Letdown flow shutoff with delayed return to service	20
Charging flow shutoff with prompt return to service	20
Charging flow shutoff with delayed return to service	20
Charging flow step decrease and return to normal	24,000
Charging flow step increase and return to normal	24,000
Letdown flow step decrease and return to normal	2,000
Letdown flow step increase and return to normal	24,000
<u>Normal Condition RCS Transients</u>	
Plant heatup and cooldown	200
Large step load decrease with steam dump	200
Refueling	80
Turbine roll test	20
Primary side leakage test	200
<u>Upset Condition RCS Transients</u>	
Loss of load	80
Loss of power	40
Partial loss of flow	80
Reactor trip A - with no inadvertent cooldown	230
Reactor trip B - with cooldown and no S.I.	160
Reactor trip C - with cooldown and S.I.	10
Inadvertent RCS depressurization - Umbrella Case	20
Inadvertent RCS depressurization - Inadvertent auxiliary spray	10
Excessive feedwater flow	30
<u>Test Condition RCS Transients</u>	
Primary side hydrostatic test	10

The detailed fatigue table for PATH5 is shown in Table 5. Allowable numbers of cycles are recalculated using the NUREG/CR-6909, Revision 1 fatigue curve [1, Table A-2]. For the load pair F_{en} calculations, the maximum service temperature for the load pair and a zero strain rate are conservatively used. For the top load pair, which includes OBE, an effective F_{en} is calculated, using the methods described in Section 2.2.1. Calculations are performed in Excel spreadsheet *Charging.xlsm*.

The resulting CUF_{en} is 0.7149, which is less than 1.0 and, therefore, acceptable for 80-years, if cycle counts remain within the limits of Table 4.

Table 5: CUF_{en} for Charging Inlet Nozzle, PATH5

I	Load Set A	Load Set B	n	S _{alt} , psi	N	U	T _{max} , °F	F _{en}	U _{en}
1	Chg&LtnSO2_p	LoffDR1_v+OBE	20	91005	1666.2	}			0.0936
2	Chg&LtnSO2_p	LtnSoffPtR_v	60	77861	2756.4				0.1947
3	LtnSoffPtR_v	LtnSoffDR2_p	20	77861	2756.4				0.0649
4	LtnSoffPtR_p	LtnSoffPtR_v	120	53832	9726.2				0.1104
5	LtnSoffPtR_p	Refueling	80	37246	35869.9				0.0199
6	LoffDR1_p	Refueling	20	37246	35869.9				0.0050
7	ExcessFWF_p	Refueling	190	37240	35891.7				0.0474
8	OBE	OBE	380	36168	40062.2				0.0095
9	InadvRCSDep	ExcessFWF_p	30	34945	45599.6			0.0062	
10	PlantHeatup	ExcessFWF_p	200	34828	46178.8			0.0387	
11	PlantCldwn	ExcessFWF_p	200	34828	46178.8			0.0387	
12	ExcessFWF_p	LeakTest	30	32943	56987.6			}	0.0047
13	ChgSoffPtR	LeakTest	20	26298	142064.2	0.0001	--		1.00
14	LtdnInc&Rtn1	LeakTest	150	24487	196776.0	0.0008	--	1.00	0.0008
15	LtdnInc&Rtn1	HydroTest	10	23420	249682.5	0.0000	--	1.00	0.0000
16	LtdnInc&Rtn1	LtdnInc&Rtn2	23840	22343	322142.9	0.0740	--	1.00	0.0740
17	ChgInc&Rtn_p	LtdnInc&Rtn2	160	20140	570679.4	0.0003	--	1.00	0.0003
18	LtnSoffDR2_v	ChgInc&Rtn_p	20	17208	1475571.4	0.0000	--	1.00	0.0000
19	Chg&LtnSO2_v	ChgInc&Rtn_p	80	17196	1482094.5	0.0001	--	1.00	0.0001
20	ChgInc&Rtn_p	LtdnDec&Rtn1	2000	17164	1499653.5	0.0013	--	1.00	0.0013
21	ChgInc&Rtn_p	LossofLoad	430	15026	4367390.7	0.0001	--	1.00	0.0001
22	ChrgDec&Rtn	ChgInc&Rtn_p	21310	14864	4811083.0	0.0044	--	1.00	0.0044
						0.1619		4.41	0.7149
						CUF		F_{en,eff}	CUF_{en}

This document previously contained proprietary information, which has been redacted.



4.2 Hot Leg Surge Nozzle

An EAF analysis for 60 years was previously performed [13][14] using the ASME fatigue curve [3b], design numbers of cycles, and F_{en} formulations provided in NUREG/CR-5704 [4]. Locations analyzed are shown in Figure 2 (excerpted from [12, Figure 12]). The maximum CUF_{en} using NUREG/CR-5704 methods was determined to be 1.0346 at the PATH4 nozzle to piping girth butt field weld [14]. Subsequent analysis using 60-year projected cycles determined the CUF_{en} to be 0.5353 [15] using the same NUREG/CR-5704 methods.

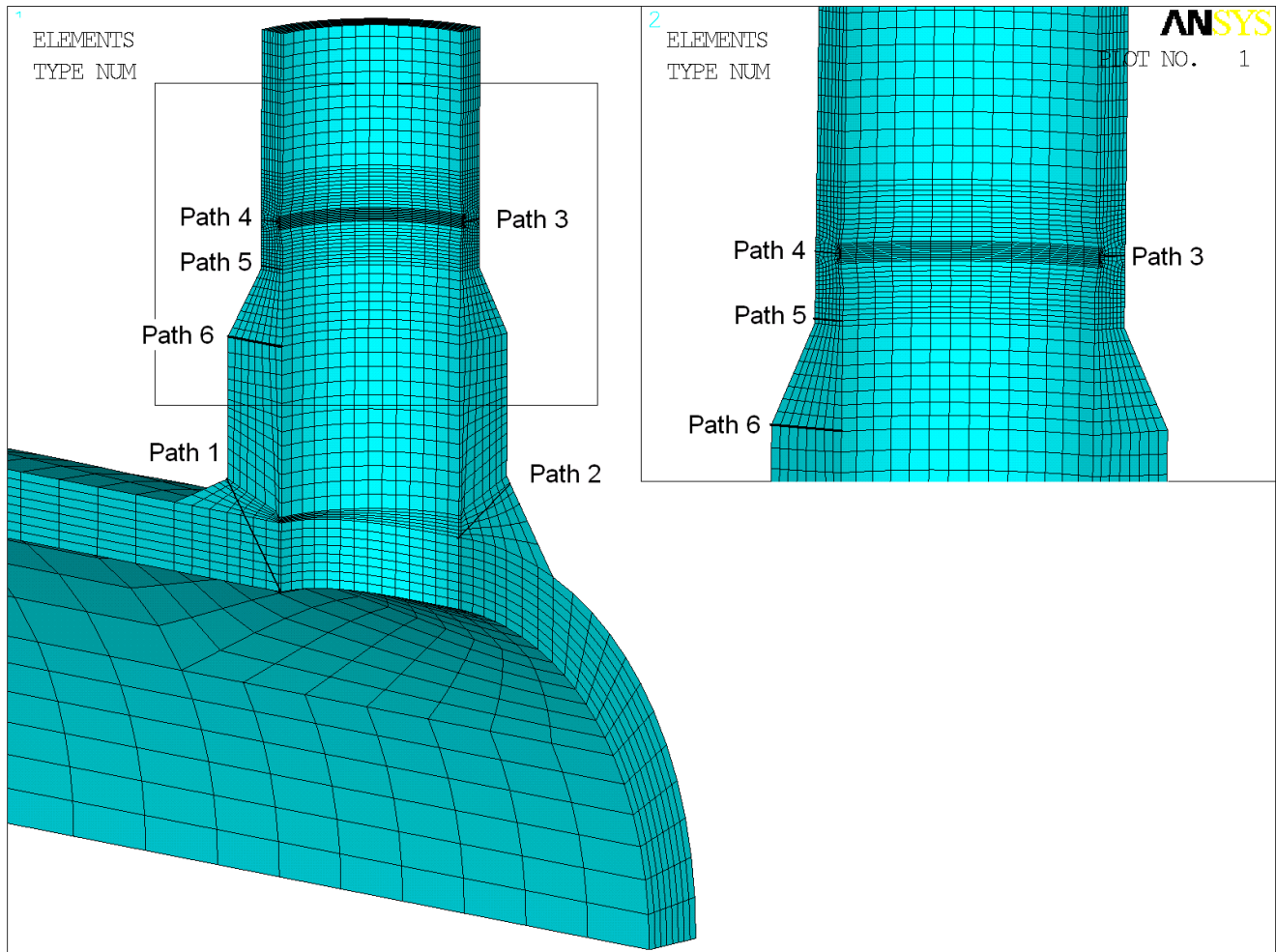


Figure 2: Hot Leg Surge Nozzle Path Locations Evaluated for EAF
(PATH4 is Limiting)

The Design Cycles applicable to the hot leg surge nozzle fatigue analysis are taken from Reference [13, Table 1] and shown in Table 6 and Table 7. In the Reference [13] fatigue analysis it was necessary to split individual transients into multiple sets, to capture the individual stress peaks and valleys. For example, for Transient #3, Plant loading, 5% power/minute, was split into 3 different cycles with abbreviated names LOAD-1, LOAD-2, LOAD-3, which each represent different portions of the transient for potential stress cycle pairing.

File No.: 2000088.310P - REDACTED Revision: 1

Page 16 of 28
F0306-01R4

This document previously contained proprietary information, which has been redacted.

Analyzed Cycles in the table are based on consideration of the Design Cycles and the Projected Cycles shown in Table 1. With respect to Projected Cycles, in some cases a bit of extra margin for additional conservatism is selected. Various numbers were experimented with to arrive at an optimum set of cycles to maximize the allowable numbers of cycles, while still maintaining the CUF_{en} under 1.0. For cycles currently being counted, the counts used in this analysis are each greater than or equal to the 80-year suggested allowable cycles in Table 1.

Table 6: Cycles Used in Hot Leg Surge Nozzle Analysis

Transient	Abbreviation	Design Cycles	Analyzed Cycles ⁽¹⁾
1. Plant heatup	HEATUP	200	120
2. Plant cooldown	COOLDOWN	200	120
3. Plant loading, 5% power/minute	LOAD-1	18,300	18300
3. Plant loading, 5% power/minute	LOAD-2	18,300	18300
3. Plant loading, 5% power/minute	LOAD-3	18,300	18300
4. Plant unloading, 5% power/minute	UNLOAD-1	18,300	18300
4. Plant unloading, 5% power/minute	UNLOAD-2	18,300	18300
5. RCS Group Transients	GROUP-1	920	920 ⁽²⁾
5. RCS Group Transients	GROUP-2	920	920 ⁽²⁾
6. Inadvertent RCS Depress.	RCSDEPRESS-1	30	2
6. Inadvertent RCS Depress.	RCSDEPRESS-2	30	2
6. Inadvertent RCS Depress.	RCSDEPRESS-3	30	2
7. Refueling	REFUELING	290	80
8. Primary Side Leak Test	LEAKTEST	200	60
9. Primary Side Hydrostatic Test	HYDROTEST	10	3
10. PIO304 Insurge	INSURGE304	}	
11. PIO285 Insurge	INSURGE285		
12. PIO275 Insurge	INSURGE275		
13. PIO250 Insurge	INSURGE250		
14. PIO200 Insurge	INSURGE200		
15. PIO175 Insurge	INSURGE175		
16. PIO150 Insurge	INSURGE150		
17. PIO150H Insurge	INSURGE150H		
18. PIO210 Insurge	INSURGE210		
19. PIO177 Insurge	INSURGE177		
20. PIO304 Outsurge	OUTSURGE304-1		
20. PIO304 Outsurge	OUTSURGE304-2		
21. PIO285 Outsurge	OUTSURGE285-1		
21. PIO285 Outsurge	OUTSURGE285-2		
22. PIO275 Outsurge	OUTSURGE275-1		
22. PIO275 Outsurge	OUTSURGE275-2		
23. PIO250 Outsurge	OUTSURGE250-1		
23. PIO250 Outsurge	OUTSURGE250-2		
24. PIO200 Outsurge	OUTSURGE200-1		
24. PIO200 Outsurge	OUTSURGE200-2		

Table 6: Cycles Used in Hot Leg Surge Nozzle Analysis

Transient	Abbreviation	Design Cycles	Analyzed Cycles ⁽¹⁾
25. PIO175 Outsurge	OUTSURGE175-1		
25. PIO175 Outsurge	OUTSURGE175-2		
26. PIO150 Outsurge	OUTSURGE150-1		
26. PIO150 Outsurge	OUTSURGE150-2		
27. PIO150H Outsurge	OUTSURGE150H-1		
27. PIO150H Outsurge	OUTSURGE150H-2		
28. PIO210 Outsurge	OUTSURGE210-1		
28. PIO210 Outsurge	OUTSURGE210-2		
29. PIO177 Outsurge	OUTSURGE177-1		
29. PIO177 Outsurge	OUTSURGE177-2		
30. OBE self cycling	OBEself		

Table 6 notes:

1. Insurge/Outsurge cycles prorated to the number of Heatups and Cooldowns.
2. RCS Group transients are shown in Table 7. Design Cycles are conservatively used.
3. 1 OBE event with 20 internal (self-cycling) cycles are used.

Table 7: Number of Cycles for RCS Group Lumped Transient

Plant Event	Design Cycles
Large Step Load Decrease (with steam dump)	200
Loss of Load (without immediate Turbine or Reactor Trip)	80
Loss of Flow (Partial Loss of Flow, One Pump)	80
Loss of Power (Blackout w/ Natural Circulation)	40
Reactor Trip at Power with No Cooldown	230
Reactor Trip with Cooldown and No SI	160
Reactor Trip with Cooldown and SI	10
Control Rod Drop	80
Excessive FW flow	30
Turbine Roll Test	10
TOTAL	920

The previously-performed fatigue analysis [13] for PATH4 (inside) was re-run with the VESLFAT software [19] but using the modified cycles in Table 6 and Table 7 and the stainless steel fatigue curve for NUREG/CR-6909 Revision 1 [1, Table A-2].

The detailed fatigue table for PATH4 is shown in Table 8. For the load pair F_{en} calculations, it was necessary to compute detailed F_{en} values using the Modified Rate methodology. For the top load pair, which includes OBE, an effective F_{en} is calculated, using the methods described in Section 2.2.1. Calculations are performed in Excel spreadsheet *HL Surge.xlsx*.

The resulting CUF_{en} is 0.9685, which is less than 1.0 and, therefore, acceptable for 80-years, if cycle counts remain within the Analyzed Cycles limits of Table 6 and Table 7.

Table 8: CUF_{en} for Hot Leg Surge Nozzle, PATH4

I	Load Set A	Load Set B	n	S _{alt} , psi	N	U	F _{en}	U _{en}
1	OUTSURGE275-1	Out150H+OBE	}			0.0004	6.27	0.0026
2	OUTSURGE275-1	OUTSURGE150H-				0.0046	6.94	0.0323
3	OUTSURGE285-1	OUTSURGE150H-				0.0008	6.92	0.0056
4	OUTSURGE304-1	OUTSURGE150H-				0.0005	6.92	0.0037
5	REFUELING	OUTSURGE150H-			0.0117	11.94	0.1402	
6	OUTSURGE150H-	OUTSURGE177-1			0.0114	6.88	0.0787	
7	GROUP-1	OUTSURGE177-1			0.0022	6.00	0.0134	
8	GROUP-1	OUTSURGE210-1			0.0107	6.15	0.0657	
9	UNLOAD-2	RCSDEPRESS-3			0.0001	11.08	0.0012	
10	HEATUP	UNLOAD-2			0.0062	5.98	0.0370	
11	COOLDOWN	UNLOAD-2			0.0062	12.58	0.0778	
12	HYDROTEST	OUTSURGE150H-			0.0001	11.94	0.0018	
13	LEAKTEST	OUTSURGE150H-			0.0029	11.94	0.0342	
14	GROUP-2	OUTSURGE304-2			0.0001	6.06	0.0006	
15	GROUP-2	INSURGE304			0.0001	9.42	0.0009	
16	GROUP-2	OUTSURGE285-2			0.0001	6.06	0.0008	
17	GROUP-2	INSURGE285			0.0001	9.42	0.0013	
18	GROUP-2	INSURGE275			0.0008	9.42	0.0078	
19	GROUP-2	OUTSURGE275-2			0.0008	6.07	0.0050	
20	GROUP-2	OUTSURGE250-1			0.0015	7.78	0.0119	
21	GROUP-2	OUTSURGE200-1			0.0002	7.92	0.0016	
22	GROUP-2	OUTSURGE175-1			0.0017	7.98	0.0134	
23	GROUP-2	OUTSURGE150-1			0.0194	8.03	0.1556	
24	GROUP-2	INSURGE210			0.0039	9.42	0.0369	
25	GROUP-2	OUTSURGE210-2			0.0035	6.15	0.0218	
26	GROUP-1	OUTSURGE210-2			0.0004	6.15	0.0023	
27	GROUP-1	OUTSURGE177-2			0.0028	6.00	0.0171	
28	GROUP-1	INSURGE177			0.0028	9.42	0.0268	
29	GROUP-1	INSURGE250			0.0005	9.42	0.0052	
30	GROUP-1	OUTSURGE250-2			0.0005	7.78	0.0043	
31	GROUP-1	INSURGE200			0.0001	9.42	0.0006	
32	GROUP-1	OUTSURGE200-2			0.0001	7.92	0.0005	
33	GROUP-1	OUTSURGE175-2			0.0005	7.98	0.0040	
34	GROUP-1	INSURGE175			0.0005	9.42	0.0048	
35	GROUP-1	OUTSURGE150-2			0.0026	8.03	0.0206	
36	UNLOAD-2	INSURGE150			0.0053	12.58	0.0672	
37	UNLOAD-2	OUTSURGE150-2			0.0029	8.39	0.0244	
38	LOAD-1	RCSDEPRESS-2			0.0000	1.00	0.0000	
39	LOAD-1	UNLOAD-2			0.0389	1.00	0.0389	
40	LOAD-1	RCSDEPRESS-1			0.0000	1.00	0.0000	

This document previously contained proprietary information, which has been redacted.



Table 8: CUF_{en} for Hot Leg Surge Nozzle, PATH4

I	Load Set A	Load Set B	n	S _{alt} , psi	N	U	F _{en}	U _{en}
41	LOAD-1	LOAD-2				0.0003	1.00	0.0003
42	LOAD-2	OUTSURGE150H-				0.0000	1.00	0.0000
						0.1487	6.513	0.9685
						CUF	F_{en,eff}	CUF_{en}

4.3 RHR Tee and ACC SI Nozzle

An ASME NB-3600 [3a] analysis was previously performed [16] using the ASME fatigue curve and design numbers of cycles. The CUF was determined to be 0.0142 for the RHR tee at node number 36 [16, Table 10] and 0.0072 for the ACC SI nozzle at node 110 [16, Table 9]. These locations are highlighted in Figure 3 and Figure 4.

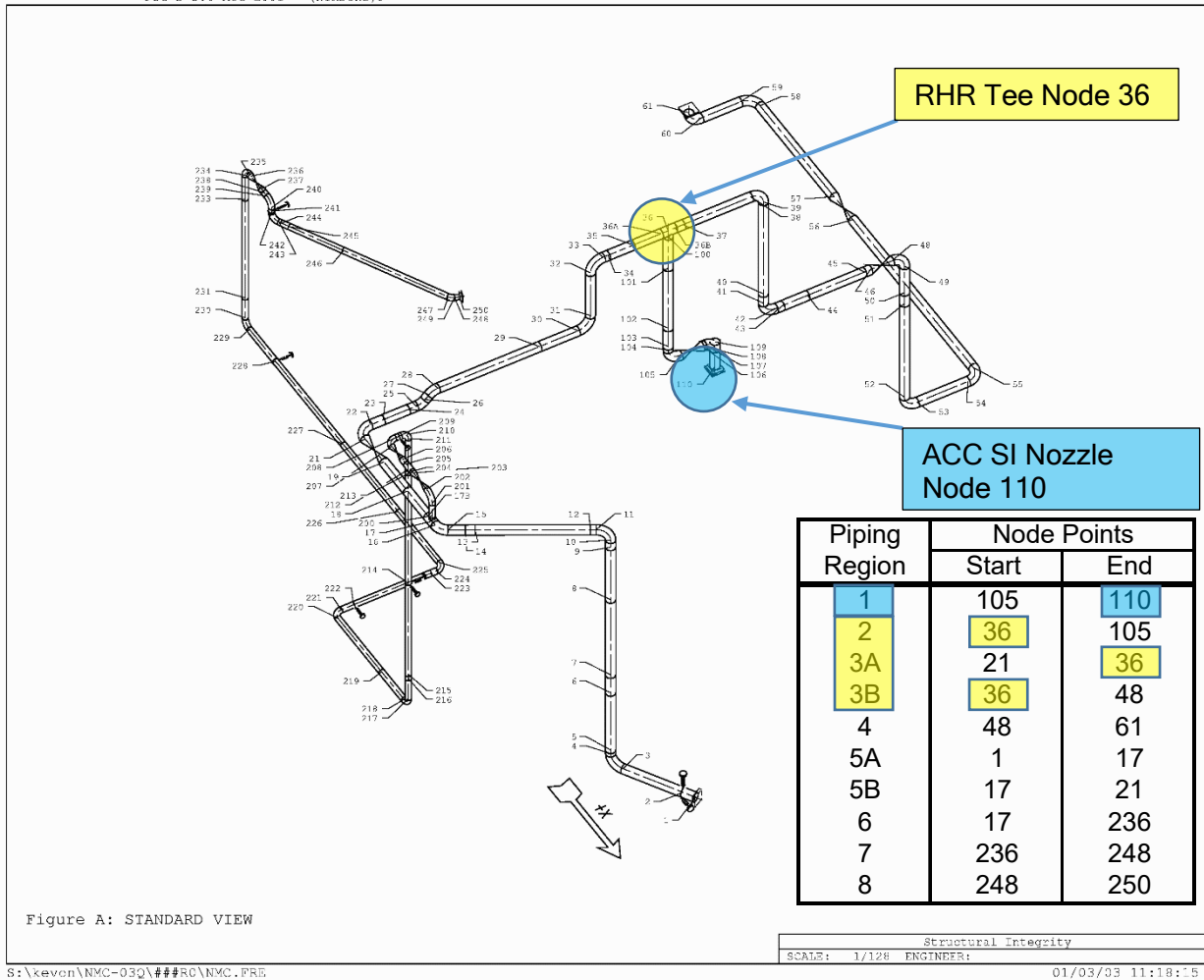


Figure 3: RHR / Safety Injection Piping Model

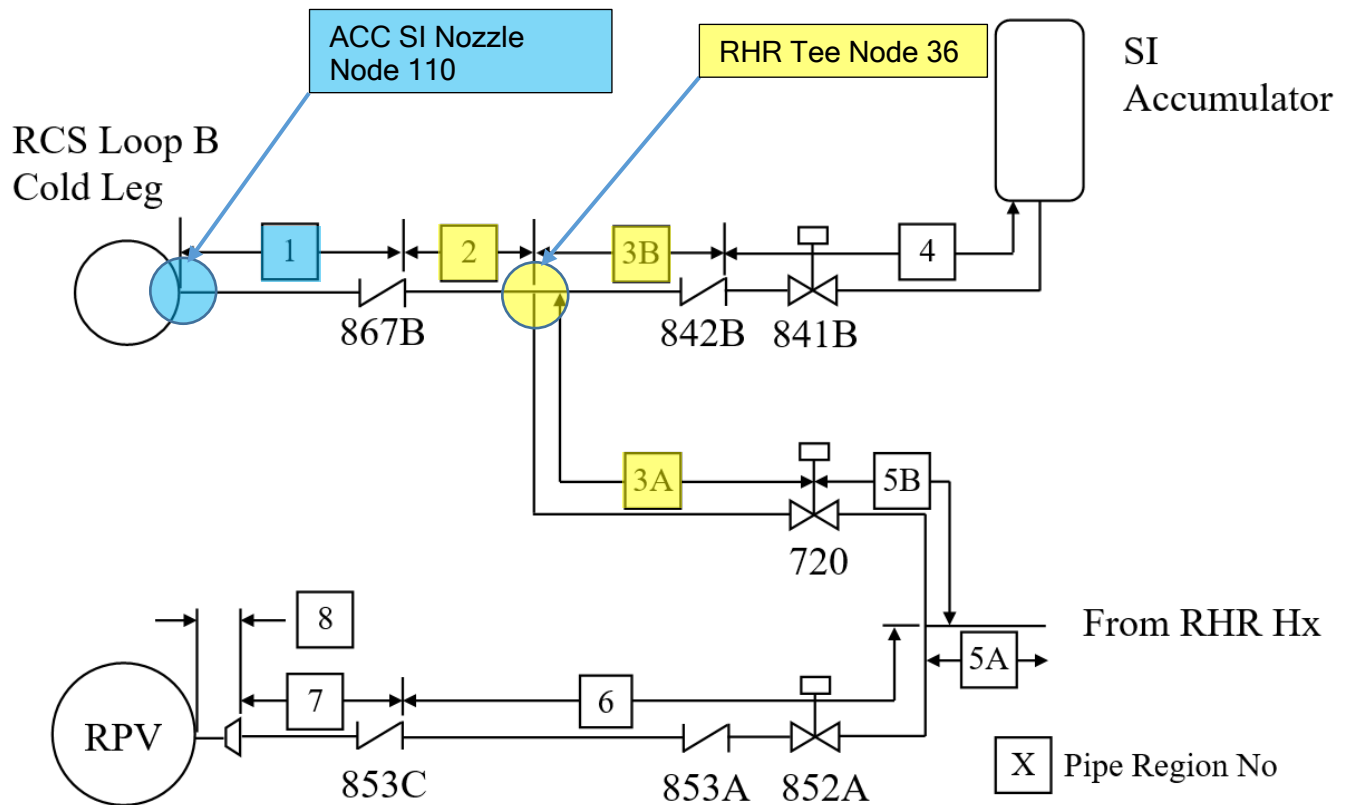


Figure 4: RHR / Safety Injection System Sketch

Cycles used for fatigue analyses are taken from Reference [16] and shown in Table 9. For cycles currently being counted, the counts used in this analysis are each greater than or equal to the 80-year suggested allowable cycles in Table 1.

Table 9: Cycles Used in RHR Tee and ACC SI Nozzle Analyses

LS #	Description	Abbrev.	Cycles
1	Inadv RCS Depress1	LS-01	30
2	Inadv RCS Depress2	LS-02	30
3	Inadv RCS Depress3	LS-03	30
4	Inadv RCS Depress4	LS-04	30
5	Inadv RCS Depress5	LS-05	30
6	Inadv RCS Depress6	LS-06	30
7	RHR Op - Cooldown1	LS-07	200
8	RHR Op - Cooldown2	LS-08	200
9	RHR Op - Cooldown3	LS-09	200
10	Refueling	LS-10	80
11	NORMAL+OBE	LS-11	5x10
12	NORMAL-OBE	LS-12	5x10
13	Inadv Accum BD1	LS-13	60
14	Inadv Accum BD2	LS-14	60

The detailed fatigue table for the RHR tee (node 36) is shown in Table 10 and for the ACC SI nozzle (node 110) is shown in Table 11. Allowable numbers of cycles are recalculated using the NUREG/CR-6909, Revision 1 fatigue curve [1, Table A-2]. For the load pair F_{en} calculations, the maximum service temperature for the load pair and a zero strain rate is conservatively used. For the RHR tee (node 36), the relevant temperatures are based on Zones 2, 3a, and 3b, and for the ACC SI nozzle (node 110), the temperature is based on Zone 1, as illustrated and highlighted in Figure 3 and Figure 4. Calculations are performed in Excel spreadsheet *RHR Tee_and_ACCSINoz.xlsm*.

The resulting CUF_{en} for RHR tee is 0.0758 and for the ACC SI nozzle is 0.0930, which are both less 1.0 and, therefore, acceptable for 80-years, if cycle counts remain within the limits of Table 9.

Table 10: CUF_{en} for RHR Tee, Node 36

Load Set A	Load Set B	F_{en}	U_{en}
Inadv RCS Depress4	RHR Op - Cooldown1	2.38	0.0173
Inadv RCS Depress5	RHR Op - Cooldown2	2.38	0.0083
Inadv RCS Depress2	RHR Op - Cooldown2	2.38	0.0077
RHR Op - Cooldown1	RHR Op - Cooldown2	2.38	0.0331
Inadv RCS Depress3	RHR Op - Cooldown1	2.38	0.0067
Inadv RCS Depress6	Refueling	1.00	0.0009
Inadv RCS Depress1	Inadv Accum BD2	1.16	0.0008
Refueling	Inadv Accum BD2	1.16	0.0007
Refueling	Inadv Accum BD1	1.00	0.0002
RHR Op - Cooldown3	Inadv Accum BD1	1.00	0.0002
RHR Op - Cooldown3	NORMAL+OBE	1.00	0.0000
RHR Op - Cooldown3	NORMAL-OBE	1.00	0.0000
NORMAL+OBE	NORMAL-OBE	1.00	0.0000
		2.28	0.0758
		$F_{en,eff}$	CUF_{en}

Table 11: CUF_{en} for ACC SI Nozzle, Node 110

I	Load Set A	Load Set B	F _{en}	U _{en}
1	Inadv RCS Depress1	Inadv Accum BD2	8.94	0.0682
7	RHR Op - Cooldown1	Inadv Accum BD2	2.70	0.0082
4	Inadv RCS Depress4	RHR Op - Cooldown1	2.38	0.0055
7	RHR Op - Cooldown1	RHR Op - Cooldown2	2.38	0.0077
8	RHR Op - Cooldown2	Inadv Accum BD1	3.27	0.0034
5	Inadv RCS Depress5	NORMAL+OBE	1.00	0.0000
5	Inadv RCS Depress5	NORMAL-OBE	1.00	0.0000
6	Inadv RCS Depress6	Refueling	1.00	0.0000
5	Inadv RCS Depress5	RHR Op - Cooldown3	1.00	0.0000
2	Inadv RCS Depress2	RHR Op - Cooldown3	1.00	0.0000
3	Inadv RCS Depress3	Refueling	1.00	0.0000
9	RHR Op - Cooldown3	Refueling	1.00	0.0000
11	NORMAL+OBE	NORMAL-OBE	1.00	0.0000
			5.39	0.0930
			F_{en,eff}	CUF_{en}

This document previously contained proprietary information, which has been redacted.

5.0 CONCLUSIONS

Environmentally-assisted fatigue usage factors (CUF_{en} values) were computed using guidance from NUREG/CR/6909, Revision 1 for the charging inlet nozzle, hot leg surge nozzle, residual heat removal to safety injection piping tee, and the accumulator safety injection nozzle.

In each case the CUF_{en} was computed to be less than 1.0 and are, therefore, acceptable. Results are summarized in Table 12.

Table 12: Summary of EAF Usage Factors

Component	CUF	$F_{en,eff}$	CUF_{en}
Charging Inlet Nozzle	0.1619	4.41	0.7149
Hot Leg Surge Nozzle	0.1487	6.51	0.9685
RHR Tee	0.0332	2.28	0.0758
ACC SI Nozzle	0.0173	5.39	0.0930

The analyses herein were performed in accordance with NRC-approved methodology for GALL SLR and adequately address all issues pertaining to NRC Regulatory Issue Summary RIS 2008-30 [20].

The usage factors in Table 12 will remain valid for 80-years of operation if cycle counts remain within the limits analyzed herein.

6.0 REFERENCES

1. NRC Contractor Report NUREG/CR-6909, Revision 1, *Effect of LWR Water Environments on the Fatigue Life of Reactor Materials*, Final Report, May 2018.
2. NRC Report NUREG-2191, Vol. 2, *Generic Aging Lessons Learned for Subsequent License Renewal (GALL-SLR) Report*, Final Report, July 2017.
3. ASME Boiler and Pressure Vessel Code
 - a. 1989 Edition
 - b. 2001 Edition with Addenda through 2003.
 - c. 2004 Edition with Addenda through 2006.
4. NRC Contractor Report NUREG/CR-5704 (ANL-98/31), *Effects of LWR Coolant Environments on Fatigue Design Curves of Austenitic Stainless Steels*, April 1999.
5. EPRI Technical Report, *Guidelines for Addressing Environmental Effects in Fatigue Usage Calculations*. EPRI, Palo Alto, CA: 2012. 1025823.
6. SI Calculation Package, *Development of 80-Year Projected Cycles for Point Beach Nuclear Plant Units 1 and 2*, Revision 1, SI File No. 2000088.301.
7. SI Calculation Package, *Loads for Charging Nozzles*, Revision 0, PROPRIETARY SI File No. 0900613.302.
8. SI Calculation Package, *Thermal and Mechanical Stress Analysis of the Charging Nozzle*, Revision 0, PROPRIETARY SI File No. 0900613.303.
9. SI Calculation Package, *Charging Nozzle Fatigue Analysis*, Revision 0, PROPRIETARY SI File No. 0900613.304.
10. SI Calculation Package, *Charging Nozzle Environmentally-Assisted Fatigue (EAF) Analysis*, Revision 0, PROPRIETARY, SI File No. 0900613.305.
11. SI Calculation Package, *Hot Leg Surge Nozzle Loads*, Revision 0, PROPRIETARY, SI File No. 0900613.307.
12. SI Calculation Package, *Thermal and Mechanical Stress Analysis of Hot Leg Surge Nozzle*, Revision 0, PROPRIETARY, SI File No. 0900613.308.
13. SI Calculation Package, *Hot Leg Surge Nozzle Fatigue Analysis*, Revision 0, PROPRIETARY, SI File No. 0900613.309.
14. SI Calculation Package, *Hot Leg Surge Nozzle Environmentally-Assisted Fatigue Analysis Calculation*, Revision 0, PROPRIETARY, SI File No. 0900613.310.
15. SI Calculation Package, *Hot Leg Surge Nozzle Environmentally-Assisted Fatigue (EAF) Analysis Using 60-Year Projected Number of Cycles*, Revision 0, PROPRIETARY, SI File No. 0900613.311.
16. SI Calculation Package, *Point Beach Safety Injection Piping Fatigue Evaluation*, Revision 2, PROPRIETARY, SI File No. NMC-03Q-302.
17. FPL Energy Point Beach, LLC, *License Amendment Request 261, Extended Power Uprate*, dated April 27, 2009. <https://www.nrc.gov/docs/ML1107/ML110750120.html>
18. NRC Letter, *POINT BEACH NUCLEAR PLANT (PBNP), UNITS 1 AND 2 - ISSUANCE OF LICENSE AMENDMENTS REGARDING EXTENDED POWER UPRATE (TAC NOS. ME1044 AND ME1045)*, Dated May 3, 2011. <https://www.nrc.gov/docs/ML1111/ML111170513.html>

19. VESLFAT, Version 2.0, 02/23/12 (build date 12/29/11), Structural Integrity Associates.
20. NRC Regulatory Issue Summary RIS-2008-30, Fatigue Analysis of Nuclear Power Plant Components, December 2008.

This document previously contained supplier proprietary information, which has been redacted.



Point Beach Nuclear Plant Units 1 and 2
Dockets 50-266 and 50-301
NRC 2020-0032 Enclosure 4, Attachment 13

Enclosure 4
Non-proprietary Reference Documents and
Redacted Versions of Proprietary Reference
Documents
(Public Version)
Attachment 13

**Structural Integrity Associates, Inc. Calculation No.
PBCH-03Q-301, Revision 3, "Evaluation of Thermal
Stratification Due to Valve Leakage," September 25,
2020**

(27 Total Pages, including cover sheets)



**STRUCTURAL
INTEGRITY
Associates, Inc.**

**CALCULATION
PACKAGE**

**FILE No.: PBCH-03Q-301
PROJECT No.: 2000088.00**

PROJECT NAME: Spray Line and Auxiliary Spray Line Fatigue Analysis

CLIENT: NextEra Point Beach, LLC

CALCULATION TITLE: Evaluation of Thermal Stratification Due to Valve Leakage


Document Revision	Affected Pages	Revision Description	Project Mgr. Approval Signature & Date	Preparer(s) & Checker(s) Signatures & Date
0	1-14 A1-A3 B1-B7 Computer Files	Original Issue	D. Gerber 7/9/03	P. Hirschberg 7/9/03 W. Weitze 7/9/03
1	Page 13	Correct results summary to match calculations	D. Gerber 1/20/05	P. Hirschberg 1/20/05 W. Weitze 1/20/05
2	1-16 Supporting File	Evaluate Fatigue and Environmentally Assisted Fatigue for 80 Years of Operation using NUREG/CR-6909 Revision 1. Revised calculation title. Added words to Sections 1-6 to clarify that scope is thermal stratification cycling fatigue, and that those sections evaluated 60 year operation. Added Section 7. Added Reference 11.	David A. Gerber 8/6/20	P. Hirschberg 8/5/20 Terry J. Herrmann 8/6/20
3	1, 4 - 5	Reworded Section 3, per client request.	<i>David A. Gerber</i> David A. Gerber 9/25/20	<i>Terry J. Herrmann</i> Terry J. Herrmann 9/25/20 <i>David A. Gerber</i> David A. Gerber 9/25/20

Table of Contents

1.0	INTRODUCTION / OBJECTIVE	3
2.0	TECHNICAL APPROACH OR METHODOLOGY	3
3.0	Assumptions / Design Inputs	4
4.0	Analysis or Calculations.....	5
5.0	Results of Analysis.....	11
6.0	Conclusions of Evaluation for 60 Years of Operation	13
7.0	Evaluation for 80 years of operation	14
8.0	References	16
APPENDIX A TOPBOT INPUT FILE		A-1
APPENDIX B TOPBOT OUTPUT EXCERPT		B-1

List of Tables

Table 1	Thermal Cycle Construction	7
Table 2	Thermal Stratification Cycle Pairing.....	8
Table 3	Stress and Fatigue Usage.....	13
Table 4	Evaluation for 80 Years of Operation	15

	Revision	0	1	2	3
	Preparer/Date	PH 7/9/03	PH 1/20/05	PH 8/5/20	TJH 9/25/20
	Checker/Date	WFW 7/9/03	WFW 1/20/05	TJH 8/6/20	DAG 9/25/20
	File No. PBCH-03Q-301	Page 2 of 16			

1.0 INTRODUCTION / OBJECTIVE

In late 1989 as a response to the NRC Bulletin 88-08 issues, Point Beach installed two sets of thermocouples on the horizontal section of the Unit 2 main and auxiliary spray piping to detect leakage and thermal stratification in the lines. Thermally stratified conditions were discovered during heatup and normal operation. Using this data [1], Sargent and Lundy performed a 40-year fatigue calculation [2] for both units for the main and auxiliary spray piping, resulting in a fatigue usage due to thermal stratification in Unit 1 of 0.66, which is more than double that of Unit 2 (0.30). If the plant licensing basis is extended to 60 years, the Unit 1 usage would extrapolate to approximately 1.0. The Sargent and Lundy calculation included a simplified hand calculation of the thermal stratification stresses. The simplifying assumptions used may or may not have been conservative.


The purpose of this calculation is to review the Sargent and Lundy work in detail, to determine a more accurate fatigue usage due to thermal stratification for a 60-year design life for Unit 1. In Revision 2 of this calculation, this evaluation is extended for 80 years of operation and the effects of environmentally assisted fatigue (EAF) is addressed.

The review consists of the following tasks:

1. The thermocouple data is reviewed to verify the basis for the stresses and contributions to fatigue of the operating parameters. The rationale for extrapolating the results of the data collection sample period to the entire plant life is revisited. Contributions to fatigue usage attributed to heatup, cooldown, auxiliary spray actuation, and thermal stratification due to valve leakage are identified.
2. The simplified hand calculation of the thermal stratification stresses done by Sargent and Lundy contains estimates of global bowing moment, radial local stress, and axial local stress. Some of the simplifying assumptions used are conservative and some are possibly unconservative. The correct thermal stratification stresses are determined using the SI program TOPBOT.
3. The evaluation for an 80-year plant life takes into account the effects of environmentally-assisted fatigue (EAF).

2.0 TECHNICAL APPROACH OR METHODOLOGY

Thermal stratification data was collected in 1989-90 using three thermocouples installed at each of two locations near the tee joining the auxiliary pressurizer spray line and one of the main spray lines in Unit 2 [3]. The thermocouples were located at the top, bottom, and midlevel of the pipe. Data was collected for a 153-day period, beginning with a plant heatup. The thermocouple data indicated that thermal stratification was present during most of the monitoring period, and the magnitude of the top-to-bottom gradient varied over time. The midlevel temperature, assumed to be indicative of the pipe

	Revision	0	1	2	3
	Preparer/Date	PH 7/9/03	PH 1/20/05	PH 8/5/20	TJH 9/25/20
	Checker/Date	WFW 7/9/03	WFW 1/20/05	TJH 8/6/20	DAG 9/25/20
	File No. PBCH-03Q-301	Page 3 of 16			

average temperature, also varied over time, not only due to plant heatup but also due to variations in spray demand. Thus, two types of thermal cycling occur: global thermal cycling, based on the midpipe temperature variations, which affects the thermal expansion moments in the pipe and the global stratification bowing effects; and thermal gradient cycling, based on the variation of the difference between the top and bottom pipe temperatures, which affects the local and global thermal stratification stresses.


Of the two monitored locations, it was apparent that the upstream location, designated as T01 and located on the auxiliary spray line between the tee and the first upstream elbow, experienced significantly more thermal stratification [3]. This is because the other location was downstream of both main spray tees, and the bypass spray flow from the two lines nearly fills the pipe. The data review is done based on T01. In the Sargent and Lundy analysis [2], node point 210 in Unit 1 was identified as the limiting location for stress and fatigue usage. Node point 210 is located on the 3-inch line between the first main spray tee and the reducer before the second tee [9]. As the calculations done here affect all locations proportionally, point 210 remains limiting and is used for determining the fatigue usage attributed to thermal stratification for extended plant life.

The thermocouple data is reviewed in detail and temperature cycles are constructed. Cycling of the mean pipe temperature is designated as Type “A” cycles, as was done in reference [3]; cycling of the top-to-bottom gradient is designated as Type “B” cycles. Type A cycles of less than 100°F and type B cycles of less than 50°F are neglected. The peaks and valleys of these cycles are paired according to the ASME method of matching highest peak with lowest valley, second highest peak with second lowest valley, etc. This is conservative because higher cyclic ranges produce exponentially higher fatigue usage.

The most severe top-to-bottom thermal stratification temperature profile is determined and modeled in the SI program TOPBOT [4]. TOPBOT is a safety related software application that is controlled by the Structural Integrity Quality Assurance program. TOPBOT calculates the fixed end thermal bowing moment and the local peak stresses due to the nonlinear, non-axisymmetric thermal gradient. The bowing moment is compared to that determined by S&L, and piping stresses that were determined are scaled according to the more accurate moment determined by TOPBOT. These results, and the local peak stresses determined by TOPBOT, are then scaled to the varied cycle amplitudes to develop stress cycles. These results are used in a revised evaluation to determine the projected fatigue usage attributed to thermal stratification for extended plant life.

3.0 ASSUMPTIONS / DESIGN INPUTS

The thermal stratification was determined to have been caused by leakage past auxiliary spray isolation valve CV-296 [3]. Although the leakage flow may initially be hot as it is taken from the charging system, the flow is sufficiently small and the valve is far enough away (80 feet [3]) from the

	Revision	0	1	2	3
	Preparer/Date	PH 7/9/03	PH 1/20/05	PH 8/5/20	TJH 9/25/20
	Checker/Date	WFW 7/9/03	WFW 1/20/05	TJH 8/6/20	DAG 9/25/20
	File No. PBCH-03Q-301	Page 4 of 16			

main spray tee that the leakage mixes with the stagnant fluid in the auxiliary spray line and arrives at the tee at containment ambient temperature. At location T01, this fluid lies along the bottom of the pipe; the hot fluid at the top of the pipe is backup of the bypass spray flow from one of the main spray lines, which is at a temperature close to the reactor coolant loop cold leg temperature. If the main spray flow increases, the bottom of pipe temperature approaches main spray temperature; if auxiliary spray flow increases, the top of pipe temperature approaches ambient (initially, until the previously stagnant fluid is flushed out). Corrective maintenance including changes to the internals has been performed on valve CV-296 after measurement of the stratification [10], and it is unlikely that leakage, and consequently thermal stratification, is continuing to occur. However, since there is no additional data available, it is conservatively assumed that valve leakage and associated thermal stratification continue to exist, and it is assumed that the stratification is of the same magnitude as measured previously. Also, the measurements were taken in Unit 2; in the Sargent and Lundy analysis it was assumed that Unit 1 also has valve leakage, and that the Unit 2 data is applicable to Unit 1.


It is also assumed that the 153-day period of data is representative of all plant operation. This is conservative because this period includes a heatup, which contains many more stress cycles than does normal steady state operation. The heatup is also considered conservatively representative of a cooldown, because the mean pipe temperature range is the same, and there are multiple main spray and auxiliary spray actuations, as well as numerous variations in spray flow rate. Heatups tend to contain more thermal cycles than cooldowns, as there are typically more procedural steps, hold points, and tests conducted than during cooldown.

4.0 ANALYSIS OR CALCULATIONS

4.1 Construction of Thermal Cycles for 60 Year Operation

The thermocouple data of reference [1] was reviewed in detail. For location T01, two types of thermal cycles were constructed: Type A cycles, which are thermal expansion moment cycles based on the midlevel pipe temperature variations; and Type B, local and global thermal stratification cycles, based on the top-to-bottom thermal gradient magnitude variations. Table 1 summarizes the construction of the thermal cycles. For each cycle, the date and hour of the beginning of the cycle (valley), the peak, and the end of the cycle (subsequent valley) are given. The mid-pipe temperature (type A cycles) and the top-to-bottom gradient (type B), and the range of the cycle are shown, along with a comment on the source of the thermal cycle. Type A cycles less than 100°F and type B cycles less than 50°F are neglected.

Looking at the temperature plots, on day 325 hour 11 for example, the top of pipe temperature drops sharply for a brief period. This indicates that an auxiliary spray has occurred, as the stagnant fluid at ambient temperature that was in the 80 feet of pipe downstream of the control valve was pushed out to the pressurizer. As the entire pipe cools then reheats, this causes a thermal expansion moment cycle.

	Revision	0	1	2	3
	Preparer/Date	PH 7/9/03	PH 1/20/05	PH 8/5/20	TJH 9/25/20
	Checker/Date	WFW 7/9/03	WFW 1/20/05	TJH 8/6/20	DAG 9/25/20
	File No. PBCH-03Q-301	Page 5 of 16			

On day 327 hour 6, the bottom of pipe temperature increases sharply to above the previous top-of-pipe temperature. This indicates that a main spray has occurred, as the spray flow at cold leg temperature is sufficiently high to fill the entire pipe. During the heatup, the top-to-bottom temperature profile varies. This is caused by variations in main spray flow. The maximum gradient occurs at minimum bypass flow (about 3.5 gpm per line) and reduces as spray flow increases. Spray flow may be increased during heatup to control the rate of pressure increase in the pressurizer.


The type A cycles thus consist of one full heatup cycle with range of 455°F, and three auxiliary spray cycles with range of up to 150°F. The latter three cycles will all be considered as 150°F.

The type B cycles were then paired according to the ASME cycle counting method. The peaks and valleys of these cycles are paired by matching highest peak with lowest valley, second highest peak with second lowest valley, etc. The philosophy of the ASME Section III Code [5] fatigue calculation considers that cyclic events are order independent. Grouping cycles in this method is conservative because it results in higher cyclic ranges which produce exponentially higher fatigue usage. Table 2 lists the reordered cycles. The result is that during the monitored period, the thermal stratification cycles are enveloped by considering three at 300°F, 17 at 230°F, and 11 at 110°F.

The above cycles represent 153 days of plant operation. To extrapolate these cycles to 60 years of operation, the following assumptions are used:

- The cycles are considered to be repeated every 153 days of operation, despite the fact that plant heatups do not occur that often
- The plant is not operated for one month per two years due to refueling outages

The cycles are therefore multiplied by a factor of $60 (365.25) (23) / [(153) (24)] = 137.3 \sim 140$.

	Revision	0	1	2	3
	Preparer/Date	PH 7/9/03	PH 1/20/05	PH 8/5/20	TJH 9/25/20
	Checker/Date	WFW 7/9/03	WFW 1/20/05	TJH 8/6/20	DAG 9/25/20
	File No. PBCH-03Q-301	Page 6 of 16			

**Table 1
Thermal Cycle Construction**

Type A Cycles - T at Center Changes > 100F

Start Date/Time	Peak Date/Time	End Date/Time	Start Temp	Peak Temp	Range, deg.F	Comments
320/12	330/7	Cooldown	65	520	455	Heatup
325/11	325/11	325/11	380	280	100	Aux spray
325/17	325/17	325/17	400	300	100	Aux spray
326/6	326/6	326/6	380	230	150	Aux spray

Type B Cycles - Top to Bottom Gradient Changes > 50F

Start Date/Time	Peak Date/Time	End Date/Time	Start Gradient	Peak Gradient	Range, deg.F	Comments
325/19	326/6	326/6	0	200	200	Heatup-aux spray
326/13	327/6	327/6	0	250	250	Heatup-main spray
327/6	327/6	328/11	0	250	250	Heatup-main spray
328/11	328/12	328/23	70	240	170	Main spray flow variation
328/23	328/24	329/2	90	180	90	Main spray flow variation
329/2	329/7.5	329/7.5	90	280	190	Main spray flow variation
329/7.5	329/8	329/8	210	280	70	Main spray flow variation
329/8	329/8	329/8.5	130	270	140	Main spray flow variation
329/8.5	329/9	329/10.5	180	280	100	Main spray flow variation
329/10.5	329/10.5	329/10.5	190	260	70	Main spray flow variation
329/10.5	329/10.5	329/11	190	260	70	Main spray flow variation
329/11	329/11.5	329/12	70	260	190	Main spray flow variation
329/12	329/12	329/12.5	80	260	180	Main spray flow variation
329/12.5	329/12.5	329/13	190	260	70	Main spray flow variation
329/13	329/13	329/13.5	130	260	130	Main spray flow variation
329/13.5	329/13.5	329/14	180	260	80	Main spray flow variation
329/14	329/14	329/16	60	260	200	Main spray flow variation
329/16	329/16	329/18	130	250	120	Main spray flow variation
329/18	329/18	329/18.5	160	230	70	Main spray flow variation
329/18.5	329/18.5	329/19	140	220	80	Main spray flow variation
329/19	329/19	329/19	160	220	60	Main spray flow variation
329/19	329/19	329/20	160	220	60	Main spray flow variation
329/20	329/20	329/20	130	220	90	Main spray flow variation
329/20.5	329/20.5	329/20.5	60	180	120	Main spray flow variation
329/20.5	329/21	329/21	50	190	140	Main spray flow variation
329/21	329/22	329/22	90	230	140	Main spray flow variation
329/22	329/23	330/1	70	220	150	Main spray flow variation
330/1	330/1	330/6	160	220	60	Main spray flow variation
330/6	330/6	330/7	140	210	70	Main spray flow variation
330/7	330/7	330/10	140	220	80	Main spray flow variation
330/10	331/2	331/5	120	300	180	Main spray flow variation
331/5	339/10	340/18	80	230	150	Main spray flow variation
340/18	341/20	342/2	90	260	170	Main spray flow variation
342/2	5/12	5/16	90	220	130	Main spray flow variation
5/16	42/24	43/2	90	200	110	Main spray flow variation
43/2	70/8	81/8	80	250	170	Main spray flow variation
81/8	84/0	91/10	50	220	170	Main spray flow variation
91/10	93/6	106/4	130	190	60	Main spray flow variation
106/4	106/6	107/0	90	160	70	Main spray flow variation



Revision	0	1	2	3
Preparer/Date	PH 7/9/03	PH 1/20/05	PH 8/5/20	TJH 9/25/20
Checker/Date	WFW 7/9/03	WFW 1/20/05	TJH 8/6/20	DAG 9/25/20
File No.	PBCH-03Q-301			Page 7 of 16

**Table 2
Thermal Stratification Cycle Pairing**

Reordered cycles using ASME method			
Valley	Peak	Range, deg,F	Comments
0	300	300	
0	280	280	
0	280	280	
50	280	230	
50	270	220	
60	260	200	
60	260	200	
70	260	190	
70	260	190	
70	260	190	
80	260	180	
80	260	180	
80	260	180	
90	260	170	
90	250	160	
90	250	160	
90	250	160	
90	250	160	
90	240	150	
90	230	140	
120	230	110	
130	230	100	
130	220	90	
130	220	90	
130	220	90	
130	220	90	
140	220	80	
140	220	80	
140	220	80	
160	220	60	
160	220	60	
160	210	50	neglect
160	200	40	neglect
180	200	20	neglect
180	190	10	neglect
190	190	0	neglect
190	180	-10	neglect
190	180	-10	neglect
210	160	-50	neglect




Revision	0	1	2	3
Preparer/Date	PH 7/9/03	PH 1/20/05	PH 8/5/20	TJH 9/25/20
Checker/Date	WFW 7/9/03	WFW 1/20/05	TJH 8/6/20	DAG 9/25/20
File No.	PBCH-03Q-301			Page 8 of 16

4.2 Thermal Stratification Analysis

In reference [6], Sargent and Lundy calculated the global thermal stratification fixed end moment, and the local thermal stratification stresses due to the nonlinear top-to-bottom thermal gradient. These calculations were done by hand and were somewhat simplified in that they assumed that the thermocouple temperatures measured at the outside of the pipe were representative of the inside fluid temperatures, and did not account for the through-wall thermal gradients. A more accurate thermal stratification stress analysis was done using the SI program TOPBOT.

TOPBOT solves the transient thermal and stress response within a pipe subjected to a step or ramp change in boundary temperatures and heat transfer coefficients. Initial temperature conditions are specified, and then a temperature change is applied to either the top or bottom fluid in the pipe, or both. The pipe is considered to be two dimensional at a pipe cross-section (or assumed to be extremely long in the axial direction). Symmetry about the pipe vertical centerline is assumed. The pipe is modeled with rectilinear elements within the R-theta coordinate system. Stresses and temperatures are computed at the center of each element (mean radius and mean angular locations). In addition, temperatures and stresses are computed at the inside and outside surfaces of the pipe, based on the "steady state" temperature distribution between the surface elements and external boundary temperatures. Required thermal input parameters include thermal conductivity and the product of the density and specific heat, modulus of elasticity, coefficient of thermal expansion, and Poisson's ratio. The thermal boundary conditions are input as internal and external temperature distributions and heat transfer distributions. For most problems, the initial pipe temperature is uniform: a uniform temperature and heat transfer coefficient is specified on the outside of the pipe, and two sets of temperature and heat transfer coefficients are specified inside the pipe, representing the top and bottom temperatures and flow rates. These two sets of temperatures, heat transfer coefficients, and their interface level can be varied linearly by specifying different values at specific points in time. The pipe temperature distribution is determined using a classical finite difference method. An energy balance is written for each element of the model.

For this analysis, the top-to-bottom temperature distribution at T01 on day 331, hour 2 was modeled, as it is representative of the most severe stratification condition. The stress results will be scaled for smaller thermal gradients. At this point in time, the outside pipe temperature at the top of the pipe is 527°F, the bottom is 227°F, and the midlevel is 502°F. In order to determine accurate thermal stratification stresses, the inside fluid temperatures that produce the temperature distribution measured at the outside of the pipe must be determined. This requires some trial and error, as it is a function of the hot-cold fluid interface level and the convective heat transfer coefficients at the top and bottom inside surface of the pipe; these coefficients in turn depend on the flow rates and temperatures of the fluid levels.

	Revision	0	1	2	3
	Preparer/Date	PH 7/9/03	PH 1/20/05	PH 8/5/20	TJH 9/25/20
	Checker/Date	WFW 7/9/03	WFW 1/20/05	TJH 8/6/20	DAG 9/25/20
	File No. PBCH-03Q-301	Page 9 of 16			

The inside surface forced convection heat transfer coefficients were determined using the following relation for turbulent flow [7]:

$$h = 0.023 Re^{0.8} Pr^{0.4} k / D$$

where

Re = Reynolds number = $\rho VD/\mu > 4000$ for turbulent flow

Pr = Prandtl number = $\mu c_p/k$

k = thermal conductivity, BTU-hr-ft/°F

D = hydraulic diameter = $4A/P$

A = flow area

P = flow perimeter

V = flow velocity, ft/sec

ρ = density, lbm/ft³

μ = dynamic viscosity, lbm /ft-sec

c_p = specific heat at constant pressure

The Reynolds number was checked to verify that the equation is applicable.

At node point 210, the pipe is 3 inch diameter schedule 160, with inside diameter = 2.624 in. Other input parameters are, for A-376 TP316 steel [6]:

$$E = 28300 - 5.12 (T-70) \text{ ksi [5]}$$

$$\alpha = 9.11 E-06 + 1.37 E-09 (T-70) \text{ in/in-°F [5]}$$

$$v = 0.3$$

$$k = 10.23 \text{ BTU/hr-ft-°F at } T=502^\circ\text{F [5]}$$

$$\rho c_p = 61.66 \text{ BTU/ft}^3\text{-°F at } T=502^\circ\text{F [5]}$$

After trial and error, the outside pipe temperature distribution is replicated if the inside fluid temperatures are 530°F at the top (some heat loss from RCS cold leg temperature) and 100°F at the bottom (containment ambient temperature), the interface level is at 148" from the top of the pipe, and the top fluid velocity is 0.516 ft/sec, or 3.1 gpm (bypass flow circulation) and the bottom fluid velocity is 0.19 ft/sec, or 0.3 gpm (leakage past auxiliary spray control valve). The actual valve leakage and the other parameters may be a little different, but as long as the temperature distribution is established in the analytical model, the stress results will be representative.

The input file, PBCH_03.IN, is attached in Appendix A.



Revision	0	1	2	3
Preparer/Date	PH 7/9/03	PH 1/20/05	PH 8/5/20	TJH 9/25/20
Checker/Date	WFW 7/9/03	WFW 1/20/05	TJH 8/6/20	DAG 9/25/20
File No.	PBCH-03Q-301			Page 10 of 16

5.0 RESULTS OF ANALYSIS

5.1 Thermal Stratification Analysis

The results of the TOPBOT thermal stratification analysis were the following:

Fixed End Moment: 108.19 in-kip (for a 300°F top-to-bottom thermal gradient)

Local Stress (maximum location): 40.31 ksi (for a 300°F top-to-bottom thermal gradient)
= 134.37 psi/°F

The steady state temperature and stress distribution results are included in Appendix B.

5.2 Stress Combinations and Fatigue Usage

The stress and fatigue usage will be computed at the limiting location, node point 210. This location is classified as ASME Code Class 2. ASME Section III, Subsection NC-3600, does not provide explicit fatigue usage criteria; however, the approach used by Markl in his fatigue testing of piping components [8] will be used, which has been implicitly adopted in NC-3600:

$$i S (N)^{0.2} = 280,000 \quad [2]$$

Where

S = stress range, psi

i = stress intensification factor = 1.0 at node point 210 (straight pipe) [5]


N = number of allowable full range stress cycles at stress S

The stress is the total of the contributions from thermal expansion moments, global thermal stratification, and local thermal stratification. Table 3 summarizes the calculation.

Per [2], the thermal expansion moment stress at node 210 is $(32113 - 6960) = 25153$ psi.

The global thermal stratification stress calculated in [2] was 6960 psi. This stress was obtained by applying the stratification fixed end moment to the piping model. A more accurate fixed end moment was calculated by TOPBOT as described above. The stresses are therefore adjusted by the ratio of the fixed end moments,

$$\text{Global stratification stress} = 6960 (108.19/104.34 [9]) = 7217 \text{ psi}$$

	Revision	0	1	2	3
	Preparer/Date	PH 7/9/03	PH 1/20/05	PH 8/5/20	TJH 9/25/20
	Checker/Date	WFW 7/9/03	WFW 1/20/05	TJH 8/6/20	DAG 9/25/20
	File No. PBCH-03Q-301	Page 11 of 16			

Per [9], the magnitude of stratification at point 210 is 0.93 of that measured at T01. The local stress is

$$= 134.37 \text{ psi/}^\circ\text{F (300) (.93) = 37,489 \text{ psi.}$$

The stress cycles for 60 years of operation are grouped in the following manner:

1x140=140 cycles of 455°F thermal expansion moment range + 300°F global stratification + 300°F local stratification

2x140=280 cycles of 150°F thermal expansion moment range + 300°F global stratification + 300°F local stratification

1x140=140 cycles of 150°F thermal expansion moment range + 230°F global stratification + 230°F local stratification

16x140=2240 cycles of 230°F global stratification + 230°F local stratification

11x140=1540 cycles of 110°F global stratification + 110°F local stratification

As shown in Table 3, the thermal expansion moment stress is scaled according to the temperature range of the cycle. For example, for a 150°F range, the thermal expansion range is


$$= 25153 (150/455) = 8292 \text{ psi.}$$

The stratification stresses, global and local, are scaled according to the top-to-bottom gradient. Thus for a 230°F gradient, the global stratification stress is

$$= 7217 (230/300) = 5533 \text{ psi}$$

and the local stratification stress is

$$= 37489 (230/300) = 28742 \text{ psi.}$$

	Revision	0	1	2	3
	Preparer/Date	PH 7/9/03	PH 1/20/05	PH 8/5/20	TJH 9/25/20
	Checker/Date	WFW 7/9/03	WFW 1/20/05	TJH 8/6/20	DAG 9/25/20
	File No. PBCH-03Q-301	Page 12 of 16			

The total stress is tabulated as shown in Table 3. The number of stress cycles for groups 2-5 are then converted into an equivalent number of full range stress cycles using equation (2) in paragraph NC-3611.2 (e) (3) of reference [5]. This relationship was developed by Markl in his fatigue testing of piping components [8] and has been incorporated into the ASME Class 2/3 piping Code:

$$N = N_1 + (S_2/S_1)^5 N_2 + (S_3/S_1)^5 N_3 + (S_4/S_1)^5 N_4 + (S_5/S_1)^5 N_5$$


Thus, following this approach, 280 cycles of group 2 are equivalent to 70.36 full range cycles, for example. As shown in Table 3, the total equivalent full range cycles of all groups is 286.9. Using Markl's equation, the allowable number of cycles at a stress of 69,859 psi is 1034. Therefore, the total implicit fatigue usage for 60 years of operation is 0.277.

**Table 3
Stress and Fatigue Usage**

Stress Combination									
Node Point	SIF	Pipe Size, in.	Local Stress per deg. F, psi	Local Stress Reduction Factor	Local Stress for 300F, psi	PIPSYS Expansion plus global stratification	Expansion only	Previous Global stratification	Revised Global stratification
210	1	3	134.37	0.93	37489	32113	25153	6960	7217
Fatigue Usage									
Cycle Group	Expansion Range	Expansion Stress	Stratification Delta, F	Global Stress	Local Stress	Total Stress, psi	No. Cycles	Equivalent Cycles	Fatigue Usage
1	455	25153	300	7217	37489	69859	140	140	
2	150	8292	300	7217	37489	52998	280	70.36	
3	150	8292	230	5533	28742	42567	140	11.76	
4	0	0	230	5533	28742	34275	2240	63.68	
5	0	0	110	2646	13746	16392	1540	1.10	
Total								286.90	0.277

6.0 CONCLUSIONS OF EVALUATION FOR 60 YEARS OF OPERATION

The result of the stress and fatigue analysis is that for the limiting location on the Unit 1 pressurizer spray line, the calculated implicit fatigue usage for thermal stratification due to leakage of the auxiliary spray control valve for a 60-year plant design life is 0.277. This value is below the allowable of 1.0 with margin. The stresses conservatively assume that a significant amount of leakage past the auxiliary spray control valve will continue to exist throughout plant life, despite maintenance actions to eliminate it. Thus, the stress and fatigue usage are acceptable for a 60-year design life.

	Revision	0	1	2	3
	Preparer/Date	PH 7/9/03	PH 1/20/05	PH 8/5/20	TJH 9/25/20
	Checker/Date	WFW 7/9/03	WFW 1/20/05	TJH 8/6/20	DAG 9/25/20
	File No. PBCH-03Q-301	Page 13 of 16			

7.0 EVALUATION FOR 80 YEARS OF OPERATION

The evaluation of the implicit fatigue usage associated with the thermal stratification measured in the pressurizer spray line in response to NRC Bulletin 88-08, as described above, is extended for 80 years of operation in this section. Since publication of Revision 1 of this calculation, the NRC has issued NUREG-6909 Revision 1 [11], which requires that the effects of reactor water environments be considered in calculating fatigue. Although the location that is the subject of this calculation is not designed to ASME Class 1 criteria (NB-3650), the environmental fatigue penalty factors, and the associated fatigue curve in air contained in the NUREG, will be used as guidance for assessing an implicit Class 2 fatigue usage.

It must be noted that the cause of the stratification measured in the thermocouple data taken in 1989 was leakage past auxiliary spray control valve CV-296. Maintenance on this valve has since been performed to eliminate this leakage, however since there is no easy way to measure whether or not this valve continues to leak, it is conservatively assumed in this evaluation that it will continue to leak throughout 80 years of plant operation.

The following methodology was used in this evaluation:

1. The numbers of cycles determined for 60 years of operation shown in Table 3 were scaled up to 80 years by multiplying by 80/60. The assumption is considered to be conservative, as maintenance has been performed on valve CV-296 to mitigate the leakage found in 1989.
2. The allowable cycles corresponding to the total stress for each group of cycles in Table 3 was determined from the fatigue curve in air published in NUREG-6909 Rev. 1 [11]. The total stress in Table 3 represents the cyclic stress due to the sum of global thermal expansion, global stratification bowing, and local thermal stratification distortion.
3. The numbers of cycles for 80 years of operation were divided by the allowable cycles for each group of cycles to arrive at a partial implicit fatigue usage for each group.
4. F_{en} multiplier factors on fatigue usage associated with reactor water environmental effects were determined using the equations in NUREG-6909 Rev. 1. For the stainless steel material of this piping location, A-376 TP 316, the F_{en} relationship is:

$$F_{en} = \exp(-T^* \epsilon^* O^*)$$

where T^* , ϵ^* , and O^* are transformed temperature, strain rate, and DO level, respectively, defined as follows:

$$T^* = 0 \quad (T \leq 100^\circ\text{C})$$

$$T^* = (T - 100)/250 \quad (100^\circ\text{C} \leq T \leq 325^\circ\text{C})$$

$$\epsilon^* = 0 \quad (\epsilon > 7\%/s)$$

$$\epsilon^* = \ln(\epsilon/7) \quad (0.0004\%/s \leq \epsilon \leq 7\%/s)$$

$$\epsilon^* = \ln(0.0004/7) \quad (\epsilon < 0.0004\%/s)$$



Revision	0	1	2	3
Preparer/Date	PH 7/9/03	PH 1/20/05	PH 8/5/20	TJH 9/25/20
Checker/Date	WFW 7/9/03	WFW 1/20/05	TJH 8/6/20	DAG 9/25/20
File No.	PBCH-03Q-301			Page 14 of 16

For DO less than 0.1 ppm (i.e., for pressurized-water reactor (PWR) or boiling-water reactor (BWR) hydrogen water chemistry (HWC) water),

$$O^* = 0.29 \text{ (all wrought and cast SSs and heat treatments and SS weld)}$$

The F_{en} is equal to 1.0 when the stress amplitude is less than 28,300 psi.

For the strain rate term, the most conservative strain rate was used, which corresponds to very slow stress cycles. In most cases, thermal stratification cycling occurs much more quickly, which would reduce the F_{en} factor.

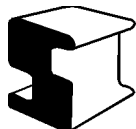
For the temperature term, an average of the maximum temperature of 530°F and the minimum midlevel temperature during the cycle (but not less than the threshold temperature of 212°F) was used, as permitted by NUREG-6909 Revision 1 [11].

- The partial implicit fatigue usage was multiplied by the F_{en} factor for each cycle group to determine an environmentally-assisted fatigue usage (EAF). The contributions from each cycle group were summed to determine a total implicit EAF fatigue usage.

The results of this calculation are shown in Table 4. The total implicit fatigue usage using the NUREG-6909 Rev. 1 air curve is 0.154, and the total fatigue usage including EAF is 0.744, which are below the allowable of 1.0.

Table 4
Evaluation for 80 Years of Operation


Cycle Group	Total Stress, psi	No. Cycles for 80 Years	Allowable Cycles per NUREG-6909	Fatigue Usage in Air	Average Temperature	F_{EN}	EAF
1	69859	187	3978	0.047	455	4.618	0.217
2	52998	373	10258	0.036	455	4.618	0.168
3	42567	187	21700	0.009	472.5	5.156	0.044
4	34275	2987	49047	0.061	472.5	5.156	0.314
5	16392	2053	2008492	0.001	502.5	1.000	0.001
Total				0.154			0.744



Revision	0	1	2	3
Preparer/Date	PH 7/9/03	PH 1/20/05	PH 8/5/20	TJH 9/25/20
Checker/Date	WFW 7/9/03	WFW 1/20/05	TJH 8/6/20	DAG 9/25/20
File No.	PBCH-03Q-301			Page 15 of 16

8.0 REFERENCES

1. Appendix to Point Beach Unit 2 Pressurizer Spray Stress Report, “Thermocouple Temperature Measurements”, WEPCO Accession Number 200057 Rev. 0, Sargent and Lundy, SI File PBCH-03Q-201.
2. Section 11.6 of Point Beach Unit 1 Pressurizer Spray Stress Report, “Local Stress Fatigue Evaluation”, WEPCO Accession Number 100066 Rev. 0, Sargent and Lundy, SI File PBCH-03Q-201.
3. Section 7 of Point Beach Unit 1 Pressurizer Spray Stress Report, “Thermal Stratification Analysis”, WEPCO Accession Number 100066 Rev. 0, Sargent and Lundy, SI File PBCH-03Q-201.
4. TOPBOT, Transient Thermal and Stress Analysis of Pipes with Stratified Flow, Version 3.0, Structural Integrity Associates.
5. ASME Boiler and Pressure Vessel Code, Section III, 1974 Edition with Addenda to Winter 1976.
6. Section 11.3 of Point Beach Unit 1 Pressurizer Spray Stress Report, “Calculations for Stratification Evaluation”, WEPCO Accession Number 100066 Rev. 0, Sargent and Lundy, SI File PBCH-03Q-201.
7. Holman, J.P., Heat Transfer, 4th Edition, McGraw-Hill, 1976.
8. Markl, A., “Fatigue Tests of Piping Components”, Transactions ASME, 1952.
9. Section 11.4 of Point Beach Unit 1 Pressurizer Spray Stress Report, “Determination of Fixed End Moments Due to Thermal Stratification”, WEPCO Accession Number 100066 Rev. 0, Sargent and Lundy, SI File PBCH-03Q-201.
10. E-mail, B. Fromm to P. Hirschberg, “Re Pressurizer Spray Stratification”, 5/2/03, SI File PBCH-03Q-102.
11. Effect of LWR Water Environments on the Fatigue Life of Reactor Materials, Final Report, NUREG/CR-6909 Revision 1, May 2018, USNRC.

	Revision	0	1	2	3
	Preparer/Date	PH 7/9/03	PH 1/20/05	PH 8/5/20	TJH 9/25/20
	Checker/Date	WFW 7/9/03	WFW 1/20/05	TJH 8/6/20	DAG 9/25/20
	File No. PBCH-03Q-301	Page 16 of 16			

APPENDIX A
TOPBOT INPUT FILE



Revision	0	1	2	3
Preparer/Date	PH 7/9/03	PH 1/20/05	PH 8/5/20	TJH 9/25/20
Checker/Date	WFW 7/9/03	WFW 1/20/05	TJH 8/6/20	DAG 9/25/20
File No. PBCH-03Q-301	Page A1 of A3			

This file is the standard input file format for TOPBOT 3.0.
 It includes instructions for running the program.
 Input is in accordance with instructions contained in the file and
 is free format style, with a blank line after each input group.

=> Input Line 1 - Inside radius and outside radius in inches:
 1.312 1.75

=> Input Line 2 - Number of radial elements in model (10 max):
 6

Following line has number of locations for 1/2 pipe (whole pipe elements
 divided by two + one) - one element each located at top and bottom
 of the pipe.

=> Input Line 3 - Number of angular locations for stress and temp. (73 max):
 37

E and alpha are input as $x = x_{not} + dxdt * (T - T_{not})$ linear functions.
 Line 4 - Tzero (F) and Nu (Poisson's ratio)
 Line 5 - Eo, and dE/dT (ksi & ksi/F) - E is modulus at temperature T
 Line 6 - ao, and da/dT (in/in-F & in/in-F/F) - alpha is mean value to T

=> Input Lines 4, 5, & 6:
 70 0.3
 28300.0 -5.12
 9.11E-6 1.37E-9

Conductivity and density * specific heat are input as constants
 Line 7 - Conductivity (BTU/Hr-ft-F)
 Line 8 - Density * Specific Heat (BTU/ft^3-F)

=> Input Lines 7 & 8:
 10.23
 61.66

Thermal condition definitions. These input lines required, but Line 9 is
 overridden if line 20 is true.
 Line 9 - Uniform pipe temperature before beginning of transient
 Line 10 - T(F) and h(Btu/hr-ft^2-F) outside
 Line 11 - Number of transient time definitions for inside pipe (40 max)
 Line 12 - time(s), level(deg), Ttop(deg.F), Tbot(deg.F), htop, hbot

=> Input Lines 9,10,11, & 12:
 530
 100 .1
 3
 0 148 530 530 127 127
 60 148 530 100 127 155
 1200 148 530 100 127 155

Output is requested at intervals requested by the user
 Line 13 - Number of output intervals (40 max)
 Line 14 (repeat Line 13 times) - end of interval - print interval

=> Input Line 13 & 14:



Revision	0	1	2	3
Preparer/Date	PH 7/9/03	PH 1/20/05	PH 8/5/20	TJH 9/25/20
Checker/Date	WFW 7/9/03	WFW 1/20/05	TJH 8/6/20	DAG 9/25/20
File No. PBCH-03Q-301	Page A2 of A3			

1
1200 60

=> Input Line 15 - Maximum time step (sec) although stable time computed:
1

=> Input Line 16 - Name of output file:
PBCH_03Q.OUT

Transient output may be requested at specific sections
Line 17 is number of requested sections (zero to maximum theta locations)
Line 18 (actually as many lines as identified in line 18) = theta element
location number with number 1 at the top (in any order)

=> Input lines 17 and 18 - number and location numbers
5
1
19
33
35
37

=> Input Line 19 - Title for Problem:
TOPBOT 3.0 Point Beach Pressurizer Spray Line

Optional input of a restart or initial temperature and heat transfer
coefficient file. (Each run creates this file at end of run as
<output filename>.rst.) Start Line 20 with T to use old restart file.

=> Input Line 21 - T (for TRUE) filename.ext - or - F (for FALSE)
F PBCH_03Q.RST

END - First three characters of this line (21) must be END or error results.
The line just preceding this line is the official end of the input file.
Any number of comments may be put in the input file following the END line.
Comment 1:
etc.



Revision	0	1	2	3
Preparer/Date	PH 7/9/03	PH 1/20/05	PH 8/5/20	TJH 9/25/20
Checker/Date	WFW 7/9/03	WFW 1/20/05	TJH 8/6/20	DAG 9/25/20
File No.	PBCH-03Q-301			Page A3 of A3

APPENDIX B
TOPBOT OUTPUT EXCERPT



Revision	0	1	2	
Preparer/Date	PH 7/9/03	PH 1/20/05	PH 9/15/20	
Checker/Date	WFW 7/9/03	WFW 1/20/05	TJH 9/15/20	
File No.	PBCH-03Q-301			Page B1 of B7

"TOP TO BOTTOM GRADIENT THERMAL STRESS ANALYSIS OUTPUT FILE"
"TOPBOT Version 3.0 - October 23, 1993"
"Written by: STRUCTURAL INTEGRITY ASSOCIATES, SAN JOSE CA (408) 978-8200"
"PROBLEM: "
" TOPBOT 3.0 Point Beach Pressurizer Spray Line"
" INPUT FILE: pbch_03q.in"
" DATE: 05-20-2003 TIME: 15:34:14"
"GEOMETRY:"
" Outside diameter (inches) = 3.5 (Radius = 1.75)"
" Inside diameter (inches) = 2.624 (Radius = 1.312)"
" Thickness (inches) = .438 "
" Area (inches^2) = 4.213366 "
" Moment of Inertia (in^4) = 5.039021 "
" Radial Elements = 6 "
" Circumferential Elements in Entire Pipe = 72 "
" NTHETA = 37 (for output angles - top to bottom)"
"MATERIAL PROPERTIES:"
" E (KSI) : 28300 + -5.12 * (T - 70)"
" Alpha (in/in-F): 9.11E-06 + 1.37E-09 * (T - 70)"
" Nu : .3 "
" Conductivity (Btu/hr-ft-F): 10.23 "
" Rho*Cp (Btu/ft^3-F) : 61.66 "
"THERMAL CONDITIONS:"
" T (F) and h (Btu/hr-ft^2-F)"
" T and h of top and bottom fluid are functions of time "
" Load *.BND to view those transient boundary values "
" Outside = 100 & .1 (effective)"
" Initial Temperature = 530 "
"OUTPUT FOLLOWS (As Free and Fixed End Cases + Temperatures):"
"-----"



Revision	0	1	2	
Preparer/Date	PH 7/9/03	PH 1/20/05	PH 9/15/20	
Checker/Date	WFW 7/9/03	WFW 1/20/05	TJH 9/15/20	
File No. PBCH-03Q-301			Page B2 of B7	

```


"TIME = 1199.995 "" ""T. Step = " .1916933 "Interface Angle = 148 "
"Stress Results - Free End Case, then Rotation-Fixed End Case"
"Moment to Fix Ends from Rotation = 108.1926 (in-kips)"

"Free End Case - R ="
"Angle"      1.312      1.349      1.421      1.495      1.567      1.640
1.714      1.750

  0.0  0.6801E+01  0.7616E+01  0.9237E+01  0.1085E+02  0.1245E+02  0.1404E+02
0.1562E+02  0.1641E+02
  5.0  0.6701E+01  0.7514E+01  0.9129E+01  0.1073E+02  0.1233E+02  0.1391E+02
0.1549E+02  0.1628E+02
 10.0  0.6403E+01  0.7208E+01  0.8807E+01  0.1039E+02  0.1197E+02  0.1354E+02
0.1510E+02  0.1588E+02
 15.0  0.5909E+01  0.6702E+01  0.8274E+01  0.9835E+01  0.1138E+02  0.1292E+02
0.1446E+02  0.1522E+02
 20.0  0.5225E+01  0.6000E+01  0.7537E+01  0.9060E+01  0.1057E+02  0.1207E+02
0.1356E+02  0.1430E+02
 25.0  0.4359E+01  0.5112E+01  0.6602E+01  0.8078E+01  0.9540E+01  0.1099E+02
0.1243E+02  0.1314E+02
 30.0  0.3319E+01  0.4045E+01  0.5481E+01  0.6900E+01  0.8304E+01  0.9693E+01
0.1107E+02  0.1175E+02
 35.0  0.2117E+01  0.2814E+01  0.4187E+01  0.5540E+01  0.6875E+01  0.8195E+01
0.9501E+01  0.1015E+02
 40.0  0.7677E+00  0.1431E+01  0.2733E+01  0.4013E+01  0.5272E+01  0.6513E+01
0.7737E+01  0.8343E+01
 45.0  -.7135E+00  -.8670E-01  0.1139E+01  0.2338E+01  0.3514E+01  0.4667E+01
0.5802E+01  0.6361E+01
 50.0  -.2308E+01  -.1720E+01  -.5754E+00  0.5373E+00  0.1622E+01  0.2681E+01
0.3718E+01  0.4226E+01
 55.0  -.3996E+01  -.3447E+01  -.2388E+01  -.1366E+01  -.3782E+00  0.5802E+00
0.1512E+01  0.1966E+01
 60.0  -.5753E+01  -.5244E+01  -.4273E+01  -.3346E+01  -.2458E+01  -.1606E+01 -
.7849E+00  -.3884E+00
 65.0  -.7554E+01  -.7085E+01  -.6201E+01  -.5370E+01  -.4586E+01  -.3844E+01 -
.3140E+01  -.2804E+01
 70.0  -.9370E+01  -.8939E+01  -.8142E+01  -.7407E+01  -.6728E+01  -.6099E+01 -
.5515E+01  -.5242E+01
 75.0  -.1117E+02  -.1077E+02  -.1006E+02  -.9418E+01  -.8845E+01  -.8330E+01 -
.7868E+01  -.7661E+01
 80.0  -.1292E+02  -.1255E+02  -.1191E+02  -.1136E+02  -.1089E+02  -.1049E+02 -
.1016E+02  -.1002E+02
 85.0  -.1457E+02  -.1423E+02  -.1366E+02  -.1320E+02  -.1282E+02  -.1254E+02 -
.1233E+02  -.1225E+02
 90.0  -.1610E+02  -.1577E+02  -.1526E+02  -.1487E+02  -.1459E+02  -.1441E+02 -
.1432E+02  -.1432E+02
 95.0  -.1744E+02  -.1712E+02  -.1664E+02  -.1631E+02  -.1612E+02  -.1605E+02 -
.1608E+02  -.1614E+02

```



	Revision	0	1	2	
	Preparer/Date	PH 7/9/03	PH 1/20/05	PH 9/15/20	
	Checker/Date	WFW 7/9/03	WFW 1/20/05	TJH 9/15/20	
	File No. PBCH-03Q-301	Page B3 of B7			

100.0 -.1854E+02 -.1822E+02 -.1776E+02 -.1748E+02 -.1736E+02 -.1738E+02 -
 .1753E+02 -.1766E+02
 105.0 -.1935E+02 -.1900E+02 -.1854E+02 -.1828E+02 -.1822E+02 -.1833E+02 -
 .1859E+02 -.1879E+02
 110.0 -.1979E+02 -.1940E+02 -.1889E+02 -.1865E+02 -.1863E+02 -.1881E+02 -
 .1918E+02 -.1944E+02
 115.0 -.1977E+02 -.1932E+02 -.1874E+02 -.1847E+02 -.1848E+02 -.1873E+02 -
 .1919E+02 -.1952E+02
 120.0 -.1921E+02 -.1867E+02 -.1798E+02 -.1766E+02 -.1766E+02 -.1796E+02 -
 .1851E+02 -.1890E+02
 125.0 -.1799E+02 -.1732E+02 -.1646E+02 -.1606E+02 -.1605E+02 -.1639E+02 -
 .1702E+02 -.1746E+02
 130.0 -.1592E+02 -.1509E+02 -.1403E+02 -.1354E+02 -.1351E+02 -.1389E+02 -
 .1460E+02 -.1510E+02
 135.0 -.1277E+02 -.1172E+02 -.1044E+02 -.9891E+01 -.9901E+01 -.1035E+02 -
 .1115E+02 -.1171E+02
 140.0 -.8047E+01 -.6692E+01 -.5323E+01 -.4908E+01 -.5121E+01 -.5760E+01 -
 .6708E+01 -.7305E+01
 145.0 -.5784E+00 0.1196E+01 0.1946E+01 0.1585E+01 0.7439E+00 -.3260E+00 -
 .1521E+01 -.2160E+01
 150.0 0.1895E+02 0.1572E+02 0.1187E+02 0.9160E+01 0.7023E+01 0.5234E+01
 0.3688E+01 0.3011E+01
 155.0 0.2813E+02 0.2468E+02 0.1966E+02 0.1592E+02 0.1305E+02 0.1078E+02
 0.8980E+01 0.8272E+01
 160.0 0.3322E+02 0.3012E+02 0.2514E+02 0.2119E+02 0.1807E+02 0.1560E+02
 0.1367E+02 0.1294E+02
 165.0 0.3655E+02 0.3370E+02 0.2894E+02 0.2504E+02 0.2189E+02 0.1937E+02
 0.1739E+02 0.1663E+02
 170.0 0.3870E+02 0.3601E+02 0.3145E+02 0.2765E+02 0.2454E+02 0.2202E+02
 0.2002E+02 0.1925E+02
 175.0 0.3992E+02 0.3732E+02 0.3288E+02 0.2916E+02 0.2609E+02 0.2358E+02
 0.2158E+02 0.2080E+02
 180.0 0.4031E+02 0.3775E+02 0.3335E+02 0.2966E+02 0.2660E+02 0.2410E+02
 0.2209E+02 0.2131E+02

"Fixed End Case - R ="

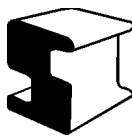
"Angle" 1.312 1.349 1.421 1.495 1.567 1.640
 1.714 1.750

0.0 -.2137E+02 -.2134E+02 -.2128E+02 -.2124E+02 -.2121E+02 -.2119E+02 -
 .2117E+02 -.2116E+02
 5.0 -.2136E+02 -.2133E+02 -.2128E+02 -.2123E+02 -.2120E+02 -.2118E+02 -
 .2116E+02 -.2116E+02
 10.0 -.2134E+02 -.2131E+02 -.2125E+02 -.2121E+02 -.2117E+02 -.2115E+02 -
 .2113E+02 -.2113E+02
 15.0 -.2130E+02 -.2127E+02 -.2121E+02 -.2116E+02 -.2112E+02 -.2110E+02 -
 .2108E+02 -.2108E+02
 20.0 -.2125E+02 -.2121E+02 -.2114E+02 -.2109E+02 -.2106E+02 -.2103E+02 -
 .2101E+02 -.2100E+02



Revision	0	1	2	
Preparer/Date	PH 7/9/03	PH 1/20/05	PH 9/15/20	
Checker/Date	WFW 7/9/03	WFW 1/20/05	TJH 9/15/20	
File No.	PBCH-03Q-301			Page B4 of B7

25.0 -.2117E+02 -.2113E+02 -.2106E+02 -.2100E+02 -.2096E+02 -.2093E+02 -
 .2091E+02 -.2091E+02
 30.0 -.2108E+02 -.2103E+02 -.2095E+02 -.2089E+02 -.2084E+02 -.2081E+02 -
 .2079E+02 -.2079E+02
 35.0 -.2096E+02 -.2090E+02 -.2081E+02 -.2075E+02 -.2069E+02 -.2066E+02 -
 .2064E+02 -.2063E+02
 40.0 -.2081E+02 -.2075E+02 -.2065E+02 -.2057E+02 -.2051E+02 -.2047E+02 -
 .2045E+02 -.2044E+02
 45.0 -.2063E+02 -.2056E+02 -.2044E+02 -.2035E+02 -.2028E+02 -.2024E+02 -
 .2021E+02 -.2021E+02
 50.0 -.2042E+02 -.2033E+02 -.2019E+02 -.2009E+02 -.2001E+02 -.1996E+02 -
 .1993E+02 -.1993E+02
 55.0 -.2015E+02 -.2005E+02 -.1989E+02 -.1977E+02 -.1968E+02 -.1962E+02 -
 .1959E+02 -.1959E+02
 60.0 -.1984E+02 -.1972E+02 -.1953E+02 -.1939E+02 -.1929E+02 -.1922E+02 -
 .1918E+02 -.1918E+02
 65.0 -.1946E+02 -.1932E+02 -.1910E+02 -.1893E+02 -.1881E+02 -.1873E+02 -
 .1869E+02 -.1868E+02
 70.0 -.1900E+02 -.1884E+02 -.1858E+02 -.1838E+02 -.1824E+02 -.1815E+02 -
 .1810E+02 -.1809E+02
 75.0 -.1846E+02 -.1827E+02 -.1796E+02 -.1772E+02 -.1756E+02 -.1745E+02 -
 .1739E+02 -.1739E+02
 80.0 -.1781E+02 -.1758E+02 -.1721E+02 -.1694E+02 -.1674E+02 -.1661E+02 -
 .1654E+02 -.1654E+02
 85.0 -.1703E+02 -.1676E+02 -.1632E+02 -.1599E+02 -.1576E+02 -.1561E+02 -
 .1553E+02 -.1553E+02
 90.0 -.1610E+02 -.1577E+02 -.1526E+02 -.1487E+02 -.1459E+02 -.1441E+02 -
 .1432E+02 -.1432E+02
 95.0 -.1498E+02 -.1460E+02 -.1398E+02 -.1352E+02 -.1319E+02 -.1298E+02 -
 .1287E+02 -.1287E+02
 100.0 -.1365E+02 -.1319E+02 -.1246E+02 -.1191E+02 -.1151E+02 -.1126E+02 -
 .1114E+02 -.1114E+02
 105.0 -.1206E+02 -.1151E+02 -.1064E+02 -.9977E+01 -.9510E+01 -.9215E+01 -
 .9071E+01 -.9067E+01
 110.0 -.1015E+02 -.9498E+01 -.8456E+01 -.7671E+01 -.7116E+01 -.6766E+01 -
 .6597E+01 -.6593E+01
 115.0 -.7869E+01 -.7087E+01 -.5846E+01 -.4913E+01 -.4254E+01 -.3840E+01 -
 .3641E+01 -.3637E+01
 120.0 -.5129E+01 -.4195E+01 -.2717E+01 -.1611E+01 -.8337E+00 -.3463E+00 -
 .1140E+00 -.1101E+00
 125.0 -.1828E+01 -.7112E+00 0.1043E+01 0.2345E+01 0.3252E+01 0.3817E+01
 0.4084E+01 0.4088E+01
 130.0 0.2182E+01 0.3521E+01 0.5587E+01 0.7091E+01 0.8122E+01 0.8755E+01
 0.9053E+01 0.9056E+01
 135.0 0.7145E+01 0.8756E+01 0.1114E+02 0.1280E+02 0.1390E+02 0.1456E+02
 0.1486E+02 0.1486E+02
 140.0 0.1353E+02 0.1549E+02 0.1806E+02 0.1967E+02 0.2066E+02 0.2122E+02
 0.2148E+02 0.2148E+02
 145.0 0.2250E+02 0.2491E+02 0.2695E+02 0.2787E+02 0.2831E+02 0.2853E+02
 0.2862E+02 0.2862E+02

	Revision	0	1	2	
	Preparer/Date	PH 7/9/03	PH 1/20/05	PH 9/15/20	
	Checker/Date	WFW 7/9/03	WFW 1/20/05	TJH 9/15/20	
	File No.	PBCH-03Q-301			Page B5 of B7

150.0 0.4335E+02 0.4079E+02 0.3830E+02 0.3695E+02 0.3617E+02 0.3574E+02
0.3555E+02 0.3555E+02
155.0 0.5366E+02 0.5092E+02 0.4732E+02 0.4501E+02 0.4355E+02 0.4270E+02
0.4232E+02 0.4233E+02
160.0 0.5969E+02 0.5733E+02 0.5382E+02 0.5135E+02 0.4970E+02 0.4870E+02
0.4824E+02 0.4825E+02
165.0 0.6376E+02 0.6167E+02 0.5842E+02 0.5604E+02 0.5440E+02 0.5339E+02
0.5292E+02 0.5293E+02
170.0 0.6644E+02 0.6453E+02 0.6150E+02 0.5925E+02 0.5768E+02 0.5671E+02
0.5625E+02 0.5625E+02
175.0 0.6798E+02 0.6617E+02 0.6329E+02 0.6113E+02 0.5962E+02 0.5867E+02
0.5823E+02 0.5823E+02
180.0 0.6848E+02 0.6670E+02 0.6387E+02 0.6175E+02 0.6025E+02 0.5932E+02
0.5888E+02 0.5889E+02

"Temperature Results Inside Pipe and at R ="


"Angle" "Inside" " ID " 1.349 1.421 1.495 1.567 1.640
1.714 " OD " "Outside" " Hin " " Hout "

0.0	530.0	527.7	527.6	527.5	527.3	527.3	527.2
527.1	527.1	100.0	127.000	1.000E-01			
5.0	530.0	527.7	527.6	527.4	527.3	527.2	527.2
527.1	527.1	100.0	127.000	1.000E-01			
10.0	530.0	527.6	527.5	527.3	527.2	527.1	527.0
527.0	527.0	100.0	127.000	1.000E-01			
15.0	530.0	527.4	527.3	527.2	527.0	526.9	526.9
526.8	526.8	100.0	127.000	1.000E-01			
20.0	530.0	527.2	527.1	526.9	526.8	526.7	526.6
526.6	526.5	100.0	127.000	1.000E-01			
25.0	530.0	526.9	526.8	526.6	526.4	526.3	526.2
526.2	526.2	100.0	127.000	1.000E-01			
30.0	530.0	526.5	526.4	526.2	526.0	525.9	525.8
525.7	525.7	100.0	127.000	1.000E-01			
35.0	530.0	526.0	525.9	525.7	525.5	525.3	525.2
525.2	525.2	100.0	127.000	1.000E-01			
40.0	530.0	525.5	525.3	525.0	524.8	524.6	524.5
524.5	524.5	100.0	127.000	1.000E-01			
45.0	530.0	524.7	524.5	524.2	524.0	523.8	523.7
523.6	523.6	100.0	127.000	1.000E-01			
50.0	530.0	523.9	523.6	523.3	523.0	522.8	522.6
522.6	522.5	100.0	127.000	1.000E-01			
55.0	530.0	522.8	522.5	522.1	521.8	521.5	521.4
521.3	521.3	100.0	127.000	1.000E-01			
60.0	530.0	521.6	521.2	520.7	520.3	520.1	519.9
519.8	519.8	100.0	127.000	1.000E-01			
65.0	530.0	520.0	519.7	519.1	518.6	518.3	518.1
518.0	517.9	100.0	127.000	1.000E-01			
70.0	530.0	518.2	517.8	517.1	516.5	516.2	515.9
515.8	515.8	100.0	127.000	1.000E-01			



Revision	0	1	2	
Preparer/Date	PH 7/9/03	PH 1/20/05	PH 9/15/20	
Checker/Date	WFW 7/9/03	WFW 1/20/05	TJH 9/15/20	
File No.	PBCH-03Q-301			Page B6 of B7

75.0	530.0	516.0	515.5	514.7	514.1	513.6	513.3
513.2	513.1	100.0	127.000	1.000E-01			
80.0	530.0	513.4	512.8	511.8	511.1	510.5	510.2
510.0	510.0	100.0	127.000	1.000E-01			
85.0	530.0	510.3	509.6	508.4	507.5	506.9	506.5
506.3	506.3	100.0	127.000	1.000E-01			
90.0	530.0	506.6	505.7	504.3	503.3	502.5	502.0
501.8	501.8	100.0	127.000	1.000E-01			
95.0	530.0	502.1	501.1	499.4	498.2	497.3	496.7
496.5	496.4	100.0	127.000	1.000E-01			
100.0	530.0	496.8	495.6	493.6	492.1	491.1	490.4
490.1	490.1	100.0	127.000	1.000E-01			
105.0	530.0	490.5	489.0	486.6	484.9	483.6	482.8
482.4	482.4	100.0	127.000	1.000E-01			
110.0	530.0	482.9	481.1	478.3	476.2	474.7	473.8
473.3	473.3	100.0	127.000	1.000E-01			
115.0	530.0	473.8	471.7	468.4	465.9	464.1	463.0
462.4	462.4	100.0	127.000	1.000E-01			
120.0	530.0	462.9	460.4	456.4	453.5	451.4	450.1
449.5	449.5	100.0	127.000	1.000E-01			
125.0	530.0	449.8	446.8	442.2	438.7	436.3	434.8
434.0	434.0	100.0	127.000	1.000E-01			
130.0	530.0	434.1	430.5	425.0	421.0	418.2	416.6
415.8	415.8	100.0	127.000	1.000E-01			
135.0	530.0	414.8	410.5	404.2	399.8	396.9	395.1
394.3	394.3	100.0	127.000	1.000E-01			
140.0	530.0	390.7	385.5	378.7	374.4	371.8	370.3
369.6	369.6	100.0	127.000	1.000E-01			
145.0	530.0	358.4	352.0	346.7	344.2	343.0	342.5
342.2	342.2	100.0	127.000	1.000E-01			
150.0	143.0	293.4	300.2	306.7	310.3	312.3	313.5
314.0	314.0	100.0	152.200	1.000E-01			
155.0	100.0	258.0	265.2	274.7	280.7	284.6	286.8
287.8	287.8	100.0	155.000	1.000E-01			
160.0	100.0	235.8	241.9	251.1	257.6	261.9	264.5
265.7	265.7	100.0	155.000	1.000E-01			
165.0	100.0	220.3	225.8	234.3	240.5	244.8	247.4
248.6	248.6	100.0	155.000	1.000E-01			
170.0	100.0	210.0	215.0	222.9	228.8	232.9	235.4
236.6	236.6	100.0	155.000	1.000E-01			
175.0	100.0	204.0	208.7	216.3	221.9	225.8	228.3
229.5	229.5	100.0	155.000	1.000E-01			
180.0	100.0	202.1	206.7	214.1	219.6	223.5	226.0
227.1	227.1	100.0	155.000	1.000E-01			

	Revision	0	1	2	
	Preparer/Date	PH 7/9/03	PH 1/20/05	PH 9/15/20	
	Checker/Date	WFW 7/9/03	WFW 1/20/05	TJH 9/15/20	
	File No.	PBCH-03Q-301			Page B7 of B7

Point Beach Nuclear Plant Units 1 and 2
Dockets 50-266 and 50-301
NRC 2020-0032 Enclosure 4, Attachment 14

Enclosure 4

**Non-proprietary Reference Documents and
Redacted Versions of Proprietary Reference
Documents**

(Public Version)

Attachment 14

**Westinghouse LTR-SDA-20-064-NP, Revision 1,
“ASME Section XI Appendix L Evaluation Results for
the Point Beach Units 1 and 2 Pressurizer Spray
Nozzles,” October 7, 2020**

(35 Total Pages, including cover sheets)



1000 Westinghouse Drive
Cranberry Twp., PA 16066

To: John T. Ahearn
cc:

Date: October 7, 2020

From: RV/CV Design and Analysis
Ext: 412-374-3631

Ref: LTR-SDA-20-064-NP Rev. 1

Subject: ASME Section XI Appendix L Evaluation Results for the Point Beach Units 1 and 2 Pressurizer Spray Nozzles

To support the Point Beach Unit 1 and Unit 2 Subsequent License Renewal (SLR) program, ASME Section XI Appendix L evaluations were performed to demonstrate that acceptable operation of the pressurizer spray nozzles is ensured. This letter report summarizes the results of ASME Appendix L flaw tolerance evaluations. In addition, discussion of transient cycles used for the Appendix L analyses and recommendations for transient cycle counting for future operation is included in Appendix A attached to this letter.

The purpose for Revision 1 of this letter is to incorporate comments from NextEra Energy. The customer comment resolution form is electronically attached to this letter in the Process, Records, and Information Management Environment (PRIME). All changes from Revision 0 to Revision 1 are denoted by revision bars in the left margin.

Author: Stephen E. Marlette*
NSSS Component Design and Analysis

Author: Eric J. Matthews (Appendix A only)*
Reactor Vessel/Containment Vessel Design and Analysis

Verifier: Gordon Z. Hall*
Structural Design and Analysis

Verifier: Thomas G. Joseph (Appendix A only)*
Functional and Systems Engineering

Manager: Lynn A. Patterson*
Reactor Vessel/Containment Vessel Design and Analysis

WESTINGHOUSE NON-PROPRIETARY CLASS 3

© 2020 Westinghouse Electric Company LLC
All Rights Reserved

***Electronically approved records are authenticated in the Process, Records, and Information Management Environment.**

Foreword:

This document contains Westinghouse Electric Company LLC proprietary information and data which has been identified in brackets. Coding ^(a,c,e) associated with the brackets sets forth the basis on which information is considered proprietary. These code letters are listed with their meanings in BMS-LGL-84, and are defined as follows:

- a. The information reveals the distinguishing aspects of a process (or component, structure, tool, method, etc.) where the prevention of its use by any of Westinghouse's competitors without license from Westinghouse constitutes a competitive economic advantage over other companies.
- c. The information, if used by a competitor, would reduce the competitor's expenditure of resources or improve the competitor's advantage in the design, manufacture, shipment, installation, assurance of quality, or licensing of a similar product.
- e. The information reveals aspects of past, present, or future Westinghouse or customer funded development plans and programs of potential commercial value to Westinghouse.

The proprietary information and data contained within the brackets of this document were obtained at considerable Westinghouse expense and its release could seriously affect our competitive position. This information is to be withheld from public disclosure in accordance with the Rules of Practice 10 CFR 2.390 and the information presented herein is to be safeguarded in accordance with 10 CFR 2.390. Withholding of this information does not affect the public interest.

This information has been provided for your internal use only and should not be released to persons or organizations outside the Directorate of Regulation and the ACRS (Advisory Committee on Reactor Safeguards) without the express written approval of Westinghouse Electric Company LLC. Should it become necessary to release this information to such persons as part of the review procedure, please contact Westinghouse Electric Company LLC, which will make the necessary arrangements required to protect the Company's proprietary interests.

The proprietary information in brackets has been deleted in this non-proprietary version. The deleted information is provided in the proprietary version of this report (LTR-SDA-20-064-P).

1.0 Introduction and Summary of Results

The purpose of this letter is to summarize the ASME Section XI Appendix L [1] flaw tolerance evaluation of the Point Beach Units 1 and 2 pressurizer spray nozzles as part of the Subsequent License Renewal (SLR) program (80 year life extension). As part of the SLR program, Point Beach Units 1 and 2 (NextEra Energy) have identified the spray nozzle safe ends as fatigue sensitive sentinel locations as part of or in addition to those identified in NUREG-6260 [2]. In lieu of conducting formal fatigue calculations to disposition the spray nozzle locations for the SLR program, NUREG-2192 [3] permits inspection as a management method for fatigue sensitive locations. NUREG-2192 requires a flaw tolerance evaluation to determine the time required between inspections. The flaw tolerance evaluation for the spray nozzles at Point Beach Units 1 and 2 will be per of Section XI Appendix L [1].

Two analysis locations (e.g. ASN 3 and ASN 2) were considered in the Appendix L fracture mechanics for the Pressurizer spray nozzle safe end region. ASN 3 (safe end) was identified as the fatigue sensitive location on the pressurizer spray nozzle with respect to environmental fatigue; therefore, the safe end (ASN 3) needs to be analyzed for Appendix L. However, the ASME Section XI inspection program considers only the safe end to pipe weld region (ASN 2); therefore, in order to justify flaw tolerance of ASN 3 (fatigue sensitive location), which is not within the inspection zone, the Appendix L fracture mechanics needs to evaluate and justify ASN 2 (inspectable weld location) to bound ASN 3

The most limiting loads for the pressurizer spray line for both units were considered for generating the fracture analysis stresses and the most limiting nozzle loads were considered for determining the end of evaluation period flaw size. Results of the Section XI Appendix L analyses are shown in Table 1-1 and the corresponding analysis section number (ASN) locations are shown in Figure 1-1. As can be seen from the results in Table 1-1, the most limiting result is for the axial flaw case at ASN 2 which demonstrates an acceptable period of at least 12 years. These results provide assurance that flaws will not grow to an unacceptable size between inservice examinations based on conservative Section XI Appendix L methodology.

Table 1-1: Summary of Limiting Section XI Appendix L Results for the Pressurizer Spray Nozzle

ASN	Flaw Configuration	Appendix L Calculated Aspect Ratio ¹	Acceptable Standards Flaw Size Section XI Table IWB-3410-1 (a/t)	Final Flaw Size (a/t)	Maximum Allowable End-of-Evaluation Flaw Size (a/t) ²	Allowable Operating Period (Years)
2	Axial Flaw	69.1	0.1214	0.171	0.173	12
	Circumferential Flaw	50.0	0.1214	0.169	0.170	21
3	Axial Flaw	42.0	0.1361	0.379	0.383	53
	Circumferential Flaw	42.6	0.1361	0.249	0.530	80

Notes:

1. Aspect ratio (AR) is defined as flaw length/depth (l/a).
2. Flaw size a/t = flaw depth (a) / wall thickness (t).

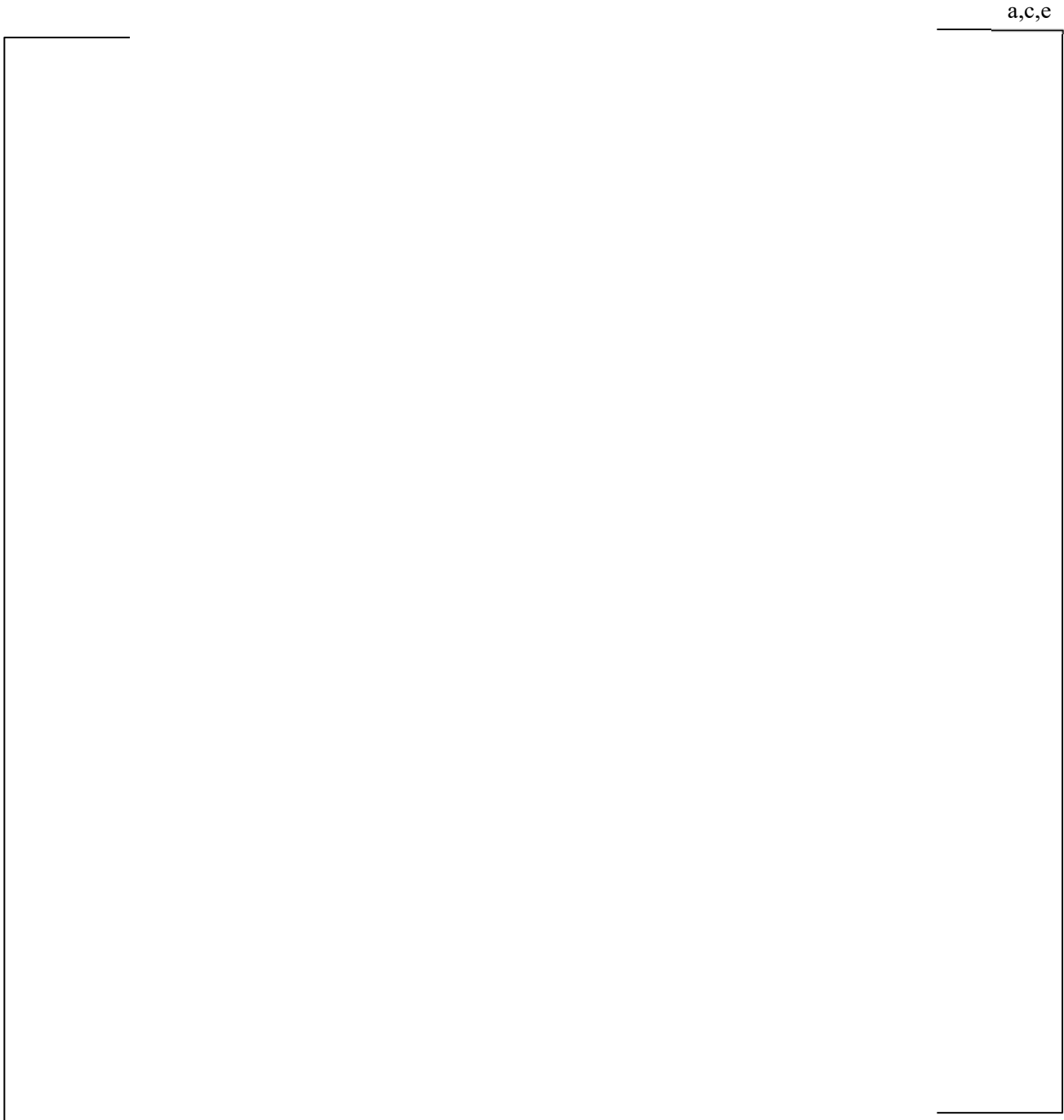


Figure 1-1 Locations of the ASN's

2.0 Flaw Tolerance Methodology

As part of the SLR program, Point Beach 1 and 2 (NextEra Energy) have identified that the Pressurizer Spray nozzle safe end regions are fatigue sensitive sentinel locations as part of and in addition to those identified in NUREG-6260 [2]. The environmentally assisted fatigue (EAF) usage value (U_{en}) for the safe ends (ASN3) is predicted to be in excess of 1.0 as required by the design code. Thus, NextEra has elected to manage the effects of fatigue by crediting the inservice inspection (ISI) programs during the SLR period. NUREG-2192 [3] permits inspection as a management method for fatigue as long as a flaw tolerance evaluation is performed to determine the time between inspections. Thus, flaw tolerance evaluations are performed for the pressurizer spray nozzle safe end based on ASME Section XI Appendix L [1]. The results of the flaw tolerance calculations determine the required inservice inspection frequency for the spray nozzles. Since the inservice inspection frequency is 10 years, the desired result of the Appendix L analysis would be to demonstrate 10 years or more for acceptable operation.

The Section XI Appendix L flaw tolerance evaluation consists of calculating the maximum allowable end-of-evaluation (EOE) period flaw size and determining the allowable operating period for a postulated flaw to grow (via fatigue crack growth (FCG) to the maximum allowable EOE period flaw size. ASME Section XI Appendix L-3212 requires the postulated initial flaw depth to be no smaller than the applicable acceptance standards in Table IWB-3410-1 using a flaw shape (a/l) equal to 0.167 (or aspect ratio, $AR = 6$). Since the analysis locations for the pressurizer spray nozzle are at the stainless steel safe end and safe-end-to-pipe welds, Section XI, Paragraph IWB-3514 is used to determine the initial flaw size for welds and adjacent base metal in austenitic piping material.

The postulated flaws used in the flaw tolerance evaluation are inside surface axial and circumferential flaws with aspect ratios (AR , flaw length/flaw depth) determined based on ASME Section XI Appendix L. Due to the nature of fatigue mechanisms, several small fatigue cracks may initiate, coalesce, and then grow like an equivalent long single crack. ASME Section XI Appendix L calculates the required aspect ratio to be used in the flaw tolerance evaluation to consider the effects of fatigue cracking. The evaluation of postulated inside surface flaws conservatively covers evaluations for embedded flaws and outside surface flaws, as the stress intensity factors for inside surface flaws are more limiting than embedded and outside surface flaws.

The primary crack growth mechanism for flaws within the spray nozzle/weld is fatigue crack growth. Crack growth due to Primary Water Stress Corrosion Crack (PWSCC) growth does not need to be investigated since the base metals (stainless steel piping and nozzles) and stainless steel weld material have a low susceptibility to stress corrosion cracking. The fatigue crack growth rate and the applicable stress intensity factor equations are needed to perform a FCG analysis. The FCG rate for stainless steel in a water environment is based on ASME Section XI Code Case N-809 [4]. The 2016 Edition of API-579 [5] is used for the stress intensity factor calculations.

2.1 ASME Section XI Appendix L Analysis

ASME Section XI IWB-3740 and Appendix L provide the methodology approved by the NRC to calculate a conservative equivalent single crack (ESC) aspect ratio for flaw tolerance evaluation. ASME Section XI Appendix L calculates the ESC AR and points to the Appendix C procedures for the flaw tolerance evaluation as described in later paragraphs of this letter.

The postulated initial flaw shape (or aspect ratio) and depth requirements are described in Appendix L-3200. For axial and circumferential initial postulated flaws in stainless steel austenitic piping, the aspect ratios (AR, l/a = flaw length/flaw depth) are determined from Table L-3210-2 of [1].

The following total membrane-to-gradient cyclic stress ratio equation is required to use Table L-3210-2:

$$\frac{\Delta\sigma_m}{\Delta\sigma_g} = \sum_i^m \frac{\Omega_i}{\Omega_{total}} * \left(\frac{\Delta\sigma_m}{\Delta\sigma_g} \right)_i \quad \text{[Equation 1]}$$

where:

$$\Omega_i = (\Delta\sigma_m + \Delta\sigma_g)_i^n * N_i$$

$$\Omega_{total} = \sum_i \Omega_i$$

$\Delta\sigma_m$ = cyclic membrane stress for i^{th} load pair or transient loading condition, psi

$\Delta\sigma_g$ = cyclic linear and nonlinear gradient stress for i^{th} load pair or transient loading condition, psi

n = fatigue crack growth rate exponent = 2.25 per ASME Code Case N-809 [4]

N_i = number of cycles for i^{th} load pair or transient loading condition

The transient through-wall stress profiles for normal, upset, emergency, faulted and test conditions are required to determine the Appendix L ESC aspect ratio per Appendix L-3110 in [1]. The Appendix L ESC aspect ratio evaluation accounts for the linear membrane portions of the stress distributions, as well as the non-membrane gradient stress portions. Both axial and circumferential flaws were calculated for the applicable ESC AR for the Point Beach spray nozzle locations shown in Figure 1-1 considering bounding nozzle loads and transient stresses.

2.2 Maximum Allowable End-of-Evaluation Period Flaw Size

The ASME Section XI Appendix L evaluation procedures for austenitic stainless steel piping allow the use of Appendix C procedures and acceptance criteria for the calculation of the maximum allowable end-of-evaluation period flaw sizes. The maximum allowable end-of-evaluation period flaw size was determined based on ASME Section XI Code [1]. Rapid, non-ductile failure is possible for ferritic materials at low temperatures but is not applicable to stainless steel materials. The Point Beach pressurizer spray nozzle safe ends and welds are fabricated from stainless steel material. For stainless steel materials, the higher ductility leads to plastic collapse being the dominant failure mechanism. Thus, a conservative combination of the limit load expressions and the elastic-plastic fracture mechanics expressions (for stainless steel flux

welds) in ASME Section XI Appendix C-5000 and C-6000 were used to calculate the maximum end-of-evaluation flow size for an axial flaw and circumferential flaw with the aspect ratio determined via the Section XI Appendix L methodology in Section 2.1.

The maximum allowable end-of-evaluation period flow sizes are based on the applicable plant specific pipe loadings and geometry, and ASME Code material properties (see further discussion in Section 3.2 of this report). Loadings under normal, upset, emergency and faulted conditions are considered in conjunction with the applicable structural factors for the corresponding service conditions required in the ASME Section XI Code. For circumferential flaws, axial stress due to pressure, deadweight, thermal expansion, seismic and pipe break loads are considered in the evaluation. Hoop stress resulting from pressure loading is used for the axial flaws. The geometry and operating parameters, material properties, and piping loads that are used in the calculation of the maximum end-of-evaluation period flow sizes are bounding loads ([13] and [14]) for Point Beach Units 1 and 2.

Axial Flaws

For axial flaws the allowable flaw depth is given by the equations in ASME Section XI Appendix C-5420:

$$\sigma_{h, \text{allow}} = \frac{\sigma_f}{SF_m} \left[\frac{1 - \frac{a}{t}}{1 - \left(\frac{a}{t}\right)/M_2} \right]$$

where:

$$\sigma_f = \text{Flow stress} = \frac{S_y + S_u}{2} \text{ (Average of yield and ultimate strengths)}$$

$$M_2 = [1 + (1.61/4R_m t) \ell^2]^{1/2}$$

$$\ell = \text{Total flaw length}$$

$$a = \text{Flaw depth}$$

$$R_m = \text{Mean radius}$$

$$t = \text{Wall thickness}$$

$$\sigma_{h, \text{allow}} = \text{Allowable nominal hoop stress}$$

$$SF_m = \text{Structural Factor for membrane stress}$$

(for Service Levels A, B, C, and D, $SF_m = 2.7, 2.4, 1.8,$ and 1.3 respectively)

The limits of applicability of the previously mentioned equation are $a/t < 0.75$ and $\ell < \ell_{\text{allow}}$, where ℓ_{allow} is the allowable axial flaw length which is given by the condition:

$$\ell_{\text{allow}} = 1.58 \sqrt{R_m t \left[\left(\frac{\sigma_f}{\sigma_h} \right)^2 - 1 \right]}$$

The actual nominal hoop stress is calculated by the following equation:

$$\sigma_h = \frac{pR_m}{t}$$

where:

p = Internal pressure
 σ_h = Applied hoop stress

Circumferential Flaws

For circumferential flaws not penetrating the compressive side of the pipe such as $(\theta+\beta)<\pi$, the relation between the applied loads and flaw depth at incipient collapse is given by equations in ASME Section XI Appendix C-5320:

$$\sigma_b^c = \frac{2\sigma_f}{\pi} \left[2 \sin \beta - \frac{a}{t} \sin \theta \right] \quad \text{[Equation 2]}$$

$$\beta = \frac{1}{2} \left(\pi - \frac{a}{t} \theta - \pi \frac{\sigma_m}{\sigma_f} \right)$$

For longer circumferential flaws which penetrate into the compressive side (see Figure 2-1) of the pipe such as $(\theta+\beta) > \pi$, the relation between the applied loads and flaw depth at incipient collapse is given by:

$$\sigma_b^c = \frac{2\sigma_f}{\pi} \left(2 - \frac{a}{t} \right) \sin \beta \quad \text{[Equation 3]}$$

$$\beta = \frac{\pi}{2 - \frac{a}{t}} \left(1 - \frac{a}{t} - \frac{\sigma_m}{\sigma_f} \right)$$

where:

σ_b^c = Bending stress at incipient plastic collapse
 θ = One-half of the final flaw angle
 β = Angle to neutral axis of flawed pipe
 a/t = Flaw depth to wall thickness ratio
 σ_f = Flow stress = $\frac{S_y + S_u}{2}$ (Average of Yield and Ultimate Strengths)
 σ_m = Applied membrane stress

Per Section XI Appendix C-6321, the allowable bending stress, S_c , which is used to calculate the maximum allowable end-of-evaluation period flaw sizes, is as follows:

$$S_c = \frac{1}{(SF_b)} \left[\frac{\sigma_b^c}{Z} - \sigma_e \right] - \sigma_m \left[1 - \frac{1}{Z(SF_m)} \right] \quad \text{[Equation 4]}$$

where:

S_c	=	Allowable bending stress
σ_m	=	Applied membrane stress
σ_e	=	Thermal expansion stress
σ_b^c	=	Bending stress at incipient plastic collapse per [Equation 2 or 3]
SF_m	=	Structural Factor for membrane stress (for Service Levels A, B, C, and D, $SF_m = 2.7, 2.4, 1.8,$ and 1.3 respectively)
SF_b	=	Structural Factor for bending stress (for Service Levels A, B, C, and D, $SF_b = 2.3, 2.0, 1.6,$ and 1.4 respectively)
Z	=	Z factor based on weld process to take into account Z factor based on NPS
	=	$1.30 [1 + 0.010 (NPS-4)]$
NPS	=	Nominal pipe size

The maximum end-of-evaluation period allowable flaw depth can then be determined by the a/t value which makes the allowable bending stress (S_c) in [Equation 4] equal to the applied bending stress (σ_b).

The upper bounds of these equations for axial and circumferential flaws, based on ASME Section XI Appendix C, are for a flaw depth of 75% of the wall thickness (e.g., $a/t < 0.75$).

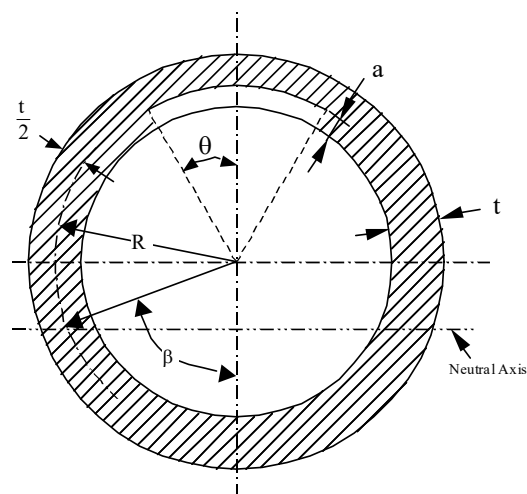


Figure 2-1 Cross Section of Flawed Pipe

2.3 Fatigue Crack Growth Analysis

A fatigue crack growth (FCG) analysis determines the allowable operating period of a postulated flaw. Fatigue crack growth is the only credible mechanism for crack growth, since both the weld and the base metals of the spray nozzles are resistant to Primary Water Stress Corrosion Cracking (PWSCC). The fatigue crack growth analysis procedure involves postulating an initial flaw at the applicable analysis location and predicting the growth based on the applicable transient stresses. The input required for a fatigue crack growth analysis is essentially the information necessary to calculate the range of crack tip stress intensity factor, which depends on the crack size and shape, geometry of the structural component where the crack is postulated, and the applied cyclic stresses. A plant specific transient stress finite element analysis (FEA) model was developed and used to calculate the stresses due to thermal and mechanical stresses (pressure and piping loads). The resulting transient stress output files from the FEA model were then used as input to the Appendix L fracture analyses. Provided below is the methodology used to calculate the stress intensity factor for the axial and circumferential surface flaws.

2.3.1 Stress Intensity Factors for Surface Flaws

The FCG analysis involves calculating growth for postulated axial and circumferential flaws on the inside surface. The postulated flaws are subjected to cyclic loads due to the transients and welding residual stresses. The inputs required for the fatigue crack growth analysis is the range in stress intensity factor (SIF, ΔK) and the R ratio (K_{Imin}/K_{Imax}).

The SIF expressions for surface flaws utilize a representation of the actual stress profile rather than a linearization between data points. The stress distribution profiles are represented by a 4th order polynomial:

$$\sigma(x/t) = \sigma_0 + \sigma_1 (x/t) + \sigma_2 (x/t)^2 + \sigma_3 (x/t)^3 + \sigma_4 (x/t)^4$$

where:

$\sigma_0, \sigma_1, \sigma_2, \sigma_3,$ and σ_4 are the stress profile curve fitting coefficients,

x is the distance from the inside wall surface,

t is the wall thickness, and

σ is the stress perpendicular to the plane of the crack.

The FCG analysis uses the stress intensity factor expressions from API-579 2016 Edition [5]. The SIF expression considered were for inside surface semi-elliptical flaws. The flaw shapes, or aspect ratios were calculated from the Appendix L methodology described in Section 2.1.

Stress intensity factors can be expressed in the general form as follows:

$$K_I = \left(\frac{\pi a}{Q} \right)^{0.5} \sum_{j=0}^4 G_j(a/c, a/t, t/R_i, \phi) \sigma_j$$

where:

- a: crack depth
- c: half of the crack length along the surface
- t: wall thickness
- R_i : inside radius of the component
- σ_j : coefficients σ_j ($\sigma_0, \sigma_1, \sigma_2, \sigma_3,$ and σ_4) for the stress profile 4th order fit
- ϕ : angular position of a point of the crack front
- G_j: boundary correction factors provided in API-579 [5]
- Q: shape factor of an elliptical crack. Q is approximated by:

$$Q = 1 + 1.464(a/c)^{1.65} \text{ for } a/c \leq 1, \text{ or } Q = 1 + 1.464(c/a)^{1.65} \text{ for } a/c > 1$$

The through-wall stress distributions used in the crack tip stress intensity factor calculation were determined by combining the transient stresses (mechanical loads included) with the welding residual stresses.

The corresponding crack tip stress intensity factors (K_I) is then calculated for each transient based on its through-wall stress profiles following the methodology in API-579 [5]. The resulting $K_{I_{max}}$, $K_{I_{min}}$, and $\Delta K_I = K_{I_{max}} - K_{I_{min}}$, is used to calculate the fatigue crack growth.

2.3.2 Fatigue Crack Growth Rate

The fatigue crack growth evaluation procedure involves postulating an initial flaw at specific regions and predicting the growth of that flaw due to an imposed series of loading transients. The input required for a fatigue crack growth analysis is the information necessary to calculate the parameter ΔK_I which depends on the crack and structure geometry, and the range of applied stresses in the area where the crack exists.

Once R (load ratio = $K_{I_{min}}/K_{I_{max}}$) and ΔK_I are calculated, the crack growth due to any given stress cycle can be calculated for each transient. This increment of crack growth is then added to the original crack size, and the analysis proceeds to the next transient.

Fatigue crack growth for each transient for a given time interval and number of cycles (N) can be computed using the following equation:

$$\text{New Crack Depth} = \text{Initial Crack Depth} + \text{Incremental Crack Depth}$$

with the incremental crack depth, Δa , given by:

$$\Delta a = C (\Delta K_I)^n N$$

The procedure is continued in this manner until all the transients known to occur in the period of evaluation have been analyzed. The above equation is the most fundamental form of fatigue crack growth law, where C and n are material constants.

Appendix L-3331 states that the procedures in Appendix C-3200 may be used for the fatigue crack growth evaluation. Currently, ASME Section XI Appendix C-3200 does not provide fatigue crack growth rates for austenitic stainless steel in water. However, fatigue crack growth rates for austenitic stainless steel in water are provided in the ASME approved Code Case N-809 [4] (the technical basis for Code Case N-809 is provided in PVP2015-45884 [6]).

The reference crack growth law used for the stainless steel in a pressurized water reactor (PWR) environment is based on ASME Code Case N-809 [4]. The following fatigue crack growth equation is based on Type 304 and Type 316 has the following generic form:

$$\frac{da}{dN} = C_o (\Delta K_I)^n$$

where:

$\frac{da}{dN}$	=	Fatigue crack growth rate, inches per cycle
C_o	=	Scaling parameter that accounts for the effect of loading rate and environment on crack growth rate = $C * S_T * S_R * S_{ENV}$, (inch/cycle) / (ksi $\sqrt{\text{in}}$) ^{2.25}
ΔK_I	=	Stress intensity factor range, ksi $\sqrt{\text{in}}$
C	=	Nominal fatigue crack growth rate constant, (inch/cycle) (ksi $\sqrt{\text{in}}$) ^{-2.25} = 4.43×10^{-7} for $\Delta K_I \geq \Delta K_{th}$ = 0 for $\Delta K_I < \Delta K_{th}$ Where ΔK_{th} = Threshold on ΔK_I $\Delta K_{th} = 1.1$ ksi $\sqrt{\text{in}}$
S_T	=	Parameter defining the effect of temperature on fatigue crack growth rate, dimensionless = $e^{(-2516/T_K)}$ for $300^\circ\text{F} \leq \text{Temperature} \leq 650^\circ\text{F}$ = $3.39 \times 10^5 * e^{((-2516/T_K) - 0.0301 * T_K)}$ for $70^\circ\text{F} \leq \text{Temperature} < 300^\circ\text{F}$ T_K = metal temperature in Kelvin = $((T-32) / 1.8) + 273.15$ T = metal temperature in Fahrenheit
S_R	=	Parameter defining the effect of R ratio on fatigue crack growth rate, dimensionless = 1.0 for $R < 0$ = $1 + e^{(8.02 * (R - 0.748))}$ for $0 \leq R < 1.0$
R	=	K_{Imin} / K_{Imax}
S_{ENV}	=	Parameter defining the environmental effects on fatigue crack growth rate, dimensionless = $T_R^{0.3}$, T_R is the loading rise time in seconds described below
n	=	Slope of the log (da/dN) versus log (ΔK) curve, = 2.25

If the rise time, T_R , is less than 1 second then $T_R = 1.0$ second. Also, per Code Case N-809, the loading rise time is the period of time in seconds for which the stress is increasing during a stress cycle. The loading rise time, which excludes hold times and time periods for which the stress is decreasing during the cycle, includes the time periods from minimum stress to steady state and from steady state to maximum stress. Hold time includes periods in which the change in stress does not exceed 1,000 psi/hr.

Therefore, to summarize the general methodology, the guidance of ASME Section XI Appendix L was used to determine the equivalent single crack aspect ratio for postulated inside axial and circumferential flaws. The ESC AR is then used to calculate the maximum allowable end-of-evaluation period flaw size (see Section 2.1) based on ASME Section XI Appendix C guidelines. The maximum allowable operating period is determined by calculating the amount of time needed for an initial flaw size, which is based on the acceptance standard table in IWB-3410, to reach the maximum allowable end-of-evaluation period flaw size (see Section 2.2) based on the fatigue crack growth mechanics per ASME Section XI Code Case N-809. If the calculated allowable operating period is equal to or greater than 10 years, the successive sampling basis inspection schedule for the piping nozzles to pipe welds shall be equal to the examination interval listed in the Point Beach ASME Section XI schedule of Inservice Inspection program of the component, which is typically every 10 years. Thus, the goal of the flaw tolerance evaluation is to demonstrate that only one inspection needs to be performed every 10 years for the pressurizer spray nozzle safe end region.

3.0 Analysis Inputs

The following sections describe that analysis inputs used for the Point Beach spray nozzle Appendix L evaluations. The inputs include geometry, material properties, piping loads, and transient stresses and applicable cycles.

3.1 Spray Nozzle and Pipe Geometry

The spray nozzle geometry consists of the pressurizer nozzle, safe end, attached piping, and welds. The original pressurizer stress reports are in [7] and [8] for Point Beach Units 1 and 2, and the applicable drawing are per [8]. A finite element analysis (FEA) model was used to generate the transient stresses at the safe end and safe-end-to-weld location. The FEA model and the analysis section numbers (ASN) used in the analyses are shown in Figure 1-1. Table 3.1-1 lists the applicable dimensions for the analyses section number (ASN) locations of the FEA model and fracture analyses described in Section 2.

Table 3.1-1 Point Beach Units 1 and 2 Spray Nozzle and Piping Geometry

a,c,e



3.2 Material Properties

The spray nozzle safe-ends are constructed from SA-182 Grade F316 ([7] and [8]) and the piping is A 376 TP 316 ([9], [10] and [11]). For Point Beach Unit 1 the CMTRs for the safe-end and piping [12] are available and are used to establish plant specific yield and ultimate strength values for evaluating the end-of-evaluation-period flow size because the nozzle loads are notably higher than those for Unit 2. The allowable end of evaluation period flow size calculations described in Section 2.2 considers the limiting material properties and load combinations for both units to provide bounding results.

3.3 Piping Loads

The applicable piping loads for the spray nozzle safe-end are given in [13] for Unit 1 and [14] for Unit 2. The most limiting loads were considered in the analyses. Note that the load sets in [13] and [14] do not include loss of coolant accident (LOCA) or pipe break loads and were therefore not included in the ASME Section XI Appendix L analysis. Spray nozzle loads used to calculate the maximum allowable end-of-evaluation-period flow size are summarized in Table 3.3-1 and Table 3.3-2 for Units 1 and 2 respectively.

Table 3.3-1 Point Beach Unit 1 Spray Nozzle Piping Loads

--

a,c,e

--

Table 3.3-2 Point Beach Unit 2 Spray Nozzle Piping Loads

--

a,c,e

--

3.4 Transient Stresses

The applicable design transients for Point Beach Units 1 and 2 are documented in [15] and are applicable for 80 years. Transient stresses for the pressurizer spray nozzle were developed specifically for the fracture evaluation based on the transient definitions from [15]. For the ASME Section XI Appendix L evaluation, projected transient cycles were provided by NextEra [16], based on past operating history and cycle counting. Since the number of transient cycles have a significant influence on the calculated Appendix L flow aspect ratios and fatigue crack growth, it is important to consider more realistic transient cycles based

on plant operating procedures and data. Table 3.4-1 list the transient cycles provided in [16] which includes actual cycles counted during operation, projected total cycles for 80 years of operation, design cycles and suggested allowable cycles.

Further refinement of transient definitions and cycles were performed based on review of plant operating procedures and data. Table 3.4-2 provides the final transient list used for the fracture evaluation. [

^{a,c,e} Note that Appendix A provides recommended revisions to the Point Beach Units 1 and 2 Fatigue Monitoring Program to address the transients and cycles considered in this evaluation.

Table 3.4-1 Point Beach Units 1 and 2 Transient Cycles Projections for 80 years Operation [16]

Row	Transient	Current Cycles as of Year End 2019		Projection Upper Bound	Design Allowable Cycles ¹	Suggested Allowable Cycles ²
		Unit 1	Unit 2			
1	10% Step Load Decrease	25	30	44	2000	100
2	10% Step Load Increase	0	1	2	2000	20
3	50% Step Load Decrease	46	20	66	200	100
4	Accumulator Safety Injection	4	1	7	89	8
5	Auxiliary Spray Actuation	0	0	0	10	2
6	HPSI Injection	2	0	4	89	4
7	Inadvertent Accumulator Blowdown	0	0	0	4	2
8	Inadvertent RCS Depressurization	0	0	0	20	2
9	Loss of Charging Flow	16	17	34	60	50
10	Loss of Letdown Flow	20	17	46	200	75
11	PZR Cooldown	78	61	115	200	120
12	PZR Heatup	79	62	116	200	120
13	Primary Side Hydrostatic Test	1	2	3	5	3
14	Primary Side Leak Test	36	38	57	94	60
15	Primary to Secondary Leak Test	2	9	14	27	15
16	RCS Cooldown	79	62	118	200	120
17	RCS Heatup	80	63	119	200	120
18	Reactor Pressure Vessel Safety Injection	0	0	0	89	2
19	Reactor Trip	68	52	107	300	120
20	Refueling	49	46	77	80	80
21	Relief Valve Actuation	1	3	7	100	8
22	Secondary to Primary Leak Test	38	33	57	128	60
23	Trip due to Loss of Reactor Coolant Pump	1	2	4	100	4
24	Unit Loading 5%/min	1691	1806	2478	11600	8000
25	Unit Unloading 5%/min	1544	1670	2295	11600	8000
26	Feedwater Cycling at Hot Standby	NC	NC	N/A	2000	Not Provided
27	Boron Concentration Equalization	NC	NC	N/A	23360	Not Provided
28	Loss of Load (Trip)	NC	NC	N/A	80	80
29	Loss of Power (Trip)	NC	NC	N/A	40	40
30	Loss of Flow (Trip)	NC	NC	N/A	80	80
31	Turbine Roll Test	NC	NC	N/A	10	10
32	Control Rod Drop	NC	NC	N/A	Not Provided	80
33	Excessive Feedwater Flow	NC	NC	N/A	Not Provided	30
34	Operational Basis Earthquake (OBE)	NC	NC	N/A	Not Provided	10

Notes:

1. Blue font in the "Design Allowable Cycles" column indicates a value from the final safety analysis report.
2. The "Suggested Allowable Cycles" column provides values of cycles that would form a reasonable basis for a maximum set of transients for analysis. For Rows 24 and 25 (i.e. Unit Loading and Unloading), the

plant does not load follow based on the current cycles to date. Therefore, the projected upper bound cycles are used with a 5% increase and the value rounded up to 2700 cycles.

3. NC = not counted via monitoring. For transients not counted, Westinghouse has proceeded with the number of cycles for 80 years not exceeding the 40-year design allowable cycles.
4. N/A = not applicable. There is no basis for computing the upper bound.

Table 3.4-2 Point Beach Units 1 and 2 Transient Cycles for Appendix L Fracture Analysis

a,c,e

No.	Transient	Service Condition	Analyzed Cycles ¹
1	Plant HU/CD Case 1 ²	Normal	
2	Plant HU/CD Case 2 ²	Normal	
3	Plant HU/CD Case 3 ²	Normal	
4	Plant HU/CD Case 4 ²	Normal	
5	Plant HU/CD Case 5 ²	Normal	
6	Plant HU/CD Case 6 ²	Normal	
7	Plant HU/CD Case 7 ²	Normal	
8	Plant HU/CD Case 8 ²	Normal	
9	Zero Stress State ⁽²⁾	Normal	
10	Plant Loading at 5% of Full Power per Minute	Normal	See Note 3
11	Plant Unloading at 5% of Full Power per Minute	Normal	See Note 3
12	Small Step Load Increase of 10% of Full Power	Normal	
13	Small Step Load Decrease of 10% of Full Power	Normal	
14	Step Load Decrease of 50% of Full Power	Normal	
15	Steady State Fluctuations – Initial	Normal	
16	Steady State Fluctuations – Random	Normal	
17	Boron Concentration Equilibrium	Normal	See Note 3
18	Feedwater Cycling at Hot Standby	Normal	
19	Turbine Roll Test	Normal	
20	Loss of Load	Upset	
21	Loss of Power	Upset	
22	Loss of Flow in One Loop	Upset	
23	Reactor Trip and Attendant Temperature Transients	Upset	
24	Inadvertent Auxiliary Spray	Upset	
25	OBE	Upset	
26	Reactor Coolant Pipe Break	Faulted	
27	Steam Line Break	Faulted	
28	SSE	Faulted	
29	Primary Side Hydrostatic Test (3107 psig)	Test	
30	Primary Side Hydrostatic Test (2485 psig)	Test	
31	Primary Side Leak Test (2250 psig)	Test	

Notes:

1. The analyzed cycles were used for the Appendix L analyses documented in this letter.
2. [

] a,c,e

3. The Plant Loading at 5% of Full Power per Minute, Plant Unloading at 5% of Full Power per Minute, and Boron Concentration Equilibrium transients were consolidated into a single representative pressurizer (PZR) spray transient (Controlling PZR Spray Transient Group) with 1800 cycles based on

review of plant data. The Controlling PZR Spray Transient Group was analyzed in place of the Boron Concentration Equilibrium transient to generate transient stress input files (i.e., frac files).

Table 3.4-3 Plant Heatup and Cooldown Transient Temperature Definitions. a,c,e



3.5 Welding Residual Stresses

Residual stresses due to the weld fabrication process are also considered in the fatigue crack growth analysis. The residual stress values were obtained from the technical basis document for austenitic steel piping flaw evaluation [17] and used in the evaluation of the heat affected zones of the spray nozzle safe end weld. The through-wall axial and circumferential residual stress profiles used in the fatigue crack growth analysis are shown in Figure 3-1.

Wall Thickness	Through-Wall Residual Stress ¹	
	Axial	Circumferential ²
< 1 inch		
≥ 1 inch	See Note 3	

Notes:

1. $S = 30$ ksi
2. Considerable variation with weld heat input
3. $\sigma = \sigma_i [1.0 - 6.91(a/t) + 8.69(a/t)^2 - 0.48(a/t)^3 - 2.03(a/t)^4]$
 σ_i = stress at inner surface ($a = 0$)
 a = distance through pipe weld thickness

Figure 3-1 Recommended Axial and Circumferential Residual Stress Distributions for Austenitic Stainless Steel Pipe Welds [17]

4.0 Analysis Results

The following sections describe the ASME Section XI Appendix L analyses performed for the Point Beach Units 1 and 2 pressurizer spray nozzles. [

] ^{a,c,e} Results for both
ASN 2 and ASN 3 are documented at each stage of the analyses described in Section 2.

4.1 ASME Section XI Appendix L Evaluation Results

The equivalent single crack (ESC) aspect ratio (AR) was determined for the spray nozzle based on ASME Section XI Appendix L methodology described in Section 2.1. The Appendix L evaluation is based on the Service Level A, B, Test, and D time history through-wall stress profiles at ASNs 2 and 3 and was calculated accounting for linear membrane stress and non-linear gradient stress. The maximum calculated aspect ratios are reported in Table 4.1-1 for ASN 2 and Table 4.1-2 for ASN 3 and are used to calculate the allowable end of evaluation period flow sizes and fatigue crack growth.

Table 4.1-1 Point Beach Unit 1 and 2¹ Appendix L Aspect Ratio for ASN 2

Axial ESC AR ²	Circumferential ESC AR ²
69.1	50.0

Notes:

- [
- Aspect ratio (AR) is defined as flaw length/depth (l/a).] ^{a,c,e}

Table 4.1-2 Point Beach Unit 1 and 2¹ Appendix L Aspect Ratio for ASN 3

Axial Flaw ESC AR	Circumferential ESC AR ³
42.0	42.6

Notes:

- [
- Aspect ratio (AR) is defined as flaw length/depth (l/a).] ^{a,c,e}

4.2 Maximum Allowable End-of-Evaluation Period Flow Sizes

The calculation of the maximum allowable end-of-evaluation (EOE) period flow sizes for the spray nozzle is based the procedures described in Section 2.2. The stainless steel safe end and weld materials were analyzed using the guidance of IWB-3740 of ASME Section XI and subsequently Appendix C of the ASME Code. The maximum allowable EOE period flow size is determined for axial and circumferential flow configurations based on the Appendix L ESC maximum AR given in Table 4.1-1 and Table 4.1-2, and the piping loads in Section 3.3. The flow sizes are determined based on the limiting Service Level A, B, Test, or D conditions, as applicable. [

] ^{a,c,e} The maximum allowable end-of-evaluation period, and axial and circumferential flaw sizes (a/t, flaw depth over wall thickness) for the Point Beach Units 1 and 2 spray nozzles are shown in Table 4.2-1 for ASN 2 and ASN 3.

Table 4.2-1 Maximum Allowable End-of-Evaluation Flaw Bounding Sizes for Units 1 and 2

ASN	Flaw Configuration	Aspect Ratio	Maximum Allowable End-of-Evaluation Flaw Size (a/t)
2	Axial	69.1	0.173
2	Circumferential	50.0	0.170
3	Axial	42.0	0.383
3	Circumferential	42.6	0.530

4.3 Fatigue Crack Growth Analysis Results

The fatigue crack growth (FCG) evaluation was performed based on the methodology described in Section 2.3.2. The FCG is determined based on ASME Section XI Code Case N-809 [4] and API-579 [5] for SIF expressions. The initial flaw sizes for the ASN cuts are provided in Table 3.1-1 and are based on the acceptance standards in Table IWB-3410-1 (for aspect ratio of 6). The allowable operating period in years is based on when the postulated flaw reaches the maximum allowable end-of-evaluation period flaw size shown in Table 4.2-1.

The FCG analyses utilized piping stress, transient stresses and residual stresses. Transient stress files containing thermal, mechanical and pressure stresses were used to calculate crack growth for both axial and circumferential flaws. The through-wall residual stress profiles discussed in Section 3.5 were also included as applicable. [

] ^{a,c,e}

The FCG results reported herein were calculated based on the transient stresses and cycles listed in Table 3.4-2. As can be seen from the results in Table 4.3-1 the most limiting result is for the ASN 2 axial flaw, which demonstrates an allowable operating period for greater than 10 years. [

] ^{a,c,e}

Table 4.3-1 Fatigue Crack Growth Results for Point Beach Unit 1 and 2 Spray Nozzles

ASN	Flaw Configuration	Appendix L Calculated Aspect Ratio	Acceptable Standards Flaw Size Section XI Table IWB-3410-1 (a/t)	Final Flaw Size (a/t)	Maximum Allowable End-of-Evaluation Flaw Size (a/t)	Allowable Operating Period (Years)
ASN 2	Axial Flaw	69.1	0.1214	0.171	0.173	12
	Circumferential Flaw	50	0.1214	0.168	0.170	22
ASN 3	Axial Flaw	42.0	0.1361	0.379	0.383	53
	Circumferential Flaw	42.6	0.1361	0.249	0.530	80

5.0 References

- 1 ASME Code Section XI, "Rules for Inservice Inspection of Nuclear Power Plant Components," 2007 Edition, with 2008 Addenda (Code edition for the Appendix L Evaluation).
- 2 NUREG/CR-6260 (INEL-95/0045), "Application of NUREG/CR-5999 Interim Fatigue Curves to Selected Nuclear Power Plant Components," February 1995.
- 3 NUREG-2192, "Standard Review Plan for Review of Subsequent License Renewal Applications for Nuclear Power Plants," July 2017.
- 4 ASME Code Case N-809, "Reference Fatigue Crack Growth Rate Curves for Austenitic Stainless Steels in Pressurized Water Reactor Environments, Section XI, Division 1," ASME International, dated June 23, 2015.
- 5 American Petroleum Institute, API-579-1/ASME FFS-1, "Fitness-For-Service," June 2016.
- 6 ASME PVP2015-45884, "Technical Basis for Code Case N-809 on Reference Fatigue Crack Growth Curves for Austenitic Stainless Steels in Pressurized Water Reactor Environments," June 19-23, 2015, Boston Massachusetts, USA.
- 7 WNET-108(WEP), "Wisconsin Electric Power Pressurizer Stress Report (for Point Beach Unit1)," Westinghouse Electric Corporation, Tampa Division, Tampa, Florida, August 1969 (Westinghouse Proprietary Class 2).
- 8 Sec. 1 & 2(WIS), "Pressurizer Stress Report Sections 1 and 2, Wisconsin Electric Power Company, Point Beach Nuclear Plant Unit No. 2," Westinghouse Electric Corporation, Large Components Division, Tampa Division, Tampa, Florida, April 1975 (Westinghouse Proprietary Class 2).
- 9 Bechtel Drawing Job No. 10447, P-143, Rev. 6, "Spray Line from Primary Loop (Cold Leg) to Pressurizer 1-T1 RC-2501R-1 (Inside CTMT) Unit 1, June 1, 1992.
- 10 Bechtel Drawing Job No. 10447, P-243, Rev. 2, "Spray Line from Primary Loop (Cold Leg) to Pressurizer 2-T1 RC-2501R-1, October 3, 1981.
- 11 Westinghouse Piping Class Summary, DG-M02, Rev. 9, "Point Beach Nuclear Plant Design and Installation Guidelines," March 24, 2006 (Westinghouse Proprietary Class 2).
- 12 NextEra Letter PBNWEC-20-0046, Rev. 0, "Point Beach Nuclear Plant Units 1 and 2 Subsequent License Renewal Project Response to Westinghouse Letters WEC-NEE-PB-SLR-20-022, NEXT-20-85 and WEC-NEE-PB-SLR-20-033, NEXT-20-103," July 22, 2020.
- 13 Sargent & Lundy Stress Report, Accession N0. 100066, Rev. 0, "Addendum A to Piping Analysis Stress Report, Spray Line from Primary Loop (Cold Leg) to Pressurizer 1-T1, Unit 1," July 10, 1990.
- 14 Sargent & Lundy Stress Report, Accession N0. 200057, Rev. 0, "Piping Analysis Stress Report, Pressurizer Spray, Spray Line from Primary Loop (Cold Leg) to Pressurizer 2-T1, Unit 2," June 15, 1990.
 - a Sargent and Lundy Piping Analysis Stress Report, 200057, Revision 0, Addendum B, "Spray Line from Primary Loop (Cold Leg) to Pressurizer 2-T1," February 21, 1996.

- 15 Westinghouse Report, WCAP-16983-P, Revision 1, "Point Beach Units 1 and 2 Extended Power Uprate (EPU) Engineering Report," October 29, 2014 (Westinghouse Proprietary Class 2).
- 16 NextEra Energy Project Letter, PBNWEC-20-0020, Rev. 1, April 21, 2020.
- 17 "Evaluation of Flaws in Austenitic Steel Piping," Trans ASME, Journal of Pressure Vessel Technology, Vol. 108, Aug. 1986, pp. 352-366.

Appendix A: Transient Cycle Discussion and Recommended Aging Management Program Modifications

A.1 Purpose:

The Point Beach Units 1 and 2 Aging Management Program (AMP), described in LR-AMP-025-FATMON [2], TRM 4.5 [3], and NP 7.7.19 [4], was established to monitor loading cycles due to thermal and pressure transients and cumulative fatigue usage for selected component locations. To demonstrate compliance with the requirements in Title 10 of the Code of Federal Regulations (10 CFR) 54.21(c)(1), the AMP provides an analytical basis for confirming that the actual number of cycles does not exceed the number of cycles used in time-limited aging analyses (TLAAs), and that the cumulative fatigue usage will be maintained below the allowable limit during the period of extended operation. The pressurizer spray nozzle ASME Code Section XI Appendix L flaw tolerance evaluation described herein is a TLAAs based on the criteria in 10 CFR 54.3(a) and must therefore demonstrate compliance with 10 CFR 54.21(c)(1) for the period of extended operation. This appendix provides a summary of the transients analyzed in the pressurizer spray nozzle ASME Section XI Appendix L flaw tolerance evaluation and provides recommended modifications to the AMP based on this flaw tolerance evaluation. AMP modifications are required to ensure adequate tracking of the Controlling PZR Spray Transient Group based on the following:

- The Controlling PZR Spray Transient Group consists of the Plant Loading at 5% of Full Power per Minute, Plant Unloading at 5% of Full Power per Minute, and Boron Concentration Equilibrium (also referred to as Boron Concentration Equalization) transients, which were all combined under a bounding set of spray parameters.
- As shown in Table A-1 and PBNWEC-20-0020 [6], all other design spray transients were analyzed separately in the flaw tolerance evaluation, many of these transients are already tracked in the AMP, and the analyzed cycles for these transients are projected to remain bounding for an 80-year period of operation.
- The Controlling PZR Spray Transient Group contributed over []^{a,c,e} of the fatigue crack growth for the pressurizer spray nozzle. No other transient contributed more than []^{a,c,e} of the fatigue crack growth.

Based on the preceding bullets, the Controlling PZR Spray Transient Group is the only transient that needs to be monitored for the spray nozzle in support of the inservice inspection program.

A.2 Summary of Recommended Aging Management Program Modifications:

The recommended modifications to the AMP are summarized as follows and should be implemented prior to the period of extended operation:

1. The Controlling PZR Spray Transient Group should be added to the transient monitoring scope of the AMP. The criteria for recording a transient event and establishing associated cycle limits should be defined as follows:
 - Criteria for recording a transient event:

- The plant is in Mode 1 or 2.
- Either of the PZR main spray valves is opened from the fully closed position (assumes that the main spray valves are fully closed during normal steady state operation).
- Cycle limit for each 10-year inspection interval: 225 cycles

The cycle count to compare for the Controlling PZR Spray Transient Group should be defined to start from the last inservice inspection.

2. The PZR spray nozzle could be removed from the stress-based fatigue monitoring scope of the AMP since the PZR spray nozzle will be included in the inservice inspection program for the subsequent period of extended operation. PZR spray nozzle stress-based fatigue monitoring is not required to support this document.

A.3 Supporting Discussion:

Table A-1 summarizes the transients and cycles considered in the pressurizer spray nozzle ASME Section XI Appendix L flaw tolerance evaluation compared to the transients tracked by the current AMP. The design transients considered in the pressurizer analysis of record (AOR) in [5] formed the basis for the transients and cycles considered in the flaw tolerance evaluation. The following refinements to the design transients were made in order to reduce conservatism in the transients and cycles and demonstrate an acceptable inspection frequency in the flaw tolerance evaluation:

1. The transient cycles were reduced from the design cycles to the suggested allowable cycles provided in PBNWEC-20-0020 [6] for some transients.
2. Based on a review of PBNWEC-20-0046 [7], OP 1A [8], and OP 3C [9], PZR spray is initiated once and continuous spray flow is maintained throughout each HU/CD cycle. Therefore, the heatup and cooldown (HU/CD) design transients were modified to reflect actual plant operation. [

] ^{a,c,e}

3. The spray flow rates were reduced from the design flow rates to more realistic flow rates by relaxing conservative assumptions utilized in the development of the design transients.
4. Based on a review of the plant data provided in PBNWEC-20-0046 [7], Modes 1 and 2 normal operating PZR spray events were determined to occur at a different rate than was assumed in the development of the design transients. Therefore, several design spray transients postulated to occur regularly in Modes 1 and 2 operation (Plant Loading at 5% of Full Power per Minute, Plant Unloading at 5% of Full Power per Minute, and Boron Concentration Equilibrium) were consolidated into a single representative PZR spray transient (Controlling PZR Spray Transient Group). The number of Controlling PZR Spray Transient Group cycles analyzed was defined based on all of the normal operating PZR spray events noted to occur in Modes 1 and 2 from the plant data provided in PBNWEC-20-0046 [7]. Therefore, all of the spray events in the plant data were

conservatively assumed to be the result of either the Plant Loading at 5% of Full Power per Minute, Plant Unloading at 5% of Full Power per Minute, or Boron Concentration Equilibrium transients. All other design spray transients were analyzed separately in the flaw tolerance evaluation as shown in Table A-1.

As shown in Table A-1, the analyzed cycles are bounding for an 80-year period of operation based on the projected 80-year cycles provided in PBNWEC-20-0020 [6] for all transients except the Plant Loading and Unloading at 5% of Full Power per Minute transients. The projected 80-year cycles in Table A-1 for the Plant Loading and Unloading at 5% of Full Power per Minute transients exceed the 1800 analyzed cycles for the Controlling PZR Spray Transient Group, which is intended to represent the Plant Loading at 5% of Full Power per Minute, Plant Unloading at 5% of Full Power per Minute, and Boron Concentration Equilibrium transients. As stated in Item 2d of PBNWEC-20-0046 [7], the operators typically energize the PZR backup heaters to initiate spray for power ramps of 10% or more. The analyzed cycles for the Controlling PZR Spray Transient Group were determined based on a review of the PZR spray events from the plant data provided in PBNWEC-20-0046 [7]. The larger number of projected 80-year cycles for the Plant Loading and Unloading at 5% of Full Power per Minute transients could be attributed to the conservative classification of events in the fatigue monitoring program or higher cycle accumulation rates in early plant operation. The analyzed cycles for the Controlling PZR Spray Transient Group are judged to be appropriate since the analyzed cycles were determined based on recent plant data, and the cycles for this transient will be tracked to verify that the inspection frequencies from the flaw tolerance evaluation remain appropriate.

Per Section X.M1 of NUREG-2191 [10], the AMP should monitor and track the number of occurrences and severity of critical thermal and pressure transients for the selected components that are used in fatigue or flaw tolerance evaluations to verify that the inspection frequencies remain appropriate. The Controlling PZR Spray Transient Group was concluded to be the only transient that requires monitoring for the spray nozzle in support of the inservice inspection program to validate the flaw tolerance evaluation based on the following:

- The Controlling PZR Spray Transient Group contributed over []^{a,c,e} of the fatigue crack growth for the pressurizer spray nozzle. No other transient contributed more than []^{a,c,e} of the fatigue crack growth.
- The Controlling PZR Spray Transient Group consists of the Plant Loading at 5% of Full Power per Minute, Plant Unloading at 5% of Full Power per Minute, and Boron Concentration Equilibrium transients, which were all combined under a bounding set of spray parameters.
- As shown in Table A-1 and PBNWEC-20-0020 [6], all other design spray transients were analyzed separately in the flaw tolerance evaluation, many of these transients are already tracked in the AMP, and the analyzed cycles for these transients are projected to remain bounding for an 80-year period of operation.
- The recommended criteria for recording an event under the Controlling PZR Spray Transient Group may conservatively include other events that are analyzed separate from the Controlling PZR Spray Transient Group. Based on the review of historical plant data, this is not expected to result in exceeding the cycle limit, but if the cycle limit is approached in a particular inspection interval, certain events may be removed if they can be attributed to the following design transients:

- Small Step Load Increase of 10% of Full Power
- Small Step Load Decrease of 10% of Full Power
- Step Load Decrease of 50% of Full Power
- Loss of Load
- Inadvertent Auxiliary Spray

It is recommended that the AMP is updated prior to the period of extended operation to monitor the Controlling PZR Spray Transient Group to verify that the inspection frequencies remain appropriate. The criteria for recording a transient event should be defined as follows:

- The plant is in Mode 1 or 2.
- Either of the PZR main spray valves is opened from the fully closed position (assumes that the main spray valves are fully closed during normal steady state operation).

To verify that the inspection frequencies remain appropriate, cycles for the Controlling PZR Spray Transient Group need to be tracked over each inspection interval. Based on a review of the 12-year period of plant data from 1/1/2008 to 12/31/2019 provided in PBNWEC-20-0046 [7], 152 cycles were accumulated for Unit 1 (12.7 cycles per year) and 135 cycles were accumulated for Unit 2 (11.3 cycles per year). The cycles accumulated from plant startup to 12/31/2019 were approximated to be 1097 cycles for Unit 1 and 922 cycles for Unit 2. The flaw tolerance evaluation considered 1800 cycles for an 80-year plant life (22.5 cycles per year). The cycle limit for each 10-year inspection interval should be defined as follows based on the cycles considered in the flaw tolerance evaluation:

$$\text{Cycle Limit} = 1800 * \frac{10}{80} = 225 \text{ cycles}$$

The cycle count to compare for the Controlling PZR Spray Transient Group should be defined to start from the last inservice inspection.

In addition, the current AMP performs stress-based fatigue monitoring for various components, including the PZR spray nozzle, to ensure that the cumulative usage factor including environmental effects (CUF_{en}) remains below the allowable limit of 1.0. However, for the subsequent period of extended operation, stress-based fatigue monitoring is no longer required for the PZR spray nozzle since it will be included in the inservice inspection program. PZR spray nozzle stress-based fatigue monitoring is not required to support this document.

Table A-1: Transient Comparison between the Pressurizer Spray Nozzle ASME Appendix L Flaw Tolerance Evaluation and Fatigue Monitoring Program

Transient ⁽¹⁾	Service Condition	Design Cycles ⁽²⁾	Included in Fatigue Monitoring Program (Y/N) ⁽³⁾	Cycle Limit ⁽⁴⁾	Projection Upper Bound ⁽¹⁰⁾	Analyzed Cycles ⁽⁵⁾
Plant HU/CD Cases 1 to 8 and Zero Stress State {RCS Heatup, RCS Cooldown, Pressurizer Heatup, Pressurizer Cooldown}	Normal	200	Y	200	119 ⁽¹¹⁾	[] ^{a,c,e (7) (12)}
Plant Loading at 5% of Full Power per Minute	Normal	11,600 ⁽⁶⁾	Y	18,300 ⁽⁶⁾	2478	[] ^{a,c,e (9)}
Plant Unloading at 5% of Full Power per Minute	Normal	11,600 ⁽⁶⁾	Y	18,300 ⁽⁶⁾	2295	[] ^{a,c,e (9)}
Small Step Load Increase of 10% of Full Power {Step Load Increase (10%)}	Normal	2000	Y	2000	2	[] ^{a,c,e (7)}
Small Step Load Decrease of 10% of Full Power {Step Load Decrease (10%)}	Normal	2000	Y	2000	44	[] ^{a,c,e (7)}
Step Load Decrease of 50% of Full Power {Step Load Reduction (50%)}	Normal	200	Y	200	66	[] ^{a,c,e (7)}
Steady State Fluctuations – Initial	Normal	150,000	N	---	---	[] ^{a,c,e (8)}
Steady State Fluctuations – Random	Normal	5,000,000	N	---	---	[] ^{a,c,e (8)}
Boron Concentration Equilibrium	Normal	23,360	N	---	---	[] ^{a,c,e (9)}
Feedwater Cycling at Hot Standby	Normal	25,000 (Unit 1) 10,000 (Unit 2)	N	---	---	[] ^{a,c,e (8)}
Turbine Roll Test	Normal	10	N	---	---	[] ^{a,c,e (7)}
Loss of Load	Upset	80	N	---	---	[] ^{a,c,e (7)}
Loss of Power	Upset	40	N	---	---	[] ^{a,c,e (7)}
Loss of Flow in One Loop	Upset	80	N	---	---	[] ^{a,c,e (7)}
Reactor Trip and Attendant Temperature Transients {Reactor Trip}	Upset	400	Y	300	107	[] ^{a,c,e (7)}
Inadvertent Auxiliary Spray {Auxiliary Spray Actuation}	Upset	10	Y	10	0	[] ^{a,c,e (7)}
OBE	Upset	50	N	---	---	[] ^{a,c,e (7)}

Transient ⁽¹⁾	Service Condition	Design Cycles ⁽²⁾	Included in Fatigue Monitoring Program (Y/N) ⁽³⁾	Cycle Limit ⁽⁴⁾	Projection Upper Bound ⁽¹⁰⁾	Analyzed Cycles ⁽⁵⁾
Reactor Coolant Pipe Break	Faulted	1	N	---	---	[] ^{a,c,e (8)}
Steam Line Break	Faulted	1	N	---	---	[] ^{a,c,e (8)}
SSE	Faulted	1	N	---	---	[] ^{a,c,e (8)}
Primary Side Hydrostatic Test (3107 psig) {Primary Side Hydro}	Test	5	Y	5	3	[] ^{a,c,e (7)}
Primary Side Hydrostatic Test (2485 psig) {Primary Side Leak Test}	Test	94	Y	94	57	[] ^{a,c,e (7)}
Primary Side Leak Test (2250 psig) {Primary to Secondary Leak Test}	Test	27	Y	27	14	[] ^{a,c,e (7)}
Controlling PZR Spray Transient Group	Normal	---	N	---	---	[] ^{a,c,e (9)}

Notes:

- (1) The transient names in {} provide correlation to transients defined in Attachment C of NP 7.7.19 [4].
- (2) This column indicates the design cycles from the pressurizer analysis of record in [5].
- (3) This column indicates if the transient is tracked by the current fatigue monitoring program as defined by Attachment C of NP 7.7.19 [4].
- (4) This column contains the cycle limit for transients tracked by the current fatigue monitoring program as defined by Attachment C of NP 7.7.19 [4].
- (5) This column contains the cycles analyzed for the pressurizer spray nozzle ASME Appendix L flaw tolerance evaluation.
- (6) Per Attachment C of NP 7.7.19 [4], 18,300 cycles is applicable for all components except the pressurizer and reactor vessel internal baffle bolts, which are 11,600 and 2,485, respectively.
- (7) []^{a,c,e}
- (8) []^{a,c,e}
- (9) The Plant Loading at 5% of Full Power per Minute, Plant Unloading at 5% of Full Power per Minute, and Boron Concentration Equilibrium transients were consolidated into a single representative PZR spray transient (Controlling PZR Spray Transient Group) based on a review of plant data.
- (10) This column contains the 80-year projected cycles for transients tracked by the current fatigue monitoring program as defined by PBNWEC-20-0020 [6].
- (11) The projection upper bound cycles for the HU/CD transients were set to the maximum projection upper bound cycles between the RCS Heatup, RCS Cooldown, Pressurizer Heatup, and Pressurizer Cooldown transients from PBNWEC-20-0020 [6].

(12) [

]a,c,e

A.4 References:

1. NextEra Energy Letter, PBNWEC-20-0027, Revision 0, "Response to Westinghouse Letter WEC-NEE-PB-SLR-20-006, NET-20-36."
2. LR-AMP-025-FATMON, Revision 10, "Fatigue Monitoring Program Basis Document for License Renewal," February 15, 2013 (electronically attached to [1]).
3. TRM 4.5, "Cyclic or Transient Limit Monitoring Program," April 2018," (electronically attached to [1]).
4. NP 7.7.19, Revision 8, "Fatigue Monitoring Program," (electronically attached to [1]).
5. Westinghouse Report, WCAP-16983-P, Revision 1, "Point Beach Units 1 and 2 Extended Power Uprate (EPU) Engineering Report." (Westinghouse Proprietary Class 2).
6. NextEra Energy Letter, PBNWEC-20-0020, Revision 1, "Response to WEC-NEE-PB-SLR-20-002."
7. NextEra Energy Letter, PBNWEC-20-0046, Revision 0, "Response to Westinghouse Letters WEC-NEE-PB-SLR-20-022, NEXT-20-85 and WEC-NEE-PB-SLR-20-033, NEXT-20-103."
8. OP 1A, Revision 19, "Cold Shutdown to Hot Standby Unit 1," (electronically attached to [7]).
9. OP 3C, Revision 17, "Hot Standby to Cold Shutdown Unit 1," (electronically attached to [7]).
10. NRC Document, NUREG-2191, Volumes 1 and 2, "Generic Aging Lessons Learned for Subsequent License Renewal (GALL-SLR) Report," July 2017 (ADAMS Accession Nos. ML17187A031 and ML17187A204).

This page was added to the quality record by the PRIME system upon its validation and shall not be considered in the page numbering of this document.

Approval Information

Author Approval Marlette Stephen Oct-07-2020 10:15:26

Author Approval Matthews Eric J Oct-07-2020 10:20:58

Verifier Approval Joseph Thomas G Oct-07-2020 10:48:12

Verifier Approval Hall Gordon Z Oct-07-2020 11:15:52

Manager Approval Patterson Lynn Oct-07-2020 12:05:59

Files approved on Oct-07-2020

*** This record was final approved on 10/7/2020 12:05:59 PM. (This statement was added by the PRIME system upon its validation)

Point Beach Nuclear Plant Units 1 and 2
Dockets 50-266 and 50-301
NRC 2020-0032 Enclosure 4, Attachment 15

Enclosure 4

**Non-proprietary Reference Documents and
Redacted Versions of Proprietary Reference
Documents**

(Public Version)

Attachment 15

**Structural Integrity Associates Calculation PBCH-
06Q-301, Revision 1, "Containment Penetration
Fatigue Evaluation," November 11, 2003**

(9 Total Pages, including cover sheets)



**STRUCTURAL
INTEGRITY
Associates**

CALCULATION PACKAGE

FILE No.: PBCH-06Q-301

PROJECT No.: PBCH-06Q

PROJECT NAME: Point Beach Units 1 and 2 Containment Penetrations

CLIENT: Nuclear Management Company

TITLE: Containment Penetration Fatigue Evaluation

Document Revision	Affected Pages	Revision Description	Project Mgr. Approval Signature & Date	Preparer(s) & Checker(s) Signatures & Date
0	1-8	Original Issue	DAG 10/9/03	JDC 10/9/03 DAG 10/9/03
1	4, 6, 7, 8	To incorporate additional design input	<i>DAG</i> 11/11/03	DAG 11/11/03 <i>DAG</i> JDC 11/11/03 <i>JDC</i>

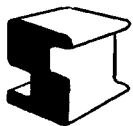
REC'D JAN 05 2004

Table of Contents

1.0	OBJECTIVE	3
2.0	TECHNICAL APPROACH.....	4
3.0	ANALYSIS.....	5
4.0	CONCLUSIONS AND DISCUSSIONS	7
5.0	REFERENCES	8

List of Figures

Figure 1:	Containment Penetration Detail	4
-----------	--------------------------------------	---



	Revision	0	1		
	Preparer/Date	JDC 10/9/03	DAG 11/11/03		
	Checker/Date	DAG 10/9/03	JDC 11/11/03		
File No. PBCH-06Q-301				Page 2 of 8	

1.0 OBJECTIVE

The containment liner, liner penetrations and liner steel components for Point Beach Units 1 and 2 comply with the ASME Code, Section III, 1965 Edition [1] for pressure boundary.

The liner plate (including penetraton extension sleeves) incorporated the design guidance of ASME Boiler and Pressure Vessel Code, Section III, 1965 edition, Nuclear Vessels, Article 4, Paragraphs; N-412(m), N-414.5, N-412(n), and N-415.1, Figures N-414, and N-415(A); and Table N-413 [1].

The containment penetrations conform to the applicable sections of ASA N6.2-1965, "Safety Standard for the Design, Fabrication, and Maintenance of Steel Containment Structures for Stationary Nuclear Power Reactors". In addition, penetration strains were limited per the ASME Boiler and Pressure Vessel Code, Section III, Nuclear Vessels, Article 4, 1965 edition [1].

The containment penetration head fittings were designed, fabricated, inspected, and tested in accordance with ASME Boiler and Pressure Vessel Code, Section III, Class B, 1968 edition and all addenda [4].

The Winter 1965 Addenda of ASME Code, Section III, Subsection B, N-1314(a), requires that the containment vessel satisfy the provisions of Subsection A, N-415.1, "Vessels Not Requiring Analysis for Cyclic Operation" in order that Subsection B rules be applicable. The purpose of this analysis is to demonstrate that the liner and penetrations satisfy the six provisions of N-415.1 through the period of extended operation.

The components relevant to this analysis are show in Figure 1 [8].



Revision	0	1		
Preparer/Date	JDC 10/9/03	DAG 11/11/03		
Checker/Date	DAG 10/9/03	JDC 11/11/03		
File No.	PBCH-06Q-301			Page 3 of 8

LOADS FROM CONCRETE (PRESTRESS,
DEAD LOAD, CREEP, SHRINKAGE,
EARTHQUAKE, PRESSURE AND TEMPERATURE)

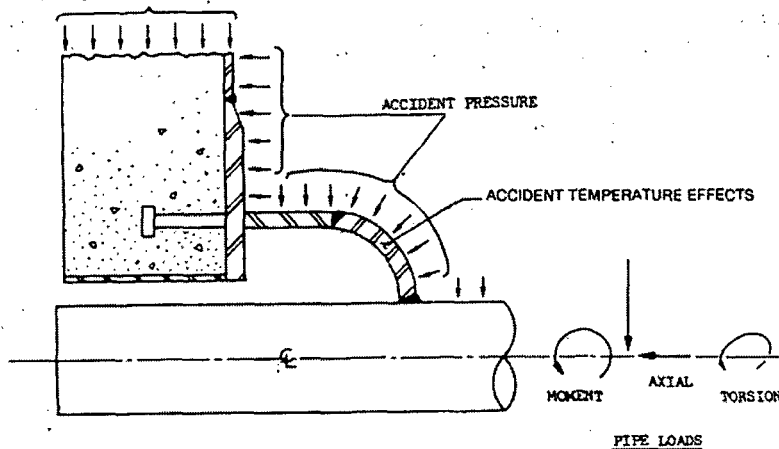


Figure 1: Containment Penetration Detail

2.0 TECHNICAL APPROACH

To determine whether or not the containment liner and penetrations satisfies the six provisions of Subsection A, N-415.1 [1], each provision will be analyzed individually. The six provisions are as follows.

1. Atmospheric to Operating Pressure Cycles
2. Normal Service Pressure Fluctuations
3. Temperature Difference – Startup and Shutdown
4. Temperature Difference – Normal Service
5. Temperature Difference – Dissimilar Materials
6. Mechanical Loads

The main steam line was analyzed since the temperature and loadings at this penetration are limiting, and thus it bounds all the other containment penetrations.

The temperatures used in this analysis are as follows [historical operating information]:

- Hot shutdown: 550°F
- Full Power: 520°F
- Containment at Startup: 90°F



Revision	0	1		
Preparer/Date	JDC 10/9/03	DAG 11/11/03		
Checker/Date	DAG 10/9/03	JDC 11/11/03		
File No.	PBCH-06Q-301			Page 4 of 8

3.0 ANALYSIS

Condition 1: Atmospheric to Operating Pressure Cycles

The specified number of times that the pressure will be cycled from atmospheric pressure to operating pressure and back to atmospheric pressure shall not exceed the number of cycles on the applicable fatigue curve corresponding to an S_a value of 3 times the S_m value for the material at operating temperature, where S_a is the allowable alternating stress amplitude, and S_m is the Design Stress Intensity.

For this analysis, 400 operating pressure cycles will be assumed for conservatism sake. The design stress intensity (S_m) at 100°F for each of the materials from which the components are constructed is listed below [2, Table 2A]. The material list was taken from Drawing 6118-M-82 [3].

- ASTM A-350 LFI $S_m = 20.0$ ksi
- ASTM A-516 $S_m = 20.0$ ksi

For an S_a equal to $3S_m$, or 60 ksi, the allowable number of cycles (N) is 2500 [4, Figure N-415(A)]. As 400 cycles is less than 2500 cycles, condition 1 is satisfied. The 1968 code edition was appropriate for use in this analysis because the head fittings were designed to this code and have the most limiting temperature profiles.

Condition 2: Normal Service Pressure Fluctuations

The specified full range of pressure fluctuations during normal operation shall not exceed the quantity $(1/3) \times \text{Design Pressure} \times (S_a/S_m)$, where S_a is the values obtained from the applicable design fatigue curve for the total specified number of significant pressure fluctuations, and S_m is the Design Stress Intensity for the material at operating temperature.

The assumed number of design cycles is 17354, which is comprised of the following transients: 14500 loading/unloading, 2200 load increase/decrease, 400 reactor trips, and 254 test [6, Table 4.1-8].

For: $S_a = 28000$ psi [5, Figure N-415(A)]
 $S_m = 20000$ psi
 Design pressure = 60 psig

Full Range of pressure fluctuations: $\frac{1}{3} \times 60 \times \frac{28000}{20000} = 28.0$ psi

Since normal pressure variation < 5 psi, condition 2 is satisfied.



Revision	0	1		
Preparer/Date	JDC 10/9/03	DAG 11/11/03		
Checker/Date	DAG 10/9/03	JDC 11/11/03		
File No.	PBCH-06Q-301			Page 5 of 8

Condition 3: Temperature Difference – Startup and Shutdown

The temperature difference in °F between any two adjacent points of the component during normal operation and during startup and shutdown, does not exceed the quantity $S_a/(2E\alpha)$, where S_a is the value obtained from the applicable design fatigue curve for the total specified number of significant startup/shutdown cycles, and E and α are the elastic modulus and coefficient of thermal expansion (instantaneous) at the mean value of temperatures at the two points.

Based on the temperature results in Reference [9], the maximum temperature difference between adjacent points in the main steam line is: $544^\circ\text{F} - 330^\circ\text{F} = 214^\circ\text{F}$. The average of these temperatures is 437°F . Assuming 400 full startup/shutdown cycles over a 60 year period, the allowable alternating stress amplitude S_a is 117 ksi [4, Figure N-415(A)]. For conservatism, the material ASTM A-516 was used because it has the highest E and α values of the carbon steel materials used in the components relevant to this analysis: $E = 27.65 \times 10^6$ [2, Table TM-1] and $\alpha = 7.465 \times 10^{-6}$ [2, Table TE-1] at the average temperature of 375°F .

$$\Delta T_{allowable} = \frac{S_a}{2E\alpha} = \frac{117000}{2(27.65 \times 10^6)(7.465 \times 10^{-6})} = 283.42^\circ\text{F}$$

The maximum temperature difference in the system of 214°F meets the maximum allowable temperature difference of 283.42°F . Condition 3, with a cycle count of 400, is met.

Condition 4: Temperature Difference – Normal Service

The temperature difference in °F between any two adjacent points of the component does not change during normal operation by more than the quantity $S_a/(2E\alpha)$, where S_a is the value obtained from the applicable design fatigue curve for the total specified number of significant temperature difference fluctuations.

The temperature difference, during normal operation, between adjacent points in the main steam line is as follows: $550^\circ\text{F} - 520^\circ\text{F} = 30^\circ\text{F}$. The average of these temperatures is 535°F . The number of significant temperature fluctuations is 17354. The allowable alternating stress amplitude $S_a = 28$ ksi for $N = 17354$. For ASTM A-516, $E = 26.89 \times 10^6$ [2, Table TM-1] and $\alpha = 8.217 \times 10^{-6}$ [2, Table TE-1] for and average temperature of 535°F .

$$\Delta T_{allowable} = \frac{S_a}{2E\alpha} = \frac{28000}{2(26.89 \times 10^6)(8.217 \times 10^{-6})} = 63.36^\circ\text{F}$$

Since $30^\circ\text{F} < 63.36^\circ\text{F}$, condition 4 is satisfied.



Revision	0	1		
Preparer/Date	JDC 10/9/03	DAG 11/11/03		
Checker/Date	DAG 10/9/03	JDC 11/11/03		
File No.	PBCH-06Q-301			Page 6 of 8

Condition 5: Temperature Difference – Dissimilar Materials

For components fabricated from materials of different moduli of elasticity and/or coefficients of thermal expansion, the total range of temperature fluctuations experienced by the component during normal operation shall not exceed the magnitude $S_a/[2(E_1\alpha_1-E_2\alpha_2)]$, there S_a is the value obtained from the applicable design fatigue curve for the total specified number of significant temperature fluctuations. A temperature fluctuation shall be considered significant if its total excursion exceeds the quantity $S/[2(E_1\alpha_1-E_2\alpha_2)]$, where S is the value obtained from the applicable design fatigue curve for 10^6 cycles.

For 10^6 cycles, the S_a is 12500 psi [4, Figure 415(A)]. Using the two carbon steel materials in this analysis, ASTM A-350 LFI, with the material properties $E = 27.98 \times 10^6$ and $\alpha = 7.156 \times 10^{-6}$, and ASTM A-516, with material properties $E = 27.98 \times 10^6$ and 7.156×10^{-6} at 320°F, ΔT is as follows.

$$\Delta T_{allowable} = \frac{S_a}{2(E_1 \alpha_1 - E_2 \alpha_2)}$$

Condition 5 is satisfied because the moduli of elasticity and the coefficients of thermal expansion are the same for both materials so there is not an issue with dissimilar materials.

Condition 6: Mechanical Loads

The specified full range of mechanical loads, excluding pressure, shall not result in load stresses whose range exceeds the S_a value obtained from the applicable design fatigue curve for the total specified number of significant load fluctuations.

The maximum number of cycles, due to the low end limit of the table, is 10. For $N = 10$, $S_a = 580$ ksi [4, Figure N-415(A)]. The maximum allowable stress intensity factor is $3S_m$, with an assumed stress concentration factor of 5 [4, N-415.3], resulting in a maximum allowable peak stress of $15S_m$. For the materials used in this analysis, the maximum S_m value is 20.0 ksi; therefore, the maximum allowable peak stress is $(15) \times (20.0 \text{ ksi}) = 300$ ksi. Condition 6 is satisfied because 300 ksi is less than 580 ksi.

4.0 CONCLUSIONS AND DISCUSSIONS

This analysis has demonstrated that the Point Beach Units 1 and 2 liner and penetrations meet all 6 conditions listed in ASME Code, Section III, 1968 Edition, N-415.1 and therefore is exempt from analysis for cyclic operation.



Revision	0	1		
Preparer/Date	JDC 10/9/03	DAG 11/11/03		
Checker/Date	DAG 10/9/03	JDC 11/11/03		
File No.	PBCH-06Q-301			Page 7 of 8

5.0 REFERENCES

1. ASME Code, Section III, 1965 Edition
2. AISC Manual of Steel Construction, 6th Edition.
3. Drawing No. 6118-M-82, Rev 10, "Piping and Mechanical Detail or Containment Piping Penetration Closure", SI File No. PBCH-06Q-201.
4. ASME Code Section III, 1968 Edition.
5. Report LR-AMP-025-FATMON, Fatigue Monitoring Program, License Renewal Aging Management Program Basis Document, Point Beach Nuclear Plant, Revision 0", June 14, 2002, SI File No. NMC-03Q-401.
6. "PBNP FSAR Reactor Coolant System – Design Basis", June 2001, SI File No. NMC-03Q-227.
7. Bechtel letter PBB-W-1240, "Point Beach Nuclear Plant Heat Transfer Calculations for Steam & Feedwater Penetrations", August 30, 1968, SI File No. PBCH-06Q-202
8. Email from Brad Fromm to David Gerber, October 8, 2003, SI File No. PBCH-06Q-103.
9. "Preventative Maintenance Inspection", November 11, 2003, SI File No. PBCH-06Q-206.



Revision	0	1		
Preparer/Date	JDC 10/9/03	DAG 11/11/03		
Checker/Date	DAG 10/9/03	JDC 11/11/03		
File No.	PBCH-06Q-301			Page 8 of 8

Enclosure 4

Non-proprietary Reference Documents and
Redacted Versions of Proprietary Reference
Documents

(Public Version)

Attachment 16

**Westinghouse WCAP-14439-NP, Revision 4,
“Technical Justification for Eliminating Large Primary
Loop Pipe Rupture as the Structural Design Basis for
the Point Beach Nuclear Plant Units 1 and 2 for the
Subsequent License Renewal Program (80 Years),”
June 2020**

(71 Total Pages, including cover sheets)

**Technical Justification for Eliminating
Large Primary Loop Pipe Rupture as
the Structural Design Basis for the
Point Beach Nuclear Plant Units 1 and 2
for the Subsequent License Renewal
Program (80 Years)**



**WCAP-14439-NP
Revision 4**

**Technical Justification for Eliminating Large Primary Loop
Pipe Rupture as the Structural Design Basis for the Point
Beach Nuclear Plant Units 1 and 2 for the Subsequent
License Renewal Program (80 Years)**

June 2020

Author: Momo Wiratmo*
Operating Plants Piping and Supports

Reviewer: Eric D. Johnson*
Reactor Vessel and Containment
Vessel Design and Analysis

Approved: Lynn A. Patterson, Manager*
Reactor Vessel and Containment
Vessel Design and Analysis

*Electronically approved records are authenticated in the electronic document management system.

Westinghouse Electric Company LLC
1000 Westinghouse Drive
Cranberry Township, PA 16066, USA

© 2020 Westinghouse Electric Company LLC
All Rights Reserved

REVISION INDEX

Revision	Date	Remarks
0	09/2003	Revision 0 of WCAP-14439-NP is the non-proprietary version of Revision 2 of WCAP-14439-P.
3	05/2020	Non-Proprietary Issue of WCAP-14439-P, Revision 3.
4	06/2020	<p>Non-Proprietary Issue of WCAP-14439-P, Revision 4.</p> <p>This revision is issued to incorporate customer review comments. The following bulleted items are provided to identify the scope of the changes due to the Subsequent License Renewal Program (80 Years) in Revisions 3 and 4:</p> <ul style="list-style-type: none"> • Additional background and summary of analysis locations, materials and evaluation types was added to the Executive summary section. • Added Section 2.4, reviewing the potential for piping degradation due to wall thinning, creep, and cleavage; as required by SRP 3.6.3. • Updated the operating temperature parameters considered in Section 3.0 and 4.0 to the latest applicable values. • Clarified the basis for limiting tensile properties and material interpolation process using ASME Code material properties (Section 4.2). • Updated the estimations of reduced fracture toughness values due to thermal aging effects; based on the methodology of NUREG/CR-4513 (Section 4.3). • Provided additional clarification related to the presence of dissimilar metal welds of alloy 82/182 material, associated susceptibility and mitigation of primary water stress corrosion effects, and confirmation that the base-metal material properties remain limiting for the Leak-Before-Break evaluations (Sections 5.1 and 7.3). • Recalculation of leakage flow sizes (Table 6-1) based on updated material properties and operating temperatures. • Documented supplemental elastic-plastic fracture mechanics evaluations used at analysis locations where the previous (Revision 2) linear-elastic fracture mechanics approach proved to be too conservative (Section 7.1 and Table 7-1). • Recalculation of critical flaw sizes (Table 7-2) based on updated material properties and operating temperatures. • Showed the previous transient set (Revision 2) remains bounding of the 80-year operating life for subsequent license renewal (Section 8.0). • Inclusion of fatigue crack growth evaluation description and results for

		<p>the dissimilar metal weld cross section, representative of the Unit 2 steam generator inlet and outlet nozzle welds (Section 8.0 and Table 8-2).</p> <ul style="list-style-type: none">• Updated report conclusions; addressing dissimilar metal welds, limiting material properties, and the evaluation of thermal aging effects (Section 10.0).
--	--	--

Note: Revisions 3 and 4 of WCAP-14439-NP have been issued to ensure consistent revision numbering between the proprietary and non-proprietary versions of the report. As such, Revisions 1 and 2 of WCAP-14439-NP were never generated and do not exist.

TABLE OF CONTENTS

1.0	Introduction.....	1-1
1.1	Purpose.....	1-1
1.2	Background Information.....	1-1
1.3	Scope and Objectives.....	1-2
1.4	References.....	1-3
2.0	Operation and Stability of the Reactor Coolant System	2-1
2.1	Stress Corrosion Cracking	2-1
2.2	Water Hammer	2-2
2.3	Low Cycle and High Cycle Fatigue.....	2-3
2.4	Wall Thinning, Creep, and Cleavage	2-3
2.5	References.....	2-3
3.0	Pipe Geometry and Loading	3-1
3.1	Introduction to Methodology	3-1
3.2	Calculation of Loads and Stresses	3-1
3.3	Loads for Leak Rate Evaluation	3-2
3.4	Load Combination for Crack Stability Analyses	3-3
3.5	References.....	3-3
4.0	Material Characterization.....	4-1
4.1	Primary Loop Pipe and Fittings Materials	4-1
4.2	Tensile Properties.....	4-1
4.3	Fracture Toughness Properties	4-2
4.4	References.....	4-5
5.0	Critical Location and Evaluation Criteria	5-1
5.1	Critical Locations.....	5-1
5.2	Evaluation Criteria.....	5-1
6.0	Leak Rate Predictions	6-1
6.1	Introduction.....	6-1
6.2	General Considerations.....	6-1
6.3	Calculation Method.....	6-1
6.4	Leak Rate Calculations	6-2
6.5	References.....	6-2
7.0	Fracture Mechanics Evaluation.....	7-1
7.1	Local Failure Mechanism	7-1
7.2	Global Failure Mechanism.....	7-3
7.3	Unit 2 SGIN and SGON Alloy 82/182 Welds.....	7-4
7.4	References.....	7-4

8.0	Fatigue Crack Growth Analysis	8-1
8.1	References.....	8-3
9.0	Assessment of Margins	9-1
10.0	Conclusions.....	10-1
	Appendix A: Limit Moment.....	A-1

LIST OF TABLES

Table ES-1	Summary of Analysis Locations, Materials, and Evaluation Types.....	ix
Table 3-1	Dimensions, Normal Loads and Stresses for Point Beach Units 1 and 2	3-4
Table 3-2	Dimensions, Faulted Loads and Stresses for Point Beach Units 1 and 2.....	3-5
Table 4-1	Measured Tensile Properties for Point Beach Unit 1 Primary Loop Pipes (A376-TP316).....	4-6
Table 4-2	Measured Tensile Properties for Point Beach Unit 2 Primary Loop Pipes (A376-TP316).....	4-7
Table 4-3	Measured Tensile Properties for Point Beach Unit 1 Primary Loop Elbows (A351-CF8M).....	4-8
Table 4-4	Measured Tensile Properties for Point Beach Unit 2 Primary Loop Elbows (A351-CF8M).....	4-9
Table 4-5	ASME Code Tensile Properties for Material A376-TP316 and A351-CF8M.....	4-10
Table 4-6	Tensile Properties for Point Beach Units 1 and 2 Materials at Operating Temperatures	4-11
Table 4-7	Point Beach Units 1 and 2 CF8M Chemical Composition	4-12
Table 4-8	Point Beach Units 1 and 2 CF8M Fracture Toughness and Tearing Modulus Properties	4-13
Table 4-9	Point Beach Units 1 and 2 CF8M Elbows with Lowest Fracture Toughness Properties	4-14
Table 4-10	J _{IC} Limiting Values NUREG/CR-4513 either per Rev. 1 or per Rev. 2.....	4-15
Table 5-1	Critical Analysis Locations for Point Beach Units 1 and 2 RCL Lines	5-3
Table 6-1	Flaw Sizes for Point Beach Units 1 and 2 Yielding a Leak Rate of 10 gpm for the RCL Lines.....	6-3
Table 7-1	Stability Results for Point Beach Units 1 and 2 Based on Elastic-Plastic J-Integral Evaluations	7-5
Table 7-2	Flaw Stability Results for Point Beach Units 1 and 2 Yielding a Leak Rate of 10 gpm for the RCL Lines Based on Limit Load.....	7-6
Table 8-1	Summary of Reactor Vessel Transients for FCG Evaluation	8-4
Table 8-2	Typical Fatigue Crack Growth at [] ^{a,c} (80 years)	8-4
Table 8-3	Point Beach Units 1 and 2 Transient Cycle Projections to 80 Years.....	8-5
Table 9-1	Leakage Flaw Sizes, Critical Flaw Sizes and Margins for Point Beach Units 1 and 2	9-2

LIST OF FIGURES

Figure 3-1	Hot Leg Coolant Pipe.....	3-6
Figure 3-2	Point Beach Units 1 and 2 RCL Weld Locations	3-7
Figure 4-1	Pre-Service J vs. Δa for SA351-CF8M Cast Stainless Steel at 600°F.....	4-16
Figure 5-1	Schematic Diagram of Point Beach Units 1 and 2 Primary Loop Showing Critical Weld Locations.....	5-4
Figure 6-1	Analytical Predictions of Critical Flow Rates of Steam-Water Mixtures	6-4
Figure 6-2	[] ^{a,c,e} Pressure Ratio as a Function of L/D	6-5
Figure 6-3	Idealized Pressure Drop Profile Through a Postulated Crack.....	6-6
Figure 7-1	[] ^{a,c,e} Stress Distribution.....	7-7
Figure 8-1	Typical Cross-Section of [] ^{a,c,e}	8-6
Figure 8-2	Reference Fatigue Crack Growth Curves for Carbon & Low Alloy Ferritic Steels.....	8-7
Figure 8-3	Reference Fatigue Crack Growth Law for Inconel 600 in a Water Environment at 600°F.....	8-8
Figure A-1	Pipe with a Through-Wall Crack in Bending	A-2

EXECUTIVE SUMMARY

The original structural design basis of the reactor coolant system for the Point Beach Units 1 and 2 Nuclear Power Plants required consideration of dynamic effects resulting from pipe break and that protective measures for such breaks be incorporated into the design. Subsequent to the original Point Beach design, additional concern of asymmetric blowdown loads was raised as described in Unresolved Safety Issue A-2 (Asymmetric Blowdown Loads on the Reactor Coolant System) and Generic Letter 84-04 (Reference 1-1). However, research by the NRC and industry coupled with operating experience determined that safety could be negatively impacted by placement of pipe whip restraints on certain systems. As a result, NRC and industry initiatives resulted in demonstrating that Leak-before-break (LBB) criteria can be applied to reactor coolant system piping based on fracture mechanics technology and material toughness. Generic analyses by Westinghouse for the application of LBB for specific plants were documented in response to Unresolved Safety Issue A-2 and approved for Point Beach in the NRC letter dated May 6, 1986 (Reference 1-2). By letter dated May 6, 1986, the NRC stated that:

"By letter dated May 30, 1985, you requested an exemption from the requirements of 10 CFR 50 Appendix A, General Design Criterion (GDC) 4, to eliminate the consideration of large reactor coolant system primary loop pipe breaks in the structural design basis of the Point Beach Nuclear Plant Units 1 and 2. You requested this exemption as directed by staff guidance contained in Generic Letter 84-04, dated February 1, 1984, "Safety Evaluation of Westinghouse Topical Reports Dealing with Elimination of Postulated Pipe Breaks in PWR Primary Main Loops." The Safety Evaluation contained in the generic letter concluded that an acceptable technical basis had been provided so that the asymmetric blowdown loads resulting from double-ended pipe breaks in main coolant loop piping need not be considered as a design basis for the Westinghouse Owner's Group plants listed (two of which were Point Beach Units 1 and 2) provided certain conditions were met. Your May 30, 1985 exemption request provided information showing that the first of these conditions was not applicable to Point Beach Units 1 and 2 and that the second condition was met for both units.

Subsequent to your submittal, the Commission has published in the Federal Register on April 11, 1986 (51 FR 12502) its final rule, "Modification of General Design Criterion 4 Requirements for Protection Against Dynamic Effects of Postulated Pipe Ruptures." This change to the rule allows use of leak-before-break technology for excluding from the design basis the dynamic effects of postulated ruptures in primary coolant loop piping in pressurized water reactors (PWRs). The new rule is effective May 12, 1986.

Based upon the Commission's issuance of the final rule modifying GDC 4 of Appendix A to 10 CFR Part 50, the staff has determined that the exemption requested in your May 30, 1985 application is no longer needed."

Westinghouse performed the original LBB analysis for the Point Beach Units 1 and 2 primary loop piping in 1996 and the results of the analysis were documented in WCAP-14439 (Reference 1-3). The report demonstrates compliance with LBB technology for the Point Beach reactor coolant system piping based on a plant specific analysis. Subsequently, the evaluation was updated to address 1.7% mini-uprating program and plant life extension for 60 years (Reference 1-4). Later, the 2003 LBB evaluation conclusions were re-examined against an extended power uprate (EPU) program in 2008.

According to the results of evaluation performed in 2008, the LBB evaluation for the power uprate and license renewal program for plant life extension for 60 years (Reference 1-4) remain applicable.

The WCAP-14439-P Revision 3 and 4 reports update the LBB evaluations provided in Reference 1-4 to demonstrate that the conclusions provided in Reference 1-4 remain applicable for the subsequent license renewal (SLR) program for the plant operation extension for 80 years.

It has been shown in this report that for 80-year plant service of Point Beach nuclear power plants, all the recommended LBB margins (margin on leak rate, margin on flaw size and margin on loads) are satisfied. For elbow material of A351-CF8M, the fracture mechanics evaluation results show that the LBB loads do not exceed the limit that can initiate a crack in elbow. For alloy 82 weld material at Unit 2 steam generator inlet and outlet nozzles that is susceptible to Primary Water Stress Corrosion Cracking (PWSCC), an inlay of alloy 52/152 material has been applied to mitigate PWSCC. The impact of transient cycles that accounts for 80-year plant service to fatigue crack growth aspect has been shown to be acceptable.

It is therefore concluded that dynamic effects of RCS primary loop pipe breaks need not be considered in the structural design basis of the Point Beach Units 1 and 2 Nuclear Power Plants for the subsequent license renewal program.

The following table presents a brief summary of the analysis locations considered in this report. This table includes the material type(s) considered for each location, as well as the specific evaluation which are used to justify the applicability of Leak-Before-Break for the full Reactor Coolant Loop (RCL) piping system.

RCL Piping	Location	Unit	Material	Evaluation Type	Results Summary
Hot Leg (HL)	1	Both	A376-TP316	Global failure ⁽¹⁾	Table 7-2
	2	Both	A351-CF8M	Local stability ⁽²⁾	Table 7-1
			A376-TP316	Global failure ⁽¹⁾	Table 7-2
3	2	Alloy 82 weld (with Alloy 52/152 inlay)	See note (3)		
Crossover Leg (XOL)	4	2	Alloy 82 weld (with Alloy 52/152 inlay)	See note (3)	
	8	Both	A351-CF8M	Local stability ⁽²⁾	Table 7-1
			A376-TP316	Global failure ⁽¹⁾	Table 7-2
Cold Leg (CL)	11	Both	A351-CF8M	Local stability ⁽²⁾	Table 7-1
			A376-TP316	Global failure ⁽¹⁾	Table 7-2

- Notes: (1) Global failure evaluation accounts for lower tensile properties. Pipe stainless steel (A376-TP316) base metal is more limiting than both the elbow cast austenitic stainless steel base-metal and the weld material, as noted in Section 4. While the global failure evaluations use the base metal material properties, the analysis also accounts for the fracture strength reductions due to the welding process used during fabrication.
- (2) Local stability evaluations accounts for the thermal aging effects on the cast austenitic stainless steel base-metal.
- (3) Point Beach Unit 2 SG inlet and outlet nozzles (locations 3 and 4) contain alloy 82/182 dissimilar metal welds which are susceptible to Primary Water Stress Corrosion Cracking (PWSCC). An inlay of the alloy 52/152 material was applied to these welds to mitigate the PWSCC. The LBB evaluations for both locations 3 and 4 are bounded by evaluations provided for locations 2 and 8, as justified in Section 5.1.

1.0 INTRODUCTION

1.1 PURPOSE

This report applies to the Point Beach Units 1 and 2 Reactor Coolant System (RCS) primary loop piping. It is intended to demonstrate that for the specific parameters of the Point Beach Units 1 and 2 Nuclear Power Plants, RCS primary loop pipe breaks need not be considered in the structural design basis for the 80-year plant life subsequent license renewal (SLR) program. The specific parameters include normal operation temperature and internal pressure conditions for 7% mini-uprating, extended power uprate programs and also NSSS design transient cycles for 80-year plant life.

In addition, this report also confirms the use of alloy 82/182 nickel-base materials which are susceptible to primary water stress corrosion cracking (PWSCC) at the dissimilar metal weld (DMW) locations at the Unit 2 Steam Generator inlet and outlet nozzles has been appropriately mitigated with inlaid alloy 52/152 weld.

1.2 BACKGROUND INFORMATION

Westinghouse has performed considerable testing and analysis to demonstrate that Reactor Coolant System (RCS) primary loop pipe breaks can be eliminated from the structural design basis of all Westinghouse plants. The concept of eliminating pipe breaks in the RCS primary loop was first presented to the NRC in 1978 in WCAP-9283 (Reference 1-5). That topical report employed a deterministic fracture mechanics evaluation and a probabilistic analysis to support the elimination of RCS primary loop pipe breaks. That approach was then used as a means of addressing Generic Issue A-2 and Asymmetric Loss of Coolant Accident (LOCA) Loads.

Westinghouse performed additional testing and analysis to justify the elimination of RCS primary loop pipe breaks. This material was provided to the NRC along with Letter Report NS-EPR-2519 (Reference 1-6).

The NRC funded research through Lawrence Livermore National Laboratory (LLNL) to address this same issue using a probabilistic approach. As part of the LLNL research effort, Westinghouse performed extensive evaluations of specific plant loads, material properties, transients, and system geometries to demonstrate that the analysis and testing previously performed by Westinghouse and the research performed by LLNL applied to all Westinghouse plants (References 1-7 and 1-8). The results from the LLNL study were released at a March 28, 1983, ACRS Subcommittee meeting. These studies, which are applicable to all Westinghouse plants east of the Rocky Mountains, determined the mean probability of a direct LOCA (RCS primary loop pipe break) to be 4.4×10^{-12} per reactor year and the mean probability of an indirect LOCA to be 10^{-7} per reactor year. Thus, the results previously obtained by Westinghouse (Reference 1-5) were confirmed by an independent NRC research study.

Based on the studies by Westinghouse, LLNL, the ACRS, and the Atomic Industrial Forum (AIF), the NRC completed a safety review of the Westinghouse reports submitted to address asymmetric blowdown loads that result from a number of discrete break locations on the PWR primary systems. The NRC Staff evaluation (Reference 1-1) concludes that an acceptable technical basis has been provided so that asymmetric blowdown loads need not be considered for those plants that can demonstrate the applicability of the modeling and conclusions contained in the Westinghouse response or can provide an equivalent fracture mechanics demonstration of the primary coolant loop integrity. In a more formal

recognition of Leak-Before-Break (LBB) methodology applicability for PWRs, the NRC appropriately modified 10 CFR 50, General Design Criterion 4, "Requirements for Protection Against Dynamic Effects for Postulated Pipe Rupture" (Reference 1-9).

For Point Beach Nuclear Power Station Units 1 and 2, the postulated pipe breaks for the RCS primary loop piping have been evaluated using LBB evaluation methods. It is demonstrated that the dynamic effects of the pipe rupture resulting from postulated breaks in the primary loop piping need not be considered in the structural design basis of Point Beach Units 1 and 2. The original LBB evaluation results for the RCS primary loop were documented in WCAP-14439 report (Reference 1-3) in 1996.

For the Subsequent License Renewal (SLR) program, this report demonstrates that the conclusions reached in References 1-3 and 1-4 remain applicable in the structural design basis for the 80-year plant life for the specific parameters of the Point Beach Units 1 and 2 Nuclear Power Stations.

1.3 SCOPE AND OBJECTIVES

The general purpose of this investigation is to demonstrate leak-before-break for the primary loops in Point Beach Units 1 and 2 on a plant specific basis for the 80-year plant life. The recommendations and criteria proposed in References 1-10 and 1-11 are used in this evaluation. These criteria and resulting steps of the evaluation procedure can be briefly summarized as follows:

1. Calculate the applied loads. Identify the locations at which the highest stress occurs.
2. Identify the limiting material profiles and the associated material properties.
3. Postulate a surface flaw at the governing locations. Determine fatigue crack growth. Show that a through-wall crack will not result.
4. Postulate a through-wall flaw at the governing locations. The size of the flaw should be large enough so that the leakage is assured of detection with margin using the installed leak detection equipment when the pipe is subjected to normal operating loads. A margin of 10 is demonstrated between the calculated leak rate and the leak detection capability.
5. Using faulted loads, demonstrate that there is a margin of 2 between the leakage flaw size and the critical flaw size.
6. Review the operating history to ascertain that operating experience has indicated no particular susceptibility to failure from the effects of corrosion, water hammer or low and high cycle fatigue.
7. For the materials actually used in the plant provide the properties including toughness and tensile test data. Evaluate long term effects such as thermal aging.
8. Demonstrate margin on the calculated applied load value; margin of 1.4 using algebraic summation of loads or margin of 1.0 using absolute summation of loads.

This report provides a fracture mechanics demonstration of primary loop integrity for the Point Beach Units 1 and 2 plants consistent with the NRC position for exemption from consideration of dynamic effects.

The LBB evaluation summarized in this report consider the limiting weld locations of the RCL piping. In general, the analyses consider the material properties of the piping base metal, which are more limiting than the weld materials. The re-evaluations were performed to ensure that the LBB evaluation conclusions remain valid for 80-year plant life in the SLR program.

It should be noted that the terms “flaw” and “crack” have the same meaning and are used interchangeably. “Governing location” and “critical location” are also used interchangeably throughout the report.

The computer codes used in this evaluation for leak rate and fracture mechanics calculations have been validated and used for all the LBB applications by Westinghouse.

1.4 REFERENCES

- 1-1 USNRC Generic Letter 84-04, Subject “Safety Evaluation of Westinghouse Topical Reports Dealing with Elimination of Postulated Pipe Breaks in PWR Primary Main Loops,” February 1, 1984.
- 1-2 Nuclear Regulatory Commission Docket #'s 50-266 and 50-301 Letter from G. E. Lear, Director PWR Project Directorate #1 Division of PWR Licensing-A, NRC, to C. W. Fay, Vice President Nuclear Power Department Wisconsin Electric Power Company.
- 1-3 WCAP-14439, ”Technical Justification for Eliminating Large Primary Loop Pipe Rupture as the Structural Design Basis for the Point Beach Units 1 and 2 Nuclear Power Plants,” December 1996.
- 1-4 WCAP-14439-P, Revision 2, “Technical Justification for Eliminating Large Primary Loop Pipe Rupture as the Structural Design Basis for the Point Beach Nuclear Plants Units 1 and 2 for the Power Uprate and License Renewal Program,” September 2003.
- 1-5 WCAP-9283, “The Integrity of Primary Piping Systems of Westinghouse Nuclear Power Plants During Postulated Seismic Events,” March 1978.
- 1-6 Letter Report NS-EPR-2519, Westinghouse (E. P. Rahe) to NRC (D. G. Eisenhut), Westinghouse Proprietary Class 2, and November 10, 1981.
- 1-7 Letter from Westinghouse (E. P. Rahe) to NRC (W. V. Johnston) dated April 25, 1983.
- 1-8 Letter from Westinghouse (E. P. Rahe) to NRC (W. V. Johnston) dated July 25, 1983.
- 1-9 Nuclear Regulatory Commission, 10 CFR 50, Modification of General Design Criteria 4 Requirements for Protection Against Dynamic Effects of Postulated Pipe Ruptures, Final Rule, Federal Register/Vol. 52, No. 207/Tuesday, October 27, 1987/Rules and Regulations, pp. 41288-41295.
- 1-10 Standard Review Plan: Public Comments Solicited; 3.6.3 Leak-Before-Break Evaluation Procedures; Federal Register/Vol. 52, No. 167/Friday August 28, 1987/Notices, pp. 32626-32633.
- 1-11 NUREG-0800 Revision 1, March 2007, Standard Review Plan: 3.6.3 Leak-Before-Break Evaluation Procedures.

2.0 OPERATION AND STABILITY OF THE REACTOR COOLANT SYSTEM

2.1 STRESS CORROSION CRACKING

The Westinghouse reactor coolant system primary loops have an operating history that demonstrates the inherent operating stability characteristics of the design. This includes a low susceptibility to cracking failure from the effects of corrosion (e.g., intergranular stress corrosion cracking (IGSCC)). This operating history totals over 1400 reactor-years, including 16 plants each having over 30 years of operation, 10 other plants each with over 25 years of operation, 11 plants each with over 20 years of operation, and 12 plants each with over 15 years of operation.

In 1978, the United States Nuclear Regulatory Commission (USNRC) formed the second Pipe Crack Study Group. (The first Pipe Crack Study Group (PCSG) established in 1975, addressed cracking in boiling water reactors only.) One of the objectives of the second PCSG was to include a review of the potential for stress corrosion cracking in Pressurized Water Reactors (PWR's). The results of the study performed by the PCSG were presented in NUREG-0531 (Reference 2-1) entitled "Investigation and Evaluation of Stress Corrosion Cracking in Piping of Light Water Reactor Plants." In that report the PCSG stated:

“The PCSG has determined that the potential for stress-corrosion cracking in PWR primary system piping is extremely low because the ingredients that produce IGSCC are not all present. The use of hydrazine additives and a hydrogen overpressure limit the oxygen in the coolant to very low levels. Other impurities that might cause stress-corrosion cracking, such as halides or caustic, are also rigidly controlled. Only for brief periods during reactor shutdown when the coolant is exposed to the air and during the subsequent startup are conditions even marginally capable of producing stress-corrosion cracking in the primary systems of PWRs. Operating experience in PWRs supports this determination. To date, no stress corrosion cracking has been reported in the primary piping or safe ends of any PWR.”

During 1979, several instances of cracking in PWR feedwater piping led to the establishment of the third PCSG. The investigations of the PCSG reported in NUREG-0691 (Reference 2-2) further confirmed that no occurrences of IGSCC have been reported for PWR primary coolant systems.

As stated above, for the Westinghouse plants there is no history of cracking failure in the reactor coolant system loop. The discussion below further qualifies the PCSG's findings.

For stress corrosion cracking (SCC) to occur in piping, the following three conditions must exist simultaneously: high tensile stresses, susceptible material, and a corrosive environment. Since some residual stresses and some degree of material susceptibility exist in any stainless steel piping, the potential for stress corrosion is minimized by properly selecting a material immune to SCC as well as preventing the occurrence of a corrosive environment. The material specifications consider compatibility with the system's operating environment (both internal and external) as well as other material in the system, applicable ASME Code rules, fracture toughness, welding, fabrication, and processing.

The elements of a water environment known to increase the susceptibility of austenitic stainless steel to stress corrosion are: oxygen, fluorides, chlorides, hydroxides, hydrogen peroxide, and reduced forms of sulfur (e.g., sulfides, sulfites, and thionates). Strict pipe cleaning standards prior to operation and careful control of water chemistry during plant operation are used to prevent the occurrence of a corrosive environment. Prior to being put into service, the piping is cleaned internally and externally. During flushes and preoperational testing, water chemistry is controlled in accordance with written specifications. Requirements on chlorides, fluorides, conductivity, and pH are included in the acceptance criteria for the piping.

During plant operation, the reactor coolant water chemistry is monitored and maintained within very specific limits. Contaminant concentrations are kept below the thresholds known to be conducive to stress corrosion cracking with the major water chemistry control standards being included in the plant operating procedures as a condition for plant operation. For example, during normal power operation, oxygen concentration in the RCS is expected to be in the parts-per-billion (ppb) range by controlling charging flow chemistry and maintaining hydrogen in the reactor coolant at specified concentrations. Halogen concentrations are also stringently controlled by maintaining concentrations of chlorides and fluorides within the specified limits. Thus, during plant operation, the likelihood of stress corrosion cracking is minimized.

The potential susceptibility to primary water stress corrosion cracking (PWSCC) in materials such as alloy 82/182 in the dissimilar metal welds in the Point Beach Units 1 and 2 RCS primary loop piping was investigated. The susceptible material is not found in the primary loop piping at the Unit 1. However, the alloy 82 weld exists at the Unit 2 between the Steam Generators (SG) nozzle-to-safe end weld locations. The PWSCC susceptibility of the alloy 82 welds was mitigated with alloy 152 buttering on the inside surfaces at the Unit 2 and the welding was performed in the shop under controlled conditions and with improved welding technology. Alloy 152 weld material, in contact with the primary coolant, is considered to have improved PWSCC resistance. Since the alloy 82 weld in the primary loop piping for Point Beach Unit 2 is not exposed to the primary coolant, PWSCC should not be a concern.

2.2 WATER HAMMER

Overall, there is a low potential for water hammer in the RCS since it is designed and operated to preclude the voiding condition in normally filled lines. The reactor coolant system, including piping and primary components, is designed for normal, upset, emergency, and faulted condition transients. The design requirements are conservative relative to both the number of transients and their severity. Relief valve actuation and the associated hydraulic transients following valve opening are considered in the system design. Other valve and pump actuations are relatively slow transients with no significant effect on the system dynamic loads. To ensure dynamic system stability, reactor coolant parameters are stringently controlled. Temperature during normal operation is maintained within a narrow range; pressure is controlled by pressurizer heaters and pressurizer spray also within a narrow range for steady-state conditions. The flow characteristics of the system remain constant during a fuel cycle because the only governing parameters, namely system resistance and the reactor coolant pump characteristics, are controlled in the design process. Additionally, Westinghouse has instrumented typical reactor coolant systems to verify the flow and vibration characteristics of the system. Preoperational testing and operating experience have verified the Westinghouse approach. The operating transients of the RCS primary piping are such that no significant water hammer can occur.

2.3 LOW CYCLE AND HIGH CYCLE FATIGUE

An assessment of the low cycle fatigue loadings was carried out as part of this study in the form of a fatigue crack growth analysis, as discussed in Section 8.0.

High cycle fatigue loads in the system would result primarily from pump vibrations. These are minimized by restrictions placed on shaft vibrations during hot functional testing and operation. During operation, an alarm signals the exceedance of the vibration limits. Field vibration measurements have been made on the reactor coolant loop piping in a number of plants during hot functional testing, including plants similar to Point Beach Units 1 and 2. Stresses in the elbow below the reactor coolant pump resulting from system vibration have been found to be very small, between 2 and 3 ksi at the highest. These stresses are well below the fatigue endurance limit for the material and would also result in an applied stress intensity factor below the threshold for fatigue crack growth.

2.4 WALL THINNING, CREEP, AND CLEAVAGE

Wall thinning by erosion and erosion-corrosion effects should not occur in the primary loop piping due to the low velocity, typically less than 1.0 ft/sec and the stainless steel material, which is highly resistant to these degradation mechanisms. The cause of wall thinning is related to high water velocity and is therefore clearly not a mechanism that would affect the primary loop piping.

Creep is typically experienced for temperatures over 700°F for stainless steel material, and the maximum operating temperature of the primary loop piping is well below this temperature value; therefore, there would be no significant mechanical creep damage in stainless steel piping.

Cleavage type failures are not a concern for the operating temperatures and the stainless steel material used in the primary loop piping.

2.5 REFERENCES

- 2-1 Investigation and Evaluation of Stress-Corrosion Cracking in Piping of Light Water Reactor Plants, NUREG-0531, U.S. Nuclear Regulatory Commission, February 1979.
- 2-2 Investigation and Evaluation of Cracking Incidents in Piping in Pressurized Water Reactors, NUREG-0691, U.S. Nuclear Regulatory Commission, September 1980.

3.0 PIPE GEOMETRY AND LOADING

3.1 INTRODUCTION TO METHODOLOGY

The general approach is discussed first. As an example, a segment of the primary coolant hot leg pipe is shown in Figure 3-1. The as-built outside diameter and minimum wall thickness of the pipe are 34.21 in. and 2.50 in., respectively, as shown in the figure. The normal stresses at the weld locations are from the load combination procedure discussed in Section 3.3 whereas the faulted loads are as described in Section 3.4. The components for normal loads are pressure, deadweight and thermal expansion (Table 3-1). An additional component, Safe Shutdown Earthquake (SSE), is considered for faulted loads (Table 3-2). Tables 3-1 and 3-2 show the enveloping loads for Point Beach Units 1 and 2. As seen from Table 3-2, the highest stressed location in the entire Point Beach Units 1 and 2 reactor coolant loops is at the reactor vessel outlet nozzle to pipe weld (Location 1). This is one of the locations at which leak-before-break is to be established. Essentially a circumferential flaw is postulated to exist at this location which is subjected to both the normal loads and faulted loads to assess leakage and stability, respectively. The loads (developed below) at this location are also given in Figure 3-1.

Since the primary loop piping are made of different materials (A376-TP316 and A351-CF8M), locations other than the highest stressed pipe location were examined by taking into consideration both fracture toughness and stress. The four most critical locations among the entire primary loop are identified after the full analysis is completed (see Section 5.0). Once loads (this section) and fracture toughnesses (Section 4.0) are obtained, the critical locations are determined (Section 5.0). At these locations, leak rate evaluations (Section 6.0) and fracture mechanics evaluations (Section 7.0) are performed per the guidance of References 3-1 and 3-2.

For global failure mechanism, all locations are evaluated using the A376-TP316 stainless steel material properties which present a limiting condition due to their lower tensile properties as shown in Section 4.2.

For local stability mechanism, the respective locations are evaluated using the A351-CF8M cast austenitic stainless steel (CASS) material properties which present a limiting condition not only due to their tensile properties in unaged condition but also the material fracture toughness and tearing modulus reductions due to the thermal aging effects for the entire 80-year plant life.

Fatigue crack growth (Section 8.0) assessment and stability margins are also evaluated (Section 9.0). All the weld locations considered for the LBB evaluation are those shown in Figure 3-2.

3.2 CALCULATION OF LOADS AND STRESSES

The stresses due to axial loads and bending moments are calculated by the following equation:

$$\sigma = \frac{F}{A} + \frac{M}{Z} \quad (3-1)$$

where,

σ	=	stress, ksi
F	=	axial load, kips
M	=	bending moment, in-kips
A	=	pipe cross-sectional area, in ²
Z	=	section modulus, in ³

The total moments for the desired loading combinations are calculated by the following equation:

$$M = \sqrt{M_X^2 + M_Y^2 + M_Z^2} \quad (3-2)$$

where,

M	=	total moment for required loading
M_X	=	X component of moment (torsion)
M_Y	=	Y component of bending moment
M_Z	=	Z component of bending moment

NOTE: X-axis is along the center line of the pipe.

The axial load and bending moments for leak rate predictions and crack stability analyses are computed by the methods to be explained in Sections 3.3 and 3.4.

3.3 LOADS FOR LEAK RATE EVALUATION

The normal operating loads for leak rate predictions are calculated by the following equations:

$$F = F_{DW} + F_{TH} + F_P \quad (3-3)$$

$$M_X = (M_X)_{DW} + (M_X)_{TH} \quad (3-4)$$

$$M_Y = (M_Y)_{DW} + (M_Y)_{TH} \quad (3-5)$$

$$M_Z = (M_Z)_{DW} + (M_Z)_{TH} \quad (3-6)$$

The subscripts of the above equations represent the following loading cases:

DW	=	deadweight
TH	=	normal thermal expansion
P	=	load due to internal pressure

This method of combining loads is often referred to as the algebraic sum method (References 3-1 and 3-2).

The loads based on this method of combination are provided in Table 3-1 at all the weld locations identified in Figure 3-2. These loads bound both loops for Point Beach Units 1 and 2.

3.4 LOAD COMBINATION FOR CRACK STABILITY ANALYSES

In accordance with Standard Review Plan 3.6.3 (References 3-1 and 3-2), the margin in terms of applied loads needs to be demonstrated by crack stability analysis. Margin on loads of 1.4 ($\sqrt{2}$) can be demonstrated if normal plus Safe Shutdown Earthquake (SSE) are applied. The 1.4 ($\sqrt{2}$) margin should be reduced to 1.0 if the deadweight, thermal expansion, internal pressure, pressure expansion, Safe Shutdown Earthquake (SSE) loads are combined based on individual absolute values as shown below.

The absolute sum of loading components is used for the LBB analysis which results in higher magnitude of combined loads and thus satisfies a margin on loads of 1.0. The absolute summation of loads is shown in the following equations:

$$F = |F_{DW}| + |F_{TH}| + |F_P| + |F_{SSEINERTIA}| + |F_{SSEAM}| \quad (3-7)$$

$$M_X = |(M_X)_{DW}| + |(M_X)_{TH}| + |(M_X)_{SSEINERTIA}| + |(M_X)_{SSEAM}| \quad (3-8)$$

$$M_Y = |(M_Y)_{DW}| + |(M_Y)_{TH}| + |(M_Y)_{SSEINERTIA}| + |(M_Y)_{SSEAM}| \quad (3-9)$$

$$M_Z = |(M_Z)_{DW}| + |(M_Z)_{TH}| + |(M_Z)_{SSEINERTIA}| + |(M_Z)_{SSEAM}| \quad (3-10)$$

where subscript SSEINERTIA refers to safe shutdown earthquake inertia, SSEAM is safe shutdown earthquake anchor motion, respectively.

The loads so determined are used in the fracture mechanics evaluations (Section 7.0) to demonstrate the LBB margins at the locations established to be the governing locations. These loads at all the weld locations (see Figure 3-2) are given in Table 3-2. The loads in these tables bound both loops for Point Beach Units 1 and 2.

3.5 REFERENCES

- 3-1 Standard Review Plan: Public Comments Solicited; 3.6.3 Leak-Before-Break Evaluation Procedures; Federal Register/Vol. 52, No. 167/Friday, August 28, 1987/Notices, pp. 32626-32633.
- 3-2 NUREG-0800 Revision 1, March 2007, Standard Review Plan: 3.6.3 Leak-Before-Break Evaluation Procedures.

Table 3-1: Dimensions, Normal Loads and Stresses for Point Beach Units 1 and 2					
Location Weld Points^a	Outside Diameter (in)	Minimum Thickness (in)	Axial Load^b (kips)	Moment (in-kips)	Total Stress (ksi)
1	34.210	2.500	1,412	13,165	12.82
2	34.210	2.500	1,412	4,102	7.90
3	37.750	3.270	1,585	6,424	6.76
4	37.630	3.210	1,713	1,310	5.41
5	36.560	2.675	1,710	1,447	6.65
6	36.560	2.675	1,707	1,609	6.71
7	36.560	2.675	1,717	1,215	6.57
8	36.560	2.675	1,713	2,449	7.10
9	37.630	3.210	1,767	4,786	6.83
10	32.460	2.375	1,361	2,804	7.85
11	32.460	2.375	1,361	4,111	8.68
12	33.560	2.925	1,362	5,182	7.45

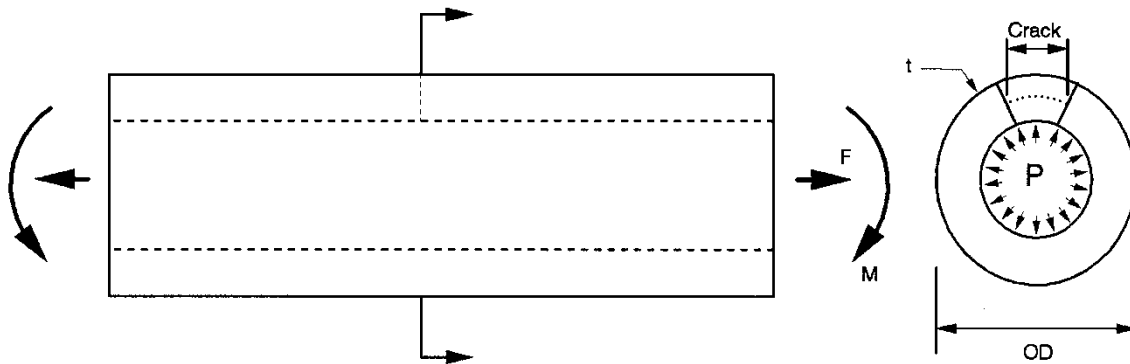
Notes:

- a. See Figure 3-2
- b. Included Pressure

Table 3-2: Dimensions, Faulted Loads and Stresses for Point Beach Units 1 and 2					
Location Weld Points^a	Outside Diameter (in)	Minimum Thickness (in)	Axial Load^b (kips)	Moment (in-kips)	Total Stress (ksi)
1	34.210	2.500	1,715	20,688	18.12
2	34.210	2.500	1,715	6,080	10.19
3	37.750	3.270	1,943	10,696	9.29
4	37.630	3.210	1,794	11,387	9.30
5	36.560	2.675	1,785	8,438	10.02
6	36.560	2.675	1,781	6,895	9.32
7	36.560	2.675	1,798	5,856	8.92
8	36.560	2.675	1,803	9,070	10.36
9	37.630	3.210	1,793	11,098	9.19
10	32.460	2.375	1,399	7,378	10.92
11	32.460	2.375	1,426	14,069	15.29
12	33.560	2.925	1,401	17,254	13.66

Notes:

- a. See Figure 3-2
- b. Included Pressure



$OD^a = 34.21$ in
 $t^a = 2.50$ in

Location 1

Normal Loads^a

Force^c: 1412 kips
 Bending Moment: 13165 in-kips

Faulted Loads^b

Force^c: 1715 kips
 Bending Moment: 20688 in-kips

^a See Table 3-1

^b See Table 3-2

^c Includes the force due to a pressure of 2235 psig

Figure 3-1 Hot Leg Coolant Pipe

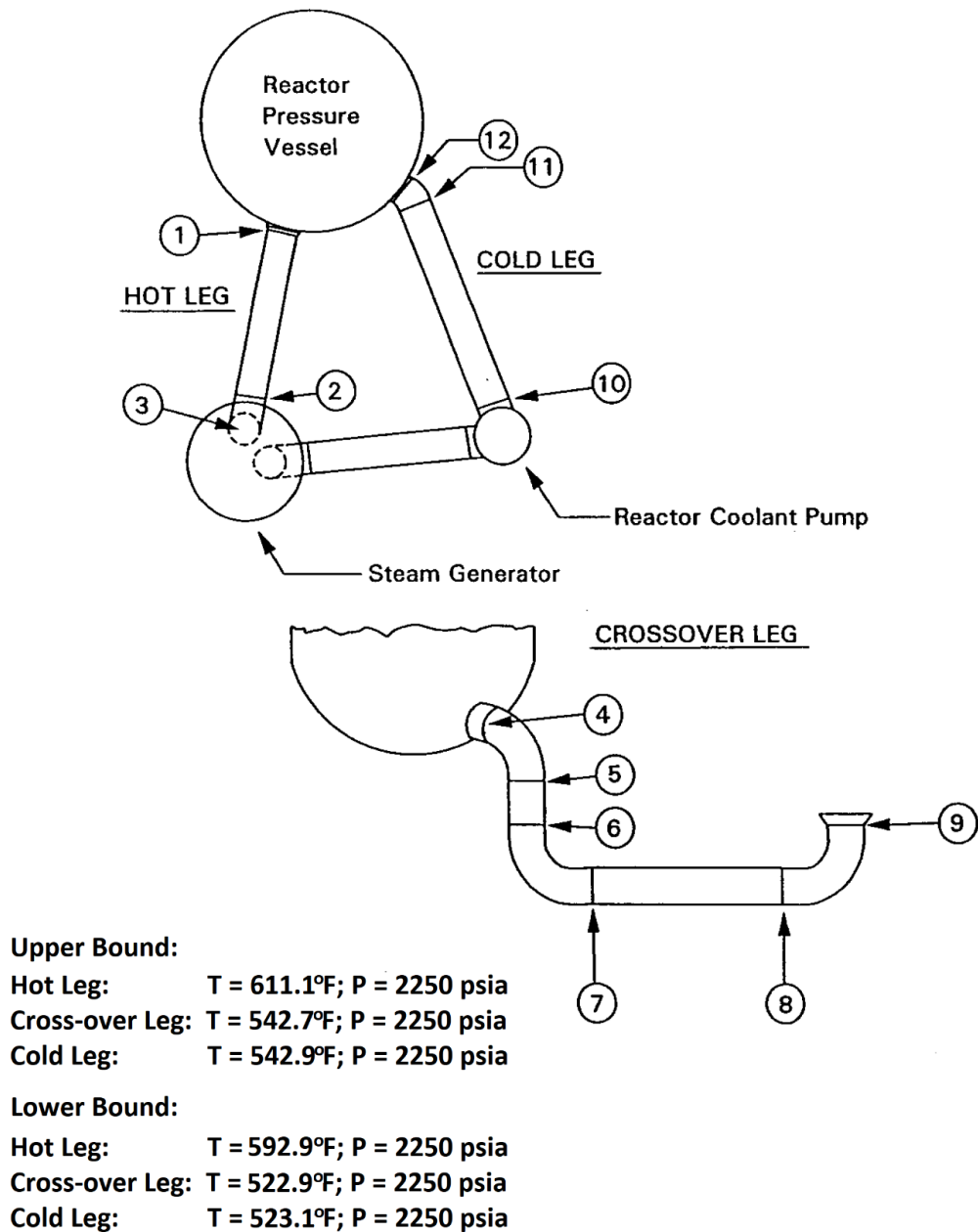


Figure 3-2 Point Beach Units 1 and 2 RCL Weld Locations

4.0 MATERIAL CHARACTERIZATION

4.1 PRIMARY LOOP PIPE AND FITTINGS MATERIALS

The Point Beach Units 1 and 2 primary loop pipe material is A376-TP316 and the elbow fitting material is A351-CF8M.

4.2 TENSILE PROPERTIES

The Certified Materials Test Reports (CMTRs) for the Point Beach Units 1 and 2 Reactor Coolant Loop Lines are used to establish the tensile properties for the Leak-Before-Break analyses. For the RCL Lines, Tables 4-1 and 4-2 provide the pipe (A376-TP316) tensile properties for Units 1 and 2; Tables 4-3 and 4-4 provide the elbows (A351-CF8M) tensile properties for Units 1 and 2.

For both materials, the applicable operating temperatures based on EPU program are 611.1°F for Hot Leg and the average value of 542.8°F to represent 542.7°F for Cross-over Leg and 542.9°F for Cold Leg.

For A376-TP316 material with material heats, CMTR data is available for the 70°F and 650°F test temperatures. To obtain conservatism in the calculation, i.e. the smallest flaw size margin, material property interpolations are based on the CMTR properties taken at 70°F temperature for the minimum and average yield strength (Sy) values; and CMTR properties taken at 650°F for the minimum ultimate strength (Su) values. The representative properties at 611.1°F or 542.8°F are established from the tensile properties either at 70°F or 650°F given in Tables 4-1 and 4-2 by utilizing Section II of the 2007 ASME Boiler and Pressure Vessel Code (Reference 4-1).

For A351-CF8M material, material interpolations are based on the CMTR properties taken at room temperature because the CMTR data does not include tensile properties at an elevated temperature. The representative properties at 611.1°F or 542.8°F are established from the tensile properties at room temperature (70°F) given in Tables 4-3 and 4-4 by utilizing Section II of the 2007 ASME Code (Reference 4-1).

Code tensile properties at temperatures for the operating conditions considered in this LBB analysis are obtained by linear interpolation of tensile properties provided in the Code. Ratios of the Code tensile properties at the operating temperatures to the corresponding properties at the CMTR temperature are then applied to obtain the Point Beach Units 1 and 2 line-specific properties at operating temperatures.

It should be noted that there is no significant impact by using the 2007 ASME Code Section II edition for material properties for the LBB analysis, as compared to the Point Beach ASME Code of record.

Material modulus of elasticity is also interpolated from ASME Code values for the operating temperatures considered, and Poisson's ratio is taken as 0.3. The temperature-dependent material properties from the ASME Code are shown in Table 4-5. The average and lower bound yield strengths, ultimate strengths, and elastic moduli for the pipe material at applicable operating temperatures are tabulated in Table 4-6.

For the SLR program that accounts for 80 years of plant operation, the more conservative material properties are used.

Conservative Evaluations:

For global failure mechanism based on limit load method, the stability of postulated cracks at critical locations for 80 years of plant operation are examined. To evaluate conservatively, it is desired to use lower tensile properties obtained from base-metals and weld materials, since lower tensile properties potentially reduce the critical flaw size/flaw size margins. Therefore, A376-TP316 material tensile (S_u and S_y) properties as shown in Table 4-6 are used.

For local stability mechanism based on J-integral method, the stability of postulated cracks at A351-CF8M CASS material at the critical locations for 80 years of plant operation is examined based on the following parameter values: J_{Ic} , J_{max} , T_{mat} , J_{app} and T_{app} (see Section 5.2), where:

- (1) If $J_{app} < J_{Ic}$, then the crack will not initiate, and the crack is stable;
- (2) If $J_{app} \geq J_{Ic}$; and $T_{app} < T_{mat}$ and $J_{app} < J_{max}$, then the crack is stable.

The A351-CF8M material is susceptible to thermal aging. J_{app} , T_{app} , and T_{mat} values (which are dependent on aging tensile (S_u and S_y) properties) will be affected. To evaluate conservatively, both unaged and aged tensile properties are used for the following reasons: (a) lower tensile properties are more conservative for the LBB evaluation by increasing the calculated J_{app} and T_{app} values; therefore, the unaged tensile properties as shown in Table 4-6 are used to calculate those values; (b) higher tensile properties are more conservative for the LBB evaluation by lowering T_{mat} values; therefore, the aged tensile properties as shown in Table 4-8 are used just to calculate T_{mat} .

4.3 FRACTURE TOUGHNESS PROPERTIES

The pre-service fracture toughness (J) of cast austenitic stainless steel CASS) that are of interest are in terms of J_{Ic} (J at Crack Initiation) and have been found to be very high at 600°F. [

]^{a,c,e} However, cast stainless steel is susceptible to thermal aging at the reactor operating temperature, that is, about 290°C (550°F). Thermal aging of cast stainless steel results in embrittlement, that is, a decrease in the ductility, impact strength, and fracture toughness of the material. Depending on the material composition, the Charpy impact energy of a cast stainless steel component could decrease to a small fraction of its original value after exposure to reactor temperatures during service.

In 1994, the Argonne National Laboratory (ANL) completed an extensive research program in assessing the extent of thermal aging of cast stainless steel materials. The ANL research program measured mechanical properties of cast stainless steel materials after they had been heated in controlled ovens for long periods of time. ANL compiled a database, both from data within ANL and from international sources, of about 85 compositions of cast stainless steel exposed to a temperature range of 290-400°C (550-750°F) for up to 58,000 hours (6.5 years). In 2015 the work done by ANL was augmented, and the fracture toughness database for CASS materials was aged to 100,000 hours at 290-350°C (554-633°F). The methodology for estimating fracture properties has been extended to cover CASS materials with a ferrite content of up to 40%. From this database (NUREG/CR-4513, Revision 2), ANL developed correlations for estimating the extent of thermal aging of cast stainless steel (Reference 4-2).

ANL developed the fracture toughness estimation procedures by correlating data in the database conservatively. After developing the correlations, ANL validated the estimation procedures by comparing the estimated fracture toughness with the measured value for several cast stainless steel plant components removed from actual plant service. The procedure developed by ANL was used to calculate the end of life fracture toughness values for this analysis. The ANL research program was sponsored and the procedure was accepted by the NRC.

The results from the ANL Research Program indicate that the lower-bound fracture toughness of thermally aged cast stainless steel is similar to that of submerged arc welds (SAWs). The applied value of the J-integral for a flaw in the weld regions will be lower than that in the base metal because the yield stress for the weld materials is much higher at the temperature.¹

Therefore, weld regions are less limiting than the cast material.

Based on Reference 4-2, the fracture toughness correlations used for the full aged condition is applicable for plants operating at ≥ 15 EFPY (effective full-power years) for the A351-CF8M materials. As of June 2020, Point Beach Units 1 and 2 are operating at > 15 EFPY. For the SLR program that accounts for 80 years of plant operation, the materials will thermally age. Therefore, the use of the fracture toughness correlations described in the following sections is applicable for the fully aged or saturated condition of the Point Beach Units 1 and 2 materials made of A351-CF8M elbow fittings.

It is noted that both Revision 1 and Revision 2 of NUREG/CR-4513 were considered in evaluating the thermal aging of the Point Beach CASS materials. Table 4-10 provides a comparison of the J_{Ic} values for each CASS material heat calculated using both Revision 1 and Revision 2 of NUREG/CR-4513. While Revision 1 may be limiting for some material heats, it was found that Revision 2 (Reference 4-2) resulted in the most limiting fracture toughness values for the critical material heats identified in Table 4-9.

Fracture Toughness Properties of Static Cast Elbows (CF8M)

The susceptibility of the material to thermal aging increases with increasing ferrite contents, and the molybdenum bearing CF8M shows increased susceptibility to thermal aging.

The chemical compositions of the Point Beach Units 1 and 2 primary loop elbow fitting material are available from CMTRs. The following equations 4-1 to 4-3 for delta ferrite calculations are taken from Reference 4-2 and applicable for CF8M type materials.

$$Cr_{eq} = Cr + 1.21(Mo) + 0.48(Si) - 4.99 = (\text{Chromium equivalent}) \quad (4-1)$$

$$Ni_{eq} = (Ni) + 0.11(Mn) - 0.0086(Mn)^2 + 18.4(N) + 24.5(C) + 2.77 = (\text{Nickel equivalent}) \quad (4-2)$$

Note: N is not included in CMTR. Value of 0.04 is assumed per Reference 4-2.

$$\delta_c = 100.3(Cr_{eq} / Ni_{eq})^2 - 170.72(Cr_{eq} / Ni_{eq}) + 74.22 \quad (4-3)$$

where the elements are in percent weight and δ_c is ferrite in percent volume.

¹ In the report all the applied J values were conservatively determined by using base metal strength properties.

The saturation room temperature (RT at 77°F) impact energies of the cast stainless steel materials are determined from the chemical compositions available from CMTRs and shown in Table 4-7.

For CF8M steel with < 10% Ni, the saturation value of RT impact energy Cv_{sat} (J/cm²) is the lower value determined from

$$\log_{10}Cv_{sat} = 0.27 + 2.81 \exp(-0.022\phi) \quad (4-4)$$

where the material parameter ϕ is expressed as

$$\phi = \delta_c (Ni + Si + Mn)^2(C + 0.4N)/5.0 \quad (4-5)$$

and from

$$\log_{10}Cv_{sat} = 7.28 - 0.011\delta_c - 0.185Cr - 0.369Mo - 0.451Si - 0.007Ni - 4.71(C + 0.4N) \quad (4-6)$$

For CF8M steel with $\geq 10\%$ Ni, the saturation value of RT impact energy Cv_{sat} (J/cm²) is the lower value determined from

$$\log_{10}Cv_{sat} = 0.84 + 2.54 \exp(-0.047\phi) \quad (4-7)$$

where the material parameter ϕ is expressed as

$$\phi = \delta_c (Ni + Si + Mn)^2(C + 0.4N)/5.0 \quad (4-8)$$

and from

$$\log_{10}Cv_{sat} = 7.28 - 0.011\delta_c - 0.185Cr - 0.369Mo - 0.451Si - 0.007Ni - 4.71(C + 0.4N) \quad (4-9)$$

Note, that the calculated Cv_{sat} value is conservatively used to represent Cv value in the following equations.

The J-R curve at RT, for static-cast CF8M steel is given by

$$J_d = 16 (Cv)^{0.67}(\Delta a)^n \quad \text{for } Cv \geq 35 \text{ J/cm}^2 \quad (4-10)$$

$$J_d = 1.44 (Cv)^{1.35}(\Delta a)^n \quad \text{for } Cv < 35 \text{ J/cm}^2 \quad (4-11)$$

$$n = 0.20 + 0.08 \log_{10} (Cv) \quad (4-12)$$

where J_d is the “deformation J” in kJ/m² and Δa is the crack extension in mm.

The J-R curve at 290-320°C (554-608°F), for static-cast CF8M steel is given by

$$J_d = 49 (Cv)^{0.41}(\Delta a)^n \quad \text{for } Cv \geq 46 \text{ J/cm}^2 \quad (4-13)$$

$$J_d = 5.5 (Cv)^{0.98}(\Delta a)^n \quad \text{for } Cv < 46 \text{ J/cm}^2 \quad (4-14)$$

$$n = 0.19 + 0.07 \log_{10} (Cv) \quad (4-15)$$

where J_d is the “deformation J” in kJ/m² and Δa is the crack extension in mm. Note that the operating temperatures used in the LBB evaluations are 611.1°F for Hot Leg and 542.8°F (for Crossover Leg and Cold Leg). Therefore, to obtain values at operating temperatures, data interpolation for 542.8°F and extrapolation for 611.1°F are performed using values calculated at RT condition (77°F) and hot condition (554-608°F). For hot condition, temperature upper bound (608°F) and temperature lower bound (554°F) are considered in the data interpolation/extrapolation processes, and then the minimum calculated value is conservatively selected.

J_{Ic} and J_{max} Calculations:

[

$$]^{a,c,e}$$

T_{mat} Calculations:

The material shearing modulus, T_{mat}, is calculated as follows:

$$T_{mat} = dJ/da \times E/(\sigma_{fa})^2$$

J_{app} and T_{app} Calculations:

The critical heats for CF8M with lowest fracture toughness property and lowest tearing modulus values from Table 4-8 on each Cold Leg, Hot Leg, and Crossover Leg are summarized in Table 4-9.

The applied J Integral value, J_{app}, is calculated and compared to the J_{Ic} and J_{max} values in Table 7-1 for Units 1 and 2.

Consideration of Dissimilar Metal Weld Material Profiles

Point Beach Unit 2 has Dissimilar Metal Weld (DMW) locations, i.e. alloy 82/182 welds at the safe-end-to Steam Generators inlet and outlet nozzles (at locations 3 and 4). However, the presence of this alloy that generates concern of Primary Water Stress Corrosion Cracking (PWSCC) has been mitigated with alloy 52/152 buttering on the inside surfaces of the welds to improve PWSCC resistance.

For local failure mechanism, the DMW locations are evaluated using the cast stainless steel material properties (A351-CF8M) as shown in Table 4-9 which present a limiting condition due to the thermal aging effects. As stated in Reference 4-3,

“The fracture resistance of Alloy 82 and 52 welds have been investigated by conducting fracture toughness J-R curve tests at 24 – 338 °C in deionized water [...]. The results indicate that these welds exhibit high fracture toughness in air and high-temperature water (> 93 °C).”

Since nickel alloys are known to have high toughness properties and because the CASS base metal of the RCL piping and elbows are susceptible to thermal aging degradation of the fracture toughness, it is determined that the CASS base metal presents the most limiting condition.

For the DMW locations 3 and 4, the evaluation is represented by J-integral evaluation for location 2 (hot leg) and location 8 (cross-over leg) based on CASS base metal (A351-CF8M) property that presents the most limiting condition. The evaluation results are presented in Table 7-1 and applicable for 80 year plant life period in SLR program.

4.4 REFERENCES

- 4-1 ASME Boiler and Pressure Vessel Code Section II, 2007 Edition through 2008 Addenda.
- 4-2 O. K. Chopra, "Estimation of Fracture Toughness of Cast Stainless Steels During Thermal Aging in LWR Systems," NUREG/CR-4513, Revision 2, U.S. Nuclear Regulatory Commission, Washington, DC, May 2016.
- 4-3 NUREG/CR-6721, "Effects of Alloy Chemistry, Cold Work, and Water Chemistry on Corrosion Fatigue and Stress Corrosion Cracking of Nickel Alloys and Welds," date published: April 2001.

Heat No.	Serial No.	Location	At Room Temperature		At 650°F	
			Yield Strength (psi)	Ultimate Strength (psi)	Yield Strength (psi)	Ultimate Strength (psi)
F0056	2627	Hot Leg	41900	82200	33100	72100
F0056	2627	Hot Leg	47600	90400	N/A	N/A
52154	1985Y	Hot Leg	32300	75000	24300	61000
52154	1985Y	Hot Leg	32400	75300	N/A	N/A
F0058	2630	Hot Leg	43500	86200	26600	71000
F0058	2630	Hot Leg	43900	85200	N/A	N/A
52154	1985X	Hot Leg	32400	75300	24300	61000
52154	1985X	Hot Leg	32300	75000	N/A	N/A
F0060	2633Y	Cold Leg	45000	89400	23100	74200
F0060	2632	Cold Leg	41600	86300	23100	74200
F0060	2632	Cold Leg	46900	89000	N/A	N/A
D8649	1475X	Cold Leg	32700	76400	20500	56700
D8649	1475X	Cold Leg	31700	75000	N/A	N/A
F0060	2633X	Cold Leg	41400	86100	23100	74200
52154	1983Y	X-Over Leg	34600	79300	20600	62200
V0246	1981	X-Over Leg	33200	75900	25300	68600
V0246	1981	X-Over Leg	31700	75500	N/A	N/A
52154	1983X	X-Over Leg	34000	75500	20600	62200
F0056	2626	X-Over Leg	40700	82200	22100	66800
F0056	2626	X-Over Leg	47000	87400	31800	74800

N/A= Not applicable

Heat No.	Serial No.	Location	At Room Temperature		At 650°F	
			Yield Strength (psi)	Ultimate Strength (psi)	Yield Strength (psi)	Ultimate Strength (psi)
F0213	2890Y	Hot Leg	41900	82500	23700	69800
F0213	2890Y	Hot Leg	46500	84500	N/A	N/A
F0227	2897Y	Hot Leg	42500	85500	20900	66600
F0227	2897Y	Hot Leg	41800	86800	N/A	N/A
F0225	2896Y	Hot Leg	44000	86900	22100	68200
F0225	2896Y	Hot Leg	48500	88900	N/A	N/A
F0225	2895Y	Hot Leg	42000	85900	22100	68200
F0225	2895Y	Hot Leg	46000	88800	N/A	N/A
F0382	3131	Cold Leg	45700	86900	25300	72600
F0382	3131	Cold Leg	45000	90500	N/A	N/A
V0631	3123	Cold Leg	37000	77200	22000	60000
V0631	3123	Cold Leg	47700	83500	N/A	N/A
F0212	2867Y	X-Over Leg	43500	84200	34400	67000
F0212	2867Y	X-Over Leg	43900	82300	N/A	N/A
F0221	2865Y	X-Over Leg	39300	82600	22600	65200
F0221	2865Y	X-Over Leg	45500	89000	N/A	N/A
F0212	2887Y	X-Over Leg	43500	84200	34400	67000
F0212	2887Y	X-Over Leg	43900	82300	N/A	N/A
E1483	3362	X-Over Leg	43200	89700	23700	52100
E1483	3362	X-Over Leg	42900	89900	N/A	N/A

N/A= Not applicable

Table 4-3: Measured Tensile Properties for Point Beach Unit 1 Primary Loop Elbows (A351-CF8M)			
Heat Number	Location	At Room Temperature	
		Yield Strength (psi)	Ultimate Strength (psi)
04258-6	Hot Leg ^a	46500	90000
04099-1	Hot Leg ^a	55500	89000
06874-2	Cold Leg ^b	45000	87000
07242-1	Cold Leg ^b	45000	85500
02710-2	X-Over Leg ^c	53000	92000
07392-1	X-Over Leg ^d	43500	85500
07896-1	X-Over Leg ^d	43500	85500
08849-1	X-Over Leg ^e	45000	92000
09439-1	X-Over Leg ^e	48000	91500
02259-1	X-Over Leg ^c	49500	88500
07599-1	X-Over Leg ^d	55500	92500
07848-1	X-Over Leg ^d	51000	88500
08325-1	X-Over Leg ^e	40500	85000
09216-1	X-Over Leg ^e	49500	92500

Note: a = 29-inch x 31-inch ID elbow - 50°
b = 27.5-inch ID elbow - 26°
c = 31-inch ID elbow - 40°
d = 31-inch ID elbow - 90°
e = 31-inch ID elbow - 90° w/ splitter

Table 4-4: Measured Tensile Properties for Point Beach Unit 2 Primary Loop Elbows (A351-CF8M)			
Heat Number	Location	At Room Temperature	
		Yield Strength (psi)	Ultimate Strength (psi)
10400-3	Hot Leg ^a	46500	89000
11007-1	Hot Leg ^a	45000	86000
11575-3	Cold Leg ^b	42000	82000
11556-4	Cold Leg ^b	43500	85000
12660-1	X-Over Leg ^c	42000	83000
12547-1	X-Over Leg ^d	43500	86500
13174-1	X-Over Leg ^d	45000	86000
11575-1	X-Over Leg ^e	40500	81500
11897-1	X-Over Leg ^e	42000	82000
12476-2	X-Over Leg ^c	40500	86000
12584-1	X-Over Leg ^d	42000	83000
12476-3	X-Over Leg ^d	42000	85500
11632-1	X-Over Leg ^e	37500	75000
12012-1	X-Over Leg ^e	42000	81500

Note: a = 29-inch x 31-inch ID elbow - 50°
b = 27.5-inch ID elbow - 26°
c = 31-inch ID elbow - 40°
d = 31-inch ID elbow - 90°
e = 31-inch ID elbow - 90° w/ splitter

Table 4-5 ASME Code Tensile Properties for Material A376-TP316 and A351-CF8M						
Temperature (°F)	A376-TP316			A351-CF8M		
	Yield Strength (ksi)	Ultimate Strength (ksi)	Elastic Modulus (ksi)	Yield Strength (ksi)	Ultimate Strength (ksi)	Elastic Modulus (ksi)
70	30.00	75.00	28300	30.00	70.00	28300
100	30.00	75.00	28300	30.00	70.00	28300
150	27.40	75.00	27900	27.30	70.00	27900
200	25.90	75.00	27500	25.80	70.00	27500
250	24.60	73.95	27250	24.50	69.00	27250
300	23.40	72.90	27000	23.30	68.00	27000
400	21.40	71.90	26400	21.40	67.20	26400
500	20.00	71.80	25900	19.90	67.20	25900
542.8 ^a	19.53	71.80	25643	19.43	67.20	25643
600	18.90	71.80	25300	18.80	67.20	25300
611.1 ^b	18.81	71.80	25245	18.71	67.20	25245
650	18.50	71.80	25050	18.40	67.20	25050
700	18.20	71.80	24800	18.10	67.20	24800

- Notes:
- a. XOL, CL operating temperature, value is interpolated.
 - b. HL operating temperature, value is interpolated.
 - c. Material properties are from the 2007 Edition of the ASME Boiler and Pressure Vessel Code (Reference 4-1).
 - d. Shaded cells are based on linear interpolation of the values provided in the ASME Code

**Table 4-6 Tensile Properties for Point Beach Units 1 and 2
Materials at Operating Temperatures**

Materials*	T** (°F)	Avg. Sy (psi)	Min. Sy (psi)	Min. Su (psi)	E (psi)	Poisson ratio
A376-TP316	542.8	26708	20636	52100	25643200	0.3
	611.1	25726	19877	52100	25244500	0.3
A351-CF8M	542.8	29259	24287	72000	25643200	0.3
	611.1	28178	23389	72000	25244500	0.3

* Material tensile properties are in unaged condition.

A376-TP316 tensile properties are unchanged in aged condition.

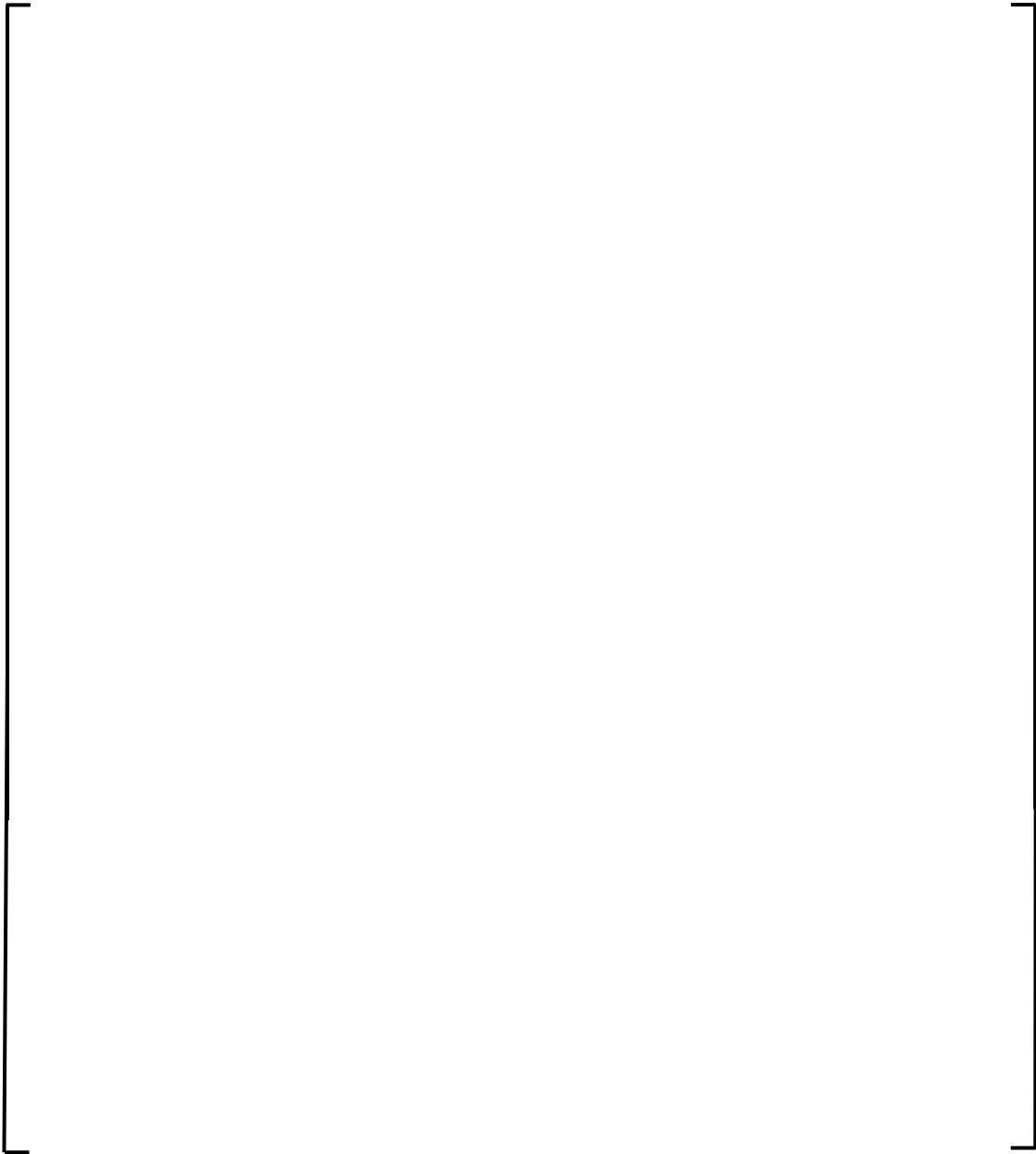
A351-CF8M tensile properties (Sy, and Su) increase due to thermal aging.

** The upper bound temperatures are used in this calculation note to reflect the operating temperature due to EPU program. The 542.8°F is the average between 542.7°F (Cross-over Leg) and 542.9°F (Cold Leg).

a.c.e

a,c,e

Note: As discussed in Section 4.3, the cast stainless steel fracture toughness properties present a limiting condition when compared to the alloys 82/182 and 52/152 fracture toughness properties found in Unit 2 SG (inlet/outlet) nozzle welds.



a,c,e

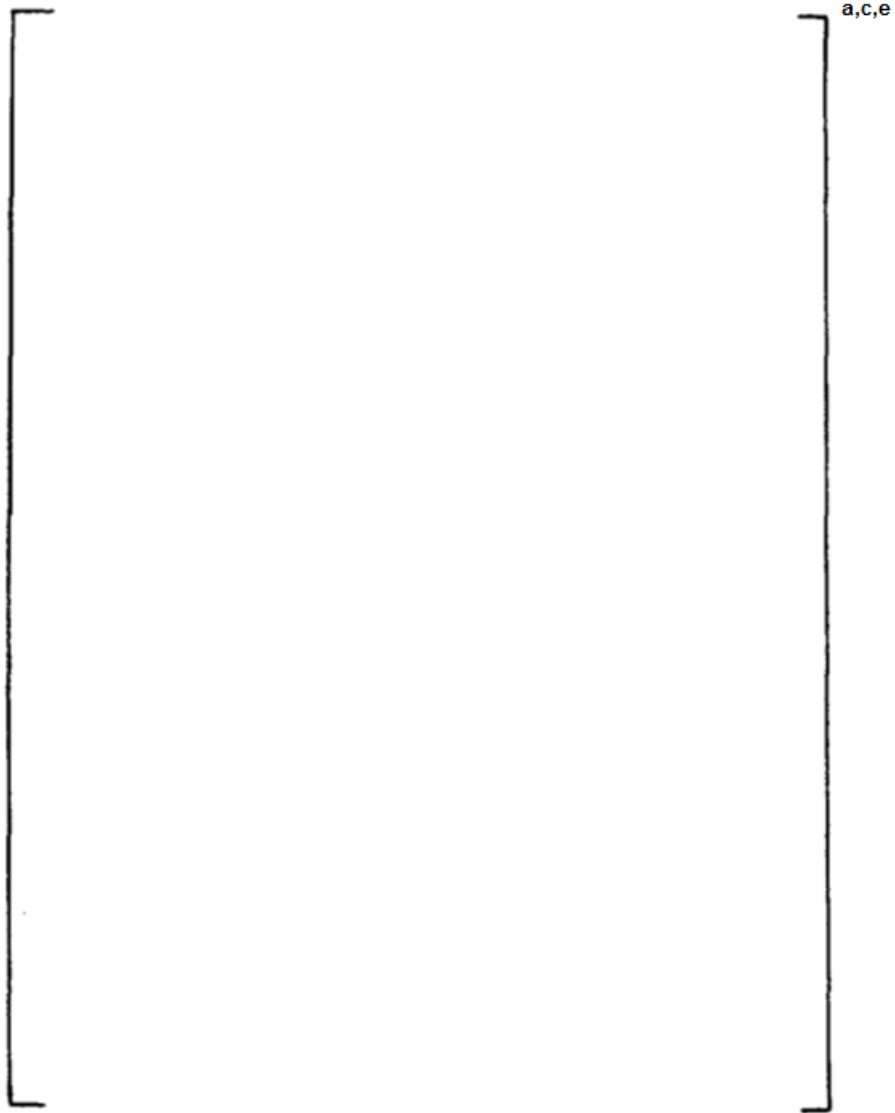


Figure 4-1 Pre-Service J vs. Δa for SA351-CF8M Cast Stainless Steel at 600°F

5.0 CRITICAL LOCATION AND EVALUATION CRITERIA

5.1 CRITICAL LOCATIONS

The governing or critical locations for the LBB evaluation are established based on the fracture toughness properties of the metal-base at the weld points and also on the basis of pipe geometry, welding process, operating temperature, operating pressure, and the highest faulted stresses at the welds.

The RCL weld points applicable for Point Beach Unit 1 and 2 are shown in Figure 3-2. However, the critical locations for LBB analysis are shown in Figure 5-1.

The highest stressed location for the entire primary loop (Figure 3-2) is at location 1 (in the hot leg) at the reactor vessel outlet nozzle to pipe weld. Location 1 is the critical location for all the weld locations in the primary loop piping. Furthermore, since it is on a straight pipe with forged material, it is a high toughness location.

Low toughness locations are at the ends of every elbow. In the case of the hot leg, low toughness are at locations 2 and 3 (Figure 3-2). Location 2 governs since it has a higher stress than location 3. In the case of cross-over leg, the lowest toughness is at locations 8 and 9. Location 8 governs since it has a higher stress than location 9. In the case of cold leg, the low toughness is at locations 11 and 12. Location 11 governs since it has a higher stress than location 12. It is thus concluded that the enveloping locations are 2, 8, and 11. The allowable toughness values for the critical locations are shown in Table 4-9.

It should be noted, that Point Beach Unit 2 SG inlet and outlet nozzles (locations 3 and 4) contain alloy 82/182 dissimilar metal welds which are susceptible to Primary Water Stress Corrosion Cracking (PWSCC). An inlay of the alloy 52/152 material was applied to these welds to mitigate the PWSCC. Based on the alloy 52/152 inlay material properties which are superior than the base-metal properties, and also the lesser faulted stresses as shown in Table 3-2, locations 3 and 4 are not critical locations.

For LBB evaluation, Table 5-1 shows the critical locations bounding both Point Beach Units 1 and 2. Figure 5-1 shows the locations of the critical welds for Point Beach Units 1 and 2.

5.2 EVALUATION CRITERIA

As will be discussed later, fracture mechanics analyses are made based on local failure mechanism as described in Section 7.1 and based on global failure mechanism as described in Section 7.2.

For local failure mechanism, stability analysis is performed using J-integral evaluation method with the criteria as follows:

- (1) If $J_{app} < J_{Ic}$, then the crack will not initiate, and the crack is stable;
- (2) If $J_{app} \geq J_{Ic}$; and $T_{app} < T_{mat}$ and $J_{app} < J_{max}$, then the crack is stable.

Where:

$$J_{app} = \text{Applied J}$$

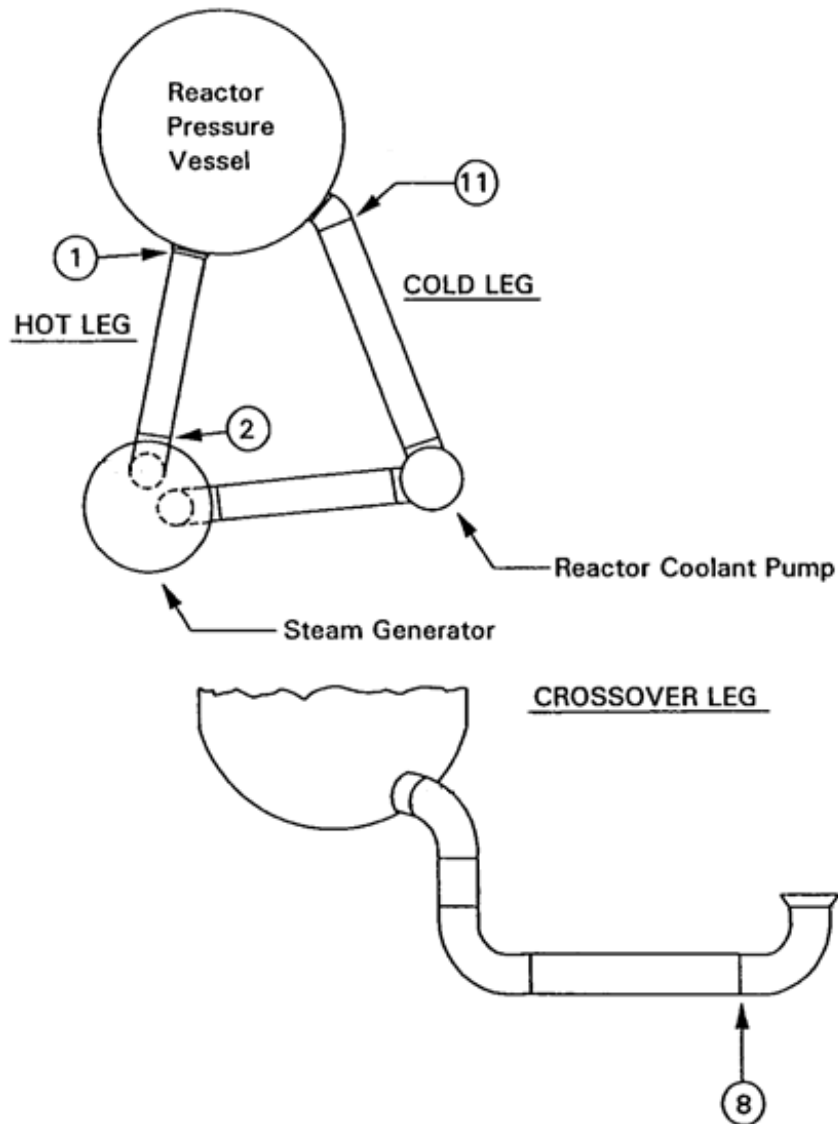
$$J_{Ic} = \text{J at Crack Initiation}$$

- T_{app} = Applied Tearing Modulus
 T_{mat} = Material Tearing Modulus
 J_{max} = Maximum J value of the material

For global failure mechanism, the stability analysis is performed using limit load method based on loads and postulated flaw sizes related to leakage, with the criteria as follows:

- Margin of 10 on the Leak Rate
- Margin of 2.0 on Flaw Size
- Margin of 1.0 on Loads (using the absolute summation method for faulted load combination).

Table 5-1 Critical Analysis Locations for Point Beach Units 1 and 2 RCL Lines						
Weld Pts.	D_o Pipe (in)	Thickness (in)	Welding Process	Operating Pressure (psia)	Operating Temperature (°F)	Maximum Faulted Stress (psi)
1	34.210	2.500	SAW	2250	611.1	18.12
2	34.210	2.500	SAW	2250	611.1	10.19
8	36.560	2.675	SAW	2250	542.8	10.36
11	32.460	2.375	SAW	2250	542.8	15.29



**Figure 5-1 Schematic Diagram of Point Beach Units 1 and 2
Primary Loop Showing Critical Weld Locations**

6.0 LEAK RATE PREDICTIONS

6.1 INTRODUCTION

The purpose of this section is to discuss the method which is used to predict the flow through postulated through-wall cracks and present the leak rate calculation results for through-wall circumferential cracks.

6.2 GENERAL CONSIDERATIONS

The flow of hot pressurized water through an opening to a lower back pressure causes flashing which can result in choking. For long channels where the ratio of the channel length, L , to hydraulic diameter, D_H , (L/D_H) is greater than [

] ^{a,c,e}

6.3 CALCULATION METHOD

The basic method used in the leak rate calculations is the method developed by [

] ^{a,c,e}

The flow rate through a crack was calculated in the following manner. Figure 6-1 from Reference 6-2 was used to estimate the critical pressure, P_c , for the primary loop enthalpy condition and an assumed flow. Once P_c was found for a given mass flow, the [^{a,c,e}] was found from Figure 6-2 (taken from Reference 6-2). For all cases considered, since [^{a,c,e}] Therefore, this method will yield the two-phase pressure drop due to momentum effects as illustrated in Figure 6-3, where P_o is the operating pressure. Now using the assumed flow rate, G , the frictional pressure drop can be calculated using

$$\Delta P_f = [\quad]^{a,c,e} \quad (6-1)$$

where the friction factor f is determined using the [^{a,c,e}] The crack relative roughness, ϵ , was obtained from fatigue crack data on stainless steel samples. The relative roughness value used in these calculations was [^{a,c,e}]

The frictional pressure drop using equation 6-1 is then calculated for the assumed flow rate and added to the [^{a,c,e}] to obtain the total pressure drop from the primary system to the atmosphere. That is, for the primary loop:

$$\text{Absolute Pressure} - 14.7 = [\quad]^{a,c,e} \quad (6-2)$$

for a given assumed flow rate G . If the right-hand side of equation 6-2 does not agree with the pressure difference between the primary loop and the atmosphere, then the procedure is repeated until equation 6-2 is satisfied to within an acceptable tolerance which in turn leads to flow rate value for a given crack size.

6.4 LEAK RATE CALCULATIONS

Leak rate calculations were made as a function of crack length at the governing locations previously identified in Section 5.1. The normal operating loads of Table 3-1 were applied in these calculations. The crack opening areas were estimated using the method of Reference 6-3, and the leak rates were calculated using the two-phase flow formulation described in the preceding section. The average material properties of Section 4.0 (see Table 4-6) were used for these calculations.

The flaw sizes to yield a leak rate of 10 gpm were calculated at the governing locations and are given in Table 6-1 for Point Beach Units 1 and 2. The flaw sizes so determined are called leakage flaw sizes (crack lengths).

The Point Beach Units 1 and 2 RCS pressure boundary leak detection system capability is 1 gpm in 4 hours. Thus, to satisfy the margin of 10 on the leak rate, the flaw sizes (leakage flaw sizes) (crack lengths) are determined which yield a leak rate of 10 gpm.

6.5 REFERENCES

- 6-1 []^{a,c,e}
- 6-2 M. M, El-Wakil, "Nuclear Heat Transport, International Textbook Company," New York, N.Y, 1971.
- 6-3 Tada, H., "The Effects of Shell Corrections on Stress Intensity Factors and the Crack Opening Area of Circumferential and a Longitudinal Through-Crack in a Pipe," Section II-1, NUREG/CR-3464, September 1983.

Table 6-1 Flaw Sizes for Point Beach Units 1 and 2 Yielding a Leak Rate of 10 gpm for the RCL Lines	
Weld Points	Leakage Flaw Size (in)
1	5.47
2	7.56
8	7.94
11	6.82

Note: The flaw size in the Table 6-1 refers to the flaw length of through-wall circumferential crack.

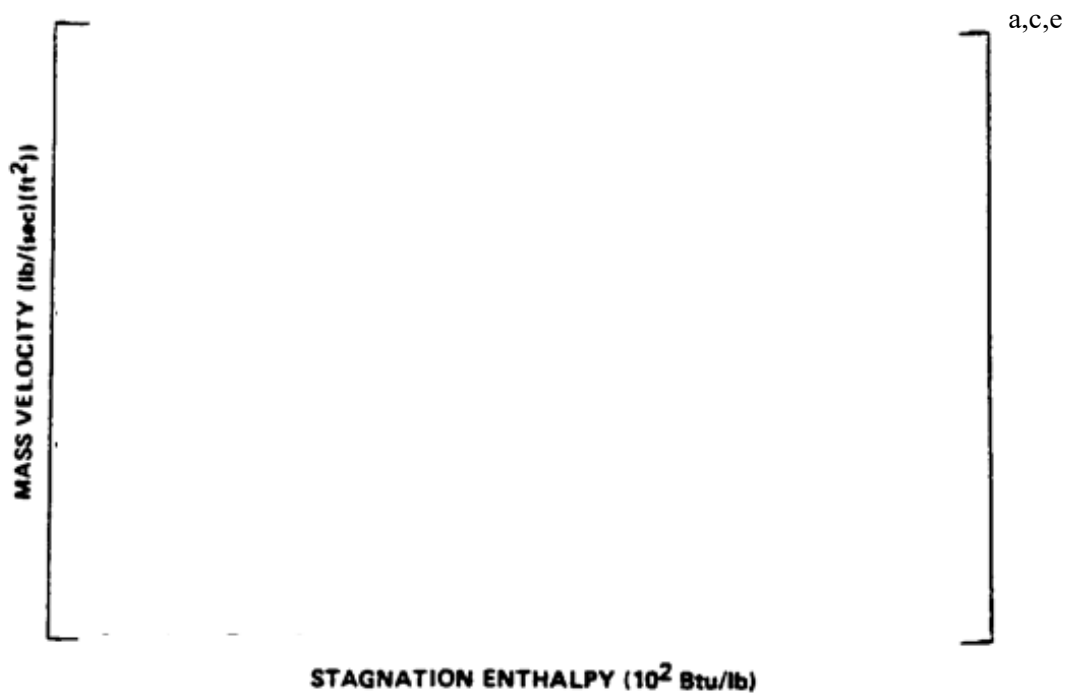


Figure 6-1 Analytical Predictions of Critical Flow Rates of Steam-Water Mixtures



Figure 6-2 [

] ^{a,c,e} Pressure Ratio as a Function of L/D

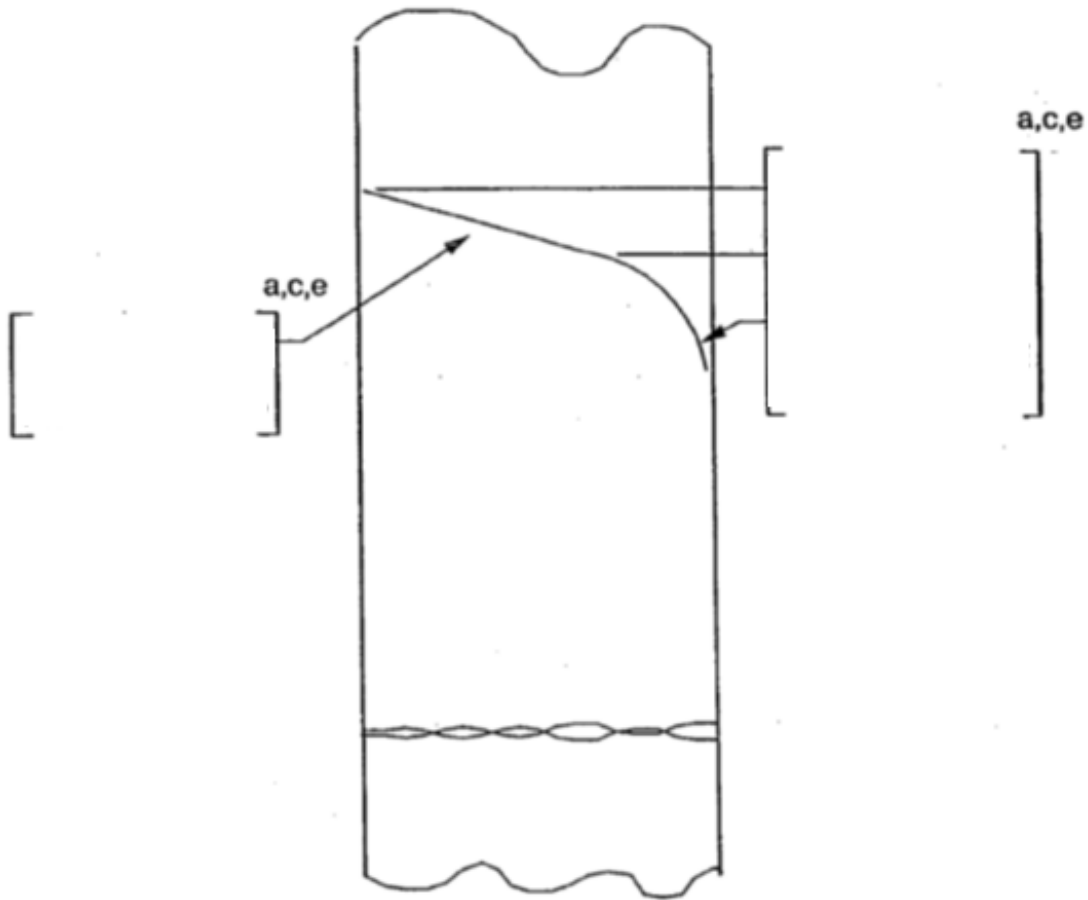


Figure 6-3 Idealized Pressure Drop Profile Through a Postulated Crack

7.0 FRACTURE MECHANICS EVALUATION

7.1 LOCAL FAILURE MECHANISM

The local mechanism of failure is primarily dominated by the crack tip behavior in terms of crack-tip blunting, initiation, extension, and final crack instability. The local stability will be assumed if the crack does not initiate at all. It has been accepted that the initiation toughness measured in terms of J_{Ic} from a J-integral resistance curve is a material parameter defining the crack initiation. If, for a given load, the calculated J-integral value is shown to be less than the J_{Ic} of the material, then the crack will not initiate. If the initiation criterion is not met, one can calculate the tearing modulus as defined by the following relation:

$$T_{app} = \frac{dJ}{da} \times \frac{E}{\sigma_f^2} \quad (7-1)$$

where:

T_{app}	=	applied tearing modulus
E	=	modulus of elasticity
σ_f	=	$0.5 (\sigma_y + \sigma_u)$ = flow stress
a	=	crack length
σ_y, σ_u	=	yield and ultimate strength of the material, respectively

Stability is said to exist when ductile tearing does not occur if T_{app} is less than T_{mat} , the experimentally determined tearing modulus. Since a constant T_{mat} is assumed a further restriction is placed in J_{app} . J_{app} must be less than J_{max} where J_{max} is the maximum value of J for which the experimental T_{mat} is greater than or equal to the T_{app} used.

As discussed in Section 5.2 the local crack stability criteria is a two-step process:

- (1) If $J_{app} < J_{Ic}$, then the crack will not initiate, and the crack is stable;
- (2) If $J_{app} \geq J_{Ic}$; and $T_{app} < T_{mat}$ and $J_{app} < J_{max}$, then the crack is stable.

Previous evaluations of local failure for the Point Beach Units 1 and 2 RCL piping were based on a conservative approach using linear elastic fracture mechanics (LEFM). While piping loads, geometry, materials, and stress are not changing for the 80-year SLR Program, the decrease in fracture toughness properties due to thermal aging (Section 4.3) has shown that LEFM is too conservative for some critical analysis locations. As needed, these locations are evaluated using a more realistic approach using elastic-plastic fracture mechanics (EPFM). The evaluation results using LEFM and EPFM approaches are provided in Table 7-1.

7.1.1 Linear Elastic Fracture Mechanics (LEFM)

[

]a,c,e

7.1.2 Elastic-Plastic Fracture Mechanics (EPFM)

At location 8, the J_{app} value of []^{a,c,e} calculated using LEFM method in Section 7.1.1 is greater than the updated J_{Ic} value of []^{a,c,e} for Cross-over leg as shown in Table 4-9; therefore, the crack stability criteria would not be satisfied. In order to meet the criteria, J_{app} value is recalculated using Elastic-Plastic Fracture Mechanics (EPFM) method, a methodology developed in References 7-5 and 7-6. The location 8 stability results based on EPFM method are provided in Table 7-1.

7.2 GLOBAL FAILURE MECHANISM

Determination of the conditions which lead to failure in stainless steel should be done with plastic fracture methodology because of the large amount of deformation accompanying fracture. One method for predicting the failure of ductile material is the plastic instability method, based on traditional plastic limit load concepts, but accounting for strain hardening and taking into account the presence of a flaw. The flawed pipe is predicted to fail when the remaining net section reaches a stress level at which a plastic hinge is formed. The stress level at which this occurs is termed as the flow stress. The flow stress is generally taken as the average of the yield and ultimate tensile strength of the material at the temperature of interest. This methodology has been shown to be applicable to ductile piping through a large number of experiments and will be used here to predict the critical flaw size in the primary coolant piping. The failure criterion has been obtained by requiring equilibrium of the section containing the flaw (Figure 7-1) when loads are applied. The detailed development is provided in Appendix A for a through-wall circumferential flaw in a pipe with internal pressure, axial force, and imposed bending moments. The limit moment for such a pipe is given by:

$$[] \quad (7-6)$$

$$(7-7)$$

$$]^{a,c,e}$$

The analytical model described above accurately accounts for the piping internal pressure as well as imposed axial force as they affect the limit moment. Good agreement was found between the analytical predictions and the experimental results (Reference 7-1). For application of the limit load methodology, the material, including consideration of the configuration, must have a sufficient ductility and ductile tearing resistance to sustain the limit load.

A stability analysis based on limit load was performed for all the critical locations (locations 1, 2, 8, and 11). For the RCL Lines of Point Beach Units 1 and 2, the SAW weld processes are conservatively assumed to be used. The "Z" factor correction for SAW was applied per References 7-7 and 7-8:

$$Z = 1.30 [1.0 + 0.01 (OD-4)] \quad \text{for SAW} \quad (7-8)$$

where OD is the outer diameter of the pipe in inches.

The Z-factors were calculated for the critical locations, using the dimensions given in Tables 3-1 and 3-2. The applied loads were increased by the Z factors. Table 7-2 summarizes the results of the stability analyses based on limit load. The leakage flaw sizes are also presented on the same table.

7.3 UNIT 2 SGIN AND SGON ALLOY 82/182 WELDS

Point Beach Unit 2 reactor coolant system primary loop piping contains alloy 82/182 dissimilar metal welds which are susceptible to Primary Water Stress Corrosion Cracking (PWSCC). The alloy 82/182 welds are at Steam Generator Inlet and Outlet Nozzles (SGIN's and SGON's). Weld inlay has been applied for both nozzles using inlay of alloy 52/152 material to prevent PWSCC. In summary, the potential PWSCC have been mitigated by weld inlay, therefore no further evaluations are required for those locations for the SLR program (80-year plant service), because the base metal properties are more limiting for the fracture mechanics evaluations.

7.4 REFERENCES

- 7-1 Kanninen, M. F., et. al., "Mechanical Fracture Predictions for Sensitized Stainless Steel Piping with Circumferential Cracks," EPRI NP-192, September 1976.
- 7-2 Johnson, W. and Mellor, P. B., Engineering Plasticity, Van Nostrand Reinhold Company, New York, (1973), pp. 83-86.
- 7-3 Tada, H., "The Effects of Shell Corrections on Stress Intensity Factors and the Crack Opening Area of Circumferential and a Longitudinal Through-Crack in a Pipe," Section II-1, NUREG/CR-3464, September 1983.
- 7-4 Irwin, G. R., "Plastic Zone Near a Crack and Fracture Toughness," Proc. 7th Sagamore Conference, P. IV-63 (1960).
- 7-5 []^{a,c,e}
- 7-6 []^{a,c,e}
- 7-7 Standard Review Plan; Public Comment Solicited; 3.6.3 Leak-Before-Break Evaluation Procedures; Federal Register/Vol. 52, No. 167/Friday, August 28, 1987/Notices, pp. 32626-32633.
- 7-8 NUREG-0800 Revision 1, March 2007, Standard Review Plan: 3.6.3 Leak-Before-Break Evaluation Procedures.

a,c,e



Table 7-2 Flaw Stability Results for Point Beach Units 1 and 2 Yielding a Leak Rate of 10 gpm for the RCL Lines Based on Limit Load		
Weld Points	Leakage Flaw Size (in)	Critical Flaw Size (in)
1	5.47	19.88
2	7.56	31.65
8	7.94	34.07
11	6.82	23.85

Note: results are based on the limiting material properties of the A376-TP316 base-metal.

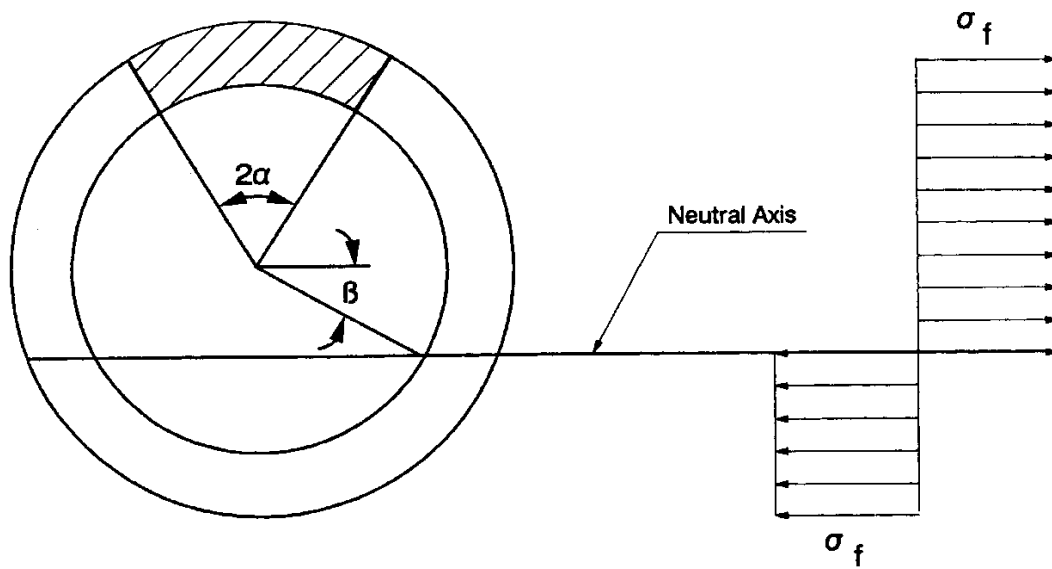


Figure 7-1 |]^{a,c,e} Stress Distribution

8.0 FATIGUE CRACK GROWTH ANALYSIS

To determine the sensitivity of the primary coolant system to the presence of small cracks, a fatigue crack growth analysis was carried out for the []^{a,c,e} region of a typical system (see Location []^{a,c,e} of Figure 3-2). This region was selected because crack growth calculated here will be typical of that in the entire primary loop. Crack growths calculated at other locations can be expected to show minimal variation.

Even-though the Point Beach plant does not have Inconel alloy 600 weld at the vessel inlet nozzle, the Inconel 600 weld exists at the Unit 2 SG inlet and outlet nozzles. From the crack growth point of view, the crack growth at the vessel inlet nozzle remains typical. Therefore, the plant typical evaluation at the vessel inlet nozzle with Inconel alloy 600 is used in this calculation note, to represent the evaluation of FCG at the primary equipment nozzles including at the SG inlet and outlet nozzles. Fatigue crack growth results for the Inconel 182 and Inconel 152 welds are expected to be about the same as Inconel 600 weld.

A []^{a,c,e} of a plant typical in geometry and operational characteristics to any Westinghouse PWR System. []

] ^{a,c,e}

The normal, upset, and test conditions were considered. Circumferentially oriented surface flaws are postulated in the region, assuming the flaw was located in three different locations, as shown in Figure 8-1.

Specifically, these are:



Fatigue crack growth rate laws were used []

] ^{a,c,e}

The law for stainless steel was derived from Reference 8-1, a compilation of data for austenitic stainless steel in a PWR water environment was presented in Reference 8-2, and it is found that the effect of the environment on the crack growth rate was very small. From this information it was estimated that the environmental factor should be conservatively set at []^{a,c,e} in the crack growth equation from Reference 8-1.

For stainless steel, the fatigue crack growth formula is:

[] (8-1)

*** This record was final approved on 6/11/2020 11:23:07 AM. (This statement was added by the PRIME system upon its validation)

[] a,c,e	
[] a,c,e	(8-2)

The calculated fatigue crack growth for semi-elliptic surface flaws of circumferential orientation and various depths is summarized in Table 8-2, and shows that the crack growth is very small, regardless of which material is assumed.

The reactor vessel transients and projected 80-year cycles for Point Beach Units 1 and 2 are shown in Table 8-3. By comparing the transients and cycles for the original Point Beach 40-year design basis analysis shown in Table 8-1 and the Point Beach transients and cycles shown in Table 8-3 for 80 years of operation, it is concluded that the transients and cycles used for the fatigue crack growth analysis enveloped the 80-year design of Point Beach.

The fatigue crack growth analysis is not a requirement for the LBB analysis (see References 8-5 and 8-6) since the LBB analysis is based on the postulation of through-wall flaws, whereas the FCG analysis is performed based on a surface flaw. In addition, Reference 8-7 has indicated that, “the Commission deleted the fatigue crack growth analysis in the proposed rule. This requirement was found to be unnecessary because it was bounded by the crack stability analysis.”

It is therefore, concluded that the fatigue crack growth analysis results shown in Table 8-2 are representative of the Point Beach plants fatigue crack growth for 80 years.

8.1 REFERENCES

- 8-1 James, L.A. and Jones, D. P., "Fatigue Crack Growth Correlations for Austenitic Stainless Steel in Air, Predictive Capabilities in Environmentally Assisted Cracking," ASME publication PVP-99, December 1985.
- 8-2 Bamford, W. H., "Fatigue Crack Growth of Stainless Steel Piping in a Pressurized Water Reactor Environment," Trans. ASME Journal of Pressure Vessel Technology, Vol. 101, Feb. 1979.
- 8-3 James, L.A., "Fatigue Crack Propagation Behavior of Inconel 600," in Hanford Engineering Development Labs Report HEDL-TME-76-43, May 1976.
- 8-4 Hale, D. A., et. al., "Fatigue Crack Growth in Piping and RPV Steels in Simulated BWR Water Environment," Report GEAP 24098/NUREG CR-0390, Jan. 1978.
- 8-5 Standard Review Plan: Public Comments Solicited; 3.6.3 Leak-Before-Break Evaluation Procedures; Federal Register/Vol. 52, No. 167/Friday August 28, 1987/Notices, pp. 32626-32633.
- 8-6 NUREG-0800, Revision 1, "Standard Review Plan: 3.6.3 Leak-Before-Break Evaluation Procedures" March 2007.
- 8-7 Nuclear Regulatory Commission, 10 CFR 50, Modification of General Design Criteria 4 Requirements for Protection Against Dynamic Effects of Postulated Pipe Ruptures, Final Rule, Federal Register/Vol. 52, No. 207/Tuesday, October 27, 1987/Rules and Regulations, pp. 41288-41295.
- 8-8 []^{a,c,e}

Table 8-1 Summary of Reactor Vessel Transients for FCG Evaluation		
Number	Transient Identification	Number of Cycles
	Normal Conditions and Upset Conditions	
1	Heat Up/Cool Down at 100° F/hr (pressurizer cool down 200° F/hr)	200
2	Load Follow Cycles (Unit loading and unloading at 5% of full power/min.)	18300
3	Step load increase and decrease	2000
4	Large step load decrease, with steam dump	200
5	Feed water Cycling at Hot Standby	25000
6	Loss of Load, without immediate turbine or reactor trip	80
7	Loss of Power (blackout with natural circulation in the Reactor Coolant System)	40
8	Loss of Flow (partial loss of flow, one pump only)	80
9	Reactor Trip from full power	400
10	Inadvertent Auxiliary Spray	10
	Test Conditions	
11	Primary Hydro @3106 psig	5
12	Primary Pressure Test @2485 psig	100
13	Secondary Hydrotest @1356 psig	10
14	Secondary Pressure Test @1085 psig	50
15	Primary-to-Secondary Leak Tests	30
16	Secondary-to-Primary Leak Tests	130

Table 8-2 Fatigue Crack Growth at []^{a,c,e} (80 years)			
Initial Flaw Depth (in.)	Final Flaw Depth (in.)		
	[] ^{a,c,e}	[] ^{a,c,e}	[] ^{a,c,e}
0.292	0.2944	0.2948	0.2924
0.300	0.3025	0.3028	0.3004
0.375	0.3785	0.3785	0.3756
0.425	0.4290	0.4288	0.4257

Table 8-3 Point Beach Units 1 and 2 Transient Cycle Projections to 80 Years		
Number	Transient Identification	Projected Cycles
	Normal Conditions and Upset Conditions	
1	RCS Heat Up	120
	RCS Cool Down	120
2	Unit Loading 5%/min	8000
	Unit Unloading 5%/min	8000
3	10% Step Load Decrease	100
	10% Step Load Increase	20
4	50% Step Load Decrease	100
5	Feed Water Cycling at Hot Standby	2000
6	Loss of Load (Trip)	80
7	Loss of Power (Trip)	40
8	Loss of Flow (Trip)	80
9	Reactor Trip	120
10	Auxiliary Spray Actuation	2
	Test Conditions	
11	Primary Side Hydrostatic Test	3
12	Primary Side Leak Test	60
13	Secondary Side Hydrostatic Test	see note (1)
14	Secondary Side Leak Test	see note (1)
15	Primary to Secondary Leak Test	15
16	Secondary to Primary Leak Test	60

Notes:

(1) Transients 13 and 14 are not in the design basis for Point Beach, but cycles are conservatively included in the FCG evaluation as shown in Table 8-1.

(2) A reduction of cycles for some transients has been applied to the Baffle Former Bolt components of Point Beach Units 1 and 2. These reductions are not applicable for the RCL piping and are not reflected in this table.



Figure 8-1 Typical Cross-Section of []^{a,c,e}

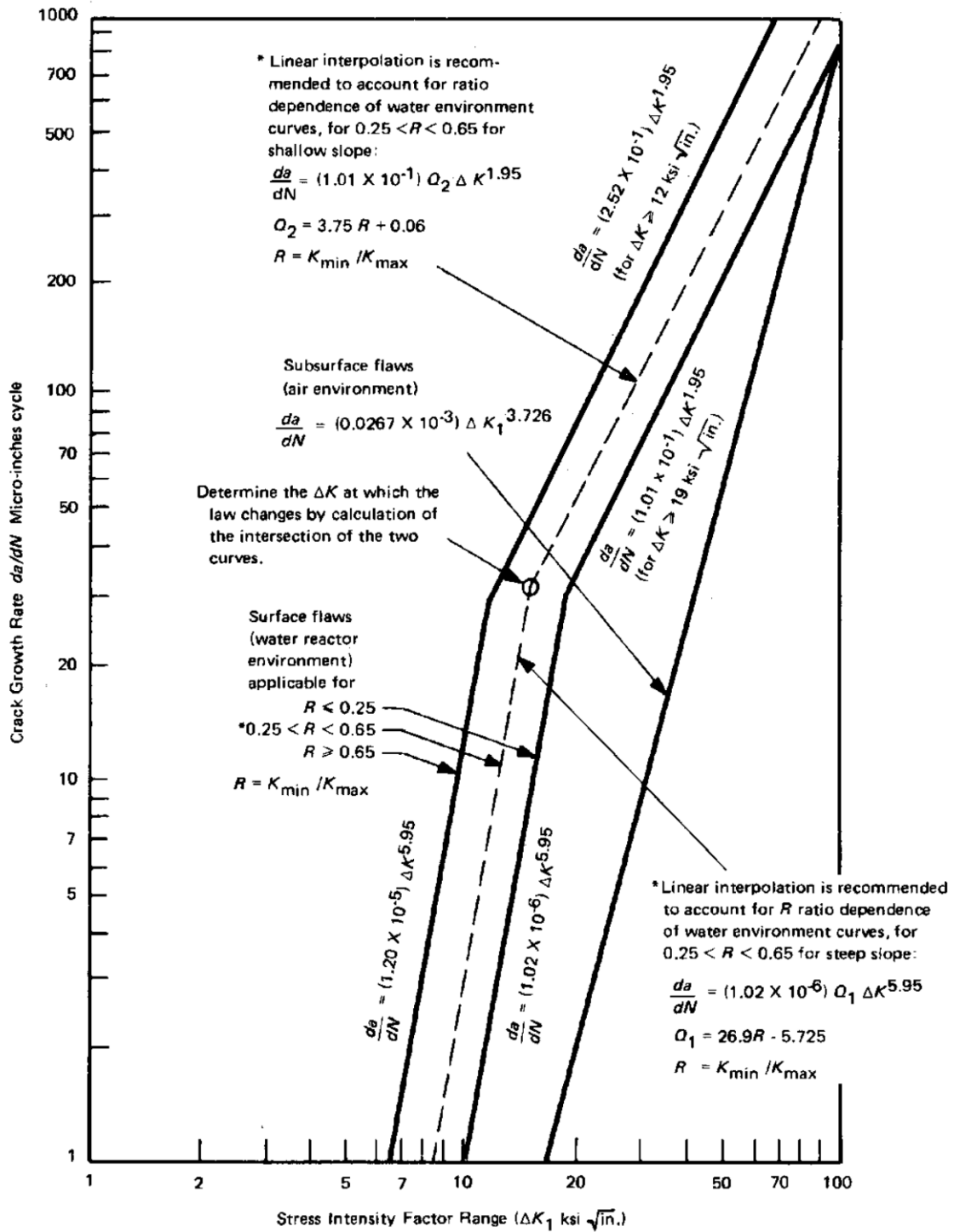
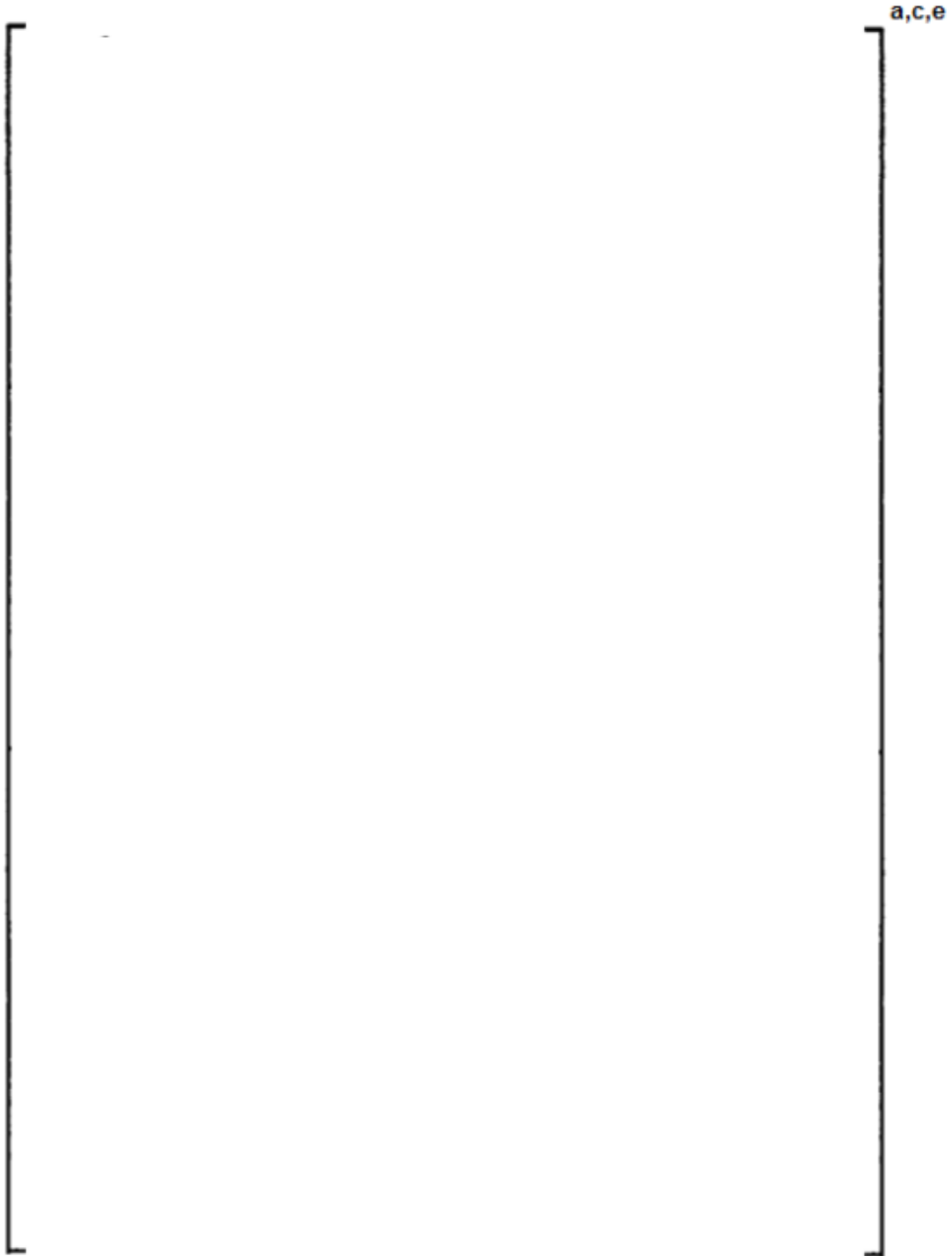


Figure 8-2 Reference Fatigue Crack Growth Curves for Carbon & Low Alloy Ferritic Steels



**Figure 8-3 Reference Fatigue Crack Growth Law for []^{a,c,e}
in a Water Environment at 600°F**

9.0 ASSESSMENT OF MARGINS

The results of the leak rates of Section 6.4 and the corresponding stability and fracture toughness evaluations of Sections 7.1 and 7.2 are used in performing the assessment of margins. Margins are shown in Table 9-1 for Units 1 and 2. All of the LBB recommended margins are satisfied. The LBB analyses results are acceptable for the subsequent license renewal program (80 years).

In summary, at all the critical locations relative to:

1. Flaw Size - Using faulted loads obtained by the absolute sum method, a margin of 2 or more exists between the critical flaw and the flaw having a leak rate of 10 gpm (the leakage flaw).
2. Leak Rate - A margin of 10 exists between the calculated leak rate from the leakage flaw and the plant leak detection capability of 1 gpm.
3. Loads - At the critical locations the leakage flaw was shown to be stable using the faulted loads obtained by the absolute sum method (i.e., a flaw twice the leakage flaw size is shown to be stable; hence the leakage flaw size is stable). A margin of 1 on loads using the absolute summation of faulted load combinations is satisfied.

Location	Leakage Flaw Size (in)	Critical Flaw Size (in)	Margin
1	5.47	19.88 ^a	3.64 ^a
2	7.56	31.65 ^a	4.19 ^a
	7.56	15.12 ^b	>2.0 ^b
8	7.94	34.07 ^a	4.29 ^a
	7.94	15.88 ^b	>2.0 ^b
11	6.82	23.85 ^a	3.50 ^a
	6.82	13.64 ^b	>2.0 ^b

^abased on limit load

^bbased on J integral evaluation

10.0 CONCLUSIONS

This report justifies the elimination of RCS primary loop pipe breaks from the structural design basis for the 80-year plant life of Point Beach Units 1 and 2 as follows:

- a. Stress corrosion cracking is precluded by use of fracture resistant materials in the piping system and controls on reactor coolant chemistry, temperature, pressure, and flow during normal operation. Alloy 82/182 welds are present at the Point Beach Unit 2 SGIN's and SGON's. The alloy 82/182 welds are susceptible to PWSCC (Primary Water Stress Corrosion Cracking).
- b. To mitigate PWSCC due to the existence of alloy 82/182, weld inlay has been applied to the Point Beach Unit 2 SGIN's and SGON's, therefore no further consideration of PWSCC effects is required for SLR program.
- c. As stated in Section 3.0, for global failure mechanisms, all locations are evaluated using the stainless steel material properties (A376-TP316). For local failure mechanisms, all locations are evaluated using the cast stainless steel material properties (A351-CF8M) which present a limiting condition due to the thermal aging effects.
- d. Evaluation of the RCS piping considering the thermal aging effects for the 80-year plant life period of the SLR program and also the use of the most limiting fracture toughness properties ensures that each materials profile is appropriately bounded by the LBB results presented in this report.
- e. Water hammer should not occur in the RCS piping because of system design, testing, and operational considerations.
- f. The effects of low and high cycle fatigue on the integrity of the primary piping are negligible.
- g. Ample margin exists between the leak rate of small stable flaws and the capability of the Point Beach Units 1 and 2 reactor coolant system pressure boundary Leakage Detection System.
- h. Ample margin exists between the small stable flaw sizes of item (e) and larger stable flaws.
- i. Ample margin exists in the material properties used to demonstrate end-of-service life (fully aged) stability of the critical flaws.

For the critical locations, flaws are identified that will be stable because of the ample margins described in e, f, and g above.

Based on the above, the Leak-Before-Break conditions and margins are satisfied for the Point Beach Units 1 and 2 primary loop piping. All the recommended margins are satisfied. It is therefore concluded that dynamic effects of RCS primary loop pipe breaks need not be considered in the structural design basis for Point Beach Units 1 and 2 Nuclear Power Plants for the 80-year plant life (subsequent license renewal program).

APPENDIX A: LIMIT MOMENT

[

]a,c,e



Figure A-1 Pipe with a Through-Wall Crack in Bending

This page was added to the quality record by the PRIME system upon its validation and shall not be considered in the page numbering of this document.

Approval Information

Author Approval Wiratmo Momo Jun-11-2020 10:51:16

Verifier Approval Johnson Eric D Jun-11-2020 10:55:15

Manager Approval Patterson Lynn Jun-11-2020 11:23:07

Files approved on Jun-11-2020

*** This record was final approved on 6/11/2020 11:23:07 AM. (This statement was added by the PRIME system upon its validation)

Enclosure 4

**Non-proprietary Reference Documents and
Redacted Versions of Proprietary Reference
Documents**

(Public Version)

Attachment 17

**Westinghouse LTR-SDA-II-20-06, Revision 1, “Leak-
Before-Break Reconciliation of the Point Beach Units
1 and 2 Pressurizer Surge Line, Residual Heat
Removal Line, and Accumulator Line Piping Systems
for the Subsequent License Renewal Program,”
May 4, 2020**

(5 Total Pages, including cover sheets)



To: John T. Ahearn

Date: May 04, 2020

From: M. Wiratmo

Ext: 412-374-4296

Fax: N/A

Our ref: LTR-SDA-II-20-06

Revision 1

Subject: Leak-Before-Break Reconciliation of the Point Beach Units 1 and 2 Pressurizer Surge Line, Residual Heat Removal Line, and Accumulator Line Piping Systems for the Subsequent License Renewal Program

References:

1. WCAP-15065-P-A, Revision 1, "Technical Justification for Eliminating Pressurizer Surge Line Rupture as the Structural Design Basis for Point Beach Units 1 and 2 Nuclear Plants," June 2001.
2. WCAP-15105-P-A, Revision 1, "Technical Justification for Eliminating Residual Heat Removal (RHR) Rupture as the Structural Design Basis for Point Beach Units 1 and 2 Nuclear Plants," June 2001.
3. WCAP-15107-P-A, Revision 1, "Technical Justification for Eliminating Accumulator Rupture as the Structural Design Basis for Point Beach Units 1 and 2 Nuclear Plants," June 2001.
4. CN-PAFM-08-54 Revision 0, "Point Beach Units 1 and 2 Extended Power Uprate (EPU) Leak-Before-Break (LBB) Evaluation for Reactor Coolant Loop, Accumulator, RHR, and Surge Line," September 25, 2008.
5. Westinghouse Performance Capability Working Group (PCWG) Letters:
 - a. PCWG-07-49, "Point Beach Units 1 & 2 (WEP/WIS): Approval of Category III (for Contract) PCWG Parameters to Support the EPU Program," October 15, 2007.
 - b. PCWG-11-9, Point Beach Units 1 & 2 (WEP/WIS): Approval of Category IV (for Implementation) PCWG Parameters to Support the Extended Power Uprate (EPU) Program," June 13, 2011.
6. LTR-CPS-08-19, "NSSS Design Transients for Point Beach Units 1 and 2 EPU Program." February 15, 2008.
7. LTR-SMT-03-6, "Deliverable for the NMC Purchase Order Number 3618 LI001, Task Number: WTN 2002/009 Rev. 0," 1/27/03 (note: the letter documents the applicability of References 1, 2, 3 for 60-year licensed operating period).
8. NextEra Energy Letter, PBNWEC-20-0020 R1, April 21, 2020 (note: the letter documents the responses to the three requests for information (RFI) as requested by Westinghouse Letter WEC-NEE-PB-SLR-20-002, NEXT20-17 dated January 27, 2020: Input Request for Leak-Before-Break Data).
9. Enercon Comment and Resolution Form, CSP 3.08 Revision 1 Attachment C, "Document Reviewed: LTR-SDA-II-20-06 Rev 0," acceptance date 5/4/2020 (electronically attached in PRIME).

The purpose of this letter is to confirm that the previous evaluations provided in References 1 to 3 remain valid for the Point Beach Units 1 and 2 during 80-year plant operation to support the Subsequent License Renewal (SLR) program.

Revision 1 of this letter is issued to incorporate the review comments provided in Comment and Resolution Form (Reference 9).

Westinghouse had performed Leak-Before-Break (LBB) evaluations for Point Beach Units 1 and 2 in the year of 2001 for Pressurizer Surge Line (Reference 1), Residual Heat Removal (RHR) Line (Reference 2), and Accumulator Line (Reference 3). References 1, 2, and 3 specifically provided the LBB evaluation results for 1.7% Uprating. Reference 7 documents the applicability of References 1, 2, 3 for 60-year licensed operating period. It was concluded that the dynamic effects of pipe breaks in the Pressurizer Surge Lines, RHR Lines and Accumulator Lines need not be considered in the structural design basis of Point Beach Units 1 and 2.

In 2008, Westinghouse also performed an LBB evaluation (Reference 4) for the Point Beach Units 1 and 2, due to the Extended Power Uprate (EPU) program. The evaluation was based on operating parameters which were provided in PCWG parameters Approval for Contract (Reference 5a) for the EPU program. The status of EPU PCWG parameters in Reference 5a was later updated as Approval for Implementation in Reference 5b. Reference 4 concluded that References 1 to 3 which were applicable for 60-year plant operation remained valid for the EPU program.

PCWG parameters (References 5a and 5b) provided the operating parameters that were intended for the Point Beach Units 1 and 2 EPU program. Based on the review of EPU PCWG parameters and the operating conditions used in References 1 to 3, it was determined in Reference 4 that the temperature differences for the hot leg, cross-over leg, and cold legs did not significantly change the pre-EPU LBB loads used in References 1 to 3. The temperature differences also did not significantly impact the material properties used in the LBB analyses. In Reference 4, it was determined that the minor changes have negligible impact on the 2001 LBB analysis results. For the SLR program, Reference 8 confirms that there are no further changes to LBB piping loads provided to Westinghouse. A review of the LBB piping loads generated by Westinghouse also confirms that those loads remain applicable for SLR.

LTR-CPS-08-19 (Reference 6) provided updated design transient definitions based on the EPU program, as well as showing the transient cycles for the 60-year license renewal period. The fatigue crack growth (FCG) analyses summarized in References 1 to 3 use similar design transients and cycles. Minor differences in the time history temperature and pressure conditions will have a negligible impact on the FCG results and conclusions. Furthermore, Reference 8 provides the projection of transient cycles for the 80-year SLR program. Based on a review of the transient inputs provided in Reference 8, the projected cycles for monitored transients remain below the 40-year design basis cycles which were applied in LBB evaluations as documented in References 1 to 3. It can be seen that there is a great amount of conservatism in the analyzed cycles for many of the transient events. Also, for transients that are not monitored, the cycles for 80 years do not exceed the 40 year design basis used in the LBB evaluation. As such it can be concluded that the FCG analyses and results in References 1 to 3 remain valid for the SLR program.

For Pressurizer Surge Line, RHR Line and Accumulator Line piping and fittings, thermal aging is not an issue because there is no cast material in any of the lines.

For the SLR program, the existing LBB loads for Pressurizer Surge Line, RHR Line and Accumulator Line piping do not change in the post-EPU program implementation, as confirmed in Reference 8.

Based on the negligible impact of the PCWG operating parameters and also based on the continued applicability of the design transients and the piping loads, it is concluded that LBB evaluation results for 1.7% uprating, 60-year LR and EPU program are also valid for the 80-year plant operation to support SLR program.

This letter demonstrates that the LBB conclusions provided in current LBB analyses for Point Beach Units 1 and 2 as documented in References 1 to 3 remain valid and applicable for the 80-year plant operation Subsequent License Renewal program. It is therefore concluded that the dynamic effects of auxiliary line pipe breaks need not be considered in the structural design basis of the Point Beach Units 1 and 2 Pressurizer Surge Line, RHR Line and Accumulator Line.

Conclusion:

TLAA Disposition: 10 CFR 54.21(c)(1)(i)

The LBB analyses associated with the pressurizer surge line, residual heat removal line, and accumulator line have been evaluated and determined to remain valid for the subsequent period of extended operation (SPEO).

If you have any questions, please call the undersigned.

Author: Momo Wiratmo*
Operating Plants Piping and Supports

Verifier: Eric D. Johnson*
Reactor Vessel and Containment Vessel Design and Analysis

Manager: Lynn A. Patterson*
Reactor Vessel and Containment Vessel Design and Analysis

****Electronically Approved Records are authenticated in the Electronic Document Management System.***

This page was added to the quality record by the PRIME system upon its validation and shall not be considered in the page numbering of this document.

Approval Information

Author Approval Wiratmo Momo May-04-2020 12:10:30

Verifier Approval Johnson Eric D May-05-2020 14:29:31

Manager Approval Patterson Lynn May-05-2020 14:32:13

Files approved on May-05-2020

*** This record was final approved on 5/5/2020 2:32:13 PM. (This statement was added by the PRIME system upon its validation)

Enclosure 4

Non-proprietary Reference Documents and
Redacted Versions of Proprietary Reference
Documents

(Public Version)

Attachment 18

**Westinghouse LTR-PAFM-05-58-NP, Revision 3,
“Flaw Tolerance Evaluation for Susceptible Reactor
Coolant Loop Cast Austenitic Stainless Steel Piping
Components in Point Beach Units 1 and 2 for 80
years,” July 2020**

(28 Total Pages, including cover sheets)

LTR-PAFM-05-58-NP
Revision 3

**Flaw Tolerance Evaluation for Susceptible Reactor Coolant Loop Cast
Austenitic Stainless Steel Piping Components in Point Beach Units 1 and 2 for
80 years**

July 2020

Author: B. Reddy Ganta*, Structural Design Analysis

Verifier: Xiaolan (Clair) Song*, RV Upper Internals Design Analysis

Reviewer: Anees Udyawar*, RV/CV Design & Analysis

Approved: Lynn A. Patterson*, Manager, RV/CV Design & Analysis

**Electronically approved records are authenticated in the electronic document management system.*

© 2020 Westinghouse Electric Company LLC
All Rights Reserved



Record of Revisions

Rev	Date	Revision Description
0	July 2005	Original Issue
1	June 2011	Revision 1 reconciles the flaw evaluation results documented in Revision 0 to Point Beach Units 1 and 2 Extended Power Uprate (EPU) condition. Appendix A and Reference 9 have been added in Revision 1 to address the impact of the EPU conditions. All changes are marked by revision bars in the left-hand margin.
2	July 2020	Revision 2 evaluates the Point Beach Units 1 and 2 reactor coolant piping CASS components for the 80-year extended plant life using the latest NRC and ASME Code requirements. No Revision bars are used since significant changes are made in this revision.
3	July 2020	Revision 3 incorporates final customer comments to Sections 2 and 6. All changes are marked by revision bars in the left-hand margin.

FOREWORD

This letter contains Westinghouse Electric Company LLC proprietary information and data which has been identified by brackets. Coding (a,c,e) associated with the brackets sets forth the basis on which the information is considered proprietary.

The proprietary information and data contained in this letter were obtained at considerable Westinghouse expense and its release could seriously affect our competitive position. This information is to be withheld from public disclosure in accordance with the Rules of Practice 10CFR2.390 and the information presented herein is to be safeguarded in accordance with 10CFR2.390. Withholding of this information does not adversely affect the public interest.

This information has been provided for your internal use only and should not be released to persons or organizations outside the Directorate of Regulation and the ACRS without the express written approval of Westinghouse Electric Company LLC. Should it become necessary to release this information to such persons as part of the review procedure, please contact Westinghouse Electric Company LLC, which will make the necessary arrangements required to protect the Company's proprietary interests.

The proprietary information in the brackets has been deleted in the non-proprietary version of this letter (LTR-PAFM-05-58-NP, Revision 3).

1 INTRODUCTION

The reactor coolant loop piping elbow components in Point Beach Nuclear Plant Units 1 and 2 are constructed from cast austenitic stainless steel (CASS) material (ASTM A-351 Grade CF8M). CASS material is susceptible to thermal aging at the reactor operating temperature. Thermal aging of CASS material results in embrittlement, that is, a decrease in the ductility, impact strength, and fracture toughness of the material. Depending on the material composition, the Charpy impact energy of a component made of CASS material could decrease to a small fraction of its original value after prolonged exposure to reactor temperatures during service. Note that the primary coolant piping material is A376 TP316 and not susceptible to thermal aging.

Susceptibility of CASS piping elbow materials in Point Beach Nuclear Plant Units 1 and 2 can be determined using the screening criteria given in Grimes's Letter [1] based on the molybdenum content, casting method and ferrite content. As stated in Reference [1], since the base metal of reactor coolant loop piping does not receive periodic inspection in accordance with Section XI of the ASME Code, the susceptibility of piping components constructed from CASS material should be assessed for each heat of material. If a specific heat is found to be "not susceptible", no additional inspections or evaluations are required to demonstrate that the material has adequate toughness. Otherwise, aging management can be accomplished through volumetric examination or plant specific flaw tolerance evaluation using plant specific geometry and stress information.

A flaw tolerance evaluation of the CASS reactor coolant loop (RCL) piping components for the subsequent license renewal (SLR) program for 80-year service life of Point Beach Units 1 and 2 is evaluated herein in Revision 2 of this letter. The Nuclear Regulatory Commission (NRC) has published Generic Aging Lessons Learned for Subsequent License Renewal (GALL-SLR) Report, NUREG-2191 [2] which provides information regarding license renewal for 80 years. NUREG-2191 Volume 2 Chapter XI.M12 contains aging management guidance for CASS materials in Class 1 piping through a component-specific flaw tolerance evaluation in accordance with ASME Code, Section XI.

The susceptibility of CASS piping components to thermal aging is determined according to molybdenum content, casting methods, and delta ferrite content per NUREG-2191, Volume 2, Table XI.M12-1. According to NUREG-2191, material heats with high molybdenum content (SA-351 Grades CF3M, CF3MA, and CF8M or other steels with approximately 2-3% molybdenum content) for statically cast elbow components which have delta ferrite content greater than 14% are potentially susceptible to thermal aging. Centrifugally cast straight piping (CF8A material) with low molybdenum content is not susceptible to thermal aging for any amount of delta ferrite.

In determining susceptibility of the CASS piping components to thermal aging, the delta ferrite content for Point Beach Units 1 and 2 is primarily estimated using Hull's Equivalent Factor in NUREG/CR-4513 Revision 1 [3] according to the Grimes's Letter and NUREG-2191. The Hull's Equivalent Factor correlations in Revision 1 of NUREG/CR-4513 are the same as Revision 2 of NUREG/CR-4513.

The evaluation procedures and acceptance criteria, contained in paragraph IWB-3640 of ASME Section XI code [4], are used to determine the maximum allowable flaw size at the end of the inspection/evaluation period. A fatigue growth analysis is then performed considering the requirements for the thermal transients and the design or projected cycles for the 80-year service life. Since the reactor coolant water chemistry is monitored and maintained within very specific limits, contaminant concentrations are kept below the thresholds known to be conducive to stress corrosion cracking, with the major water chemistry control standards being included in the plant operating procedures as a condition for plant operation. The CASS

pipng material in pressurized water reactors is therefore not susceptible to stress corrosion cracking and only fatigue crack growth needs to be considered. The maximum acceptable initial flaw size for a given service life can then be determined such that the corresponding end of the inspection/evaluation period flaw size does not exceed the maximum allowable flaw size determined per Appendix C of ASME Section XI Code [4, 5]. Based on the guidance of ASME Section XI, this letter report provides flaw tolerance charts that show the maximum acceptable flaw size for a range of flaw shapes at the susceptible CASS piping locations in the hot leg, crossover leg and cold leg of the reactor coolant loop. Bounding evaluations applicable to both Point Beach Units 1 and 2 were performed for the susceptible elbow locations in each leg (hot leg, crossover leg and cold leg) of the reactor coolant loop. The objective of the flaw tolerance evaluation is to demonstrate that even with thermal aging, the susceptible CASS components are flaw tolerant for 80 years of service.

2 GEOMETRY, LOADING AND STRESSES

Point Beach Units 1 and 2 reactor coolant loop piping layouts for the hot leg, cross-over leg and cold leg components are shown in Figure 2-1. The limiting locations for flaw evaluation are identified in Table 2-1 based on limiting geometry, material properties and loading.

The elbow geometry along with the operating parameters are shown in Table 2-1. In developing the flaw tolerance charts in this report, all the applicable loadings are being considered. The piping loads considered in the flaw tolerance evaluation consist of loads due to [

] ^{a,c,e} The bounding piping loads are given in Table 2-2. [

] ^{a,c,e}

Thermal transients and the number of cycles applied during the design life of the plants are required in performing fatigue crack growth analysis. The Nuclear Steam Supply System (NSSS) design transients applicable for Point Beach Units 1 and 2 are shown in Table 2-3. Note that the design cycles listed in Table 2-3 are conservatively used in the fatigue crack growth (FCG) analysis, [

] ^{a,c,e}

Residual stresses due to the weld fabrication process are also considered in the fatigue crack growth analysis. The residual stress values were obtained from the technical basis document for austenitic steel piping flaw evaluation [6] and used in the evaluation of the heat affected zones of the susceptible CASS piping components. The through-wall axial and circumferential residual stress profiles used in the fatigue crack growth analysis are shown in Figure 2-2.

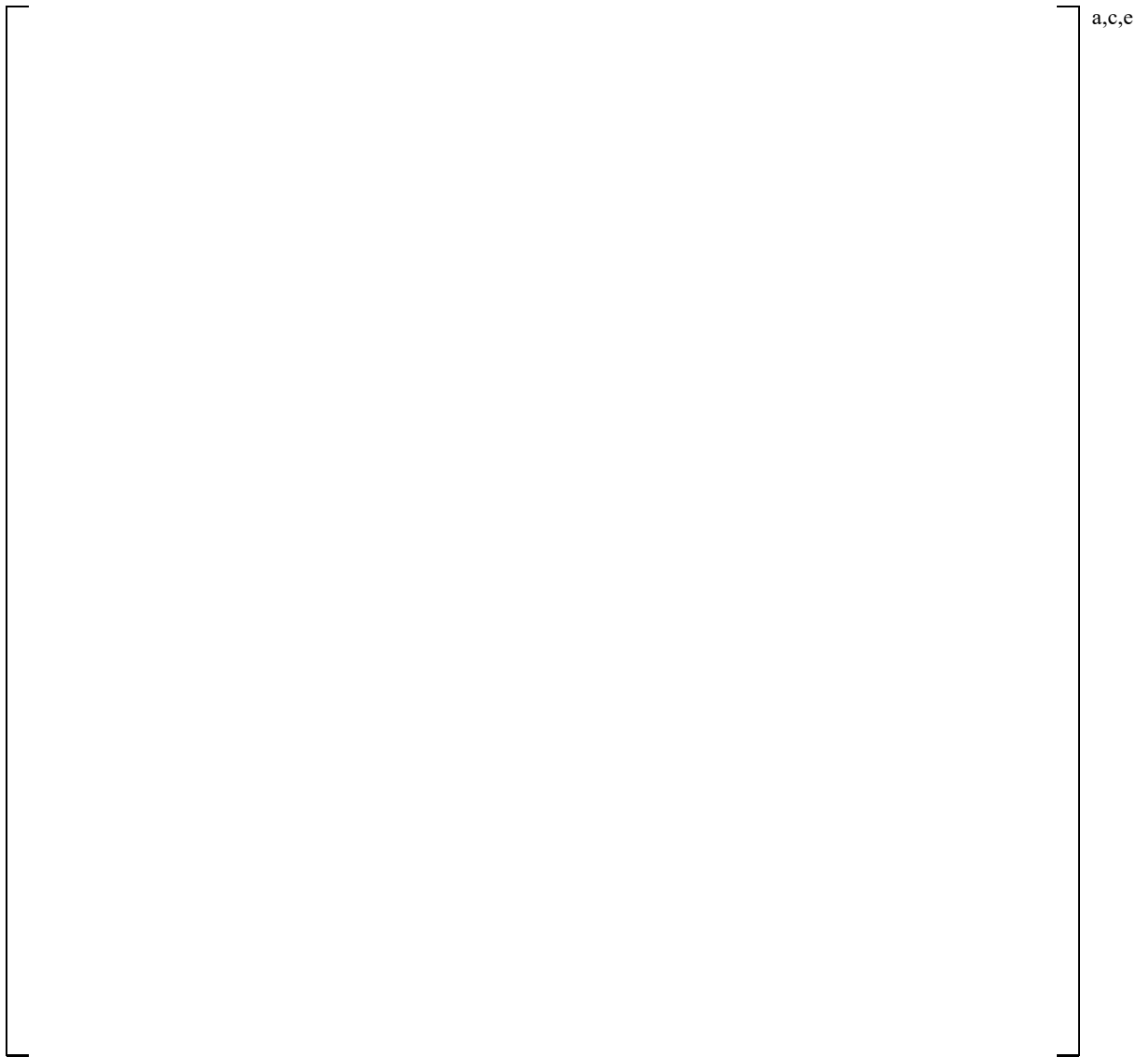


Figure 2-1: Schematic Diagram for Units 1 and 2 Primary Loop with Weld Locations

Wall Thickness	Through-Wall Residual Stress ¹	
	Axial	Circumferential ²
< 1 inch		
≥ 1 inch	See Note 3	

¹S = 30 ksi

²Considerable variation with weld heat input.

³ $\sigma = \sigma_i [1.0 - 6.91(a/t) + 8.69(a/t)^2 - 0.48(a/t)^3 - 2.03(a/t)^4]$
 $\sigma_i = \text{stress at inner surface (a = 0)}$

Note: "a/t" = distance through pipe weld thickness

Figure 2-2: Axial and Circumferential Residual Stress Distributions for Austenitic Stainless Steel Pipe Welds [6]

Table 2-1: Geometry and Operating Parameters for Point Beach Units 1 and 2 at Susceptible Critical Locations

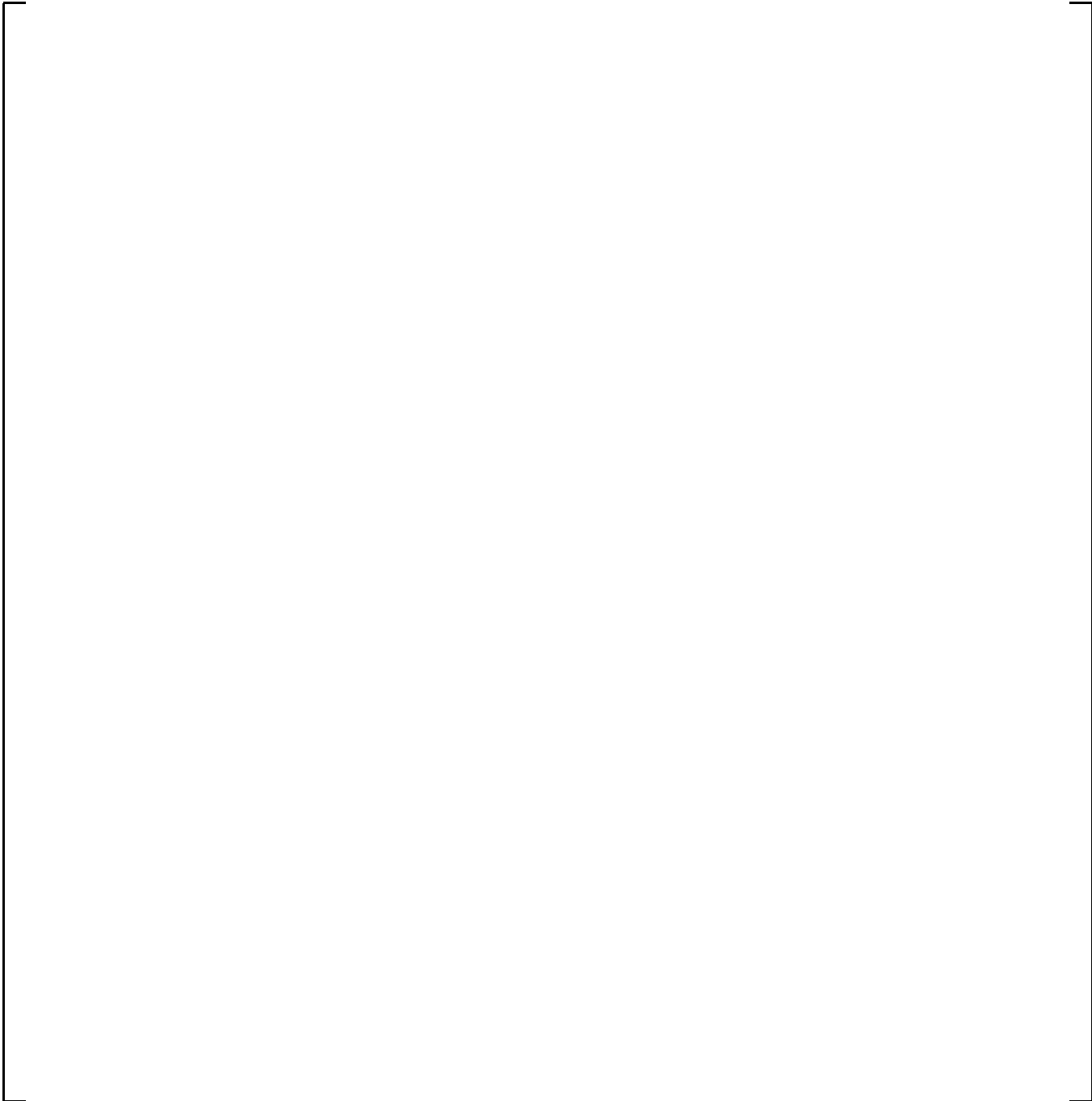
	a,c,e
--	-------

Table 2-2: Bounding Point Beach Units 1 and 2 Piping Loads for Susceptible Components in Each Leg of the Reactor Coolant Looping

	a,c,e
--	-------

Table 2-3: Summary of Point Beach Nuclear Plant Units 1 and 2 Design Transients for 80 Years⁽¹⁾

a,c,e



3 MATERIAL PROPERTIES

3.1 Screening Criteria

The pre-service fracture toughness of cast stainless steels has been found to be very high at operating temperatures. However, cast stainless steel is susceptible to thermal aging at the reactor coolant temperature. Thermal aging of cast stainless steel results in embrittlement, that is, a decrease in the ductility, impact strength and fracture toughness of the material. Depending on the material composition, the Charpy impact energy of a cast stainless steel component could decrease to a small fraction of its original value after prolonged exposure to high temperature during service.

According to the NUREG-2191, Volume 2, AMP XI.M12 [2], aging management is accomplished through a component specific flaw tolerance evaluation of susceptible CASS materials in accordance with the ASME Code, Section XI. The screening criteria used for all the RCL CASS components is shown in Table 3-1. This screening criteria will be used for the Point Beach Units 1 and 2 to determine susceptibility of the RCL elbows fabricated from A351 CF8M.

3.2 Thermal Aging Susceptibility

For Point Beach Nuclear Plant Units 1 and 2, the primary coolant loop piping material is A376 TP316 which is not CASS material and therefore not susceptible to thermal aging, while the piping elbow material A351 CF8M may be susceptible. The susceptibility of the A351 CF8M material to thermal aging increases with increasing ferrite content. The molybdenum bearing CF8M materials shows increased susceptibility to thermal aging. Susceptibility of RCL CASS piping components in Point Beach Units 1 and 2 are determined using the screening criteria given in Table 3-1 [2] based on the molybdenum content, casting method, and ferrite content. The δ -ferrite content was estimated using Hull's Equivalent Factor in the NUREG/CR-4513 Revision 1 [3]. For Point Beach Units 1 and 2, reactor coolant loop piping elbow CASS material is susceptible and the δ -ferrite content for all the heats have been computed and shown in Table 3-2a for Unit 1 and Table 3-2b for Unit 2. Material thermal aging susceptibility is also shown in these tables.

Table 3-1: Screening Criteria for Thermal Embrittlement of CASS Materials

Molybdenum (Mo) Content wt. %	δ_c Content	Casting Method	Not Significant (Screens out)	Potentially Significant (Screens in)
Low, ≤ 0.5	$\leq 20\%$	Static	X	
	$> 20\%$			Yes
	Any	Centrifugal	X	
High, 2.0-3.0	$\leq 14\%$	Static	X	
	$> 14\%$			Yes
	$\leq 20\%$	Centrifugal	X	
	$> 20\%$			Yes

Table 3-2a: Chemistry and Delta Ferrite Content for Point Beach Unit 1 Elbows

The table area is mostly empty, consisting of a large rectangular frame. On the right side of this frame, there is a vertical line extending from the top to the bottom. To the right of the top of this vertical line, the text 'a,c,e' is written.

Table 3-2b: Chemistry and Delta Ferrite Content for Point Beach Unit 2 Elbows



a,c,e

4 ACCEPTANCE CRITERIA

Per NUREG-2191, Volume 2, AMP XI.M12, the CASS components are to be evaluated in accordance with the applicable procedures in ASME Code, Section XI. The acceptance criteria for the determination of allowable flaw sizes in high toughness base materials are contained in paragraph IWB-3640 in the ASME Section XI Code. Although rapid, nonductile failure is possible for ferritic materials at low temperatures, it is not applicable to stainless steels. In high toughness material, the higher ductility leads to two possible modes of failure: plastic collapse or unstable ductile tearing. The second mechanism can occur when the applied J integral exceeds the material property, fracture toughness J_{Ic} , and some stable tearing occurs prior to failure. If this mode of failure is dominant, the load carrying capacity is less than that predicted by the plastic collapse mechanism. The allowable flaw sizes of paragraph IWB-3640 for the high toughness base materials were determined based on the assumption that plastic collapse would be achieved and would be the dominant mode of failure. However, due to the reduced toughness of the submerged arc and shielded metal arc welds, it is possible that crack extension and unstable ductile tearing could occur and be the dominant mode of failure. To account for this effect, penalty feature called “Z factors” were developed in ASME Section XI code Appendix C, which are used as multiplying factors for the applied loadings at these welds. Thus, the effects of unstable ductile tearing due to reduced toughness of thermally aged cast stainless steel can therefore be addressed through the use of “Z” factors for submerged arc welds in accordance with the IWB-3640 flaw evaluation procedure and acceptance criteria.

According to the Grimes’s Letter [1], the results from the ANL Research Program indicate that the lower-bound fracture toughness of thermally aged cast stainless steel is similar to that of submerged arc welds (SAW). The evaluation procedures and acceptance criteria for indications in submerged arc welds are contained in paragraph IWB-3640 of ASME Section XI and are used in the generation of the flaw tolerance charts for Point Beach Units 1 and 2 reactor coolant loop elbows made of CASS material. As previously discussed, the susceptibility of CASS elbow components to thermal aging the delta ferrite content is estimated per Hull’s Equivalent Factor in NUREG/CR-4513, Rev. 1 [3] per NUREG-2191 AMP XI.M12.

The in-service inspection code of record for Point Beach Units 1 and 2 is the 2007 ASME Section XI with 2008 addendum [4], which will be used in the evaluation. However, the evaluation method for the case with the δ -ferrite content $\geq 20\%$ is not provided in Appendix C of 2007 Edition with 2008 addendum of ASME Code Section XI [4]. Appendix C of the 2019 Edition of the ASME Code Section XI [5] provides flaw evaluation of procedures for CASS with δ -ferrite content $\geq 20\%$. The NRC is in the process of changing GALL-SLR aging management program (AMP) XI.M12 in NUREG-2191 [10] to add the 2019 Edition of ASME Code, Section XI [5], Non-mandatory Appendix C. Therefore, the flaw evaluation for the heats with δ -ferrite content $\geq 20\%$ would be in accordance with the procedures specified in the 2019 edition of the ASME Section XI Appendix C [5].

5 FATIGUE CRACK GROWTH

In applying the ASME Code Section XI [4, 5] acceptance criteria, the final flaw size (a_f) used is defined as the flaw size to which the detected or postulated flaw is calculated to grow until the next inspection period. For CASS piping components in pressurized water reactors, only the fatigue crack growth needs to be considered as the RCL CASS piping component material in pressurized water reactors is unlikely to be susceptible to stress corrosion cracking as discussed in Section 1.

To determine fatigue crack growth for the susceptible CASS piping components, the loadings used consist of loads due to []^{a,c,e}

The design transients shown in Table 2-3 are used in the fatigue crack growth analysis. The analysis procedure involves postulating an initial flaw at the susceptible piping components and predicting the flaw growth due to an imposed series of loading transients. The input required for a fatigue crack growth analysis is basically the information necessary to calculate the crack tip stress intensity factor range (ΔK_I), which depends on the geometry of the crack, its surrounding structure, and the range of applied stresses in the crack area.

The stress intensity factor calculations were performed for semi elliptical inside surface axial and circumferential flaws using the stress intensity factor expressions from [8]. The fatigue crack growth rate for embedded and outside surface flaws in an air environment is lower than that for inside surface flaws exposed to the Pressurized Water Reactor (PWR) water environment. Therefore, embedded flaw and outside surface flaw evaluations are conservatively bounded by the inside surface flaw tolerance analysis in this letter.

Once ΔK_I is calculated, the growth for inside surface flaws due to a particular stress cycle can be calculated using the applicable fatigue crack growth reference curves for stainless steel in PWR water environments. To represent the PWR water environment for stainless steel, an environment factor of 2 for PWR environment [9] was applied to the reference fatigue crack growth curve for austenitic stainless steel in an air environment, as provided in Appendix C of ASME Section XI. The incremental growth from fatigue crack growth is then added to the original crack size, and the analysis proceeds to the next cycle or transient. The procedure is continued in this manner until all of the analytical transients known to occur in the 80 years of operation have been analyzed.

6 FLAW TOLERANCE EVALUATION

Longitudinal and circumferential surface flaws are defined respectively as flaws oriented along and perpendicular to the centerline axis of the piping location of interest. Two basic dimensionless parameters, flaw shape parameter (a/ℓ) and flaw depth parameter (a/t) can fully address the characteristics of a surface flaw, where:

t	=	wall thickness
a	=	flaw depth
ℓ	=	flaw length

Flaw tolerance evaluations were performed for the susceptible CASS elbows (A351 CF8M) with the bounding end-of-life (80 years) fracture toughness and the highest stress values in each leg of the reactor coolant loop piping. [

]^{a,c,e} The flaw tolerance charts for these critical susceptible locations in the hot leg, cold leg and crossover legs are shown in Figure 6-1 through Figure 6-6 for the longitudinal and circumferential flaws. The purpose of these flaw tolerance charts is to identify the maximum acceptable initial flaw size for the total 80-years' service life. The results presented in Figure 6-1 through Figure 6-6 represent the limiting results for inside surface, outside surface, and embedded flaws which are defined in accordance with IWA-3300 of the ASME Code Section XI. For a typical flaw tolerance chart, the flaw shape parameter (a/ℓ) was plotted as the abscissa from 0.1 to 0.5 and the flaw depth parameter (a/t) in percentage (%) through-wall thickness was plotted as the ordinate. Therefore, the flaw tolerance charts encompass various postulated flaw cases based on different aspect ratios (ranging in ℓ/a from 2 to 10). The lower curve was the ASME Code acceptable flaw depth tabulated in Table IWB-3514-2 for austenitic steels from ASME Section XI [4]. This curve indicates the acceptance standard of the Code, below which analytical evaluation is not required. The upper boundary curves show the maximum acceptable flaw depth beyond which repair is required for continued service. Any flaw which falls between the upper and lower boundary curves will be acceptable in accordance with the IWB-3640 criteria.

The following is an explanation of how to use the flaw tolerance charts, using Figure 6-3 as an example. Assume a hypothetical axial flaw in an elbow on the cross-over leg with aspect ratio of 2 (or a/ℓ of 0.5) and flaw depth of 30% through the wall thickness is to be evaluated per ASME Section XI. The flaw dimensions of $a/\ell = 0.5$ and $a/t = 0.3$ can be plotted in Figure 6-3 in order to determine flaw tolerance evaluation of the axial flaw in the cross-over leg. This particular flaw falls below the allowable initial flaw size curve in Figure 6-3; the allowable initial flaw size curve which is shown as red solid line in Figure 6-3 indicates that with $a/\ell = 0.5$, the largest initial flaw size (a/t) that will be acceptable for 80 years of fatigue crack growth per the guidance of ASME Section XI is about 65%. Thus, the hypothetical axial flaw that is 30% of the wall is demonstrated to be flaw tolerant for at least 80 years. Thus, in general, any flaw with a combination of flaw size (a/t) and aspect ratio that is below the allowable initial flaw size curve is flaw tolerant for at least 80 years.

The maximum acceptable initial flaw depths as a percentage of wall thickness for postulated flaws with aspect ratio (ℓ/a) of 6 and a remaining service life of 80 years at the susceptible locations in the hot leg, crossover leg and cold leg are summarized in Table 6-1. An aspect ratio of 6 is frequently considered for flaw tolerance analysis of hypothetical flaws in ASME Section XI. The maximum acceptable initial flaw

sizes for all other analyzed aspect ratios can be obtained directly from Figure 6-1 through Figure 6-6 for the susceptible CASS piping components in the hot leg, crossover leg and cold leg. As discussed in Section 4, the allowable end-of-life final flaw sizes shown in Table 6-1 were determined in accordance with the flaw evaluation guidelines and acceptance criteria contained in IWB-3640 with plastic collapse as the dominant mode of failure. The acceptable initial flaw sizes shown in Table 6-1 were then obtained by subtracting the fatigue crack growth for 80 years of service life from the allowable final flaw sizes.

Based on the results tabulated in Table 6-1 for a hypothetical postulated flaw with an aspect ratio of 6, the most limiting maximum acceptable initial flaw depth is for an axial flaw in the susceptible CASS piping components of the crossover leg, which is 27.2% of the wall thickness. [

]^{a,c,e} The “Acceptable Initial Flaw Size” in Table 6-1 represents the largest allowable flaw sizes that will take 80 years to grow to the maximum allowable end-of-evaluation period flaw size. As a result, a lower value for “Acceptable Initial Flaw Size” is more conservative (i.e., 27.2% flaw depth through the wall thickness compared to, for example, 29.9% for hot leg, axial flaw). The “Maximum Allowable End-of-Evaluation Period Flaw Size” in Table 6-1 represents the largest flaw size that will result in plastic collapse of the piping component. The difference between the acceptable initial flaw sizes and the maximum allowable end-of-evaluation period flaw sizes in Table 6-1 is the amount of fatigue crack growth over 80 years of plant life. Thus, as-found flaw sizes less than the “Acceptable Initial Flaw Size” will take longer than 80 years to reach the critical flaw size that will result in plastic collapse of the component.

Table 6-1: Summary of Maximum Acceptable Initial Flaw Sizes and Allowable Final Flaw Sizes (% through wall thickness) for AR (l/a) of 6, 80-yr Plant Life

Location	Longitudinal Flaw		Circumferential. Flaw	
	Acceptable Initial Flaw Size	Allowable Final Flaw Size	Acceptable Initial Flaw Size	Allowable Final Flaw Size
Hot Leg	29.9%	56.0%	45.5%	75.0%
Crossover Leg	27.2%	53.0%	44.6%	75.0%
Cold Leg	29.2%	55.0%	45.1%	75.0%

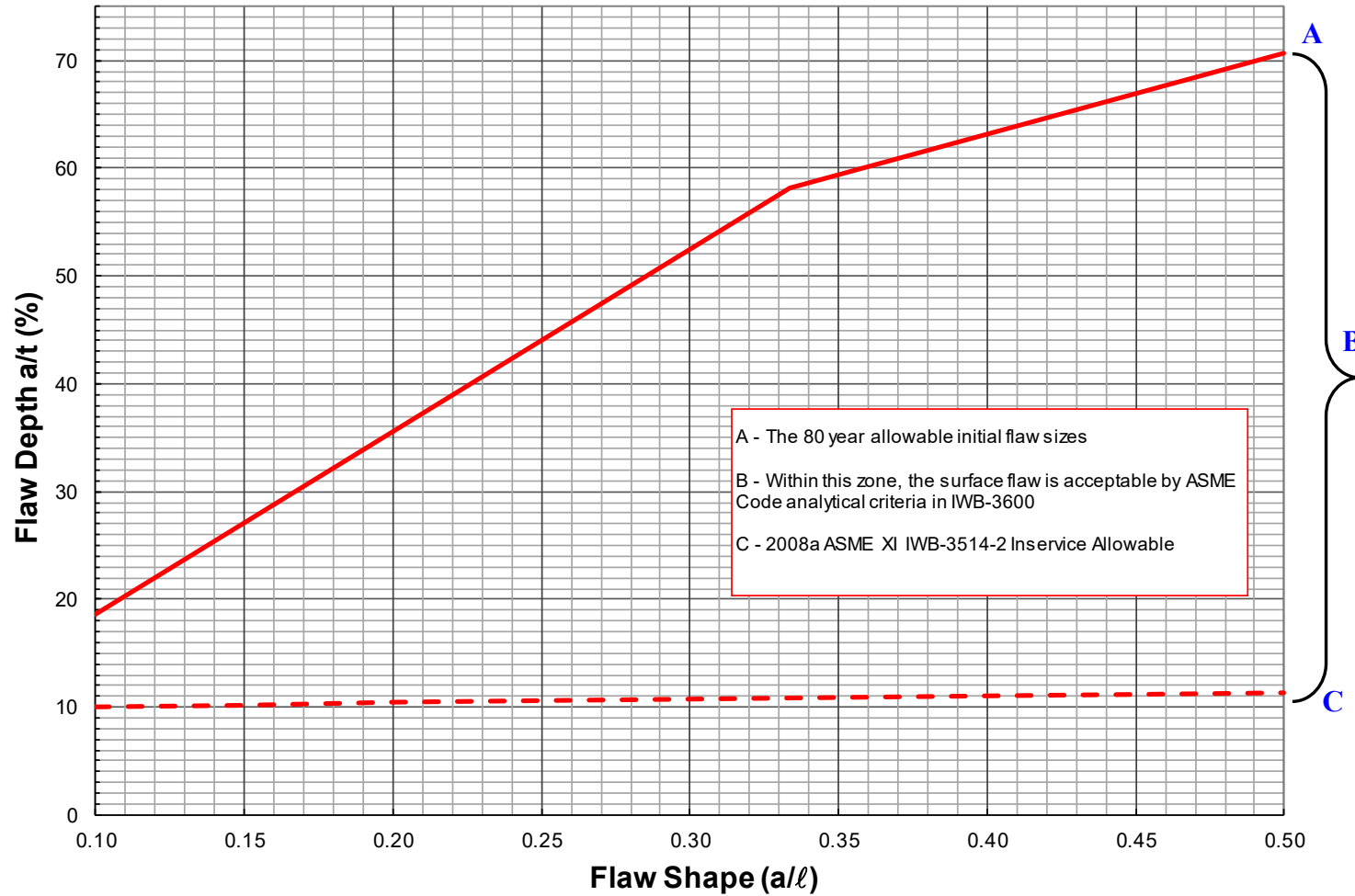


Figure 6-1: Longitudinal Flaw Tolerance Chart for Hot Leg

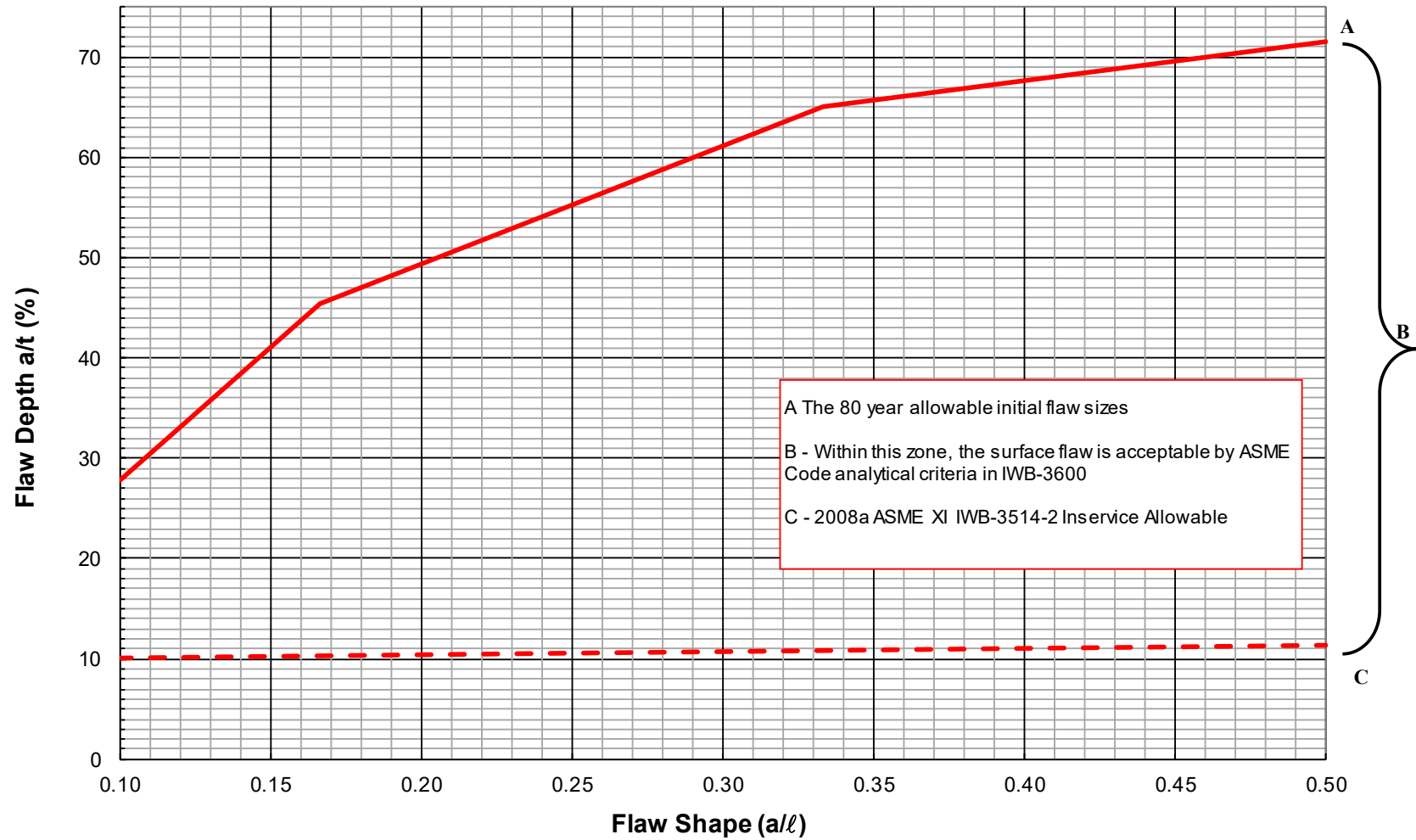


Figure 6-2: Circumferential Flaw Tolerance Chart for Hot Leg

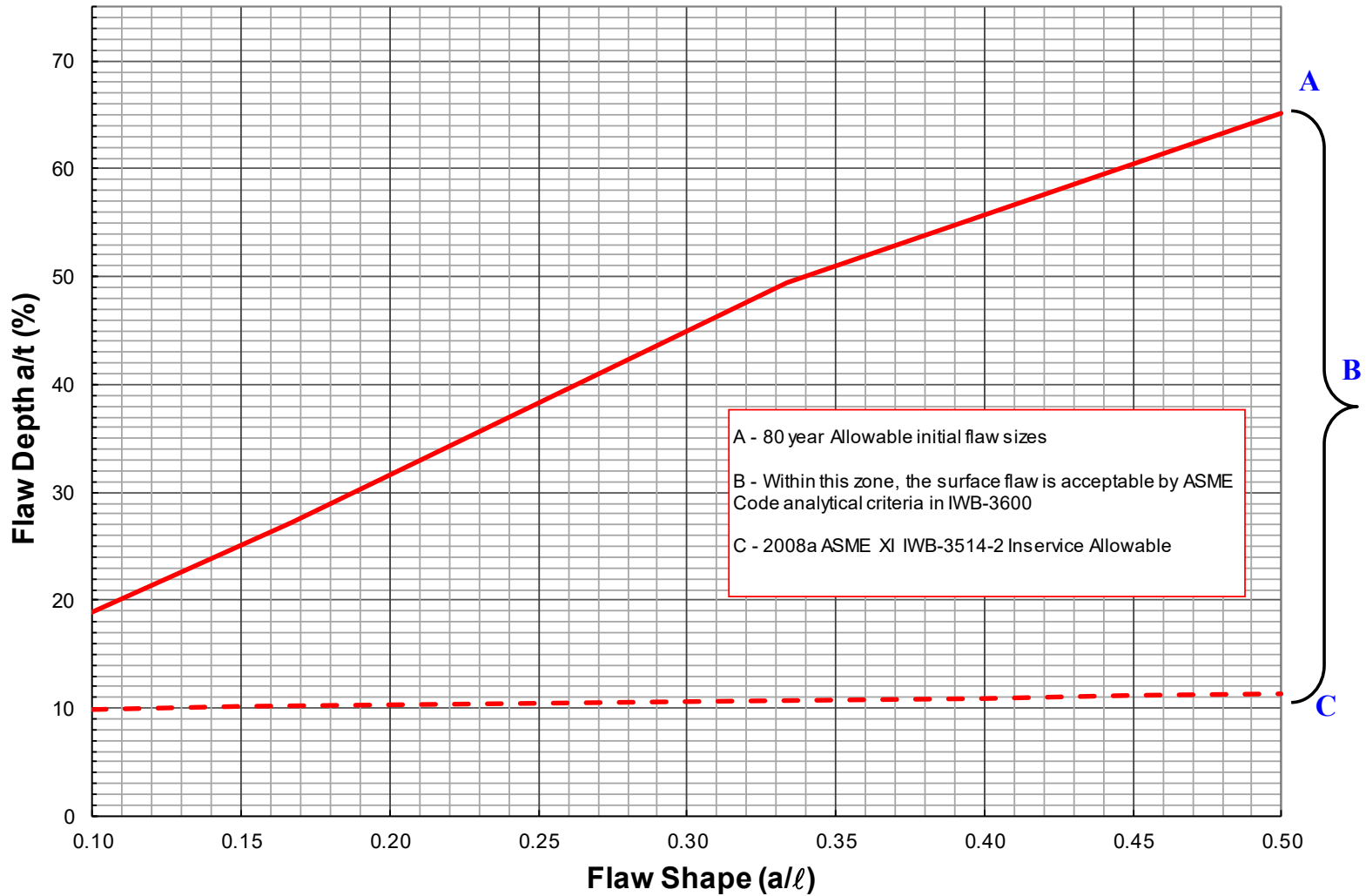


Figure 6-3: Longitudinal Flaw Tolerance Chart for Crossover Leg

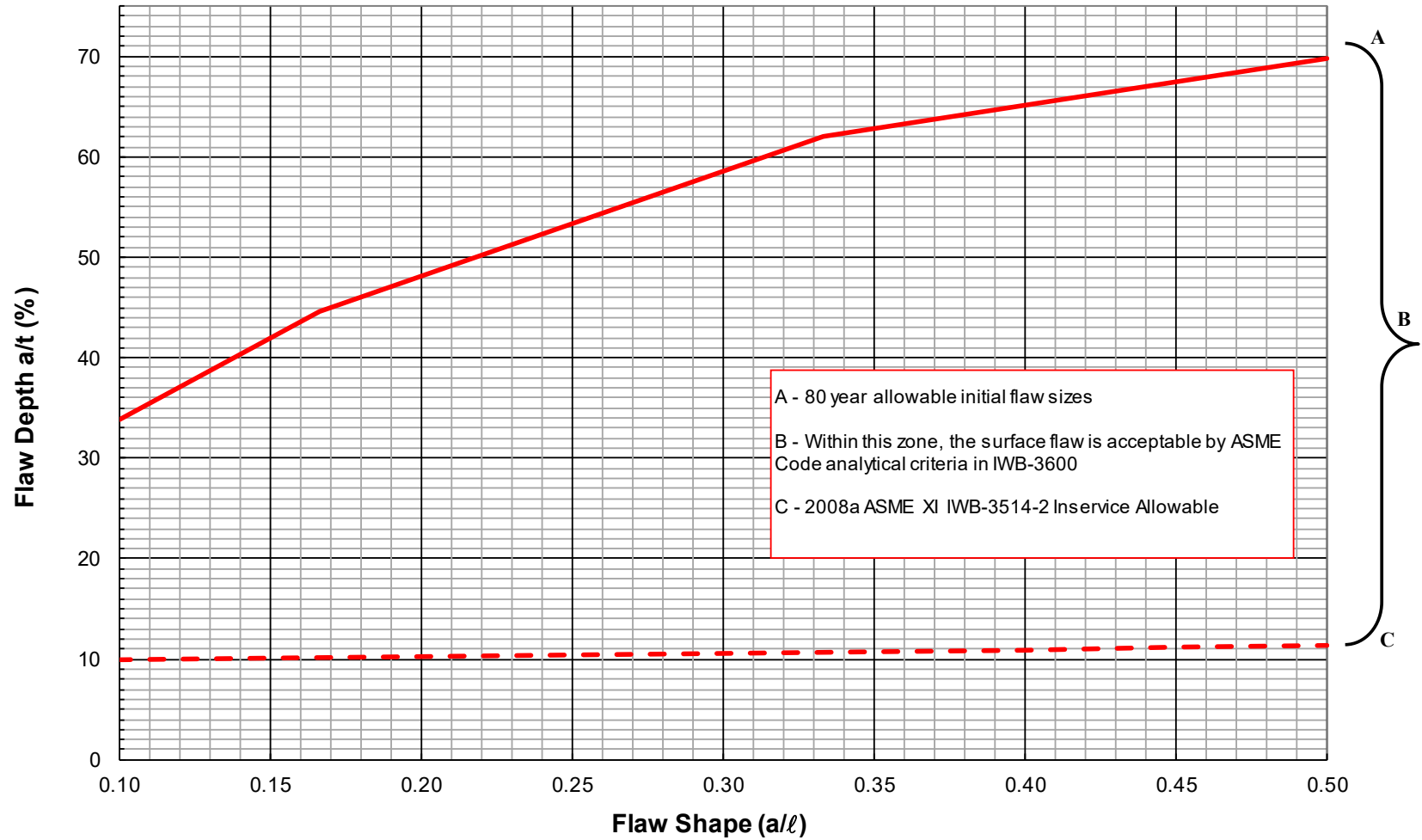


Figure 6-4: Circumferential Flaw Tolerance Chart for Crossover Leg

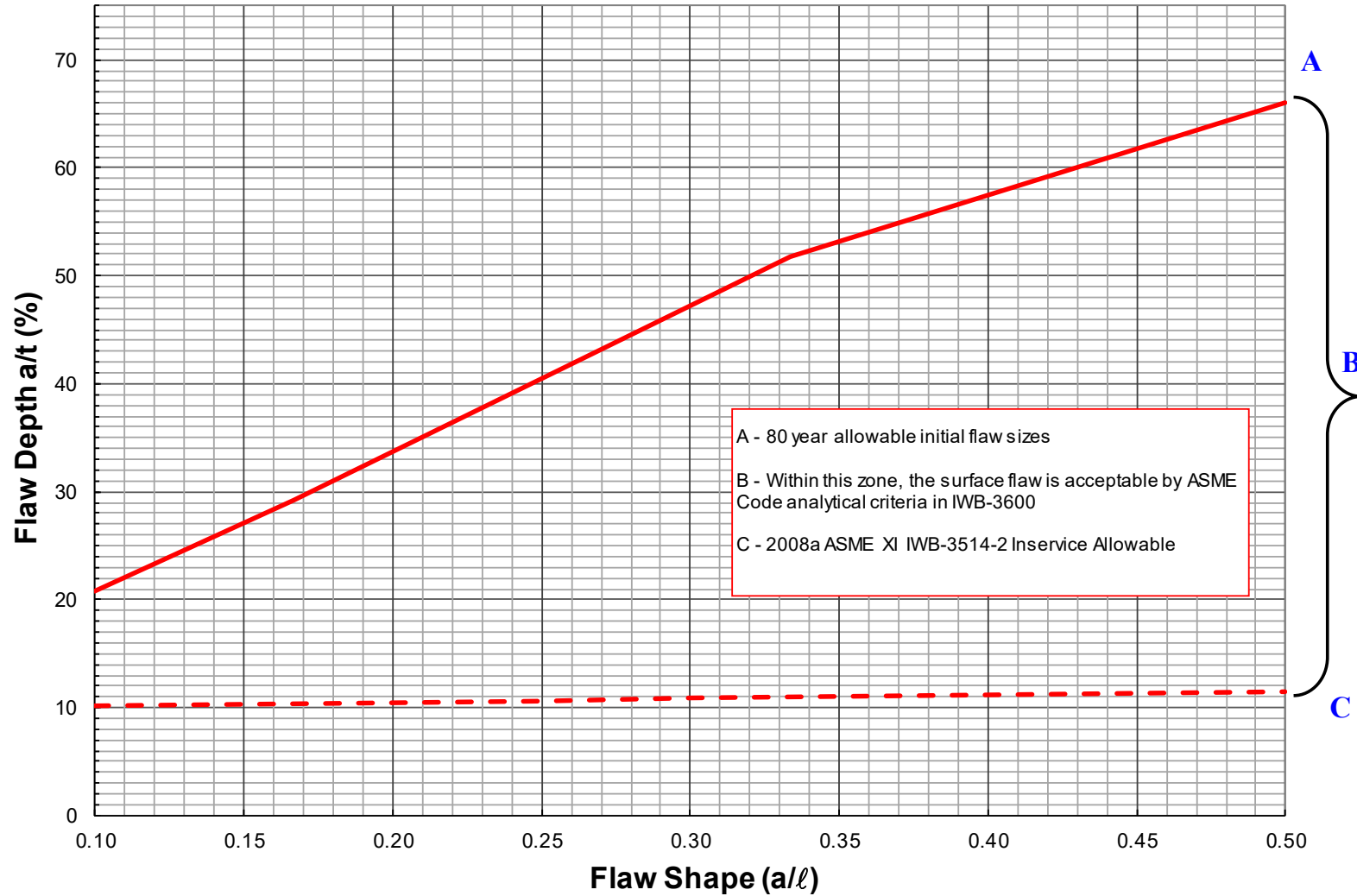


Figure 6-5: Longitudinal Flaw Tolerance Chart for Cold Leg

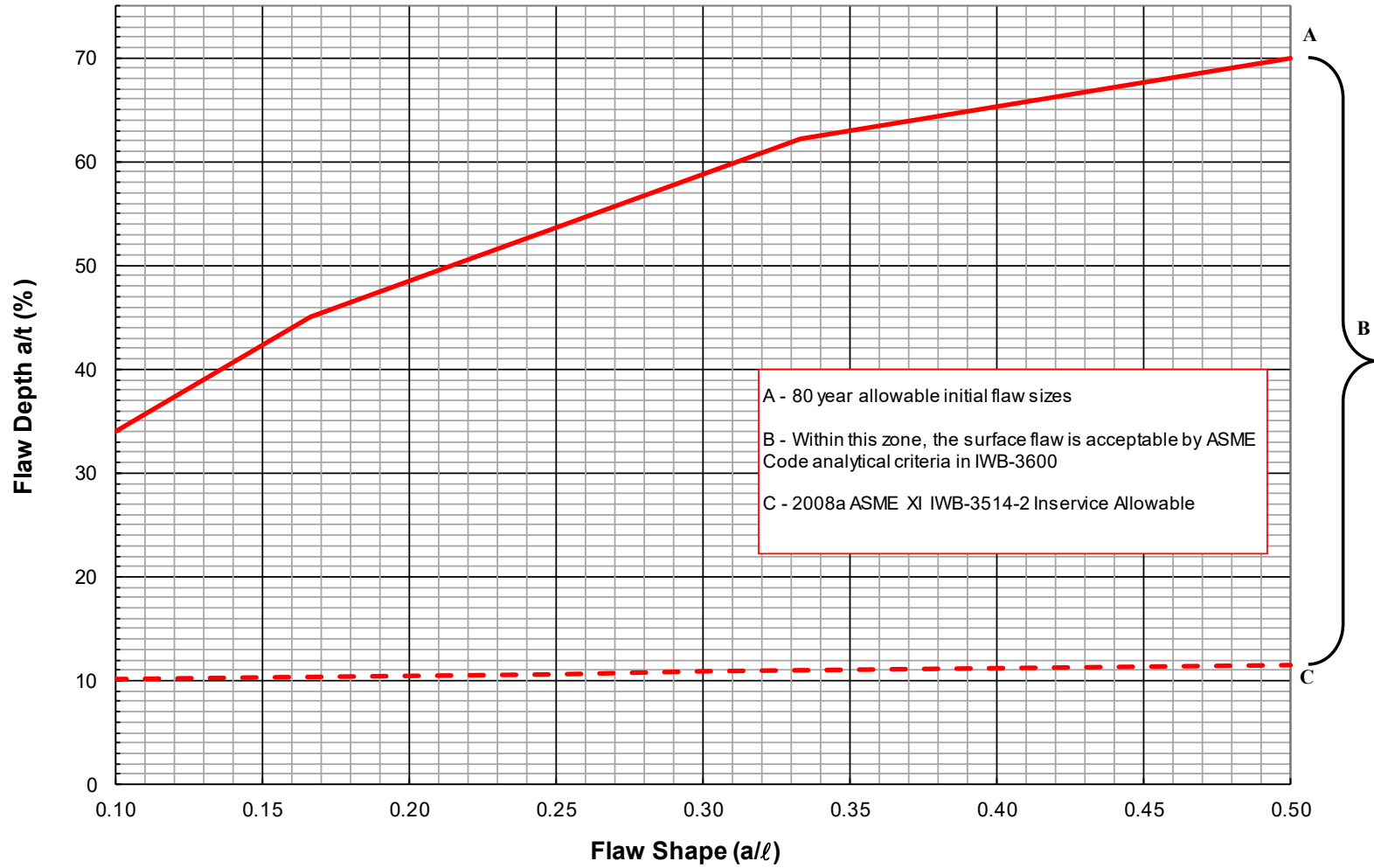


Figure 6-6: Circumferential Flaw Tolerance Chart for Cold Leg

7 SUMMARY AND CONCLUSION

The susceptible piping locations in the reactor coolant loop piping system of Point Beach Nuclear Plant Units 1 and 2 were evaluated in accordance with the evaluation procedures and acceptance criteria in paragraph IWB-3640 of ASME Section XI code. The reactor coolant loop piping material is A376 TP316, which is not CASS material and therefore not susceptible to thermal aging. However, several of the A351 CF8M piping elbow components are susceptible due to the δ -ferrite content level. The maximum acceptable flaw size for a range of flaw shapes for the susceptible CASS piping locations in the hot leg, crossover leg and cold leg are shown in Figure 6-1 through Figure 6-6. The limiting flaw size for a given aspect ratio (l/a) of 6 is for the cross-over leg axial flaw with an acceptable size of 27.2% of the wall thickness for an operating period of 80 years. These maximum acceptable initial flaw depth in all the three CASS components are deeper than the allowable flaw standards for the volumetric examination method in Table IWB-3514-2 in Section XI of the ASME Code 2007 Edition with 2008 Addendum [4]. Therefore, even with thermal aging in the susceptible reactor coolant loop CASS piping material for Point Beach Units 1 and 2, the susceptible piping locations have been shown to be tolerant of large flaws for 80-year plant life.

8 REFERENCES

1. Letter from Christopher I. Grimes, U.S. Nuclear Regulatory Commission License Renewal and Standardization Branch, to Douglas J. Walters, Nuclear Energy Institute, , License Renewal Issue No. 98-0030, “Thermal Aging Embrittlement of Cast Austenitic Stainless-Steel Components.” ML003717179, May 19, 2000.
2. U.S. Nuclear Regulatory Commission, NUREG-2191, Volume 2, “Generic Aging Lessons Learned for Subsequent License Renewal (GALL-SLR) Report – Final Report,” July 2017. (Section XI.M12 Thermal Aging Embrittlement of Cast Austenitic Stainless Steel (CASS)).
3. O. K. Chopra, “Estimation of Fracture Toughness of Cast Stainless Steels During Thermal Aging in LWR Systems,” NUREG/CR-4513, Rev. 1, U. S. Nuclear Regulatory Commission, Washington DC, August 1994.
4. ASME Boiler and Pressure Vessel Code, Section XI, “Rules for Inservice Inspection of Nuclear Power Plant Components,” 2007 Edition with 2008 Addendum.
5. ASME Boiler and Pressure Vessel Code, Section XI, “Rules for Inservice Inspection of Nuclear Power Plant Components,” 2019 Edition.
6. “Evaluation of Flaws in Austenitic Steel Piping,” Trans ASME, Journal of Pressure Vessel Technology, Vol. 108, August 1986, pp. 352-366.
7. Westinghouse WCAP-14439-P, Rev. 4, “Technical Justification for Eliminating Large Primary Loop Pipe Rupture as the Structural Design Basis for the Point Beach Nuclear Plant Units 1 and 2 for the Power Uprate and License Renewal Program (80 Years),” June 2020.
8. Raju, I. S. and Newman, J. C., “Stress Intensity Factor Influence Coefficients for Internal and External Surface Cracks in Cylindrical Vessels” in Aspects of Fracture Mechanics in Pressure Vessels and Piping, ASME publication PVP. Vol. 58, 1982.
9. Bamford, W. H., “Fatigue Crack Growth of Stainless Steel Piping in a Pressurized Water Reactor Environment,” Trans ASME, Journal of Pressure Vessel Technology, February 1979.
10. U.S. NRC Document SLR-ISG-Mechanical-2020-XX, “Updated Aging Management Criteria for Mechanical Portions of Subsequent License Renewal Guidance. Draft Interim Staff Guidance,” June 2020. ADAMS Accession No. ML20156A330.

This page was added to the quality record by the PRIME system upon its validation and shall not be considered in the page numbering of this document.

Approval Information

Author Approval Ganta B Reddy Jul-23-2020 10:00:31

Verifier Approval Song Xiaolan Jul-23-2020 10:44:55

Reviewer Approval Udyawar Anees Jul-23-2020 11:50:27

Manager Approval Patterson Lynn Jul-23-2020 12:34:27

Files approved on Jul-23-2020

*** This record was final approved on 7/23/2020 12:34:27 PM. (This statement was added by the PRIME system upon its validation)

Point Beach Nuclear Plant Units 1 and 2
Dockets 50-266 and 50-301
NRC 2020-0032 Enclosure 4, Attachment 19

Enclosure 4

**Non-proprietary Reference Documents and
Redacted Versions of Proprietary Reference
Documents**

(Public Version)

Attachment 19

**Westinghouse LTR-SDA-20-020-NP, Revision 1,
“Point Beach Units 1 and 2 Reactor Coolant Pump
Casings ASME Code Case N-481 Analysis for 80-year
Subsequent License Renewal (SLR),” July 2020**

(21 Total Pages, including cover sheets)

LTR-SDA-20-020-NP
Revision 1

**Point Beach Units 1 and 2 Reactor Coolant Pump Casings ASME Code Case
N-481 Analysis for 80-year Subsequent License Renewal (SLR)**

July 2020

Author: Jennifer J. Zhang*, AP1000 Concrete/R-bar Design & Seismic Analysis

Reviewer: Anees Udyawar*, Reactor Vessel/Containment Vessel Design & Analysis

Verifier: Stephen E. Marlette*, NSSS Component Design, Analysis & Aging Management

Manager: Lynn A. Patterson*, Reactor Vessel/Containment Vessel Design & Analysis

****Electronically approved records are authenticated in the electronic document management system.***

© 2020 Westinghouse Electric Company LLC
All Rights Reserved



RECORD OF REVISIONS

Rev	Date	Revision Description
0	June 2020	Original Issue.
1	July 2020	Revision 1 incorporates minor non-technical comments from NextEra Energy (Point Beach) on Revision 0. The comments are saved within Westinghouse internal documentation system.

FOREWORD

This document contains Westinghouse Electric Company LLC proprietary information and data which has been identified by brackets. Coding (a,c,e) associated with the brackets sets forth information which is considered proprietary.

The proprietary information and data contained within the brackets in this report were obtained at considerable Westinghouse expense and its release could seriously affect our competitive position. This information is to be withheld from public disclosure in accordance with the Rules of Practice 10CFR2.390 and the information presented herein is safeguarded in accordance with 10CFR2.390. Withholding of this information does not adversely affect the public interest.

This information has been provided for your internal use only and should not be released to persons or organizations outside the Directorate of Regulation and the ACRS without the express written approval of Westinghouse Electric Company LLC. Should it become necessary to release this information to such persons as part of the review procedure, please contact Westinghouse Electric Company LLC, which will make the necessary arrangements required to protect the Company's proprietary interests.

The proprietary information in the brackets is provided in the proprietary version of the report (LTR-SDA-20-020-P).

1 BACKGROUND AND INTRODUCTION

The ASME Code Case, N-481 (Alternate Examination Requirements for Cast Austenitic Pump Casings) (Reference 1), allowed the replacement of volumetric examinations of primary loop pump casing welds with fracture mechanics-based integrity evaluations supplemented by specific visual inspections. In March 2004, Code Case N-481 was annulled by ASME, and the information in Code Case N-481 was implemented into the 2008 Addenda of ASME Code Section XI. Note that the ASME Section XI 2000 Addenda replaced the pump casing weld B-L-1 volumetric examinations with visual examinations, while the ASME Section XI 2008 Addenda eliminated the pump casing weld (B-L-1) examinations completely. The only required examination is a visual examination of the pump casing (B-L-2) when the pump is disassembled for maintenance or repair.

During the early 1990's when the Code Case N-481 was approved by the ASME, the Westinghouse Owners Group (WOG) performed a generic fracture mechanics analysis per Code Case N-481 for the various primary loop pump casing models found in Westinghouse-designed Nuclear Steam Supply Systems (NSSS). The generic fracture mechanics analyses are documented in WCAP-13045 (Reference 2), in which [

] ^{a,c,e} in WCAP-13045.

For the Westinghouse-designed RCP, the majority of the casings are fabricated from [

] ^{a,c,e}

A plant-specific flaw tolerance evaluation of the Point Beach Units 1 and 2 RCP casings was completed in WCAP-14705 (Reference 3) to demonstrate compliance to ASME Code Case N-481 based on the generic evaluation completed in WCAP-13045. The NRC staff reviewed WCAP-14705 in the 1st license renewal application for the Point Beach Units 1 and 2 in NUREG-1839 (Reference 4). The NRC concluded in Section 4.4.3 of NUREG-1839 that

The RCP casings are not considered susceptible to thermal aging. Therefore, a structural integrity analysis is not necessary. The staff concluded that the RCP casing analysis is not identified as a TLAA, in accordance with the definitions of 10 CFR 54.3.

However, Loss-of-Fracture toughness due to thermal aging embrittlement of CASS RCP casings is identified as an aging mechanism in NUREG-2191, Volume 2, AMP XI.M12, "Generic Aging Lessons Learned for Subsequent License Renewal (GALL-SLR) Report," (Reference 5). Specifically, GALL-SLR provides an allowance for continued use of flaw tolerance evaluations performed as part of implementation of Code Case N-481 to address thermal aging embrittlement:

For pump casings, as an alternative to the screening and other actions described above, no further actions are needed if applicants demonstrate that the original flaw tolerance evaluation performed as part of Code Case N-481 implementation remains bounding and applicable for the subsequent license renewal (SLR) period or the evaluation is revised to be applicable for 80 years.

For the Subsequent License Renewal (SLR) program to extend an operating license to 80 years, further updates to WCAP-13045 was recently completed in the Pressurized Water Reactor Owners Group (PWROG) report PWROG-17033-P-A (Reference 6) and approved by the NRC.

In this letter report, a reconciliation analysis is performed for Point Beach Units 1 and 2 RCP casings to the generic fracture mechanics evaluation completed in PWROG-17033-P-A and WCAP-13045 to address the thermal aging embrittlement concern for the SLR period of 80 years. The latest plant-specific piping loads, and 80-year design transients and cycles are considered in the analysis to satisfy the NRC-required conditions on the use of the PWROG-17033-P-A (see Section 2). Furthermore, the plant-specific fracture toughness values are determined based on NUREG/CR-4513, Rev.1 (Reference 7) and NUREG/CR-4513, Rev.2 (Reference 8), which is consistent with the calculation of the limiting fracture toughness values in PWROG-17033-P-A.

Herein, Section 2 describes the general methodology applied in the fracture mechanics analysis of the Point Beach Units 1 and 2 RCP casings. More specifically, Section 2 outlines the steps to demonstrate the NRC-required conditions are met so that the generic fracture mechanics analyses completed in PWROG-17033 and WCAP-13045 can be applied to the Point Beach Units 1 and 2. Sections 3, 4, and 5 present the flaw stability evaluation and fatigue crack growth discussions. The conclusions are given in Section 6. The references are listed in Section 7.

2 GENERAL METHODOLOGY

The report PWROG-17033-P-A extends the generic fracture mechanics analysis of WCAP-13045 to an 80-year plant life. To address thermal aging embrittlement concern for the Point Beach Units 1 and 2 RCP casings with the use of PWROG-17033-P-A, the following four NRC-required conditions should be met:

1. The licensee must confirm that its RCPs are Westinghouse-designed models.

The applicability of ASME Code Case N-481 to the Point Beach Units 1 and 2 RCP casings was demonstrated in WCAP-14705. It is confirmed in WCAP-14705 that the Point Beach Units 1 and 2 RCPs are the Westinghouse []^{a,c,e} design.

2. The licensee must confirm that the Westinghouse-designed RCP is either a Model 63, Model 70, Model 93, Model 93A, Model 93A-1, Model 93D, Model 100A, or Model 100D, and fabricated with SA-351 CF8 or CF8M material.

It is confirmed in WCAP-14705 that the Point Beach Units 1 and 2 RCP casings are the Westinghouse []^{a,c,e} design which consist of []^{a,c,e} which is given in Figure 1.

3. For the crack stability analysis, the licensee must confirm that the screening loadings (force, moment, J_{app} and T_{app}) used in WCAP-13045 bound the plant-specific loadings. The licensee must confirm the limiting material fracture toughness values (J_{IC} , T_{mat} , and J_{max}) used in WCAP-13045 and PWROG-17033-P-A, Revision 1, bound the plant-specific fracture toughness values. If the screening loadings and material fracture toughness values in the WCAP-13045 and PWROG-17033 reports bound plant-specific values, the licensee needs to discuss how the Technical Reports (TRs) are bounding in the subsequent license renewal application. If the screening loadings or material fracture toughness value in the WCAP-13045 and PWROG-17033-P-A reports do not bound plant-specific values, the licensee needs to submit a plant-specific crack stability analysis to demonstrate structural integrity of the RCP casing as part of the subsequent license renewal application.

Refer to Sections 3 and 4 for the plant-specific compliance to these requirements.

4. For the fatigue crack growth (FCG) analysis, the licensee must confirm that the transient cycles specified in the WCAP-13045 or PWROG-17033 report bound the plant-specific transient cycles for the 80 years of operation. The licensee must confirm that the loadings used in the FCG analysis in WCAP-13045 bound the plant-specific applied loadings, considering potential increase in applied loading caused by plant-specific system operational changes, power uprate or piping modifications. If the FCG analysis inputs in WCAP-13045 bound the plant-specific conditions, the licensee must discuss how they are bounding in the subsequent license renewal application. If the FCG analysis inputs in WCAP-13045 do not bound the plant-specific conditions, the plant owner must provide a plant-specific analysis to demonstrate the FCG of the postulated flaw is within acceptable criteria as part of the subsequent license renewal application.

Refer to Section 5 for the plant-specific compliance to these requirements.

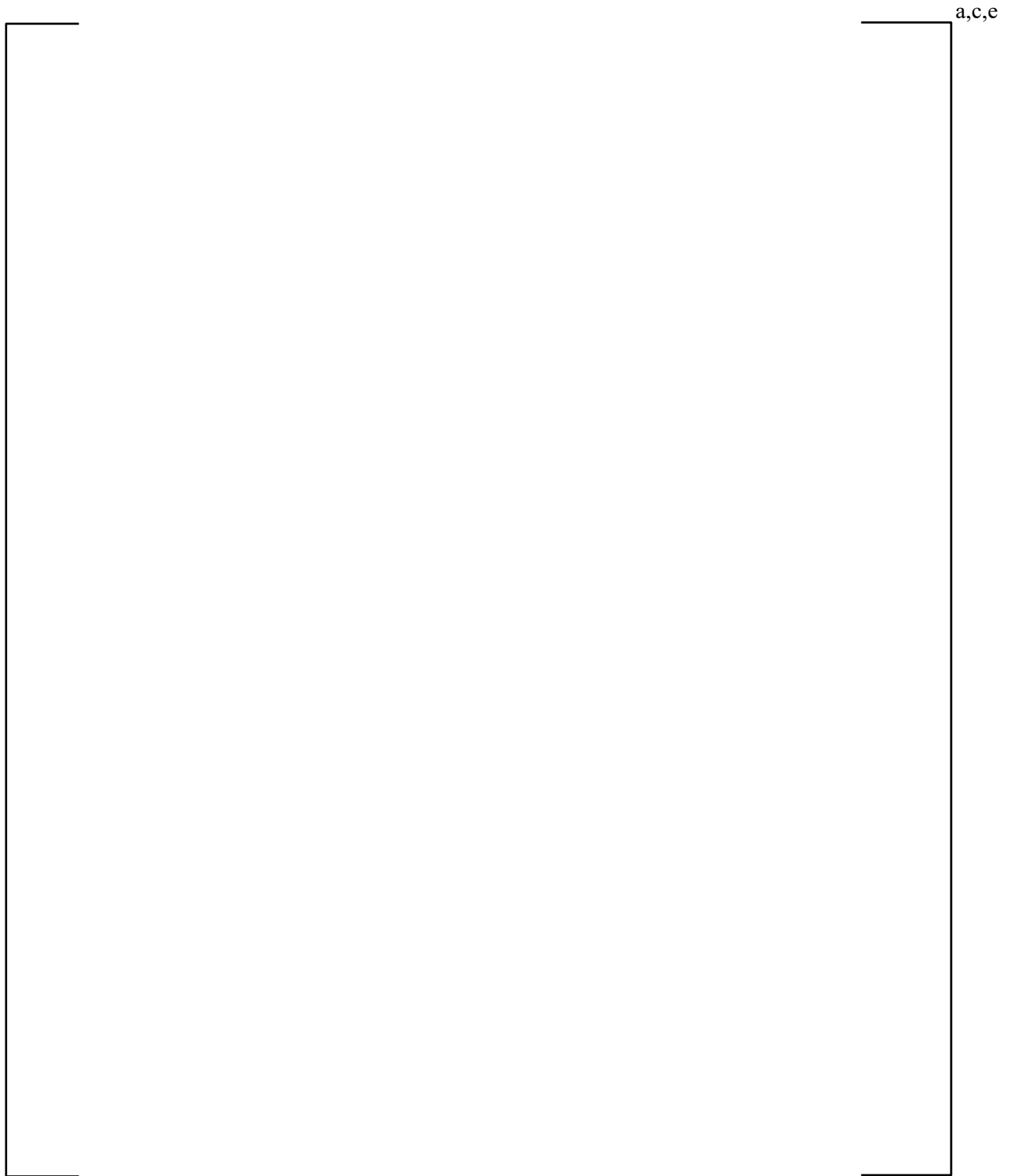


Figure 1 Typical Dimensions of a []^{a,c,e} Pump (Reference 2)

3 POINT BEACH UNITS 1 AND 2 PLANT-SPECIFIC LOADINGS ON THE PUMP CASING NOZZLES

In WCAP-13045, [

] ^{a,c,e} applied J-integral (J_{app}) and Tearing Modulus (T_{app}). If the Point Beach Units 1 and 2 plant-specific loads are less than the generic screening loads, the generic applied J-integral (J_{app}) and Tearing Modulus (T_{app}) calculated in WCAP-13045 can be applied to Point Beach Units 1 and 2 RCP casings crack stability analysis in Section 4.

In this section, the Point Beach Units 1 and 2 plant-specific [

] ^{a,c,e} as documented in WCAP-13045.

[

] ^{a,c,e}

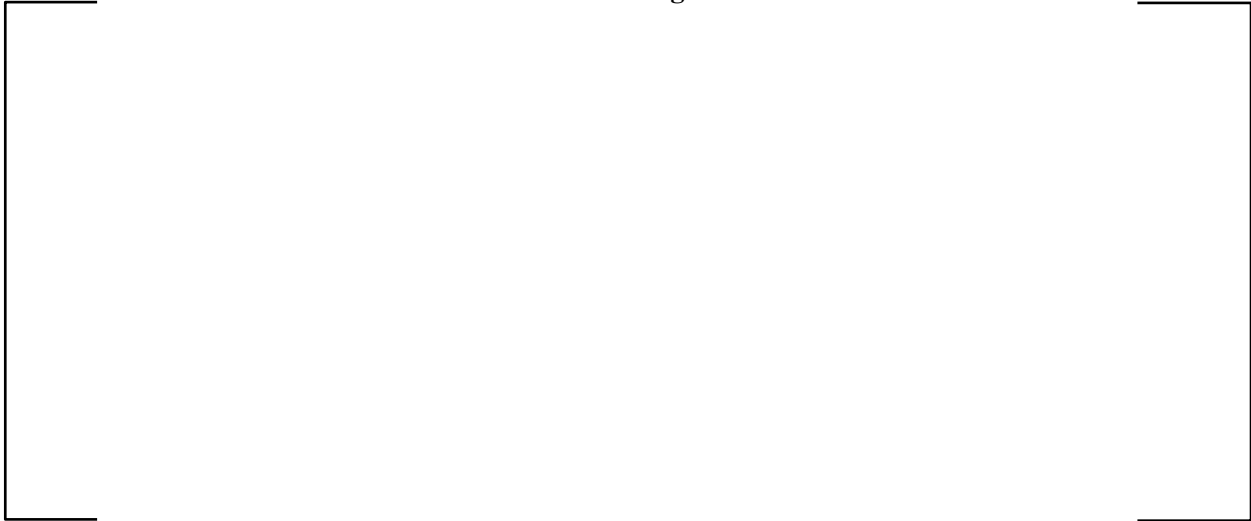
In Table 1, the Point Beach Units 1 and 2 plant-specific [

] ^{a,c,e} In Table 2, the Point Beach Units 1 and 2 plant-specific [

] ^{a,c,e}

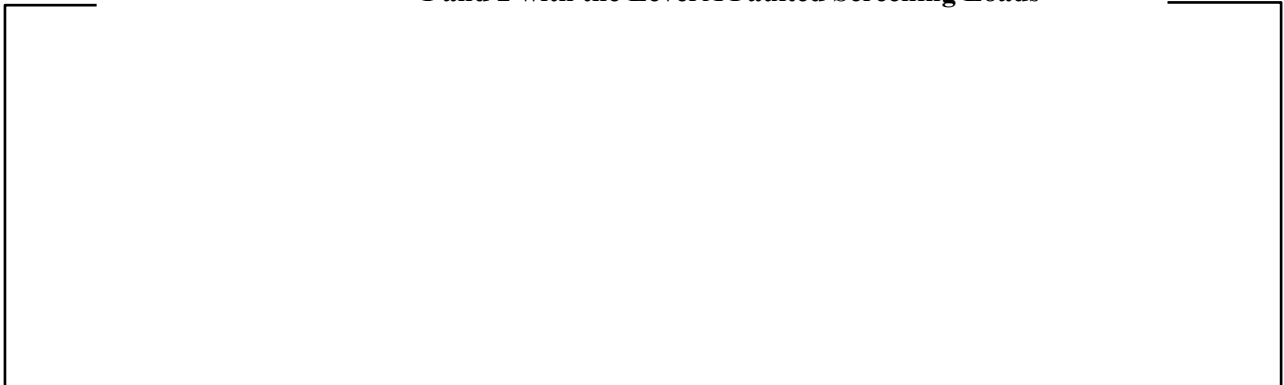
Since both of Level A and Level C screening nozzle loads reported in WCAP-13045 adequately bound the corresponding Point Beach Units 1 and 2 plant-specific faulted and normal RCP nozzles loads, the generic applied J-integral (J_{app}) and Tearing Modulus (T_{app}) as calculated in WCAP-13045 are conservatively applicable to the Point Beach Units 1 and 2 RCP casings for 80 years of operation.

Table 1 Comparison of the Normal Loads for the Pump Casing Nozzles of Point Beach Units 1 and 2 with the Screening Level C Normal Loads

An empty rectangular table frame with a thin black border, intended for the data of Table 1.

a,c,e

Table 2 Comparison of the Faulted Loads for the Pump Casing Nozzles of Point Beach Units 1 and 2 with the Level A Faulted Screening Loads

An empty rectangular table frame with a thin black border, intended for the data of Table 2.

a,c,e

4 CRACK STABILITY EVALUATION

For the Point Beach Units 1 and 2 SLR of 80 years, the plant-specific fracture toughness values of the RCP casings are determined with fracture toughness correlations for thermal aging of CASS from both NUREG/CR-4513, Rev. 1 and Rev. 2. [

] ^{a,c,e} Per NUREG/CR-4513, Rev.1 and Rev. 2, a Nitrogen concentration equal to 0.04% is assumed for the calculation of CASS fracture toughness.

The Point Beach Units 1 and 2 plant-specific fracture toughness values (J_{IC} , T_{mat} , J_{max}) of the critical heat, which envelop all the heats of the Point Beach Units 1 and 2 RCP casings, are listed in Table 3.

The end-of-service life fracture toughness values for [

] ^{a,c,e} This comparison indicates that the limiting fracture toughness values of WCAP-13045 and PWROG-17033-P-A bound the Point Beach Units 1 and 2 plant-specific values.

In WCAP-13045, [

] ^{a,c,e}.

As mentioned in Section 3, the Point Beach Units 1 and 2 plant-specific normal and faulted loads at the inlet and outlet RCP casings nozzles are bounded by the respective screening loads of WCAP-13045. Therefore, the stability analyses performed for pump [] ^{a,c,e} in WCAP-13045 are conservatively applicable to the Point Beach Units 1 and 2 RCP casings.

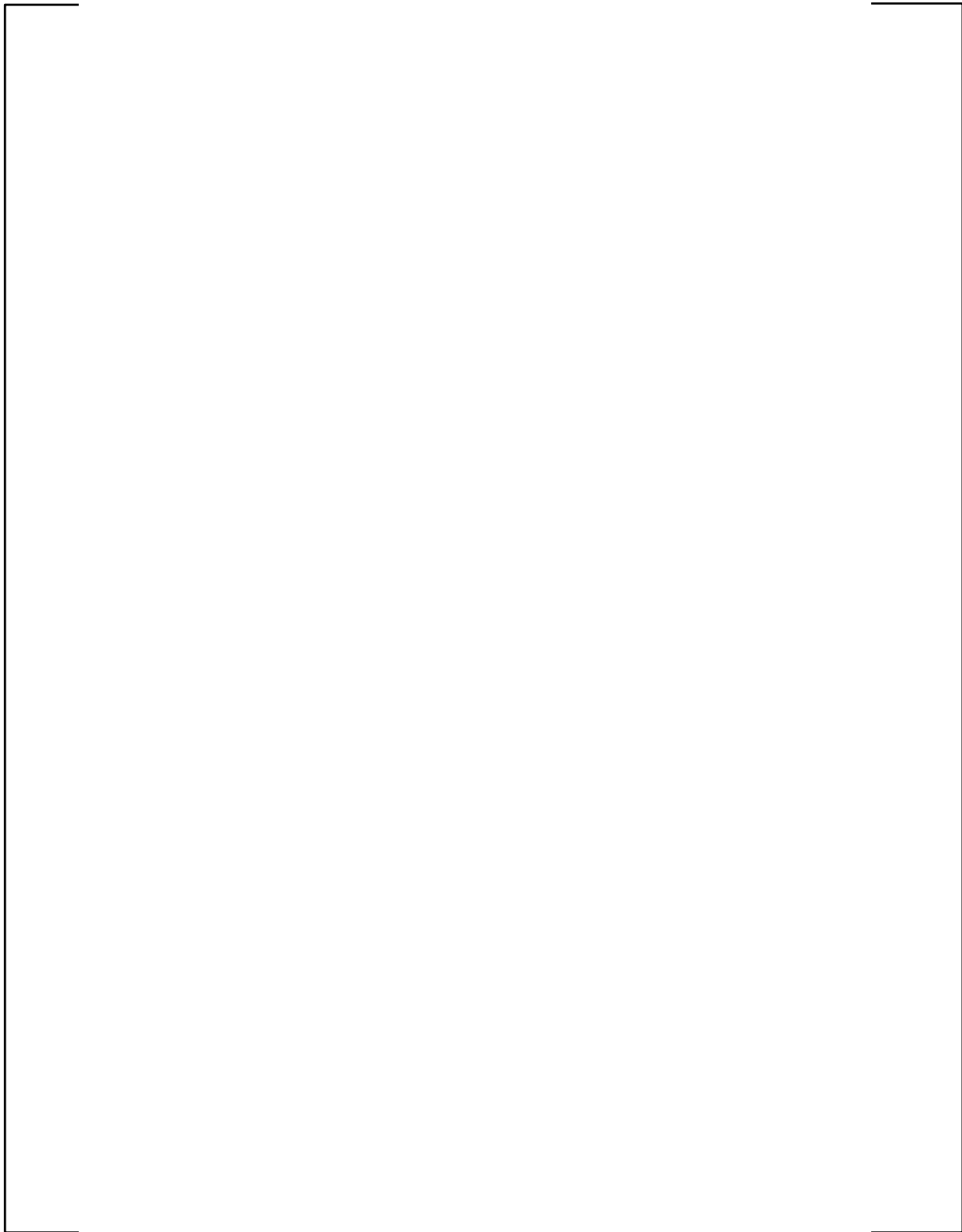
As explained in Section 10 of WCAP-13045, a postulated flaw is stable if

1. $J_{app} < J_{IC}$ or
2. If $J_{app} > J_{IC}$ then $T_{app} < T_{material}$ and $J_{app} < J_{max}$

The crack stability analysis results of the Point Beach Units 1 and 2 RCP casings are shown in Table 4. The most limiting stability results for the pump casings material are [

]^{a,c,e} The J_{app} and T_{app} values are less than the Point Beach Units 1 and 2 plant-specific values of [^{a,c,e}. Thus, all the crack stability criteria are met.

It can be concluded that flaws postulated in the Point Beach Units 1 and 2 RCP casings per Code Case N-481, when subjected to the plant-specific normal and faulted loadings, are determined to be stable for the 80-year plant life when considering the plant-specific fracture toughness values. Consequently, the Point Beach Units 1 and 2 RCP casings have sufficient fracture toughness with consideration of thermal aging embrittlement of CASS for the extended life of 80 years.



a,c,e

Figure 2 Location of Flaws Postulated in the []^{a,c,e} Pump Casing (Reference 2)

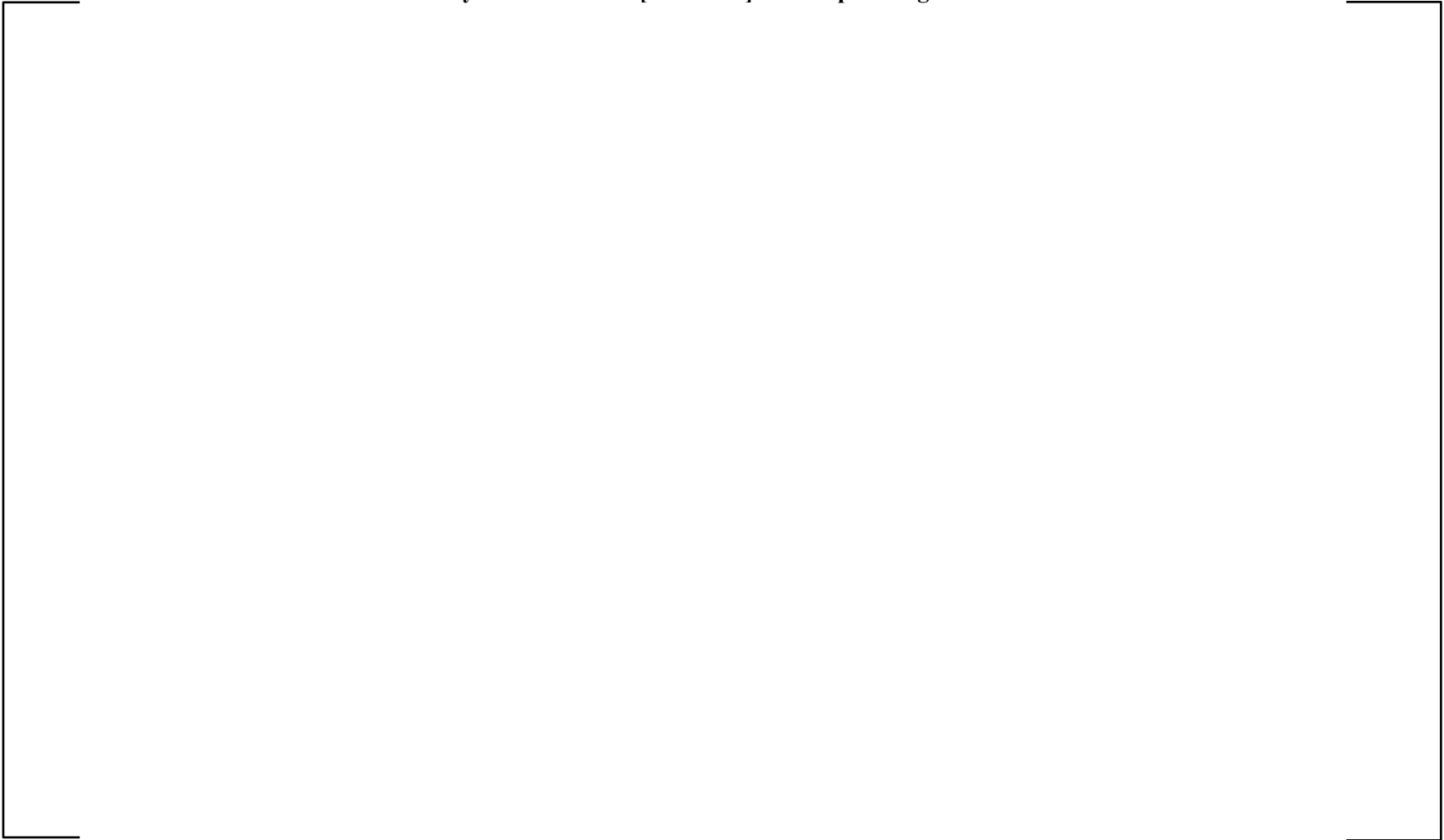
Table 3 Comparison of WCAP-13045 & PWROG-17033 Fracture Toughness versus Point Beach Units 1 & 2 Plant-specific Values

a,c,e



Table 4 Crack Stability Results for the []^{a,c,e} Pump Casing of Point Beach Units 1 & 2

a,c,e



5 FATIGUE CRACK GROWTH ASSESSMENT

A generic Fatigue Crack Growth (FCG) analysis is performed for []^{a,c,e} The report PWROG-17033-P-A re-evaluated and confirmed that the generic FCG evaluation performed in WCAP-13045 remains applicable for 80 years of operation in terms of the stresses, Stress Intensity Factor (SIF) equations, transient definitions and cycles, and FCG rates.

The report PWROG-17033-P-A indicated that the SIF correlations of FCG rates used for the FCG analysis in WCAP-13045 were consistent with the current correlations provided in the ASME Code, Section XI, Appendix A. The transient stresses used in the FCG analysis were generic and encompassed the various pump designs. In general, these stresses had not changed for the subsequent period of extended operation.

The transients and cycles considered in the generic FCG analysis of []

[]^{a,c,e}

Table 6 presents the Nuclear Steam Supply Systems (NSSS) design transients and cycles of the Point Beach Units 1 and 2 applicable for the 60-year plants life, which envelop the 80-year projection transient.

[]

[]^{a,c,e}

Consequently, the generic FCG evaluations performed in WCAP-13045 can be applied to the Point Beach Units 1 and 2 RCP casings for 80 years of operation per PWROG-17033-P-A. []

[]^{a,c,e}

In conclusion, the postulated flaws in RCP casings would exhibit only minimal crack extension during service life of 80 years. The end-of-service life flaws would remain well below the stable flaw size []

[]

[]^{a,c,e}

Table 5 Summary of Transients Used in the Fatigue Crack Growth Analysis (Ref. 2)

a,c,e



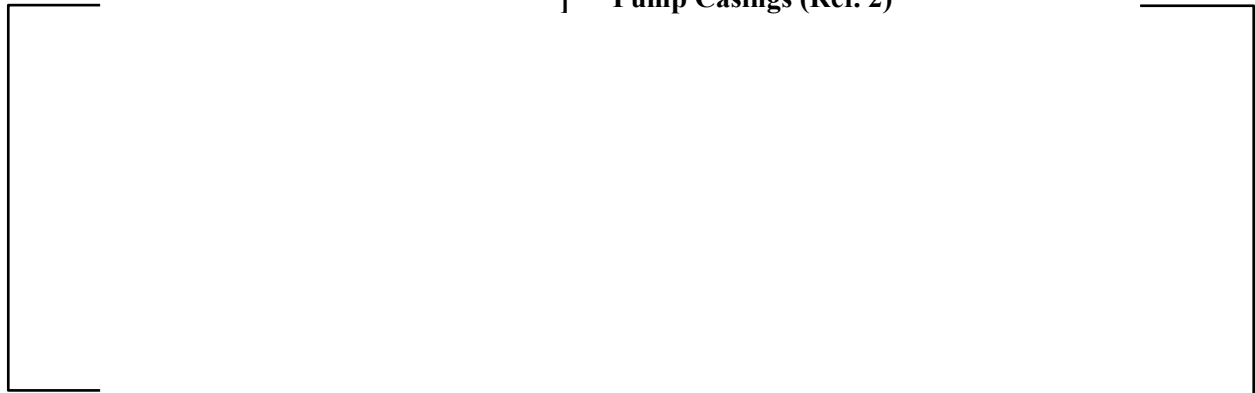
Table 6 Summary of Point Beach Units 1&2 NSSS Design Transients

a,c,e



Table 7 Fatigue Crack Growth for Postulated Flaws in the [
]^{a,c,e} Pump Casings (Ref. 2)

a,c,e



6 CONCLUSIONS

This report provides an assessment for the Point Beach Units 1 and 2 Reactor Coolant Pump (RCP) casings for the thermal aging embrittlement concern on long-term operation (80 years). Westinghouse-designed RCP casings were generically evaluated for fracture mechanics-based structural stability in WCAP-13045. The generic fracture mechanics evaluations of WCAP-13045 was re-evaluated for 80 years of operation in PWROG-17033-P-A. The NRC approved PWROG-17033-P-A for Subsequent License Renewal and provided conditions on the plant-specific applicability of the PWROG-17033-P-A and WCAP-13045 in terms of assessing the plant-specific loadings, material fracture toughness and transients.

The results presented in Sections 3 through 5 justify the plant-specific applicability of PWROG-17033-P-A and WCAP-13045 for Point Beach Units 1 and 2 RCP casings. The effect of thermal aging embrittlement has been evaluated and addressed in this report. No other mechanism is known to degrade the properties of the pump casings during the remaining service. Thus, it is concluded that the Point Beach Units 1 and 2 RCP casings are in compliance with ASME Code Case N-481 for the SLR program of 80-year operations.

7 REFERENCES

1. ASME Boiler & Pressure Vessel Code Section XI, Code Case N-481, "Alternative Examination Requirements for Cast Austenitic Pump Casings," Approval Date: March 5, 1990.
2. Westinghouse Report WCAP-13045, "Compliance to ASME Code Case N-481 of the Primary Loop Pump Casings of Westinghouse Type Nuclear Steam Supply Systems", September, 1991.
3. Westinghouse Report WCAP-14705, "A Demonstration of Applicability of ASME Code Case N-481 to the Primary Loop Pump Casings of the Point Beach Units 1 & 2," August, 1996.
4. NUREG-1839, Rev. 0, "Safety Evaluation Report Related to the License Renewal of the Point Beach Nuclear Plant, Units 1 and 2, Docket Nos. 50-266 and 50-301," December, 2005.
5. NUREG-2191, Vol. 2, Rev.0, "Generic Aging Lessons Learned for Subsequent License Renewal (GALL-SLR) Report," July, 2017.
6. a. Westinghouse Report PWROG-17033-P-A, Rev.1, "Update for Subsequent License Renewal: WCAP-13045, "Compliance to ASME Code Case N-481 of the Primary Loop Pump Casings of Westinghouse Type Nuclear Steam Supply Steams," November, 2019.
b. Westinghouse Report PWROG-17033-NP-A, Rev.1, "Update for Subsequent License Renewal: WCAP-13045, "Compliance to ASME Code Case N-481 of the Primary Loop Pump Casings of Westinghouse Type Nuclear Steam Supply Steams," November, 2019.
7. NUREG/CR-4513 ANL-93/22, Rev. 1, "Estimation of Fracture Toughness of Cast Stainless Steels During Thermal Aging in LWR Systems," August, 1994.
8. NUREG/CR-4513 ANL-15/08, Rev. 2, "Estimation of Fracture Toughness of Cast Stainless Steels During Thermal Aging in LWR Systems," May, 2016.
9. Westinghouse Report WCAP-14439-NP, Rev. 4, "Technical Justification for Eliminating Large Primary Loop Pipe Rupture as the Structural Design Basis for the Point Beach Nuclear Plant Units 1 and 2 for the Subsequent License Renewal Program (80 Years)," June, 2020.
10. Westinghouse Report WCAP-16983-P, Rev.1, "Point Beach Units 1 and 2 Extended Power Uprate (EPU) Engineering Report", October 2014.
11. ASME Boiler and Pressure Vessel Code, Section XI, "Rules for Inservice Inspection of Nuclear Power Plant Components."

This page was added to the quality record by the PRIME system upon its validation and shall not be considered in the page numbering of this document.

Approval Information

Author Approval Zhang Jennifer J Jul-07-2020 13:43:00

Reviewer Approval Udyawar Anees Jul-07-2020 14:12:54

Verifier Approval Marlette Stephen Jul-07-2020 14:36:59

Manager Approval Patterson Lynn Jul-08-2020 14:31:46

Files approved on Jul-08-2020

*** This record was final approved on 7/8/2020 2:31:46 PM. (This statement was added by the PRIME system upon its validation)

Point Beach Nuclear Plant Units 1 and 2
Dockets 50-266 and 50-301
NRC 2020-0032 Enclosure 4, Attachment 20

Enclosure 4
Non-proprietary Reference Documents and
Redacted Versions of Proprietary Reference
Documents
(Public Version)
Attachment 20

**Westinghouse LTR-AMLR-20-26-NP, Revision 1,
“Transmittal of Results from the MRP-191 Revision 2
Review in Support of Subsequent License Renewal
for Point Beach Units 1 and 2,” June 11, 2020**

(99 Total Pages, including cover sheets)



To: John T. Ahearn
Cc: Gregory M. Imbrogno

Date: June 11, 2020

From: Lance S. Harbison
Ext: (412) 374-2648
Fax: (724) 940-8660

Our ref: LTR-AMLR-20-26-NP, Rev. 1

Subject: Transmittal of Results from the MRP-191 Revision 2 Review in Support of Subsequent License Renewal for Point Beach Units 1 and 2

References:

1. U.S. Nuclear Regulatory Commission Report, NUREG-2191, "Generic Aging Lessons Learned for Subsequent License Renewal (GALL-SLR) Report," July 2017 (ADAMS Accession Number ML17187A031).
2. Nuclear Regulatory Commission Report, NUREG-2192, "Standard Review Plan for Review of Subsequent License Renewal Applications for Nuclear Power Plants," July 2017 (ADAMS Accession Number ML17188A158).
3. Materials Reliability Program: Pressurized Water Reactor Internals Inspection and Evaluation Guidelines (MRP-227-A). EPRI, Palo Alto, CA: 2011. 1022863.
4. Materials Reliability Program: Pressurized Water Reactor Internals Inspection and Evaluation Guidelines (MRP-227, Revision 1-A). EPRI, Palo Alto, CA: 2019. 3002017168.
5. Materials Reliability Program: Screening, Categorization, and Ranking of Reactor Internals Components for Westinghouse and Combustion Engineering PWR Design (MRP-191, Revision 2). EPRI, Palo Alto, CA: 2018. 3002013220.
6. Westinghouse Calculation Note, CN-RIDA-13-87, Revision 3, "Point Beach Units 1 and 2 Support for Reactor Internals Aging Management – Applicant/Licensee Action Items 1 and 2," October 18, 2016.
7. Materials Reliability Program: Pressurized Water Reactor Internals Inspection and Evaluation Guidelines (MRP-227, Revision 0). EPRI, Palo Alto, CA: 2008. 1016596.
8. PBNWEC-20-0009, Revision 1, "Response to Westinghouse Letter WEC-NEE-PB-SLR-20-005, NEXT-20-35," May 7, 2020.
9. Westinghouse Report, WCAP-16983-P, Revision 1, "Point Beach Units 1 and 2 Extended Power Uprate (EPU) Engineering Report," October 2014.
10. Materials Reliability Program: Screening, Categorization, and Ranking of Reactor Internals Components for Westinghouse and Combustion Engineering PWR Design (MRP-191). EPRI, Palo Alto, CA: 2006. 1013234.
11. Materials Reliability Program: Screening, Categorization, and Ranking of Reactor Internals Components for Westinghouse and Combustion Engineering PWR Design (MRP-191, Revision 1). EPRI, Palo Alto, CA: 2016. 3002007960.

Attachments: 1. Point Beach Components Compared to MRP-191, Revision 2 Results
2. Comparison of MRP-191 Revisions

Per the USNRC guidance for subsequent license renewal (SLR), NUREG-2191 [1] and NUREG-2192 [2], MRP-227-A [3] is the initial reference basis for developing a reactor vessel internals (RVI) aging management program (AMP) for operation beyond the first period of extended operation. The reference basis of the approved inspection and evaluation guidelines is supplemented with a gap analysis to determine the changes required to provide reasonable assurance that aging degradation effects will be managed during SLR. The USNRC-approved revision to the internals inspection and evaluation guidelines, MRP-227,

Revision 1-A [4] was recently published, providing an updated starting point for the gap analysis. The conclusions of the USNRC safety evaluation on MRP-227, Revision 1-A states:

“The NRC staff finds MRP-227, Revision 1, as modified by this SE and subject to the A/LAI detailed in Section 4.0 of this SE, provides an acceptable baseline or starting point for an AMP for SLR subject to a gap analysis as described in the SRP-SLR Section 3.1.2.2.9 and GALL-SLR, AMP XI.M16A. An exception to GALL-SLR AMP XI.16A must be identified in such cases.” [4]

CN-RIDA-13-87, Revision 3 [6] provided the technical support to NextEra Energy Point Beach, LLC, Point Beach Nuclear Plant (PBNP) Units 1 and 2 with respect to Applicant/Licensee Action Items (A/LAIs) 1 and 2 from the United States (U.S.) Nuclear Regulatory Commission’s (NRC’s) Safety Evaluation (SE) on revision 0 of MRP-227 [7]. This letter presents the gap analysis between CN-RIDA-13-87, Revision 3 [6] and MRP-191, Revision 2 [5] in Support of SLR for Point Beach Units 1 and 2. The results are presented as attachments in table form as follows:

Attachment 1 contains Table 1 and Table 2 which compare Point Beach Unit 1 and Unit 2 reactor vessel internal (RVI) components/materials [6] with the RVI components/materials listed in Table 4-4 of the latest revision of MRP-191 [5]. Table 1 and Table 2 also list the applicability of each MRP-191, Revision 2 [5] RVI component/material for Point Beach Unit 1 and Unit 2. All changes from CN-RIDA-13-87, Revision 3 [6] to MRP-191, Revision 2 [5] are designated by gray-shaded cells. Note, Point Beach has confirmed in PBNWEC-20-0009, Revision 1 [8] that no major changes have been made to the reactor vessel internals components since WCAP-16983-P, Revision 1 [9]. WCAP-16983-P, Revision 1 was issued in October 2014, thus the starting data of CN-RIDA-13-87, Revision 3 is valid. For information, calculation note CN-RIDA-13-87, Revision 3 [6] was revised in 2016 to document a baffle former bolt drawing discrepancy; however, there is no impact to the earlier revision used by the licensee to address LAI #1 and #2 as part of the first license renewal program basis approved by the NRC in 2015 (refer to ADAMS Accession Number ML15079A087).

Attachment 2 contains Tables 3 through 8 which compare MRP-191, Revision 2 [5] with the previous MRP-191 revisions (Revision 0 and 1) [10 and 11, respectively]. All changes from MRP-191, Revisions 0 [10] and 1 [11] to MRP-191, Revision 2 [5] are designated by gray-shaded cells.

The purpose of revision 1 of this document is to incorporate comments received from NextEra Energy Point Beach, LLC (comments and their resolution are attached in PRIME).

If you have any questions, please contact the undersigned.

Authored by: ELECTRONICALLY APPROVED*
Lance S. Harbison
Materials and Aging Management

Verified by: ELECTRONICALLY APPROVED*
Taylor Zindren
Materials and Aging Management

Approved by: ELECTRONICALLY APPROVED*
Kaitlyn M. Musser, Manager
Materials and Aging Management

*Electronically approved records are authenticated in the electronic document management system.

Attachment 1
Point Beach Components Compared to MRP-191, Revision 2 Results

The PWR Inspection and Evaluation Guidelines, MRP-227, Revision 1-A [1] requires comparison of the reactor vessel internal components that are within the scope of license renewal for Point Beach Units 1 and 2 to those components contained in MRP-191, Revision 2 [2]. Table 1 and Table 2 contain a tabulation of Westinghouse PWR reactor vessel internals components and materials that are listed in Revision 2 of MRP-191 [2] and indicate their applicability to Point Beach Units 1 and 2. The Point Beach Unit 1 and Unit 2 data within Table 1 and Table 2 originates from Table 5-1 and Table 5-2 in CN-RIDA-13-87, Revision 3 [3]. This data has been updated within Table 1 and Table 2 of this attachment to reflect the additional information within Table 4-4 of MRP-191, Revision 1 [4] and Revision 2 [2] denoted by gray-shaded highlight.

The upper core plate insert locking devices & dowel pins material is listed in MRP-191, Revision 2 [2], as Type 304 SS and Type 316 SS. However, according to the Point Beach Unit 1 and Unit 2 RVI component drawings, the component material is Type 304L SS. There are two degradation mechanisms of concern for the upper core plate insert locking devices & dowel pins, as shown in Table 5-1 of MRP-191, Revision 2 [2]. Type 304 SS and Type 304L SS fall under the austenitic stainless steel category and there are no differences in the screening criteria for either material. Thus, no additional degradation mechanisms are applicable. With no changes to the susceptibility or to the degradation mechanisms of concern, the FMECA and functionality analysis are still applicable. Therefore, all Point Beach Unit 1 and Unit 2 RVI components are addressed by MRP-191, Revision 1 and Revision 2. Although MRP-191, Revision 0 [5], did not include all Point Beach Unit 1 and Unit 2 component materials, these materials differences were considered within the expert panel for MRP-191, Revision 2, and there is no impact on the applicability of MRP-227, Revision 1-A [1] for Point Beach Unit 1 and Unit 2.

Table 1: Point Beach Unit 1 Material and Component Comparison with MRP-191, Revision 2					
Assembly	Sub-Assembly (Note 1)	Component (Note 1)	Material (Note 1)	Applicable (Note 1)	LRA Component (Based on [6])
Upper Internals Assembly	Control Rod Guide Tube Assemblies and Flow Downcomers	Anti-rotation studs and nuts	304 SS	No	
		Anti-rotation studs and nuts	316 SS	No	
		Bolts	316 SS	Yes	RVI RCCA Guide Tube Bolts
		Bolts	304 SS	No	
		C-tubes	304 SS	Yes	
		Enclosure pins	304 SS	No	
		Guide tube enclosures	304 SS	Yes	
		Guide tube enclosures	CF8	No	
		Flanges, intermediate	304 SS	Yes	
		Flanges, intermediate	CF8	Yes	
		Flanges, lower	304 SS	Yes	
		Flanges, lower	CF8	Yes	
		Flexureless inserts	304 SS	Yes	RVI RCCA Guide Tubes, Inserts, and Flow Downcomers
		Flexureless inserts (spring)	Alloy 718	Yes	
		Flexures	X-750	No	
		Guide plates/cards	304 SS	Yes	RVI RCCA Flexures, GT Support pin (split pin)
		Guide plates/cards	CF8	Yes	
		Guide plates/cards	316L SS	No	
		Guide tube support pins	X-750	No	
		Guide tube support pins	316 SS	Yes	
Housing plates	304 SS	Yes			
Housing plates	CF8	Yes			

Table 1: Point Beach Unit 1 Material and Component Comparison with MRP-191, Revision 2 (cont.)

Assembly	Sub-Assembly (Note 1)	Component (Note 1)	Material (Note 1)	Applicable (Note 1)	LRA Component (Based on [6])
Upper Internals Assembly (cont.)	Control Rod Guide Tube Assemblies and Flow Downcomers (cont.)	Inserts	304 SS	No	
		Inserts	CF8	No	
		Lock bars	304 SS	No	
		Sheaths	304 SS	Yes	
		Cover plates	304 SS	No	
		Cover plate cap screws	316 SS	No	
		Cover plate locking caps and tie straps	304 SS	No	
		Support pin nuts	X-750	No	
		Support pin nuts	316 SS	Yes	
		Support pin nuts	304 SS	No	
		Water flow slot ligaments	304 SS	No	
		Probe holder shroud	304 SS	No	
		Mixing Devices	Mixing devices	CF8	Yes
	Mixing devices		304 SS	Yes	
	Upper Core Plate and Fuel Alignment Pins	Fuel alignment pins	316 SS	No	RVI Upper Core Plate Fuel Alignment Pin
		Fuel alignment pins	304 SS	Yes	
		Upper core plate	304 SS	Yes	RVI Upper Core Plate
		Upper core plate insert	304 SS	Yes	
		Upper core plate insert	Stellite	Yes	
		Upper core plate insert bolts	316 SS	Yes	
		Upper core plate insert locking devices & dowel pins	304 SS (Note 2)	No	

Table 1: Point Beach Unit 1 Material and Component Comparison with MRP-191, Revision 2 (cont.)					
Assembly	Sub-Assembly (Note 1)	Component (Note 1)	Material (Note 1)	Applicable (Note 1)	LRA Component (Based on [6])
Upper Internals Assembly (cont.)	Upper Core Plate and Fuel Alignment Pins (cont.)	Upper core plate insert locking devices & dowel pins	316 SS	Yes	RVI Upper Instrumentation Column, Conduit (tubing and supports), Spacers/Clamps
		Protective skirt	304 SS	No	
		Protective skirt bolts	316 SS	No	
		Protective skirt lock bars	304 SS	No	
		Protective skirt dowel pins	304 SS	No	
		Protective skirt dowel pins	316 SS	No	
	Upper Instrumentation Conduit and Supports	Bolting	316 SS	Yes	
		Bolting	304 SS	Yes	
		Brackets, clamps, terminal blocks, and conduit straps	304 SS	Yes	
		Brackets, clamps, terminal blocks, and conduit straps	CF8	Yes	
		Brackets, clamps, terminal blocks, and conduit straps	302 SS	No	
		Conduit seal assembly: body, tubesheets, tubesheet welds	304 SS	Yes	
		Conduit seal assembly – tubes	304 SS	Yes	
		Conduits	304 SS	Yes	
		Flange base	304 SS	Yes	
		Locking caps	304 SS	No	
		Locking caps	304L SS	Yes	
		Support tubes	304 SS	Yes	

Table 1: Point Beach Unit 1 Material and Component Comparison with MRP-191, Revision 2 (cont.)

Assembly	Sub-Assembly (Note 1)	Component (Note 1)	Material (Note 1)	Applicable (Note 1)	LRA Component (Based on [6])
Upper Internals Assembly (cont.)	Upper Plenum	UHI flow column bases	CF8	No	
		UHI flow columns	304 SS	No	
	Upper Support Column Assemblies	Adapters	304 SS	Yes	
		Bolts	316 SS	Yes	RVI Upper Support Column Bolts
		Column bases	CF8	Yes	RVI Upper Support Column- USC Base castings
		Column bases	304 SS	No	
		Column bodies	304 SS	Yes	RVI Upper Support Column and Bottom Nozzle
		Extension tubes	304 SS	Yes	
		Flanges	304 SS	Yes	
		Lock keys	304 SS	No	
		Lock keys	304L SS	No	
		Nuts	304 SS	Yes	
		Nuts	302 SS	No	
	Upper Support Plate Assembly - Inverted Top Hat Design	ITH flange	304 SS	No	
		ITH upper support plate	304 SS	No	
		ITH upper support ring or skirt	304 SS	No	
		ITH upper support ring or skirt	CF8	No	
	Upper Support Plate Assembly - Top Hat Design	Flange	304 SS	No	
		Flange	CF8	No	
		Upper support plate	304 SS	No	
		Upper support plate	CF8	No	
		Upper support ring or skirt	304 SS	No	
		Upper support ring or skirt	CF8	No	

Table 1: Point Beach Unit 1 Material and Component Comparison with MRP-191, Revision 2 (cont.)					
Assembly	Sub-Assembly (Note 1)	Component (Note 1)	Material (Note 1)	Applicable (Note 1)	LRA Component (Based on [6])
Upper Internals Assembly (cont.)	Upper Support Plate Assembly - Top Hat Design (cont.)	Deep beam ribs	304 SS	No	
		Deep beam stiffeners	304 SS	No	
		Bolts	316 SS	No	
		Locking device	316 SS	No	
		Locking device	304 SS	No	
	Upper Support Plate Assembly - Flat Plate Design	Bolts	316 SS	Yes	RVI Upper Instrumentation Column, Conduit (tubing and supports), Spacers/Clamps
		Deep beam ribs	304 SS	Yes	RVI Upper Support Plate, deep beam weldment, top plate, ribs, hollow rounds
		Deep beam stiffeners	304 SS	Yes	
		Locking device	316 SS	No	
		Locking device	304 SS	No	
		Upper support plate	304 SS	Yes	
		Upper support plate	CF8	No	
		Upper support ring or skirt	304 SS	No	
Upper support ring or skirt	CF8	No			
Lower Internals Assembly	Baffle and Former Assembly	Baffle bolting lock devices	304 SS	No	
		Baffle-edge bolts	316 SS	Yes	
		Baffle-edge bolts	347 SS	No	
		Bracket bolts	347 SS	No	
		Baffle plates	304 SS	Yes	RVI Baffle and Former Plates
		Baffle-former bolts	316 SS	No	RVI Baffle/Barrel-Former Bolts
		Baffle-former bolts	347 SS	Yes	
		Corner bolts	347 SS	No	
		Barrel-former bolts	316 SS	No	RVI Baffle/Barrel-Former Bolts
		Barrel-former bolts	347 SS	Yes	

Table 1: Point Beach Unit 1 Material and Component Comparison with MRP-191, Revision 2 (cont.)					
Assembly	Sub-Assembly (Note 1)	Component (Note 1)	Material (Note 1)	Applicable (Note 1)	LRA Component (Based on [6])
Lower Internals Assembly (cont.)	Baffle and Former Assembly (cont.)	Former dowel pins	302 SS	No	
		Former dowel pins	304 SS	Yes	
		Former plates	304 SS	Yes	RVI Baffle and Former Plates
	Bottom-Mounted Instrumentation (BMI) Column Assemblies	BMI column bodies	304 SS	Yes	RVI Bottom Mounted Instrumentation Columns
		BMI column bolts	316 SS	Yes	
		BMI column collars	304 SS	No	
		BMI column cruciforms	CF8	Yes	RVI Bottom Mounted Instrumentation Column Cruciforms
		BMI column cruciforms	304 SS	Yes	
		BMI column extension bars	304 SS	Yes	
		BMI column extension tubes	304 SS	Yes	
		BMI column locking devices	304L SS	Yes	
		BMI column nuts	304 SS	Yes	
	Core Barrel	Core barrel flange	304 SS	Yes	RVI Core Barrel Flange – ring forging, Core Barrel (guide key)
		Upflow conversion core barrel plug body	304 SS	Yes	
		Upflow conversion core barrel plug mandrel	316 SS	Yes	
		Core barrel outlet nozzles	304 SS	Yes	RVI Core Barrel Outlet Nozzle
		Upper core barrel (includes UAW)	304 SS	Yes	
		Upper core barrel (includes UFW and UGW)	304 SS	Yes	
		Lower core barrel (includes MAW and LAW)	304 SS	Yes	
		Lower core barrel (includes LGW and LFW)	304 SS	Yes	

Table 1: Point Beach Unit 1 Material and Component Comparison with MRP-191, Revision 2 (cont.)						
Assembly	Sub-Assembly (Note 1)	Component (Note 1)	Material (Note 1)	Applicable (Note 1)	LRA Component (Based on [6])	
Lower Internals Assembly (cont.)	Core Barrel (cont.)	Safety injection nozzle interface	304 SS	Yes		
	Diffuser Plate	Diffuser plate	304 SS	Yes	RVI Secondary Core Support - base plate, energy absorber, Diffuser Plate (Flow Mixer Plate)	
	Flux Thimbles (Tubes)	Flux thimble tube plugs	Flux thimble tube plugs	304 SS	Yes	RVI Flux Thimbles
		Flux thimble tube plugs	Flux thimble tube plugs	316 SS	No	
		Flux thimble tube plugs	Flux thimble tube plugs	308 SS	No	
		Flux thimble tube plugs	Flux thimble tube plugs	A600	No	
		Flux thimbles (tubes)	Flux thimbles (tubes)	316 SS	Yes	
		Flux thimbles (tubes)	Flux thimbles (tubes)	A600	No	
		Flux thimble anti-vibration sleeve	Flux thimble anti-vibration sleeve	304 SS	No	
	Head Cooling Spray Nozzles	Head cooling spray nozzles	304 SS	Yes	RVI (Head-Cooling) Spray nozzle bodies and nozzle tips	
	Irradiation Specimen Guides	Irradiation specimen guides	Irradiation specimen guides	304 SS	Yes	
		Irradiation specimen guide bolts	Irradiation specimen guide bolts	316 SS	No	
		Irradiation specimen guide lock caps	Irradiation specimen guide lock caps	304L SS	No	
		Irradiation specimen plug (spring)	Irradiation specimen plug (spring)	X-750	Yes	
		Irradiation specimen plug (dowel pin)	Irradiation specimen plug (dowel pin)	316 SS	Yes	
		Irradiation specimen plug (plug)	Irradiation specimen plug (plug)	304 SS	Yes	
	Lower Core Plate and Fuel Alignment Pins	Fuel alignment pins	Fuel alignment pins	316 SS	No	RVI Lower Core Plate Fuel Alignment Pins
		Fuel alignment pins	Fuel alignment pins	304 SS	Yes	
		XL LCP fuel alignment pins	XL LCP fuel alignment pins	316 SS	No	

Table 1: Point Beach Unit 1 Material and Component Comparison with MRP-191, Revision 2 (cont.)						
Assembly	Sub-Assembly (Note 1)	Component (Note 1)	Material (Note 1)	Applicable (Note 1)	LRA Component (Based on [6])	
Lower Internals Assembly (cont.)	Lower Core Plate and Fuel Alignment Pins (cont.)	LCP and manway bolts	316 SS	Yes		
		LCP and manway locking devices	304L SS	No		
		Lower core plate	304 SS	Yes	RVI Lower Core Plate	
		XL lower core plate	304 SS	No		
	Lower Support Column Assemblies	Lower support column bodies	Lower support column bodies	CF8	No	
			Lower support column bodies	304 SS	Yes	
		Lower support column bolts	Lower support column bolts	304 SS	No	RVI Lower Support Plate Column Bolts/Nuts
			Lower support column bolts	316 SS	Yes	
			Lower support column nuts	304 SS	Yes	
		Lower support column bolt locking devices	Lower support column bolt locking devices	304L SS (Note 3)	Yes	
			Lower support column bolt locking devices	304 SS (Note 3)	No	
		Lower support column sleeves	304 SS	Yes	RVI Lower Support Columns, Sleeves	
		Lower Support Casting or Forging	Lower support casting	CF8	No	
	Lower support forging		304 SS	Yes	RVI Lower Support Forging	
	Neutron Panels/Thermal Shield	Neutron panel bolts	Neutron panel bolts	316 SS	No	
			Neutron panel lock devices	304 SS	No	
		Neutron panel lock devices	304L SS	No		
		Thermal shield bolts	316 SS	Yes		
		Thermal shield dowels	316 SS	Yes	RVI Thermal shield – plate material, flexures, Dowel Pin	
		Thermal shield dowels	304 SS	Yes		

Table 1: Point Beach Unit 1 Material and Component Comparison with MRP-191, Revision 2 (cont.)					
Assembly	Sub-Assembly (Note 1)	Component (Note 1)	Material (Note 1)	Applicable (Note 1)	LRA Component (Based on [6])
Lower Internals Assembly (cont.)	Neutron Panels/ Thermal Shield (cont.)	Thermal shield flexures	304 SS	Yes	RVI Thermal shield – plate material, flexures, Dowel Pin
		Thermal shield flexures	316 SS	No	
		Thermal shield flexure bolts	316 SS	Yes	
		Thermal shield flexure locking devices and dowel pins	304 SS	No	
		Thermal shield flexure locking devices and dowel pins	304L SS	Yes	
		Thermal shield or neutron panels	304 SS	Yes	
	Radial Support Keys	Radial support key bolts	304 SS	No	RVI Radial Support Keys
		Radial support key bolts	316 SS	Yes	
		Radial support key dowels	304 SS	No	
		Radial support key lock keys	304 SS (Note 4)	No	RVI Radial Support Keys
		Radial support keys	304 SS	Yes	
		Radial support keys	Stellite	Yes	
	Secondary Core Support (SCS) Assembly	SCS base plate	304 SS	Yes	RVI Secondary Core Support - base plate, energy absorber, Diffuser Plate (Flow Mixer Plate)
		SCS bolts	316 SS	No	
		SCS energy absorber	304 SS	Yes	
		SCS guide post	304 SS	Yes	RVI Secondary Core Support Assy – guide post, housing
		SCS guide post	CF8	No	
		SCS housing	304 SS	Yes	
		SCS housing	CF8	No	
		SCS lock keys	304 SS	No	
	Upper and lower tie plates	304 SS	Yes		

Table 1: Point Beach Unit 1 Material and Component Comparison with MRP-191, Revision 2 (cont.)

Assembly	Sub-Assembly (Note 1)	Component (Note 1)	Material (Note 1)	Applicable (Note 1)	LRA Component (Based on [6])
Interfacing Components	Interfacing Components	Clevis insert bolts	X-750	Yes	RVI Clevis Insert Bolts
		Clevis insert dowels	A600	Yes	
		Clevis insert locking devices	A 600	Yes	RVI Clevis Insert Bolt Locking Mechanisms
		Clevis insert locking devices	316 SS	No	
		Clevis inserts	A 600	Yes	RVI Clevis Inserts
		Clevis inserts	304 SS	No	
		Clevis inserts	Stellite	Yes	
		Head and vessel alignment pin bolts	316 SS	Yes	RVI Head and Vessel Alignment Pins
		Head and vessel alignment pin lock caps	304L SS	No	
		Head and vessel alignment pins	304 SS	Yes	
		Head and vessel alignment pins	Stellite	No	
		Internals hold-down spring	304 SS	No	RVI Hold-down Spring
		Internals hold-down spring	403 SS	Yes	
		Internals hold-down spring	F6NM	No	
		Upper core plate alignment pins	304 SS	Yes	RVI Upper Core Plate Alignment Pin
		Upper core plate alignment pins	Stellite	Yes	
		Thermal sleeves	304 SS	Yes	
		Thermal sleeve guide funnels	304 SS	No	
		Thermal sleeve guide funnels	CF8	Yes	

Table 1: Point Beach Unit 1 Material and Component Comparison with MRP-191, Revision 2 (cont.)					
Assembly	Sub-Assembly (Note 1)	Component (Note 1)	Material (Note 1)	Applicable (Note 1)	LRA Component (Based on [6])
Interfacing Components (cont.)	Interfacing Components (cont.)	Instrumentation nozzle funnels	304 SS	No	
		Replacement reactor vessel head (RRVH) extension tubes	304 SS	No	

Notes:

1. Cells that are shaded gray represent additional information from Table 4-4 of MRP-191, Revision 1 [4] and Revision 2 [2], that was not within MRP-191, Revision 0 [5]. This includes component name changes, component material additions, and new components or sub-assemblies.
2. Upper core plate insert locking devices at Unit 1 are 304L SS.
3. The lower support column bolt locking devices are listed as 304 SS within Table 4-6, Table 5-1, Table 6-10, and Table 7-2 of MRP-191, Revision 2 [2] and also as 304L SS in Table 4-4 of MRP-191, Revision 2 [2]. Both materials are listed in this table.
4. The radial support key lock keys was listed as 316 SS within Table 6-10 and Table 7-2 of MRP-191, Revision 2 [2] but should be 304 SS.

Table 2: Point Beach Unit 2 Material and Component Comparison with MRP-191, Revision 2					
Assembly	Sub-Assembly (Note 1)	Component (Note 1)	Material (Note 1)	Applicable (Note 1)	LRA Component (Based on [6])
Upper Internals Assembly	Control Rod Guide Tube Assemblies and Flow Downcomers	Anti-rotation studs and nuts	304 SS	No	
		Anti-rotation studs and nuts	316 SS	No	
		Bolts	316 SS	Yes	RVI RCCA Guide Tube Bolts
		Bolts	304 SS	No	
		C-tubes	304 SS	Yes	
		Enclosure pins	304 SS	No	
		Guide tube enclosures	304 SS	Yes	
		Guide tube enclosures	CF8	No	
		Flanges, intermediate	304 SS	Yes	
		Flanges, intermediate	CF8	Yes	
		Flanges, lower	304 SS	Yes	
		Flanges, lower	CF8	Yes	
		Flexureless inserts	304 SS	Yes	RVI RCCA Guide Tubes, Inserts, and Flow Downcomers
		Flexureless inserts (spring)	Alloy 718	Yes	
		Flexures	X-750	No	
		Guide plates/cards	304 SS	Yes	RVI RCCA Flexures, GT Support pin (split pin)
		Guide plates/cards	CF8	Yes	
		Guide plates/cards	316L SS	No	
		Guide tube support pins	X-750	No	
		Guide tube support pins	316 SS	Yes	
		Housing plates	304 SS	Yes	
		Housing plates	CF8	Yes	

Table 2: Point Beach Unit 2 Material and Component Comparison with MRP-191, Revision 2 (cont.)

Assembly	Sub-Assembly (Note 1)	Component (Note 1)	Material (Note 1)	Applicable (Note 1)	LRA Component (Based on [6])
Upper Internals Assembly (cont.)	Control Rod Guide Tube Assemblies and Flow Downcomers (cont.)	Inserts	304 SS	No	
		Inserts	CF8	No	
		Lock bars	304 SS	No	
		Sheaths	304 SS	Yes	
		Cover plates	304 SS	No	
		Cover plate cap screws	316 SS	No	
		Cover plate locking caps and tie straps	304 SS	No	
		Support pin nuts	X-750	No	
		Support pin nuts	316 SS	Yes	
		Support pin nuts	304 SS	No	
		Water flow slot ligaments	304 SS	No	
		Probe holder shroud	304 SS	No	
		Mixing Devices	Mixing devices	CF8	Yes
	Mixing devices		304 SS	Yes	
	Upper Core Plate and Fuel Alignment Pins	Fuel alignment pins	316 SS	No	RVI Upper Core Plate Fuel Alignment Pin
		Fuel alignment pins	304 SS	Yes	
		Upper core plate	304 SS	Yes	RVI Upper Core Plate
		Upper core plate insert	304 SS	Yes	
		Upper core plate insert	Stellite	Yes	
		Upper core plate insert bolts	316 SS	Yes	
		Upper core plate insert locking devices & dowel pins	304 SS (Note 2)	No	
	Upper core plate insert locking devices & dowel pins	316 SS	Yes		

Table 2: Point Beach Unit 2 Material and Component Comparison with MRP-191, Revision 2 (cont.)

Assembly	Sub-Assembly (Note 1)	Component (Note 1)	Material (Note 1)	Applicable (Note 1)	LRA Component (Based on [6])
Upper Internals Assembly (cont.)	Upper Core Plate and Fuel Alignment Pins (cont.)	Protective skirt	304 SS	No	RVI Upper Instrumentation Column, Conduit (tubing and supports), Spacers/Clamps
		Protective skirt bolts	316 SS	No	
		Protective skirt lock bars	304 SS	No	
		Protective skirt dowel pins	304 SS	No	
		Protective skirt dowel pins	316 SS	No	
	Upper Instrumentation conduit and supports	Bolting	316 SS	Yes	
		Bolting	304 SS	Yes	
		Brackets, clamps, terminal blocks, and conduit straps	304 SS	Yes	
		Brackets, clamps, terminal blocks, and conduit straps	CF8	Yes	
		Brackets, clamps, terminal blocks, and conduit straps	302 SS	No	
		Conduit seal assembly: body, tubesheets, tubesheet welds	304 SS	Yes	
		Conduit seal assembly – tubes	304 SS	Yes	
		Conduits	304 SS	Yes	
		Flange base	304 SS	Yes	
		Locking caps	304 SS	No	
		Locking caps	304L SS	Yes	
		Support tubes	304L SS	Yes	
		Upper plenum	UHI flow column bases	CF8	
	UHI flow columns		304 SS	No	
	Upper Support Column Assemblies	Adapters	304 SS	Yes	

Table 2: Point Beach Unit 2 Material and Component Comparison with MRP-191, Revision 2 (cont.)

Assembly	Sub-Assembly (Note 1)	Component (Note 1)	Material (Note 1)	Applicable (Note 1)	LRA Component (Based on [6])
Upper Internals Assembly (cont.)	Upper Support Column Assemblies (cont.)	Bolts	316 SS	Yes	RVI Upper Support Column Bolts
		Column bases	CF8	Yes	RVI Upper Support Column- USC Base castings
		Column bases	304 SS	No	
		Column bodies	304 SS	Yes	RVI Upper Support Column and Bottom Nozzle
		Extension tubes	304 SS	Yes	
		Flanges	304 SS	Yes	
		Lock keys	304 SS	No	
		Lock keys	304L SS	No	
		Nuts	304 SS	Yes	
		Nuts	302 SS	No	
	Upper support plate assembly - inverted top hat design	ITH flange	304 SS	No	
		ITH upper support plate	304 SS	No	
		ITH upper support ring or skirt	304 SS	No	
		ITH upper support ring or skirt	CF8	No	
	Upper support plate assembly - top hat design	Flange	304 SS	No	
		Flange	CF8	No	
		Upper support plate	304 SS	No	
		Upper support plate	CF8	No	
		Upper support ring or skirt	304 SS	No	
		Upper support ring or skirt	CF8	No	
		Deep beam ribs	304 SS	No	
		Deep beam stiffeners	304 SS	No	
		Bolts	316 SS	No	

Table 2: Point Beach Unit 2 Material and Component Comparison with MRP-191, Revision 2 (cont.)					
Assembly	Sub-Assembly (Note 1)	Component (Note 1)	Material (Note 1)	Applicable (Note 1)	LRA Component (Based on [6])
Upper Internals Assembly (cont.)	Upper support plate assembly - top hat design (cont.)	Locking device	316 SS	No	
		Locking device	304 SS	No	
	Upper support plate assembly - flat plate design	Bolts	316 SS	Yes	RVI Upper Instrumentation Column, Conduit (tubing and supports), Spacers/Clamps
		Deep beam ribs	304 SS	Yes	RVI Upper Support Plate, deep beam weldment, top plate, ribs, hollow rounds
		Deep beam stiffeners	304 SS	Yes	
		Locking device	316 SS	No	
		Locking device	304 SS	No	
		Upper support plate	304 SS	Yes	
		Upper support plate	CF8	No	
		Upper support ring or skirt	304 SS	No	
		Upper support ring or skirt	CF8	No	
Lower Internals Assembly	Baffle and Former Assembly	Baffle bolting lock devices	304 SS	No	
		Baffle-edge bolts	316 SS	Yes	
		Baffle-edge bolts	347 SS	No	
		Bracket bolts	347 SS	No	
		Baffle plates	304 SS	Yes	RVI Baffle and Former Plates
		Baffle-former bolts	316 SS	No	RVI Baffle/Barrel-Former Bolts
		Baffle-former bolts	347 SS	Yes	
		Corner bolts	347 SS	No	
		Barrel-former bolts	316 SS	No	RVI Baffle/Barrel-Former Bolts
		Barrel-former bolts	347 SS	Yes	
		Former dowel pins	302 SS	No	
		Former dowel pins	304 SS	Yes	
		Former plates	304 SS	Yes	RVI Baffle and Former Plates

Table 2: Point Beach Unit 2 Material and Component Comparison with MRP-191, Revision 2 (cont.)

Assembly	Sub-Assembly (Note 1)	Component (Note 1)	Material (Note 1)	Applicable (Note 1)	LRA Component (Based on [6])
Lower Internals Assembly (cont.)	Bottom Mounted Instrumentation (BMI) column assemblies	BMI column bodies	304 SS	Yes	RVI Bottom Mounted Instrumentation Columns
		BMI column bolts	316 SS	Yes	
		BMI column collars	304 SS	No	
		BMI column cruciforms	CF8	Yes	RVI Bottom Mounted Instrumentation Column Cruciforms
		BMI column cruciforms	304 SS	Yes	
		BMI column extension bars	304 SS	Yes	
		BMI column extension tubes	304 SS	Yes	
		BMI column locking devices	304L SS	Yes	
		BMI column nuts	304 SS	Yes	
	Core Barrel	Core barrel flange	304 SS	Yes	RVI Core Barrel Flange – ring forging, Core Barrel (guide key)
		Upflow conversion core barrel plug body	304 SS	Yes	
		Upflow conversion core barrel plug mandrel	316 SS	Yes	
		Core barrel outlet nozzles	304 SS	Yes	RVI Core Barrel Outlet Nozzle
		Lower core barrel (includes MAW and LAW)	304 SS	Yes	
		Lower core barrel (includes LGW and LFW)	304 SS	Yes	
		Upper core barrel (includes UAW)	304 SS	Yes	
		Upper core barrel (includes UFW and UGW)	304 SS	Yes	
		Safety injection nozzle interface	304 SS	Yes	
	Diffuser Plate	Diffuser plate	304 SS	Yes	RVI Secondary Core Support - base plate, energy absorber, Diffuser Plate (Flow Mixer Plate)

Table 2: Point Beach Unit 2 Material and Component Comparison with MRP-191, Revision 2 (cont.)					
Assembly	Sub-Assembly (Note 1)	Component (Note 1)	Material (Note 1)	Applicable (Note 1)	LRA Component (Based on [6])
Lower Internals Assembly (cont.)	Flux Thimbles (Tubes)	Flux thimble tube plugs	304 SS	Yes	RVI Flux Thimbles
		Flux thimble tube plugs	316 SS	No	
		Flux thimble tube plugs	308 SS	No	
		Flux thimble tube plugs	A600	No	
		Flux thimbles (tubes)	316 SS	Yes	
		Flux thimbles (tubes)	A600	No	
		Flux thimble anti-vibration sleeve	304 SS	No	
	Head Cooling Spray Nozzles	Head cooling spray nozzles	304 SS	Yes	RVI (Head-Cooling) Spray nozzle bodies and nozzle tips
	Irradiation Specimen Guides	Irradiation specimen guides	304 SS	Yes	
		Irradiation specimen guide bolts	316 SS	No	
		Irradiation specimen guide lock caps	304L SS	No	
		Irradiation specimen plug (spring)	X-750	Yes	
		Irradiation specimen plug (dowel pin)	316 SS	Yes	
		Irradiation specimen plug (plug)	304 SS	Yes	
	Lower Core Plate and Fuel Alignment Pins	Fuel alignment pins	316 SS	No	RVI Lower Core Plate Fuel Alignment Pins

Table 2: Point Beach Unit 2 Material and Component Comparison with MRP-191, Revision 2 (cont.)

Assembly	Sub-Assembly (Note 1)	Component (Note 1)	Material (Note 1)	Applicable (Note 1)	LRA Component (Based on [6])
Lower Internals Assembly (cont.)	Lower Core Plate and Fuel Alignment Pins (cont.)	Fuel alignment pins	304 SS	Yes	RVI Lower Core Plate Fuel Alignment Pins
		XL LCP fuel alignment pins	316 SS	No	
		LCP and manway bolts	316 SS	Yes	
		LCP and manway locking devices	304L SS	No	
		Lower core plate	304 SS	Yes	RVI Lower Core Plate
		XL lower core plate	304 SS	No	
	Lower Support Column Assemblies	Lower support column bodies	CF8	No	
		Lower support column bodies	304 SS	Yes	
		Lower support column bolts	304 SS	No	RVI Lower Support Plate Column Bolts/Nuts
		Lower support column bolts	316 SS	Yes	
		Lower support column nuts	304 SS	Yes	
		Lower support column bolt locking devices	304L SS Note 3	Yes	
		Lower support column bolt locking devices	304 SS Note 3	No	
		Lower support column sleeves	304 SS	Yes	RVI Lower Support Columns, Sleeves
	Lower Support Casting or Forging	Lower support casting	CF8	No	
		Lower support forging	304 SS	Yes	RVI Lower Support Forging

Table 2: Point Beach Unit 2 Material and Component Comparison with MRP-191, Revision 2 (cont.)						
Assembly	Sub-Assembly (Note 1)	Component (Note 1)	Material (Note 1)	Applicable (Note 1)	LRA Component (Based on [6])	
Lower Internals Assembly (cont.)	Neutron Panels/ Thermal Shield	Neutron panel bolts	316 SS	No		
		Neutron panel locking devices	304 SS	No		
		Neutron panel locking devices	304L SS	No		
		Thermal shield bolts	316 SS	Yes		
		Thermal shield dowels	316 SS	Yes		
		Thermal shield dowels	304 SS	Yes		
		Thermal shield flexures	304 SS	Yes		
		Thermal shield flexures	316 SS	No		
		Thermal shield flexure bolts	316 SS	Yes		
		Thermal shield flexure locking devices and dowel pins	304 SS	No		
		Thermal shield flexure locking devices and dowel pins	304L SS	Yes		
		Thermal shield or neutron panels	304 SS	Yes		
						RVI Thermal shield – plate material, flexures, Dowel Pin
		Radial Support Keys	Radial support key bolts	304 SS	No	
			Radial support key bolts	316 SS	Yes	
			Radial support key dowels	304 SS	No	
			Radial support key lock keys	304 SS Note 4	No	
			Radial support keys	304 SS	Yes	
			Radial support keys	Stellite	Yes	
						RVI Radial Support Keys
					RVI Radial Support Keys	

Table 2: Point Beach Unit 2 Material and Component Comparison with MRP-191, Revision 2 (cont.)

Assembly	Sub-Assembly (Note 1)	Component (Note 1)	Material (Note 1)	Applicable (Note 1)	LRA Component (Based on [6])
Lower Internals Assembly (cont.)	Secondary Core Support (SCS) Assembly	SCS base plate	304 SS	Yes	RVI Secondary Core Support - base plate, energy absorber, Diffuser Plate (Flow Mixer Plate)
		SCS bolts	316 SS	No	
		SCS energy absorber	304 SS	Yes	
		SCS guide post	304 SS	No	RVI Secondary Core Support Assy – guide post, housing
		SCS guide post	CF8	Yes	
		SCS housing	304 SS	No	
		SCS housing	CF8	Yes	
		SCS lock keys	304 SS	No	
		Upper and lower tie plates	304 SS	Yes	
Interfacing Components	Interfacing Components	Clevis insert bolts	X-750	Yes	RVI Clevis Insert Bolts
		Clevis insert dowels	Alloy 600	Yes	
		Clevis insert locking devices	A 600	Yes	RVI Clevis Insert Bolt Locking Mechanisms
		Clevis insert locking devices	316 SS	No	
		Clevis inserts	A 600	Yes	RVI Clevis Inserts
		Clevis inserts	304 SS	No	
		Clevis inserts	Stellite	Yes	
		Head and vessel alignment pin bolts	316 SS	Yes	RVI Head and Vessel Alignment Pins
		Head and vessel alignment pin lock caps	304L SS	No	
		Head and vessel alignment pins	304 SS	Yes	
		Head and vessel alignment pins	Stellite	No	
		Internals hold-down spring	304 SS	No	RVI Hold-down Spring

Table 2: Point Beach Unit 2 Material and Component Comparison with MRP-191, Revision 2 (cont.)

Assembly	Sub-Assembly (Note 1)	Component (Note 1)	Material (Note 1)	Applicable (Note 1)	LRA Component (Based on [6])
Interfacing Components (cont.)	Interfacing Components (cont.)	Internals hold-down spring	403 SS	Yes	RVI Hold-down Spring
		Internals hold-down spring	F6NM	No	
		Upper core plate alignment pins	304 SS	Yes	RVI Upper Core Plate Alignment Pin
		Upper core plate alignment pins	Stellite	Yes	
		Thermal sleeves	304 SS	Yes	
		Thermal sleeve guide funnels	304 SS	No	
		Thermal sleeve guide funnels	CF8	Yes	
		Instrumentation nozzle funnels	304 SS	No	
		Replacement reactor vessel head extension tubes	304 SS	No	

Notes:

1. Cells that are shaded gray represent additional information from Table 4-4 of MRP-191, Revision 1 [4] and Revision 2 [2] that was not within MRP-191, Revision 0 [5]. This includes component name changes, component material additions, and new components or sub-assemblies.
2. Upper core plate insert locking devices at Unit 2 are 304L SS.
3. The lower support column bolt locking devices are listed as 304 SS within Table 4-6, Table 5-1, Table 6-10, and Table 7-2 of MRP-191, Revision 2 [2] and also as 304L SS in Table 4-4 of MRP-191, Revision 2 [2]. Both materials are listed in this table.
4. The radial support key lock keys was listed as 316 SS within Table 6-10 and Table 7-2 of MRP-191, Revision 2 [2] but should be 304 SS..

References for Attachment 1:

1. Materials Reliability Program: Pressurized Water Reactor Internals Inspection and Evaluation Guidelines (MRP-227, Revision 1-A). EPRI, Palo Alto, CA: 2019. 3002017168.
2. Materials Reliability Program: Screening, Categorization, and Ranking of Reactor Internals Components for Westinghouse and Combustion Engineering PWR Design (MRP-191, Revision 2), EPRI, Palo Alto, CA, 2018. 3002013220.
3. Westinghouse Calculation Note, CN-RIDA-13-87, Revision 3, "Point Beach Units 1 and 2 Support for Reactor Internals Aging Management – Applicant/Licensee Action Items 1 and 2," October 18, 2016.
4. Materials Reliability Program: Screening, Categorization, and Ranking of Reactor Internals Components for Westinghouse and Combustion Engineering PWR Design (MRP-191, Revision 1). EPRI, Palo Alto, CA: 2016. 3002007960.
5. Materials Reliability Program: Screening, Categorization, and Ranking of Reactor Internals Components for Westinghouse and Combustion Engineering PWR Design (MRP-191). EPRI, Palo Alto, CA: 2006. 1013234.
6. License Renewal Application Point Beach Nuclear Generating Station, "Application for Renewed Operating Licenses," February 26, 2004.

Attachment 2
Comparison of MRP-191 Revisions

Table 3: MRP-191 Revision – Component and IMT Consequence of Failure Comparison

Assembly	Subassembly (Note 1)	MRP-191 Rev. 0 Component	MRP-191 Rev. 1 Component	MRP-191 Rev. 2 Component (Note 1)	Material	MRP-191 Rev. 0 IMT Conseq. of Failure	MRP-191 Rev. 1 IMT Conseq. of Failure	MRP-191 Rev. 2 IMT Conseq. of Failure (Note 2)
Upper internals assembly	Control rod guide tube assemblies and flow downcomers	Anti-rotation studs and nuts	Anti-rotation studs and nuts	Anti-rotation studs and nuts	304 SS	G	G	G
		--	Anti-rotation studs and nuts	Anti-rotation studs and nuts	316 SS	--	G	G
		Bolts	Bolts	Bolts	316 SS	NONE	NONE	NONE
		--	Bolts	Bolts	304 SS	--	NONE	NONE
		C-tubes	C-tubes	C-tubes	304 SS	G	G	G
		Enclosure pins	Enclosure pins	Enclosure pins	304 SS	NONE	NONE	NONE
		Upper guide tube enclosures	Upper guide tube enclosures	Guide tube enclosures (Note 3)	304 SS	NONE	NONE	NONE
		--	Upper guide tube enclosures	Guide tube enclosures (Note 3)	CF8	--	NONE	NONE
		Flanges, intermediate	Flanges, intermediate	Flanges, intermediate	304 SS	G	G	G
		Flanges, intermediate	Flanges, intermediate	Flanges, intermediate	CF8	G	G	G
		Flanges, lower	Flanges, lower	Flanges, lower	304 SS	G	G	G
		Flanges, lower	Flanges, lower	Flanges, lower	CF8	G	G	G
		Flexureless inserts	Flexureless inserts	Flexureless inserts	304 SS	G	NONE	NONE
		--	--	Flexureless inserts (spring)	Alloy 718	--	--	N/A
		Flexures	Flexures	Flexures	X-750	G	NONE	NONE
Guide plates/cards	Guide plates/cards	Guide plates/cards	304 SS	G	G	G		

Table 3 (continued): MRP-191 Revision – Component and IMT Consequence of Failure Comparison

Assembly	Subassembly (Note 1)	MRP-191 Rev. 0 Component	MRP-191 Rev. 1 Component	MRP-191 Rev. 2 Component (Note 1)	Material	MRP-191 Rev. 0 IMT Conseq. of Failure	MRP-191 Rev. 1 IMT Conseq. of Failure	MRP-191 Rev. 2 IMT Conseq. of Failure (Note 2)
Upper internals assembly (cont.)	Control rod guide tube assemblies and flow downcomers (cont.)	--	Guide plates/cards	Guide plates/cards	316L SS	--	G	G
		--	Guide plates/cards	Guide plates/cards	CF8	--	G	G
		Guide tube support pins	Guide tube support pins	Guide tube support pins	X-750	NONE	NONE	NONE
		Guide tube support pins	Guide tube support pins	Guide tube support pins	316 SS	NONE	NONE	NONE
		Housing plates	Housing plates	Housing plates	304 SS	G	G	G
		--	Housing plates	Housing plates	CF8	--	G	G
		Inserts	Inserts	Inserts	304 SS	N/A	N/A	N/A
		--	--	Inserts	CF8	--	--	N/A
		Lock bars	Lock bars	Lock bars	304 SS	NONE	NONE	NONE
		Sheaths	Sheaths	Sheaths	304 SS	G	G	G
		Support pin cover plates	Support pin cover plates	Cover plates (Note 4)	304 SS	NONE	NONE	NONE
		Support pin cover plate cap screws	Support pin cover plate cap screws	Cover plate cap screws (Note 4)	316 SS	NONE	NONE	NONE
		Support pin cover plate locking caps and tie straps	Support pin cover plate locking caps and tie straps	Cover plate locking caps and tie straps (Note 4)	304 SS	NONE	NONE	NONE
		Support pin nuts	Support pin nuts	Support pin nuts	X-750	NONE	NONE	NONE
		--	Support pin nuts	Support pin nuts	304 SS	--	NONE	NONE
		Support pin nuts	Support pin nuts	Support pin nuts	316 SS	NONE	NONE	NONE
		Water flow slot ligaments	Water flow slot ligaments	Water flow slot ligaments	304 SS	N/A	N/A	N/A
		--	--	Probe holder shroud	304 SS	--	--	N/A
		Mixing Devices	Mixing devices	Mixing devices	Mixing devices	CF8	NONE	NONE
	--	Mixing devices	Mixing devices	Mixing devices	304 SS	--	NONE	NONE

Table 3 (continued): MRP-191 Revision – Component and IMT Consequence of Failure Comparison

Assembly	Subassembly (Note 1)	MRP-191 Rev. 0 Component	MRP-191 Rev. 1 Component	MRP-191 Rev. 2 Component (Note 1)	Material	MRP-191 Rev. 0 IMT Conseq. of Failure	MRP-191 Rev. 1 IMT Conseq. of Failure	MRP-191 Rev. 2 IMT Conseq. of Failure (Note 2)
Upper Internals Assembly (cont.)	UCP and fuel alignment pins	Fuel alignment pins	Fuel alignment pins	Fuel alignment pins	316 SS	NONE	NONE	NONE
		--	Fuel alignment pins	Fuel alignment pins	304 SS	--	NONE	NONE
		UCP	UCP	UCP	304 SS	A, G	A, G	A, G
		--	--	Upper core plate insert	304 SS	--	--	N/A
		--	--	Upper core plate insert	Stellite	--	--	N/A
		--	--	Upper core plate insert bolts	316 SS	--	--	N/A
		--	--	Upper core plate insert locking devices & dowel pins	304 SS	--	--	N/A
		--	--	Upper core plate insert locking devices & dowel pins	316 SS	--	--	N/A
		--	Protective skirt	Protective skirt	304 SS	--	N/A	N/A
		--	Bolts	Protective skirt bolts (Note 5)	316 SS	--	N/A	N/A
		--	Lock bars	Protective skirt lock bars (Note 5)	304 SS	--	N/A	N/A
		--	Dowel pins	Protective skirt dowel pins (Note 5)	304 SS	--	N/A	N/A
		--	Dowel pins	Protective skirt dowel pins (Note 5)	316 SS	--	N/A	N/A

Table 3 (continued): MRP-191 Revision – Component and IMT Consequence of Failure Comparison

Assembly	Subassembly (Note 1)	MRP-191 Rev. 0 Component	MRP-191 Rev. 1 Component	MRP-191 Rev. 2 Component (Note 1)	Material	MRP-191 Rev. 0 IMT Conseq. of Failure	MRP-191 Rev. 1 IMT Conseq. of Failure	MRP-191 Rev. 2 IMT Conseq. of Failure (Note 2)
Upper internals assembly (cont.)	Upper instrumentation conduit and supports	Bolting	Bolting	Bolting	316 SS	NONE	NONE	NONE
		--	Bolting	Bolting	304 SS	--	NONE	NONE
		Brackets, clamps, terminal blocks, and conduit straps	Brackets, clamps, terminal blocks, and conduit straps	Brackets, clamps, terminal blocks, and conduit straps	304 SS	NONE	NONE	NONE
		--	Brackets, clamps, terminal blocks, and conduit straps	Brackets, clamps, terminal blocks, and conduit straps	302 SS	--	NONE	NONE
		--	Brackets, clamps, terminal blocks, and conduit straps	Brackets, clamps, terminal blocks, and conduit straps	CF8	--	NONE	NONE
		Conduit seal assembly: body, tubesheets	Conduit seal assembly: body, tubesheets	Conduit seal assembly: body, tubesheets, tubesheet welds	304 SS	NONE	NONE	NONE
		Conduit seal assembly: tubes	Conduit seal assembly: tubes	Conduit seal assembly: tubes	304 SS	NONE	NONE	NONE
		Conduits	Conduits	Conduits	304 SS	NONE	NONE	NONE
		Flange base	Flange base	Flange base	304 SS	NONE	NONE	NONE
		Locking caps	Locking caps	Locking caps	304 SS	NONE	NONE	NONE
		--	Locking caps	Locking caps	304L SS	--	NONE	NONE
		Support tubes	Support tubes	Support tubes	304 SS	NONE	NONE	NONE
	Upper plenum	UHI flow column bases	UHI flow column bases	UHI flow column bases	CF8	G	G	G
		UHI flow columns	UHI flow columns	UHI flow columns	304 SS	G	G	G
	Upper support column assemblies	Adapters	Adapters	Adapters	304 SS	G	G	G
		Bolts	Bolts	Bolts	316 SS	G	G	G
		Column bases	Column bases	Column bases	CF8	G	G	G

Table 3 (continued): MRP-191 Revision – Component and IMT Consequence of Failure Comparison

Assembly	Subassembly (Note 1)	MRP-191 Rev. 0 Component	MRP-191 Rev. 1 Component	MRP-191 Rev. 2 Component (Note 1)	Material	MRP-191 Rev. 0 IMT Conseq. of Failure	MRP-191 Rev. 1 IMT Conseq. of Failure	MRP-191 Rev. 2 IMT Conseq. of Failure (Note 2)
Upper internals assembly (cont.)	Upper support column assemblies (cont.)	--	Column bases	Column bases	304 SS	--	G	G
		Column bodies	Column bodies	Column bodies	304 SS	G	G	G
		Extension tubes	Extension tubes	Extension tubes	304 SS	G	G	G
		Flanges	Flanges	Flanges	304 SS	G	G	G
		Lock keys	Lock keys	Lock keys	304 SS	G	G	G
		Lock keys	Lock keys	Lock keys	304L SS	G	G	G
		Nuts	Nuts	Nuts	304 SS	G	G	G
		--	Nuts	Nuts	302 SS	--	G	G
	Upper support plate assembly - Inverted Top Hat Design (Note 6)	ITH flange	ITH flange	ITH flange	304 SS	N/A	G	G
		ITH upper support plate	ITH upper support plate	ITH upper support plate	304 SS	N/A	G	G
		Upper support ring or skirt	Upper support ring or skirt	ITH Upper support ring or skirt	304 SS	G	G	G
		--	Upper support ring or skirt	ITH Upper support ring or skirt	CF8	--	G	G
	Upper support plate assembly - Top Hat Design (Note 6)	Flange	Flange	Flange	304 SS	N/A	G	G
		--	Flange	Flange	CF8	--	G	G
		Upper support plate	Upper support plate	Upper support plate	304 SS	G	G	G
		--	Upper support plate	Upper support plate	CF8	--	G	G
		Upper support ring or skirt	Upper support ring or skirt	Upper support ring or skirt	304 SS	G	G	G
		--	Upper support ring or skirt	Upper support ring or skirt	CF8	--	G	G
		Deep beam ribs	Deep beam ribs	Deep beam ribs (Note 7)	304 SS	G	G	G
		Deep beam stiffeners	Deep beam stiffeners	Deep beam stiffeners	304 SS	G	G	G

Table 3 (continued): MRP-191 Revision – Component and IMT Consequence of Failure Comparison

Assembly	Subassembly (Note 1)	MRP-191 Rev. 0 Component	MRP-191 Rev. 1 Component	MRP-191 Rev. 2 Component (Note 1)	Material	MRP-191 Rev. 0 IMT Conseq. of Failure	MRP-191 Rev. 1 IMT Conseq. of Failure	MRP-191 Rev. 2 IMT Conseq. of Failure (Note 2)	
Upper internals assembly (cont.)	Upper support plate assembly - Top Hat Design (Note 6) (cont.)	Bolts	Bolts	Bolts	316 SS	NONE	NONE	NONE	
		Lock keys	Lock keys	Locking device	316 SS	NONE	NONE	G	
		--	Lock keys	Locking device	304 SS	--	NONE	G	
	Upper support plate assembly - Flat Plate Design (Note 6)	Upper support plate	Upper support plate	Upper support plate	Upper support plate	304 SS	G	G	G
		--	Upper support plate	Upper support plate	Upper support plate	CF8	--	G	G
		Upper support ring or skirt	Upper support ring or skirt	Upper support ring or skirt	Upper support ring or skirt	304 SS	G	G	G
		--	Upper support ring or skirt	Upper support ring or skirt	Upper support ring or skirt	CF8	--	G	G
		Deep beam ribs	Deep beam ribs	Deep beam ribs (Note 7)	Deep beam ribs	304 SS	G	G	G
		Deep beam stiffeners	Deep beam stiffeners	Deep beam stiffeners	Deep beam stiffeners	304 SS	G	G	G
		Bolts	Bolts	Bolts	Bolts	316 SS	NONE	NONE	NONE
		Lock keys	Lock keys	Locking device	Locking device	316 SS	NONE	NONE	G
	--	Lock keys	Locking device	Locking device	304 SS	--	NONE	G	
	Lower Internals Assembly	Baffle and former assembly	Baffle bolting lock bars	Baffle bolting lock devices	Baffle bolting locking devices	304 SS	NONE	NONE	NONE
Baffle-edge bolts			Baffle-edge bolts	Baffle-edge bolts	316 SS	NONE	NONE	NONE	
Baffle-edge bolts			Baffle-edge bolts	Baffle-edge bolts	347 SS	NONE	NONE	NONE	
--			--	Bracket bolts	347 SS	--	--	N/A	
Baffle plates			Baffle plates	Baffle plates	304 SS	G	G	G	
Baffle-former bolts			Baffle-former bolts	Baffle-former bolts	316 SS	G	G	G	
Baffle-former bolts			Baffle-former bolts	Baffle-former bolts	347 SS	G	G	G	
--			--	Corner bolts	347 SS	--	--	N/A	
Barrel-former bolts			Barrel-former bolts	Barrel-former bolts	316 SS	N/A	G	G	
Barrel-former bolts	Barrel-former bolts	Barrel-former bolts	347 SS	N/A	G	G			

Table 3 (continued): MRP-191 Revision – Component and IMT Consequence of Failure Comparison

Assembly	Subassembly (Note 1)	MRP-191 Rev. 0 Component	MRP-191 Rev. 1 Component	MRP-191 Rev. 2 Component (Note 1)	Material	MRP-191 Rev. 0 IMT Conseq. of Failure	MRP-191 Rev. 1 IMT Conseq. of Failure	MRP-191 Rev. 2 IMT Conseq. of Failure (Note 2)	
Lower Internals Assembly (cont.)	Baffle and former assembly (cont.)	--	--	Former dowel pins	302 SS	--	--	N/A	
		--	--	Former dowel pins	304 SS	--	--	N/A	
		Former plates	Former plates	Former plates	304 SS	G	G	G	
	BMI column assemblies	BMI column bodies	BMI column bodies	BMI column bodies	BMI column bodies	304 SS	G	G	G
		BMI column bolts	BMI column bolts	BMI column bolts	BMI column bolts	316 SS	NONE	NONE	NONE
		BMI column collars	BMI column collars	BMI column collars	BMI column collars	304 SS	G	G	G
		--	BMI column cruciforms	BMI column cruciforms	BMI column cruciforms	304 SS	--	G	G
		BMI column cruciforms	BMI column cruciforms	BMI column cruciforms	BMI column cruciforms	CF8	G	G	G
		BMI column extension bars	BMI column extension bars	BMI column extension bars	BMI column extension bars	304 SS	G	G	G
		BMI column extension tubes	BMI column extension tubes	BMI column extension tubes	BMI column extension tubes	304 SS	G	G	G
		BMI column lock caps	BMI column lock caps	BMI column locking devices	BMI column locking devices	304L SS	NONE	NONE	NONE
		BMI column nuts	BMI column nuts	BMI column nuts	BMI column nuts	304 SS	NONE	NONE	NONE
	Core barrel	Core barrel flange	Core barrel flange	Core barrel flange	Core barrel flange	304 SS	A, G	A, G	A, G
		--	--	Upflow conversion core barrel plug body	Upflow conversion core barrel plug body	304 SS	--	--	N/A
		--	--	Upflow conversion core barrel plug mandrel	Upflow conversion core barrel plug mandrel	316 SS	--	--	N/A

Table 3 (continued): MRP-191 Revision – Component and IMT Consequence of Failure Comparison

Assembly	Subassembly (Note 1)	MRP-191 Rev. 0 Component	MRP-191 Rev. 1 Component	MRP-191 Rev. 2 Component (Note 1)	Material	MRP-191 Rev. 0 IMT Conseq. of Failure	MRP-191 Rev. 1 IMT Conseq. of Failure	MRP-191 Rev. 2 IMT Conseq. of Failure (Note 2)
Lower Internals Assembly (cont.)	Core barrel (cont.)	Core barrel outlet nozzles	Core barrel outlet nozzles	Core barrel outlet nozzles	304 SS	G	G	G
		Lower core barrel	Lower core barrel (includes LGW, LFW, MAW, and LAW)	Lower core barrel (includes MAW and LAW)	304 SS	A, G	A, G	A, G
				Lower core barrel (includes LGW and LFW)				A, G
		Upper core barrel	Upper core barrel (includes UFW, UGW, and UAW)	Upper core barrel (includes UAW)	304 SS	A, G	A, G	A, G
				Upper core barrel (includes UFW and UGW)	304 SS	A, G	A, G	A, G
		--	--	Safety injection nozzle interface	304 SS	--	--	N/A
	Diffuser plate	Diffuser plate	Diffuser plate	Diffuser plate	304 SS	NONE	NONE	NONE
	Flux thimbles (tubes)	Flux thimble tube plugs	Flux thimble tube plugs	Flux thimble tube plugs	304 SS	G	G	G
		--	Flux thimble tube plugs	Flux thimble tube plugs	316 SS	--	G	G
		--	Flux thimble tube plugs	Flux thimble tube plugs	308 SS	--	G	G
		--	Flux thimble tube plugs	Flux thimble tube plugs	A600	--	G	G
		Flux thimbles (tubes)	Flux thimbles (tubes)	Flux thimbles (tubes)	316 SS	G	G	G
		--	Flux thimbles (tubes)	Flux thimbles (tubes)	A600	--	G	G
	--	--	--	Flux thimble anti- vibration sleeve	304 SS	--	--	N/A

Table 3 (continued): MRP-191 Revision – Component and IMT Consequence of Failure Comparison

Assembly	Subassembly (Note 1)	MRP-191 Rev. 0 Component	MRP-191 Rev. 1 Component	MRP-191 Rev. 2 Component (Note 1)	Material	MRP-191 Rev. 0 IMT Conseq. of Failure	MRP-191 Rev. 1 IMT Conseq. of Failure	MRP-191 Rev. 2 IMT Conseq. of Failure (Note 2)
Lower Internals Assembly (cont.)	Head cooling spray nozzles	Head cooling spray nozzles	Head cooling spray nozzles	Head cooling spray nozzles	304 SS	NONE	NONE	NONE
	Irradiation specimen guides	Irradiation specimen guides	Irradiation specimen guides	Irradiation specimen guides	304 SS	NONE	NONE	NONE
		Irradiation specimen guide bolts	Irradiation specimen guide bolts	Irradiation specimen guide bolts	316 SS	NONE	NONE	NONE
		Irradiation specimen guide lock caps	Irradiation specimen guide lock caps	Irradiation specimen guide lock caps	304L SS	NONE	NONE	NONE
		--	--	Irradiation specimen access plug (spring) (Note 8)	X-750	--	--	N/A
		--	--	Irradiation specimen access plug (dowel pin) (Note 8)	316 SS	--	--	N/A
		Specimen plugs	Specimen plugs	Irradiation specimen access plug (plug) (Note 8)	304 SS	NONE	NONE	NONE
		LCP and fuel alignment pins	Fuel alignment pins	Fuel alignment pins	Fuel alignment pins	316 SS	NONE	NONE
	--		Fuel alignment pins	Fuel alignment pins	304 SS	--	NONE	NONE
	--		--	XL LCP fuel alignment pins	316 SS	--	--	N/A
	LCP, fuel alignment pin bolts		LCP, fuel alignment pin bolts	LCP and manway bolts	316 SS	NONE	NONE	NONE
	LCP, fuel alignment pin lock caps		LCP, fuel alignment pin lock caps	LCP and manway locking devices	304L SS	NONE	NONE	NONE

Table 3 (continued): MRP-191 Revision – Component and IMT Consequence of Failure Comparison

Assembly	Subassembly (Note 1)	MRP-191 Rev. 0 Component	MRP-191 Rev. 1 Component	MRP-191 Rev. 2 Component (Note 1)	Material	MRP-191 Rev. 0 IMT Conseq. of Failure	MRP-191 Rev. 1 IMT Conseq. of Failure	MRP-191 Rev. 2 IMT Conseq. of Failure (Note 2)	
Lower Internals Assembly (cont.)	LCP and fuel alignment pins (cont.)	Lower core plate	Lower core plate	Lower core plate	304 SS	A, F, G	A, F, G	A, F, G	
		XL lower core plate	XL lower core plate	XL lower core plate	304 SS	N/A	N/A	N/A	
	Lower support column assemblies	Lower support column bodies	Lower support column bodies	Lower support column bodies	Lower support column bodies	304 SS	G	G	G
		Lower support column bodies	Lower support column bodies	Lower support column bodies	Lower support column bodies	CF8	G	G	G
		Lower support column bolts	Lower support column bolts	Lower support column bolts	Lower support column bolts	304 SS	G	G	G
		--	Lower support column bolts	Lower support column bolts	Lower support column bolts	316 SS	--	G	G
		--	--	--	Lower support column bolt locking devices	304L SS (Note 10)	--	--	N/A
		--	--	--	Lower support column bolt locking devices	304 SS (Note 10)	--	--	N/A
		Lower support column nuts	Lower support column nuts	Lower support column nuts	Lower support column nuts	304 SS	G	G	G
		Lower support column sleeves	Lower support column sleeves	Lower support column sleeves	Lower support column sleeves	304 SS	G	G	G
		Lower support casting or forging	Lower support casting	Lower support casting	Lower support casting	Lower support casting	CF8	A, G	A, G
	Lower support forging		Lower support forging	Lower support forging	Lower support forging	304 SS	A, G	A, G	A, G
	Neutron panels/thermal shield	Neutron panel bolts	Neutron panel bolts	Neutron panel bolts	Neutron panel bolts	316 SS	NONE	NONE	NONE
		Neutron panel lock caps	Neutron panel lock caps	Neutron panel lock caps	Neutron panel locking devices	304 SS	NONE	NONE	NONE

Table 3 (continued): MRP-191 Revision – Component and IMT Consequence of Failure Comparison

Assembly	Subassembly (Note 1)	MRP-191 Rev. 0 Component	MRP-191 Rev. 1 Component	MRP-191 Rev. 2 Component (Note 1)	Material	MRP-191 Rev. 0 IMT Conseq. of Failure	MRP-191 Rev. 1 IMT Conseq. of Failure	MRP-191 Rev. 2 IMT Conseq. of Failure (Note 2)
Lower Internals Assembly (cont.)	Neutron panels/thermal shield (cont.)	--	Neutron panel lock caps	Neutron panel locking devices	304L SS	--	NONE	NONE
		Thermal shield bolts	Thermal shield bolts	Thermal shield bolts	316 SS	NONE	NONE	NONE
		Thermal shield dowels	Thermal shield dowels	Thermal shield dowels	316 SS	NONE	NONE	NONE
		--	Thermal shield dowels	Thermal shield dowels	304 SS	--	NONE	NONE
		Thermal shield flexures	Thermal shield flexures	Thermal shield flexures	304 SS	N/A	NONE	NONE
		--	Thermal shield flexures	Thermal shield flexures	316 SS	--	NONE	NONE
		--	--	Thermal shield flexure bolts	316 SS	--	--	N/A
		--	--	Thermal shield flexure locking devices and dowel pins	304 SS	--	--	N/A
		--	--	Thermal shield flexure locking devices and dowel pins	304L SS	--	--	N/A
		Thermal shield or neutron panels	Thermal shield or neutron panels	Thermal shield or neutron panels	304 SS	G	G	G
	Radial support keys	Radial support key bolts	Radial support key bolts	Radial support key bolts	304 SS	G	G	G
		--	Radial support key bolts	Radial support key bolts	316 SS	--	G	G

Table 3 (continued): MRP-191 Revision – Component and IMT Consequence of Failure Comparison

Assembly	Subassembly (Note 1)	MRP-191 Rev. 0 Component	MRP-191 Rev. 1 Component	MRP-191 Rev. 2 Component (Note 1)	Material	MRP-191 Rev. 0 IMT Conseq. of Failure	MRP-191 Rev. 1 IMT Conseq. of Failure	MRP-191 Rev. 2 IMT Conseq. of Failure (Note 2)
Lower Internals Assembly (cont.)	Radial support keys (cont.)	--	--	Radial support key dowels	304 SS	--	--	N/A
		Radial support key lock keys	Radial support key lock keys	Radial support key lock keys	304 SS (Note 9)	G	G	G
		Radial support keys	Radial support keys	Radial support keys	304 SS	G	G	G
		--	--	Radial support keys	Stellite	--	--	G
	SCS assembly	SCS base plate	SCS base plate	SCS base plate	304 SS	NONE	NONE	NONE
		SCS bolts	SCS bolts	SCS bolts	316 SS	NONE	NONE	NONE
		SCS energy absorber	SCS energy absorber	SCS energy absorber	304 SS	NONE	NONE	NONE
		SCS guide post	SCS guide post	SCS guide post	304 SS	NONE	NONE	NONE
		--	SCS guide post	SCS guide post	CF8	--	NONE	NONE
		SCS housing	SCS housing	SCS housing	304 SS	NONE	NONE	NONE
--		SCS housing	SCS housing	CF8	--	NONE	NONE	
SCS lock keys	SCS lock keys	SCS lock keys	304 SS	NONE	NONE	NONE		
--	Upper and lower tie plates	Upper and lower tie plates	304 SS	--	N/A	N/A		
Interfacing components	Interfacing components	Clevis insert bolts	Clevis insert bolts	Clevis insert bolts	X-750	G	G	G
		--	--	Clevis insert dowels	Alloy 600	--	--	G
		Clevis insert lock keys	Clevis insert lock keys	Clevis insert locking devices	Alloy 600	G	G	G
		Clevis insert lock keys	Clevis insert lock keys	Clevis insert locking devices	316 SS	G	G	G
		Clevis inserts	Clevis inserts	Clevis inserts	Alloy 600	G	G	G
		Clevis inserts	Clevis inserts	Clevis inserts	304 SS	G	G	G
		Clevis inserts	Clevis inserts	Clevis inserts	Stellite	G	G	G
Head and vessel alignment pin bolts	Head and vessel alignment pin bolts	Head and vessel alignment pin bolts	316 SS	NONE	NONE	NONE		

Table 3 (continued): MRP-191 Revision – Component and IMT Consequence of Failure Comparison

Assembly	Subassembly (Note 1)	MRP-191 Rev. 0 Component	MRP-191 Rev. 1 Component	MRP-191 Rev. 2 Component (Note 1)	Material	MRP-191 Rev. 0 IMT Conseq. of Failure	MRP-191 Rev. 1 IMT Conseq. of Failure	MRP-191 Rev. 2 IMT Conseq. of Failure (Note 2)
Interfacing components (cont.)	Interfacing components (cont.)	Head and vessel alignment pin lock caps	Head and vessel alignment pin lock caps	Head and vessel alignment pin lock caps	304L SS	NONE	NONE	NONE
		Head and vessel alignment pins	Head and vessel alignment pins	Head and vessel alignment pins	304 SS	NONE	NONE	NONE
		--	--	Head and vessel alignment pins	Stellite	--	--	N/A
		Internals hold-down spring	Internals hold-down spring	Internals hold-down spring	304 SS	G	G	G
		Internals hold-down spring	Internals hold-down spring	Internals hold-down spring	403 SS	G	G	G
		--	--	Internals hold-down spring	F6NM	--	--	G
		UCP alignment pins	UCP alignment pins	UCP alignment pins	304 SS	NONE	NONE	NONE
		--	--	UCP alignment pins	Stellite	--	--	NONE
		--	--	Thermal sleeves	304 SS	--	--	N/A
		--	--	Thermal sleeve guide funnels	304 SS	--	--	N/A
		--	--	Thermal sleeve guide funnels	CF8	--	--	N/A
		--	--	Instrumentation nozzle funnels	304 SS	--	--	N/A
		--	--	Replacement reactor vessel head extension tubes	304 SS	--	--	N/A

Table 3 (continued): MRP-191 Revision – Component and IMT Consequence of Failure Comparison

Assembly	Subassembly (Note 1)	MRP-191 Rev. 0 Component	MRP-191 Rev. 1 Component	MRP-191 Rev. 2 Component (Note 1)	Material	MRP-191 Rev. 0 IMT Conseq. of Failure	MRP-191 Rev. 1 IMT Conseq. of Failure	MRP-191 Rev. 2 IMT Conseq. of Failure (Note 2)
-----------------	---------------------------------	---	---	--	-----------------	--	--	---

Notes:

1. Cells that are gray shaded represent changes between MRP-191, Revision 2 [1], and previous revisions of MRP-191 (Revisions 0 [2] and 1 [3]). This includes additions of subassemblies and components or component name changes.
2. Cells that are gray shaded represent changes in consequence of failure between MRP-191, Revision 2 [1], and previous revisions of MRP-191 (Revisions 0 [2] and 1 [3]).
3. Component name modified to eliminate “upper” from its name to further clarify the actual component in MRP-191, Revision 2 [1].
4. Component name modified to eliminate “support pin” from its name to further clarify the actual component in MRP-191, Revision 2 [1].
5. “Protective skirt” was added to the component name for clarification in MRP-191, Revision 2 [1].
6. The upper support plate assembly was separated out to identify specific components applicable to the three design variations (inverted top hat, top hat, and flat plate).
7. The component “ribs” was listed in MRP-191, Revision 0 [2] and Revision 1 [3]; however, with splitting up the upper support plate assembly into the three design variations, the “deep beam ribs” component captures the previously listed “ribs” in MRP-191, Revision 2 [1].
8. This was originally listed as “specimen plugs” in MRP-191, Revision 1 [3]. However, due to the materials comprising this component, it was divided out into its subcomponents in MRP-191, Revision 2 [1].
9. The radial support key lock keys was listed as 316 SS within Table 6-10 and Table 7-2 of MRP-191, Revision 2 [1] but should be 304 SS.
10. The lower support column bolt locking devices are listed as 304 SS within Table 4-6, Table 5-1, Table 6-10, and Table 7-2 of MRP-191, Revision 2 [1] and also as 304L SS in Table 4-4 of MRP-191, Revision 2 [1]. Both materials are listed in this table.

Consequences of Failure*

A	Precludes the ability to reach safe shutdown due to loss of a coolable geometry, inability to control reactivity, or loss of instrumentation
F	Breaches fuel cladding
G	Causes significant economic impact
None	None identified
N/A	These are items not listed in the IMT
*More complete descriptions of these consequences are provided in Section 2.1.4 of MRP-205	

References for Table 3:

1. Materials Reliability Program: Screening, Categorization, and Ranking of Reactor Internals Components for Westinghouse and Combustion Engineering PWR Design (MRP-191, Revision 2). EPRI, Palo Alto, CA: 2018. 3002013220.
2. Materials Reliability Program: Screening, Categorization, and Ranking of Reactor Internals Components for Westinghouse and Combustion Engineering PWR Design (MRP-191). EPRI, Palo Alto, CA: 2006. 1013234.
3. Materials Reliability Program: Screening, Categorization, and Ranking of Reactor Internals Components for Westinghouse and Combustion Engineering PWR Design (MRP-191, Revision 1). EPRI, Palo Alto, CA: 2016. 3002007960.

Table 4: MRP-191 Revision – Screened-in Degradation Mechanisms Comparison						
Assembly	Subassembly	MRP-191 Rev. 2 Component	Material	MRP-191 Rev. 0 Screened-in Degradation Mechanisms	MRP-191 Rev. 1 Screened-in Degradation Mechanisms	MRP-191 Rev. 2 Screened-in Degradation Mechanisms (Note 1)
Upper internals assembly	Control rod guide tube assemblies and flow downcomers	Anti-rotation studs and nuts	304 SS	NONE	NONE	NONE
		Anti-rotation studs and nuts	316 SS	--	NONE	NONE
		Bolts	316 SS	NONE	NONE	1, 4
		Bolts	304 SS	--	NONE	4
		C-tubes	304 SS	3	3	3, 4
		Enclosure pins	304 SS	1A, 3	1A, 3	1A, 3
		Guide tube enclosures (Note 2)	304 SS	1A, 3	1A	1A, 4
		Guide tube enclosures (Note 2)	CF8	--	1A, 5, 6	1A, 4, 5
		Flanges, intermediate	304 SS	1A, 4	1A, 4	1A, 4
		Flanges, intermediate	CF8	1A, 4, 5	1A, 4, 5	1A, 4, 5
		Flanges, lower	304 SS	1A, 4	1A, 4	1A, 2, 4, 6
		Flanges, lower	CF8	1A, 4, 5, 6	1A, 4, 5, 6	1A, 2, 4, 5, 6
		Flexureless inserts	304 SS	NONE	NONE	4
		Flexureless inserts (spring)	Alloy 718	--	--	1
		Flexures	X-750	1	1	1, 4
		Guide plates/cards	304 SS	1A, 3, 4	1A, 3, 4	1A, 3, 4
		Guide plates/cards	316L SS	--	1A, 3, 4	1A, 3, 4
		Guide plates/cards	CF8	--	1A, 3, 4, 5, 6	1A, 3, 4, 5
		Guide tube support pins	X-750	1, 3, 4, 8	1, 3, 4, 8	1, 2, 3, 4, 6, 8
		Guide tube support pins	316 SS	3, 4, 8	3, 4, 8	2, 3, 4, 6, 8
		Housing plates	304 SS	NONE	NONE	NONE
		Housing plates	CF8	--	5	5
		Inserts	304 SS	NONE	NONE	NONE
		Inserts	CF8	--	--	5
		Lock bars	304 SS	NONE	NONE	4
		Sheaths	304 SS	3	3	3, 4
Cover plate (Note 3)	304 SS	NONE	NONE	4		
Cover plate cap screws (Note 3)	316 SS	NONE	NONE	4		

Table 4 (continued): MRP-191 Revision – Screened-in Degradation Mechanisms Comparison						
Assembly	Subassembly	MRP-191 Rev. 2 Component	Material	MRP-191 Rev. 0 Screened-in Degradation Mechanisms	MRP-191 Rev. 1 Screened-in Degradation Mechanisms	MRP-191 Rev. 2 Screened-in Degradation Mechanisms (Note 1)
Upper internals assembly (cont.)	Control rod guide tube assemblies and flow downcomers (cont.)	Cover plate guide tube locking caps and tie straps (Note 3)	304 SS	NONE	NONE	4
		Support pin nuts	X-750	NONE	NONE	4, 6
		Support pin nuts	304 SS	--	NONE	4, 6
		Support pin nuts	316 SS	NONE	NONE	4, 6
		Water flow slot ligaments	304 SS	NONE	NONE	NONE
		Probe holder shroud	304 SS	--	--	1A, 4, 6
	Mixing Devices	Mixing devices	CF8	1A, 5, 6	1A, 5, 6	1A, 4, 5, 6
		Mixing devices	304 SS	--	1A, 6	1A, 4, 6
	UCP and fuel alignment pins	Fuel alignment pins	316 SS	3	3	2, 3, 4, 6
		Fuel alignment pins	304 SS	--	3	2, 3, 4, 6
		UCP	304 SS	3, 4	3, 4, 6	2, 4, 6
		Upper core plate insert	304 SS	--	--	3, 6
		Upper core plate insert	Stellite	--	--	3, 6
		Upper core plate insert bolts	316 SS	--	--	2, 4, 6, 8
		Upper core plate insert locking devices & dowel pins	304 SS	--	--	4, 6
		Upper core plate insert locking devices & dowel pins	316 SS	--	--	4, 6
		Protective skirt	304 SS	--	1A, 6	1A, 4, 6
		Protective skirt bolts (Note 4)	316 SS	--	3, 4, 6, 8	1, 2, 3, 4, 6, 8
		Protective skirt lock bars (Note 4)	304 SS	--	NONE	4, 6
		Protective skirt dowel pins (Note 4)	304 SS	--	NONE	2, 4, 6

Table 4 (continued): MRP-191 Revision – Screened-in Degradation Mechanisms Comparison						
Assembly	Subassembly	MRP-191 Rev. 2 Component	Material	MRP-191 Rev. 0 Screened-in Degradation Mechanisms	MRP-191 Rev. 1 Screened-in Degradation Mechanisms	MRP-191 Rev. 2 Screened-in Degradation Mechanisms (Note 1)
Upper internals assembly (cont.)	UCP and fuel alignment pins (cont.)	Protective skirt dowel pins (Note 4)	316 SS	--	NONE	2, 4, 5
	Upper instrumentation conduit and supports	Bolting	316 SS	NONE	NONE	NONE
		Bolting	304 SS	--	NONE	NONE
		Brackets, clamps, terminal blocks, and conduit straps	304 SS	NONE	NONE	1, 4
		Brackets, clamps, terminal blocks, and conduit straps	302 SS	--	NONE	1, 4
		Brackets, clamps, terminal blocks, and conduit straps	CF8	--	5	1, 4, 5, 6
		Conduit seal assembly: body, tubesheets, tubesheet welds	304 SS	NONE	NONE	1, 4
		Conduit seal assembly: tubes	304 SS	NONE	NONE	1, 4
		Conduits	304 SS	NONE	NONE	NONE
		Flange base	304 SS	NONE	NONE	4
		Locking caps	304 SS	NONE	NONE	4
		Locking caps	304L SS	--	NONE	4
		Support tubes	304 SS	NONE	NONE	4
	Upper plenum	UHI flow column bases	CF8	5, 6	5, 6	4, 5, 6
		UHI flow columns	304 SS	NONE	NONE	4
	Upper support column assemblies	Adapters	304 SS	NONE	NONE	NONE
		Bolts	316 SS	3, 4, 8	3, 4, 8	2, 3, 4, 6, 8
		Column bases	CF8	1, 5, 6	1, 5, 6	1, 2, 5, 6
		Column bases	304 SS	--	1, 6	1, 2, 6
		Column bodies	304 SS	NONE	NONE	1A, 4
		Extension tubes	304 SS	1A	1A	1A
		Flanges	304 SS	NONE	NONE	NONE
		Lock keys	304 SS	NONE	NONE	4

Table 4 (continued): MRP-191 Revision – Screened-in Degradation Mechanisms Comparison						
Assembly	Subassembly	MRP-191 Rev. 2 Component	Material	MRP-191 Rev. 0 Screened-in Degradation Mechanisms	MRP-191 Rev. 1 Screened-in Degradation Mechanisms	MRP-191 Rev. 2 Screened-in Degradation Mechanisms (Note 1)
Upper internals assembly (cont.)	Upper support column assemblies (cont.)	Lock keys	304L SS	NONE	NONE	4
		Nuts	304 SS	NONE	NONE	4
		Nuts	302 SS	--	NONE	4
	Upper support plate assembly - Inverted Top Hat Design (Note 5)	ITH flange	304 SS	1A, 4	1A, 4	4
		ITH upper support plate	304 SS	1A	1A	4
		ITH Upper support ring or skirt	304 SS	1A, 4	1A, 4	1A, 4
		ITH Upper support ring or skirt	CF8	--	1A, 4, 5	1A, 4, 5
	Upper support plate assembly - Top Hat Design (Note 5)	Flange	304 SS	NONE	NONE	4
		Flange	CF8	--	5	4, 5
		Upper support plate	304 SS	NONE	NONE	4
		Upper support plate	CF8	--	5	4, 5
		Upper support ring or skirt	304 SS	1A, 4	1A, 4	1A, 4
		Upper support ring or skirt	CF8	--	1A, 4, 5	1A, 4, 5
		Deep beam ribs (Note 6)	304 SS	1A	1A	1A
		Deep beam stiffeners	304 SS	1A	1A	1A
		Bolts	316 SS	NONE	NONE	1, 4
		Locking device	316 SS	NONE	NONE	4
		Locking device	304 SS	--	NONE	4
	Upper support plate assembly - Flat Plate Design (Note 5)	Upper support plate	304 SS	NONE	NONE	4
		Upper support plate	CF8	--	5	4, 5
		Upper support ring or skirt	304 SS	1A, 4	1A, 4	1A, 4
		Upper support ring or skirt	CF8	--	1A, 4, 5	1A, 4, 5
		Deep beam ribs (Note 6)	304 SS	1A	1A	1A
		Deep beam stiffeners	304 SS	1A	1A	1A
		Bolts	316 SS	NONE	NONE	1, 4
		Locking device	316 SS	NONE	NONE	4
	Locking device	304 SS	--	NONE	4	

Table 4 (continued): MRP-191 Revision – Screened-in Degradation Mechanisms Comparison						
Assembly	Subassembly	MRP-191 Rev. 2 Component	Material	MRP-191 Rev. 0 Screened-in Degradation Mechanisms	MRP-191 Rev. 1 Screened-in Degradation Mechanisms	MRP-191 Rev. 2 Screened-in Degradation Mechanisms (Note 1)
Lower internals assembly	Baffle and former assembly	Baffle bolting locking devices	304 SS	2, 6, 7	2, 6, 7	2, 4, 6, 7
		Baffle, edge bolts	316 SS	2, 3, 4, 6, 7, 8	2, 3, 4, 6, 7, 8	2, 3, 4, 6, 7, 8
		Baffle, edge bolts	347 SS	2, 3, 4, 6, 7, 8	2, 3, 4, 6, 7, 8	2, 3, 4, 6, 7, 8
		Bracket bolts	347 SS	--	--	2, 3, 4, 6, 7, 8
		Baffle plates	304 SS	2, 6, 7	2, 6, 7	2, 4, 6, 7
		Baffle, former bolts	316 SS	2, 3, 4, 6, 7, 8	2, 3, 4, 6, 7, 8	2, 3, 4, 6, 7, 8
		Baffle, former bolts	347 SS	2, 3, 4, 6, 7, 8	2, 3, 4, 6, 7, 8	2, 3, 4, 6, 7, 8
		Corner bolts	347 SS	--	--	2, 3, 4, 6, 7, 8
		Barrel, former bolts	316 SS	2, 3, 4, 6, 7, 8	2, 3, 4, 6, 7, 8	2, 3, 4, 6, 7, 8
		Barrel, former bolts	347 SS	2, 3, 4, 6, 7, 8	2, 3, 4, 6, 7, 8	2, 3, 4, 6, 7, 8
		Former dowel pins	302 SS	--	--	2, 4, 6, 7
		Former dowel pins	304 SS	--	--	2, 4, 6, 7
		Former plates	304 SS	2, 6, 7	2, 6, 7	2, 4, 6, 7
		BMI column assemblies	BMI column bodies	304 SS	1A, 2, 4, 6, 7	1A, 2, 4, 6, 7
	BMI column bolts		316 SS	4	4	2, 3, 4, 6, 7, 8
	BMI column collars		304 SS	2, 6, 7	2, 6, 7	2, 4, 6, 7
	BMI column cruciforms		304 SS	--	2, 6, 7	2, 3, 4, 6, 7
	BMI column cruciforms		CF8	2, 5, 6, 7	2, 5, 6, 7	2, 3, 4, 5, 6, 7
	BMI column extension bars		304 SS	2, 6, 7	2, 6, 7	2, 4, 6, 7
	BMI column extension tubes		304 SS	1A, 2, 4, 6, 7	1A, 2, 4, 6, 7	1A, 4
	BMI column locking devices		304L SS	NONE	NONE	2, 6, 7
	Core barrel	BMI column nuts	304 SS	2, 3, 4, 6, 7, 8	2, 3, 4, 6, 7, 8	2, 3, 4, 6, 7, 8
		Core barrel flange	304 SS	1A, 3	1A, 3	1A, 3, 4
		Upflow conversion core barrel plug body	304 SS	--	--	2, 3, 4, 6, 8
		Upflow conversion core barrel plug mandrel	316 SS	--	--	2, 3, 6, 8

Table 4 (continued): MRP-191 Revision – Screened-in Degradation Mechanisms Comparison						
Assembly	Subassembly	MRP-191 Rev. 2 Component	Material	MRP-191 Rev. 0 Screened-in Degradation Mechanisms	MRP-191 Rev. 1 Screened-in Degradation Mechanisms	MRP-191 Rev. 2 Screened-in Degradation Mechanisms (Note 1)
Lower internals assembly (cont.)	Core barrel (cont.)	Core barrel outlet nozzles	304 SS	1A, 4	1A, 4	1A, 3, 4
		Lower core barrel (includes MAW and LAW)	304 SS	1A, 2, 6	1A, 2, 6	1A, 2, 4, 6, 7
		Lower core barrel (includes LGW and LFW)	304 SS	1A, 2, 6	1A, 2, 6	1A, 2, 4, 6, 7
		Upper core barrel (includes UAW)	304 SS	1A, 2, 6	1A, 6	1A, 4
		Upper core barrel (includes UFW and UGW)	304 SS	1A, 2, 6	1A, 6	1A, 4
		Safety injection nozzle interface	304 SS	--	--	1A, 3, 4
	Diffuser plate	Diffuser plate	304 SS	NONE	NONE	NONE
	Flux thimbles (tubes)	Flux thimble tube plugs	304 SS	1A, 2, 6, 7	1A, 2, 6, 7	1A, 2, 4, 6, 7
		Flux thimble tube plugs	316 SS	--	1A, 2, 6, 7	1A, 2, 4, 6, 7
		Flux thimble tube plugs	308 SS	--	1A, 2, 6, 7	1A, 2, 4, 6, 7
		Flux thimble tube plugs	A600	--	1A, 2, 6, 7	1A, 2, 4, 6, 7
		Flux thimbles (tubes)	316 SS	1A, 2, 3, 6, 7	1A, 2, 3, 6, 7	1A, 2, 3, 4, 6, 7
		Flux thimbles (tubes)	A600	--	1A, 2, 3, 6, 7	1A, 2, 3, 4, 6, 7
		Flux thimble anti-vibration sleeve	304 SS	--	--	2, 3, 4, 6, 7, 8
	Head cooling spray nozzles	Head cooling spray nozzles	304 SS	NONE	NONE	4
	Irradiation specimen guides	Irradiation specimen guide	304 SS	3, 6	3, 6	1A, 3, 4
		Irradiation specimen guide bolts	316 SS	2, 3, 4, 6, 8	2, 3, 4, 6, 8	3, 4, 8
		Irradiation specimen guide lock caps	304L SS	6	6	NONE
		Irradiation specimen plug (spring) (Note 7)	X-750	--	--	NONE
		Irradiation specimen access plug (dowel pin) (Note 7)	316 SS	--	--	NONE

Table 4 (continued): MRP-191 Revision – Screened-in Degradation Mechanisms Comparison						
Assembly	Subassembly	MRP-191 Rev. 2 Component	Material	MRP-191 Rev. 0 Screened-in Degradation Mechanisms	MRP-191 Rev. 1 Screened-in Degradation Mechanisms	MRP-191 Rev. 2 Screened-in Degradation Mechanisms (Note 1)
Lower internals assembly (cont.)	Irradiation specimen guides (cont.)	Irradiation specimen access plug (plug) (Note 7)	304 SS	6	6	NONE
	LCP and fuel alignment pins	Fuel alignment pins	316 SS	2, 3, 6, 7	2, 3, 6, 7	2, 3, 4, 6, 7
		Fuel alignment pins	304 SS	--	2, 3, 6, 7	2, 3, 6, 7
		XL LCP fuel alignment pins	316 SS	--	--	2, 3, 4, 6, 7
		LCP and manway bolts	316 SS	2, 3, 4, 6, 7, 8	2, 3, 4, 6, 7, 8	2, 3, 4, 6, 7, 8
		LCP and manway locking devices	304L SS	2, 6, 7	2, 6, 7	2, 6, 7
		Lower core plate	304 SS	1A, 2, 3, 4, 6, 7	1A, 2, 3, 4, 6, 7	2, 3, 4, 6, 7
		XL lower core plate	304 SS	1A, 2, 3, 4, 6	1A, 2, 3, 4, 6	1A, 2, 3, 4, 6, 7
	Lower support column assemblies	Lower support column bodies	304 SS	2, 6, 7	2, 6, 7	2, 4, 6, 7
		Lower support column bodies	CF8	2, 5, 6, 7	2, 5, 6, 7	2, 4, 5, 6, 7
		Lower support column bolts	304 SS	2, 3, 4, 6, 7, 8	2, 3, 4, 6, 7, 8	2, 3, 4, 6, 7, 8
		Lower support column bolts	316 SS	--	2, 3, 4, 6, 7, 8	2, 3, 4, 6, 7, 8
		Lower support column bolt locking devices	304L SS (Note 9)	--	--	2, 4, 6, 7
		Lower support column bolt locking devices	304 SS (Note 9)	--	--	2, 4, 6, 7
		Lower support column nuts	304 SS	NONE	NONE	4
		Lower support column sleeves	304 SS	NONE	NONE	NONE
	Lower support casting or forging	Lower support casting	CF8	5	5	4, 5
		Lower support forging	304 SS	NONE	NONE	4
	Neutron panels/thermal shield	Neutron panel bolts	316 SS	2, 3, 4, 6, 8	2, 3, 4, 6, 8	2, 3, 4, 6, 8
		Neutron panel locking devices	304 SS	6	6	NONE
		Neutron panel locking devices	304L SS	--	6	NONE
		Thermal shield bolts	316 SS	2, 3, 4, 6, 8	2, 3, 4, 6, 8	4, 8
		Thermal shield dowels	316 SS	6	6	4
		Thermal shield dowels	304 SS	--	6	4

Table 4 (continued): MRP-191 Revision – Screened-in Degradation Mechanisms Comparison							
Assembly	Subassembly	MRP-191 Rev. 2 Component	Material	MRP-191 Rev. 0 Screened-in Degradation Mechanisms	MRP-191 Rev. 1 Screened-in Degradation Mechanisms	MRP-191 Rev. 2 Screened-in Degradation Mechanisms (Note 1)	
Lower internals assembly (cont.)	Neutron panels/thermal shield (cont.)	Thermal shield flexures	304 SS	2, 3, 4, 6, 8	2, 3, 4, 6, 8	1A, 4	
		Thermal shield flexures	316 SS	--	2, 3, 4, 6, 8	1A, 4	
		Thermal shield flexure bolts	316 SS	--	--	4, 8	
		Thermal shield flexure locking devices and dowel pins	304 SS	--	--	4	
		Thermal shield flexure locking devices and dowel pins	304L SS	--	--	4	
		Thermal shield or neutron panels	304 SS	6	6	1A, 4, 6	
	Radial support keys	Radial support key bolts	304 SS	3	3	4	
		Radial support key bolts	316 SS	--	3	4	
		Radial support key dowels	304 SS	--	--	4	
		Radial support key lock keys	304 SS (Note 8)	NONE	NONE	4	
		Radial support keys	304 SS	1A, 3	1A, 3	1A, 3, 4	
		Radial support keys	Stellite	--	--	3	
	SCS assembly	SCS base plate	304 SS	1A	1A	1A, 3	
		SCS bolts	316 SS	NONE	NONE	4	
		SCS energy absorber	304 SS	NONE	NONE	NONE	
		SCS guide post	304 SS	NONE	NONE	NONE	
		SCS guide post	CF8	--	5	5	
		SCS housing	304 SS	NONE	NONE	NONE	
		SCS housing	CF8	--	5	5	
		SCS lock keys	304 SS	NONE	NONE	4	
		Upper and lower tie plates	304 SS	--	NONE	4	
	Interfacing components	Interfacing components	Clevis insert bolts	X-750	1, 3	1, 3	1, 3
			Clevis insert dowels	Alloy 600	--	--	4
Clevis insert locking devices			Alloy 600	NONE	NONE	4	

Table 4 (continued): MRP-191 Revision – Screened-in Degradation Mechanisms Comparison						
Assembly	Subassembly	MRP-191 Rev. 2 Component	Material	MRP-191 Rev. 0 Screened-in Degradation Mechanisms	MRP-191 Rev. 1 Screened-in Degradation Mechanisms	MRP-191 Rev. 2 Screened-in Degradation Mechanisms (Note 1)
Interfacing components (cont.)	Interfacing components (cont.)	Clevis insert locking devices	316 SS	NONE	NONE	4
		Clevis inserts	Alloy 600	3	3	3, 4
		Clevis inserts	304 SS	3	3	3, 4
		Clevis inserts	Stellite	3	3	3, 4
		Head and vessel alignment pin bolts	316 SS	NONE	NONE	4
		Head and vessel alignment pin lock caps	304L SS	NONE	NONE	NONE
		Head and vessel alignment pins	304 SS	NONE	NONE	4
		Head and vessel alignment pins	Stellite	--	--	3
		Internals hold-down spring	304 SS	3	3	3, 4
		Internals hold-down spring	403 SS	3, 5	3, 5	3, 4, 5
		Internals hold-down spring	F6NM	--	--	3, 4, 5
		UCP alignment pins	304 SS	1A, 3	1A, 3	1A, 3, 4
		UCP alignment pins	Stellite	--	--	3
		Thermal sleeves	304 SS	--	--	3
		Thermal sleeve guide funnels	304 SS	--	--	3
		Thermal sleeve guide funnels	CF8	--	--	3, 5
		Instrumentation nozzle funnels	304 SS	--	--	NONE
Replacement reactor vessel head extension tubes	304 SS	--	--	NONE		

Table 4 (continued): MRP-191 Revision – Screened-in Degradation Mechanisms Comparison						
Assembly	Subassembly	MRP-191 Rev. 2 Component	Material	MRP-191 Rev. 0 Screened-in Degradation Mechanisms	MRP-191 Rev. 1 Screened-in Degradation Mechanisms	MRP-191 Rev. 2 Screened-in Degradation Mechanisms (Note 1)

Notes:

1. Cells that are gray shaded represent changes in screened-in degradation mechanisms between MRP-191, Revision 2 [1], and previous revisions of MRP-191 (Revisions 0 [2] and 1 [3]).
2. Component name modified to eliminate “upper” from its name to further clarify the actual component in MRP-191, Revision 2 [1].
3. Component name modified to eliminate “support pin” from its name to further clarify the actual component in MRP-191, Revision 2 [1].
4. “Protective skirt” was added to the component name for clarification in MRP-191, Revision 2 [1].
5. The upper support plate assembly was separated out to identify specific components applicable to the three design variations (inverted top hat, top hat, and flat plate).
6. The component “ribs” was listed in MRP-191, Revision 0 [2] and Revision 1 [3]; however, with splitting up the upper support plate assembly into the three design variations, the “deep beam ribs” component captures the previously listed “ribs” in MRP-191, Revision 2 [1].
7. This was originally listed as “specimen plugs” in MRP-191, Revision 1 [3]. However, due to the materials comprising this component, it was divided out into its subcomponents in MRP-191, Revision 2 [1].
8. The radial support key lock keys was listed as 316 SS within Table 6-10 and Table 7-2 of MRP-191, Revision 2 [1] but should be 304 SS.
9. The lower support column bolt locking devices are listed as 304 SS within Table 4-6, Table 5-1, Table 6-10, and Table 7-2 of MRP-191, Revision 2 [1] and also as 304L SS in Table 4-4 of MRP-191, Revision 2 [1]. Both materials are listed in this table.

Degradation Mechanism	
SCC	1
SCC welds	1A
IASCC	2
Wear	3
Fatigue	4
Thermal embrittlement	5
Irradiation embrittlement	6
Void swelling	7
Irradiation ISR/IC; thermal SR	8
None (values for mechanisms did not exceed screening threshold values)	None

References for Table 4:

1. Materials Reliability Program: Screening, Categorization, and Ranking of Reactor Internals Components for Westinghouse and Combustion Engineering PWR Design (MRP-191, Revision 2). EPRI, Palo Alto, CA: 2018. 3002013220.
2. Materials Reliability Program: Screening, Categorization, and Ranking of Reactor Internals Components for Westinghouse and Combustion Engineering PWR Design (MRP-191). EPRI, Palo Alto, CA: 2006. 1013234.
3. Materials Reliability Program: Screening, Categorization, and Ranking of Reactor Internals Components for Westinghouse and Combustion Engineering PWR Design (MRP-191, Revision 1). EPRI, Palo Alto, CA: 2016. 3002007960.

Table 5: MRP-191 Revision – Likelihood of Failure Comparison

Assembly	Subassembly	MRP-191 Rev. 2 Component	Material	MRP-191 Rev. 0 Likelihood of Failure L,M,H	MRP-191 Rev. 1 Likelihood of Failure L,M,H	MRP-191 Rev. 2 Likelihood of Failure L,M,H (Note 1)
Upper internals assembly	Control rod guide tube assemblies and flow downcomers	Anti-rotation studs and nuts	304 SS	Note 2	Note 2	Note 2
		Anti-rotation studs and nuts	316 SS	Note 3	Note 2	Note 2
		Bolts	316 SS	Note 2	Note 2	L
		Bolts	304 SS	Note 3	Note 2	L
		C-tubes	304 SS	M	M	M
		Enclosure pins	304 SS	L	L	L
		Guide tube enclosures (Note 4)	304 SS	L	L	L
		Guide tube enclosures (Note 4)	CF8	Note 3	L	L
		Flanges, intermediate	304 SS	L	L	L
		Flanges, intermediate	CF8	L	L	L
		Flanges, lower	304 SS	L	L	M
		Flanges, lower	CF8	M	M	M
		Flexureless inserts	304 SS	Note 2	Note 2	L
		Flexureless inserts (spring)	Alloy 718	Note 3	Note 3	L
		Flexures	X-750	H	H	H
		Guide plates/cards	304 SS	H	H	H
		Guide plates/cards	316L SS	Note 3	H	H
		Guide plates/cards	CF8	Note 3	H	H
		Guide tube support pins	X-750	H	H	H
		Guide tube support pins	316 SS	L	L	L
		Housing plates	304 SS	Note 2	Note 2	Note 2
		Housing plates	CF8	Note 3	L	L
		Inserts	304 SS	Note 2	Note 2	Note 2
		Inserts	CF8	Note 3	Note 3	L
Lock bars	304 SS	Note 2	Note 2	L		
Sheaths	304 SS	M	M	H		
Cover plate (Note 5)	304 SS	Note 2	Note 2	L		

Table 5 (continued): MRP-191 Revision – Likelihood of Failure Comparison						
Assembly	Subassembly	MRP-191 Rev. 2 Component	Material	MRP-191 Rev. 0 Likelihood of Failure L,M,H	MRP-191 Rev. 1 Likelihood of Failure L,M,H	MRP-191 Rev. 2 Likelihood of Failure L,M,H (Note 1)
Upper internals assembly (cont.)	Control rod guide tube assemblies and flow downcomers (cont.)	Cover plate cap screws (Note 5)	316 SS	Note 2	Note 2	L
		Cover plate guide tube locking caps and tie straps (Note 5)	304 SS	Note 2	Note 2	L
		Support pin nuts	X-750	Note 2	Note 2	L
		Support pin nuts	304 SS	Note 3	Note 2	L
		Support pin nuts	316 SS	Note 2	Note 2	L
		Water flow slot ligaments	304 SS	Note 2	Note 2	Note 2
		Probe holder shroud	304 SS	Note 3	Note 3	L
	Mixing Devices	Mixing devices	CF8	L	L	L
		Mixing devices	304 SS	Note 3	L	L
	UCP and fuel alignment pins	Fuel alignment pins	316 SS	L	L	L
		Fuel alignment pins	304 SS	Note 3	L	H
		UCP	304 SS	L	M	M
		Upper core plate insert	304 SS	Note 3	Note 3	M
		Upper core plate insert	Stellite	Note 3	Note 3	M
		Upper core plate insert bolts	316 SS	Note 3	Note 3	L
		Upper core plate insert locking devices & dowel pins	304 SS	Note 3	Note 3	L
		Upper core plate insert locking devices & dowel pins	316 SS	Note 3	Note 3	L
		Protective skirt	304 SS	Note 3	L	L
		Protective skirt bolts (Note 6)	316 SS	Note 3	M	M
		Protective skirt lock bars (Note 6)	304 SS	Note 3	Note 2	L
		Protective skirt dowel pins (Note 6)	304 SS	Note 3	Note 2	L
		Protective skirt dowel pins (Note 6)	316 SS	Note 3	Note 2	L

Table 5 (continued): MRP-191 Revision – Likelihood of Failure Comparison						
Assembly	Subassembly	MRP-191 Rev. 2 Component	Material	MRP-191 Rev. 0 Likelihood of Failure L,M,H	MRP-191 Rev. 1 Likelihood of Failure L,M,H	MRP-191 Rev. 2 Likelihood of Failure L,M,H (Note 1)
Upper internals assembly (cont.)	Upper instrumentation conduit and supports	Bolting	316 SS	Note 2	Note 2	Note 2
		Bolting	304 SS	Note 3	Note 2	Note 2
		Brackets, clamps, terminal blocks, and conduit straps	304 SS	Note 2	Note 2	H
		Brackets, clamps, terminal blocks, and conduit straps	302 SS	Note 3	Note 2	M
		Brackets, clamps, terminal blocks, and conduit straps	CF8	Note 3	L	L
		Conduit seal assembly: body, tubesheets, tubesheet welds	304 SS	Note 2	Note 2	H
		Conduit seal assembly: tubes	304 SS	Note 2	Note 2	H
		Conduits	304 SS	Note 2	Note 2	Note 2
		Flange base	304 SS	Note 2	Note 2	L
		Locking caps	304 SS	Note 2	Note 2	L
		Locking caps	304L SS	Note 3	Note 2	L
	Support tubes	304 SS	Note 2	Note 2	L	
	Upper plenum	UHI flow column bases	CF8	L	L	L
		UHI flow columns	304 SS	Note 2	Note 2	L
	Upper support column assemblies	Adapters	304 SS	Note 2	Note 2	Note 2
		Bolts	316 SS	L	L	L
		Column bases	CF8	L	L	L
		Column bases	304 SS	Note 3	L	L
		Column bodies	304 SS	Note 2	Note 2	L
		Extension tubes	304 SS	L	L	L
		Flanges	304 SS	Note 2	Note 2	Note 2
		Lock keys	304 SS	Note 2	Note 2	L
	Lock keys	304L SS	Note 2	Note 2	L	
Nuts	304 SS	Note 2	Note 2	L		

Table 5 (continued): MRP-191 Revision – Likelihood of Failure Comparison						
Assembly	Subassembly	MRP-191 Rev. 2 Component	Material	MRP-191 Rev. 0 Likelihood of Failure L,M,H	MRP-191 Rev. 1 Likelihood of Failure L,M,H	MRP-191 Rev. 2 Likelihood of Failure L,M,H (Note 1)
Upper internals assembly (cont.)	Upper support column assemblies (cont.)	Nuts	302 SS	Note 3	Note 2	L
	Upper support plate assembly - Inverted Top Hat Design (Note 7)	ITH flange	304 SS	L	L	L
		ITH upper support plate	304 SS	L	L	L
		ITH Upper support ring or skirt	304 SS	M	M	L
		ITH Upper support ring or skirt	CF8	Note 3	M	L
	Upper support plate assembly - Top Hat Design (Note 7)	Flange	304 SS	Note 2	Note 2	L
		Flange	CF8	Note 3	L	L
		Upper support plate	304 SS	Note 2	Note 2	L
		Upper support plate	CF8	Note 3	L	L
		Upper support ring or skirt	304 SS	M	M	L
		Upper support ring or skirt	CF8	Note 3	M	L
		Deep beam ribs (Note 8)	304 SS	L	L	L
		Deep beam stiffeners	304 SS	L	L	L
		Bolts	316 SS	Note 2	Note 2	L
		Locking device	316 SS	Note 2	Note 2	L
		Locking device	304 SS	Note 3	Note 2	L
		Upper support plate assembly - Flat Plate Design (Note 7)	Upper support plate	304 SS	Note 2	Note 2
	Upper support plate		CF8	Note 3	L	L
	Upper support ring or skirt		304 SS	M	M	L
	Upper support ring or skirt		CF8	Note 3	M	L
	Deep beam ribs (Note 8)		304 SS	L	L	L
	Deep beam stiffeners		304 SS	L	L	L
	Bolts		316 SS	Note 2	Note 2	L
Locking device	316 SS		Note 2	Note 2	L	
Lower internals assembly	Baffle and former assembly	Baffle bolting locking devices	304 SS	L	L	H
		Baffle, edge bolts	316 SS	H	H	H

Table 5 (continued): MRP-191 Revision – Likelihood of Failure Comparison						
Assembly	Subassembly	MRP-191 Rev. 2 Component	Material	MRP-191 Rev. 0 Likelihood of Failure L,M,H	MRP-191 Rev. 1 Likelihood of Failure L,M,H	MRP-191 Rev. 2 Likelihood of Failure L,M,H (Note 1)
Lower internals assembly (cont.)	Baffle and former assembly (cont.)	Baffle, edge bolts	347 SS	H	H	H
		Bracket bolts	347 SS	Note 3	Note 3	H
		Baffle plates	304 SS	M	M	L
		Baffle, former bolts	316 SS	H	H	H
		Baffle, former bolts	347 SS	H	H	H
		Corner bolts	347 SS	Note 3	Note 3	H
		Barrel, former bolts	316 SS	H	H	H
		Barrel, former bolts	347 SS	H	H	H
		Former dowel pins	302 SS	Note 3	Note 3	L
		Former dowel pins	304 SS	Note 3	Note 3	L
		Former plates	304 SS	M	M	L
	BMI column assemblies	BMI column bodies	304 SS	M	M	M
		BMI column bolts	316 SS	L	L	M
		BMI column collars	304 SS	M	M	M
		BMI column cruciforms	304 SS	Note 3	M	M
		BMI column cruciforms	CF8	M	M	M
		BMI column extension bars	304 SS	L	L	L
		BMI column extension tubes	304 SS	M	M	L
		BMI column locking devices	304L SS	Note 2	Note 2	L
	Core barrel	BMI column nuts	304 SS	L	L	L
		Core barrel flange	304 SS	L	L	L
		Upflow conversion core barrel plug body	304 SS	Note 3	Note 3	L
		Upflow conversion core barrel plug mandrel	316 SS	Note 3	Note 3	L
		Core barrel outlet nozzles	304 SS	M	M	L

Table 5 (continued): MRP-191 Revision – Likelihood of Failure Comparison						
Assembly	Subassembly	MRP-191 Rev. 2 Component	Material	MRP-191 Rev. 0 Likelihood of Failure L,M,H	MRP-191 Rev. 1 Likelihood of Failure L,M,H	MRP-191 Rev. 2 Likelihood of Failure L,M,H (Note 1)
Lower internals assembly (cont.)	Core barrel (cont.)	Lower core barrel (includes MAW and LAW)	304 SS	M	M	M
		Lower core barrel (includes LGW and LFW)	304 SS	M	M	M
		Upper core barrel (includes UAW)	304 SS	M	M	M
		Upper core barrel (includes UFW and UGW)	304 SS	M	M	M
		Safety injection nozzle interface	304 SS	Note 3	Note 3	L
	Diffuser plate Flux thimbles (tubes)	Diffuser plate	304 SS	Note 2	Note 2	Note 2
		Flux thimble tube plugs	304 SS	M	M	M
		Flux thimble tube plugs	316 SS	Note 3	M	M
		Flux thimble tube plugs	308 SS	Note 3	M	M
		Flux thimble tube plugs	A600	Note 3	M	M
		Flux thimbles (tubes)	316 SS	H	H	H
		Flux thimbles (tubes)	A600	Note 3	H	H
		Flux thimble anti-vibration sleeve	304 SS	Note 3	Note 3	L
	Head cooling spray nozzles	Head cooling spray nozzles	304 SS	Note 2	Note 2	L
	Irradiation specimen guides	Irradiation specimen guides	304 SS	L	L	L
		Irradiation specimen guide bolts	316 SS	L	L	L
		Irradiation specimen guide lock caps	304L SS	L	L	Note 2
		Irradiation specimen access plug (spring) (Note 9)	X-750	Note 3	Note 3	Note 2
		Irradiation specimen access plug (dowel pin) (Note 9)	316 SS	Note 3	Note 3	Note 2
		Irradiation specimen access plug (plug) (Note 9)	304 SS	L	L	Note 2

Table 5 (continued): MRP-191 Revision – Likelihood of Failure Comparison						
Assembly	Subassembly	MRP-191 Rev. 2 Component	Material	MRP-191 Rev. 0 Likelihood of Failure L,M,H	MRP-191 Rev. 1 Likelihood of Failure L,M,H	MRP-191 Rev. 2 Likelihood of Failure L,M,H (Note 1)
Lower internals assembly (cont.)	LCP and fuel alignment pins	Fuel alignment pins	316 SS	L	L	L
		Fuel alignment pins	304 SS	Note 3	L	H
	LCP and fuel alignment pins (cont.)	XL LCP fuel alignment pins	316 SS	Note 3	Note 3	H
		LCP and manway bolts	316 SS	L	L	M
		LCP and manway locking devices	304L SS	L	L	L
		Lower core plate	304 SS	M	M	L
		XL lower core plate	304 SS	M	M	L
		Lower support column assemblies	Lower support column bodies	304 SS	M	M
	Lower support column bodies		CF8	M	M	L
	Lower support column bolts		304 SS	M	M	M
	Lower support column bolts		316 SS	Note 3	M	M
	Lower support column bolt locking devices		304L SS (Note 11)	Note 3	Note 3	L
	Lower support column bolt locking devices		304 SS (Note 11)	Note 3	Note 3	L
	Lower support column nuts		304 SS	Note 2	Note 2	L
	Lower support column sleeves		304 SS	Note 2	Note 2	Note 2
	Lower support casting or forging	Lower support casting	CF8	L	L	L
		Lower support forging	304 SS	L	L	L
	Neutron panels/thermal shield	Neutron panel bolts	316 SS	L	L	L
		Neutron panel locking devices	304 SS	L	L	Note 2
		Neutron panel locking devices	304L SS	Note 3	L	Note 2
		Thermal shield bolts	316 SS	L	L	H
		Thermal shield dowels	316 SS	L	L	L
		Thermal shield dowels	304 SS	Note 3	L	L
		Thermal shield flexures	304 SS	M	M	M
		Thermal shield flexures	316 SS	Note 3	M	M
	Thermal shield flexure bolts	316 SS	Note 3	Note 3	L	

Table 5 (continued): MRP-191 Revision – Likelihood of Failure Comparison						
Assembly	Subassembly	MRP-191 Rev. 2 Component	Material	MRP-191 Rev. 0 Likelihood of Failure L,M,H	MRP-191 Rev. 1 Likelihood of Failure L,M,H	MRP-191 Rev. 2 Likelihood of Failure L,M,H (Note 1)
Lower internals assembly (cont.)	Neutron panels/thermal shield (cont.)	Thermal shield flexure locking devices and dowel pins	304 SS	Note 3	Note 3	L
		Thermal shield flexure locking devices and dowel pins	304L SS	Note 3	Note 3	L
		Thermal shield or neutron panels	304 SS	L	L	L
	Radial support keys	Radial support key bolts	304 SS	L	L	L
		Radial support key bolts	316 SS	Note 3	L	L
		Radial support key dowels	304 SS	Note 3	Note 3	L
		Radial support key lock keys	304 SS (Note 10)	Note 2	Note 2	L
		Radial support keys	304 SS	L	L	L
		Radial support keys	Stellite	Note 3	Note 3	H
		SCS assembly	SCS base plate	304 SS	L	L
	SCS bolts	316 SS	Note 2	Note 2	L	
	SCS energy absorber	304 SS	Note 2	Note 2	Note 2	
	SCS guide post	304 SS	Note 2	Note 2	Note 2	
	SCS guide post	CF8	Note 3	L	L	
	SCS housing	304 SS	Note 2	Note 2	Note 2	
	SCS housing	CF8	Note 3	L	L	
	SCS lock keys	304 SS	Note 2	Note 2	L	
Upper and lower tie plates	304 SS	Note 3	Note 2	L		
Interfacing components	Interfacing components	Clevis insert bolts	X-750	M	H	H
		Clevis insert dowels	Alloy 600	Note 3	Note 3	M
		Clevis insert locking devices	Alloy 600	Note 2	Note 2	L
		Clevis insert locking devices	316 SS	Note 2	Note 2	L
		Clevis inserts	Alloy 600	L	L	L
		Clevis inserts	304 SS	L	L	L

Table 5 (continued): MRP-191 Revision – Likelihood of Failure Comparison						
Assembly	Subassembly	MRP-191 Rev. 2 Component	Material	MRP-191 Rev. 0 Likelihood of Failure L,M,H	MRP-191 Rev. 1 Likelihood of Failure L,M,H	MRP-191 Rev. 2 Likelihood of Failure L,M,H (Note 1)
Interfacing components (cont.)	Interfacing components (cont.)	Clevis inserts	Stellite	L	L	H
		Head and vessel alignment pin bolts	316 SS	Note 2	Note 2	L
		Head and vessel alignment pin lock caps	304L SS	Note 2	Note 2	Note 2
		Head and vessel alignment pins	304 SS	Note 2	Note 2	L
		Head and vessel alignment pins	Stellite	Note 3	Note 3	M
		Internals hold-down spring	304 SS	L	L	H
		Internals hold-down spring	403 SS	L	L	L
		Internals hold-down spring	F6NM	Note 3	Note 3	L
		UCP alignment pins	304 SS	M	M	L
		UCP alignment pins	Stellite	Note 3	Note 3	M
		Thermal sleeves	304 SS	Note 3	Note 3	H
		Thermal sleeve guide funnels	304 SS	Note 3	Note 3	H
		Thermal sleeve guide funnels	CF8	Note 3	Note 3	H
		Instrumentation nozzle funnels	304 SS	Note 3	Note 3	Note 2
Replacement reactor vessel head extension tubes	304 SS	Note 3	Note 3	Note 2		

Table 5 (continued): MRP-191 Revision – Likelihood of Failure Comparison						
Assembly	Subassembly	MRP-191 Rev. 2 Component	Material	MRP-191 Rev. 0 Likelihood of Failure L,M,H	MRP-191 Rev. 1 Likelihood of Failure L,M,H	MRP-191 Rev. 2 Likelihood of Failure L,M,H (Note 1)

Notes:

1. Cells that are gray shaded represent changes in likelihood of failure between MRP-191, Revision 2 [1], and previous revisions of MRP-191 (Revisions 0 [2] and 1 [3]).
2. This component exists within MRP-191, Revision 0 [2], and/or Revision 1 [3], and/or Revision 2 [1], and had no degradation mechanisms. Therefore this component was not provided a likelihood ranking by the MRP-191 Expert Panel.
3. This component is not within MRP-191, Revision 0 [2], and/or Revision 1 [3].
4. Component name modified to eliminate “upper” from its name to further clarify the actual component in MRP-191, Revision 2 [1].
5. Component name modified to eliminate “support pin” from its name to further clarify the actual component in MRP-191, Revision 2 [1].
6. “Protective skirt” was added to the component name for clarification in MRP-191, Revision 2 [1].
7. The upper support plate assembly was separated out to identify specific components applicable to the three design variations (inverted top hat, top hat, and flat plate).
8. The component “ribs” was listed in MRP-191, Revision 0 [2] and Revision 1 [3]; however, with splitting up the upper support plate assembly into the three design variations, the “deep beam ribs” component captures the previously listed “ribs” in MRP-191, Revision 2 [1].
9. This was originally listed as “specimen plugs” in MRP-191, Revision 1 [3]. However, due to the materials comprising this component, it was divided out into its subcomponents in MRP-191, Revision 2 [1].
10. The radial support key lock keys was listed as 316 SS within Table 6-10 and Table 7-2 of MRP-191, Revision 2 [1] but should be 304 SS.
11. The lower support column bolt locking devices are listed as 304 SS within Table 4-6, Table 5-1, Table 6-10, and Table 7-2 of MRP-191, Revision 2 [1] and also as 304L SS in Table 4-4 of MRP-191, Revision 2 [1]. Both materials are listed in this table.

References for Table 5:

1. Materials Reliability Program: Screening, Categorization, and Ranking of Reactor Internals Components for Westinghouse and Combustion Engineering PWR Design (MRP-191, Revision 2). EPRI, Palo Alto, CA: 2018. 3002013220.
2. Materials Reliability Program: Screening, Categorization, and Ranking of Reactor Internals Components for Westinghouse and Combustion Engineering PWR Design (MRP-191). EPRI, Palo Alto, CA: 2006. 1013234.
3. Materials Reliability Program: Screening, Categorization, and Ranking of Reactor Internals Components for Westinghouse and Combustion Engineering PWR Design (MRP-191, Revision 1). EPRI, Palo Alto, CA: 2016. 3002007960.

Table 6: MRP-191 Revision – Likelihood of Damage/Consequence Comparison

Assembly	Subassembly	MRP-191 Rev. 2 Component	Material	MRP-191 Rev. 0 Likelihood of Damage L,M,H	MRP-191 Rev. 1 Likelihood of Damage L,M,H	MRP-191 Rev. 2 Safety Consequence L,M,H (Note 1)	MRP-191 Rev. 2 Economic Consequence L,M,H (Note 1)
Upper internals assembly	Control rod guide tube assemblies and flow downcomers	Anti-rotation studs and nuts	304 SS	Note 2	Note 2	Note 2	Note 2
		Anti-rotation studs and nuts	316 SS	Note 3	Note 2	Note 2	Note 2
		Bolts	316 SS	Note 2	Note 2	M	L
		Bolts	304 SS	Note 3	Note 2	L	L
		C-tubes	304 SS	M	M	M	M
		Enclosure pins	304 SS	M	M	M	M
		Guide tube enclosures (Note 4)	304 SS	M	M	M	M
		Guide tube enclosures (Note 4)	CF8	Note 3	M	M	M
		Flanges, intermediate	304 SS	M	M	M	M
		Flanges, intermediate	CF8	M	M	M	M
		Flanges, lower	304 SS	M	M	M	M
		Flanges, lower	CF8	M	M	M	M
		Flexureless inserts	304 SS	Note 2	Note 2	L	L
		Flexureless inserts (spring)	Alloy 718	Note 3	Note 3	L	L
		Flexures	X-750	M	M	L	M
		Guide plates/cards	304 SS	M	M	H	M
		Guide plates/cards	316L SS	Note 3	M	H	M
		Guide plates/cards	CF8	Note 3	M	H	M
		Guide tube support pins	X-750	M	M	L	M
		Guide tube support pins	316 SS	M	M	L	M
		Housing plates	304 SS	Note 2	Note 2	Note 2	Note 2
		Housing plates	CF8	Note 3	M	L	M
		Inserts	304 SS	Note 2	Note 2	Note 2	Note 2
Inserts	CF8	Note 3	Note 3	L	L		
Lock bars	304 SS	Note 2	Note 2	L	M		

Table 6 (continued): MRP-191 Revision – Likelihood of Damage/Consequence Comparison							
Assembly	Subassembly	MRP-191 Rev. 2 Component	Material	MRP-191 Rev. 0 Likelihood of Damage L,M,H	MRP-191 Rev. 1 Likelihood of Damage L,M,H	MRP-191 Rev. 2 Safety Consequence L,M,H (Note 1)	MRP-191 Rev. 2 Economic Consequence L,M,H (Note 1)
Upper internals assembly (cont.)	Control rod guide tube assemblies and flow downcomers (cont.)	Sheaths	304 SS	M	M	H	M
		Cover plate (Note 5)	304 SS	Note 2	Note 2	L	L
		Cover plate cap screws (Note 5)	316 SS	Note 2	Note 2	L	L
		Cover plate guide tube locking caps and tie straps (Note 5)	304 SS	Note 2	Note 2	L	L
		Support pin nuts	X-750	Note 2	Note 2	L	M
		Support pin nuts	304 SS	Note 3	Note 2	L	M
		Support pin nuts	316 SS	Note 2	Note 2	L	M
		Water flow slot ligaments	304 SS	Note 2	Note 2	Note 2	Note 2
		Probe holder shroud	304 SS	Note 3	Note 3	L	M
		Mixing Devices	Mixing devices	CF8	L	L	L
	Mixing devices		304 SS	Note 3	L	L	M
	UCP and fuel alignment pins	Fuel alignment pins	316 SS	L	L	L	M
		Fuel alignment pins	304 SS	Note 3	L	L	M
		UCP	304 SS	M	M	M	H
		Upper core plate insert	304 SS	Note 3	Note 3	M	M
		Upper core plate insert	Stellite	Note 3	Note 3	M	M
		Upper core plate insert bolts	316 SS	Note 3	Note 3	L	M
		Upper core plate insert locking devices & dowel pins	304 SS	Note 3	Note 3	L	M
		Upper core plate insert locking devices & dowel pins	316 SS	Note 3	Note 3	L	M
		Protective skirt	304 SS	Note 3	L	L	L
		Protective skirt bolts (Note 6)	316 SS	Note 3	L	L	L

Table 6 (continued): MRP-191 Revision – Likelihood of Damage/Consequence Comparison

Assembly	Subassembly	MRP-191 Rev. 2 Component	Material	MRP-191 Rev. 0 Likelihood of Damage L,M,H	MRP-191 Rev. 1 Likelihood of Damage L,M,H	MRP-191 Rev. 2 Safety Consequence L,M,H (Note 1)	MRP-191 Rev. 2 Economic Consequence L,M,H (Note 1)
Upper internals assembly (cont.)	UCP and fuel alignment pins (cont.)	Protective skirt lock bars (Note 6)	304 SS	Note 3	Note 2	L	L
		Protective skirt dowel pins (Note 6)	304 SS	Note 3	Note 2	L	L
		Protective skirt dowel pins (Note 6)	316 SS	Note 3	Note 2	L	L
	Upper instrumentation conduit and supports	Bolting	316 SS	Note 2	Note 2	Note 2	Note 2
		Bolting	304 SS	Note 3	Note 2	Note 2	Note 2
		Brackets, clamps, terminal blocks, and conduit straps	304 SS	Note 2	Note 2	L	H
		Brackets, clamps, terminal blocks, and conduit straps	302 SS	Note 3	Note 2	L	H
		Brackets, clamps, terminal blocks, and conduit straps	CF8	Note 3	L	L	H
		Conduit seal assembly: body, tubesheets, tubesheet welds	304 SS	Note 2	Note 2	M	M
		Conduit seal assembly: tubes	304 SS	Note 2	Note 2	M	M
		Conduits	304 SS	Note 2	Note 2	Note 2	Note 2
		Flange base	304 SS	Note 2	Note 2	L	M
		Locking caps	304 SS	Note 2	Note 2	L	M
		Locking caps	304L SS	Note 3	Note 2	L	M
	Support tubes	304 SS	Note 2	Note 2	L	M	
	Upper plenum	UHI flow column bases	CF8	L	L	L	L
		UHI flow columns	304 SS	Note 2	Note 2	L	L
Upper support column assemblies	Adapters	304 SS	Note 2	Note 2	Note 2	Note 2	
	Bolts	316 SS	M	M	L	M	
	Column bases	CF8	M	M	L	H	

Table 6 (continued): MRP-191 Revision – Likelihood of Damage/Consequence Comparison							
Assembly	Subassembly	MRP-191 Rev. 2 Component	Material	MRP-191 Rev. 0 Likelihood of Damage L,M,H	MRP-191 Rev. 1 Likelihood of Damage L,M,H	MRP-191 Rev. 2 Safety Consequence L,M,H (Note 1)	MRP-191 Rev. 2 Economic Consequence L,M,H (Note 1)
Upper internals assembly (cont.)	Upper support column assemblies (cont.)	Column bases	304 SS	Note 3	M	L	H
		Column bodies	304 SS	Note 2	Note 2	L	H
		Extension tubes	304 SS	M	M	L	H
		Flanges	304 SS	Note 2	Note 2	Note 2	Note 2
		Lock keys	304 SS	Note 2	Note 2	L	M
		Lock keys	304L SS	Note 2	Note 2	L	M
		Nuts	304 SS	Note 2	Note 2	L	M
		Nuts	302 SS	Note 3	Note 2	L	M
	Upper support plate assembly - Inverted Top Hat Design (Note 7)	ITH flange	304 SS	M	M	L	H
		ITH upper support plate	304 SS	M	M	L	H
		ITH Upper support ring or skirt	304 SS	M	M	L	H
		ITH Upper support ring or skirt	CF8	Note 3	M	L	H
	Upper support plate assembly - Top Hat Design (Note 7)	Flange	304 SS	Note 2	Note 2	M	H
		Flange	CF8	Note 3	M	M	H
		Upper support plate	304 SS	Note 2	Note 2	L	H
		Upper support plate	CF8	Note 3	M	L	H
		Upper support ring or skirt	304 SS	M	M	M	H
		Upper support ring or skirt	CF8	Note 3	M	M	H
		Deep beam ribs (Note 8)	304 SS	M	M	L	L
		Deep beam stiffeners	304 SS	M	M	L	L
		Bolts	316 SS	Note 2	Note 2	L	L
		Locking device	316 SS	Note 2	Note 2	L	L
	Locking device	304 SS	Note 3	Note 2	L	L	

Table 6 (continued): MRP-191 Revision – Likelihood of Damage/Consequence Comparison							
Assembly	Subassembly	MRP-191 Rev. 2 Component	Material	MRP-191 Rev. 0 Likelihood of Damage L,M,H	MRP-191 Rev. 1 Likelihood of Damage L,M,H	MRP-191 Rev. 2 Safety Consequence L,M,H (Note 1)	MRP-191 Rev. 2 Economic Consequence L,M,H (Note 1)
Upper internals assembly (cont.)	Upper support plate assembly - Flat Plate Design (Note 7)	Upper support plate	304 SS	Note 2	Note 2	L	H
		Upper support plate	CF8	Note 3	M	L	H
		Upper support ring or skirt	304 SS	M	M	L	H
		Upper support ring or skirt	CF8	Note 3	M	L	H
		Deep beam ribs (Note 8)	304 SS	M	M	L	L
		Deep beam stiffeners	304 SS	M	M	L	L
		Bolts	316 SS	Note 2	Note 2	L	L
		Locking device	316 SS	Note 2	Note 2	L	L
		Locking device	304 SS	Note 3	Note 2	L	L
Lower internals assembly	Baffle and former assembly	Baffle bolting locking devices	304 SS	L	L	L	M
		Baffle, edge bolts	316 SS	M	M	L	M
		Baffle, edge bolts	347 SS	M	M	L	M
		Bracket bolts	347 SS	Note 3	Note 3	L	M
		Baffle plates	304 SS	L	L	L	L
		Baffle, former bolts	316 SS	L	M	M	M
		Baffle, former bolts	347 SS	L	M	M	M
		Corner bolts	347 SS	Note 3	Note 3	M	M
		Barrel, former bolts	316 SS	L	L	L	M
		Barrel, former bolts	347 SS	L	L	L	M
		Former dowel pins	302 SS	Note 3	Note 3	L	L
		Former dowel pins	304 SS	Note 3	Note 3	L	L
		Former plates	304 SS	L	L	L	L
	BMI column assemblies	BMI column bodies	304 SS	L	L	L	L
		BMI column bolts	316 SS	L	L	L	M
		BMI column collars	304 SS	L	L	L	L
BMI column cruciforms		304 SS	Note 3	L	L	L	
BMI column cruciforms		CF8	L	L	L	L	
		BMI column extension bars	304 SS	L	L	L	L

Table 6 (continued): MRP-191 Revision – Likelihood of Damage/Consequence Comparison								
Assembly	Subassembly	MRP-191 Rev. 2 Component	Material	MRP-191 Rev. 0 Likelihood of Damage L,M,H	MRP-191 Rev. 1 Likelihood of Damage L,M,H	MRP-191 Rev. 2 Safety Consequence L,M,H (Note 1)	MRP-191 Rev. 2 Economic Consequence L,M,H (Note 1)	
Lower internals assembly (cont.)	BMI column assemblies (cont.)	BMI column extension tubes	304 SS	L	L	L	L	
		BMI column locking devices	304L SS	Note 2	Note 2	L	L	
		BMI column nuts	304 SS	L	L	L	L	
	Core barrel	Core barrel flange	304 SS	H	H	M	H	
		Upflow conversion core barrel plug body	304 SS	Note 3	Note 3	L	L	
		Upflow conversion core barrel plug mandrel	316 SS	Note 3	Note 3	L	L	
		Core barrel outlet nozzles	304 SS	M	M	M	H	
		Lower core barrel (includes MAW and LAW)	304 SS	H	H	M	H	
		Lower core barrel (includes LGW and LFW)	304 SS	H	H	M	H	
		Upper core barrel (includes UAW)	304 SS	H	H	M	H	
		Upper core barrel (includes UFW and UGW)	304 SS	H	H	M	H	
		Safety injection nozzle interface	304 SS	Note 3	Note 3	M	H	
		Diffuser plate	Diffuser plate	304 SS	Note 2	Note 2	Note 2	Note 2
		Flux thimbles (tubes)	Flux thimble tube plugs	304 SS	L	L	L	L
	Flux thimble tube plugs		316 SS	Note 3	L	L	L	
	Flux thimble tube plugs		308 SS	Note 3	L	L	L	
	Flux thimble tube plugs		A600	Note 3	L	L	L	
	Flux thimbles (tubes)		316 SS	L	L	L	L	
	Flux thimbles (tubes)		A600	Note 3	L	L	L	

Table 6 (continued): MRP-191 Revision – Likelihood of Damage/Consequence Comparison

Assembly	Subassembly	MRP-191 Rev. 2 Component	Material	MRP-191 Rev. 0 Likelihood of Damage L,M,H	MRP-191 Rev. 1 Likelihood of Damage L,M,H	MRP-191 Rev. 2 Safety Consequence L,M,H (Note 1)	MRP-191 Rev. 2 Economic Consequence L,M,H (Note 1)
Lower internals assembly (cont.)	Flux thimbles (tubes) (cont.)	Flux thimble anti-vibration sleeve	304 SS	Note 3	Note 3	L	L
	Head cooling spray nozzles	Head cooling spray nozzles	304 SS	Note 2	Note 2	L	L
	Irradiation specimen guides	Irradiation specimen guides	304 SS	L	L	L	L
		Irradiation specimen guide bolts	316 SS	L	L	L	L
		Irradiation specimen guide lock caps	304L SS	L	L	Note 2	Note 2
		Irradiation specimen access plug (spring) (Note 9)	X-750	Note 3	Note 3	Note 2	Note 2
		Irradiation specimen access plug (dowel pin) (Note 9)	316 SS	Note 3	Note 3	Note 2	Note 2
		Irradiation specimen access plug (plug) (Note 9)	304 SS	L	L	Note 2	Note 2
		LCP and fuel alignment pins	Fuel alignment pins	316 SS	L	L	L
	Fuel alignment pins		304 SS	Note 3	L	L	M
	XL LCP fuel alignment pins		316 SS	Note 3	Note 3	L	M
	LCP and manway bolts		316 SS	L	L	L	M
	LCP and manway locking devices		304L SS	L	L	L	M
	Lower core plate		304 SS	M	M	M	H
	XL lower core plate		304 SS	M	M	M	H
	Lower support column assemblies	Lower support column bodies	304 SS	L	L	L	L
		Lower support column bodies	CF8	L	L	L	L
		Lower support column bolts	304 SS	L	L	L	M
		Lower support column bolts	316 SS	Note 3	L	L	M

Table 6 (continued): MRP-191 Revision – Likelihood of Damage/Consequence Comparison							
Assembly	Subassembly	MRP-191 Rev. 2 Component	Material	MRP-191 Rev. 0 Likelihood of Damage L,M,H	MRP-191 Rev. 1 Likelihood of Damage L,M,H	MRP-191 Rev. 2 Safety Consequence L,M,H (Note 1)	MRP-191 Rev. 2 Economic Consequence L,M,H (Note 1)
Lower internals assembly (cont.)	Lower support column assemblies (cont.)	Lower support column bolt locking devices	304L SS (Note 11)	Note 3	Note 3	L	L
		Lower support column bolt locking devices	304 SS (Note 11)	Note 3	Note 3	L	L
		Lower support column nuts	304 SS	Note 2	Note 2	L	L
		Lower support column sleeves	304 SS	Note 2	Note 2	Note 2	Note 2
	Lower support casting or forging	Lower support casting	CF8	H	H	M	H
		Lower support forging	304 SS	H	H	M	H
	Neutron panels/thermal shield	Neutron panel bolts	316 SS	L	L	L	L
		Neutron panel locking devices	304 SS	L	L	Note 2	Note 2
		Neutron panel locking devices	304L SS	Note 3	L	Note 2	Note 2
		Thermal shield bolts	316 SS	L	L	L	L
		Thermal shield dowels	316 SS	L	L	L	L
		Thermal shield dowels	304 SS	Note 3	L	L	L
		Thermal shield flexures	304 SS	L	L	L	H
		Thermal shield flexures	316 SS	Note 3	L	L	H
		Thermal shield flexure bolts	316 SS	Note 3	Note 3	L	L
		Thermal shield flexure locking devices and dowel pins	304 SS	Note 3	Note 3	L	L
		Thermal shield flexure locking devices and dowel pins	304L SS	Note 3	Note 3	L	L
		Thermal shield or neutron panels	304 SS	L	L	L	L
		Radial support keys	Radial support key bolts	304 SS	L	L	L
	Radial support key bolts		316 SS	Note 3	L	L	L

Table 6 (continued): MRP-191 Revision – Likelihood of Damage/Consequence Comparison							
Assembly	Subassembly	MRP-191 Rev. 2 Component	Material	MRP-191 Rev. 0 Likelihood of Damage L,M,H	MRP-191 Rev. 1 Likelihood of Damage L,M,H	MRP-191 Rev. 2 Safety Consequence L,M,H (Note 1)	MRP-191 Rev. 2 Economic Consequence L,M,H (Note 1)
Lower internals assembly (cont.)	Radial support keys (cont.)	Radial support key dowels	304 SS	Note 3	Note 3	L	L
		Radial support key lock keys	304 SS (Note 10)	Note 3	Note 3	Note 2	Note 2
		Radial support keys	304 SS	L	L	M	M
		Radial support keys	Stellite	Note 3	Note 3	M	M
	SCS assembly	SCS base plate	304 SS	L	L	L	L
		SCS bolts	316 SS	Note 2	Note 2	L	L
		SCS energy absorber	304 SS	Note 2	Note 2	Note 2	Note 2
		SCS guide post	304 SS	Note 2	Note 2	Note 2	Note 2
		SCS guide post	CF8	Note 3	L	L	L
		SCS housing	304 SS	Note 2	Note 2	Note 2	Note 2
		SCS housing	CF8	Note 3	L	L	L
		SCS lock keys	304 SS	Note 2	Note 2	L	L
		Upper and lower tie plates	304 SS	Note 3	Note 2	L	L
Interfacing components	Interfacing components	Clevis insert bolts	X-750	L	L	L	H
		Clevis insert dowels	Alloy 600	Note 3	Note 3	L	L
		Clevis insert locking devices	Alloy 600	Note 2	Note 2	L	L
		Clevis insert locking devices	316 SS	Note 2	Note 2	L	L
		Clevis inserts	Alloy 600	L	L	L	H
		Clevis inserts	304 SS	L	L	L	H
		Clevis inserts	Stellite	L	L	M	H
		Head and vessel alignment pin bolts	316 SS	Note 2	Note 2	L	L
		Head and vessel alignment pin lock caps	304L SS	Note 2	Note 2	Note 2	Note 2
		Head and vessel alignment pins	304 SS	Note 2	Note 2	L	L

Table 6 (continued): MRP-191 Revision – Likelihood of Damage/Consequence Comparison							
Assembly	Subassembly	MRP-191 Rev. 2 Component	Material	MRP-191 Rev. 0 Likelihood of Damage L,M,H	MRP-191 Rev. 1 Likelihood of Damage L,M,H	MRP-191 Rev. 2 Safety Consequence L,M,H (Note 1)	MRP-191 Rev. 2 Economic Consequence L,M,H (Note 1)
Interfacing components (cont.)	Interfacing components (cont.)	Head and vessel alignment pins	Stellite	Note 3	Note 3	L	L
		Internals hold-down spring	304 SS	L	L	L	H
		Internals hold-down spring	403 SS	L	L	L	H
		Internals hold-down spring	F6NM	Note 3	Note 3	L	H
		UCP alignment pins	304 SS	L	L	L	M
		UCP alignment pins	Stellite	Note 3	Note 3	L	M
		Thermal sleeves	304 SS	Note 3	Note 3	H	H
		Thermal sleeve guide funnels	304 SS	Note 3	Note 3	L	L
		Thermal sleeve guide funnels	CF8	Note 3	Note 3	L	L
		Instrumentation nozzle funnels	304 SS	Note 3	Note 3	Note 2	Note 2
		Replacement reactor vessel head extension tubes	304 SS	Note 3	Note 3	Note 2	Note 2

Table 6 (continued): MRP-191 Revision – Likelihood of Damage/Consequence Comparison							
Assembly	Subassembly	MRP-191 Rev. 2 Component	Material	MRP-191 Rev. 0 Likelihood of Damage L,M,H	MRP-191 Rev. 1 Likelihood of Damage L,M,H	MRP-191 Rev. 2 Safety Consequence L,M,H (Note 1)	MRP-191 Rev. 2 Economic Consequence L,M,H (Note 1)

Notes:

1. Cells that are gray shaded represent changes in safety or economic consequence between MRP-191, Revision 2 [1], and previous revisions of MRP-191 (Revisions 0 [2] and 1 [3]). MRP-191, Revision 0 [2] and 1 [3] determined one combined consequence ranking and FMECA group; however, the safety-related consequences and economic consequences were separated for MRP-191, Revision 2 [1].
2. This component exists within MRP-191, Revision 0 [2], and/or Revision 1 [3], and/or Revision 2 [1], and had no degradation mechanisms. Therefore, this component was not provided a likelihood ranking by the MRP-191 Expert Panel.
3. This component is not within MRP-191, Revision 0 [2], and/or Revision 1 [3].
4. Component name modified to eliminate “upper” from its name to further clarify the actual component in MRP-191, Revision 2 [1].
5. Component name modified to eliminate “support pin” from its name to further clarify the actual component in MRP-191, Revision 2 [1].
6. “Protective skirt” was added to the component name for clarification in MRP-191, Revision 2 [1].
7. The upper support plate assembly was separated out to identify specific components applicable to the three design variations (inverted top hat, top hat, and flat plate).
8. The component “ribs” was listed in MRP-191, Revision 0 [2] and Revision 1 [3]; however, with splitting up the upper support plate assembly into the three design variations, the “deep beam ribs” component captures the previously listed “ribs” in MRP-191, Revision 2 [1].
9. This was originally listed as “specimen plugs” in MRP-191, Revision 1 [3]. However, due to the materials comprising this component, it was divided out into its subcomponents in MRP-191, Revision 2 [1].
10. The radial support key lock keys was listed as 316 SS within Table 6-10 and Table 7-2 of MRP-191, Revision 2 [1] but should be 304 SS.
11. The lower support column bolt locking devices are listed as 304 SS within Table 4-6, Table 5-1, Table 6-10, and Table 7-2 of MRP-191, Revision 2 [1] and also as 304L SS in Table 4-4 of MRP-191, Revision 2 [1]. Both materials are listed in this table.

References for Table 6:

1. Materials Reliability Program: Screening, Categorization, and Ranking of Reactor Internals Components for Westinghouse and Combustion Engineering PWR Design (MRP-191, Revision 2). EPRI, Palo Alto, CA: 2018. 3002013220.
2. Materials Reliability Program: Screening, Categorization, and Ranking of Reactor Internals Components for Westinghouse and Combustion Engineering PWR Design (MRP-191). EPRI, Palo Alto, CA: 2006. 1013234.
3. Materials Reliability Program: Screening, Categorization, and Ranking of Reactor Internals Components for Westinghouse and Combustion Engineering PWR Design (MRP-191, Revision 1). EPRI, Palo Alto, CA: 2016. 3002007960.

Table 7: MRP-191 Revision – FMECA Group Comparison							
Assembly	Subassembly	MRP-191 Rev. 2 Component	Material	MRP-191 Rev. 0 FMECA Group	MRP-191 Rev. 1 FMECA Group	MRP-191 Rev. 2 Safety FMECA Group (Note 1)	MRP-191 Rev. 2 Economic FMECA Group (Note 1)
Upper internals assembly	Control rod guide tube assemblies and flow downcomers	Anti-rotation studs and nuts	304 SS	0	0	0	0
		Anti-rotation studs and nuts	316 SS	--	0	0	0
		Bolts	316 SS	0	0	1	1
		Bolts	304 SS	--	0	1	1
		C-tubes	304 SS	2	2	2	2
		Enclosure pins	304 SS	1	1	1	1
		Guide tube enclosures (Note 2)	304 SS	1	1	1	1
		Guide tube enclosures (Note 2)	CF8	--	1	1	1
		Flanges, intermediate	304 SS	1	1	1	1
		Flanges, intermediate	CF8	1	1	1	1
		Flanges, lower	304 SS	1	1	2	2
		Flanges, lower	CF8	2	2	2	2
		Flexureless inserts	304 SS	0	0	1	1
		Flexureless inserts (spring)	Alloy 718	--	--	1	1
		Flexures	X-750	3	3	3	3
		Guide plates/cards	304 SS	3	3	3	3
		Guide plates/cards	316L SS	--	3	3	3
		Guide plates/cards	CF8	--	3	3	3
		Guide tube support pins	X-750	3	3	3	3
		Guide tube support pins	316 SS	1	1	1	1
		Housing plates	304 SS	0	0	0	0
		Housing plates	CF8	--	1	1	1
		Inserts	304 SS	0	0	0	0
		Inserts	CF8	--	--	1	1
Lock bars	304 SS	0	0	1	1		
Sheaths	304 SS	2	2	3	3		
Cover plate (Note 3)	304 SS	0	0	1	1		

Table 7 (continued): MRP-191 Revision – FMECA Group Comparison							
Assembly	Subassembly	MRP-191 Rev. 2 Component	Material	MRP-191 Rev. 0 FMECA Group	MRP-191 Rev. 1 FMECA Group	MRP-191 Rev. 2 Safety FMECA Group (Note 1)	MRP-191 Rev. 2 Economic FMECA Group (Note 1)
Upper internals assembly (cont.)	Control rod guide tube assemblies and flow downcomers (cont.)	Cover plate cap screws (Note 3)	316 SS	0	0	1	1
		Cover plate guide tube locking caps and tie straps (Note 3)	304 SS	0	0	1	1
		Support pin nuts	X-750	0	0	1	1
		Support pin nuts	304 SS	--	0	1	1
		Support pin nuts	316 SS	0	0	1	1
		Water flow slot ligaments	304 SS	0	0	0	0
		Probe holder shroud	304 SS	--	--	1	1
	Mixing Devices	Mixing devices	CF8	1	1	1	1
		Mixing devices	304 SS	--	1	1	1
	UCP and fuel alignment pins	Fuel alignment pins	316 SS	1	1	1	1
		Fuel alignment pins	304 SS	--	1	3	3
		UCP	304 SS	1	2	2	3
		Upper core plate insert	304 SS	--	--	2	2
		Upper core plate insert	Stellite	--	--	2	2
		Upper core plate insert bolts	316 SS	--	--	1	1
		Upper core plate insert locking devices & dowel pins	304 SS	--	--	1	1
		Upper core plate insert locking devices & dowel pins	316 SS	--	--	1	1
		Protective skirt	304 SS	--	1	1	1
		Protective skirt bolts (Note 4)	316 SS	--	1	2	2
		Protective skirt lock bars (Note 4)	304 SS	--	0	1	1
		Protective skirt dowel pins (Note 4)	304 SS	--	0	1	1

Table 7 (continued): MRP-191 Revision – FMECA Group Comparison							
Assembly	Subassembly	MRP-191 Rev. 2 Component	Material	MRP-191 Rev. 0 FMECA Group	MRP-191 Rev. 1 FMECA Group	MRP-191 Rev. 2 Safety FMECA Group (Note 1)	MRP-191 Rev. 2 Economic FMECA Group (Note 1)
Upper internals assembly (cont.)	UCP and fuel alignment pins (cont.)	Protective skirt dowel pins (Note 4)	316 SS	--	0	1	1
	Upper instrumentation conduit and supports	Bolting	316 SS	0	0	0	0
		Bolting	304 SS	--	0	0	0
		Brackets, clamps, terminal blocks, and conduit straps	304 SS	0	0	3	3
		Brackets, clamps, terminal blocks, and conduit straps	302 SS	--	0	2	3
		Brackets, clamps, terminal blocks, and conduit straps	CF8	--	1	1	2
		Conduit seal assembly: body, tubesheets, tubesheet welds	304 SS	0	0	3	3
		Conduit seal assembly: tubes	304 SS	0	0	3	3
		Conduits	304 SS	0	0	0	0
		Flange base	304 SS	0	0	1	1
		Locking caps	304 SS	0	0	1	1
		Locking caps	304L SS	--	0	1	1
		Support tubes	304 SS	0	0	1	1
	Upper plenum	UHI flow column bases	CF8	1	1	1	1
		UHI flow columns	304 SS	0	0	1	1
	Upper support column assemblies	Adapters	304 SS	0	0	0	0
		Bolts	316 SS	1	1	1	1
		Column bases	CF8	1	1	1	2
		Column bases	304 SS	--	1	1	2
		Column bodies	304 SS	0	0	1	2
		Extension tubes	304 SS	1	1	1	2
		Flanges	304 SS	0	0	0	0

Table 7 (continued): MRP-191 Revision – FMECA Group Comparison							
Assembly	Subassembly	MRP-191 Rev. 2 Component	Material	MRP-191 Rev. 0 FMECA Group	MRP-191 Rev. 1 FMECA Group	MRP-191 Rev. 2 Safety FMECA Group (Note 1)	MRP-191 Rev. 2 Economic FMECA Group (Note 1)
Upper internals assembly (cont.)	Upper support column assemblies (cont.)	Lock keys	304 SS	0	0	1	1
		Lock keys	304L SS	0	0	1	1
		Nuts	304 SS	0	0	1	1
		Nuts	302 SS	--	0	1	1
	Upper support plate assembly - Inverted Top Hat Design (Note 5)	ITH flange	304 SS	1	1	1	2
		ITH upper support plate	304 SS	1	1	1	2
		ITH Upper support ring or skirt	304 SS	2	2	1	2
		ITH Upper support ring or skirt	CF8	--	2	1	2
	Upper support plate assembly - Top Hat Design (Note 5)	Flange	304 SS	0	0	1	2
		Flange	CF8	--	1	1	2
		Upper support plate	304 SS	0	0	1	2
		Upper support plate	CF8	--	1	1	2
		Upper support ring or skirt	304 SS	2	2	1	2
		Upper support ring or skirt	CF8	--	2	1	2
		Deep beam ribs (Note 6)	304 SS	1	1	1	1
		Deep beam stiffeners	304 SS	1	1	1	1
		Bolts	316 SS	0	0	1	1
		Locking device	316 SS	0	0	1	1
		Locking device	304 SS	--	0	1	1
		Upper support plate assembly - Flat Plate Design (Note 5)	Upper support plate	304 SS	0	0	1
	Upper support plate		CF8	--	1	1	2
	Upper support ring or skirt		304 SS	2	2	1	2
	Upper support ring or skirt		CF8	--	2	1	2
	Deep beam ribs (Note 6)		304 SS	1	1	1	1
	Deep beam stiffeners		304 SS	1	1	1	1
	Bolts		316 SS	0	0	1	1
	Locking device		316 SS	0	0	1	1

Table 7 (continued): MRP-191 Revision – FMECA Group Comparison							
Assembly	Subassembly	MRP-191 Rev. 2 Component	Material	MRP-191 Rev. 0 FMECA Group	MRP-191 Rev. 1 FMECA Group	MRP-191 Rev. 2 Safety FMECA Group (Note 1)	MRP-191 Rev. 2 Economic FMECA Group (Note 1)
Upper internals assembly (cont.)	Upper support plate assembly - Flat Plate Design (Note 5)(cont.)	Locking device	304 SS	--	0	1	1
Lower internals assembly	Baffle and former assembly	Baffle bolting locking devices	304 SS	1	1	3	3
		Baffle, edge bolts	316 SS	3	3	3	3
		Baffle, edge bolts	347 SS	3	3	3	3
		Bracket bolts	347 SS	--	--	3	3
		Baffle plates	304 SS	1	1	1	1
		Baffle, former bolts	316 SS	2	3	3	3
		Baffle, former bolts	347 SS	2	3	3	3
		Corner bolts	347 SS	--	--	3	3
		Barrel, former bolts	316 SS	2	2	3	3
		Barrel, former bolts	347 SS	2	2	3	3
		Former dowel pins	302 SS	--	--	1	1
		Former dowel pins	304 SS	--	--	1	1
		Former plates	304 SS	1	1	1	1
	BMI column assemblies	BMI column bodies	304 SS	1	1	2	2
		BMI column bolts	316 SS	1	1	2	2
		BMI column collars	304 SS	1	1	2	2
		BMI column cruciforms	304 SS	--	1	2	2
		BMI column cruciforms	CF8	1	1	2	2
		BMI column extension bars	304 SS	1	1	1	1
		BMI column extension tubes	304 SS	1	1	1	1
		BMI column locking devices	304L SS	0	0	1	1
	Core barrel	BMI column nuts	304 SS	1	1	1	1
		Core barrel flange	304 SS	2	2	1	2
	Upflow conversion core barrel plug body	304 SS	--	--	1	1	

Table 7 (continued): MRP-191 Revision – FMECA Group Comparison							
Assembly	Subassembly	MRP-191 Rev. 2 Component	Material	MRP-191 Rev. 0 FMECA Group	MRP-191 Rev. 1 FMECA Group	MRP-191 Rev. 2 Safety FMECA Group (Note 1)	MRP-191 Rev. 2 Economic FMECA Group (Note 1)
Lower internals assembly (cont.)	Core barrel (cont.)	Upflow conversion core barrel plug mandrel	316 SS	--	--	1	1
		Core barrel outlet nozzles	304 SS	2	2	1	2
		Lower core barrel (includes MAW and LAW)	304 SS	3	3	2	3
		Lower core barrel (includes LGW and LFW)	304 SS	3	3	2	3
		Upper core barrel (includes UAW)	304 SS	3	3	2	3
		Upper core barrel (includes UFW and UGW)	304 SS	3	3	2	3
		Safety injection nozzle interface	304 SS	--	--	1	2
	Diffuser plate	Diffuser plate	304 SS	0	0	0	0
	Flux thimbles (tubes)	Flux thimble tube plugs	304 SS	1	1	2	2
		Flux thimble tube plugs	316 SS	--	1	2	2
		Flux thimble tube plugs	308 SS	--	1	2	2
		Flux thimble tube plugs	A600	--	1	2	2
		Flux thimbles (tubes)	316 SS	2	2	3	3
		Flux thimbles (tubes)	A600	--	2	3	3
	Flux thimble anti-vibration sleeve	304 SS	--	--	1	1	
	Head cooling spray nozzles	Head cooling spray nozzles	304 SS	0	0	1	1
	Irradiation specimen guides	Irradiation specimen guides	304 SS	1	1	1	1
		Irradiation specimen guide bolts	316 SS	1	1	1	1
		Irradiation specimen guide lock caps	304L SS	1	1	0	0
		Irradiation specimen access plug (spring) (Note 7)	X-750	--	--	0	0

Table 7 (continued): MRP-191 Revision – FMECA Group Comparison							
Assembly	Subassembly	MRP-191 Rev. 2 Component	Material	MRP-191 Rev. 0 FMECA Group	MRP-191 Rev. 1 FMECA Group	MRP-191 Rev. 2 Safety FMECA Group (Note 1)	MRP-191 Rev. 2 Economic FMECA Group (Note 1)
Lower internals assembly (cont.)	Irradiation specimen guides (cont.)	Irradiation specimen access plug (dowel pin) (Note 7)	316 SS	--	--	0	0
		Irradiation specimen access plug (plug) (Note 7)	304 SS	1	1	0	0
	LCP and fuel alignment pins	Fuel alignment pins	316 SS	1	1	1	1
		Fuel alignment pins	304 SS	--	1	3	3
		XL LCP fuel alignment pins	316 SS	--	--	3	3
		LCP and manway bolts	316 SS	1	1	2	2
		LCP and manway locking devices	304L SS	1	1	1	1
		Lower core plate	304 SS	2	2	1	2
		XL lower core plate	304 SS	2	2	1	2
		Lower support column assemblies	Lower support column bodies	304 SS	1	1	1
	Lower support column bodies		CF8	1	1	1	1
	Lower support column bolts		304 SS	1	1	2	2
	Lower support column bolts		316 SS	--	1	2	2
	Lower support column bolt locking devices		304L SS (Note 9)	--	--	1	1
	Lower support column bolt locking devices		304 SS (Note 9)	--	--	1	1
	Lower support column nuts		304 SS	0	0	1	1
	Lower support column sleeves		304 SS	0	0	0	0
	Lower support casting or forging	Lower support casting	CF8	2	2	1	2
		Lower support forging	304 SS	0	0	1	2
	Neutron panels/thermal shield	Neutron panel bolts	316 SS	1	1	1	1
		Neutron panel locking devices	304 SS	1	1	0	0
		Neutron panel locking devices	304L SS	--	1	0	0
		Thermal shield bolts	316 SS	1	1	3	3
		Thermal shield dowels	316 SS	1	1	1	1

Table 7 (continued): MRP-191 Revision – FMECA Group Comparison							
Assembly	Subassembly	MRP-191 Rev. 2 Component	Material	MRP-191 Rev. 0 FMECA Group	MRP-191 Rev. 1 FMECA Group	MRP-191 Rev. 2 Safety FMECA Group (Note 1)	MRP-191 Rev. 2 Economic FMECA Group (Note 1)
Lower Internals Assembly (cont.)	Neutron panels/thermal shield (cont.)	Thermal shield dowels	304 SS	--	1	1	1
		Thermal shield flexures	304 SS	1	1	2	3
		Thermal shield flexures	316 SS	--	1	2	3
		Thermal shield flexure bolts	316 SS	--	--	1	1
		Thermal shield flexure locking devices and dowel pins	304 SS	--	--	1	1
		Thermal shield flexure locking devices and dowel pins	304L SS	--	--	1	1
		Thermal shield or neutron panels	304 SS	1	1	1	1
	Radial support keys	Radial support key bolts	304 SS	1	1	1	1
		Radial support key bolts	316 SS	--	1	1	1
		Radial support key dowels	304 SS	--	--	1	1
		Radial support key lock keys	304 SS (Note 8)	0	0	1	1
		Radial support keys	304 SS	1	1	1	1
		Radial support keys	Stellite	--	--	3	3
	SCS assembly	SCS base plate	304 SS	1	1	1	1
		SCS bolts	316 SS	0	0	1	1
		SCS energy absorber	304 SS	0	0	0	0
		SCS guide post	304 SS	0	0	0	0
		SCS guide post	CF8	--	1	1	1
		SCS housing	304 SS	0	0	0	0
		SCS housing	CF8	--	1	1	1
		SCS lock keys	304 SS	0	0	1	1
Upper and lower tie plates		304 SS	--	0	1	1	
Interfacing components	Interfacing components	Clevis insert bolts	X-750	1	2	3	3
		Clevis insert dowels	Alloy 600	--	--	2	2

Table 7 (continued): MRP-191 Revision – FMECA Group Comparison							
Assembly	Subassembly	MRP-191 Rev. 2 Component	Material	MRP-191 Rev. 0 FMECA Group	MRP-191 Rev. 1 FMECA Group	MRP-191 Rev. 2 Safety FMECA Group (Note 1)	MRP-191 Rev. 2 Economic FMECA Group (Note 1)
Interfacing components (cont.)	Interfacing components (cont.)	Clevis insert locking devices	Alloy 600	0	0	1	1
		Clevis insert locking devices	316 SS	0	0	1	1
		Clevis inserts	Alloy 600	1	1	1	2
		Clevis inserts	304 SS	1	1	1	2
		Clevis inserts	Stellite	1	1	3	3
		Head and vessel alignment pin bolts	316 SS	0	0	1	1
		Head and vessel alignment pin lock caps	304L SS	0	0	0	0
		Head and vessel alignment pins	304 SS	0	0	1	1
		Head and vessel alignment pins	Stellite	--	--	2	2
		Internals hold-down spring	304 SS	1	1	3	3
		Internals hold-down spring	403 SS	1	1	1	2
		Internals hold-down spring	F6NM	--	--	1	2
		UCP alignment pins	304 SS	1	1	1	1
		UCP alignment pins	Stellite	--	--	2	2
		Thermal sleeves	304 SS	--	--	3	3
		Thermal sleeve guide funnels	304 SS	--	--	3	3
		Thermal sleeve guide funnels	CF8	--	--	3	3
		Instrumentation nozzle funnels	304 SS	--	--	0	0
		Replacement reactor vessel head extension tubes	304 SS	--	--	0	0

Table 7 (continued): MRP-191 Revision – FMECA Group Comparison							
Assembly	Subassembly	MRP-191 Rev. 2 Component	Material	MRP-191 Rev. 0 FMECA Group	MRP-191 Rev. 1 FMECA Group	MRP-191 Rev. 2 Safety FMECA Group (Note 1)	MRP-191 Rev. 2 Economic FMECA Group (Note 1)

Notes:

1. Cells that are gray shaded represent changes in safety or economic FMECA grouping between MRP-191, Revision 2 [1], and previous revisions of MRP-191 (Revisions 0 [2] and 1 [3]). MRP-191, Revision 0 [2] and 1 [3] determined one combined consequence ranking and FMECA group; however, the safety-related consequences and economic consequences were separated for MRP-191, Revision 2 [1].
2. Component name modified to eliminate “upper” from its name to further clarify the actual component in MRP-191, Revision 2 [1].
3. Component name modified to eliminate “support pin” from its name to further clarify the actual component in MRP-191, Revision 2 [1].
4. “Protective skirt” was added to the component name for clarification in MRP-191, Revision 2 [1].
5. The upper support plate assembly was separated out to identify specific components applicable to the three design variations (inverted top hat, top hat, and flat plate).
6. The component “ribs” was listed in MRP-191, Revision 0 [2] and Revision 1 [3]; however, with splitting up the upper support plate assembly into the three design variations, the “deep beam ribs” component captures the previously listed “ribs” in MRP-191, Revision 2 [1].
7. This was originally listed as “specimen plugs” in MRP-191, Revision 1 [3]. However, due to the materials comprising this component, it was divided out into its subcomponents in MRP-191, Revision 2 [1].
8. The radial support key lock keys was listed as 316 SS within Table 6-10 and Table 7-2 of MRP-191, Revision 2 [1] but should be 304 SS.
9. The lower support column bolt locking devices are listed as 304 SS within Table 4-6, Table 5-1, Table 6-10, and Table 7-2 of MRP-191, Revision 2 [1] and also as 304L SS in Table 4-4 of MRP-191, Revision 2 [1]. Both materials are listed in this table.

References for Table 7:

1. Materials Reliability Program: Screening, Categorization, and Ranking of Reactor Internals Components for Westinghouse and Combustion Engineering PWR Design (MRP-191, Revision 2). EPRI, Palo Alto, CA: 2018. 3002013220.
2. Materials Reliability Program: Screening, Categorization, and Ranking of Reactor Internals Components for Westinghouse and Combustion Engineering PWR Design (MRP-191). EPRI, Palo Alto, CA: 2006. 1013234.
3. Materials Reliability Program: Screening, Categorization, and Ranking of Reactor Internals Components for Westinghouse and Combustion Engineering PWR Design (MRP-191, Revision 1). EPRI, Palo Alto, CA: 2016. 3002007960.

Table 8: MRP-191 Revision – Category Comparison

Assembly	Subassembly	MRP-191 Rev. 2 Component	Material	MRP-191 Rev. 0 Category	MRP-191 Rev. 1 Category	MRP-191 Rev. 2 Safety Category (Note 1)	MRP-191 Rev. 2 Economic Category (Note 1)
Upper internals assembly	Control rod guide tube assemblies and flow downcomers	Anti-rotation studs and nuts	304 SS	A	A	A	A
		Anti-rotation studs and nuts	316 SS	--	A	A	A
		Bolts	316 SS	A	A	A	A
		Bolts	304 SS	--	A	A	A
		C-tubes	304 SS	C	C	B	B
		Enclosure pins	304 SS	A	A	A	A
		Guide tube enclosures (Note 2)	304 SS	A	A	A	A
		Guide tube enclosures (Note 2)	CF8	--	A	A	A
		Flanges, intermediate	304 SS	A	A	A	A
		Flanges, intermediate	CF8	A	A	A	A
		Flanges, lower	304 SS	A	A	B	B
		Flanges, lower	CF8	B	B	B	B
		Flexureless inserts	304 SS	A	A	A	A
		Flexureless inserts (spring)	Alloy 718	--	--	A	A
		Flexures	X-750	C	C	C	C
		Guide plates/cards	304 SS	C	C	C	C
		Guide plates/cards	316L SS	--	C	C	C
		Guide plates/cards	CF8	--	C	C	C
		Guide tube support pins	X-750	C	C	C	C
		Guide tube support pins	316 SS	A	A	A	A
		Housing plates	304 SS	A	A	A	A
		Housing plates	CF8	--	A	A	A
		Inserts	304 SS	A	A	A	A
		Inserts	CF8	--	--	A	A
		Lock bars	304 SS	A	A	A	A
		Sheaths	304 SS	C	C	C	C
		Cover plate (Note 3)	304 SS	A	A	A	A
		Cover plate cap screws (Note 3)	316 SS	A	A	A	A

Table 8 (continued): MRP-191 Revision – Category Comparison							
Assembly	Subassembly	MRP-191 Rev. 2 Component	Material	MRP-191 Rev. 0 Category	MRP-191 Rev. 1 Category	MRP-191 Rev. 2 Safety Category (Note 1)	MRP-191 Rev. 2 Economic Category (Note 1)
Upper internals assembly (cont.)	Control rod guide tube assemblies and flow downcomers (cont.)	Cover plate guide tube locking caps and tie straps (Note 3)	304 SS	A	A	A	A
		Support pin nuts	X-750	A	A	A	A
		Support pin nuts	304 SS	--	A	A	A
		Support pin nuts	316 SS	A	A	A	A
		Water flow slot ligaments	304 SS	A	A	A	A
		Probe holder shroud	304 SS	--	--	A	B
	Mixing Devices	Mixing devices	CF8	A	A	A	A
		Mixing devices	304 SS	--	A	A	A
	UCP and fuel alignment pins	Fuel alignment pins	316 SS	A	A	A	A
		Fuel alignment pins	304 SS	--	A	B	B
		UCP	304 SS	A	B	B	C
		Upper core plate insert	304 SS	--	--	B	B
		Upper core plate insert	Stellite (Note 9)	--	--	B	B
		Upper core plate insert bolts	316 SS	--	--	A	A
		Upper core plate insert locking devices & dowel pins	304 SS	--	--	A	A
		Upper core plate insert locking devices & dowel pins	316 SS	--	--	A	A
		Protective skirt	304 SS	--	A	A	A
		Protective skirt bolts (Note 4)	316 SS	--	A	B	B
		Protective skirt lock bars (Note 4)	304 SS	--	A	A	A
		Protective skirt dowel pins (Note 4)	304 SS	--	A	A	A

Table 8 (continued): MRP-191 Revision – Category Comparison							
Assembly	Subassembly	MRP-191 Rev. 2 Component	Material	MRP-191 Rev. 0 Category	MRP-191 Rev. 1 Category	MRP-191 Rev. 2 Safety Category (Note 1)	MRP-191 Rev. 2 Economic Category (Note 1)
Upper internals assembly (cont.)	Upper instrumentation conduit and supports (cont.)	Bolting	316 SS	A	A	A	A
		Bolting	304 SS	--	A	A	A
		Brackets, clamps, terminal blocks, and conduit straps	304 SS	A	A	B	C
		Brackets, clamps, terminal blocks, and conduit straps	302 SS	--	A	B	C
		Brackets, clamps, terminal blocks, and conduit straps	CF8	--	A	A	B
		Conduit seal assembly: body, tubesheets, tubesheet welds	304 SS	A	A	B	B
		Conduit seal assembly: tubes	304 SS	A	A	B	B
		Conduits	304 SS	A	A	A	A
		Flange base	304 SS	A	A	A	A
		Locking caps	304 SS	A	A	A	A
		Locking caps	304L SS	--	A	A	A
		Support tubes	304 SS	A	A	A	A
	Upper plenum	UHI flow column bases	CF8	A	A	A	A
		UHI flow columns	304 SS	A	A	A	A
	Upper support column assemblies	Adapters	304 SS	A	A	A	A
		Bolts	316 SS	A	A	A	A
		Column bases	CF8	A	A	A	B
		Column bases	304 SS	--	A	A	B
		Column bodies	304 SS	A	A	A	B
		Extension tubes	304 SS	A	A	A	B
		Flanges	304 SS	A	A	A	A
	Lock keys	304 SS	A	A	A	A	

Table 8 (continued): MRP-191 Revision – Category Comparison							
Assembly	Subassembly	MRP-191 Rev. 2 Component	Material	MRP-191 Rev. 0 Category	MRP-191 Rev. 1 Category	MRP-191 Rev. 2 Safety Category (Note 1)	MRP-191 Rev. 2 Economic Category (Note 1)
Upper internals assembly (cont.)	Upper support column assemblies (cont.)	Lock keys	304L SS	A	A	A	A
		Nuts	304 SS	A	A	A	A
		Nuts	302 SS	--	A	A	A
	Upper support plate assembly - Inverted Top Hat Design (Note 5)	ITH flange	304 SS	A	A	A	B
		ITH upper support plate	304 SS	A	A	A	B
		ITH Upper support ring or skirt	304 SS	B	B	A	B
		ITH Upper support ring or skirt	CF8	--	B	A	B
	Upper support plate assembly - Top Hat Design (Note 5)	Flange	304 SS	A	A	A	B
		Flange	CF8	--	A	A	B
		Upper support plate	304 SS	A	A	A	B
		Upper support plate	CF8	--	A	A	B
		Upper support ring or skirt	304 SS	B	B	A	B
		Upper support ring or skirt	CF8	--	B	A	B
		Deep beam ribs (Note 6)	304 SS	A	A	A	A
		Deep beam stiffeners	304 SS	A	A	A	A
		Bolts	316 SS	A	A	A	A
		Locking device	316 SS	A	A	A	A
	Upper support plate assembly - Flat Plate Design (Note 5)	Locking device	304 SS	--	A	A	A
		Upper support plate	304 SS	A	A	A	B
		Upper support plate	CF8	--	A	A	B
		Upper support ring or skirt	304 SS	B	B	A	B
		Upper support ring or skirt	CF8	--	B	A	B
		Deep beam ribs (Note 6)	304 SS	A	A	A	A
		Deep beam stiffeners	304 SS	A	A	A	A
		Bolts	316 SS	A	A	A	A
		Locking device	316 SS	A	A	A	A
	Locking device	304 SS	--	A	A	A	

Table 8 (continued): MRP-191 Revision – Category Comparison							
Assembly	Subassembly	MRP-191 Rev. 2 Component	Material	MRP-191 Rev. 0 Category	MRP-191 Rev. 1 Category	MRP-191 Rev. 2 Safety Category (Note 1)	MRP-191 Rev. 2 Economic Category (Note 1)
Lower internals assembly	Baffle and former assembly	Baffle bolting locking devices	304 SS	A	A	B	B
		Baffle, edge bolts	316 SS	C	C	B	C
		Baffle, edge bolts	347 SS	C	C	B	C
		Bracket bolts	347 SS	--	--	B	C
		Baffle plates	304 SS	B	B	A	A
		Baffle, former bolts	316 SS	C	C	C	C
		Baffle, former bolts	347 SS	C	C	C	C
		Corner bolts	347 SS	--	--	C	C
		Barrel, former bolts	316 SS	C	C	B	C
		Barrel, former bolts	347 SS	C	C	B	C
		Former dowel pins	302 SS	--	--	A	A
		Former dowel pins	304 SS	--	--	A	A
		Former plates	304 SS	B	B	A	A
		BMI column assemblies	BMI column bodies	304 SS	B	B	B
	BMI column bolts		316 SS	A	A	B	B
	BMI column collars		304 SS	B	B	B	B
	BMI column cruciforms		304 SS	--	B	B	B
	BMI column cruciforms		CF8	B	B	B	B
	BMI column extension bars		304 SS	A	A	A	A
	BMI column extension tubes		304 SS	B	B	A	A
	BMI column locking devices		304L SS	A	A	A	A
	BMI column nuts		304 SS	A	A	A	A
	Core barrel	Core barrel flange	304 SS	B	B	B	B
		Upflow conversion core barrel plug body	304 SS	--	--	A	A
		Upflow conversion core barrel plug mandrel	316 SS	--	--	A	A
		Core barrel outlet nozzles	304 SS	B	B	B	B

Table 8 (continued): MRP-191 Revision – Category Comparison							
Assembly	Subassembly	MRP-191 Rev. 2 Component	Material	MRP-191 Rev. 0 Category	MRP-191 Rev. 1 Category	MRP-191 Rev. 2 Safety Category (Note 1)	MRP-191 Rev. 2 Economic Category (Note 1)
Lower internals assembly (cont.)	Core barrel (cont.)	Lower core barrel (includes MAW and LAW)	304 SS	C	C	B	C
		Lower core barrel (includes LGW and LFW)	304 SS	C	C	B	C
		Upper core barrel (includes UAW)	304 SS	C	C	B	C
		Upper core barrel (includes UFW and UGW)	304 SS	C	C	B	C
		Safety injection nozzle interface	304 SS	--	--	B	B
	Diffuser plate	Diffuser plate	304 SS	A	A	A	A
	Flux thimbles (tubes)	Flux thimble tube plugs	304 SS	B	B	B	B
		Flux thimble tube plugs	316 SS	--	B	B	B
		Flux thimble tube plugs	308 SS	--	B	B	B
		Flux thimble tube plugs	A600	--	B	B	B
		Flux thimbles (tubes)	316 SS	C	C	B	B
		Flux thimbles (tubes)	A600	--	C	B	B
		Flux thimble anti-vibration sleeve	304 SS	--	--	A	A
	Head cooling spray nozzles	Head cooling spray nozzles	304 SS	A	A	A	A
	Irradiation specimen guides	Irradiation specimen guides	304 SS	A	A	A	A
		Irradiation specimen guide bolts	316 SS	A	A	A	A
		Irradiation specimen guide lock caps	304L SS	A	A	A	A
		Irradiation specimen access plug (spring) (Note 7)	X-750	--	--	A	A
		Irradiation specimen access plug (dowel pin) (Note 7)	316 SS	--	--	A	A
		Irradiation specimen access plug (plug) (Note 7)	304 SS	A	A	A	A

Table 8 (continued): MRP-191 Revision – Category Comparison							
Assembly	Subassembly	MRP-191 Rev. 2 Component	Material	MRP-191 Rev. 0 Category	MRP-191 Rev. 1 Category	MRP-191 Rev. 2 Safety Category (Note 1)	MRP-191 Rev. 2 Economic Category (Note 1)
Lower internals assembly (cont.)	LCP and fuel alignment pins	Fuel alignment pins	316 SS	A	A	A	A
		Fuel alignment pins	304 SS	--	A	B	B
		XL LCP fuel alignment pins	316 SS	--	--	B	B
		LCP and manway bolts	316 SS	A	A	B	B
		LCP and manway locking devices	304L SS	A	A	A	A
		Lower core plate	304 SS	C	B	A	B
		XL lower core plate	304 SS	C	B	A	B
	Lower support column assemblies	Lower support column bodies	304 SS	B	B	A	A
		Lower support column bodies	CF8	B	B	A	A
		Lower support column bolts	304 SS	B	B	B	B
		Lower support column bolts	316 SS	--	B	B	B
		Lower support column bolt locking devices	304L SS (Note 10)	--	--	A	A
		Lower support column bolt locking devices	304 SS (Note 10)	--	--	A	A
		Lower support column nuts	304 SS	A	A	A	A
		Lower support column sleeves	304 SS	A	A	A	A
	Lower support casting or forging	Lower support casting	CF8	A	A	A	B
		Lower support forging	304 SS	A	A	A	B
	Neutron panels/thermal shield	Neutron panel bolts	316 SS	A	A	A	A
		Neutron panel locking devices	304 SS	A	A	A	A
		Neutron panel locking devices	304L SS	--	A	A	A
		Thermal shield bolts	316 SS	A	A	B	B
		Thermal shield dowels	316 SS	A	A	A	A
		Thermal shield dowels	304 SS	--	A	A	A
		Thermal shield flexures	304 SS	B	B	B	C
		Thermal shield flexures	316 SS	--	B	B	C

Table 8 (continued): MRP-191 Revision – Category Comparison							
Assembly	Subassembly	MRP-191 Rev. 2 Component	Material	MRP-191 Rev. 0 Category	MRP-191 Rev. 1 Category	MRP-191 Rev. 2 Safety Category (Note 1)	MRP-191 Rev. 2 Economic Category (Note 1)
Lower internals assembly (cont.)	Neutron panels/thermal shield (cont.)	Thermal shield flexure bolts	316 SS	--	--	A	A
		Thermal shield flexure locking devices and dowel pins	304 SS	--	--	A	A
		Thermal shield flexure locking devices and dowel pins	304L SS	--	--	A	A
		Thermal shield or neutron panels	304 SS	A	A	A	A
	Radial support keys	Radial support key bolts	304 SS	A	A	A	A
		Radial support key bolts	316 SS	--	A	A	A
		Radial support key dowels	304 SS	--	--	A	A
		Radial support key lock keys	304 SS (Note 8)	A	A	A	A
		Radial support keys	304 SS	A	A	A	A
		Radial support keys	Stellite	--	--	C	C
	SCS assembly	SCS base plate	304 SS	A	A	A	A
		SCS bolts	316 SS	A	A	A	A
		SCS energy absorber	304 SS	A	A	A	A
		SCS guide post	304 SS	A	A	A	A
		SCS guide post	CF8	--	A	A	A
		SCS housing	304 SS	A	A	A	A
		SCS housing	CF8	--	A	A	A
		SCS lock keys	304 SS	A	A	A	A
		Upper and lower tie plates	304 SS	--	A	A	A
	Interfacing components	Interfacing components	Clevis insert bolts	X-750	B	B	B
Clevis insert dowels			Alloy 600	--	--	B	B
Clevis insert locking devices			Alloy 600	A	A	A	A
Clevis insert locking devices			316 SS	A	A	A	A
Clevis inserts			Alloy 600	A	A	A	B

Table 8 (continued): MRP-191 Revision – Category Comparison							
Assembly	Subassembly	MRP-191 Rev. 2 Component	Material	MRP-191 Rev. 0 Category	MRP-191 Rev. 1 Category	MRP-191 Rev. 2 Safety Category (Note 1)	MRP-191 Rev. 2 Economic Category (Note 1)
Interfacing components (cont.)	Interfacing components (cont.)	Clevis inserts	304 SS	A	A	A	B
		Clevis inserts	Stellite	A	A	C	C
		Head and vessel alignment pin bolts	316 SS	A	A	A	A
		Head and vessel alignment pin lock caps	304L SS	A	A	A	A
		Head and vessel alignment pins	304 SS	A	A	A	A
		Head and vessel alignment pins	Stellite	--	--	A	A
		Internals hold-down spring	304 SS	B	B	B	C
		Internals hold-down spring	403 SS	A	A	A	A
		Internals hold-down spring	F6NM	--	--	A	A
		UCP alignment pins	304 SS	B	B	A	A
		UCP alignment pins	Stellite	--	--	A	B
		Thermal sleeves	304 SS	--	--	C	C
		Thermal sleeve guide funnels	304 SS	--	--	B	B
		Thermal sleeve guide funnels	CF8	--	--	B	B
		Instrumentation nozzle funnels	304 SS	--	--	A	A
Replacement reactor vessel head extension tubes	304 SS	--	--	A	A		

Table 8 (continued): MRP-191 Revision – Category Comparison							
Assembly	Subassembly	MRP-191 Rev. 2 Component	Material	MRP-191 Rev. 0 Category	MRP-191 Rev. 1 Category	MRP-191 Rev. 2 Safety Category (Note 1)	MRP-191 Rev. 2 Economic Category (Note 1)

Notes:

1. Cells that are gray shaded represent changes in safety or economic category between MRP-191, Revision 2 [1], and previous revisions of MRP-191 (Revisions 0 [2] and 1 [3]). MRP-191, Revision 0 [2] and 1 [3] determined one combined consequence ranking and FMECA group; however, the safety-related consequences and economic consequences were separated for MRP-191, Revision 2 [1]. Therefore, MRP-191 Revision 2 [1] includes a Safety Category and Economic Category.
2. Component name modified to eliminate “upper” from its name to further clarify the actual component in MRP-191, Revision 2 [1].
3. Component name modified to eliminate “support pin” from its name to further clarify the actual component in MRP-191, Revision 2 [1].
4. “Protective skirt” was added to the component name for clarification in MRP-191, Revision 2 [1].
5. The upper support plate assembly was separated out to identify specific components applicable to the three design variations (inverted top hat, top hat, and flat plate).
6. The component “ribs” was listed in MRP-191, Revision 0 [2] and Revision 1 [3]; however, with splitting up the upper support plate assembly into the three design variations, the “deep beam ribs” component captures the previously listed “ribs” in MRP-191, Revision 2 [1].
7. This was originally listed as “specimen plugs” in MRP-191, Revision 1 [3]. However, due to the materials comprising this component, it was divided out into its subcomponents in MRP-191, Revision 2 [1].
8. The radial support key lock keys was listed as 316 SS within Table 6-10 and Table 7-2 of MRP-191, Revision 2 [1] but should be 304 SS.
9. MRP-191, Revision 2 [1] does not list Stellite in Table 7-2. The Safety and Economic ratings are assumed to match the 304 SS insert.
10. The lower support column bolt locking devices are listed as 304 SS within Table 4-6, Table 5-1, Table 6-10, and Table 7-2 of MRP-191, Revision 2 [1] and also as 304L SS in Table 4-4 of MRP-191, Revision 2 [1]. Both materials are listed in this table.

References for Table 8:

1. Materials Reliability Program: Screening, Categorization, and Ranking of Reactor Internals Components for Westinghouse and Combustion Engineering PWR Design (MRP-191, Revision 2). EPRI, Palo Alto, CA: 2018. 3002013220.
2. Materials Reliability Program: Screening, Categorization, and Ranking of Reactor Internals Components for Westinghouse and Combustion Engineering PWR Design (MRP-191). EPRI, Palo Alto, CA: 2006. 1013234.
3. Materials Reliability Program: Screening, Categorization, and Ranking of Reactor Internals Components for Westinghouse and Combustion Engineering PWR Design (MRP-191, Revision 1). EPRI, Palo Alto, CA: 2016. 3002007960.

This page was added to the quality record by the PRIME system upon its validation and shall not be considered in the page numbering of this document.

Approval Information

Author Approval Harbison Lance S Jun-12-2020 08:54:30

Verifier Approval Zindren Taylor Jun-12-2020 08:59:57

Manager Approval Musser Kaitlyn M Jun-12-2020 09:13:54

Files approved on Jun-12-2020

*** This record was final approved on 6/12/2020 9:13:54 AM. (This statement was added by the PRIME system upon its validation)

Point Beach Nuclear Plant Units 1 and 2
Dockets 50-266 and 50-301
NRC 2020-0032 Enclosure 4, Attachment 21

Enclosure 4
Non-proprietary Reference Documents and
Redacted Versions of Proprietary Reference
Documents
(Public Version)
Attachment 21

**Westinghouse LTR-REA-20-29-NP, Revision 0,
“Comparison of Point Beach Unit 1 Reactor Internals
Fluence Values to the Representative 3-Loop Plant
for MRP-191, Revision 2”, July 7, 2020**

(16 Total Pages, including cover sheets)



To: John T. Ahearn
cc: Gregory M. Imbrogno

Date: July 7, 2020

From: Nuclear Operations and Radiation Analysis (NORA)
Phone: (412) 374-5851
Email: hawkae@westinghouse.com
Our Ref: **LTR-REA-20-29-NP, Revision 0**

Subject: **Comparison of Point Beach Unit 1 Reactor Internals Fluence Values to the Representative 3-Loop Plant for MRP-191, Revision 2**

Reference(s): 1. Electric Power Research Institute (EPRI) Technical Report, "Materials Reliability Program: Screening, Categorization, and Ranking of Reactor Internals Components for Westinghouse and Combustion Engineering PWR Design (MRP-191, Revision 2)," EPRI, Palo Alto, CA: 2018. 3002013220.

Attachment(s): 1. Comparison of Point Beach Unit 1 Reactor Internals Fluence Values to the Representative 3-Loop Plant for MRP-191, Revision 2

Attachment 1 provides a comparison of Point Beach Unit 1 reactor internals fluence values to the representative 3-loop plant for MRP-191, Revision 2 (Reference 1). This comparison concludes that the reactor internals fluence values determined for the representative Westinghouse 3-loop pressurized water reactor (PWR) of Reference 1 are applicable to Point Beach Units 1 and 2. As such, the estimated reactor internals fluence ranges documented in Reference 1 as being applicable to Westinghouse-designed plants are also applicable to Point Beach Units 1 and 2. The information in Attachment 1 is intended to be provided to NextEra Energy Point Beach, LLC in support of the Point Beach subsequent license renewal (SLR) project.

Please contact the undersigned if there are any questions regarding this information.

Author: *(Electronically Approved)**
Andrew E. Hawk
NORA

Reviewer: *(Electronically Approved)**
Riley I. Benson
NORA

Approver: *(Electronically Approved)**
Laurent P. Houssay
NORA

**Electronically approved records are authenticated in the electronic document management system.*

Attachment 1

Comparison of Point Beach Unit 1 Reactor Internals Fluence Values to the Representative 3-Loop Plant for MRP-191, Revision 2

1.0 Introduction and Background

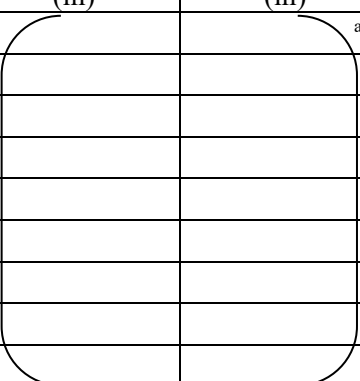
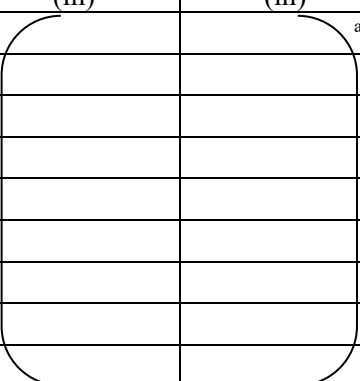
NextEra Energy Point Beach, LLC intends to pursue a subsequent license renewal (SLR) for Point Beach Units 1 and 2 to extend their current operating license to a plant lifetime of 80 years (72 effective full-power years (EFPY)). Reactor internals fluence projections were determined for a representative Westinghouse 3-loop pressurized water reactor (PWR) and incorporated into MRP-191, Revision 2 (Reference 1) as part of a materials reliability program (MRP) project developed to manage irradiation-assisted and irradiation-induced material degradation. Reactor internals fluence projections for Westinghouse 2-loop PWRs were not, however, specifically calculated as part of developing Reference 1. Therefore, this attachment compares select reactor internals fluence projections determined for the representative Westinghouse 3-loop PWR of Reference 1 to the corresponding projections determined for Point Beach Unit 1. The purpose of this comparison is to demonstrate that the reactor internals fluence projections that were determined for the representative 3-loop PWR and used when establishing the estimated fluence ranges reported in Table 4-6 of Reference 1 are applicable to Point Beach Units 1 and 2.

2.0 Evaluation

2.1 Reactor Geometry Comparison

Table 2-1 provides a comparison of several dimensions used in the model of the representative 3-loop PWR with the corresponding dimensions from the model of the Point Beach Unit 1 and Unit 2 reactor geometries. The information provided in Table 2-1 was used to establish the locations of, and points along, the reactor internals components included in the comparison of the fluence projections for the representative 3-loop PWR and Point Beach Unit 1.

Table 2-1
Reactor Geometry Comparison

Description	Representative 3-Loop Plant (in)	Point Beach Units 1 & 2 (in)
Core Centerline to Baffle Inner Surface at 0° Azimuth		 ^{a,c}
Core Barrel Inner Radius (IR)		
Core Barrel Outer Radius (OR)		
Thermal Shield IR		
Thermal Shield OR		
Reactor Pressure Vessel (RPV) IR		
Top of Lower Core Plate (LCP) to Bottom of Fuel		
Core Height		
Top of LCP to Bottom of Upper Core Plate (UCP)		

2.2 Reactor Internals Fluence Comparison

Reactor internals fast neutron ($E > 1.0$ MeV) fluence projections at 72 EFPY of operation were determined for the representative 3-loop PWR using the three-dimensional fluence rate synthesis methodology described in WCAP-14040-A (Reference 2). The WCAP-14040-A methodology adheres to the guidance of Regulatory Guide 1.190 (Reference 3). The projections for the representative 3-loop PWR were then compared with the plant-specific ones that were determined for Point Beach Unit 1 using the three-dimensional discrete ordinates methodology described in WCAP-18124-A (Reference 4).

Since the purpose of the comparison was to determine if the reactor internals fluence projections for the representative 3-loop PWR are appropriately representative for Point Beach, the majority of the points used in the comparison were limited to locations and components surrounding the fuel region. For example, various points along the core barrel, baffle, UCP, and LCP were included in the comparison. A series of points extending from the core barrel outer radius to the reactor vessel inner radius were also included. In addition, and consistent with the representative 3-loop plant projections determined for Reference 1, the 0° azimuthal angle was used in the comparison. Note that the maximum reactor pressure vessel neutron exposures for Point Beach Units 1 and 2 occur at the 0° azimuthal angle.

The results of the reactor internals fast neutron fluence comparison are provided in Table 2-2 through Table 2-6. As indicated by the fluence ratios shown in these tables, the fast neutron fluence values at 72 EFPY determined for the representative 3-loop PWR are, with one exception, significantly greater than the values determined for Point Beach Unit 1. However, as shown in Table 2-6, the fast neutron fluence projection determined at the core midplane elevation of the Point Beach Unit 1 thermal shield inner surface is slightly greater than the one determined for the representative 3-loop PWR. This is because the downcomer water gap between the core barrel outer surface and thermal shield inner surface is approximately []^{a,c} thinner for Point Beach than it is for the representative 3-loop PWR. Even so, the fast neutron fluence projection determined at the core midplane elevation of the Point Beach Unit 1 thermal shield inner surface is easily within the thermal shield estimated fluence range of $1E+21$ n/cm² to $1E+22$ n/cm² reported in Table 4-6 of Reference 1. Therefore, this estimated fluence range is applicable to Point Beach Unit 1.

Since the fast neutron fluence projection determined at the core midplane elevation of the Point Beach Unit 1 thermal shield inner surface is slightly greater than the one determined for the representative 3-loop PWR, fluence projections at several additional elevations along the thermal shield inner surface were also compared. The results of this comparison are provided in Table 2-7. As indicated by the fluence ratios shown in Table 2-7, for elevations at/above the top or at/below the bottom of the active core, the fast neutron fluence projections determined for the inner surface of the representative 3-loop PWR thermal shield are significantly greater than the ones determined for Point Beach Unit 1 (note that, for these elevations, the representative 3-loop PWR fast neutron fluence projections were determined using a flat axial power distribution with a 1.3 multiplier (see Section 4.3.2 of Reference 1)). Therefore, the estimated fluence ranges reported in Table 4-6 of Reference 1 for the thermal shield components located near/above the top or near/below the bottom of the active core (e.g., thermal shield bolts, dowels, flexures, etc.) are applicable to Point Beach Unit 1.

Table 2-2
Fast Neutron ($E > 1.0$ MeV) Fluence at 72 EFPY – Core Baffle Plate Inner Surface at 0° Azimuth

Component	Axial Elevation (cm)	Fast Neutron Fluence (n/cm^2)		Fluence Ratio	
		Representative PWR	Point Beach Unit 1 ^[1]		
Baffle					
		a,c	2.52E+22	9.93E+21	2.54
			5.11E+22	2.45E+22	2.09
			5.81E+22	3.41E+22	1.70
			6.43E+22	3.93E+22	1.63
			6.71E+22	4.21E+22	1.59
			6.87E+22	4.38E+22	1.57
			7.60E+22	4.39E+22	1.73
			7.02E+22	4.41E+22	1.59
			6.93E+22	4.42E+22	1.57
			6.96E+22	4.44E+22	1.57
			8.76E+22	4.50E+22	1.95
			7.01E+22	4.50E+22	1.56
			6.92E+22	4.55E+22	1.52
			7.04E+22	4.61E+22	1.53
			7.20E+22	4.70E+22	1.53
			6.90E+22	4.70E+22	1.47
			7.02E+22	4.66E+22	1.51
			7.51E+22	4.64E+22	1.62
			6.82E+22	4.65E+22	1.47
		6.81E+22	4.58E+22	1.49	
		7.15E+22	4.37E+22	1.64	
		6.18E+22	4.04E+22	1.53	
		5.77E+22	3.50E+22	1.65	
		5.27E+22	2.44E+22	2.16	
		2.62E+22	1.02E+22	2.58	
		1.25E+22	2.05E+21	6.11	
Note(s): 1. The projection cycle design used to determine these values is based on the average core power distributions and reactor operating conditions of Unit 1 Cycle 37, but includes a 10% bias on the peripheral and re-entrant corner assembly relative powers.					

Table 2-3
Fast Neutron (E > 1.0 MeV) Fluence at 72 EFPY – Core Barrel Inner Surface at 0° Azimuth

Component	Axial Elevation (cm)	Fast Neutron Fluence (n/cm ²)		Fluence Ratio
		Representative PWR	Point Beach Unit 1 ^[1]	
Barrel		3.48E+20	6.62E+19	5.26
		1.53E+21	3.82E+20	4.01
		4.46E+21	1.91E+21	2.34
		8.34E+21	4.08E+21	2.05
		1.10E+22	5.67E+21	1.94
		1.23E+22	6.65E+21	1.85
		1.29E+22	7.20E+21	1.79
		1.32E+22	7.58E+21	1.74
		1.31E+22	7.54E+21	1.74
		1.33E+22	7.58E+21	1.76
		1.34E+22	7.60E+21	1.76
		1.33E+22	7.67E+21	1.74
		1.34E+22	7.83E+21	1.71
		1.33E+22	7.75E+21	1.72
		1.34E+22	7.82E+21	1.71
		1.32E+22	7.92E+21	1.67
		1.31E+22	8.09E+21	1.62
		1.33E+22	8.09E+21	1.64
		1.31E+22	8.00E+21	1.64
		1.30E+22	7.97E+21	1.63
		1.31E+22	8.01E+21	1.64
		1.29E+22	7.84E+21	1.64
		1.23E+22	7.44E+21	1.65
		1.17E+22	6.83E+21	1.71
		1.03E+22	6.02E+21	1.71
		8.97E+21	4.05E+21	2.21
	5.19E+21	1.92E+21	2.71	
	2.29E+21	6.69E+20	3.43	
	6.43E+20	1.36E+20	4.73	

Note(s):

- The projection cycle design used to determine these values is based on the average core power distributions and reactor operating conditions of Unit 1 Cycle 37, but includes a 10% bias on the peripheral and re-entrant corner assembly relative powers.

Table 2-4
Fast Neutron (E > 1.0 MeV) Fluence at 72 EFPY – UCP Bottom Surface at 0° Azimuth

Component	Representative PWR		Point Beach Unit 1		Fluence Ratio
	Radius (cm)	Fast Neutron Fluence (n/cm ²)	Radius ^[1] (cm)	Fast Neutron Fluence ^[2] (n/cm ²)	
UCP		^{a,c} 1.60E+21		^{a,c} 1.04E+21	1.53
		1.59E+21		1.02E+21	1.56
		1.63E+21		1.00E+21	1.62
		1.63E+21		9.85E+20	1.65
		1.60E+21		9.61E+20	1.67
		1.57E+21		9.19E+20	1.71
		1.46E+21		8.41E+20	1.74
		1.31E+21		7.15E+20	1.83
		1.23E+21		5.24E+20	2.35
		1.35E+21		3.43E+20	3.93

Note(s):

1. Radial dimensions are scaled down based on the ratio of the core barrel IRs for Point Beach and the representative 3-loop PWR.
2. The projection cycle design used to determine these values is based on the average core power distributions and reactor operating conditions of Unit 1 Cycle 37, but includes a 10% bias on the peripheral and re-entrant corner assembly relative powers.

Table 2-5
Fast Neutron (E > 1.0 MeV) Fluence at 72 EFPY – LCP Top Surface at 0° Azimuth

Component	Representative PWR		Point Beach Unit 1		Fluence Ratio
	Radius (cm)	Fast Neutron Fluence (n/cm ²)	Radius ^[1] (cm)	Fast Neutron Fluence ^[2] (n/cm ²)	
LCP	[] ^{a,c}	2.73E+22	[] ^{a,c}	9.01E+21	3.03
	[]	2.77E+22	[]	8.96E+21	3.09
	[]	2.85E+22	[]	8.96E+21	3.18
	[]	2.85E+22	[]	8.98E+21	3.17
	[]	2.80E+22	[]	8.94E+21	3.13
	[]	2.79E+22	[]	8.85E+21	3.15
	[]	2.72E+22	[]	8.51E+21	3.19
	[]	2.48E+22	[]	7.58E+21	3.27
	[]	2.14E+22	[]	5.29E+21	4.05
	[]	1.49E+22	[]	2.79E+21	5.35

Note(s):

1. Radial dimensions are scaled down based on the ratio of the core barrel IRs for Point Beach and the representative 3-loop PWR.
2. The projection cycle design used to determine these values is based on the average core power distributions and reactor operating conditions of Unit 1 Cycle 37, but includes a 10% bias on the peripheral and re-entrant corner assembly relative powers.




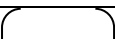
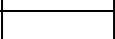
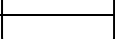
Table 2-6
Fast Neutron (E > 1.0 MeV) Fluence at 72 EFPY – Reactor Components at 0° Azimuth

Component	Axial Elevation (cm)	Fast Neutron Fluence (n/cm ²)		Fluence Ratio
		Representative PWR	Point Beach Unit 1 ^[1]	
Core Barrel OR	0	5.77E+21	3.75E+21	1.54
Thermal Shield IR		2.15E+21	2.28E+21	0.94 ^[2]
Thermal Shield OR		6.37E+20	5.22E+20	1.22 ^[3]
RPV IR		1.42E+20	7.62E+19	1.86

Note(s):

1. The projection cycle design used to determine these values is based on the average core power distributions and reactor operating conditions of Unit 1 Cycle 37, but includes a 10% bias on the peripheral and re-entrant corner assembly relative powers.
2. The water gap between the core barrel OR and thermal shield IR is approximately []^{a,c} thinner for Point Beach than it is for the representative 3-loop PWR.
3. The thermal shield for Point Beach is approximately []^{a,c} thicker than the thermal shield for the representative 3-loop PWR.

Table 2-7
Fast Neutron (E > 1.0 MeV) Fluence at 72 EFPY – Thermal Shield Inner Surface at 0° Azimuth

Component	Axial Elevation (cm)	Fast Neutron Fluence (n/cm ²)		Fluence Ratio
		Representative PWR	Point Beach Unit 1 ^[1]	
Thermal Shield	 a,c	7.61E+19	2.76E+19	2.75
		2.80E+20	1.46E+20	1.92
		6.45E+20	5.42E+20	1.19
	0	2.15E+21	2.28E+21	0.94
	 a,c	8.39E+20	5.87E+20	1.43
		3.63E+20	2.09E+20	1.74
		1.25E+20	4.88E+19	2.56
Note(s): 1. The projection cycle design used to determine these values is based on the average core power distributions and reactor operating conditions of Unit 1 Cycle 37, but includes a 10% bias on the peripheral and re-entrant corner assembly relative powers.				

2.3 MRP-191 Applicability Criteria

The Point Beach Unit 1 and Unit 2 projection cycle designs were evaluated against the applicability criteria for core operation provided in Section 4.3.2 of Reference 1. These cycle designs were chosen for this evaluation since they contribute more to the plant-specific fluence projections at 72 EFPY than any other cycle design. For example, because it is used for the time period beginning at the end of Cycle 39 and ending at 72 EFPY, the projection cycle design for Point Beach Unit 1 contributes more than 30 EFPY to the plant-specific values used for the reactor internals fluence comparison performed in Section 2.2. The specific criteria provided in Section 4.3.2 of Reference 1 for key reactor internals components of Westinghouse-designed reactors are as follows:

- Heat generation rate (HGR) figure of merit (FOM) $\leq 68 \text{ W/cm}^3$
- Average core power density $< 124 \text{ W/cm}^3$
- Active fuel to fuel alignment plate distance > 12.2 inches

2.3.1 Heat Generation Rate FOM

Table 2-8 provides a comparison of the HGR-FOMs determined for the Point Beach Unit 1 and Unit 2 projection cycle designs with the corresponding HGR-FOMs determined for the representative 3-loop PWR projection cycle design. Note that MRP 2013-025 (Reference 5), which is cited in Section 4.3.2 of Reference 1, describes the corner type (i.e., Type 1 or Type 2) and associated assembly weighting factors listed in Table 2-8.

Table 2-8 shows that the Point Beach Unit 1 projection cycle design meets the HGR-FOM applicability criterion of Reference 1. Note that this cycle design is based on the average core power distributions and reactor operating conditions of Unit 1 Cycle 37, but includes a 10% bias on the peripheral and re-entrant corner assembly relative powers. Since this cycle design meets the HGR-FOM applicability criterion of Reference 1, future reload cycle designs at Point Beach Unit 1 would also be expected to meet this criterion providing they are similar—especially with respect to core power and peripheral and re-entrant corner assembly cycle-average relative powers—to Unit 1 Cycle 37.

Table 2-8 also shows that the Point Beach Unit 2 projection cycle design meets the HGR-FOM applicability criterion of Reference 1. Note that this cycle design is based on the average core power distributions and reactor operating conditions of Unit 2 Cycle 38, but includes a 10% bias on the peripheral and re-entrant corner assembly relative powers. Since this cycle design meets the HGR-FOM applicability criterion of Reference 1, future reload cycle designs at Point Beach Unit 2 would also be expected to meet this criterion providing they are similar—especially with respect to core power and peripheral and re-entrant corner assembly cycle-average relative powers—to Unit 2 Cycle 38.

Finally, Table 2-8 shows that the HGR-FOMs determined for the Point Beach Unit 1 and Unit 2 projection cycle designs are not bounded by the ones determined for the representative 3-loop PWR projection cycle design. This is acceptable, however, since the HGR-FOMs determined for the Point Beach Unit 1 and Unit 2 projection cycle designs are less than the HGR-FOM applicability criterion of Reference 1. In addition, the fluence comparison performed in Section 2.2 shows that the reactor internals fast neutron fluence values determined for Point Beach Unit 1 are bounded by (or in the case of the thermal shield, easily within the applicable fluence ranges reported in Table 4-6 of Reference 1) the fluence values determined for the representative 3-loop PWR.

**Table 2-8
 Projection Cycle HGR-FOM**

Corner C1-A								
HGR Weight (Wi)		0.36	0.19	0.35	0.05	ΣWi·Ri	PD·ΣWi·Ri (W/cm ³)	Above Criterion
Projection Cycle	PD (W/cm ³)	Relative Core Power (Ri)						
		F1	F2	E2	D2			
Unit 1	[]						a,c	No
Unit 2	[]							No
Rep. PWR	[]							No
Corner C1-B								
HGR Weight (Wi)		0.36	0.19	0.35	0.05	ΣWi·Ri	PD·ΣWi·Ri (W/cm ³)	Above Criterion
Projection Cycle	PD (W/cm ³)	Relative Core Power (Ri)						
		A6	B6	B5	B4			
Unit 1	[]						a,c	No
Unit 2	[]							No
Rep. PWR	[]							No
Corner C2-A								
HGR Weight (Wi)		0.37	0.21	0.37		ΣWi·Ri	PD·ΣWi·Ri (W/cm ³)	Above Criterion
Projection Cycle	PD (W/cm ³)	Relative Core Power (Ri)						
		D2	D3	C3				
Unit 1	[]						a,c	No
Unit 2	[]							No
Rep. PWR	[]							No
Corner C2-B								
HGR Weight (Wi)		0.37	0.21	0.37		ΣWi·Ri	PD·ΣWi·Ri (W/cm ³)	Above Criterion
Projection Cycle	PD (W/cm ³)	Relative Core Power (Ri)						
		C3	C4	B4				
Unit 1	[]						a,c	No
Unit 2	[]							No
Rep. PWR	[]							No

2.3.2 Average Core Power Density

The average core power density for the Point Beach Unit 1 and Unit 2 projection cycle designs is []^{a,c}. This is less than the average core power density applicability criterion of Reference 1.

2.3.3 Active Fuel to Fuel Alignment Plate Distance

The active fuel to fuel alignment plate distance for the Point Beach Unit 1 and Unit 2 projection cycle designs is []^{a,c}. In addition, the active fuel to fuel alignment plate distance for the last 5 cycles at Point Beach Units 1 and 2 is also []^{a,c}. This is greater than the active fuel to fuel alignment plate distance applicability criterion of Reference 1.

3.0 Conclusion

The reactor internals fast neutron ($E > 1.0$ MeV) fluence projections determined for the representative 3-loop PWR were used when establishing the reactor internals estimated fluence ranges reported in Table 4-6 of Reference 1. The comparison performed in Section 2.2 shows that the fast neutron fluence projections at 72 EFPY determined for the representative 3-loop PWR are, with one exception, significantly greater than the ones determined for Point Beach Unit 1.

However, the fast neutron fluence projection determined at the core midplane elevation of the Point Beach Unit 1 thermal shield inner surface is slightly greater than the one determined for the representative 3-loop PWR. This is because the downcomer water gap between the core barrel outer surface and thermal shield inner surface is approximately []^{a,c} thinner for Point Beach than it is for the representative 3-loop PWR. Even so, the fast neutron fluence projection determined at the core midplane elevation of the Point Beach Unit 1 thermal shield inner surface is easily within the thermal shield estimated fluence range of $1E+21$ n/cm² to $1E+22$ n/cm² reported in Table 4-6 of Reference 1. In addition, fast neutron fluence projections decrease as the radial distance from the core increases. Therefore, the thermal shield estimated fluence range reported in Table 4-6 of Reference 1 is applicable to Point Beach.

Since the fast neutron fluence projection determined at the core midplane elevation of the Point Beach Unit 1 thermal shield inner surface is slightly greater than the one determined for the representative 3-loop PWR, fluence values at several additional elevations along the thermal shield inner surface were also compared. The results of this comparison show that for elevations at/above the top or at/below the bottom of the active core, the fast neutron fluence projections determined for the inner surface of the representative 3-loop PWR thermal shield are significantly greater than the ones determined for Point Beach Unit 1. Therefore, the estimated fluence ranges reported in Table 4-6 of Reference 1 for the thermal shield components located near/above the top or near/below the bottom of the active core (e.g., thermal shield bolts, dowels, flexures, etc.) are applicable to Point Beach.

Therefore, based on the result of the fluence comparison performed in Section 2.2, the reactor internals estimated fluence ranges reported in Table 4-6 of Reference 1 are applicable to Point Beach Unit 1. Note that given the margins shown in Section 2.2, this conclusion would remain valid even if relatively small (e.g., 5%) increases in the Point Beach Unit 1 fluence projections were to occur. In addition, and for the following reasons, the reactor internals estimated fluence ranges reported in Table 4-6 of Reference 1 are also applicable to Point Beach Unit 2:

- Point Beach Units 1 and 2 have similar reactor internals geometries.
- Point Beach Units 1 and 2 employ similar fuel management plans.

- Point Beach Units 1 and 2 operate under similar conditions (e.g., reactor power, inlet temperature, outlet temperature).
- Since Point Beach Units 1 and 2 have similar reactor internals geometries, employ similar fuel management plans, and operate under similar conditions, the reactor internals fluence projections for Point Beach Unit 2 would be similar to the ones determined for Point Beach Unit 1.
- With the exception of the thermal shield inner surface at the core midplane, the reactor internals fast neutron fluence projections determined for the representative 3-loop PWR are significantly greater than the ones determined for Point Beach Unit 1.
- The thermal shield fast neutron fluence projections determined for Point Beach Unit 1 are easily within the applicable estimated fluence ranges reported in Table 4-6 of Reference 1.

The Point Beach Unit 1 projection cycle design meets the applicability criteria for core operation provided in Section 4.3.2 of Reference 1. Note that these criteria are the same as the applicability guidelines for Westinghouse-designed reactors specified in Appendix B of MRP-227, Revision 1-A (Reference 6). Also note that the Unit 1 projection cycle design evaluated herein is based on the average core power distributions and reactor operating conditions of Unit 1 Cycle 37, but includes a 10% bias on the peripheral and re-entrant corner assembly relative powers. Since this cycle design meets the applicability criteria for core operation provided in Reference 1, future reload cycle designs at Point Beach Unit 1 would also be expected to meet these criteria providing they are similar—especially with respect to core power, peripheral and re-entrant corner assembly cycle-average relative powers, and fuel design—to Unit 1 Cycle 37.

The Point Beach Unit 2 projection cycle design meets the applicability criteria for core operation provided in Section 4.3.2 of Reference 1. Note that these criteria are the same as the applicability guidelines for Westinghouse-designed reactors specified in Appendix B of Reference 6. Also note that the Unit 2 projection cycle design evaluated herein is based on the average core power distributions and reactor operating conditions of Unit 2 Cycle 38, but includes a 10% bias on the peripheral and re-entrant corner assembly relative powers. Since this cycle design meets the applicability criteria for core operation provided in Reference 1, future reload cycle designs at Point Beach Unit 2 would also be expected to meet these criteria providing they are similar—especially with respect to core power, peripheral and re-entrant corner assembly cycle-average relative powers, and fuel design—to Unit 2 Cycle 38.

4.0 References

1. Electric Power Research Institute (EPRI) Technical Report, "Materials Reliability Program: Screening, Categorization, and Ranking of Reactor Internals Components for Westinghouse and Combustion Engineering PWR Design (MRP-191, Revision 2)," EPRI, Palo Alto, CA: 2018. 3002013220.
2. WCAP-14040-A, Revision 4, "Methodology Used to Develop Cold Overpressure Mitigating System Setpoints and RCS Heatup and Cooldown Limit Curves," May 2004.
3. Regulatory Guide 1.190, "Calculational and Dosimetry Methods for Determining Pressure Vessel Neutron Fluence," March 2001.
4. WCAP-18124-NP-A, Revision 0, "Fluence Determination with RAPTOR-M3G and FERRET," July 2018.
5. ERPI Letter MRP 2013-025, "MRP-227-A Applicability Template Guideline," October 2013. (ADAMS Accession No. ML13322A454)
6. EPRI Technical Report, "Materials Reliability Program: Pressurized Water Reactor Internals Inspection and Evaluation Guidelines (MRP-227, Revision 1-A)," EPRI, Palo Alto, CA: 2019. 3002017168. (ADAMS Accession No. ML19339G350)

This page was added to the quality record by the PRIME system upon its validation and shall not be considered in the page numbering of this document.

Approval Information

Author Approval Hawk Andrew E Jul-07-2020 13:58:50

Reviewer Approval Benson Riley Jul-07-2020 15:35:23

Manager Approval Houssay Laurent Jul-07-2020 20:38:05

Files approved on Jul-07-2020

*** This record was final approved on 7/7/2020 8:38:05 PM. (This statement was added by the PRIME system upon its validation)